Green Chemistry and Sustainable Technology

Hongzhang Chen

High-solid and Multi-phase Bioprocess Engineering

Theory and Practice

Springer

Green Chemistry and Sustainable Technology

Aims and Scope

The series *Green Chemistry and Sustainable Technology* aims to present cutting-edge research and important advances in green chemistry, green chemical engineering and sustainable industrial technology. The scope of coverage includes (but is not limited to):

- Environmentally benign chemical synthesis and processes (green catalysis, green solvents and reagents, atom-economy synthetic methods etc.)
- Green chemicals and energy produced from renewable resources (biomass, carbon dioxide etc.)
- Novel materials and technologies for energy production and storage (bio-fuels and bioenergies, hydrogen, fuel cells, solar cells, lithium-ion batteries etc.)
- Green chemical engineering processes (process integration, materials diversity, energy saving, waste minimization, efficient separation processes etc.)
- Green technologies for environmental sustainability (carbon dioxide capture, waste and harmful chemicals treatment, pollution prevention, environmental redemption etc.)

The series *Green Chemistry and Sustainable Technology* is intended to provide an accessible reference resource for postgraduate students, academic researchers and industrial professionals who are interested in green chemistry and technologies for sustainable development.

More information about this series at http://www.springer.com/series/11661

Hongzhang Chen

High-solid and Multi-phase Bioprocess Engineering

Theory and Practice

Springer

Hongzhang Chen
Institute of Process Engineering
Chinese Academy of Sciences
Beijing
China

ISSN 2196-6982 ISSN 2196-6990 (electronic)
Green Chemistry and Sustainable Technology
ISBN 978-981-10-6351-0 ISBN 978-981-10-6352-7 (eBook)
https://doi.org/10.1007/978-981-10-6352-7

Library of Congress Control Number: 2018939314

Printed on acid-free paper

This Springer imprint is published by the registered company Springer Nature Singapore Pte Ltd.
part of Springer Nature
The registered company address is: 152 Beach Road, #21-01/04 Gateway East, Singapore 189721, Singapore

Preface

High water consumption, high energy consumption, and high cost of product purification are main problems in traditional low concentration of bioprocess system, which has great hindered development of bio-industry. Therefore, new sustainable strategies must be developed so as to promote green bio-industry both in academic and industrial fields. Based on the author's work, high-solid and multi-phase bioprocess is proposed. High-solid and multi-phase bioprocess is featured by high-solid loading, less water, and full utilization of biomass resources. In this system, economic raw materials (such as lignocellulose) are used as the substrate in a high loading which contributes to higher product concentration and less waste discharge. This book systematically elaborates principle and application of high-solid and multi-phase process and the process intensification method.

Starting with proposed conception of high-solid and multi-phase bioprocess, features and problems of high-solid and multi-phase system are elaborated first, followed by corresponding solutions for the problems. Particularly, novel intensification strategies (including periodical peristalsis and gas double dynamic) in high-solid and multi-phase system take a big part in this book. Additionally, several models of high-solid and multi-phase process chains are summarized and analyzed in this book. Consequently, this book provides academic and industrial introduction of high-solid and multi-phase bioprocess and could be the reference for readers in related fields.

This book is a monograph that systematically discusses the theory of high-solid and multi-phase bioprocess engineering and its application. First, Chap. 1 gives brief introduction and problems in high-solid and multi-phase bioprocess engineering. Chapters 2 and 3 describe the features of high-solid multi-phase bioprocess based on characteristics of solid substrates. Chapter 4 emphasizes the construction of microorganism and enzyme catalysis which is suitable for high-solid and multi-phase system. Chapters 5–7 elaborate the function of periodical stimuli and new methods, process engineering, and parameters monitoring in high-solid and multi-phase bioprocess, respectively. Finally, Chap. 8 reviews the industrial application of high-solid multi-phase bioprocess.

My Ph.D. and Masters' research work was essential precondition for publishing this book. In particular, Dr. Yang Liu, Dr. Wenjie Sui, Dr. Zhihua Liu, Dr. Zhimin Zhao, Dr. Menglei Xia, Dr. Yuzhen Zhang, Master Feng Kong, Dr. Qihong Zhao, and Master Jun Xie participated in writing some chapters. Additionally, Prof. Lan Wang gave kind suggestion on contents and layout of this book. Many references have been cited by our predecessors and colleagues. And I wish to express my sincere thanks to all of them.

Beijing, China Hongzhang Chen

Contents

Chapter 1
Introduction

Abstract High-solid and multi-phase bioprocess system refers to the system with more than 15% solid loading. Usually, the system is composed of solid, liquid, and gas phases. It has become the hot topic in bioprocess due to the merits of environmental friendly, water saving, and energy saving. However, "solid effect" caused by high-solid loading results in a series of problems such as high viscosity, high stirring energy consumption, and low conversion. In this chapter, overview of high-solid and multi-phase bioprocess, as well as some characteristics, is elaborated. Additionally, novel enhancement measures and integration concept for high-solid and multi-phase system are briefly introduced from the aspect of process engineering scientific theory.

Keywords High-solid and multi-phase bioprocess · Solid effect
Bioprocess intensification

1.1 Propose of High-solid and Multi-phase Bioprocess

China, the second-largest economy in the world, has played important role in global biological industry for many years. Although it is the largest producer of fermented products in the world, energy consumption in industrial process is also huge. For example, a 50 million m^3 industrial reactor will consume 1.3 billion m^3 and discharge 1 billion m^3 of wastewater every year. The resource and environmental pressure are the bottleneck to realize the sustainable development of Chinese bio-industry. Biological reaction is the core of chemical production by fermentation, waste biodegradation, and resource-oriented utilization, which is also the important choice of producing biofuels and biological chemicals, in case of the shortage of oil resources and the deterioration of the atmospheric environment caused by the usage of petroleum-based products especially gasoline and diesel. In conclusion, biological reaction is essential to industrial upgrade and sustainable development of economy and society.

H. Chen, *High-solid and Multi-phase Bioprocess Engineering*,
Green Chemistry and Sustainable Technology,
https://doi.org/10.1007/978-981-10-6352-7_1

In general, solid material content of traditional biological reaction system is 5%, compared to the chemical and oil processing process, the biological fermentation, and enzyme catalysis reaction which are low substrate concentration, causing the problem of resources and environment. Moreover, the drawback of the low substrate concentration reaction system is low apparent efficiency and high energy consumption and water waste.

High-solid and multi-phase bioprocess system refers to the system with more than 15% solid loading. Usually, the system consists of solid, liquid, and gas phase. It could become a breakthrough and dominant strategy for solving problems in traditional fermentation industry. Taking ethanol production with starch materials, for example, in high-solid system, wastewater decreased from 9 to 7 tons for every ton of ethanol, emission is reduced by over 20%, and steam consumption is reduced by one-third. Up to now, most researches in domestic and aboard are exploring reaction process conditions from perspective of mechanical agitation. However, a series of technological difficulties were resulted from the normal mechanical agitation in the high-solid multi-phase system, e.g., energy consumption exponentially increased with the solid loading; mixed scale could only achieve cm level which could not be favorable to heat and mass transfer intra-particle. Therefore, the low efficiency of heat and mass transfer in the system composed of solid, liquid, gas and microorganism, and the inapplicability of the mixing methods of traditional mechanical agitation (energy consumption increased exponentially with high-solid content) are the main difficulties in the development of high-solid biological reaction.

Considering the above obstacles of technology and cost, we developed new methods to enhance the high-solid and multi-phase bioprocess based on solid substrate effect and innovated new systems of theory and technology for optimization and amplification of biological process based on periodic force, so as to solve the current problems of efficiency during the high-solid biological reaction process. The results present basic problem in engineering: the mechanism of biological reaction in high-solid system.

Aiming at the break, the restriction of heat and mass transfer in high-solid reaction, the author enhanced the accessibility of the solid substrate biological reaction of fermenting materials by steam explosion and established a material refining platform with the core technology of steam explosion; proposed novel methods to enhance the high-solid and multi-phase system with periodic force which breaks through the key technology, such as periodic agitation and pressure pulsation; and also put forward a new way to simulate numerical amplification of the high-solid multi-phase bioprocess, which finally realizes the comprehensive research of integrated industrialization technology foundation of high-solid multi-phase biological reaction process and lays the scientific and technological foundation for high-solid multi-phase bioprocess.

1.2 Specificity of High-solid and Multi-phase Bioprocess

1.2.1 The Porous Characteristics and "Solid Effect" of Solid Substrate

Traditional enzymatic hydrolysis and fermentation of biomass are usually carried out under the low-solid loading (less than 15% (w/w)). Low-solid loading conversion process has caused several problems. First of all, low substrate concentration results in low product concentration, increasing separation cost. Second, it can cause much water consumption, large amount of wastewater emissions, environmental pollution, and high cost for wastewater treatment. In addition, the large equipment with low utilization results in low production efficiency. For example, in the process of lignocellulosic ethanol production, the separation process is economic when ethanol concentration is greater than 4% (w/w), implying that fermentable sugar concentration must be higher than 8%, for the majority of lignocellulose biomass, and the initial solid load should be above 20%. When solid load is higher than 15%, the system is no longer a liquid or slurry state, but keeps in solid state, called high-solid reaction. High-solid bioprocess has many advantages, such as high production efficiency, small equipment with high efficiency, less wastewater, and low cost. High-solid reaction process is the inevitable trend of lignocellulosic ethanol with a cost advantage and has become the hot topics in the study of lignocellulose biomass refining [1].

Despite the many advantages of high-solid system, it also causes some problems. Porous heterogeneity and poor liquidity of biomass cause "solid effect" due to the increased complexity of liquid–solid multi-phase system, which hinder the mass transfer and reduce reaction efficiency. The bound water of high-solid reaction system is not beneficial for mass transfer, while high viscosity affects stirring. Low conversion is caused by product inhibition. More importantly, enzymes and microorganisms with biological activity are sensitive to the environment and dependencies; the presence of enzymes and microorganisms in high-solid reaction system make system more complex. The traditional mixing methods using shear force as the power source and mixing energy consumption rapidly increased with increase of solid load; it cannot strengthen the transfer in lignocellulose porous channel to lignocellulose biomass porous channel or even stirred under the high-solid loading condition. Besides mechanical shear force of mechanical stirring, shear mixing damages the enzyme activity and microbial activity, reducing the reaction efficiency. Therefore, scientific cognition and analysis of high-solid reaction system are needed urgently, and efficient new way strengthening measures and the reactors are also needed to improve the efficiency of high-solid reaction [1].

1.2.2 Water-Binding Effect in High-solid and Multi-phase System

Water played a key role in the enzymatic hydrolysis process, which is the medium for the enzyme and product spread diffusing or leaving to the site or diffusion from leaving the reaction sites and also the substrates of enzymatic hydrolysis of glycosidic bond hydrolysis reaction, and thus decided the enzymatic hydrolysis reaction efficiency. In lignocellulosic biomass enzymatic hydrolysis system, water present in five different states, including primary combined water, limited secondary combined water, capillary water, gravity water, and free water. Water which connected cellulose or other chitosan via hydrogen bond is known as the primary combined water. Water adsorbed by the cell wall or chitosan surface is known as the secondary combined water or water film. Water existed in microporous capillary pores or space between cells fettered by capillary force is called capillary water. Water in macroporous channel is known as restricted gravity water. Water free from the solid effect or other solutes is called free water. Water and other substances can lead to its liquidity reduced; the phenomenon is called water-binding effect, and the water is referred to as bound water. With the increase of solid loading, water is bound to the matrix, and free water becomes less or disappeared, such that phenomenon is called water-binding effect, which affect in reducing the efficiency of enzymatic hydrolysis.

There are some researches on water binding in lignocellulose hydrolysis process. Selig et al. [2] studied the influence of lignocellulose polymer to water bound and its relation with the efficiency of the enzymatic hydrolysis. Results showed that when adding polymer under 10% solid content, the low-field NMR determination of T2 relaxation time curve determined by the low-field NMR soon become close to zero, implying that the water-binding effect is increased with polymer's increased water-binding effect. Water is closely related to the binding effect and cellulose enzyme inhibition causes the decrease of enzymatic hydrolysis conversion rate. Roberts et al. [3] studied the relationship among the variation of water distribution, mass transfer efficiency, and enzymatic hydrolysis efficiency. It was found that water bondage increased with the increase of solid load. In addition, bond water was found closely related to the enzyme system and the spread of monosaccharide. With solid load increased from 5 to 20%, the effective diffusion coefficient of bovine serum protein was reduced by 61.5% and the calculation of intrinsic diffusion coefficient was decreased by 51.2%. It showed that water distribution and status in high-solid reaction system is closely related to the enzymatic hydrolysis efficiency of enzymatic hydrolysis. However, the mechanisms are still not clear and the conclusions about that are far from being standardized [4]. There is much confusion about water bondage in high-solid reaction system that needs to be further studied, for example, what are the key factors of bound water, the key role of these factors in the digestion hydrolysis process? Whether water with different positions and status in the hydrolysis process has its unique function?

What measures need to be taken to reduce water bondage to improve the efficiency of enzymatic hydrolysis?

1.2.3 The Rheological Property of High-solid and Multi-phase System

Rheology is one branch of mechanics, which studies the change rules of the substrate form and flow under conditions such as stress, strain, temperature, and humidity. In high-solid system, the in-depth analysis of rheological properties is helpful for process design, process optimization, and reactor development. The rheological properties of high-solid reaction system depend on the physical properties of raw materials, pretreatment methods and conditions, solid particle size and distribution and fiber softness, etc. Solid loading can significantly affect the rheological properties. When solid loading is higher than 15%, free water content decreased to zero, and solid lubrication among the solid particles disappears, the mixture no longer in liquid or slurry state but in solid state. Rheological models of high-solid enzymatic hydrolysis such as the Bingham model, the Herschel–Bulkley model, the Wildemuth–Williams, and the Casson model [5, 6] can be used to describe the rheological properties of high-solid reaction system of lignocellulose. Roche et al. [7] investigated the relation between the changes of yield stress and the solid particle concentration during the enzymatic hydrolysis of corn stover with the 20% (w/w) solid loading after dilute-acid pretreatment, and found that when the enzymatic conversion rate was near 40%, the enzymatic hydrolysis system of corn stover could reach the yield stress ($\tau\ y < 10$ Pa) after saccharification for about 2 days. The Wildemuth–Williams model, a semi-empirical rheological model, describes the relationship between yield stress ($\tau\ y$) and volume fraction (ϕ) as follows [8]:

$$\tau \times y(\phi) = \frac{A}{m} \times \frac{\left(\frac{\phi}{\phi m0-1}\right)}{\left(1 - \frac{\phi}{\phi m\infty}\right)} \tag{1.1}$$

where $\Phi m0$ is the maximum volume fraction with no shear; $\Phi m\infty$ is the maximum packing fraction with ultimate shear; and A and m are related to the microstructural changes of the system under the ultimate shear action. The yield stress decreased with the decrease of the volume fraction in the high-solid enzymatic hydrolysis process. By establishing the material balance and the semi-empirical model, high-solid enzymatic hydrolysis processes can be connected with particle concentration and yield stress, providing guidance for the process design and optimization. Viamajala studied the relationship between the rheological properties and initial solid concentration, the relation between pretreatment extent and the particle size by enzymatic hydrolysis of corn stover pretreatment by the dilute acid, and the results

showed that there was shear thinning of the enzymatic hydrolysis of corn stover, described as by Casson model [8]:

$$\tau^{0.5} = \tau_{\mathrm{Cy}}^{0.5} + K_C \gamma^{0.5} \tag{1.2}$$

where τ is the shear stress (Pa), τ_{Cy} is the apparent Casson yield stress (Pa), γ is the shear rate (s^{-1}), and K_C is a Casson constant ($Pa^2\ s^2$). Apparent viscosity and yield stress increased with the increase of solid loading. Under the same solid loading, dilute-acid pretreatment and smaller particle size can make apparent viscosity and yield stress smaller. With the increase of solid loading, the particle interaction can cause the increase of the apparent viscosity and yield stress. In addition, the rheological properties are also closely related to the composition and physical properties (such as porosity) of solid substrate. Um et al. investigated the relations among viscosity, shear stress, and shear rate with 10–20% solid loading; the viscosities in the 10%, 15%, and 20% enzymatic hydrolysis systems are 0.0418–0.0144, 0.233–0.0348, and 0.292–0.0447 Pa•s, respectively. The enzymatic hydrolysis system showed pseudoplastic behaviors, and the rheological analysis suggested that apparent viscosity was closely related to solid loading [6]. Above studies indicated that the rheological properties of high-solid bioprocess system are closely related to solids loading and can affect the enzymatic hydrolysis efficiency. The increased solid loading can significantly affect the rheological properties of the enzymatic hydrolysis system and bring new challenges for process design and operations. Therefore, the rheological studies on high-solid enzymatic hydrolysis reaction system should be carried out to look for new and effective strategies to promote the rheological properties, so as to improve the enzymatic hydrolysis efficiency.

1.2.4 Transformation Efficiency of High-solid and Multi-phase System

The sugar conversion rate and sugar yields are two important evaluation criteria of enzymatic hydrolysis process, and significantly influence the cost of unit operation of enzymatic hydrolysis. During the enzymatic hydrolysis process, with the increase of the solid-to-liquid ratio, the influences of washing pretreated material, the addition of matrix, and the synergetic effects on sugar conversion rate and sugar yield will be more significant and influence the final sugar concentration of enzymatic hydrolysis. In enzymatic hydrolysis process, the washing of the pretreated materials and the detoxification of the hydrolysate after the enzymatic hydrolysis are usually needed to reduce inhibitors, while the costs of washing and detoxification processes account for over 22% of the total cost of ethanol production [5]. Hodge et al. [9] compared the glucose yield of the enzymatic hydrolysis of pretreated biomass with and without washing, to investigate the influences of inhibitors

on the enzymatic hydrolysis. The results showed that though the inhibition of glucose concentration could cause the "leveling-off" of enzymatic hydrolysis rate, the enzymatic hydrolysis rate decreased more obviously during enzymatic hydrolysis of pretreated biomass without washing. In addition, it was found that soluble composition had more contribution to the mass transfer and hydrolysis limitations. Lu et al. [10] proved that the sugar conversion rate of the enzymatic hydrolysis of pretreated biomass without washing was significantly lower than that of with washing. However, Pristavka et al. [11] believed that the non-washing process had two advantages: first, it could save water with low costs and more environmental friendly; second, it could remove some soluble sugars. Recently, domestic and international scholars have studied the influences of different feeding ways on the conversion rate in high-solid enzymatic hydrolysis process. Compared with one-time feeding strategy, the batch strategy has many advantages in improving the conversion rate, such as low initial viscosity to avoid mixing and mass transfer limitations; batch feeding can provide sufficient time for the liquefaction between the batches, so as to maintain a certain degree of free water to improve the mass diffusion efficiency [9, 12]. Wang et al. [13] found that with the feeding of materials with 50% final solid-to-liquid ratio in the beginning, and the feeding of materials with 25% final solid-to-liquid ratio at 24 and 48 h, the final sugar concentration could reach 115 g/L with conversion rate only 5% lower than the materials with 15 and 20% final solid-to-liquid ratio. Zhang et al. [14] studied the enzymatic hydrolysis of corn stover pretreated by NaOH, batch feed materials with 9, 8, 7, and 6% during the first 24 h to 30% solid loading, and results showed that the enzymatic hydrolysis rate of the initial feeding reached 60% of the maximum, while the rate dropped with the batch feeding and significantly decreased to 39% at 72 h after the final feeding. It is worth noticed that in the enzymatic hydrolysis with batch feeding, the time of the feeding of raw materials and cellulose must be taken into account to ensure the increase of conversion rates, of which there has not been a consensus of the previous studies. Problems still exist besides advantages of enzymatic hydrolysis with feeding. Because of the decreased enzymatic synergies with high solid-to-liquid ratio, large amount of oligosaccharides produced in the enzymatic hydrolysis affects the conversion rate, indicating the essential importance of the synergy of cellulase in the enzymatic hydrolysis. Previous studies showed that the synergy of β-glucosidase and cellulase can reduce inhibition of products on cellulose enzyme and then increase conversion efficiency. Garcia-Aparicio et al. [15] studied the influences of cellulase, β-glucosidase, and xylan glycosidase on the enzymatic hydrolysis of steam-exploded barley straw. It was found that the addition of xylan glycosidase improved the efficiency of enzymatic hydrolysis and increased the conversion rate of cellulase. Di Risio et al. [16] compared the sugar yield of enzymatic hydrolysis under high solid-to-liquid ratio with the additions of both cellulase and xylan glycosidase, all of cellulase β-glucosidase and xylan glycosidase and only xylan glycosidase, and the results showed that the xylose yield of the xylan glycosidase group was lower than the other two groups, while the glucose yield showed the same trend. Studies have shown that the synergetic conversion with different enzymes can avoid the high

enzyme load while achieving a higher conversion rate of enzymatic hydrolysis. However, the absorption/desorption efficiency, mass transfer, and diffusion efficiency of enzymes are very low, and the synergetic effects of the enzymes reduced in high solid-to-liquid ratio. Cellulase plays an important role in the biomass conversion process. The process integration and intensification depend on the use of cellulase, while the efficiency of enzymes is the balance of the amount and the costs.

1.2.5 Intensification of High-solid and Multi-phase Bioprocess and New Bioreactors

During the high-solid reaction process (such as high-solid enzymatic hydrolysis), the effects of various limiting factors are interactive, and the change of rheological properties mainly represented by the increase of apparent viscosity can decrease the mass transfer efficiency and increase the power consumption of the mixing and blending. Physical properties of lignocellulose biomass can influence the water distributions and the status, while tight bond water can reduce the diffusion of products and enzymes in the high-solid reaction system, decrease the synergetic effects and increase the feedback inhibition, and influence the rheological properties of the system. These limiting factors can lead to obviously low efficiency of high-solid reaction.

In the process of high-solid reactions, the power of mixing is not only influenced by the high viscosity of the reaction system but also need to overcome the interface resistance (the surface tension which increases with the increase of solid loading). In addition, shear forces were usually used in traditional mixing methods, which cannot effectively act on the intra-particles, resulting in low transfer efficiency and nonuniform mixing. Meanwhile, the shear forces can deactivate the enzymes easily, decrease the adsorption/desorption efficiency of the enzymes with the substrates, and hence lower the product efficiency of high-solid reaction processes.

High-solid and multi-phase bioprocess demand higher requirements for the mixing methods, reactor design, reactor amplification, and process design. Scholars have carried out related studies at home and abroad. Mixing power is influenced by viscosity and resistance of the high-solid enzymatic hydrolysis. During the mixing process, because of the incompatibility of solids and liquids, the interface resistance which also known as the surface tension should be overcome and the resistance increased with the increase of solid contents. According to calculations, the solid loading of traditional enzymatic hydrolysis is 5–15% and the mechanical mixing power increases sharply by 300%, while the solid loading is over 20%, e.g., when solid loading is 25% and 30%, compared with 5%, the mechanical mixing power increases by 415% and 545%, respectively, indicating that with higher solid loading, the power for the mixing increases exponentially. Therefore, new requirements for mixing, reactor design, and process design of high-solid reaction

system are put forward. Development of new intensification measures is important way to improve the efficiency of high-solid reaction and to achieve large-scale production.

Efficient mixture depends on the geometric shape of the impeller, which can lead to the differences in mixing speed, shear forces, and mixing energy consumption. Zhang et al. [17] investigated the influences of the spiral blade impeller on the high-solid (30%) enzymatic hydrolysis efficiency in vertical reactor and found that the mixing power was decreased by 4/5 than traditional Rushton impeller, and spiral blade impeller was more suitable for high-viscosity non-Newtonian fluids. It also found that the geometric shape of blades was essential to efficient mixing. Wang et al. [13] investigated the influences of the plate and frame blade impellers and double-curved blade impellers on the high-solid enzymatic hydrolysis of sweet sorghum pretreated by hydrothermal method, and found that the glucose yield of which used the plate and frame blade impellers was 10% higher than the other, indicating that the geometric shape of blades could significantly affect the mixing efficiency. Compared with the double-curved blade impeller, the plate and frame blade impellers could produce bigger homogeneous mixing areas and hence improved the mass transfer in the reactor at different depths. Zhang et al. [18] investigated the rule of influences of nail-shaped mixer on the high-solid enzymatic hydrolysis of hardwood biomass and found that higher glycan conversion rate achieved at the endpoint of enzymatic hydrolysis with nail-shaped. Compared with flask shaking, it could significantly shorten the liquefaction time of unbleached hardwood with 20% solid loading and increase the mass transfer efficiency of the high-solid reaction system. In addition, parameters including the rotation speed and the size of impeller and its diameter ratio with the reactor could also influence the mass transfer efficiency of high-solid enzymatic hydrolysis. The above results indicated that developing new mixing method is an effective strategy to improve the efficiency of high-solid enzymatic hydrolysis.

There have been some studies on the new high-solid enzymatic reactors. In the study of Jørgensen et al. [19], the influence of rotor drum reactor which mixed material by free falling on the high-solid enzymatic hydrolysis efficiency was investigated. Results showed that there were no obvious influences on glycan conversion rate with rotation speed of 3.3–11.5 rpm for 24 h; while 7 FPU/g dry matter with 40% solid loading, enzymatic hydrolysis for 96 h, the glucose concentration reached 86 g/kg. Roche et al. [20] found the horizontal reactor which mixed by gravity or free falling had many advantages over conventional vertical reactors, such as minimized particle sedimentation, local product accumulation, and the distribution of enzymes are more uniform. With 20% solid loading, glycan conversion rate reached 80–85% in the flask rotation reaction system with free-falling mixing. Dasari et al. [21] found that compared with vertical reactors, with 25% solid loading, the enzymatic hydrolysis glucose conversion rates of horizontal reactors could increase by 10%, and power reduced significantly. Although the above reactors are proved to have a certain effect in the intensification of the high-solid enzymatic hydrolysis, they cannot be scaled up. Further research of new mixing methods and reactors are needed to meet the requirements of

high-solid enzymatic hydrolysis and process economy. In recent years, the pilot-trial-level or demonstration-level operational platform of high-solid enzymatic hydrolysis has been established in some countries. In Denmark, the demonstration plant with the annual output of 5.3 million liters of ethanol was established. It can deal with 1 L fermentation liquid by distillation per hour, when the solid-to-liquid ratio is at 25–30%, and the consumption of enzyme is 3–6 FPU/g dry matter. The National Renewable Energy Laboratory of USA (NREL) built a 4000 L reactor, with the solid-to-liquid ratio over 20% and daily capacity of 0.5–1.0 t dry matter [8]. However, the research on high-solid enzymatic hydrolysis is still relatively backward in China.

1.3 Fundamental Engineering Theories of High-solid and Multi-phase Bioprocess

Traditional enzymatic hydrolysis and fermentation industry could not meet the demand of sustainable development because of the disadvantage of large amount of wastewater, serious environmental pollution, and high energy cost. Taking ethanol production, for example, the ethanol concentration of industrial separation process must be over 4% (w/w) for the advantages of process cost, requiring more than 20% solid loading in system. High-solid and multi-phase bioprocess could be a potential solution to those problems. However, traditional technology is unsuitable for high-solid and multi-phase bioprocess because of large shear forces, low the enzyme adsorption/desorption efficiency, intermittent operation, and low production efficiency.

High-solid and multi-phase system has advantages of high substrates and product concentration, low product separation cost, and high productivity. However, the high loads of porous biomass can cause "solid effect" (such as composition and matrix effect, product inhibition effect, bound water effect, and enzyme absorption/desorption effect). Viscosity caused by high-solid loading ("solid effect") in high-solid enzymatic hydrolysis system can affect transfer characteristics, increase mixing power consumption, and reduce enzymatic hydrolysis efficiency. It also increases the difficulties in process design and amplification as well as the large-scale production.

There have been preliminary progress on high-solid enzymatic hydrolysis both at home and abroad, however, before the large-scale industrialization, the intensification methods, and mechanism of the enzymatic hydrolysis should be investigated based on the porosity of lignocellulose, and the new reactor and process integration strategies should be developed, so as to solve the problems in high-solid and multi-phase bioprocess system and provide theoretical basis and technological experiences for the industrialization refining and conversion of lignocellulose.

According to the principles of process engineering and sciences, scientific cognition of the porous structure of lignocellulose and high-solid enzymatic hydrolysis behaviors can be obtained by the researches on the porosity of lignocellulose, the mass transfer, and high-solid enzymatic hydrolysis efficiency. Meanwhile, the new mixing methods (periodic peristalsis) for the intensification of enzymatic hydrolysis should be developed, with the analysis and descriptions of the porosity of lignocellulose and the intensification mechanism. With studies and mechanism description of the process, the new technologies and methods can be acquired to solve the bottleneck of the limitations in the enzymatic hydrolysis and conversion. The periodic peristalsis reactor of high-solid enzymatic hydrolysis should be studied and developed, meanwhile, exploring the principles of system integration and process amplification of high-solid enzymatic hydrolysis.

1.4 Development Bottleneck and Tendency of High-solid and Multi-phase Bioprocess

Development bottleneck of high-solid and multi-phase bioprocess is mainly caused by the characteristics of the system which is described in Sect. 1.2. From the perspective of reducing consumption, energy conservation, and reducing emission, the researches should be conducted on process intensification, system integration, and process amplification of high-solid enzymatic hydrolysis and fermentation of biomass.

Apart from solving the problem of "competition for food against people, competition for land against food" in bio-based products conversion, solving the problems (including wastewater discharge, high consumption, and low efficiency of the current materials) is also the urgency. High-solid and multi-phase bioprocess system can increase the proportion of sustainable resources in energy resources, accelerating the industrialization of cellulosic ethanol and bio-based products in China, as well as make significant contribution to improve the competitiveness of biotechnology industry in the world.

References

1. Liu ZH (2016) Process intensification of high solids enzymatic hydrolysis and fermentation of steam exploded straw. Institute of Process Engineering, Chinese Academy of Sciences
2. Selig MJ, Thygesen LG, Felby C (2014) Correlating the ability of lignocellulosic polymers to constrain water with the potential to inhibit cellulose saccharification. Biotechnol Biofuels 7 (1):1–10
3. Roberts KM, Lavenson DM, Tozzi EJ et al (2011) The effects of water interactions in cellulose suspensions on mass transfer and saccharification efficiency at high solids loadings. Cellulose 18(3):759–773

4. Felby C, Thygesen LG, Kristensen JB et al (2008) Cellulose–water interactions during enzymatic hydrolysis as studied by time domain NMR. Cellulose 15(5):703–710
5. Modenbach AA, Nokes SE (2013) Enzymatic hydrolysis of biomass at high-solids loadings—a review. Biomass Bioenerg 56(38):526–544
6. Um BH, Hanley TR (2008) A comparison of simple rheological parameters and simulation data for Zymomonas mobilis fermentation broths with high substrate loading in a 3-L bioreactor. Appl Biochem Biotechnol 145(1):29–38
7. Roche CM, Dibble CJ, Knutsen JS et al (2009) Particle concentration and yield stress of biomass slurries during enzymatic hydrolysis at high-solids loadings. Biotechnol Bioeng 104 (2):290
8. Viamajala S, Mcmillan J, Schell D et al (2009) Rheology of corn stover slurries at high solids concentrations—Effects of saccharification and particle size. Bioresource Technol 100(2):925
9. Hodge DB, Karim MN, Schell DJ et al (2009) Model-based fed-batch for high-solids enzymatic cellulose hydrolysis. App Biochemistry Biotechnol 152(1):88–107
10. Lu Y, Wang Y, Xu G et al (2010) Influence of high solid concentration on enzymatic hydrolysis and fermentation of steam-exploded corn stover biomass. App Biochem Biotechnol 160(2):360–369
11. Pristavka A, Kodituvakky PA, Kozlov YP et al (2000) High-solids enzymatic hydrolysis of steam-exploded willow without prior water washing. App Biocheme Microbiol 36(2):101–108
12. Yang J, Zhang X, Yong Q et al (2010) Three-stage enzymatic hydrolysis of steam-exploded corn stover at high substrate concentration. Bioresource Technol 102(7):4905–4908
13. Zhuang X, Qiang Y, Wei Q et al (2012) High consistency enzymatic saccharification of sweet sorghum bagasse pretreated with liquid hot water. Bioresource Technol 108(2):252
14. Zhang Y, Liu Y, Xu JL et al (2011) High solid and low enzyme loading based saccharification of agricultural biomass. In: Symposium on enzyme engineering in China. pp 345–353
15. García-Aparicio MP, Oliva JM, Manzanares P et al (2011) Second-generation ethanol production from steam exploded barley straw by Kluyveromyces marxianus CECT 10875. Fuel 90(4):1624–1630
16. Risio SD, Hu CS, Saville BA et al (2011) Large-scale, high-solids enzymatic hydrolysis of steam-exploded poplar. Biofuel Bioprod Bior 5(6):609–620
17. Zhang J, Chu D, Huang J et al (2010) Simultaneous saccharification and ethanol fermentation at high corn stover solids loading in a helical stirring bioreactor. Biotechnol Bioeng 105 (4):718–728
18. Zhang X, Qin W, Paice MG et al (2009) High consistency enzymatic hydrolysis of hardwood substrates. Bioresource Technol 100(23):5890–5897
19. Jørgensen H, Vibe-Pedersen J, Larsen J et al (2007) Liquefaction of lignocellulose at high-solids concentrations. Biotechnol Bioeng 96(5):862–870
20. Roche CM, Dibble CJ, Stickel JJ (2009) Laboratory-scale method for enzymatic saccharification of lignocellulosic biomass at high-solids loadings. Biotechnol Biofuels 2(1):28
21. Dasari RK, Dunaway K, Berson RE (2008) A scraped surface bioreactor for enzymatic saccharification of pretreated corn stover slurries. Energ Fuel 23(1):492–497

Chapter 2
Physical–Chemical Properties of Solid Substrates

Abstract Physical–chemical properties of solid substrates are important parameters of high-solid and multi-phase bioprocess. The chemical properties refer to the biomass recalcitrance and heterogeneity which caused by its chemical composition. The physical properties include porous properties, rheology properties, and water state. In this chapter, the composition and recalcitrance of the solid substrates are analyzed, and the change laws of physical–chemical properties such as porous properties, rheology properties, and water states are revealed, which is significant for bioconversion of biomass in high-solid and multi-phase bioprocess. In addition, solid effects caused by physical–chemical properties of solid substrates were also systematically discussed and investigated with the expectation of guiding bioconversion process of biomass.

Keywords High solid · Chemical composition · Physical property
Recalcitrance · Solid effects

High-solid and multi-phase bioprocess has merits of high concentration of substrate and production. In high-solid and multi-phase bioprocess, "solid effect" is caused by the increase of solid substrates, which is critical to the bioconversion efficiency of high-solid and multi-phase bioprocess. Researches indicated that the "solid effect" includes solid substrates composition effects, adsorption and desorption effects of cellulolytic enzymes, water-binding effects, and inhibitor effects [1, 2]. These can be the challenge of the large-scale utilization of renewable solid resources, changing transfer and reaction characteristics of the system, increasing process energy consumption, and reducing efficiency of the reaction.

Traditional researches on renewable resources aimed to improve the process efficiency with little cognition of the solid substrates' properties. Therefore, it could not solve the bottleneck problems in bioconversion of lignocellulose, resulting in the economic infeasibility of the large-scale utilization of renewable resources. The factors, influencing the efficiency of renewable solid resources conversion, include porous structure (e.g., pore size and volume, curvature, grain size, and specific surface area), chemical component (e.g., lignin, hemicellulose, acetyl, and

H. Chen, *High-solid and Multi-phase Bioprocess Engineering*,
Green Chemistry and Sustainable Technology,
https://doi.org/10.1007/978-981-10-6352-7_2

pectin), and chemical structure (crystallinity and the degree of polymerization of cellulose) [3]. It is closely related to the multicomponent and porous characteristics of renewable solid resources. The complex multicomponent characteristics of the renewable solid resources determine that using single technology and component is not benefit to the efficiency of the conversion process. Biomass is the typical porous medium material in which mass and heat transfer are different from the traditional liquid system; this phenomenon is more obvious in the situation of high-solid content. "Solid effect" is related to the intrinsic characteristics of renewable solid resources. Therefore, analyzing the relationship between the intrinsic characteristics of renewable solid resources and "solid effect" is essential to break down the "solid effect" and realize the efficient conversion of renewable resources.

2.1 Composition and Preparation of Solid Substrates

2.1.1 Solid Substrates Composition and Recalcitrance

Lignocellulose is a typical biomass with complex chemical and physical properties. Chemical components mainly include cellulose (30–50% of the total), hemicellulose (10–40% of the total), lignin (10–30% of the total), and other components such as wax, pectin, protein, pigment, and ash. The multicomponents of lignocellulose are macromolecules with specific functions, which are consisted of different monomers. There are differences among these multicomponents of different types of lignocellulosic biomass, while hardly differences exist in their basic elements (including carbon, hydrogen, oxygen, and nitrogen) [4–6].

Lignocellulosic materials include softwoods, hardwoods, and herbal plant biomass. Softwood contains 43% cellulose, 29% hemicellulose, and 28% lignin averagely. Hardwood contains about 45% cellulose, 34% hemicellulose, and 21% lignin, and cellulose content is similar to the softwoods. Hardwood has higher content of hemicellulose than softwood. In hardwood hemicellulose, there are 20–25% poly4-O-Methylglucuronic acid and 1–3% polydextrose mannose, while hemicellulose of softwoods has 15–20% poly-galactosidase-glucose mannose–acetate, 10% poly4-O-methyl-glucuronide arab xylose, and 1–3% arabinogalactan [5]. Therefore, there is more polyxylose in the softwoods but a higher content of polymannose, polygalactose, and araban in the hardwoods. Lignin content of softwoods is higher than that of hardwoods. The main components of lignin in softwoods are guaiacol propane and some phydroxyphenyl propane. The main components of lignin in hardwood are guaiacol propane, lilac propane, and small phydroxyphenyl propane [5]. The components of herbal plants are similar to that in hardwood. Cellulose content of most herbal plants is close to wood, except for straw (corn stalks and sorghum stalks) [5]. The chemical compositions of different types of biomass fiber raw materials are summarized in Table 2.1.

Table 2.1 Chemical composition of different biomasses

	Softwoods fibrous materials	Hardwoods fiber materials	Gramineae fiber materials
Carbohydrate	65–80%	65–80%	50–80%
Cellulose	40–45% (averagely 43%)	40–45% (averagely 45%)	30–45%
	length of the molecular chain is about 5000 nm, average polymerization degree is 10000	Similar to softwoods	Low polymerization degree of cellulose averagely
Hemicellulose	25–30% (averagely 28%), A high content of Poly-galactosidase-glucose mannose–acetate (15–20%), 10% content of glucuronic acid as well as galacturonic acid and araban-4-O-methylglucuronic acid xylose. Less content of arabinogalactan is about 1–3%	30–35% (averagely 34%), large amount of araban-4-O-methylglucuronic acid xylose (20–25%), less polydextrose mannose (1–3%)	20–35%, mainly component is polyxylose, small molecular weight, low polymerization degree
Lignin	25–30%(averagely 29%), mainly contains guaiacyl propane and a little phydroxyphenyl propane	20–25% (averagely 21%), mainly contains guaiacyl propane, syringyl, and a little phydroxyphenyl propane	10–25%, mostly at a low content level which are closely to that of hardwoods, except for the bamboo that is similar to softwoods
Extractives	Low content of hot water extractives and 1% NaOH extractives. High content of organic extractives, which main component are abietic acid, terpenoid, fatty acid and unsaponifiable matter, etc., which are existing in resin duct and xylem ray parenchymal cell.	Low content of hot water extractives and 1% NaOH extractives. Less than 1% content of organic extractives than softwoods which mainly contains free or esterifiable aliphatic acids and neutral components, without or few terpenoid compounds, mainly existing in xylem ray cell and parenchymal cell.	High content of hot water extractives and 1% NaOH extractives, and less than 1% ether extractives which mainly contains wax and few higher aliphatic acid and higher alcohols et al. And with quite high content of benzene–ethanol extractives (3–6%).
Protein	<0.5%		5–10%
Inorganic substance	0.1–1.0%		0.5–10%

Cellulose is the main component of the cell wall, which binds to hemicellulose, lignin, and pectin. The binding mode determines the property of lignocellulosic biomass. Cellulose is linear polymer which composed of D-glucose by 1, 4-β-glycosidic bond, and its chemical formula is $(C_6H_{10}O_5)_n$, where *n* is the degree of polymerization. Cellulose is composed of 44.4% carbon, 6.2% hydrogen, and 49.4% oxygen. Structure of cellulose is shown in Fig. 2.1 [5, 6].

Cellulose and lignin are linked together closely by hemicellulose. Hemicellulose almost exists in all plant cell wall. It is one of the main components of cell wall, and the content is lower than cellulose. Content, component, and structure of hemicellulose in various materials are different. The structure units of hemicellulose mainly contain D-xylose, D-mannose, D-glucose, D-galactose, L-arabinose, L-rhamnose, and L-fucose.

Taking herb plant cell wall as an example (Fig. 2.2), xylan is the main component of hemicellulose. The degree of polymerization of hemicellulose is only 150–200, much smaller than that of cellulose.

Lignin is a natural polymer with three-dimensional structure which is consisted of phenylpropane structure unit linked by ether bond and carbon–carbon bond. Phenylpropane structure unit forms the basic skeleton of nature hemicellulose, but there is a little difference in aromatic part. Based on the number of $–OCH_3$, structure units are divided into three kinds including guaiacyl propane (G), syringyl (S), and phydroxyphenyl propane (H) (Fig. 2.3). As a natural adhesive, lignin exists in microfiber and intercellular layer of plant cell walls, sticking adjacent cells together.

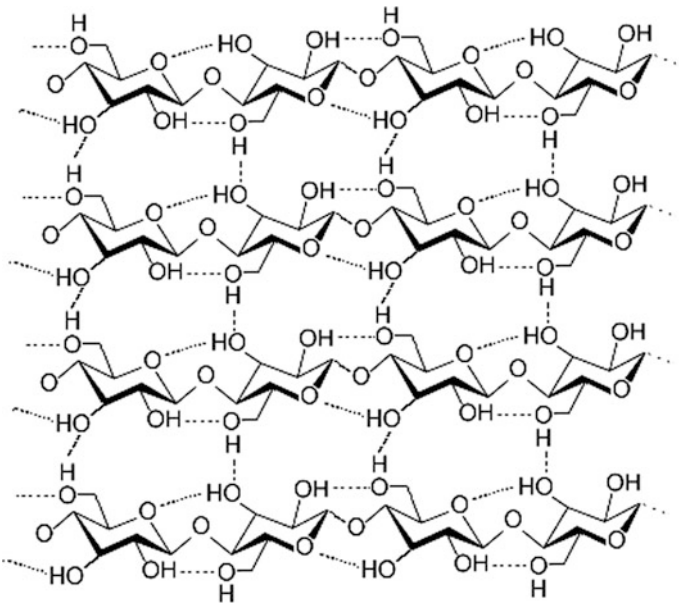

Fig. 2.1 Chemical structure of cellulose

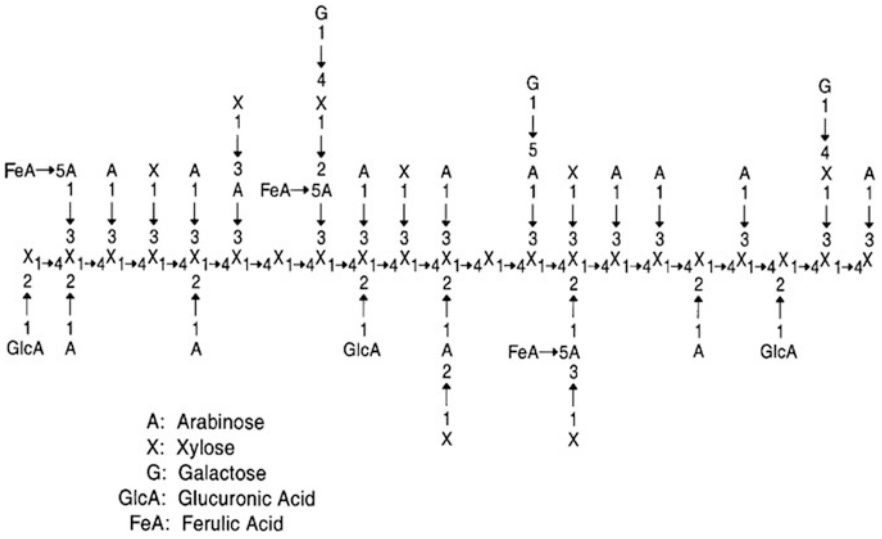

Fig. 2.2 Schematic structure of hemicellulose in maize fiber. Reprinted from Ref. [7]. Copyright 2003, with permission from Springer

Lignin plays a supporting role in maintaining the mechanical properties of the plant cell wall and reduces the transverse water permeability of cell wall. Besides, lignin can help to prevent microbial attack to glycan. The distribution of lignin in plant cell wall is inhomogeneous. The content and component of lignin of plant differ from each other, which depend on the plant species, growth time, and grown zone. Above all, lignin is the third largest nature polymer, whose content is only lower than cellulose and chitin in nature [4–6, 8].

According to the aromatic nuclear structure, lignin can be divided into guaiacyl propane, syringyl, and phydroxyphenyl propane type. And lignin has various functional groups (including aromatic ring and side chain), such as methoxy group ($-OCH_3$), phenolic hydroxyl group (–OH), and carbonyl group (–C=O), which is

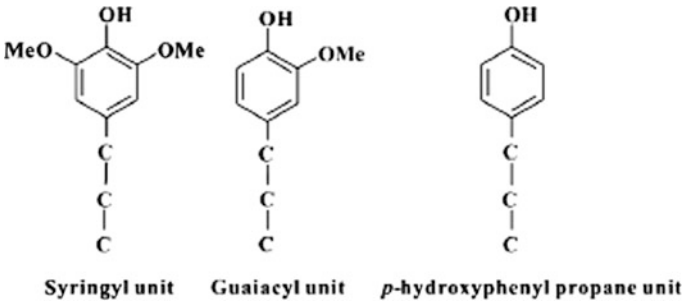

Fig. 2.3 Typical lignin aromatic polymer: syringyl (S), guaiacyl (G), and hydroxyphenyl (H)

shown in Fig. 2.4. Lignin is the biggest obstacle to the utilization of chitosan. To achieve efficient utilization of chitosan, it must change the structure of lignin or remove lignin.

Complex physical structure and chemical features of lignocellulose show different protection mechanisms against microbial attack and polysaccharide degradation, which is called biomass recalcitrance [9]. Recalcitrance determines the efficiency of refining and economical efficiency of conversion process. Himmel et al. have put forward various key factors which can measure lignocellulosic biomass recalcitrance to chemical reagents, microorganism, and enzyme [9], including (1) epidermal tissue of plant, especially cuticle and cuticular wax; (2) the arrangement and location of vascular bundle; (3) the relative content of parenchymatous tissue; (4) degree of lignification; (5) structural heterogeneity and complexity of cell wall components; (6) challenge of enzyme action in insoluble substrate; (7) inhibitory effect of the fermentation process from the inhibitor which exits naturally in cell wall or being generated in transformation process; and (8) crystalline cellulose of cytoderm

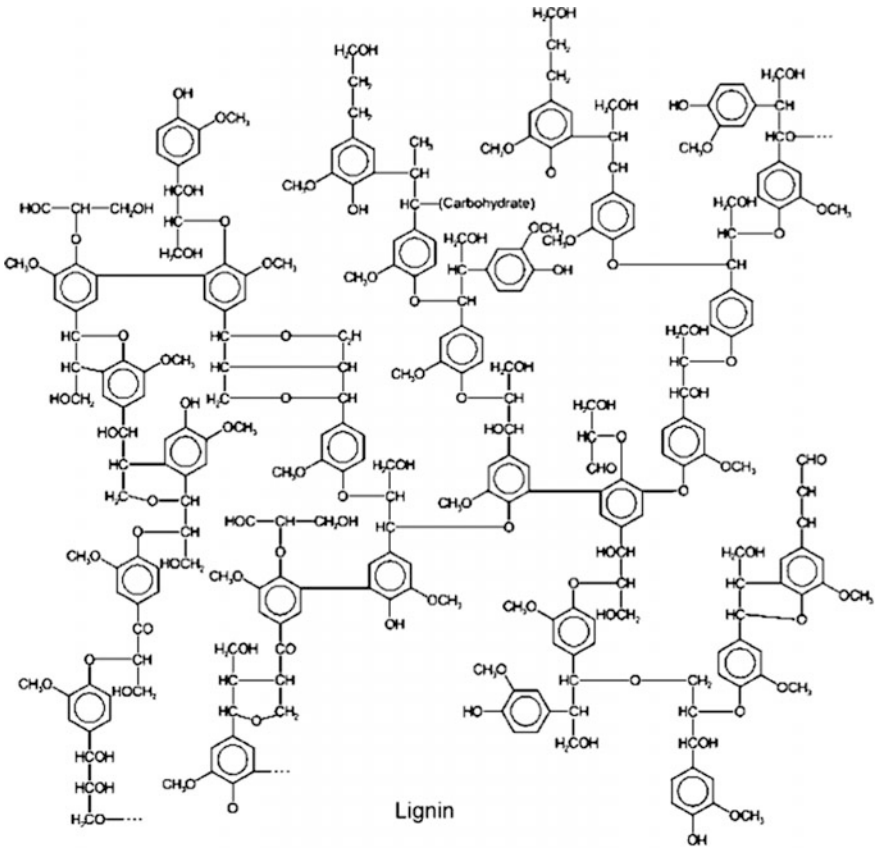

Fig. 2.4 Structure characterizations of lignin fraction in plant cell wall

microfiber hinders the chemical and biological degradation in molecular level. In conclusion, biomass recalcitrance, in the macroscopic and microscopic level, hinders the transmission of chemical reagent and enzyme, which reduces the transformation efficiency. Thus, in order to realize the efficient utilization of lignocellulosic biomass, it is necessary to develop the most efficient technology to overcome recalcitrance of lignocellulose.

Chemical composition and physical structure of lignocellulosic biomass are different in various organs, tissues, and cells, and even the same organ tissue cells. Additionally, linkage mode between monomers changes with monomer and chemical components of functional macromolecule. These qualitative differences are defined as heterogeneity of lignocellulosic biomass which influences the refining efficiency of lignocellulose biomass.

Complex structure of organs, tissues, cells, and cell wall of the plant was formed in the process of evolution. Take herb plants as example; the straw consists of several joints with a relative poor intensity. Internode and node are joined with growth band, which consists of parenchyma cells. Second, the midsection of internode will shrink in most herb plants. Vascular bundle in stick distributes scattered without epidermis and stele boundary, which mainly contains epidermis, parenchyma, and vascular bundle. Epidermis is the outer layer of the herb plants stick, which is arranged alternately by one long cell and two short cells. Vascular bundle is a vascular tissue system consisted of xylem and phloem, where intra-xylem tightly packages the outside phloem. Herb plants cell can be divided into several kinds: (1) fibrocyte, which is taper off both sides; (2) parenchymal cell, with varieties of shapes rhabditiform, rectangle, square, and spheroidal; (3) duct, channel organization in plant with ringlike structure, heliciform, trapezoid, and reticulate, whose diameter is larger than that of fibrocyte; (4) epidermal cells; (5) sieve tube and companion cell; and (6) sclereid, it is sclerenchyma cell contrary to fibriform with spheroidal, oval shape, and quite much lignification, phellemmication, or cornification. The size is quite small.

Plant cell walls mainly contain middle lamella, primary wall, secondary outer layer, central layer, and inlayer. (1) The adhesion layer between cells is middle lamella where lignin and pectin are the main chemical components, and the corner of cell is called corner aero of middle lamella. (2) Primary wall is a sac-like matter formed at the primary growth of cell with amount of hemicellulose and lignin, which links with middle lamella closely. (3) Secondary wall is the wall layer formed in primary wall. It is the metabolic sedimentation of protoplast which is the major structure of cell wall. Secondary wall can be divided into three layers. The outer layer consists of cellulose and hemicellulose. Cellulose microfibers interlacedly wrapped around the fiber cell walls in order forming into inter-helix. The cellulose microfibers of central layer of secondary are helical arrangement parallel structure, which is almost parallel to the fiber axis, and the angle between microfibers and the fiber axis presents a gradient trend from inner to outer. The inlayer takes a small part compared to the whole cell wall. However, the wrapping pattern of microfibers is similar to that of the outer layer. Cellulose macromolecule chains regularly arrange in the protofibril which arranged in microfiber. Cellulose is formed by several microfibers arranged in

different ways. Previous researches proved that one protofibril with a 3 nm diameter consisted of about forty cellulose macromolecules. One sub-microfiber with a 12 nm diameter consists of 16 protofibrils, and one protofibril with 25 nm diameter consisted of four sub-microfibers. Hemicellulose monomolecular layer exists inside of protofibril which exists inside of sub-microfiber. Inter-microfiber is filled with hemicellulose and lignin, which are linked by chemical bond to form lignin–glycan complex polymer.

In order to recognize heterogeneity, corn stover is split into five morphological fractions based on functional and structural property at the plant organ level (Fig. 2.5). Table 2.2 shows that the chemical compositions of corn stover were significantly different at the plant organ level ($P < 0.05$). Among whole corn stover and five morphological fractions, stem rind had the highest glucan content and total sugar content (61.8%), while leaf sheath had the lowest glucan content and total sugar content (49.5%). Xylan and araban contents increase as follows: stem node < stem pith < stem rind < whole corn stover < leaf < leaf sheath. Acetyl content in different fractions showed a similar trend to xylan and araban. High acetyl content could facilitate the dissolution of hemicellulose, and hence the auto-hydrolysis effect in steam explosion [10]. Stem node had the highest lignin content, whereas stem pith had the lowest ($P < 0.05$). Higher lignification may hinder chemicals or enzymes permeating into plant cell wall and decrease the conversion efficiency [11]. Water extractives content increased in the order of leaf

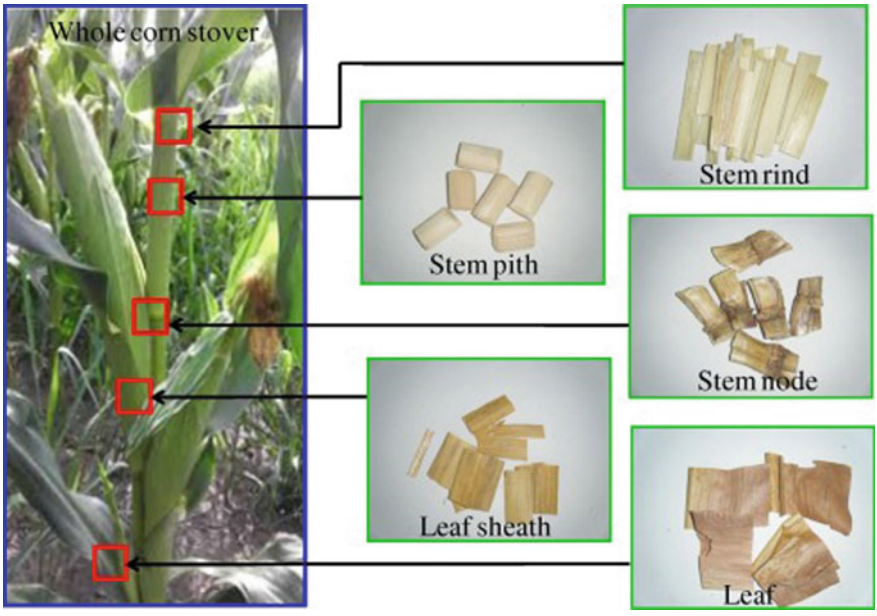

Fig. 2.5 Selective structure fractionation of corn stover biomass into five morphological fractions on the plant organ level

Table 2.2 Chemical compositions of whole corn stover and different morphological fractions before steam explosion

Compositions (% of total)	Different morphological fractions					
	Stem rind	Stem pith	Stem node	Leaf sheath	Leaf	Whole corn stover
Glucan	41.4 (0.6)	36.5 (0.9)	33.6 (0.5)	25.9 (1.2)	27.1 (0.8)	33.6 (1.1)
Xylan	17.7 (0.5)	16.6 (0.4)	15.9 (0.3)	20.2 (0.5)	19.8 (0.4)	19.1 (0.7)
Araban	2.7 (0.2)	3.0 (0.1)	2.8 (0.2)	3.4 (0.3)	3.1 (0.2)	3.1 (0.1)
Acetyl	2.7 (0.1)	2.4 (0.1)	2.4 (0.2)	3.5 (0.3)	3.2 (0.1)	2.9 (0.3)
Acid-insoluble lignin	17.9 (0.7)	13.8 (0.5)	18.0 (0.2)	14.4 (0.3)	15.3 (0.6)	16.1 (0.5)
Acid-soluble lignin	1.2 (0.1)	0.8 (0.1)	1.2 (0.2)	0.9 (0.1)	1.3 (0.1)	1.1 (0.1)
Water extractives	17.8 (0.3)	22.5 (0.5)	20.7 (0.4)	7.1 (0.6)	10.9 (0.5)	17.9 (0.7)
Glucose	8.1 (0.1)	9.5 (0.4)	8.2 (0.2)	2.4 (0.2)	1.7 (0.1)	7.7 (0.4)
Xylose	2.5 (0.3)	2.9 (0.2)	2.8 (0.3)	1.7 (0.1)	1.6 (0.2)	2.3 (0.1)
Ash	3.7 (0.1)	3.1 (0.2)	3.4 (0.2)	6.9 (0.3)	7.3 (0.2)	4.6 (0.1)
Total	105.1 (–)	98.6 (–)	97.9 (–)	82.3 (–)	88.0 (–)	98.4 (–)

Note Water-extractable glucose and xylose contents were calculated based on the total dry matter weight of feedstock; standard deviations are shown in parentheses

Table 2.3 Chemical compositions of whole corn stover and different morphological fractions after steam explosion

Steam explosion conditions	Steam-exploded solids	Glucan	Xylan	Araban	Acetyl	Lignin	Ash	Total
1.5 MPa, 6 min	Stem rind	53.4 (1.0)	5.9 (0.2)	1.1 (0.2)	0.2 (0.1)	31.2 (1.0)	2.3 (0.3)	94.1 (–)
	Stem pith	52.8 (0.9)	2.6 (0.3)	0.8 (0.1)	–	33.8 (1.1)	1.7 (0.1)	91.7 (–)
	Stem node	45.0 (0.3)	6.3 (0.5)	1.2 (0.2)	0.8 (0.1)	30.8 (1.3)	1.9 (0.2)	86.0 (–)
	Leaf sheath	39.5 (1.4)	7.6 (0.4)	1.4 (0.2)	–	26.5 (1.5)	3.1 (0.2)	78.1 (–)
	Leaf	41.5 (1.1)	7.0 (0.3)	1.3 (0.1)	–	27.4 (1.1)	3.2 (0.1)	80.4 (–)
	Whole corn stover	46.4 (1.0)	5.6 (0.2)	1.3 (0.2)	0.3 (0.1)	29.8 (1.0)	2.8 (0.1)	86.2 (–)
1.2 MPa, 6 min	Stem rind	48.4 (0.6)	7.3 (0.3)	2.0 (0.1)	1.1 (0.1)	27.8 (1.2)	2.4 (0.2)	89.0 (–)
	Stem pith	46.1 (1.0)	3.7 (0.5)	1.9 (0.1)	0.5 (0.1)	29.3 (0.9)	1.8 (0.1)	83.3 (–)
	Stem node	39.9 (0.7)	7.6 (0.4)	2.0 (0.2)	1.2 (0.2)	25.1 (1.3)	2.1 (0.2)	77.9 (–)
	Leaf sheath	35.3 (0.9)	9.1 (0.2)	2.7 (0.1)	1.0 (0.1)	22.7 (1.4)	3.5 (0.3)	74.3 (–)
	Leaf	36.7 (1.2)	9.5 (0.1)	2.6 (0.2)	0.8 (0.1)	23.6 (1.1)	3.6 (0.2)	76.8 (–)
	Whole corn stover	42.1 (1.1)	7.5 (0.3)	2.1 (0.2)	1.0 (0.1)	26.1 (1.2)	3.3 (0.2)	82.1 (–)

Note Lignin is acid-insoluble lignin; Standard deviations are shown in parentheses

sheath, leaf, stem rind, whole corn stover, stem node, and stem pith. Free sugars (glucose and xylose) showed a similar trend to water extractives. Interestingly, glucose content in stem pith, stem rind, and stem node is more than 8.0%, which is 3–4 times higher than that in leaf sheath and leaf. Free glucose content is easily degradable at high temperature, which should be adverse to the efficiency of steam explosion. The efficiency of auto-hydrolysis effect in steam explosion is closely related to the amount of ash content [8, 12]. Leaf sheath and leaf have higher ash content compared with other morphological fractions. These results suggested that different morphological fractions have different compositions and their unique effect on the efficiency of pretreatment and hydrolysis.

Chemical compositions of whole corn stover and different morphological fractions after steam explosion are given in Table 2.3. Results suggested that steam explosion increased glucan and lignin content while selectively dissolved xylan, araban, and ash. Glucan content in steam-exploded corn stover increased at 1.5 MPa and 1.2 MPa which were 11.5–16.3 and by 6.4–9.6%, respectively. Lignin content increased by 11.2–20.0% (1.5 Mpa) and 7.1–15.5% (1.2 MPa). However, xylan content in steam-exploded corn stover decreased by 9.6–13.9% (1.5 MPa) and 8.3–12.8% (1.2 Mpa) compared with that in untreated cornstalk. After steam explosion treatment, stem pith had the highest increased glucan and lignin content and the highest decreased xylan content at both 1.5 and 1.2 MPa, whereas stem node had the lowest. Acetyl content in stem pith, leaf sheath, and leaf was not detected at 1.5 MPa (Table 2.3), suggesting that all acetyl groups were removed after steam explosion. Ash content was also decreased after steam explosion especially in leaf sheath and leaf.

2.1.2 Solid-Medium Preparation Principles

High-solid and multi-phase is a bio-reaction process including solid matrix degradation and microbial growth. In general, solid matrix has complex structure caused by compact intertwine among the macro-molecular components. This natural structural feature exposed physical recalcitrance for degradation of the solid matrix and mycelium expand. In traditional solid-sate fermentation process, chemical nutrients have been focussed in culture medium preparation. However, physical properties of solid matrix are featured by porosity which has significant effect on matrix degradation and microbial growth. Specifically, accessibility governed by surface area and pore affects matrix degradation, while porosity affects mass and heat transfer in high-solid and multi-phase system. Therefore, apart from chemical nutrients in high-solid and multi-phase system, physical properties should also be paid attention. To be specific, large surface should be provided for enzyme binding or mycelium expanding, while pores are provided for enhancing heat and mass transfer.

2.2 Porous Properties of Solid Substrates

2.2.1 Cognition on Porous Properties of Solid Substrates

Porous medium is the common space occupied by the multi-phase materials and also a combination of coexisted multi-phase material. The space without solid skeleton is called pore, which is occupied by liquid phase or gas phase. Porous media has the characteristics such as porosity and heterogeneity. Porosity is the ratio of pore volume to total volume of porous media. The effective pore refers to part pore interconnected porous medium and not occupied by water, which is the ratio of effective pore volume to total volume of porous media. The dead-end pore is that one side of the porous media connects to other pores and another side of the porous media is sealed. Heterogeneity refers to the three phases, solid, liquid, and gas phases that can coexist. In porous medium, solid phase is the skeletons and the gas phase distributes in the unsaturated zone.

2.2.2 Correlation Between Substrate Porous Properties and Bioprocess

The lignocellulosic material is the typical multiscale porous material, which has the porous and frame construction. From crystalline region, amorphous region of cellulose, cell pit, cell lumen, cell wall, and vascular bundle to pellet, each scale of lignocellulosic biomass reflects the concepts of porous material such as porosity, pore size, and specific surface area. Lignocellulose aperture distribution with different dimensions is shown in Table 2.4.

There are obvious differences among coniferous wood, hardwood, and herbaceous plants in the organization structure.

In general, there are few types of cell in coniferous wood. Resin canal exists in coniferous wood, while catheter does not. Tracheid, the main component, has

Table 2.4 Lignocellulose aperture distribution with different dimensions

Level	Source of the pore size	Width (μm)	Level	Source of the pore size	Width (μm)
Tissue cell	Epidermis cell	20–35		Pit	0.5–50.0
	Pore	2–10		Plasmodesmata	0.03–0.06
	Vessel cell	30–130	Cell wall	Porosity between macrofibrils	0.001–0.100
	Sieve tube	5–50			
	Cribrate cell	5–50		Porosity between microfibrils	0.001–0.030
	Fiber cell	13			
	Intercellular layer	<1		Porosity between macromolecule	0.001–0.030
	Cube corner	≈1			

function of conducting and mechanical support, which accounted for over 90% of the timber volume; a typical cell is 3–5 mm long and 0.03–0.05 mm wide [5]. Hardwood consists of many types cell with high evolution degree. There is not resin canal in hardwood. However, catheter exists in hardwood which has function of conducting moisture, mechanical support to wood fiber. Broadleaf wood also contain three kinds of fiber cells including toughness wood fiber, fiber tracheid, and tracheid, which is known as wood fiber. Wood fiber is one of the important anatomical molecules of broadleaf timber with average length of 1 mm and the width of less than 20 μ. It accounts for 60–80% of timber volume [5]. Herbaceous plants have many cell types, including fiber cells, catheters, parenchyma cells, skin cells, screen, and companion cells. Catheter cell content in herbaceous plants is high and its diameter is much bigger than fiber cells. Stems, for example, their common characteristic is scattered identify vascular bundle throughout a large number of basic organization, not the boundaries between the cortex and the stele. Fiber cells distribute in exterior subcortical and vascular bundle, the average fiber length is 1.0–1.5 mm, and the average width is 10–20 μm, general accounting for volume content of 40–70% [5]. Basic organization takes a significant share in the stem and consists of parenchyma cells. Herbaceous plants in Gramineae stem center of basic parenchyma tend to fracture in the process of development and form hollow medullary cavity. Table 2.5 summarizes the different biomass fiber raw materials. Fiber closely packed in coniferous wood due to relatively few types of cells and is also known as the “non-pored wood”. The fiber is long and the content is high in coniferous wood. It is the structural support of the plant material organization. Fiber cells usually have secondary wall due to the high lignification thickness and compact structure. Water vapor is difficult to penetrate the material inside the pore, causing a large thermal mass transfer resistance in steam explosion process. Hardwood has catheter tissue which plays the role of conveying water. Catheter cells are large and long pipe, affected by fiber arrangement regularity than coniferous wood, known as “porous wood”. Parenchyma cell content is two times much more than that of softwood. Parenchyma cell is large with thin cell wall and short cavity. It plays the role of storing nutrition in plant growth. Those features in parenchyma cell are conducive to heat and mass transfer and water vapor in the flash physical tear. In herbaceous plants, the secondary xylem is embedded basic tissue (parenchyma). Large number of parenchyma is good for the heat transfer via water. At present, in the research of relationship of biomass physical structure and steam explosion, judgement of difficulty in material explosion is still based on qualitative analytic. Related structural parameters or specific theoretical model has not been formed to reflect the effect of multiscale physical structure of biomass on the steam explosion process transfer, the reaction, and blasting effect. Therefore, further cognitive about the structure foundation of steam-exploded biomass still has a long way to go.

Table 2.5 Structural characteristics of different kinds of biomass

	Fibrous materials of coniferous wood	Fibrous materials of broad-leaved wood	Fibrous materials of poaceae
Cell types	Simple composition,tracheid occupied about 90–95%, xylem ray occupied about 1.5–7%, axial parenchyma cells occupied about 7–8%, and epithelial cell occupied about 0–1.5%	Complex composition, wood fiber occupied about 60–80%, vessel element occupied about 20%, xylem ray occupied about 17%, and parenchymal cell occupied about 13%	Complex composition, fibrocyte occupied about 40–70%, with high content of parenchymal cell, and vessel, sieve tube, companion cells, and chrotoplast
Characteristics of arrangement	Lined up along the radial on the transverse section	As affected by the catheter, regularity of fiber is not good than coniferous wood, and big difference of different material regularities	Misaligned and scattered of vascular bundle
Parenchyma cells	Relative low content of xylem parenchyma, whose volume account for 7–8%	Relative high content of xylem parenchyma within 20%, more than twice as coniferous wood	High content of parenchymal cell, up to 46% in straw. Parenchymatous tissue is easily to be fractured and hollow medullary space is formed of Gramineae stem center in the development process
Fiber cells	Fiber is thick and long, playing a support and conducting role, with average length 3–5 mm and width 0.03–0.05 mm about 1/100 of its length	Fiber is short and thin。 wood fiber account for 60–80% of broad-leaved wood, with about average length of 1 mm and width within 20 μm	Average fiber length of 1–1.5 mm and average width of 10–20 μm. General fiber cells account for 40–70% of the total cells. And low content of corn stalk is about 30%
Duct	Nothing	There are ring, thread, scalariform, checker, and pitted vessel inner the duct. Duct cells arrange end, perforation and pit shape and size of the catheter itself pattern vary with tree species, are important basis for hardwood species identification	Relative high content of vessel cells, its diameter is much bigger than fiber cells, with shapes of circular, spiral, trapezoidal, and checker

(continued)

Table 2.5 (continued)

	Fibrous materials of coniferous wood	Fibrous materials of broad-leaved wood	Fibrous materials of poaceae
Pit	Obvious fiber pit, the tracheid wall pit are bordered pit, wood ray parenchyma cells in the pit to pit, in the cross field are connected to the wood rays to pit tracheid form half of bordered pit. Different tree species with different shapes and sizes is the main basis to identify needles	Most of the fiber pit is not obvious	Fiber cell walls have a single pit, and some without pit
Resin duct	Part of coniferous possess with volume composition less than 1%	None	None

2.2.3 *Enhancement of Seepage Transfer of Porous Solid Substrates for Bioprocess*

Porous solid substrates of high-solid and multi-phase bioprocess may exist in some fluid; these may be condensed water which flows on the surface of porous solid substrates or penetrate into the pores. The movement of the fluid abides by certain rules which have a great impact on the heat and mass transfer in high-solid and multi-phase bioprocess. The rule of seepage fluid in porous solid substrates is called Darcy's law. The microorganisms and nutrients needed are present in the water phase as the form of solute, which transport with water as the carrier. Periodical dynamic change of air is a method to strengthen mass transfer and heat transfer for high-solid and multi-phase bioprocess, which is based on hydrostatics, and its power source is the normal force. High-solid and multi-phase bioprocess could be a biogeocenose in which quality, heat, and energy exchange can be in progress. The force of periodical dynamic changes of air with air pressure pulsation on the closed pressure vessel could make the molecular diffusion into forced convection diffusion, which could enhance heat transfer and mass transfer performance [13].

2.3 Water Properties of Solid Substrates

2.3.1 *Cognition on Water States in Solid Substrates*

Water is critical factor in high-solid and multi-phase bioprocess, but often being overlooked. Functions of water in pretreatment are concluded as follows:

(1) reactant, forming mild acidic conditions due to a decrease in the pKw of water at high temperature [14, 15]; (2) solvent or mass transfer medium of intermediates, end products, and inserted catalytic substances [16]; (3) heat transfer medium, determining the heat pattern and efficiency throughout the cellular structure [17, 18]; (4) plasticizer, maintaining a moist and soft texture of fibers which influence cell size and fiber strength [19]; and (5) explosion medium for analogous explosion pretreatments, tearing materials into small pieces and disrupting microstructures when immediate discharge of high pressure occurs [20]. As water is directly related to the interaction between substrate and pretreatment medium, most pretreated materials are dry substrates with water content (WC) $\leq 15\%$. Rehydration operation before pretreatment is necessary for enhancing pretreatment efficiency.

In recent years, in terms of relationship between water state and steam explosion, many researches have been conducted on the mechanism of auto-hydrolysis and optimization of water content in target materials [17, 21–23]. Cullis et al. evaluated the effect of water content on the bioconversion efficiency of softwood. Increased water content reduced the relative severity of steam explosion pretreatment, generating improved recovery efficiency of solids and hemicellulose-derived carbohydrate due to a "buffering effect" of the water [21]. Ewanick and Bura confirmed that SO_2 steam pretreated biomass increases ethanol yield by 18–28% after simultaneous saccharification and fermentation, indicating the positive effect of increasing water content on SO_2 permeability into biomass [22]. Ferreira et al. found that straw with high water content increased methane yield by 4–10%. However, high water content also increased heating energy, leading to high cost of the process [23]. The author has previously reported water transfer mechanism during multistage steam explosion process of corn stover and its contribution to processing bottlenecks because it gives important insights for designing industrial processes to impregnate cellulosic feedstocks with pure water, preservatives, or other materials [18].

Though scholars have recognized critical importance of water in biomass pretreatment technologies, their strides made from the point of water content are far from enough in elucidating water's acting essence in pretreatments, due to the complex interactions between water and plant biomass.

When water is adsorbed to lignocellulosic matrix, it is subjected to interactions caused by the chemical and physical compositions and the structure and composition of the plant produce different states and locations of water in turn [15]. Within the matrix, these associated water molecules have properties highly different from properties of bulk water. They become localized, more structured, and comparatively limited in available degrees of freedom, kinetic motion, and ability to exchange with other water molecules compared to water in the bulk [24]. These different water states certainly influence the feedstock properties and closely relate to pretreatment process, which should be the key issue that affects the extent of pretreatment efficiency. Thus, a deep understanding of water functions in pretreatment requires an adequate consideration of water states in the architecture of biomass, which provides insights into fundamental mechanism of water function contributing to the development of pretreatments.

2.3.2 Correlation Between Substrate Water States and Bioprocess

One of the main factors that influence high-solid enzymatic hydrolysis efficiency is the mass transfer [20]. Fully contact between substrate and enzyme is the premise of effective enzymatic hydrolysis [25]. However, free water decreases with increased solid content. When solid–liquid ratio is above 15%, water bound by lignocellulose turns into bound water and capillary water, resulting in hardly free water exists in the system, which is called "water-binding effect" of high-solid enzymatic hydrolysis [25–27]. In high-solid and multi-phase system, there are five main forms of water, including primary bound water, secondary bound water, capillary water, gravity water, and free water. Water-binding effect is closely related to lignocellulosic materials species, pretreatment method and condition, chemical composition, and physical structure of the solid. Reduced free water significantly affects the mass transfer efficiency and rheological properties of enzymatic hydrolysis process. On one hand, water is the diffusion medium of enzymes and product, and takes part in the reaction in the enzymatic hydrolysis process as substrate. Reduced free water can slow down dissolution rate and transmission efficiency of product and enzymes, affecting the enzymatic hydrolysis efficiency. On the other hand, low free water content increases the viscosity of the system, increasing the requirement for mixing yield stress and energy consumption of mixing [26–28].

Roberts et al. studied the effect of combination of solid water and cellulose on mass transfer and enzymatic hydrolysis efficiency. High solid–liquid ratio increases the physical restriction of water in the system, and addition of glucose and mannose increases the water bound effect [25, 28]. Inhibition of enzymatic hydrolysis rate and increased water bound caused by monosaccharide showed the same tendency. Cellobiose was not found in the system, indicating that monosaccharide reduces the efficiency of saccharification by increasing water bound effect. There was a positive correlation between water bound and diffusion of monosaccharide and enzymes. Due to interaction between water and cellulose, water and soluble content, the system viscosity increased, leading to the increase of diffusion resistance and decrease of enzymatic and hydrolysis efficiency. Effective diffusion coefficient of BSA decreased by two-thirds with the solid–liquid ratio increased from 5 to 20%, and the intrinsic diffusion coefficient reduces by nearly 1/2 [28, 29]. Selig et al. investigated the relationship between water bound caused by macromolecule polymers and its inhibition on enzymatic hydrolysis. Relaxation time curve (T2) of added polymer system measured by low-field nuclear magnetic resonance close to zero within a short time and conversion rate of cellulose was decreased by adding polymer. The trend is consistent with water bound and reduced conversion rate, proving that water bound reduces the efficiency of high-solid enzymatic hydrolysis [30]. Selig et al. studied the influence of water availability and soluble substances on high-solid lignocellulosic saccharification. Effect of solute produced by enzymatic hydrolysis on water availability plays a determinative role in conversion rate during high-solid enzymatic hydrolysis process [31]. In addition, Hodge et al. studied

enzymolysis of corn stalk pretreated by dilute acid, finding that mass transfer become one of the main factors limiting conversion rate when solid–liquid ratio is higher than 20%. This can be explained as that mass transfer mainly depends on diffusion due to low degree liquefaction of the system, while convection efficiency is low. In addition, decreased water content limits the diffusion of the sugar from enzyme activity sites, inhibiting saccharification is suppressed, and enzyme is unreachable to new catalytic site [11]. Different types of lignocellulose, pretreatment, physics structure, and chemical composition also affect the water state and distribution of high-solid enzymatic hydrolysis process, and then affect the quality of mass transfer [31–34]. Mass transfer limit in high-solid enzymatic hydrolysis process significantly inhibits hydrolysis efficiency. Therefore, new strategies need to be developed to tackle this problem.

In order to investigate biomass–water interactions, the water pool (T2 relaxation time) distributions of untreated corn stover and steam-exploded corn stover under different moisture contents were determined, and the results are shown in Figs. 2.6 and 2.7, and Supplementary material 2 [35]. Results showed that the peak height and peak area of water pools in untreated corn stover and steam-exploded corn stover increased with the increase of moisture content. Figure 2.6 also shows that the T2 relaxation time of each water pool in steam-exploded corn stover and untreated corn stover increased with the increase of moisture content. The observations of extended relaxation times with the increase of moisture content may be due to the interactions between water molecules, which would be more frequent at higher moisture content. It is interesting to note that untreated corn stover had two peaks below fiber saturation point while steam-exploded corn stover had one peak (Fig. 2.6A, B). The reason may be that the order and rigid untreated corn stover makes the interactions of cellulose and water difficult. A part of water entered into the inner of cellulose fiber and the other part of water adsorbed to the surface of cellulose fiber. As for steam-exploded corn stover, the order and rigid structure were disrupted and cellulose fiber was obviously exposed by steam explosion, generating more accessible area for water. When moisture content was above 23%, the peak height of water pool in steam-exploded corn stover was higher than that in untreated corn stover (Fig. 2.6), while the peak width at half-height (Wh/2) was lower. Additionally, the T2 relaxation time of water pool in steam-exploded corn stover was obviously shorter than that in untreated corn stover under low moisture content (10–50%) (Supplementary material 2). These results indicated that the interactions of steam-exploded corn stover and water were stronger than those of untreated corn stover and water under low moisture content (10–50%).

Figures 2.6 and 2.7 show that water pools 1, 2, and 3 have appeared sequentially with the increase of moisture content. The result should be due to the fact that as water continues to be added and moisture content of biomass increases further, the biomass–water interactions in inner and/or surface of cellulose eventually reach an equilibrium state where water begins to accumulate in micropore and macropore thereafter. It is interesting to note that the peak height of main water pool in steam-exploded corn stover (pool 2 in Fig. 2.7B1, pool 2 in Fig. 2.7B2, and pool 3 in Fig. 2.7B3) was lower than that in untreated corn stover (pool 2 in Fig. 2.7A1, pool 3

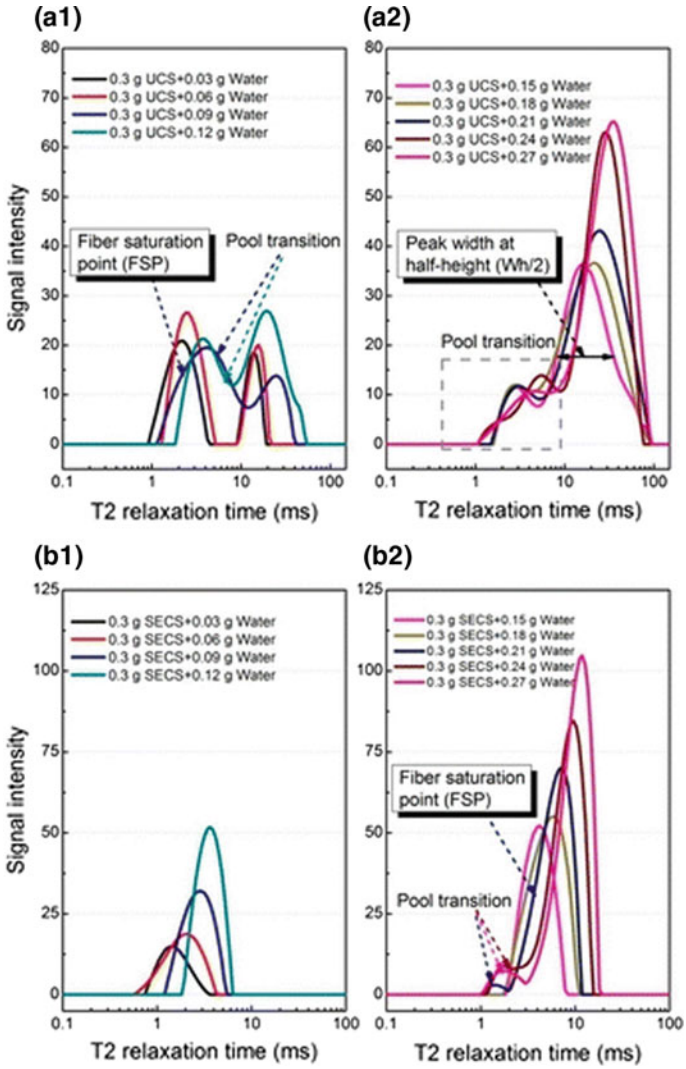

Fig. 2.6 Water pool distribution (T_2 relaxation time) and fiber saturation point of untreated (A1 and A2) and steam-exploded (B1 and B2) corn stover below 50% moisture content. UCS is untreated corn stover and SECS is steam-exploded corn stover. "0.3 g UCS + 0.03 g Water" stands for the mixture of 0.3 g of UCS and 0.03 g of water. Reprinted from Ref. [36]. Copyright 2013, with permission from Elsevier

in Fig. 2.7A2, and pool 3 in Fig. 2.7A3) at the same moisture content, respectively, while the peak width at half-height (Wh/2) of main water pool showed an opposite trend. Additionally, the T2 relaxation time of main water pool in steam-exploded corn stover was shorter than that in untreated cornstalk. It should be noticed that the peak height of water pool 3 in untreated corn stover was about 6–7 times higher than that of

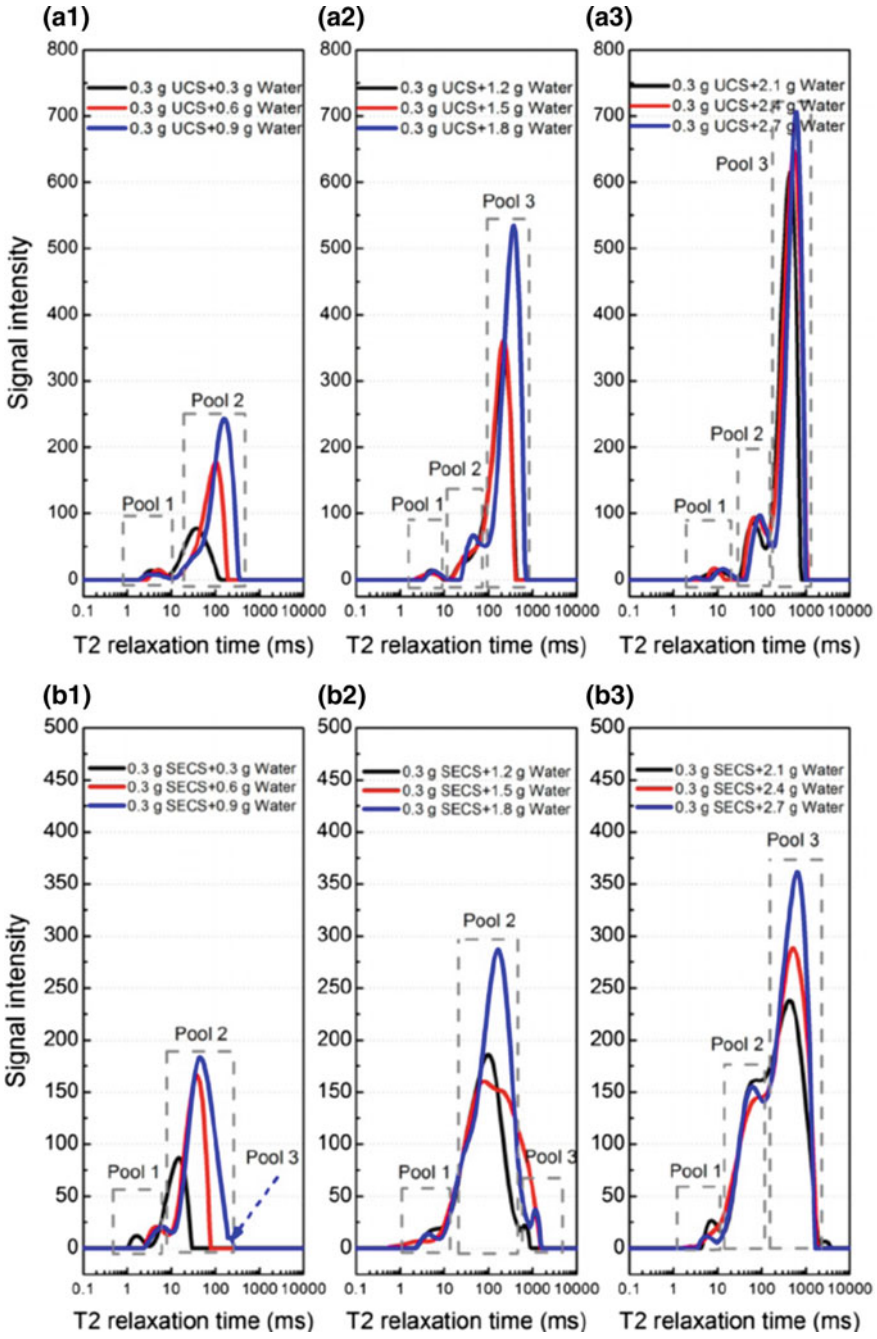

Fig. 2.7 Water pool distribution (T_2 relaxation time) of untreated (A1, A2, and A3) and steam-exploded (B1, B2, and B3) corn stover above 50% moisture content. UCS is untreated corn stover, and SECS is steam-exploded corn stover. Reprinted from Ref. [36]. Copyright 2013, with permission from Elsevier

water pool 2 beyond 87.5% of moisture content (Fig. 2.7A3), while the peak height of water pool 3 in steam-exploded corn stover was only 1.5–2.3 times higher than that of water pool 2 (Fig. 2.7B3). The states and locations of water in steam-exploded corn stover were obviously changed by steam explosion compared with these untreated cornstalks. Therefore, these results also indicated that the interactions of steam-exploded corn stover and water were stronger than those of untreated corn stover and water under high moisture content (50–90%).

The total peak area of water pools is closely related to moisture content, and the relations between total peak area and moisture content should reflect the interactions of biomass and water. The total peak area of water pools in both untreated corn stover and steam-exploded corn stover has positive correlation with the increase of moisture content (Fig. 2.8A), and the corresponding relations should conform to the exponential model as follows:

$$M(t) = A \times \exp(-t/T_0) + C_0 \tag{1}$$

where M is the total peak area; t is the moisture content, %; and A, T_0, and C_0 are the constants. The fitting results for the total peak area of untreated corn stover and steam-exploded corn stover with the increase of moisture content are given in Table 2.6, and the fitting exponential model was shown as follows (Fig. 2.8A):

$$M_{\text{ucs}} = 122.5 \times \exp(t/19.7) + 192.6 \tag{2}$$

$$M_{\text{secs}} = 105.3 \times \exp(t/18.9) + 127.3 \tag{3}$$

The correlation coefficient R^2 was 0.9990 for untreated corn stover and 0.9999 for steam-exploded cornstalk, respectively, which suggested that the exponential model can express untreated cornstalk–water interactions and steam-exploded cornstalk–water interactions well. Furthermore, it gave a conclusion that the interactions of untreated cornstalk/steam-exploded corn stover and water under lower moisture content were stronger than those under higher moisture content.

Compared with untreated cornstalk, the decreased total peak area of water pools in steam-exploded corn stover was also fitted with moisture content by exponential model (Fig. 2.8B). The correlation coefficient R^2 was 0.9338, and the fitting exponential model was given as follows:

$$\text{MDTPA} = 87.5 \times \exp(t/22.6) - 1.3 \tag{4}$$

Results suggested that the steam-exploded cornstalk–water interactions were stronger than the untreated corn stover–water interactions below 87.5% of moisture content especially below 50% of moisture content. The reason may be that steam explosion modified the structure and altered the composition of steam-exploded corn stover, and hence enhanced the interaction of steam-exploded corn stover and water under low moisture content. With the increase of moisture content, the

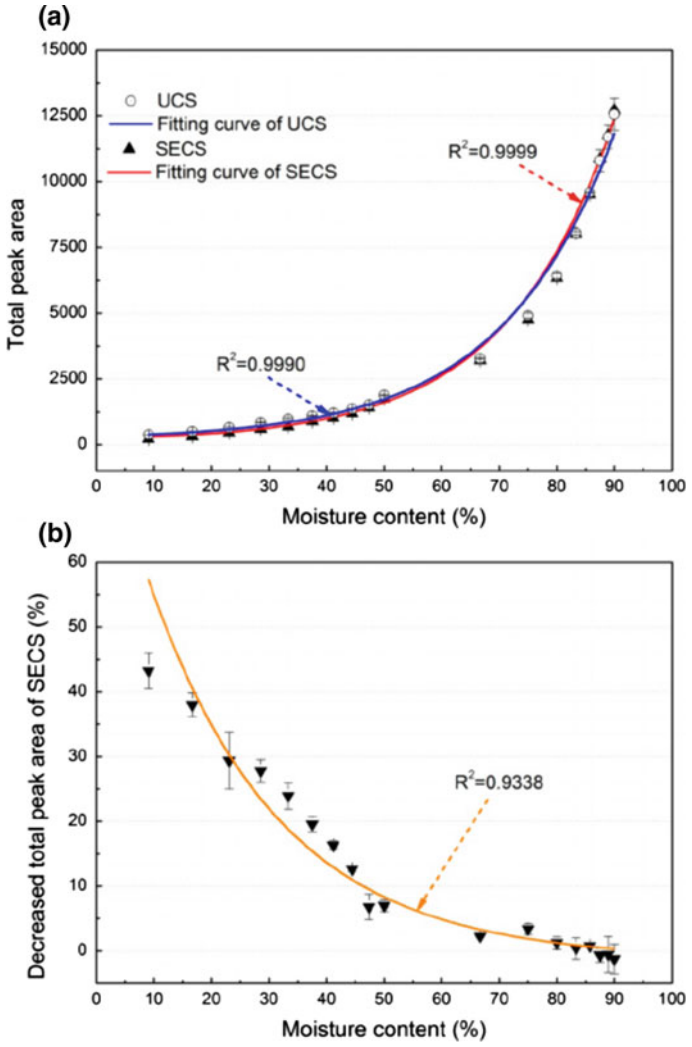

Fig. 2.8 Fitting model for the total peak area of water pools in untreated or steam-exploded corn stover with an increase in moisture content (A) and for the decreased total peak area of water pools in steam-exploded corn stover compared with untreated corn stover (B). UCS is untreated cornstalk, and SECS is steam-exploded corn stover [35]

interactions between water molecules became significant, resulting in the approximate total peak area of water pools for untreated corn stover and steam-exploded corn stover. Therefore, the exponential model can express the interactions of untreated cornstalk/steam-exploded corn stover and water well and also suggested that the interactions were stronger under lower moisture content.

Table 2.6 Exponential model fitting results for relations between total peak area of water pools in untreated and steam-exploded corn stover and moisture content. Reprinted from Ref. [35]. Copyright 2017, with permission from Elsevier

Samples	A	Standard error 1	T_0	Standard error 2	C_0	Standard error 3	R^2
M_{UCS}	122.5	9.8	−19.7	0.36	192.6	20.7	0.9990
M_{SECS}	105.3	13.6	−18.9	0.49	127.3	81.6	0.9999
M_{DTPA}	87.5	12.4	−22.6	2.2	−1.3	0.5	0.9338

2.3.3 *Water-Binding Effects of Solid Substrates for Bioprocess*

Water plays a key role in the enzymatic hydrolysis process. It is the medium for enzyme into the reaction site and the medium for product diffusing away from the reaction site. Additionally, water takes part in reaction and is the substrate of glycosidic bond hydrolysis during the enzymatic hydrolysis process, which determines the efficiency of enzymolysis reaction. Water existing in the lignocellulosic biomass enzymolysis system has five different states: primary bound water, secondary bound water, capillary water, limited gravity water, and free water, which is shown in Fig. 2.9. The water bonding with cellulose or other polysaccharides by hydrogen bonds is called primary bound water. Water adsorbed on the cell wall or surface glycan is called secondary bound water or film water. Water restricted in pores or voids by capillary force is called capillary water. The water restricted by macropore is called limited gravity water. Water which is not affected by solid or other solutes is called free water. The phenomenon that water reacts with other substances and causes fluidity reduced is called bound water effect, and the water is called bound water. With the increase of solid loading, the water is bound in the matrix and the free water reduces or even disappears, affecting the enzymatic hydrolysis efficiency.

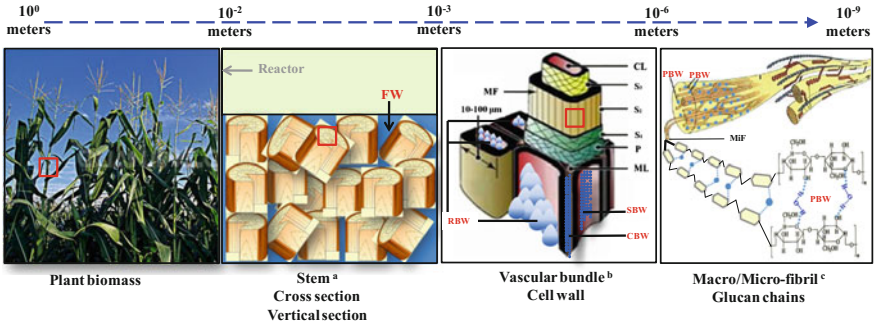

FW, Free water; RBW, Restricted bulk water; CBW, Capillary bound water; SBW, Secondary bound water; PBW, Primary bound water; MF, Macro-fibril; MiF, Micro-fibril; CL, Cell lumen; S, Secondary cell wall (S1, S2, S3); P, Primary cell wall; ML, Middle lamella.

Fig. 2.9 Schematic displaying water pools of lignocellulosic biomass in multi-length scale of its conversion process

2.4 Solid Rheology Properties in High-solid and Multi-phase Bioprocess

2.4.1 Solid Rheology Properties Variation in High-solid and Multi-phase Bioprocess

The rheology property of high-solid and multi-phase system is one of the key factors influencing enzymatic hydrolysis efficiency of lignocellulose conversion. It is also an important index of reactor design [29, 36]. Rheological property of high-solid and multi-phase system is influenced by physical and chemical properties of matrix, such as particle size and distribution, flexibility of fiber, elasticity of matrix skeleton, and material composition [36]. The water holdup affects rheological properties of mixture significantly when solid–liquid ratio is over 15%. The disappearance of solid particles lubrication results in a solid state of the enzymatic hydrolysis system. Rheological models were used to describe the enzymatic hydrolysis process of solid. Um and Hanley have studied rheological properties of enzymolysis, while the solid–liquid ratio is 15–20% and found that it conformed to the pseudoplastic fluid model [37]. Viamajala et al. found that particle size could significantly affect the rheological properties of mixture and further affect the energy consumption of agitation. Small particle size resulted in little viscosity, improving transformation efficiency. Knutsen and Liberatore found that adding surfactant can effectively reduce the yield stress of enzymatic hydrolysis, and elevated temperature can reduce viscosity to some extent [38, 39]. Increased solid–liquid ratio affects rheological properties significantly, affecting local material concentration, product removal, and heat transfer. In addition, rheological transformation demands higher stirring power and energy consumption, even agitation method is subversive, which brings new challenges to the process design and operations. Therefore, new strategy must be developed to alter the rheological properties so as to improve the efficiency of high-solid enzymatic hydrolysis.

Lignocellulosic mechanical properties (such as winding, intensification, tensile, compression, shear, and torsion) are the important parameters affecting process intensification. Although a few study of lignocellulosic mechanical properties has been reported (such as the bending force, moment of inertia, modulus of elasticity, flexural rigidity, shear strength, bending strength, the relationship between the straw stalk lodging resistance and compression characteristics, and the relationship between straw mechanical properties and harvesting and processing equipment with low energy consumption and high efficiency), the researches of intrinsic characteristics of lignocellulose mechanics are still less and dispersed. Particularly, the scholars did not recognize the intrinsic characteristics of lignocellulose mechanics for its important role on conversion process. There is no report about the inner relationship of lignocellulosic mechanical characteristics, rheology of system, and process intensification.

Plant biomass is a biological composite with multiscale structure and special molecular mechanics phenomenon [40]. In macro-scale, it is formed by intercellular

layer cells cohered into highly anisotropic natural porous materials. In microscopic scale, the plant cell wall can be regarded as natural fiber-reinforced composites composed of hemicellulose, lignin, and microfibril. In nanoscale, the plant biomass is high polymer materials composed of cellulose, hemicellulose, and lignin. The multistage structure shows that mechanism of macro- and micro-mechanical behavior is closely related to the steam explosion process. The macro- and micro-mechanical performance of biomass material directly determines the macro- and microphysical tear effect of steam explosion process. The effects include microlevel of material, the cracking damage degree, and the broken degree of cell wall. Biomass is featured by heterogeneous, anisotropic, and natural existence of micro- and macropore, defect, or damage. The irregular evolution behavior of initial pore, defect, or damage when biomass is loaded decides the macroscopic mechanical behavior [41]. Although mechanical properties of biomass have important influence on steam explosion effect, little related research has been reported. It is unclear that the resistance is based on biomass to steam explosion from the perspective of mechanics and physical damage mechanism of steam explosion.

At present, physical and mechanical properties of plant have been thoroughly and deeply studied, such as pulping, the drying process in wood processing areas. It could provide the reference and ideas for the studying of relationship between material mechanical properties and steam explosion process. The mechanical characteristics of raw material are greatly affected by the structure and composition change.

Wood is a multiple cell-layered biological composite material. From the view of mechanics, wood cells can be divided into two main kinds: one is wood fiber composed of vascular bundle, thick-walled cells, which is the main component in determining mechanical properties of wood. The other is the parenchyma cell which plays the role of uploading and buffer between the vascular bundle. Therefore, if the wood fiber is considered as reinforced body and the other parts are substrate material, timber can be seen as strong structural features of biological composite material. Its performance and damage rule depend not only on the mechanical properties of component materials, but also on its structural characteristics including the volume fraction, distribution, and shape of enhancement, as well as the nature of the interface.

Therefore, wood microstructure consists of many cells with different functions. In cell walls, orderly arranged cellulose chains form microfibril bundles, which is the main source of cell wall strength. Lignin fills in cellulose and enhances the mechanical strength of the cell wall. Besides cellulose, hemicellulose is another carbohydrate in the cell walls. It penetrates in the skeleton of material in an amorphous state and plays the role of cementation, enhancing the overall strength of fiber [40]. Factors influencing the mechanical properties of wood mainly include density, microfibril angle, chemical composition, and moisture content. Distribution, combination method, and the quality of wood cell wall components have important influence on its macroscopic mechanical properties. Water is one of important factors that affect the mechanical properties of the tracheid. Cell walls affect the intensity and elastic modulus. It affects mechanical properties of the tracheid through affecting structure and chemical composition performance. Microfibril angle is a micro-cellular structure characterization, which is closely related to the mechanical properties of the cell wall [40].

The efficiency of steam explosion is determined by the physicochemical property of plant biomass. Steam explosion included auto-hydrolysis stage and explosion stage after penetration of high-pressure steam into plant cell wall [42]. During auto-hydrolysis at high temperature and pressure, hemicellulose was solubilized and degraded. Acetic acid generated from acetyl groups further catalyzed the hydrolysis of hemicellulose. Lignin was melt, solubilized, and recondensed partly. Water soluble compositions were dissolved [10, 43]. The reaction rate (k) of these compositions was related with activation energy (Ea) according to Arrhenius formula:

$$\ln k = -Ea/RT + \ln A \tag{5}$$

Each chemical composition has its unique chemical potential energy and activation energy of reaction, resulting in the difference of reaction rate (k). Chemical compositions of whole corn stover and morphological fractions were varied, leading to a different reaction rate (k) during auto-hydrolysis at high temperature and pressure. Additionally, chemical bond connection mode of polymers in whole corn stover and morphological fractions is also different. Chemical bond mainly determined the reaction rate (k) of compositions. These results suggested that the auto-hydrolysis efficiency of steam explosion was determined by morphological fractions and the utilization of whole corn stover may be unsatisfactory. Selective fractionation can split plant biomass into different morphological fractions, which had their respective optimal steam explosion conditions for obtaining the high auto-hydrolysis efficiency.

During explosion stage in steam explosion, plant biomass particles are exploded into small pieces, the ordered structure is disrupted, and the cellulose fibers are separated by mechanical effect [10, 43]. The mechanical property of morphological fractions was measured by the compression method (Tables 2.7 and 2.8). Hardness of first cycle, reflecting the highest force used to fracture material, increased in the order of leaf < stem pith < leaf sheath < stem rind < stem node under 30% moisture content (Table 2.7). Stem node and stem rind had the maximum hardness, suggesting higher pretreatment severity was needed to achieve the same pretreatment performance as other morphological fractions. Hardness deformation percentage, reflecting the deformation of objects from force bearing point to fracture point, showed an opposite trend to hardness. Compression work of first cycle, which is the work to overcome the internal structure force of material, also increased in the order of leaf < stem pith < leaf sheath < stem rind < stem node. Results suggested that in order to obtain the same pretreatment efficiency, more work was needed in steam explosion to overcome the internal structure force of stem node and stem rind compared with other morphological fractions. Interestingly, adhesive force and adhesiveness showed a similar trend to hardness.

The mechanical property of stem pith with different moisture contents was determined by the compression method (Table 2.8). Hardness of first cycle increased with moisture content increasing from 5–90%. However, hardness deformation percentage and compression work of first cycle increased with moisture content

Table 2.7 Mechanical property of whole corn stover and different morphological fractions before steam explosion by compression method mode test. Reprinted from Ref. [42]. Copyright 2015, with permission from American Chemical Society

Parameters	Different morphological fractions (30% moisture content)					
	Steam rind	Steam pith	Stem node	Leaf sheath	Leaf	Whole cornstalk
Hardness of first cycle (g)	4085	244	6648.5	1261	190	–
Hardness deformation percentage (%)	19.4	30.7	21.2	30.7	31.3	–
Compression work done of first cycle (mJ)	49	5.1	67.5	21.9	3.4	–
Total work of 1st cycle (mJ)	49.1	5.1	67.6	22.9	3.8	–
Adhesive force (g)	68.5	12	220.1	32	2.5	–
Adhesiveness (mJ)	1.49	0.12	2.2	0.22	0.03	–
Elastic work done (mJ)	1	0.02	1.23	0.18	0.01	–
First fracture work done (mJ)	9.9	2.4	12.6	8.8	0.8	–
First fracture deformation percentage (%)	7.4	24.1	4.3	25.7	7.5	–

Table 2.8 Mechanical property of stem pith under different moisture contents before steam explosion by compression method mode test. Reprinted from Ref. [42]. Copyright 2015, with permission from American Chemical Society

Parameters	Moisture content of stem pith			
	5%	30%	60%	90%
Hardness of first cycle (g)	84	244	311	358
Hardness deformation percentage (%)	14.3	30.7	39.1	10.2
Compression work done of first cycle (mJ)	1.7	5.1	5.4	2.4
Total work of first cycle (mJ)	1.7	5.1	6.2	2.4
Adhesive force (g)	15.5	12	3	10
Adhesiveness (mJ)	0.29	0.12	0.11	0.2
Elastic work done (mJ)	0.14	0.02	0.06	0.17
First fracture work done (mJ)	0.4	2.4	2.3	0.9
First fracture deformation percentage (%)	8.2	24.1	24.2	9

increasing from 5 to 60%, and then decreased with the further increase of moisture content. Elastic work showed a similar trend to adhesive force and adhesiveness. Results suggested that moisture content significantly affected the mechanical property of stem pith because moisture can enter into plant cell wall and interact with the macromolecules by hydrogen bond and van der Waals force [15, 44], which changed the internal structure force of plant biomass. Furthermore, the swelling effect of cellulose should contribute to altering the mechanical property of plant biomass.

Mechanical property of plant biomass is key factor affecting the design and process optimization [45, 46]. It affects the energy consumption of stirring and hence the efficiency of mass transfer in enzymatic hydrolysis. The results of mechanical property measured by TPA method showed that hardness of first cycle of untreated solids increased in the order of stem pith < leaf < leaf sheath < stem rind < whole corn stover < stem node (Table 2.9). Apparent modulus, reflecting the difficulty of compression, showed the similar trend to hardness and total work of first cycle. Interestingly, apparent modulus of steam-exploded solids was 20–90% lower than that of untreated ones. Untreated stem node and stem rind obtained higher adhesive force and adhesiveness, while steam-exploded stem pith and whole corn stover showed higher adhesive force and adhesiveness. Elastic work reached the maximum value for whole corn stover before and after steam explosion.

Elasticity index is used to indicate the recovery of deformation. Before steam explosion treatment, stem pith had the highest springiness index, while whole corn stover had the lowest one. After steam explosion treatment, stem pith had the lowest springiness index, while stem rind had the highest one. Elasticity index increased by 14–65% after steam explosion treatment except for stem pith, whose elasticity index decreased by 50%. The reason was that SE disrupted the physical structure and changed the chemical composition of different morphological fractions and hence changed the springiness index.

Mechanical properties of whole corn stover at different solid loadings were determined using TPA method (Table 2.10). Hardness of first cycle of untreated whole corn stover decreased from 5800.0 to 434.0 g with decrease of solid loading from 95 to 40%. It increased to 702.0 g at 20% solid loading and then decreased to 32.0 g at 10% solid loading. Hardness of first cycle of steam-exploded whole corn stover decreased from 336.0 to 222.0 g with decrease of solid loading from 95 to 70%, and increased to 592.0 g at 20% solid loading and then decreased to 266.0 g at 10% solid loading. The possible reason was that whole corn stover mixture was swelled and the bulk density decreased with solid loading decreasing from 95 to 40%, resulting in the decrease of hardness. Along with decrease of solid loading from 40 to 20%, the bulk density increased, resulting in the increase of hardness. When solid loading was below 10%, whole corn stover mixture shows a slurry state, resulting in the decrease of hardness.

2.4.2 *Correlation Between Solid Rheology Properties and Bioprocess*

Rheology refers to the physical mechanics of material deformation or flow from the aspects of stress and strain. Stress–strain behaviors of steam-exploded whole corn stover and different morphological fractions were evaluated in enzymolysis. Hardness and total work of first cycle at 0 h in incubator shaker enzymolysis and periodic peristalsis enzymolysis with 10% solid loading increased in the order

Table 2.9 Mechanical property of whole corn stover and different morphological fractions before and after steam explosion with 5% (w/w) moisture content by texture profile analysis (TPA) method. Reprinted from Ref. [41]. Copyright 2015, with permission from American Chemical Society

Parameters	Untreated morphological fractions						Steam-exploded morphological fractions					
	Stem rind	Steam pith	Stem node	Leaf sheath	Leaf	Whole cornstalk	Stem rind	Steam pith	Stem node	Leaf sheath	Leaf	Whole cornstalk
Hardness of first cycle (g)	2666	352	8374	2598	2162	5800	358	564	1446	574	654	336
Compression work done of first cycle (mJ)	48	9.5	146.9	49.4	42	86	11.1	14.1	27.2	14.6	15.5	10.1
Recoverable work done of first cycle (mJ)	7.4	1.4	16.3	7.1	7.9	9	2.6	1.9	4.6	3	3.7	2.1
Total work of first cycle (mJ)	55.3	10.9	163.2	56.5	49.9	95	13.6	16	31.8	17.5	19.1	12.2
Apparent modulus (kPa)	118	18	391	111	89	317	29	15	61	16	20	24
Adhesive force (g)	20	4	10	6	6	6	8	14	6	8	6	8
Adhesiveness (mJ)	2.1	0.8	2.7	1.1	1.1	1.8	1.1	2.2	1.2	1.2	0.3	2.5
Elastic work done (mJ)	1.2	0.7	1.5	1	1.1	1.7	1	2.1	1.1	1	0.1	2.4
Hardness of second cycle (g)	1586	248	5718	1504	1320	3262	272	384	1032	404	494	252
Compression work done of second cycle (mJ)	10.4	3.9	46.4	12.2	11.6	16.1	6.5	3.7	8.8	5.2	7	1.9
Cohesiveness	0.22	0.41	0.32	0.25	0.28	0.19	0.59	0.27	0.32	0.35	0.45	0.18
Recoverable work done of second cycle (mJ)	3	0.8	8.6	3.7	4.5	4.4	1.8	1.6	2.7	1.9	2.3	1.3
Total work of second cycle (mJ)	13.4	4.7	55	15.9	16	20.5	8.4	5.3	11.5	7.1	9.3	3.2
Springiness index	0.33	5.02	0.39	0.38	0.41	0.25	0.48	0.29	0.33	0.46	0.47	0.41
Mean peak (g)	2126	300	7046	2051	1741	4531	315	474	1239	489	574	294

Table 2.10 Mechanical property of whole corn stover before and after steam explosion at different solid loadings by texture profile analysis (TPA) method

Parameters	Solid loading (w/w) of whole cornstalk before steam explosion					Solid loading (w/w) of whole cornstalk after steam explosion				
	95%	70%	40%	20%	10%	95%	70%	40%	20%	10%
Hardness of first cycle (g)	5800	610	434	702	32	336	222	260	592	266
Compression work done of first cycle (mJ)	86	15.8	12.2	18.5	0.6	10.1	6.8	7.6	13.5	8.8
Recoverable work done of first cycle (mJ)	9	1.2	0.9	0.6	0.5	2.1	0.5	0.9	1.7	0.2
Total work of first cycle (mJ)	95	17	13.1	19	1.2	12.2	7.4	8.5	15.2	9.1
Apparent modulus (kPa)	317	19	12	22	1	24	5.8	7	19	6
Adhesive force (g)	6	8	12	22	12	8	22	12	10	12
Adhesiveness (mJ)	1.8	0.6	1.7	2.3	1	2.5	2.6	4	0.3	2.3
Elastic work done (mJ)	1.7	0.4	1.6	2.1	0.7	2.4	2.5	3.3	0.1	0.4
Hardness of second cycle (g)	3262	550	402	514	20	252	194	244	530	246
Compression work done of second cycle (mJ)	16.1	4.7	2.7	5.2	0.1	1.9	2.9	3.3	5.8	2.9
Cohesiveness	0.19	0.3	0.22	0.28	0.17	0.18	0.42	0.43	0.43	0.32
Recoverable work done of second cycle (mJ)	4.4	1	0.9	0.4	0.5	1.3	0.5	0.6	1.3	0.3
Total work of second cycle (mJ)	20.5	5.6	3.5	5.5	0.6	3.2	3.3	3.9	7	3.1
Springiness index	0.25	0.35	0.35	0.49	0.91	0.41	0.29	0.26	0.37	0.54
Mean peak (g)	4531	580	418	608	26	294	208	252	561	256

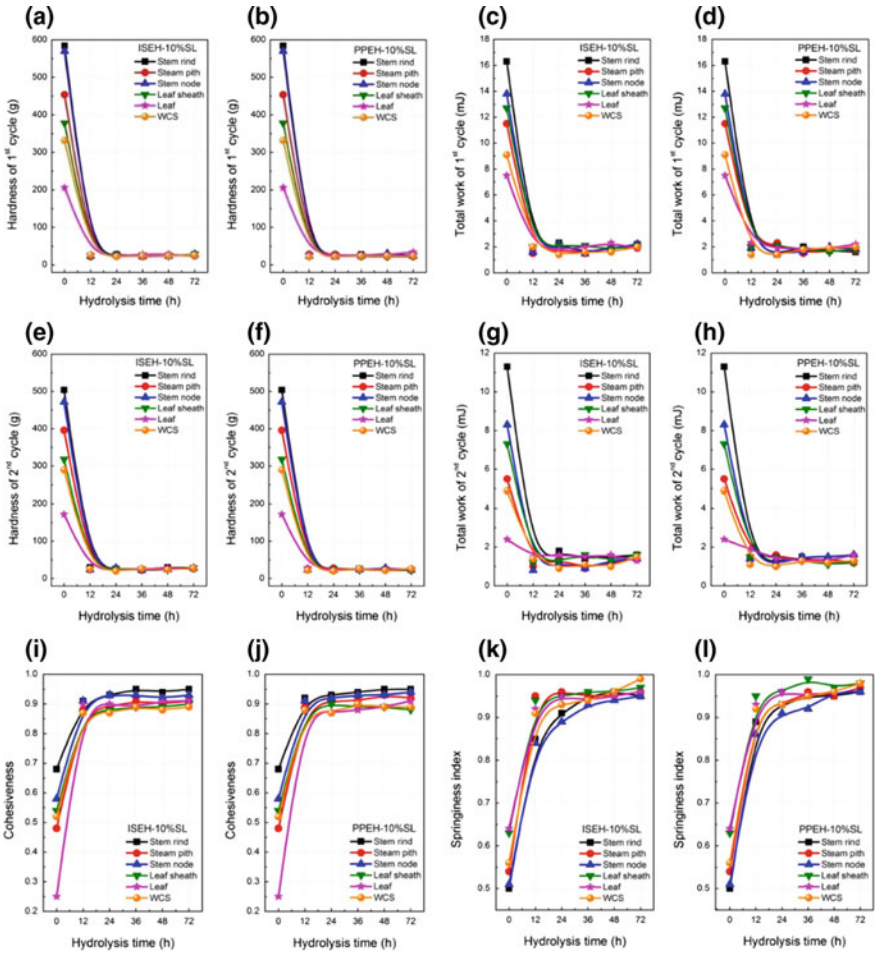

Fig. 2.10 Mechanical properties of steam-exploded whole corn stover (WCS) and morphological fractions in enzymolysis at 10% solid loading. ISEH, incubator shaker enzymolysis; PPEH, periodic peristalsis enzymolysis; SL, solid loading. Reprinted from Ref. [43]. Copyright 2015, with permission from American Chemical Society

leaf < whole corn stover < leaf sheath < stem pith < stem node < stem rind (Fig. 2.10A–D), and decreased to similar value after 12 h. Results suggested that treatment of stem mode and stem rind should be more difficult than that of whole corn stover and other morphological fractions. Hardness and total work of second cycle was lower than those of first cycle, showing same trends to those of first cycle (Fig. 2.10E–H). Interestingly, the maximum decrease of hardness and total work of hydrolysis mixture at 12 h was consisted with the maximum increase of glucan conversion. Results indicated that the mechanical property of corn stover was closely related to the enzymolysis performance. Viscidity increased in the order of

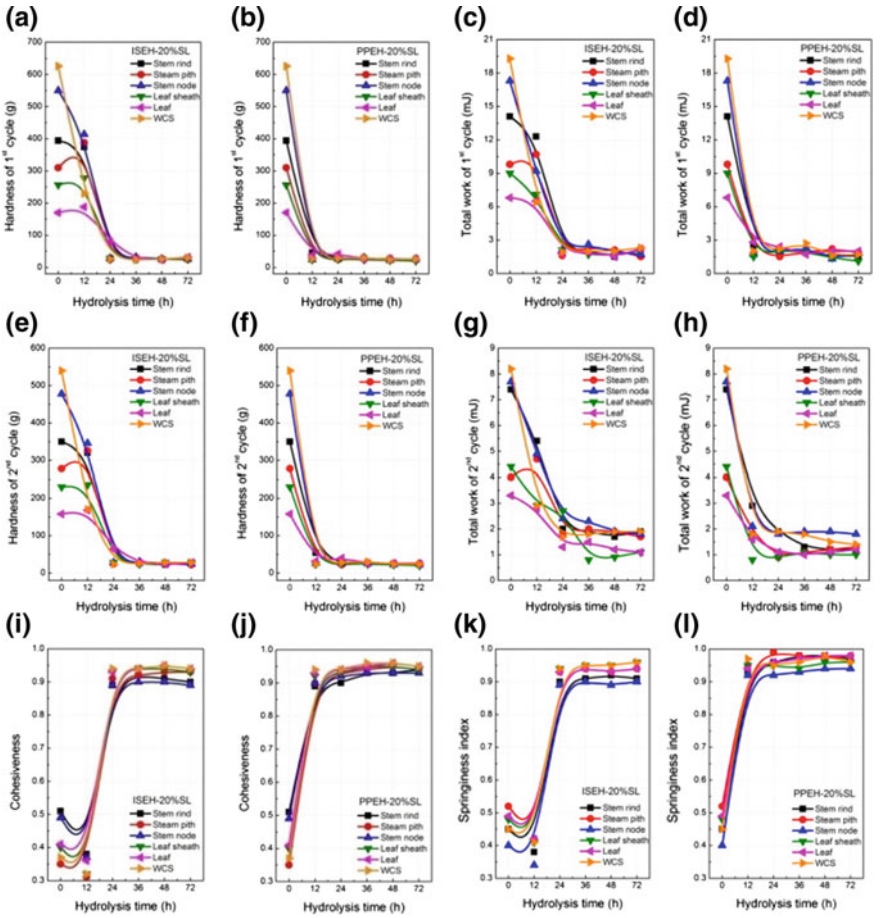

Fig. 2.11 Mechanical properties of steam-exploded whole corn stover (WCS) and morphological fractions in high-solid enzymolysis at 20% solid loading. ISEH, incubator shaker enzymolysis; PPEH, periodic peristalsis enzymolysis; SL, solid loading. Reprinted from Ref. [43]. Copyright 2015, with permission from American Chemical Society

leaf < stem pith < whole corn stover < leaf sheath < stem node < stem rind at 0 h in incubator shaker enzymolysis and periodic peristalsis enzymolysis (Fig. 2.10I, J). But it increased to 0.85–1.0 with hydrolysis progression. The higher cohesiveness indicated the stronger inner structure force of solid matrixes. The reason was that the hydrolysis mixture showed slurry state after 12 h and the hydrolyzed solid was effectively mixed with water. Elasticity index increased in the order of stem rind < stem node < stem pith < whole corn stover < leaf sheath < leaf at 0 h in incubator shaker enzymolysis and periodic peristalsis enzymatic hydrolysis (Fig. 2.10K, L), showing an opposite trend to hardness and total work. Results suggested that the mixing efficiency of steam-exploded stem mode and stem rind

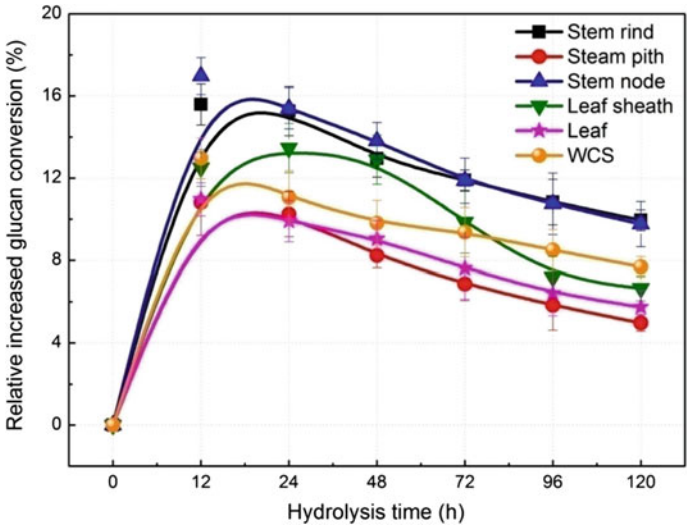

Fig. 2.12 Relative increased glucan conversions in periodic peristalsis enzymolysis compared with incubator shaker enzymolysis at 20% solid loading with an enzyme loading of 15 FPU/g glucan. ISEH, incubator shaker enzymolysis; PPEH, periodic peristalsis enzymolysis; WCS, whole corn stover. Reprinted from Ref. [43]. Copyright 2015, with permission from American Chemical Society

may lower than that of steam-exploded whole corn stover and other morphological fractions. Elasticity index increased to 0.9–1.0 after 12 h in incubator shaker enzymolysis and periodic peristalsis enzymatic hydrolysis.

As for 20% solid loading, hardness and total work of first cycle at 0 h in incubator shaker enzymolysis and periodic peristalsis enzymolysis increased in the order leaf < leaf sheath < stem pith < stem rind < stem node < whole corn stover (Fig. 2.11A–D). However, it should be noticed that they decreased with hydrolysis progress from 0 to 24 h in incubator shaker and 0–12 h in periodic peristalsis enzymatic hydrolysis. Hardness and total work of second cycle was lower than that of first cycle, showing same trends to those of first cycle (Fig. 2.11E–H). Results showed that periodic peristalsis enzymolysis reduced hardness and total work at 12 h compared with incubator shaker enzymolysis. The above results showed that periodic peristalsis increased the glucan conversion compared with incubator shaker enzymolysis at 12 h (Fig. 2.12). The reduction of hardness and total work by periodic peristalsis enzymolysis compared with incubator shaker enzymolysis was consistent with the increased glucan conversion. Interestingly, hardness and total work at 0 h showed the same trends to glucan conversion at the final stage of enzymatic hydrolysis except for whole cornstalk. Higher glucan conversion of whole corn stover can be explained as that the decrease of hardness and total work of whole corn stover were more rapid than that of five morphological fractions during hydrolysis process. Viscidity increased in the order of stem pith < whole corn stover < leaf sheath < leaf < stem node < stem rind at 0 h in incubator shaker

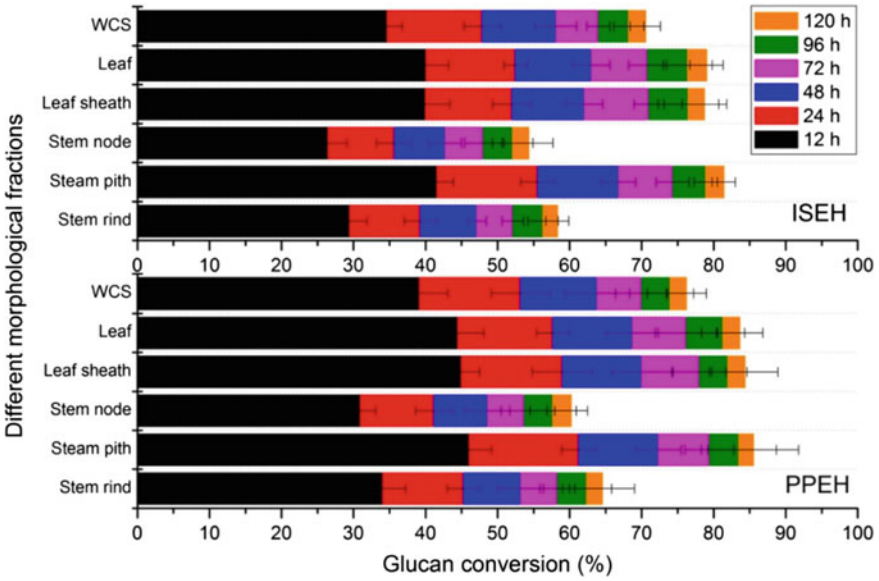

Fig. 2.13 Enzymatic hydrolysis kinetics of steam-exploded whole corn stover (WCS) and different morphological fractions at 20% solid loading. Steam explosion conditions: 1.5 MPa and 6 min; enzymolysis conditions: 15 FPU/g glucan, 120 h, and 30 rpm for periodic peristalsis enzymolysis and 200 rpm for ISEH. ISEH, incubator shaker enzymolysis; PPEH, periodic peristalsis enzymolysis. Reprinted from Ref. [43]. Copyright 2015, with permission from American Chemical Society

and periodic peristalsis enzymatic hydrolysis (Fig. 2.11I, J). The viscidity in incubator shaker decreased with hydrolysis time increasing from 0 to 12 h, and then increased to 0.9–1.0 with hydrolysis progression. But it increased from 0 to 12 h in periodic peristalsis enzymolysis. It can be explained that incubator shaker led to the agglomeration of steam-exploded solid before 12 h while periodic peristalsis rapidly converted the solid into slurry. Elasticity index increased in the order of stem node < stem rind < whole cornstalk < leaf sheath < leaf < stem pith at 0 h in incubator shaker and periodic enzymatic hydrolysis (Fig. 2.11K, L), showing an opposite trend to hardness and total work. Results suggested that the mixing efficiency of steam-exploded stem mode and stem rind may be lower than that of steam-exploded whole corn stover and other morphological fractions.

2.4.3 From Shearing-Force Stirring of Low Solids to Normal-Force Peristalsis of High Solids

The traditional mechanical agitation enhances molecular relative motion and admixture on the interfaces of gas–liquid and liquid–solid, and strengthens the mass

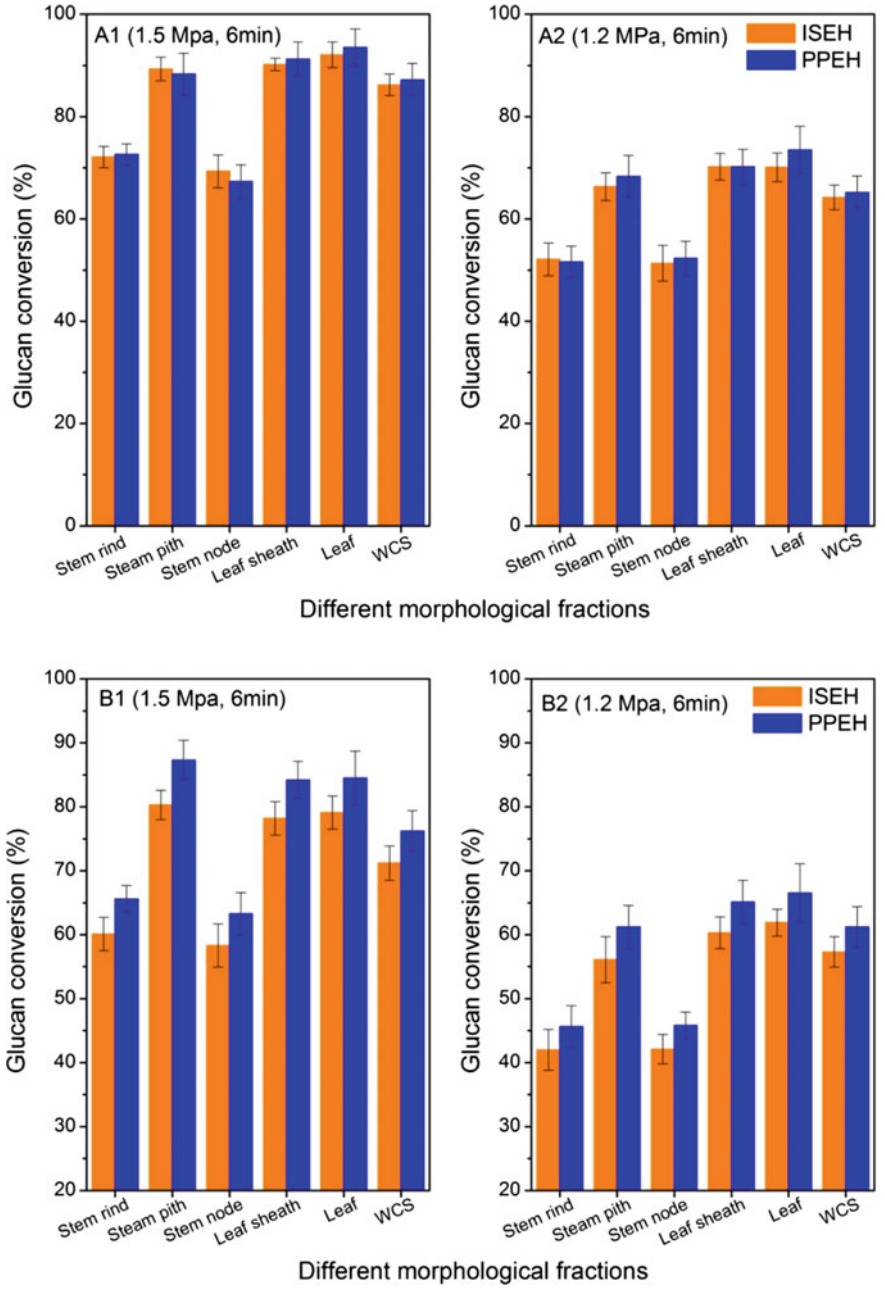

Fig. 2.14 Enzymatic hydrolysis of steam-exploded whole corn stover (WCS) and different morphological fractions at 1% (A) and 20% (B) solid loading. Steam explosion conditions: 1.5 or 1.2 MPa and 6 min. ISEH, incubator shaker enzymolysis; PPEH, periodic peristalsis enzymolysis. Reprinted from Ref. [43]. Copyright 2015, with permission from American Chemical Society

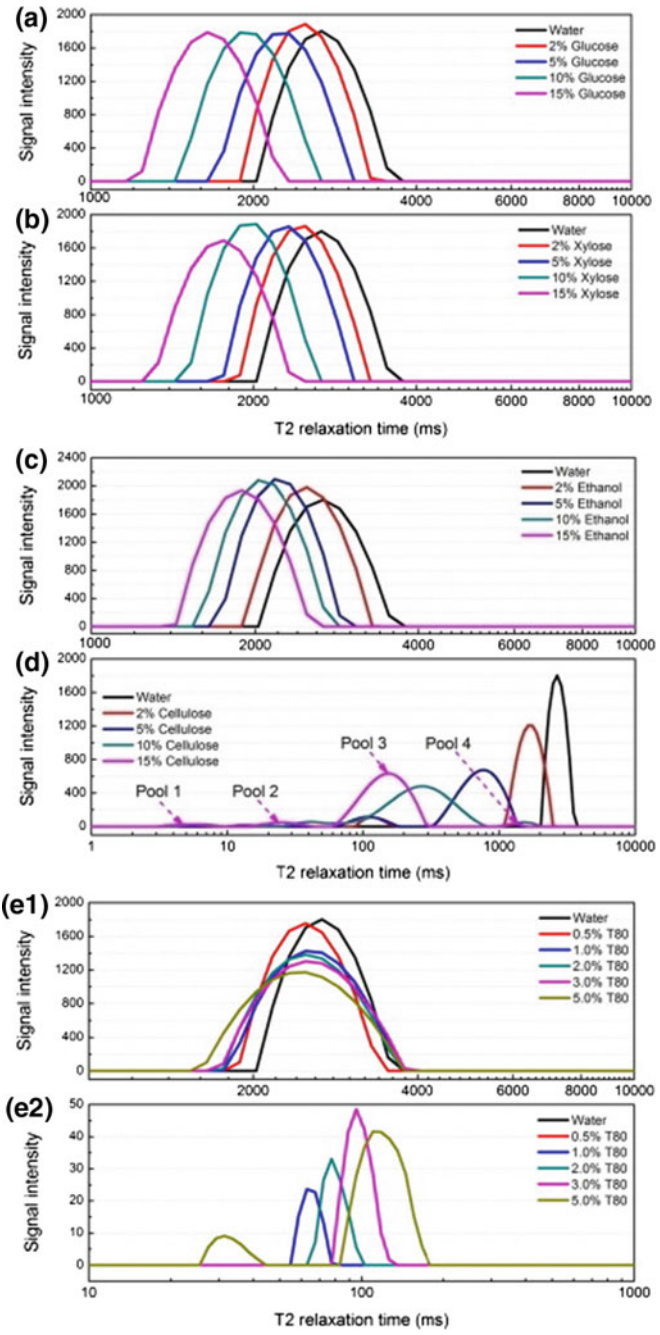

Fig. 2.15 Effects of chemicals (A for glucose, B for xylose, C for ethanol, D for cellulose, and E for Tween 80) on T_2 relaxation time of water pools in different solute concentrations (w/w). 2% glucose means that glucose concentration is 2% (w/w). T 80 is Tween 80. Reprinted from Ref. [48]. Copyright 2017, with permission from Elsevier

transfer and the heat transfer by tangential friction of momentum transfer. When mechanical stirring is applied to biological reactor, the organisms suffer the larger damage from stirring shear stress, leading to worse performance secondary metabolites synthesis. In high-solid and multi-phase bioprocess, in order to eliminate the destructive effect of shear stress caused by mechanical stirring on microbial, and enhance heat and mass transfer in reactor, periodic peristalsis is proposed. Periodic peristaltic avoids the effect of shear stress on microorganisms, which strengthens heat and mass transfer by periodic normal-force peristalsis [47].

Enzymolysis kinetics at 20% solid loading showed that glucan conversion of steam-exploded whole corn stover and five morphological fractions increased with the hydrolysis time in periodic peristalsis enzymolysis and incubator shaker enzymolysis (Fig. 2.13). Glucan conversion at the initial (at 12 h) and final (at 120 h) stage of enzymatic hydrolysis increased in the following order: stem node < stem rind < whole corn stover < stem pith < leaf sheath < leaf, which showed the same trend to the above results (Fig. 2.14).

Relative increased glucan conversion in periodic peristalsis enzymolysis compared with incubator shaker enzymolysis was calculated (Fig. 2.15). The relative increased glucan conversion among steam-exploded whole corn stover and five morphological fractions in periodic peristalsis enzymolysis compared with incubator shaker enzymolysis reached 10–17% before 24 h and then decreased to 5–10% with hydrolysis progression. Results indicated that periodic peristalsis significantly improved the glucan conversion before 24 h compared with incubator shaker. The relative increased glucan conversion at a specific hydrolysis time increased according to the order of stem pith < leaf < whole corn stover < leaf sheath < stem rind < stem node, which showed an opposite trend to glucan conversion. The possible reason was that stem node and stem rind had higher hardness compared with other morphological fractions, which reduced the mixing efficiency in incubator shaker enzymolysis at high-solid loading. Periodic peristalsis enhanced the mixing efficiency compared with incubator shaker, and hence increased the relative glucan conversion. Results suggested that the increase of glucan conversion by periodic peristalsis varied depending on morphological fractions.

References

1. Koppram R, Tomás-Pejó E, Xiros C et al (2014) Lignocellulosic ethanol production at high-gravity: challenges and perspectives. Trends Biotechnol 32(1):46–53
2. Mood SH, Golfeshan AH, Tabatabaei M et al (2013) Lignocellulosic biomass to bioethanol, a comprehensive review with a focus on pretreatment. Renew Sust Energy Rev 27(6):77–93
3. Zhao XB, Zhang L, Liu D (2012) Biomass recalcitrance, Part I: the chemical compositions and physical structures affecting the enzymatic hydrolysis of lignocellulose. Biofuel Bioprod Bior 6(4):561–579
4. Chen HZ, Wang L (2016) Technologies for biochemical conversion of biomass. Chemical Industry Press, Beijing
5. Pei JC, Ping QW, Tang AM (2012) Plant fiber chemistry. China Light Industry Press, Beijing

6. Liu RQ (1985) Chemistry basis for cellulose. Science Press, Beijing
7. Saha BC (2003) Hemicellulose bioconversion. J Ind Microbiol Biotechnol 30(5):279–291
8. O'sullivan AC (1997) Cellulose: the structure slowly unravels. Cellulose 4(3):173–207
9. Himmel ME, Adney WS, Ding SY et al (2007) Biomass recalcitrance: barrier to economic ethanol biorefineries. In: ACS National meeting book of abstracts
10. Chen HZ, Liu ZH (2015) Steam explosion and its combinatorial pretreatment refining technology of plant biomass to bio-based products. Biotechnol J 10(6):866–885
11. Himmel M, Ding S, Johnson D et al (2007) Biomass recalcitrance: engineering plants and enzymes for biofuels production. Science 315(5813):804–807
12. Yu B, Chen HZ (2010) Effect of the ash on enzymatic hydrolysis of steam-exploded rice straw. Bioresource Technol 101(23):9114–9119
13. Chen HZ, Li ZH (2002) Study on solid-state fermentation and fermenter. Cheml Ind Eng Prog 21(1):37–39
14. Alvira P, Tomás-Pejó E, Ballesteros M et al (2010) Pretreatment technologies for an efficient bioethanol production process based on enzymolysis: a review. Bioresource Technol 101 (13):4851–4861
15. Felby C, Thygesen LG, Kristensen JB et al (2008) Cellulosewater interactions during enzymolysis as studied by time domain NMR. Cellulose 15(5):703–710
16. Kristensen JB, Felby C, Jørgensen H (2009) Yield-determining factors in high-solids enzymolysis of lignocellulose. Biotechnol Biofuel 2(1):11
17. Brownell HH, Yu EKC, Saddler JN (1986) Steam-explosion pretreatment of wood: effect of chip size, acid, moisture content and pressure drop. Biotechnol Bioeng 28(6):792–801
18. Sui WJ, Chen HZ (2014) Multi-stage energy analysis of steam explosion process. Chem Eng Sci 116(SEP):254–262
19. Berry SL, Roderick ML (2005) Plant-water relations and the fibre saturation point. New Phytol 168(1):25–37
20. Zhang YZ, Chen HZ (2012) Multiscale modeling of biomass pretreatment for optimization of steam explosion conditions. Chem Eng Sci 75(25):177–182
21. Cullis IF, Saddler JN, Mansfield SD (2004) Effect of initial moisture content and chip size on the bioconversion efficiency of softwood lignocellulosics. Biotechnol Bioeng 85(4):413–421
22. Ewanick S, Bura R (2011) The effect of biomass moisture content on bioethanol yield from steam pretreated switchgrass and sugarcane bagasse. Bioresource Technol 102(3):2651–2658
23. Ferreira LC, Nilsen PJ, Fdz-Polanco F et al (2014) Biomethane potential of wheat straw: influence of particle size, water impregnation and thermal hydrolysis. Chem Eng J 242 (8):254–259
24. Selig MJ, Thygesen LG, Felby C (2014) Correlating the ability of lignocellulosic polymers to constrain water with the potential to inhibit cellulose saccharification. Biotechnol Biofuel 7 (1):1–10
25. Roche CM, Dibble CJ, Knutsen JS et al (2009) Particle concentration and yield stress of biomass slurries during enzymatic hydrolysis at high-solids loadings. Biotechnol Bioeng 104 (2):290–300
26. Deng YY, Koper M, Haigh M et al (2015) Country-level assessment of long-term global bioenergy potential. Biomass Bioenergy 74:253–267
27. Nicholls D (2015) Bioenergy from forests: the power potential of wood biomass. Science Findings-Pacific Northwest Research Station, USDA Forest Service
28. Viamajala S, McMillan JD, Schell DJ et al (2009) Rheology of corn stover slurries at high-solids concentrations-effects of saccharification and particle size. Bioresource Technol 100(2):925–934
29. Roche CM, Dibble CJ, Stickel JJ (2009) Laboratory-scale method for enzymatic saccharification of lignocellulosic biomass at high-solids loadings. Biotechnol Biofuel 2(1):28
30. Hodge DB, Karim MN, Schell DJ et al (2008) Soluble and insoluble solids contributions to high-solids enzymatic hydrolysis of lignocellulose. Bioresource Technol 99(18):8940–8948
31. Yang J, Zhang X, Yong Q et al (2011) Three-stage enzymatic hydrolysis of steam-exploded corn stover at high substrate concentration. Bioresource Technol 102(7):4905–4908

32. Wang W, Zhuang XS, Yuan ZH et al (2012) High consistency enzymatic saccharification of sweet sorghum bagasse pretreated with liquid hot water. Bioresource Technol 108(2):252–257
33. Tai C, Keshwani DR, Voltan DS et al (2015) Optimal control strategy for fed-batch enzymatic hydrolysis of lignocellulosic biomass based on epidemic modeling. Biotechnol Bioeng 112 (7):1376–1382
34. Gao YS, Xu JL, Yuan ZH et al (2014) Optimization of fed-batch enzyrnatic hydrolysis from alkali-pretreated sugarcane bagasse for high-concentration sugar production. Bioresource Technol 167(3):41–45
35. Liu ZH, Chen HZ (2016) Biomass–water interaction and its correlations with enzymatic hydrolysis of steam-exploded corn stover. Acs Sustain Chem Eng 4(3):1274–1285
36. Modenbach A, Nokes S (2013) Enzymatic hydrolysis of biomass at high-solids loadings–a review. Biomass Bioenergy 56(38):526–544
37. Um B, Hanley T (2008) A comparison of simple rheological parameters and simulation data for Zymomonas mobilis fermentation broths with high substrate loading in a 3-L bioreactor. App Biochem Biotechnol 145(1):29–38
38. Knutsen JS, Liberatore MW (2010) Rheology modification and enzyme kinetics of high-solids cellulosic slurries. Energy Fuel 24(12):6506–6512
39. Szijarto N, Horan E, Zhang JH et al (2011) Thermostable endoglucanases in the liquefaction of hydrothermally pretreated wheat straw. Biotechnol Biofuel 4(1):2
40. Fei BH (2014) Technology used for characterization of mechanical properties of wood cell wall and its application. Science Press, Beijing
41. Shao ZP (2012) Plant Materials (wood, bamboo) fracture mechanics. Science Press, Beijing
42. Liu ZH, Chen HZ (2016) Mechanical property of different corn stover morphological fractions and its correlations with high-solids enzymatic hydrolysis by periodic peristalsis. Bioresource Technol 214(AUG):292–302
43. Jacquet N, Maniet G, Vanderghem C et al (2015) Application of steam explosion as pretreatment on lignocellulosic material: a review. Ind Eng Chem Res 54(10):2593–2598
44. Roberts K, Lavenson D, Tozzi E et al (2011) The effects of water interactions in cellulose suspensions on mass transfer and saccharification efficiency at high-solids loadings. Cellulose 18(3):759–773
45. Mani S, Tabil LG, Sokhansanj S (2006) Effects of compressive force, particle size and moisture content on mechanical properties of biomass pellets from grasses. Biomass Bioenergy 30(7):648–654
46. Miao Z, Grift TE, Hansen AC et al (2011) Energy requirement for comminution of biomass in relation to particle physical properties. Ind Crop Prod 33(2):504–513
47. Chen HZ, Fu XG (2010) Periodic peristaltic stirring method. China Patent, CN101773799A
48. Liu ZH, Chen HZ (2016) Periodic peristalsis releasing constrained water in high solids enzymolysis of steam exploded corn stover. Bioresource Technol 205(APR):142–152

Chapter 3
Intensify Bioreaction Accessibility and Feedstock Refinery Process

Abstract Biomass is a kind of material featured by diversity, multicomponent, and multi-scale. Various flow, complex flow characteristics, and coupling effects between solid matrix and flow movement make it being the limitation in solving mass transfer. In this chapter, based on analysis of chemical and physical characteristics of biomass, the principle and methods of enhancing the accessibility of solid substrate in high-solid and multi-phase bioprocesses are introduced. The novel process and the steam explosion refining platform for the utilization of multicomponents of solid substrate have been established, which are based on the relationship of characteristics of solid substrate and enhanced process of accessibility of the biological reaction.

Keywords Coupling effects · Accessibility · Steam explosion

3.1 Intensification Principle of Enhancing Substrate Accessibility

3.1.1 Breakthrough from Biomass Reaction Recalcitrance to Seepage Recalcitrance

In the long-term research and practice of high-solid multi-phase reaction system, it has been found that the limiting factors for its applicability are the complexity of biomass raw materials and the lack of cognition of the essence of the refining process. Therefore, lacking the suitable process engineering theories of solid complex materials prevents the breakthrough of the key process of biomass refining. Plants have formed the natural barrier against physical, chemical, and biological unfavorable environments in long-term evolution. Chemical composition and structure characteristics, from the dense structure of epidermal cell wall to the hydrophobic epidermis tissue, have affected the transfer and reaction process of the medium. The effects of chemical composition and interface characteristics of materials on adsorption and reaction medium are defined as an intrinsic reaction

H. Chen, *High-solid and Multi-phase Bioprocess Engineering*,
Green Chemistry and Sustainable Technology,
https://doi.org/10.1007/978-981-10-6352-7_3

barrier of biomass refining and that of solid structure of materials on fluid flow and heat and mass transfer are defined as transfer barrier, which codetermine the biomass refining effect [1]. Therefore, the fundamental problem of biomass refining is to cognize physical, chemical, and biological methods of breaking the barrier in the refining process and mechanism of resistant to reaction and mass transfer. In short, the essence of biomass refining is to deeply cognize the gambling relations between solid phase material and the fluid (gas, liquid or even microorganism), so as to realize optimization and control process to strengthen refining efficiency [1].

Current researches on high-solid multi-phase bioreaction process include interaction, adsorption, desorption, and reaction between solid biomass materials and enzymes or microorganism. Taking biomass recalcitrance (first proposed by Michael R. Himmel in 2007) as an example, various properties of resistance to microbial and enzyme degradation process in different stages of refining was studied [2–4]. However, the mass transfer within the complex porous solid material is ignored, including the state, migration path, and fluid–solid coupling effect of fluid medium and microorganism in solid structure, and the change of mass transfer rule limiting factors, and impact on the efficiency in the refining process (Fig. 3.1). In biomass steam explosion refining, all procedures involve in mass transfer in complex solid porous materials [4–7], such as rehydration, steam explosion pretreatment, bioconversion processes (enzymatic hydrolysis and fermentation), and the extraction and separation of soluble constituents. Reaction behavior of target molecules contacting with the single cellulose chain is set as a theoretical yield while then the mass transfer behavior of the target molecules determine the actual yield and process efficiency Therefore, mass transfer in complex solid material may be the limiting step for biomass refining.

Diversity, multicomponent, and multi-scale structure of solid biomass, a variety of flow patterns and complex flow characteristics within solid materials, and coupling effect between solid structure and fluid flow result in problems while solving these mass transfer problems with traditional chemical theory. Simple mass transfer process is mainly modeled based on Fick's law. The premise is that homogeneity of solid materials and each point state is consistent, regardless of the mass transfer in intra-particle, the interaction of solid structure with fluid, and phase inversion. Fick's law aims to analyze the operation and mass transfer regularity in external macro environment and fails to describe the fluid behavior accurately. Taking enzymatic hydrolysis as an example, Fick's law focuses on reaction kinetics of enzyme absorption, while the influence of the mass transfer is still staying at initial stage of cognition because of lacking no systematized supported theory [5, 6, 8].

Therefore, breaking through the limitations of traditional chemical transfer theory and establishing suitable methods and theory for biomass refining process based on analyzing biomass structure characteristics and internal fluid characteristics are the urgent problems needed to be solved, for achieving high-effective transformation of biomass resources.

For complex solid materials, how to characterize the multi-scale structure features and analysis of the internal flow characteristics is one of the key steps to solve mass transfer problems in refining process [1]. Lignocellulose biomass is a typical

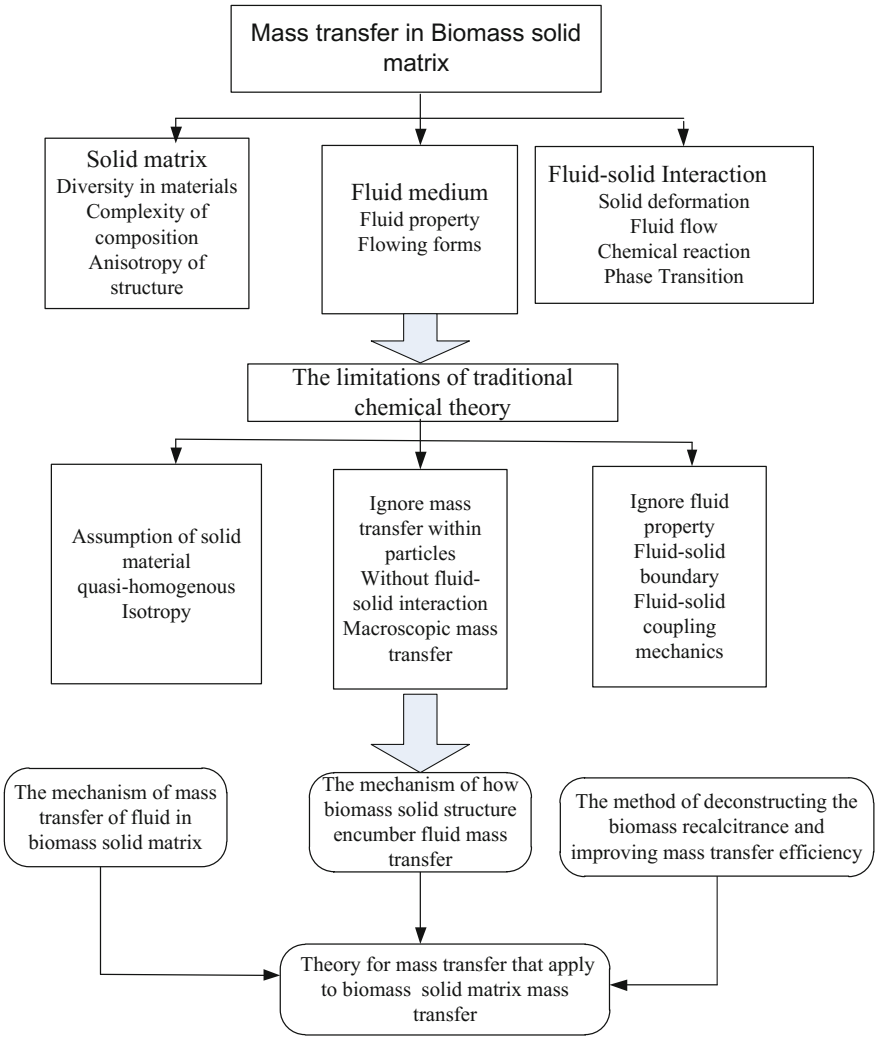

Fig. 3.1 Biomass mass transfer problems in solid material [1]

natural porous medium, from pores between particles (diameter 20–400 μm), catheter, cell cavity, plasmodesmata, elliptical pit to pores in cell walls with diameter 1–10 nm. Therefore, the authors have put forward the concept of biomass porous media: a kind of porous media based on cell walls and intercellular material as the solid skeleton to form complex pore diameter distribution for fluid transfer and flow [1]. A variety of advanced scanning technology and porous structure characterization methods such as solvent displacement method, the mercury intrusion, nitrogen adsorption has been used to get a preliminary cognition of biomass morphology and porous structure. Zhao and Chen characterized straw leaf,

stem, and cornstalk and summarized the pore size distribution of tissue, cells, and cell wall within 6 nm–360 μm [9]. Ding et al. and Chundawat et al. represented the size distribution of cell walls of corn straw at 10–1000 nm through a variety of scanning imaging techniques (SEM, TEM, CLSM, SRS, AFM, and ESCA) [5, 10].

With the development of three-dimensional tomography technology, based on microscopic image data, Ciesielski et al. and Liu et al. reconstructed three-dimensional structure of straw cellulose microfibril and honeycomb-like shape of three-dimensional structure of straw collenchyma and sclerenchyma under the action of white-rot fungus by computer simulation [7, 11]. The studies above have provided an effective guidance for material multi-scale porous structure characterization as well as cognition of biomass mass transfer behavior.

Pore structure of biomass has unique pore effects: (1) Migration channel effects. It provides pathways for fluid transport in porous structure, closely related to the pore volume, size, and shape. (2) Field effects. Biomass pores have functions for providing the place for chemical reaction. (3) Mechanics effects. Fluid migration in the pore and physical state has influence on the solid mechanics structure and, in turn, influence the fluid flow. Therefore, in view of the flow characteristics and the fluid-structure coupling effect in biomass porous medium, how to study the mass transfer behavior in intra-particles so as to explore mass transfer laws at various scales is the key for solving the mass transfer problems in lignocellulose biomass refining process [1]. Due to the complex flow channels, large specific surface area and obvious viscosity seepage theories in porous media were widely used to reflect the flow characteristics [12]. In order to cognize interaction between fluid-structure and mass transfer, more seepage theories of porous media are needed. The actual state of process through the deformation of medium, mass transfer, and chemical reaction is more extensive and deeper than the research method on a single field [13]. Therefore, based on the theory of seepage of porous media, mass transfer problems in solid biomass material is converted to seepage behaviors of mass in porous medium, which provides new methods for cognition of mass transfer during biomass refining.

Based on many years of research about the cognition of biomass structural characteristics, the conception of “Biomass Anti-Seepage” was put forward by the authors: resistance effect of biomass porous media on the mass transfer [1]. This concept embodies the biomass dynamic degradation process and the dynamic mass transfer characteristics, which is different from “Biomass Recalcitrance”. For example, during enzymatic hydrolysis process of lignocellulose, the action of enzymes on cellulose is considered mainly through the pore in intra-particles but not the pore surface, and more than 90% of the hydrolysis was contributed to the intra-particle pores areas [6]. Thus, highly ordered and compact biomass structure could reduce the enzymatic hydrolysis efficiency. Relevant pretreatment methods could increase the enzyme accessibility of the substrate through forming porous structure [4, 9, 10, 14, 15]. Therefore, the concept of “Biomass Anti-Seepage” is meaningful for key process of biomass refining, such as hydrolysis, rehydration, pretreatment, and extraction and separation of products. It is important to analyze the essence of anti-seepage at different refining stages, revealing the destruction

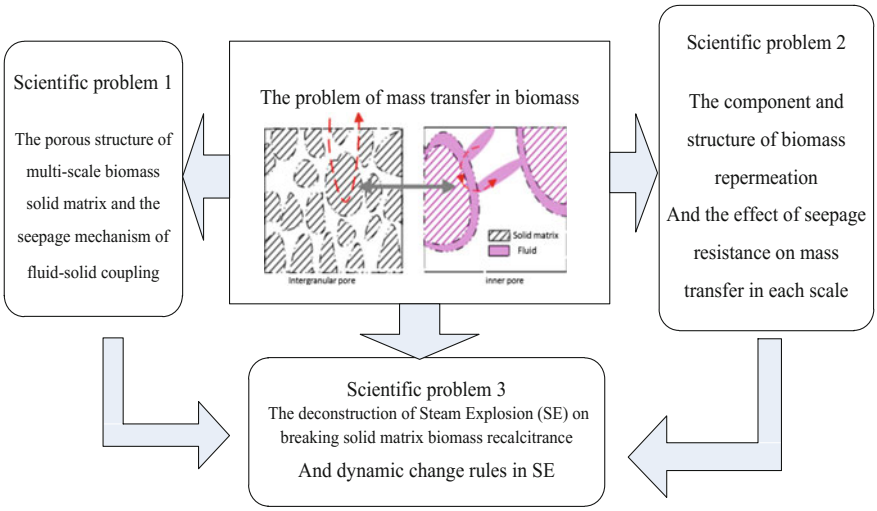

Fig. 3.2 The key scientific problems of biomass seepage [1]

mechanism and key factors of anti-seepage to improve the efficiency of refining and guiding the integrated innovation of biomass refining. Therefore, getting a deep knowledge of "Biomass Anti-Seepage" is the breakthrough for biomass refining technology, also the key to realize the industrialization production of biomass.

The key scientific problems of seepage in biomass (Fig. 3.2)are given as follows:

(1) Fluid transfer in biomass porous medium: to describe fluid seepage and transfer behavior under fluid–solid coupling effect in multi-scale pore structure of biomass based on a well knowledge of structural features of biomass. Biomass materials possess characteristics of complex composition and heterogeneous structure, determining complex flow characteristics within the pores. In turn, fluid–solid coupling effect affects the structure of solid materials under different flow conditions, which makes traditional chemical transfer theories unsuitable for analyzing and guiding the actual mass transfer behavior of biomass. Two chief questions involved are cognizing structural features of complex solid materials and describing mass transfer behavior under fluid–solid coupling effect. Only if the two cognitive problems are fully solved, scientific basis could be provided for analyzing and strengthening transfer behavior within biomass solid.

(2) How biomass solid structure prevents fluid transfer?: systematically describing the composition, structure, and mechanical properties of biomass, with quantitative description of mass transfer resistance under various scales during biomass refining process.

Lignocellulose biomass has formed some resistance barriers (chemical composition, structure characteristics, and mechanical characteristics) during

long-term evolution, which becomes the foundation for biomass anti-seepage. Therefore, systematic analysis is the foundation of biomass seepage and mass transfer resistance helps to find out the limiting step and key factors in the process of biomass refining. The targeted mass transfer strengthening measures are proposed to improve the efficiency of refining process, which would drive the breakthrough of biomass refining.

(3) The methods of overcoming seepage resistance and improving the mass transfer efficiency.
As a key pretreatment method of biomass refining, steam explosion technology can destroy the biomass anti-seepage from the source. Establishing quantitative relationships among operating parameters of steam explosion, fluid transfer behavior, and fluid-structure interaction, from the perspective of stress and strain, and analyzing the mechanism of steam explosion against seepage barrier are helpful to find the essential factors for breaking the barrier. Cognition of anti-seepage would break through the original inefficient multicomponents separation and conversion modes of biomass, to redesign and build efficient integrated innovative system of biomass refining system, and provide new ways to realize the industrialization of biomass refining.

The complex structure of biomass and lack of awareness of nature of refining is the root source of biomass refining industry, making it unable to realize large-scale industrialization. Therefore, it is the solution to problems of biomass refining industrialization to analyze the essence of biomass refining process and establishing solid phase engineering theory suitable for the complex medium. Based on many years of study on the cognition of the structural characteristics of biomass raw materials and steam explosion pretreatment, the biomass anti-seepage barrier was put forward expecting to give scientific guidance from theory level, technology level, and industrialization level of biomass refining process. At the theory level, analyzing the relationship between biomass porous structure, fluid properties, and mass transfer behavior and revealing mass transfer law in porous media, help to break through the traditional chemical transfer theory so as to establish foundation for mass transfer in complex solid phase biomass. At the technical level, based on composition analysis, structure and seepage characteristics in refining process, building relationships between anti-seepage barrier and the law of mass transfer help to find out the limiting step and key factors for mass transfer in refining process and provide scientific guidance for strengthening the refining process. An industrial level, developing economic and efficient steam explosion technology to break the barrier and establishing innovative and integrate biomass steam explosion refining system are of great importance to the development of biomass refining industrialization.

3.1.2 Prevention of the Second Recalcitrance Production

The composition of the biomass feedstock is very complicated. Appropriate pretreatment is needed to destroy the recalcitrance of biomass so as to achieve comprehensive utilization by enzymatic hydrolysis. However, a lot of potential inhibitors (such as weak acids, phenols, and furan) during enzymatic fermentation process were produced in the pretreatment process. It has been a crucial factor that inhabits the biotransformation and utilization of lignocellulosic materials. Among them, formic acid, acetic acid, hydroxymethylfurfural, and furfural, which come from hemicellulose degradation are the main inhibitors in steam explosion hydrolyzate; coumaric acid, vanillin, p-hydroxybenzoic acid, and syringic acid, which come from lignin degradation are important composition in steam explosion hydrolyzate. Eight model inhibitors were selected to study the inhibitor's generating kinetic laws during the steam explosion. The result shows that transformation of weak acid and furan degradation products is first-order reaction. Phenolic degradation products are produced by continuous reaction (the syringic acid is produced by first-order reaction), the conversion rate is influenced by the activation energy, temperature, and time of the secondary reaction. Therefore, the conversion rate is not positively correlated with time or temperature. Comparing the dilute acid or hydrothermal pretreatment with steam explosion in the respect of inhibitor production, same rule of inhibitor production was observed but there is difference in quantity. The equation can be established to predict and compute the inhibitor conversion rate in different steam explosion condition.

Steam explosion can degrade stalks into xylose and xylooligosaccharides. In this process, lignin is degraded into phenolic compounds which can be the inhibitor for fermentation. The effectiveness of xylose or phenolic compounds or other fermentation inhibitors is associated with the content and energy level. Especially, for dissolution of degradation molecules or sugars of enzymatic hydrolysis during pretreatment process, the state of sugar's energy is a key factor in inhibiting its availability. From the thermodynamics point of view, energy state and dissolution rule of degradation products in steam explosion pretreatment are analyzed. It is found that there are some common factors for adsorption and desorption: chemical potential and activity, the partial molar free energy of the degradation product was obtained. In the dissolution process, ΔG is always a negative value, implying that with the reduction of free energy, the dissolution of steam explosion degradation such as soluble molecules process occurs spontaneously. It can be seen from Eq. 3.1, the factors affecting the dissolution process include the melting temperature T, the activity coefficient γ_2, and the solid-to-liquid ratio χ_2. Ionic strength, pH value, temperature, and liquid to solid ratio and its effect on the dissolution of degradation products were studied. The temperature is conducive to the dissolution of phenolic substances, but not conducive to the dissolution of the sugar. Besides, according to Van't Hoff equation, the dissolution of phenolic substances is an endothermic process and the dissolution of carbohydrate molecules is an exothermic process. Therefore, washing steam explosion material with room temperature water can reach the

maximum dissolution of carbohydrate molecules. Minimum dissolution of phenolic molecules could be obtained by washing steam-exploded materials with water at room temperature. Secondary-level separation was achieved in this dissolution process, which will eliminate detoxification process of the fermentation industry. On the other hand, it gave us new ideas about efficient dissolution of carbohydrates and tackles the barrier effect of cellulose hydrolysis.

$$\Delta G = RT\ln(\gamma_2 * 0.6/\gamma_1 * \chi_2) \tag{3.1}$$

In steam explosion pretreatment, lignin was degraded into phenolic substances. Besides cellulose, hemicellulose, and lignin, there is 1.5% the phenolic substance. Part of phenolic substance connects hemicellulose and lignin, forming the anti-degradation barrier of cellulose, while the other is in a free state. Therefore, it is necessary to study the effects of phenolic compounds on enzyme activity and enzymatic hydrolysis which is not clear for now. Analyzing the types and contents of phenols in steam explosion straw washing liquid, model phenolic monomer material was used to prove that the effect of phenolic acids on cellulose FPU was related to its concentration. Slight inhibitory effect on the FPU of cellulase was observed when the concentration of phenolics is 0.05–8 g/L. Comparing smashing with steam explosion pretreatment in different condition, as well as before and after enzymatic hydrolysis, it was found that phenolics produced in pretreatment can promote the enzymatic hydrolysis. Small molecular phenolic substances produced during steam explosion should be retained to promote enzymatic hydrolysis, but it should be removed before fermentation in case of that it inhibits the fermentation. The results provide a reference for studying the effect of small molecular phenolic substances produced by other pretreatment processes on cellulose hydrolysis.

In steam explosion pretreatment process, based on changes in structure and composition of lignocellulose and its effect on enzymatic hydrolysis, the concept of secondary anti-degradation barrier was put forward in order to make a distinction between the lignocellulosic anti-degradation barrier and fermentation inhibitor.

In plant biomass refining process, in order to avoid the influence of intermediates, structures, and properties of substrate on operating units, following aspects during biomass refining should be paid attention:

(1) Cellulose at high temperatures or catalyzed can be converted to new products including 5-HMF and levulinic acid;
(2) Hemicellulose at high temperatures or catalyzed can be converted to new products including 5-HMF, furfural, levulinic acid, formic acid, and acetic acid;
(3) Lignin at high temperatures or catalyzed can be converted to small molecule phenolic substances;
(4) Cellulose macromolecules at high temperatures or catalyzed be converted to benzene ring;
(5) Lignin and cellulose can be combined, forming new macromolecules such as lignin–polysaccharide complex;
(6) New substances can be produced during refining process or by the interaction between the new substance and the original substance;

(7) Due to degradation or dissolution of the components, molecules rearranged by free hydrogen bond, produce a new structure and change the original interface properties and porous structure properties;
(8) Due to the combination of the new intermediates produced in the refining process or combination of new substances with the original macromolecules, the original interface performance and porous structure performance is changed;
(9) Due to changes in the composition, there is difference in capillary force, saturated water content, mass transfer performance, heat transfer performance, and momentum transfer performance in the different operating units of substances;
(10) Due to structural changes in composition, the materials in different operating units even the same operating units have different rheological properties, requiring new intensification methods;
(11) Due to structural changes in composition, mechanical properties of materials are different, requiring new equipment and process parameters.

The above changes of new composition, structure, and performance have effects on subsequent refining unit, so we need a comprehensive evaluation. First, changes in the composition, structure, and performance of the different units of action to promoting or blocking function are different. Second, changes in the composition, structure, or performance caused by changes of one or more fundamental parameters may result in a change in different operating units. So, even an operating unit can promote subsequent operating units it does not mean all changes are facilitated for subsequent operating units. Vice versa, the operating unit's influence on the subsequent operation unit is negative does not mean that influence of all changes on the subsequent operation unit is negative.

Moreover, lignocellulose refinery is a dynamic process, in other words, the whole process keeps changing. So only checking of key factors throughout the process can help us regulate results.

3.2 Intensification Methods for Enhancing Substrate Accessibility

3.2.1 Novel Steam Explosion Sterilization Improving Solid-State Fermentation Performance

Sterilization is essential to all industrial fermentation processes, which require the pure culture maintenance [16]. It is defined as the complete elimination of all microbial lives by physical or chemical methods [17]. Moist heat sterilization is widely used in submerged fermentation (SmF), and it is an effective way to eliminate microbes with the high thermal conductivity of liquid medium. Solid-state

fermentation (SSF) is considered as a promising process for producing various products such as fuel, feed, industrial chemicals, and pharmaceutical products [18]. The fact that lignocellulosic biomass can be converted to biofuels or biomaterials by SSF has attracted substantial interests from the government and private sectors, what is more, the abundance and renewability of raw materials and the urgent demand for energy make SSF more important [19, 20]. Unlike liquid medium, the complete sterilization of SSF medium has some other problems due to its low thermal conductivity and multi-compositions.

There are many sterilization methods, such as dry heat sterilization, moist heat sterilization, ultrasonic sterilization, microwave sterilization, radiations, and chemical disinfectants sterilization, all of them are proper only when it is based on the property of medium. Mechanisms and characteristics of these common sterilization methods are shown in Table 3.1. Moist heat sterilization's heating medium is steam, which is very reliable and very easy to control on a large scale, so the fermentation industry usually chooses it as a main sterilization method. Spherical

Table 3.1 Mechanisms and characteristics of different sterilization methods [146]

Sterilization methods	Mechanisms	Advantages and disadvantages	References
Dry heat sterilization	Coagulation of proteins, thus destroy microorganisms by hot air	Simple operation; no corrosion; lengthy time (about 1 h); nutrients degradation	[148]
Moist heat sterilization	Denaturation of proteins in microorganisms by steam	Large latent heat; strong penetrating power; low operation cost; lengthy time for solid materials; nutrients degradation	[149]
Ultrasonic sterilization	Killing microorganisms by radiation pressure, ultrasonic pressure, heat effect, cavitation effect, and chemical effect	Convenient operation; no pollution; high cost	[150]
Microwave sterilization	Denaturation of protein by thermal effect and changing cell membrane permeability by nonthermal effect	Short time; convenient operation; non uniform action; harmful to human body	[151]
Radiation sterilization	Penetrate microorganism cells by radiations	Simple operation; limited application area; harmful to human body	[152]
Chemical disinfectants sterilization	Oxidation of microorganisms or damaging cells by chemical disinfectants	Applicable to materials that cannot be heated; pollution to materials	[148]
Steam explosion sterilization	Deactivation of microorganisms by the high-temperature steam; destroy cells by the instant pressure relief	Short time; improving nutrition of solid medium; energy saving; applicable to solid materials	[146]

Reprinted from Ref. [21]. Copyright 2015, with permission from Elsevier

digester has been commonly used for sterilization of solid medium on an industrial scale. The solid medium will be heated to 121 °C and kept for 20 min or more with the saturated steam in spherical digester, and then they will be naturally cooled. The spherical digester rotates and that will accelerate heat transfer in the whole process so that the microorganisms will be killed by the moist. However, the main drawbacks of this technique include the long cycle time, incomplete discharge, and high energy consumption [21]. Previous research also pointed out that long-time heating has an adverse effect on nutrients for the thermal degradation of nutrients [22]. Therefore, all the above things are the main problems of traditional thermal sterilization of solid medium. According to the Arrhenius equation, rate constant of chemical degradation is less influenced by temperature than that of microbial inactivation because the activation energy of chemical degradation is lower than that of microbial inactivation [23, 24]. Therefore, the sterilization with high temperature and short time period could make it possible to minimize the degradation of nutrients while killing the microorganisms. Mann et al. studied the thermal sterilization of heat-sensitive products and suggested that the degradation of nutrients can be substantially reduced by high-temperature and short-time sterilization [23]. Kjellstrand et al. also found that the high-temperature short-time strategy should be used for sterilization to minimize the decomposition of products [25]. Steam explosion is one of the most efficient methods for lignocellulosic biomass, and it has been developed into commercial scale [26]. In steam explosion reactor, solid materials are heated by high-pressure saturated steam for a relatively short time (normally 2–8 min). Until it reached the desired residence time, the reaction system was depressurized instantaneously. This is a typical high-temperature short-time process. In steam explosion process, there are two steps which are high-temperature steam heating and explosion [27]. Besides high-temperature heating, the change of materials' structure by physical collision in explosion may also help to break the microbial cells.

In this study, we aim to exploit a novel and potential sterilization strategy for solid medium which we called it as high-temperature and short-time steam explosion process. Effects of the temperature and time of sterilization were studied and the steam explosion conditions for complete sterilization were determined. Kinetics of steam explosion sterilization was established and the effect of explosion in SE was investigated [28, 29].

The nutrient content in the medium was considered as a very important standard to evaluate the sterilization performance [30]. Additionally, fermentation performance after steam explosion and conventional thermal sterilization (121°C, 20 min) were compared to examine the feasibility of steam explosion sterilization. Finally, sterilization efficiency and energy utilization were analyzed from the point of industrial scale.

3.2.1.1 Evaluation of Sterilization Effect by Image Processing

In order to conveniently evaluate the sterilization effect and choose a proper parameter to predict the sterilization performance, the color-changing of SIT under different steam explosion conditions were investigated. SIT is exposed in steam moist heat during the steam explosion sterilization. The greater the heat intensity, the more obvious the color-changing of SIT is, which results in the smaller gray value of the heat-sensitive area in SIT. Therefore, the average gray value of the heat-sensitive area could be relevant to the sterilization performance. Figure 3.3 shows that the gray value decreased obviously after either steam explosion sterilization or conventional thermal sterilization. In steam explosion sterilization, the gray value decreased monotonically with the increase of SE temperature at the same residence time. Results showed that the complete sterilization of steam explosion sterilization was obtained above 172 °C for 2 min and above 128 °C for 5 min or 8 min, while the corresponding average gray value of the sensitive area in SIT was 41.30, 59.06, and 58.71, respectively. It was noticed that the average gray value under 172 °C for 2 min was obviously lower than that under 128 °C for 5 and 8 min. This phenomenon may be attributed to that the color-changing of SIT is more sensitive to the temperature than time. Nevertheless, when the SE residence time was 2 min, the average gray value of the sensitive area in SIT was not above 41.30 for meaning complete sterilization. Correspondingly, the threshold value was 59.06 and 58.71 for complete sterilization when the SE residence time was 5 min and 8 min, respectively. Therefore, an effective parameter, average gray value of

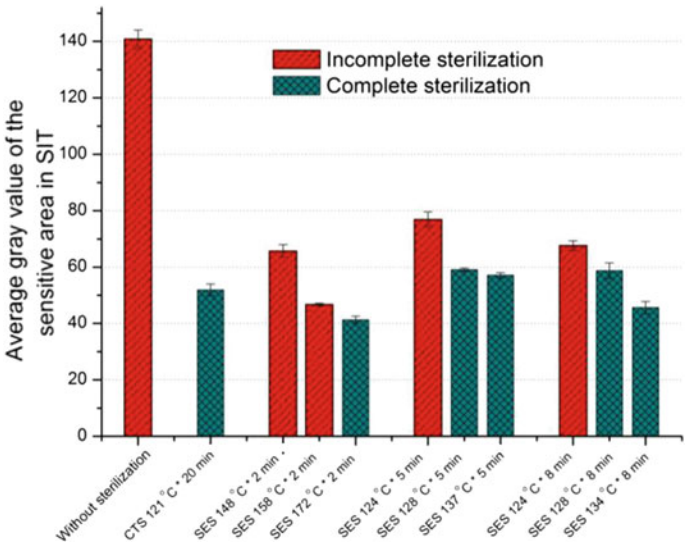

Fig. 3.3 Average gray value of the sensitive area in SIT before and after sterilization. CTS, conventional thermal sterilization; SES, steam explosion sterilization

the sensitive area in SIT was successful to indicate SE sterilization effect conveniently and rapidly.

3.2.1.2 Determination of Steam Explosion Conditions for Complete Sterilization

Effects of steam explosion temperature and explosion on sterilization efficiency were investigated. As shown in Table 3.2, the sterilization efficiency improved with the increase of SE temperature at the same residence time. The reason for this result was that coagulation and denaturation of proteins in microbes became serious at higher temperature. Therefore, microbes were more likely to be killed, resulting in the better sterilization efficiency at the higher temperature. It is interesting to note that, from number 7 and 15 in Table 3.2, the solid medium was completely sterilized by steam explosion sterilization with 128 °C for 5 min, while not by conventional thermal sterilization with the same temperature and time. This phenomenon clearly indicated that the explosion step in SE helped to break the microbial cells and thus improved the sterilization efficiency. Overall, Table 3.2

Table 3.2 Effects of residence time and temperature of steam explosion on sterilization performance [23]

Number	Residence time (min)	Temperature (°C)	LgR_0	Colony-forming units (CFU)[a]
1	2	135	1.33	++
2	2	148	1.71	++
3	2	158	2.01	++
4	2	165	2.21	+
5	2	172	2.42	ND
6	5	124	1.41	+
7	5	128	1.52	ND
8	5	134	1.70	ND
9	5	137	1.79	ND
10	5	141	1.91	ND
11	8	124	1.61	+
12	8	128	1.73	ND
13	8	134	1.90	ND
14[b]	20	121	–	ND
15[c]	5	128	–	+
16[d]	–	–	–	+++

[a]+++ means lawn; ++ means CFU ≧ 30 but lawn was not formed; + means 30 > CFU > 0; ND means not determined (CFU = 0)
[b]Conventional thermal sterilization (CTS) at 121 °C for 20 min
[c]CTS at 128 °C for 5 min
[d]Medium without sterilization treatment
Reprinted from Ref. [21]. Copyright 2015, with permission from Elsevier

shows that the complete sterilization conditions by steam explosion sterilization were above 172 °C for 2 min or above 128 °C for 5 and 8 min. Compared with the commonly used conventional thermal sterilization condition (121 °C, 20 min), the time of steam explosion sterilization was shortened dramatically, with sterilization efficiency improved.

Effect of steam explosion residence time on sterilization efficiency Residence time of steam explosion is another key factor in determining the sterilization effect. It was found in Table 3.2 that the temperature needs to reach 172 °C with 2 min residence time, while the temperature was 128 °C with the residence time of 5 min it can achieve complete sterilization. The results demonstrated that the temperature required for complete sterilization decreased apparently with longer residence time. The Arrhenius equation can be used to estimate the inactivation of microorganisms for heat sterilization process [23].

Where k is the microorganisms inactivation rate constant, s^{-1}; A is the Arrhenius frequency factor, s^{-1}; E is the activation energy, J/mol; R is the universal gas constant, J/(mol·K); and T is the absolute temperature, K, according to the Arrhenius equation, higher sterilization temperature T resulted in larger microorganisms inactivation rate constant k, requiring shorter residence time. In turn, longer residence time required lower sterilization temperature, which was consistent with the results described above.

On the other hand, severity factor which combines temperature and residence time is a concept to express the severity of a given steam explosion treatment. It was reported that severity factor was a potential parameter for SE scale-up [31–33]. As seen from number 2 and 8 in Table 3.2, the temperature and time combination of 134 °C × 5 min resulted in better sterilization effect than that of 148 °C × 2 min with almost the same steam explosion severity factor R_0. The possible reason was that although the temperature was higher in group 2, the heat could not transfer evenly in the medium within 2 min due to the low thermal conductivity of solid medium, which led to the incomplete sterilization. While for group 8, despite the lower temperature, heat could transfer uniformly during the longer residence time. Therefore, there were no blind spots within the medium. Then complete sterilization was achieved.

It also can be seen in number 7 and 11 from Table 3.2 that the sterilization effect of group 11 with the temperature and time combination of 124 °C × 8 min was worse than that of group 7 with 128 °C × 5 min, although the residence time was longer and the steam explosion severity factor was larger of group 11 than that of group 7. Number 11 and 12 showed that temperature needed to reach 128 °C for complete sterilization with the residence time of 8 min. These results implied that when the time was long enough, it was not the limiting factor for sterilization efficiency anymore. Overall, combining the effects of steam explosion temperature and residence time on sterilization efficiency, it can be concluded that using steam explosion technique for solid medium sterilization was effective. Steam explosion conditions for complete sterilization were temperature and time combination of 172 °C × 2 min and 128 °C × 5 min.

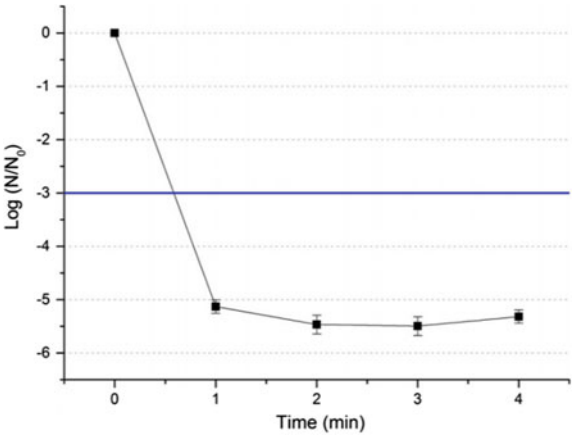

Fig. 3.4 Survival curve of microorganisms in solid medium after steam explosion treatment at 128 °C. The blue horizontal line represents the survival rate of 0.001, below which is acceptable for sterilization. Reprinted from Ref. [21]. Copyright 2015, with permission from Elsevier

Steam explosion sterilization kinetics The logarithm of microorganism survivors in solid medium after SE treatment at 128 °C was plotted in Fig. 3.4. It was shown that the inactivation curve exhibited a nonlinear behavior. Microorganism inactivation by SE progressed rapidly during pressure-hold for 1 min. 5.1-log reduction was observed after SE treatment at 128 °C for 1 min, while greater holding times had comparatively limited effect. There was no CFU observed when the holding time reached to 5 min. Similar trends in inactivation have been observed in other work involving high pressure and temperature treatments of *Clostridium sporogenes* spores in ground beef and bacillus stearothermophilus spores in egg patties [10, 34]. The nonlinear survivor curve may indicate that SE has multiple targets of action on microbial cells. The observed tailing phenomenon could be attributed to cell damage by the instant pressure release. Overall, it was noticed that the survival rate of SE treatments at 128 °C for more than 1 min were all lower than 0.001, which was generally acceptable in sterilization evaluation. Rajan et al. reported that only 1.5-log reduction was observed under the conventional thermal treatment of B [35]. *Stearothermophilus* spores in egg patties at 121 °C for 15 min. Therefore, it was indicated that using SE treatment for SM sterilization could result in a much quicker processing and better sterilization effect.

3.2.1.3 Nutrients Contents Before and After Sterilization

Heat processing also has a detrimental effect on nutrients since thermal degradation of nutrients can and does occur [22]. The effects of steam explosion sterilization and conventional thermal sterilization on nutrient contents of medium were investigated. As shown in Fig. 3.5, both glucose and xylose contents decreased more apparently after conventional thermal sterilization than those of raw medium, suggesting that conventional thermal sterilization was adverse for nutrients. It was noted that the glucose and xylose contents after conventional thermal sterilization at

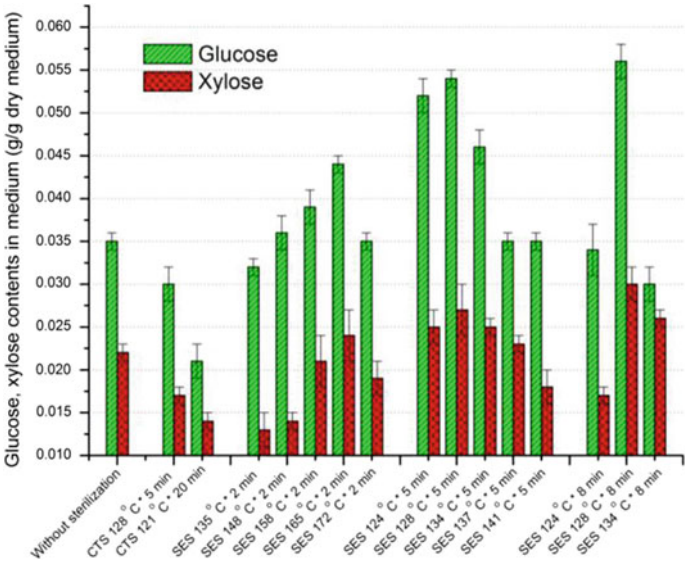

Fig. 3.5 Effects of steam explosion sterilization (SES) on nutrients contents in medium compared with conventional thermal sterilization (CTS) [146]

128 °C for 5 min were higher than those after conventional thermal sterilization at 121 °C for 20 min, which confirmed that the high-temperature short-time heat process decreased the destruction of the nutrients. With the same residence time of steam explosion, glucose and xylose contents increased initially and then decreased with the temperature increase. This phenomenon implied that SE may affect nutrient contents by two steps: degrading polysaccharides into glucose and xylose and degrading glucose and xylose into small molecules. First, the polysaccharides were degraded more and more intensely as steam explosion severity increased, thus release more glucose and xylose. However, when the SE severity reached a certain value, the degradation of glucose and xylose began to increase drastically, leading to the reduction of glucose and xylose contents in medium. Nevertheless, results clearly showed that steam explosion sterilization improved glucose and xylose contents in medium, especially compared with conventional thermal sterilization. It is interesting to note that the glucose and xylose content after steam explosion sterilization at 128 °C for 5 min increased by 80.0% and 58.8% than those after conventional thermal sterilization with the same temperature and time, respectively. This result revealed that the instant pressure relief in steam explosion helped to release glucose and xylose from the SM efficiently. From the perspective of nutrients and efficiency, combination of temperature and residence time of 128 °C × 5 min was chosen as the preferable SE condition for sterilization, under which the glucose and xylose contents were 2.57 and 1.93 times of those treated by the effective conventional thermal sterilization condition (121 °C, 20 min). The results

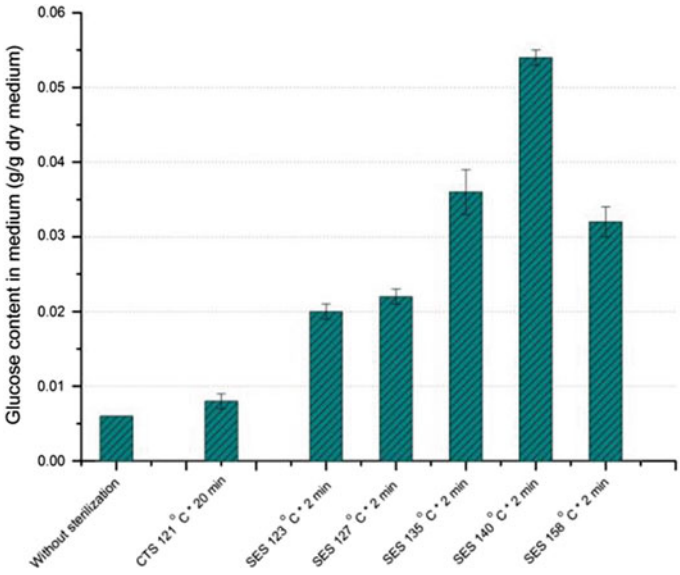

Fig. 3.6 Effects of steam explosion sterilization on glucose generation in wheat bran and soybean meal. CTS, conventional thermal sterilization; SES, steam explosion sterilization [146]

clearly indicated that steam explosion sterilization improved the solid medium nutrition.

In order to reveal the effect of steam explosion sterilization on glucose release explicitly, the medium containing only wheat bran and soybean meal with moisture of 60% (w/w) were used for steam explosion treatment. Figure 3.6 shows that steam explosion sterilization obviously converted glucan into glucose in the medium. At the residence time of 2 min, the glucose content increased first and then began to decrease with the temperature increase, of which the trends coincided with the results described above. The possible reason was that the released glucose was further degraded under the higher SE severity. Additionally, it was noticed that the conventional thermal sterilization (121 °C, 20 min) could also convert glucan to glucose, but this effect was negligible compared with steam explosion sterilization. Overall, steam explosion sterilization increased nutrients contents in medium, which must be beneficial to the subsequent fermentation.

Previous works have also suggested that inhibitors, such as weak acids, furan derivatives may generate during the steam treatment of the lignocelluloses [36, 37]. These compounds are inhibitory to microorganisms and will limit the fermentation performance. Negro et al. observed that inhibitors generated in the liquid fractions of steam-exploded olive tree pruning, the concentrations of acetic acid, formic acid, furfural, and HMF ranged from 2.7–3.5 g/L, 0.1–0.4 g/L, 0.7–1.4 g/L, and 0.1–0.3 g/L under the steam explosion conditions of 175 °C and 195 °C for 10 min, respectively [38]. The liquid fractions were then fermented with the xylose-fermenting microorganism, *Scheffersomyces stipitis,* for ethanol production.

However, neither ethanol nor growth was observed, indicating that the presence of toxic compounds inhibited the growth and fermentation of microorganisms [38]. While in the present work, the inhibitors were not detected out, in which it was beneficial to the subsequent fermentation process. The possible reason was that the SE severity for sterilization in the present work was much lower than that used in pretreatment. Therefore, the generation reactions of inhibitors were not stimulated.

3.2.1.4 FTIR Analysis of Solid Medium Before and After Sterilization

FTIR, which is a quite convenient and frequently used analysis technique for structural characterization, was applied in this study to investigate the structural changes of SM before and after sterilization. As shown in Table 3.3, the spectra presented peaks at 3342 cm^{-1} (OH), 1658 cm^{-1} (CO, CN), 1541 cm^{-1} (CN, NH),1421 cm^{-1}(CH_2), and 1103 cm^{-1} (OH), which indicated the presence of cellulose (3342 cm^{-1} and 1421 cm^{-1}), polysaccharides (3342 cm^{-1} and 1103 cm^{-1}), and proteins (1658 cm^{-1} and 1541 cm^{-1}) [39]. A semiquantitative analysis of the FTIR spectra was established and the band at 1515 cm^{-1} (aromatic skeletal stretching) was used as a reference band to estimate the relative intensities of other bands [40, 41]. Table 3.3 showed that some bands underwent detectable relative intensity changes as a result of different sterilization methods. The relative intensity A3342/A1515 of band attributed to the hydroxyl groups in polysaccharides of solid medium decreased from 1.4652 to 1.2673 after steam explosion sterilization, which indicated that steam explosion sterilization degraded polysaccharides and may help to release glucose. Whereas the A_{3342}/A_{1515} value of solid medium after conventional thermal sterilization was 1.4616, which was little lower than that of raw solid medium. The information showed that conventional thermal sterilization can also help to degrade polysaccharides, but the effect was little to neglect, which was consistent with the results described in Fig. 3.6. Moreover, the relative intensities of the 1421 cm^{-1} band originating from CH_2 bending vibrations of cellulose and 1103 cm^{-1} band attributed to the C–OH skeletal vibration decreased more obviously after steam explosion sterilization, which confirmed the polysaccharides degraded by steam explosion sterilization again. Both steam explosion sterilization and conventional thermal sterilization reduced the intensities of the 1658 cm^{-1} and 1541 cm^{-1} bands attributed to the C–O stretching, C–N stretching, and N–H bending vibrations, respectively of amide groups in proteins or protein-like compounds. The information indicated that steam explosion sterilization and conventional thermal sterilization could break down the long-chain protein into the short, of which the effect by steam explosion sterilization was more obvious. This can be confirmed by the relatively lower absorbance of C–N stretching vibration band at 1155 cm^{-1} in SM after steam explosion sterilization compared with that after conventional thermal sterilization. This effect may make microbes utilized amino acids in SM more effective after steam explosion sterilization. In addition, steam explosion sterilization obviously reduced the intensity of the 1242 cm^{-1} band attributed to the C–O stretching band (guaiacyl units), which

Table 3.3 FTIR semiquantitative analysis of raw solid medium (SM), SM after conventional thermal sterilization (CTS, 121 °C, 20 min) and SM after steam explosion sterilization (SES, 128 °C, 5 min) [146]

Bond (cm^{-1})	Assignment	A_x/A1515[a]		
		Raw SM	SM after CTS (121 °C, 20 min)	SM after SES (128 °C, 5 min)
3342	OH stretching and hydrogen bonds [39]	1.4652	1.4616	1.2673
1658	CO stretching of amide groups in proteins or protein-like compounds, i.e., amide I [39]	1.3930	1.2732	1.2095
1541	CN stretching and NH bending vibrations of amide groups in proteins or protein-like compounds, i.e., amide II [39]	0.9937	0.9828	0.9627
1515	Aromatic skeletal vibration [40, 41]	1.0000	1.0000	1.0000
1421	CH_2 bending vibrations of cellulose [39]	1.4704	1.3843	1.3788
1242	CO stretching in the acetyl and phenolic groups [20, 153]	1.1528	1.1129	1.0379
1155	CN stretching vibration of the protein fractions [154]	1.6630	1.5930	1.4803
1103	OH skeletal vibration [39, 154]	1.8662	1.7187	1.5758
1034	COC stretching typical of glucan and xylan [20]	2.1208	2.0341	1.8460

Reprinted from Ref. [21]. Copyright 2015, with permission from Elsevier

indicated that the relative content of guaiacyl lignin units after steam explosion sterilization had significant changes compared with that after conventional thermal sterilization. steam explosion sterilization also reduced the intensity of peak at 1034 cm^{-1} attributed to the C–O–C stretching typical of glucan and xylan significantly. The modification may correspond to the degradation of glucan and xylan, which facilitated the release of glucose and xylose. Thus, these results indicated that steam explosion sterilization helped to disrupt the structure of polysaccharides more efficiently than conventional thermal sterilization, which contributed to the nutrients improvement in SM. This information also corresponded to the data in Fig. 3.5 that the glucose and xylose contents increased more in SM after steam explosion sterilization than those after conventional thermal sterilization.

3.2.1.5 Comparison of Fermentation Performance on Steam Explosion Sterilization and Conventional Thermal Sterilization Medium

Fermentation performance is the key metric to evaluate the steam explosion sterilization and conventional thermal sterilization. As shown in Fig. 3.7, *B. subtilis* fermented on steam explosion sterilization medium grew fast after the fermentation for 24 h, and the maximum number reached 2.66×10^{11}/g DM at 48 h and

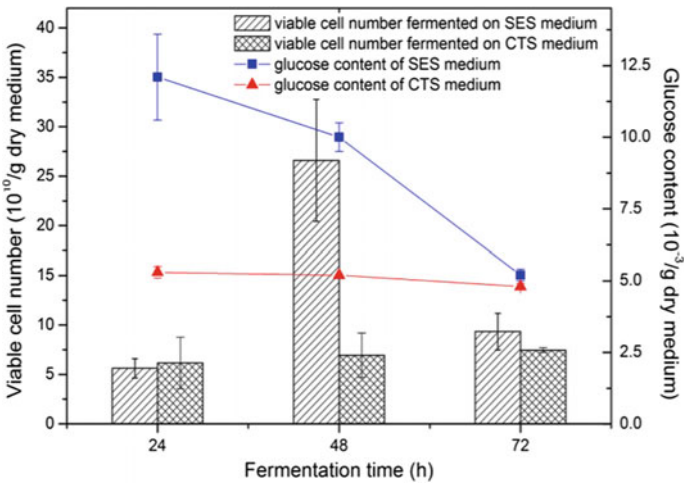

Fig. 3.7 Fermentation kinetics on solid medium after steam explosion sterilization (SES, 128 °C, 5 min) and conventional thermal sterilization (CTS, 121 °C, 20 min) [146]

decreased thereafter. While for conventional thermal sterilization medium, the bacteria number increased slowly during the fermentation process and reached 6.94×10^{10}/g DM at 48 h. It was reported that the optimum fermentation period for *B. subtilis* growth was 48 h [42, 43]. The number of *B. subtilis* fermented on conventional thermal sterilization medium reached the maximum of 6.67×10^{10}/g DM at 48 h, which was in accordance with the result of the present study [42]. Therefore, the bacteria number on steam explosion sterilization medium was 2.83 times larger than that on conventional thermal sterilization medium, which implied that steam explosion sterilization improved the fermentation performance apparently. Figure 3.7 also showed that the glucose content of steam explosion sterilization medium was 2.28 times of that of conventional thermal sterilization medium at the fermentation time of 24 h. Then, it was decreased due to the consumption by *B. subtilis* growth, and the value was 1.92 times of that of conventional thermal sterilization medium at 48 h. Finally, the glucose content of steam explosion sterilization medium was 1.08 times of that of conventional thermal sterilization medium when the fermentation time reached 72 h. In view of above results, it was found that the glucose content of steam explosion sterilization medium was higher than that of conventional thermal sterilization medium during the fermentation process. That means, the medium after steam explosion sterilization was more nutritional for *B. subtilis* fermentation, which should be an important reason for the enhanced *B. subtilis* growth on steam explosion sterilization medium than that on conventional thermal sterilization medium. Therefore, the results demonstrated that steam explosion sterilization facilitated the fermentability of solid medium and improved SSF performance efficiently.

3.2.1.6 Comparison of Production Efficiency Between Steam Explosion Sterilization and Conventional Thermal Sterilization on Large Scale

Sterilization time and energy consumption have great influence on the production efficiency and economic cost, especially for industrialization. The sterilization time and energy utilization of conventional thermal sterilization and steam explosion sterilization for SM on large scale, spherical digester, were analyzed and compared. Table 3.4 showed the process flow of the conventional spherical digester sterilization and steam explosion sterilization. The significant difference between these two processes occurred on the following two aspects. First, there was no cooling stage for steam explosion sterilization. In spherical digester sterilization, pressure inside the spherical digester was about 0.11 MPa (gauge pressure) after the temperature maintenance stage. Therefore, the spherical digester should be cooled for 30 min before discharge for security. It is noted that the cooling operation not only consumes time but also wastes the energy for heating. As for steam explosion sterilization, the high pressure was used to transport the materials aseptically and help to destroy the microbe cells. After the instant pressure relief, the temperature of the moist air inside the steam explosion reactor was still high, which saved energy for heating in the next batch operation. Besides, the time for temperature maintenance was shortened by 75% of steam explosion sterilization than that of spherical digester to the enhanced sterilization performance. It could be indicated from Table 3.4 that the time needed for a batch operation of spherical digester sterilization was 63 min while the time was only 19 min of steam explosion sterilization. That means steam explosion sterilization could save time by 69.8%, suggesting that the utilization efficiency of equipment obviously increased in steam explosion sterilization process. Therefore, steam explosion sterilization could not only save energy efficiently but also reduce operation time dramatically. This is conductive to improve industrial production efficiency and reduce the economic cost (Table 3.5).

This study clearly showed that the feasibility of steam explosion technology for solid medium sterilization. Owing to the higher temperature and physical collision effect, steam explosion sterilization shortened sterilization time by 69.8%. Meanwhile, it was worth noting that the glucose and xylose contents in solid

Table 3.4 Processes and time consumption of conventional spherical digester sterilization and novel steam explosion sterilization (SES) in a batch operation (data in this table with the unit of min) [146]

	Feedstock	Steam heating	Temperature maintenance	Cooling	Discharge	Total
Conventional spherical digester sterilization	5	5 (heating to 121 °C)	20	30	3	63
Steam explosion sterilization	5	6 (heating to 128 °C)	5	0	3	19

Reprinted from Ref. [21]. Copyright 2015, with permission from Elsevier

Table 3.5 The effects of different pretreatment on lignocellulosic biomass

	Increase specific surface area	Decrease the degree of crystallinity of cellulose	Solubility of Hemicellulose	Remove lignin	Produce inhibitors	Change the structure of lignin
crushing	■	■				
SE	■		■	■	■	■
Hydrothermal	■	n.d.	■	■	■	■
Acid pretreatment	■		■	■	■	■
Alkali pretreatment	■		■	■	■	■
Wet oxidation	■	n.d.		■	■	■
AFEX	■	■	■	■	■	■
ARP	■	■	■	■	■	■
Lime method	■	n.d.	■	■	■	■

medium after steam explosion sterilization were 2.57 and 1.93 times of those after conventional thermal sterilization (121 °C, 20 min), which suggested that steam explosion sterilization improved the fermentability of solid medium. *B. subtilis*, fermentation productivity on steam explosion sterilization medium increased by 2.83 times than that on conventional thermal sterilization medium. Therefore, steam explosion technology could be a new way in future for solid medium sterilization, which could promote the economy of solid-state fermentation.

3.2.2 Pretreatment Intensification Accessibility of Substrate in High-solid and Multi-phase Bioreaction

For the limitation of mass transfer process, it is essential to establish an effective pretreatment method to improve the bioavailability offer mentation materials.

(1) Physical pretreatment

Crushing process Most of the material needs to be crushed to reduce particle size before they are put in pretreatment reactor. Agricultural waste, herb, and other raw material can be crushed during or after harvest. And whether to further crush them or not, that depends on the type of raw material, and the heat or mass transfer. The crushing process, as the common pretreatment before enzymatic hydrolysis, has many different types which include ball mill (dry grinding, wet grinding, and vibration processing), different disc refiners and others. Although we can use these devices to increase the bioavailability of cellulose and the surface area, reduce the crystallinity of cellulose, which makes it easier for enzyme to degrade cellulose,

however, many studies show that these methods do not suit ethanol bioconversion process in terms of economy, for the grinding process is energy-intensive.

Radiation Some people studied to use high-energy electron beam and the microwave as the pretreatment of biomass. These methods are supposed to mechanically destroy the structure of plant cell walls and reduce the crystallinity of cellulose, and then increase the hydrolysis efficiency of cellulase. But when we think about the cost, energy intensity, and the feasibility to put that into commercial applications, it is obvious that radiation is not a good method.

(2) Quick depressurization pretreatment

Steam explosion

Ammonia fiber explosion (AFEX) In AFEX, anhydrous ammonia is used to pretreat the substrate. The reaction temperature ranges from 60 to 100 °C, pressure changes from 250 to 300 psig and with a few minutes of retention time usually. High pressure is released quickly, which could cause ammonia quickly spread and then the expansion of the fiber structure and physical damage to the substrate. At the same time, crystalline structure of cellulose was partly destroyed, some lignin dissolved and hemicellulose was partly degraded into oligosaccharide. The AFEX method can remove the acetyl from substrate and increase the degradability. Because of the AFEX modified hemicellulose in the process of processing, it limits the hydrolysis of hemicellulose and comprehensive utilization of biomass to hemicellulose. The AFEX pretreatment is very effective for agricultural waste and herb, but for the wood material or other materials with high content of linin, it is ineffective. The AFEX mainly worked in the environment where solid content is high (40%) and the ammonia content also is high(about 1.0 g ammonia per 1 g dry material). Although these ammonia can be recycled completely, this operation is costly, so when it extends to commercial area, the consideration of the cost is needed. AFEX is usually carried in the lab, but now people have developed a new technology for application, which is called FIBEX.

(3) Autolysis

Not only steam explosion pretreatment do not need people to add catalyst to it but also the high-pressure liquid do not need extra catalyst, what is more, the rapid decompression operation is not required. The hydrolysis of cellulose needs high temperature which is around 260 °C, but hemicellulose hydrolysis required relatively low temperature (200–230 °C). Although we can obtain high yield of soluble sugars from hemicellulose, these sugar which experienced the hydrothermal pretreatment mainly are in the form of oligosaccharide, so further acid hydrolysis or enzyme hydrolysis is needed to produce fermentable monosaccharides. Another way of hydrothermal pretreatment is to add some chemicals to control the pH within 4–7. For some materials such as corn straw, it has the buffer ability of pH, so no additional chemicals are needed. The purpose of control reaction pH value is to keep hemicellulose release mainly in the form of oligomer, so that we can reduce the loss of sugar for its dehydration and avoid producing fermentation inhibitors.

However, the method has little effect on improving the efficiency of enzymatic hydrolysis of corn stalk. From an economic point of view, hydrothermal pretreatment is attractive because of its low spending on catalyst and low corrosive to reactors which reduce the reactor cost. But these saved costs might just equal to the loss of sugar.

(4) Acid pretreatment

(5) Alkali pretreatment

Alkali In general, alkali pretreatment is less effective for cellulose hydrolysis than acid pretreatment, but it is very effective for removing lignin and then improve the efficiency of the degradation of solid substrates obviously. There are reports and summary about pretreatment by sodium hydroxide. The pretreatment can cause the expansion of the fiber, the increase of the internal surface area, low polymerization degree, reduced crystallinity degree, the separation between lignin and carbohydrate and the destruction of the lignin structure. The efficiency of sodium hydroxide pretreatment is closely related to the lignin content in substrates. This method is less effective to the substrate with high lignin content, especially the soft wood. This method shows obvious advantages when we pretreat the material with low lignin content (10–18%), such as straw, but we have not evaluated the cost-benefit yet.

Ammonia The simplest ammonia pretreatment is to use ammonia (the mass fraction of NH_4OH is 30%) with low temperature (about 90 °C) to soak the materials, the solid content is between 10 and 50%, the reaction time can vary from a few hours to a day. A study reported that lignin can be removed as high as 80% with a lower amount of dissolved hemicellulose when wheat straw and corn straw were pretreated by this method. Ammonia Recycled Percolation (ARP) is to pretreat biomass by dilute Ammonia solution (<15% NH_3) under 150–170 °C. Due to the fluid properties and chemical properties of ammonia, ARP is a good way to remove the lignin (above 80%) of corn stalk, at the same time, some hemicellulose was degraded to oligosaccharides, but it still needs further treatment to transform into monosaccharide. The efficiency of commercial cellulase for ARP-treated corn straw is high (about 90% cellulose convert into glucose, about 70% hemicellulose convert into xylose). However, economic analysis shows that the ARP process needs large amount of liquid, but the liquid will be continuously diluted in subsequent steps, which makes the ARP process have no competitive advantage when it is in competition with other methods.

Lime Lime pretreatment is a low-value processing, it is mainly used for dissolving acetyl and lignin. The range of the operating temperature of lime pretreatment is very board(25–130°C).The lime content is usually about 10% (by dry substrate), and the solid content is about 20% or less. At high temperature, pretreatment time will be significantly reduced (a few hours to a few minutes), but under the low temperature it could last for several weeks. The lime pretreatment does not require expensive reactor and be carried in the process of raw material storage. Herbaceous plants or agricultural waste materials with the low lignin content are usually good substrates for lime pretreatment. The acetyl can be almost completely removed and lignin can be removed by about 30%. If you want to make it more effective, oxygen or air should be sent to reaction system. For the low-temperature

lime pretreatment process, it needs some fresh air because lime pretreatment can remove a lot of lignin in aerobic environment. The technology can be used for some refractory substrates, such as bagasse and hardwood. Compared with other means using alkaline, this catalyst is cheap, but its reaction time is longer, at the same time, the regeneration and recycling of lime will increase the investment and running cost.

(6) Solvent pretreatment

(7) Supercritical fluid pretreatment

(8) Oxide pretreatment

(9) Biological pretreatment

Considering the chemical composition characteristics of lignocellulose, we used low-pressure steam explosion as a pretreatment and controlled the moisture content of the materials, and finally make SE pressure fell to 0.6–1.5 MPa. After steam explosion, the granularity of raw material was reduced, the surface area was increased and the conversion rate of cellulose and hemicellulose of the biomass straw was increased. So it can make about 85% hemicellulose in the straw can be degraded to hydrosoluble and low molecular weight of sugar. As we can see, this method will improve the bioavailability of SM to a great extent. A lot of works have proved that the technology is very effective to break the lignocellulose materials' porous structures and improve the bioavailability. Besides the low cost, this method fundamentally solved secondary pollution problem which is caused by adding chemicals and is almost pollution-free. Further research reveals answer to that why SE can break the porous medium. Compared with the original corn stalk, steam explosion changed the distribution of pore size, and it also increased porosity by 10.1%, increase the aperture by 3.7 times, decreased the specific surface area by 81.8%, and decreased the degree of bending by 55.3%. The above changes make the key parameter of mass transfer of maize straw improved: percolation probability is increased by 21.3%; permeability is increased by 44.2 times. Based on the theory of mass and heat transfer in porous media, we found that SE can break the barrier of plant biomass and result that it improves the mass transfer rate in enzymatic hydrolysis.

3.3 Relationship Between Solid Matrix and the Strengthen Process of Bioavailability

3.3.1 Chemical Composition

Biomass material mainly refers to softwood, hardwood, and herbaceous, and their main chemical components include cellulose, hemicellulose, and lignin. In common plants, these three components usually account for 80–95% of their total mass, which form the supporting skeleton of a plant: the cellulose forms microfine fibers and hemicellulose and lignin serve as the adhesive and fillers which are filled between the fiber and microfiber [44]. Besides, there are other components (e.g., resins, fats, waxes, pectins, starches, proteins, inorganic substances, tannins, and

pigments [45]. Differences of chemical composition of these three types make significant differences in the aspect of the mechanism and process of steam explosion.

Based on absolutely dry wood, coniferous wood content 43% cellulose, 28% hemicellulose, and 29% lignin, while hardwood contains about 45% cellulose, 34% hemicellulose, and 21% lignin. They have similar content of cellulose, except poplar, their polydextrose is also stable. The content of hemicellulose in hardwood was higher than that in coniferous wood. In the hemicellulose, hardwood contains a large amount of poly-4-O-methylglucuronic acid (20–25%) and less polyglucose or mannose (1–3%); coniferous wood contains a lot polygalactomucrose and mannose acetate (15–20%)and about 10% poly-4-O-methylglucuronic and little arabino-galactan(1–3%) [45]. Therefore, hardwoods contain more polyxylose, while coniferous wood contains more polymannose, polygalactose, and polyarabinose. The lignin content of coniferous wood is higher than that of hardwood and coniferous wood lignin mainly include guaiacyl propane and a small amount of p-hydroxyphenyl propane, the lignin of hardwood mainly include guaiacyl propane and syringyl propane and a small amount of p-hydroxyphenyl propane [45]. Herbaceous plants are similar to the hardwood in terms of the composition, but the cellulose content of straw, corn stalks or sorghum stalks is much lower, however, they have more pentosan than softwood, and that is equivalent to the high value of hardwood. Herbal biomass materials have the following characteristics: (1) High content of hemicellulose, low lignin content. During the SE, the acetyl groups in the hemicellulose chain was hydrolyzed and produced a lot of acetic acid, which catalyzes the hydrolysis of the glucosidic linkages of hemicellulose and the β-ester bonds of lignin. Therefore, materials with more hemicellulose have stronger acid catalysis, so it is easier to be degraded in the steam explosion process. (2) Compared with woody plants, the herbaceous plants' molecular weight of lignin is lower but phenol hydroxyl content is higher. Therefore, herbaceous plants have high lyophilicity and can be dissolved in the hot acid environment [46]. Compared with coniferous wood, herbaceous plants, in aspect of chemical composition, shows a strong resistance to pretreatment: (1) In coniferous wood the hemicellulose content is relatively low so the available acetyl content is low and then Polydextrose-mannose is more difficult than xylose to be degraded in acid environment, which will influence the SE results. (2) Fibrous cells are highly lignified and these kinds of lignin have higher molecular weight so that they are difficult to be dissolved during SE process. What is more, lignin contains more guaiacyl which make it difficult to be degraded. Therefore, lignin is hard to be degraded and is not conductive to stem explosion. (3) A lot of fillers are in the resin dust of softwood which will inhibit the heat and mass transfer.

Based on these differences between straw and wood, the author has improved the traditional steam explosion process and proposed that low pressure (3.0 MPa down to 1.5 MPa or below) steam explosion technology which can treat straw without any chemicals. The mechanism of autolysis of straw has been also revealed [46]. The hemicelluloses are hydrolyzed by some released acetic acid and other weak acids. In the steam explosion process, hot water also plays the role of acid catalyst.

Eventually, more than 80% of the hemicellulose can be separated and the rate of cellulose hydrolysis can reach more than 90%. At present, the steam explosion equipment has been successfully amplified to the industrial scale, which is the biggest steam explosion equipment around the world. What is more, the authors developed a set of efficient and clean steam explosion technology and a new combined pretreatment method based on steam explosion. The author also integrated the alkaline hydrogen peroxide, ultra-fine grinding, mechanical carding, and other methods in the steam explosion process, which achieve the hierarchical separation of straw chemical components, cell types and tissue layers [47–49], and laid the foundation for clean and efficient use of straw. Based on this method, the authors have developed straw-multilevel production of corrugated base paper, oriented strand board and others, and applied steam explosion refining platform to tobacco processing, extraction of Chinese herbal medicine, hemp bast degumming and other fields [46].

3.3.2 Composition Structure

The structures of softwood, broadleaf, and herbaceous plants are obviously different. Coniferous wood have few cell types, generally speaking, coniferous wood have resin ducts but no catheters. Its main tracheids have both the transport function and the mechanical support function and the tracheids account for more than 90% of timber volume, what is more, the typical cell are 3–5 mm long and 0.03–0.05 mm wide [45, 46]. The two adjacent cells are usually separated by five layers, two of these layers are fibrous and what followed them are two layers of corkification layer, and the middle layer is xylem. In addition, there are more than 50 million cells per 1 cm^3. Hardwood has lots of cell types which usually are at high degree of evolution. But the hardwood only has some vessel but no resin dust. The vessel can transport water and wood fiber provides the mechanical support. Hardwood fiber contains three kinds of fiber cell (including libriform fiber, fiber tracheid, and vasicentric tracheid) which are collectively called the wood fiber. Wood fiber is one of the important anatomical molecules that make up hardwood. On average they are 1 mm long and generally less than 20 μm wide. They account for 60–80% of timber volume, and libriform fiber accounts for the largest proportion [45]. Herbaceous plants are composed of many cell types, including fibroblasts, ducts, parenchyma cells, epidermal cells, sieve tubes, and companion cells. The ducts are higher in content and larger in diameter than fibroblasts. Taking stems as an example, the common feature is that vascular bundles are widely distributed in basic tissues, and they do not have any boundaries of the cortex or the stele. Fibroblasts are distributed in the outer epidermis and vascular bundles. On average they are 1.0–1.5 mm long and 10–20 μm wide and they usually account for 40–70% of the volume. The basic parenchyma, which is in stem center of Gramineae, often rupture and form some hollow medullary cavities [45].

Based on the above analysis, the plant biomass is porous and each cell is a cavity which is composed of cell lumen and cell wall [1]. In fact, steam explosion process is a process of forming holes and breaking holes, which involves the heat and mass transfer and some reaction in the porous structures. In order to analyze the relationship between the pore structure of plant biomass and steam explosion process, the concept of biomass porous medium is proposed: cell wall and intercellular material are their solid skeleton which can form pores with different apertures so that they can provide porous media, where the fluid may be present or conveyed. Cell walls, pits, plasmodesmata, and cell cavities are all interconnected, and they can make it possible that gas, liquid or gas-liquid can transfer in them [9]. The main properties of the porous media are porous structure and of fluid flow. Softwood is usually called "non-porous material" because the softwood have few kinds of cell and the fiber is closely and regularly arranged. Fiber is long, high in content, and is supporting tissue of plants. Due to the high degree of lignification, fibroblasts generally have developed secondary walls, they have compact structure and the water vapor is difficult to penetrate into the material pores. As a result, in the steam explosion process, the resistance to heat and mass transfer is very large, making it hard to form a target for filling with high-pressure steam. That will make the tissue difficult to be torn. There is ductal tissue that can transport water in hardwood, the vessel is very large and long and they are also known as "porous wood". And in hardwood, the content of parenchyma cell is twice more than in coniferous wood. For parenchyma cells, the cell lumen is large and cell wall is thin and short, and it can store nutrient for plant. So that is conducive not only to heat and mass transfer but also to steam to break the structure. In the herbaceous plants, secondary xylem is embedded in some basic tissues, so it is conductive to the transmission of steam and SE are more efficient than that for woody plants. Fibrous cells and parenchyma cells are the most important and basic cells in lignocellulosic biomass materials. However, in different raw materials, the content and structure are different. All of these determine the difference in the processing conditions. It can be seen that the same pretreatment intensity on these two types of cells will result in inconsistent effect. If the aim is to degrade fibroblasts, parenchyma cells will be over-degraded, which will produce a large number of inhibitors which are not conducive to the subsequent transformation. Based on this, we developed a two-stage steam explosion carding process [50]. Using the more moderate steam explosion conditions for the first stage, and the material of first stage will be carded by air flow classification device producing parenchyma and fibrous tissue. Then, we adjusted the fiber structure to a right condition for the second paragraph. The results showed that the two-stage steam explosion carding process can effectively pretreat biomass which was based on the structural characteristics of different tissues. This method can get good pretreatment performance for the fibrous tissue, and effectively control the generation of inhibitors, so it does not need detoxification operation. In addition, this method ensures that the separation and pretreatment of fibrous and parenchyma tissue can be achieved selectively, providing a new way for the multi-level transformation of lignocellulose [50].

3.3.3 Water State

As water is critical but often overlooked, research efforts have seen a gained interest in water responsible for complicating pretreatment efficiency recent years, where these researches have recognized the water's critical importance in the development of biomass pretreatment technologies. However, their strides are far from enough in elucidating water's acting essence in pretreatments, due to the complex interactions between water and plant biomass.

With this part, we aim to highlight the criticality of water states in pretreatments of lignocellulosic biomass. Through investigating the lignocellulose–water interactions in tandem with feedstock physicochemical characterization and pretreatment process features, we explored the degree with which water state can impact the development of pretreatment process; and in this context, to determine the optimal water states and rehydration conditions. We used low-field nuclear magnetic resonance (LF-NMR) measurement to address this fundamental issue on cornstalk samples subjected to steam explosion pretreatments. We chose to analyze chips from cornstalk due to their potential as an abundant, low-cost feedstock. Steam explosion applied in the conditions is used as the core technology for fractionation process of lignocelluloses. It applies only water and heat during process to break the crystalline structure of lignocelluloses through autohydrolysis effects and mechanical forces attributed from sudden explosive decompression, which avoids handling and recycling chemicals at either acidic or alkaline conditions, minimizing equipment corrosion [44, 51, 52]. In our previous publications, the pretreatment method has been proved to be very efficient to improve hydrolysis yields on lignocellulosic feedstocks [53, 54]. Herein, LF-NMR was employed to probe the interaction between water molecules and lignocellulosic matrices during rehydration process. The spin-spin relaxation information (T_2) measured can be used to discriminate between the various states in which water exists in the complex environment and trace their dynamic migration in rehydrated preparations [55, 56]. Through correlating these water state data to lignocellulosic feedstock properties and processing parameters, we explored the underlying water functions in SE and achieved the optimal rehydration strategies. The work highlights the critical importance of water in biomass pretreatment process and gives important insights for designing industrial processes to achieve the desired water states of lignocelluloses for the development of pretreatments. The involved lignocellulose–water interactions not only contribute to pretreatments with water participation but embody value in biorefining process including feedstock storage, smash, and bioconversion process. A greater attention to the complexity and role of water may be beneficial in the design of experimental testing and industrial processes and may help elucidate practical solutions to common cost-impacting bottlenecks.

3.3.3.1 Water States Decided by Rehydration of Lignocellulosic Biomass

Dynamic variation of water states Figure 3.8 shows the continuous T_2-distribution obtained for cornstalk samples that were submitted to rehydrating procedures with different water amounts for 24 h. T_2 relaxation time represents water constraint along the sample and relaxation value reflects water amount. In this data, distilled water molecules exhibit the longest relaxation times around 2,000 ms, while water molecules that are more constrained by the lignocellulosic polymers exhibit shorter relaxation times. In Fig. 3.8, transverse relaxation components of water within substrate can be evidently separated into two main population groups, represented by T_{21} (1–10 ms) and T_{22} (10–100 ms). It is worth mentioning that T_{22} appears at WC around 30% (see Fig. 3.8III) and its value gradually increases with rehydrated amount. According to the description of Sun and Wang, the water content of 30% is thus supposed to be fiber saturated point (FSP) originally described by the American forester, H. D. Tiemann, as "the water content at which the cell cavities contained no water, but the cell walls were fully saturated with liquid moisture" [57, 58]. At the FSP, all of the liquid water is bound water, as this represents the maximum amount of water that can be taken up from the vapor phase by a unit mass of fiber at a given temperature [59]. Based on the description, T_{21} is thus defined as "bound" water in the cell wall matrix and T_{22} is defined as "free" or "bulk" liquid water in the voids. The integrated mixture of cell wall materials and "bound" water is also recognized as a distinct phase and has been called a "solid solution" by Stamm [60]. In addition, the water that exists as vapor in the gas-filled voids is called "gas" water but is unable to be detected by LF-NMR.

With rehydration amount increased, T_{21} relaxation value is increased as water content does not exceed FSP. Upon water content reaching FSP, T_{22} population merges and shows a higher relaxation value as water content increases and its distribution leans toward longer and broader relaxation times, whereas T_{21} relaxation time and value remain almost constant. This presumably reflects, upon rehydrating with more water, water molecules were initially bound to cell wall until they filled all the binding sites and then started to accumulate in voids of samples as free water; besides, the bound water did not undergo significant mobility changes, while those located in the cores of vessels kept continuously increasing mobility until saturation is reached.

With rehydration time increased, water molecules in cornstalk matrix show a continuous dynamic distribution change, from very mobile molecules to constraint ones and from spatially distributed relaxation times to two main T_2 components. These indicate a growing water affinity during rehydration procedure. Continuous rehydration of samples introduces a fast equilibrium in T_{21} value associated with bound water until it reached FSP, and then introduces a steady increase in T_{22} value associated with free water. They suggest that bound water molecules are easily absorbed during the initial steps of rehydration procedure and, free water begin to emerge in voids until bound water reaches FSP with no more increase. Comparison of the curves along with rehydration time shows that after rehydration for 6–10 h,

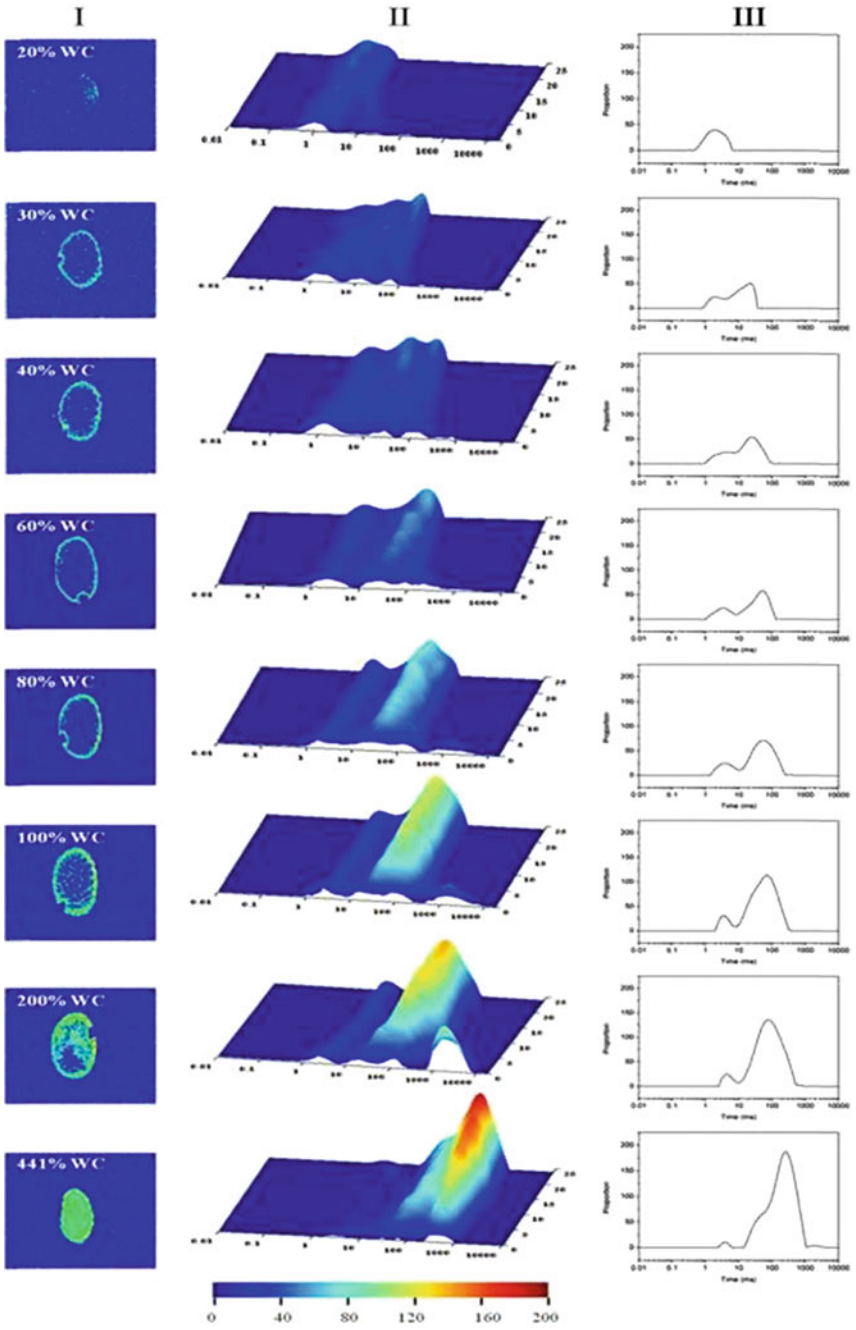

Fig. 3.8 I: Water-selective transverse images of different water content (WC) rehydrated cornstalk samples after rehydration for 24 h. II: Continuous T2-distribution obtained for cornstalk samples that were submitted to rehydrating procedures with different water content for 24 h; III: T2-distribution at the terminal of rehydration procedures and every set of curves corresponds to a different rehydration amount. Reprinted from Ref. [73]. Copyright 2016 with permission from Elsevier

relaxation time and value of T_{21} and T_{22} are almost invariable, inferring the rehydration equilibrium is achieved.

The nature of the forces that hold the water preferentially in cellular structure is supposed to be chemical bonding and capillary forces [57, 59, 61]. When dried fibrous tissues are exposed to water, the bound water molecules form strong hydrogen bonds with the exposed hydroxyl groups of the cell wall molecules. This bonding occurs because the attractive forces between the surface hydroxyl groups and water molecules exceed the attractive forces between molecules for themselves [57, 59]. Additionally, the fact that the heat of wetting evolves when water is added to dry wood, also implies the existence of chemical reactions [60]. The existence of free water in various sizes and shapes of pores in fibrous tissues is considered a capillary phenomenon [57]. Some engineers and material scientists have recognized that for the typical dimensions of conduits in timber (of the order of 1–10 μm), the reduction in vapor pressure estimated using the Kelvin capillary equation is very modest [59, 60]. So free water amount is closely related to porous structure with inner capillary forces and presents strong mobility.

As fibrous structure is rehydrated from absolute dry state to FSP, the motion of water is mostly by diffusion, including diffusion of water vapor within the void structure and diffusion of water in the "solid solution"; when fiber is wetted from FSP to higher water content, the motion of water is driven by capillary force [57]. In which the diffusion of bound water in the "solid solution" is more interesting. If the water is chemically bound to cell walls, then a "diffusion" process presumably involves a series of discrete jumps from one binding site to the next. The final equilibrium would equate to a thermodynamic state of maximum entropy [60]. Other's experiments showed a tendency that the rate of diffusion of the "bound" water in the longitudinal (fiber) direction is about twice that in the radical direction and three times that in the tangential direction [60], which was also observed in cornstalk samples in this work. The faster rate along the longitudinal direction presumably means that there are a greater number of available binding sites in that direction and the binding energy per binding site in that direction could be less than the other directions. Thus, it is the distinguishing of holding forces and driving forces of two kinds of water that contribute to the mobility behavior of fast rehydration of bound water and slow equilibrium of free water during rehydration.

Water distribution sites

As water rehydration sites bind with where the water play roles in, the spatial arrangement of water in cornstalk is important for identifying water action sites. According to the definition of bound water and free water, bound water chemically binds to cell wall and free water occurs in capillary tubes. Herein, we discuss water distribution sites at multi-length scales of cornstalk sample. (1) At tissue scale, quantitative information of water compartment along the chip was monitored by MRI. Figure 3.8I shows the water-selective transverse images collected at rehydration's beginning and equilibrium. A bright red image signal is associated to the higher water content while a dark blue image signal is associated with a more rigid structure. The water molecules are found majorly distributed in rinds of cornstalk at

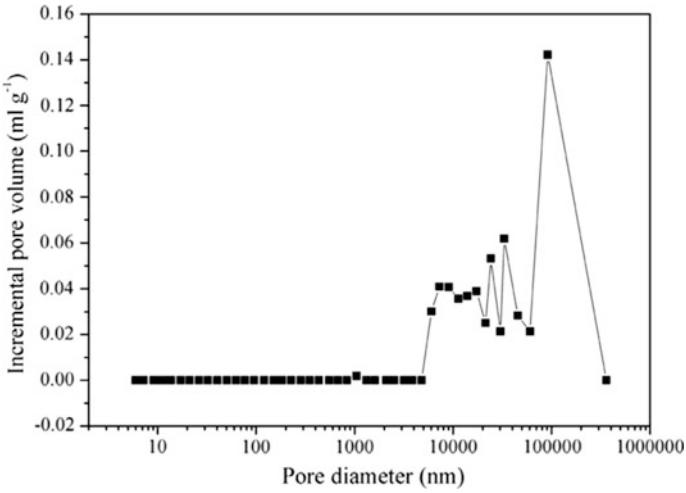

Fig. 3.9 Pore size distribution of dry cornstalk determined by MIP [147]

initial rehydration. As rehydration reaches the equilibrium, abundant water occurred at rinds and pith vascular bundles in cornstalk, which are tissues rich in fibers. This distribution is corresponding to water amount but cannot define water state. (2) At cell scale, analysis of rehydration sites depends on the one-to-one correspondence of T_2 values with the lumen sizes of water-filled cells. The amplitude of relaxation time over a period relates to the amount of water filled in certain pore sizes and the relaxation time reflects the pore size [62]. By a rough comparison between pore size distribution of dry cornstalk (see Fig. 3.9) and T_2 relaxation distribution of fully saturated sample (see Fig. 3.8III), T_2s of 10 ms, 1000 ms, and 100000 ms may be associated to pore sizes of 1 μm, 5–50 μm, and 50–300 μm at dry samples, respectively. Research of Zhao and Chen on morphological analysis of pore distribution in cornstalk indicated that pores around 1 μm corresponded to intercellular space, cell corner, and plasmodesma; 5–50 μm pores mainly referred to pits, fiber cells, and sieve tubes; 50–300 μm pores corresponded to vessel cells in vascular bundles [9]. Thus, a probably quantitative connection between water at certain T_2 relaxation time and pore size attained from differential mercury intrusion spectra is obtained for cornstalk sample. (3) At cell wall scale, the cell wall is a laminated structure, and the number of layers and their thickness vary with the cell type. Much of water in woody tissues are supposed to be held in the S2 layer of fiber cells and tracheid, owing to the thick central S2 layer of the secondary wall layer which constitutes the bulk (70–80% by volume) of cell wall and contains high proportions of cellulose [63]. (4) At component scale, of the three major components of lignocelluloses, lignin has the lowest affinity for water and hemicellulose the highest, the affinity of cellulose for water is between these two. The reason is attributed to the spatial arrangement of components (amorphous or crystalline) and exposed hydroxyl groups [57]. The early data for *Eucalyptus regnans* showed that the sorption capacity of lignin, hemicellulose, and cellulose was 0.60, 1.56, and 0.94,

respectively [59, 64]. This means that the FSP would increase as the relative proportion of hemicellulose increased, and decrease as the relative proportion of lignin increased. Hence, the observed fact that lignocellulose often has a FSP similar to cellulose arises because the two other major components have sorption capacities either side of the value for cellulose, is conducive to the guide the rehydration process for different materials.

Quantitative relationship of water states
Results from some experiments show that FSP remains almost constant for a plant sample at certain temperature, regardless of whether the sample is intact or pulverized. Hence, given an estimate of fresh volume, fresh mass, dry mass, and FSP of a piece of sample, it is straightforward to estimate volume fractions of the three bulk phases (gas, liquid, solid) of water in the sample, and calculations have remained more or less the same over the years done by engineers and material scientists [65]. The estimated results according to the calculation framework in Fig. 3.10I have been validated by LF-NMR in this work with minor measurement errors. Figure 3.10II shows the calculated volume fractions of free water, bound water, gas water, and dry matter as a function of water content of cornstalk samples that achieve the rehydration equilibrium. The conclusion is in accordance with results from Fig. 3.8 that the bound water first increases and keeps unvaried after FSP, the free water appears at FSP and since then keeps the growing momentum. It is interesting to view Fig. 3.10II with possibly different perspectives. For biologists, the fundamental starting point is the liquid phase because that is the ultimate source of biochemical activity in plants. However, the fundamental starting point for engineers is the "solid" phase because that is the principal source of mechanical strength of plant. Such constraints of water on plant architecture and function lay the foundation for the following research of water function in pretreatment process.

3.3.3.2 Relationship Between Water States and Mechanical Property of Lignocellulosic Biomass

In lignocellulosic biorefining process, engineering-oriented research on the correlation between inner water and mechanical property of feedstock focus on (1) dry feedstock swells when exposed to water, and (2) dry feedstock is stronger (i.e., it has increased strength at elastic limits in endwise compression and cross-bending, and has an increased modulus of rupture in bending) than wet feedstock. In the study, mechanical strength analysis was performed on rehydrated samples to acquire the relationship between water states and mechanical property of cornstalk and its key guiding point to pretreatment. The data depicted in Fig. 3.11 represent that rehydrating decreased the force required to penetrate the chip, reflected by the decreased hardness and fracturability, thereby increasing the chip plasticity. The downward trends of chip strength show two successive stages referring to the drastic reduction and slow reduction, and the important turning point is around FSP. This also points one of determining methods of FSP by the mechanical method.

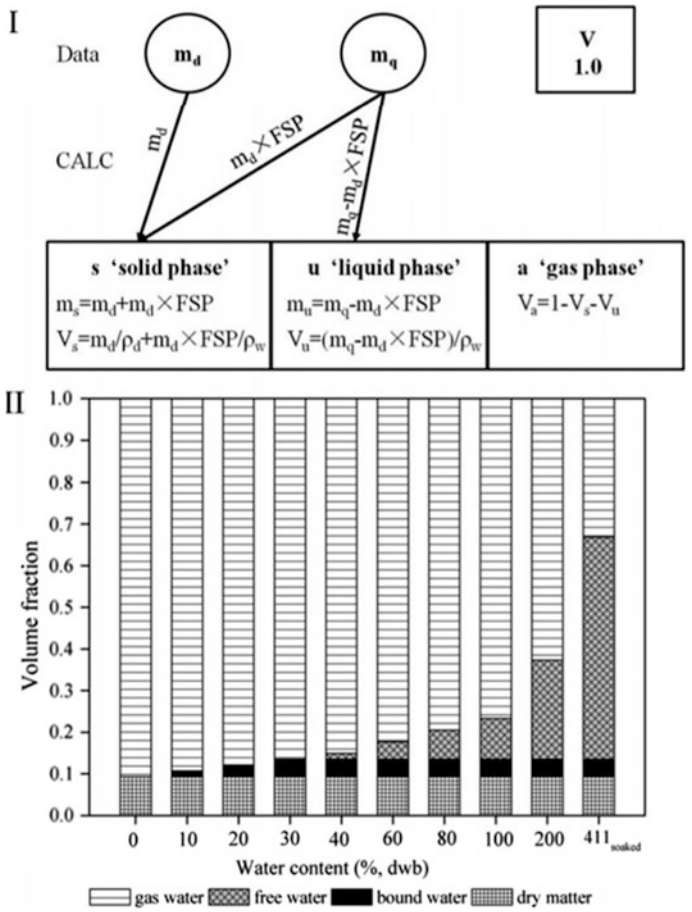

Fig. 3.10 I: Example calculations for estimating the volume of the three bulk phases (gas, liquid, solid) in cornstalk sample. In this sample, m_d and m_q refer to dry mass and liquid mass; V_a, V_u, and V_s refer to the volume of the "gas" phase, the "liquid" phase and the "solid solution" phase, respectively; qd and qw refer to the density of the dry matter and pure liquid water. II: Resultant variations in the volume fractions of free water, bound water, gas water and dry matter as a function of water content, given measurements of the fresh volume (1 cm^3), dry mass (0.14 g), density of dry matter (1.5 g cm^3), density of liquid water (1 g cm^3) and FSP (0.3) [147]

In typical fiber structure, when a small amount of liquid water is poured onto dry fiber, the water must, by default, be located inside the cell wall matrix as "bound" water as analyzed before. Hence, the mass of cell walls increases, as does the volume, which is observed macroscopically as swelling of fiber sample. Concurrently, the strength of sample progressively declines as water content increases. As water continues to be added, the system eventually reaches the equilibrium where liquid water begins to accumulate in the voids as free water. When that occurs, the cell wall ceases swelling and the strength of sample no longer

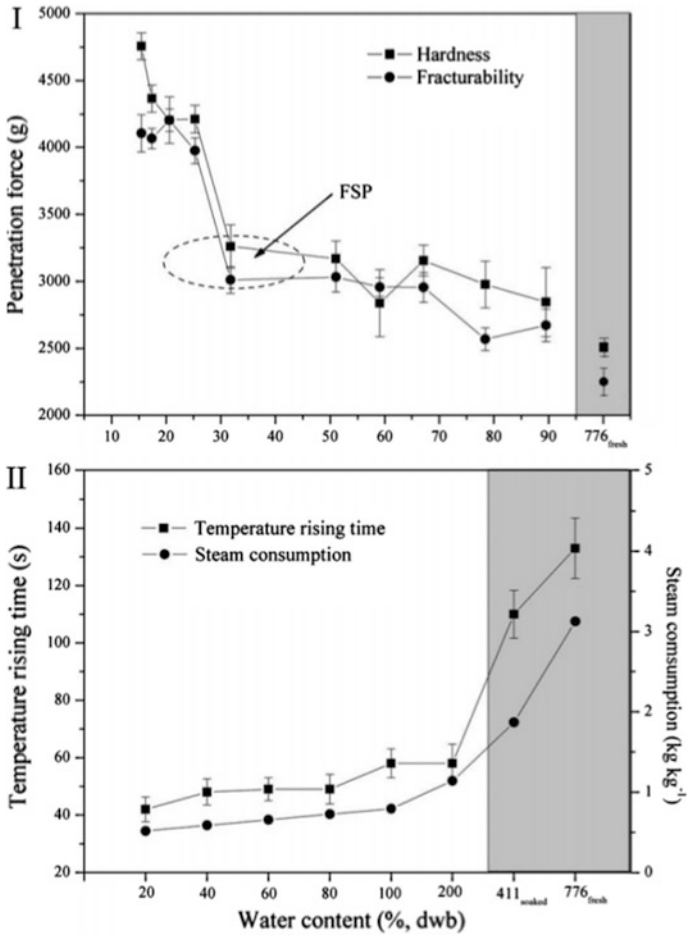

Fig. 3.11 I: Mechanical strength of rehydrated cornstalk with different water content determined by TPA. II: Temperature rising time and steam consumption during steam explosion process of rehydrated cornstalk with different water content [147]

changes with water content. The water content at which this occurs is the FSP [57]. Hence, as noted above, water is the excellent plasticizer that maintains a moist and soft texture of fibers and FSP is the turning point of fiber strength and swelling. The swelling and strength changes of cellulosic sample when exposed to water are mostly attributed to the increase in the mass of bound water while the contribution of free water is little. Since the rehydration induced the swelling of fiber and enlarged the pores in sample, thus increasing the water mobility in capillary tubes, this explains the prolongation of T_{22} relaxation time as water content increases. Especially for SE pretreatment, the reduction of structure rigidity and the enlargement of pores caused by rehydration would allow the steam to penetrate into

superfine voids and guarantee the adequate heating at cooking stage, and in the following decompression stage allow the explosion to occur by flash evaporation and vapor expansion so enhancing the physical tearing force. In the work, hardness and fracturability still slowly descend as water content increases beyond FSP, which might be attributed to rehydration inhomogeneity.

3.3.3.3 Relationship Between Water States and Steam Explosion Process of Lignocellulosic Biomass

SE applies water as the only transfer and reaction medium without adding other media and chemicals. Water here refers to inserted steam and rehydrated liquid water. The high-temperature steam is consumed to warm up wet materials and the internal water resulted from rehydration influences steam penetration, and thus relates to a series of autohydrolysis reactions and explosion effects [66]. Thus, water in lignocelluloses takes vital effects on transfer and reaction behavior during SE process.

Transfer process Variation trends of temperature rising time and steam consumption during steam explosion of cornstalk with different rehydrated amount are demonstrated in Fig. 3.11. Long temperature rising time and high amount of steam consumption are observed on cornstalk samples with increased rehydrated water. This phenomenon is owing to the heat transfer pattern and efficiency in lignocellulosic substrate influenced by its water amount and states. When water content is sufficiently low and the vessels are unblocked by liquid water, the steam enters the end chip and passes rapidly through the chip until it condenses and gives up its latent heat of vaporization inside the stalk. If the vessels are initially filled with liquid water or if sufficient condensate accumulates to fill the chip before the steam temperature is reached, further heat transfer is by the slower process of conduction [67]. If all the heat required to heat the moist stalk to steam temperature was supplied by condensation inside the chip, final water content of pretreated samples would rise with increased initial water. The increase of condensed water means the increment of consumed steam or energy. According to our previous research, there is a correlation between water amount in materials and energy demand of steam explosion, which is expressed as the steam amount consumed by per unit mass of dry materials, m' (kg/kg) [66].Therefore, much water rehydrated in samples result in a substantial decrease in heat transfer speed and energy utilization efficiency. One significant effect of the reduced ability of heat to penetrate the chips is the shortening of actual steaming time at settled temperature, causing a deteriorate severity of pretreatment and an uneven treatment of the substrate (which can potentially result in the selective degradation of the outer portion of the chips, while at the same time the interior is less affected by the treatment) [67, 68]. Since the maximum amplitude of bound water cannot exceed FSP, while free water can be aggregated in the connecting capillary tubes until reaching complete saturation and exerts hurdles to steam penetration and heat transfer, thus free water creates a greater negative impact on steam and heat transfer process due to the wider variation range.

Table 3.6 The compositions of the pretreated biomass and liquid fraction after SE of cornstalk rehydrated with different water contents [70]

Water content (%)	Filtrate composition (g/100 g feedstock)					Water-insoluble fiber composition (g/100 g feedstock)			
	Glucose	Xylose	Furfural	HMF	Acetic acid	Glucan	Xylan	ASL	AIL
20	1.38 (0.05)	3.85 (0.07)	0.18 (0.03)	1.75 (0.02)	2.50 (0.06)	28.20 (0.37)	3.38 (0.42)	2.37 (0.29)	26.03 (0.13)
30	1.35 (0.02)	3.98 (0.01)	0.18 (0.01)	1.86 (0.04)	2.38 (0.03)	28.86 (0.22)	3.44 (0.23)	2.25 (0.17)	25.37 (0.11)
40	1.65 (0.05)	4.04 (0.06)	0.17 (0.02)	1.91 (0.05)	2.21 (0.02)	28.72 (0.73)	3.76 (0.24)	2.19 (0.58)	25.01 (0.49)
60	1.78 (0.03)	4.21 (0.02)	0.19 (0.04)	1.81 (0.03)	2.07 (0.01)	29.42 (0.46)	4.27 (0.35)	2.05 (0.36)	24.12 (0.56)
80	2.03 (0.05)	4.13 (0.07)	0.17 (0.03)	1.69 (0.08)	1.73 (0.05)	29.42 (0.55)	4.25 (0.50)	2.04 (0.41)	23.67 (0.26)
100	2.12 (0.02)	4.48 (0.05)	0.15 (0.05)	1.50 (0.09)	1.80 (0.04)	29.24 (0.18)	4.38 (0.46)	1.99 (0.29)	21.78 (0.34)
200	2.20 (0.01)	4.81 (0.01)	0.12 (0.03)	1.82 (0.06)	1.06 (0.09)	32.14 (0.68)	7.03 (0.77)	1.97 (0.44)	20.79 (0.25)
411 soaked	2.64 (0.05)	4.33 (0.07)	0.12 (0.05)	2.41 (0.08)	0.68 (0.05)	32.71 (0.78)	9.02 (0.43)	1.60 (0.76)	18.04 (0.61)
776 fresh	10.89 (0.09)	5.31 (0.08)	0.05 (0.02)	6.18 (0.02)	0.69 (0.03)	30.57 (0.21)	9.04 (0.25)	1.05 (0.63)	16.53 (0.13)

Reaction process Steam explosion is usually carried out at relatively high temperature (140–220 °C) under mild acidic conditions which come about largely from the decrease in the pK_w of water at the elevated temperature and the release of organic acids from biomass components ([39, 52]). This high-temperature and acidic environment are effective in triggering a series of hydrothermal reactions. Hemicellulose was thought to be hydrolyzed into monomeric, oligomeric sugars, and partial furfural by autohydrolysis effects with the acidic water, acetic, and other acids catalysis derived from acetyl groups. The ester linkages between carbohydrates and lignin were disrupted, and hence lignin was melted, solubilized, and recondensed ([52]). The chemical composition for all the cornstalk samples is given in Table 3.6. Wet pretreated solids show high glucan and xylan content and low ASL content compared with the dry ones. This indicates that samples after rehydration with more water were less hydrolysable during pretreatment. While, samples underwent wild hydrolysis of cellulose and hemicelluloses, their SE hydrolysates show an increased amount of soluble sugars (glucose and xylose). This is due to the weakened degradation reactions, which are also supported by the decreased amount of degradation products (furfural and HMF). In addition, acetic acids produced from the removal of acetyl group show a substantial decrease as water content increased. The observed changes in chemical compositions are likely related to a "buffering effect" of water proposed by Cullis et al. (2004), whereby

water buffers against carbohydrate solubilization, decomposition, and autohydrolysis due to slower rates of heating in the interior of the chips, which causing the predetermined high-temperature and acidic environment is not accessible in a relatively short time [69]. The buffering ability of water, thereby, weakens SE severity and takes detrimental impact on pretreatment efficacy.

Resultant pretreatment performance Effect of water states on SE transfer and reaction behavior was reflected in the pretreatment performance. The cellulose recovery in pretreatment, cellulose conversion after enzymatic hydrolysis and glucose yield of the whole process (pretreatment + enzymatic hydrolysis) have been evaluated as presented in Fig. 3.12 Increasing water content has been shown to have a desirable effect on the recovery of glucose during pretreatment by its percentage increased from 93.12 to 100%. It has been confirmed an opposite relation existing between cellulose recovery and SE severity in previous research [54, 67, 70]. High water results in a substrate that demonstrates a decreased yield of enzymatic hydrolysis from 89.93 to 67.21%, which agrees with our previous findings [54]. This unfavorable hydrolysis can be attributed to the buffering effect of rehydrated water for SE as noted before. On one hand, high water impedes effective heat transfer and thus negatively affects thermo-chemical reactions during SE process. Since hemicellulose and lignin are not effectively removed from the substrates owing to the deficient solubilization and degradation, their residues impede the accessibility of hydrolytic enzymes to cellulosic substrate [4, 44, 71]. On the other hand, high water hinders the effective penetration of high-temperature

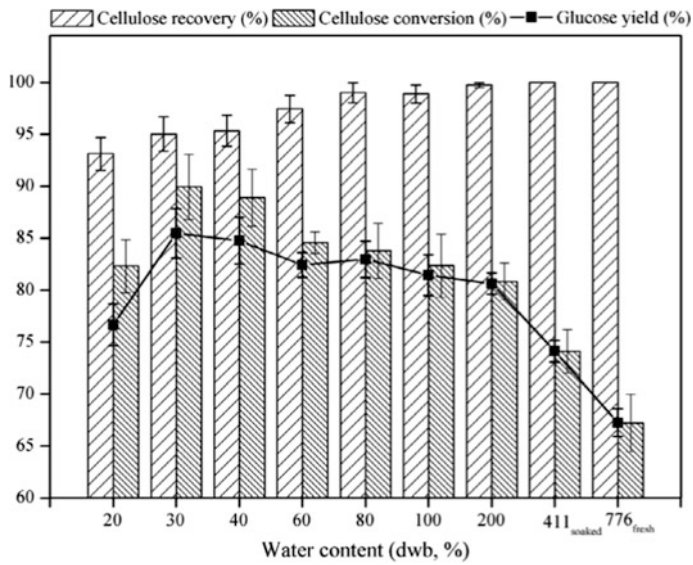

Fig. 3.12 Cellulose recovery in pretreatment, cellulose conversion after enzymatic hydrolysis and glucose yield of the whole process (pretreatment + enzymatic hydrolysis) of rehydrated cornstalk with different water content [147]

steam, the pressure difference driving the evaporation and expansion of water inside the biomass is difficult to reach between the inside and outside of each cell. This is not conducive to the physical tearing action in the decompression step on the rigid and highly ordered fibrils, thus not resulting in a loose and porous structure exposed to enzymes. These insufficient chemical and physical changes lead to the low efficiency of biomass utilization. It is worth noting that, the yield of enzymatic hydrolysis remains almost invariable when the samples were rehydrated from initial water content to FSP, after then experiences a substantial decrease. This tendency is similar to the periodical upward trend of cellulose recovery in pretreated materials. These indicate the twofold effects of free water occurring after FSP on impairing SE efficacy: the first effect being a buffering ability on hindering the normal proceeding of transfer and reaction during SE, and the second effect attributing to the no more changeable mechanical strength of rehydrated materials with occurrence of free water. Finally, as the combined result of glucose recovery and conversion yield, the overall glucose yield of the whole process is increased from 76.65 to 85.44% by increasing water content to FSP, and then decreased to 74.11% with the increase of water content from FSP to totally saturation. Thus, considering the effects on pretreatment efficacy and energy consumption, the importance of FSP for SE pretreatment is evident, the bound water it determined being the excellent plasticizer that maintains the soft texture of fibers is conducive to steam explosion effects, while the free water it determined presenting the buffering effects on pretreatment and consuming abundant energy is not conducive.

Two main water states with different mobility existed corn stalk and decided by rehydration. Bound water reducing the mechanical strength of fibers by over 30% with its increase is conducive to SE pretreatment; free water hindering heat transfer by increasing temperature rising time by 2.33 folds and increasing steam consumption by 1.44 folds is not conducive, and the distinguished point of these two water is FSP. By considering pretreatment efficacy and energy consumption, the optimal water states for SE pretreatment is achieved by rehydrating to FSP for 6-10 h.

3.3.4 Loading Coefficient

Significant advances have been done in last 30 years on expanding the application fields and enhancing the efficacy of steam explosion pretreatment by optimizing key factors (mainly retention time and holding temperature) that attributed to the "severity factor" [46, 51, 72]. There are still some studies relevant to effects of addition of acids or weak alkali salts, moisture content, and chip size of feedstocks on steam explosion [15, 27, 67, 69, 73]. While few works focused on the loading coefficient of steam explosion apparatus and its vital role played in steam explosion process and subsequent disposal effects. In this study, we recognize the importance of loading coefficient as it significantly influences transfer and reaction issues in steam explosion process. The heat and moisture transfer pattern and efficiency are

largely affected by loading coefficient, resulting in changes of energy consumption of steam explosion process and the final moisture content of steam-exploded materials. In which, the former majorly determines pretreatment economic efficiency, the latter is a crucial regulating parameter related to following drying, enzymatic hydrolysis, and other operations, especially in industrial scale. Meanwhile, loading coefficient is still related to explosion effectiveness, since it contributes to the steam deflation speed and influences the physical action of crowded materials during the sudden explosion. These effects of loading coefficient on steam explosion process inevitably alter the pretreatment effects and hence contribute to subsequent disposal effects of pretreated materials. In addition, loading coefficient is restricted by practical handling, transporting, and storing capacity of biorefinery plant and should guarantee the mutual connection of production procedures with respect to time and equipment. Therefore, to realize, control, and optimize the loading coefficient is very important in both the experimental research and industrial production, while has always been neglected.

The loading coefficient is influenced by many aspects including apparatus parameters, operational parameters, and material property. For a certain apparatus and operation condition, it should be determined by loading pattern and material property. To our best knowledge, there is no reference on evaluating the loading pattern's effect on steam explosion process and previous research on material property like moisture and chip size were limited [27, 67, 68, 73, 74] since the narrow investigation range cannot completely reflect the overall influence trend. In addition, to optimize relevant loading parameters, previous evaluation taking steam explosion efficacy as the only standard is far from enough. From an economic point of view, efficient pretreatment should make the utilization process less costly. The optimization of loading parameters would better be compromised between the economical and processing efficiency of steam explosion to meet the requirement of the economy of process. Therefore, it would also be desirable to in-depth analyze the parameters that influence loading coefficient and explore their innovative optimization strategies for improving the economics of steam explosion process.

3.3.4.1 Loading Coefficient's Relation with Loading Pattern and Material Property

The loading coefficient of steam explosion apparatus ∅ is defined as follows:

$$\phi = k\rho_0'(1+w) \tag{3.2}$$

$$\rho_0' = \rho_0(1-\varepsilon_p-\varepsilon_v), \tag{3.3}$$

where ∅ is the loading coefficient, kg/m^3, k is the compaction degree of loading materials and is expressed as loading pattern in this study. It is calculated as the loading amount divided by the bulk density of materials at certain chip size and certain volume of reactor. ρ_0' and ρ_0 are the bulk density and real density of dry

materials, kg/m^3; ε_p and ε_v are the porosity inside particles and the voidage of materials(%); w is the moisture content (dry basis) of materials (%).

According to the expression of loading coefficient, it is related to loading pattern and material property. In which loading pattern is influenced by the production capacity of process; material property includes the moisture content of materials depending on the initial moisture content and added water and the bulk density of materials determined by material type and chip size. In this study, corn stalk is the objective substrate and steam explosion is done in a 20 L reactor at 1.5 MPa for 5 min. Under this condition, loading coefficient is only determined by loading pattern, moisture content, and chip size. The bulk density of corn stalks corresponding to different chip sizes (5–8 cm, 3–5 cm, 1–2 cm, 0.5–0.8 cm, and milled powders) was measured as 64.69 kg/m^3, 72.33 kg/m^3, 85.48 kg/m^3, 112.1 kg/m^3, and 140.0 kg/m^3.

3.3.4.2 Relationship Between Loading Parameters and Transfer Process of Steam Explosion

Heat transfer and energy consumption of steam explosion process

Heat transfer and energy consumption of steam explosion process under different loading parameters are analyzed and derived from our previous research on multi-stage heat transfer model of steam explosion process [66]. In this model, total energy consumption of steam explosion process Q_t is composed of heating steam energy Q_1, heating air energy Q_2, heating materials energy Q_3, heating reactor energy Q_4, and radiation energy of reactor Q_5. In which the value of Q_2 is small and hence is negligible in this study. All the parameters involved are illustrated in Table 3.7.

According to our deduction, loading coefficient only has impact on heating materials energy Q_3 which is expressed as

$$Q_3 = (C_p kV\rho_0' + C_w kV\rho_0' w)(T_e - T_0) \tag{3.4}$$

The total energy consumption of steam explosion process taking loading coefficient into accounts, Q_t is written as

$$Q_t = \underbrace{m_g(h_{ge} - h_{f0})}_{Q_1} + \underbrace{(C_p kV\rho_0' + C_w kV\rho_0' w)(T_e - T_0)}_{Q_3} + \underbrace{C_r M_r (T_e - T_0)}_{Q_4} + \underbrace{\varepsilon C_0 (T_e/100)^4 A_r t/1000}_{Q_5} \tag{3.5}$$

And the corresponding steam consumed by per unit mass of dry materials in steam explosion process m' is changed to

Table 3.7 The model symbols [54]

Parameters	Description	Units	Value	Sources
A_r	Heating area of reactor	m^2	≈0.45	[54]
C_0	Blackbody radiation coefficient	W/(m_2 K_4)	5.67	[66]
C_p	Specific heat of material	kJ/ (kg K)	1.62	[66]
C_r	Specific heat of reactor's material	kJ/ (kg K)	0.46	[66]
C_w	Specific heat of water	kJ/ (kg K)	4.2	[66]
h_{f0}	Enthalpy of water at T	kJ/kg	83.96	[66]
h_{fe}	Enthalpy of water at T_e	kJ/kg	844.89	[155]
h_{fg}	Evaporation enthalpy at T_e	kJ/kg	1946.65	[155]
h_{ft}	Enthalpy of water at T_t	kJ/kg	376.78	[155]
h_{ge}	Enthalpy of steam at T_e	kJ/kg	2791.54	[155]
h_{gt}	Enthalpy of steam at T_t	kJ/kg	2659.60	[155]
k	Loading pattern	%		
M_r	Weight of reactor	kg	≈60	[54]
m_1	Condensed water	kg		
m_2	Flash water	kg		
m_g	Amount of steam in reactor	kg	0.15	[54]
m'	Steam consumed by per unit mass of dry materials	kg		
P_0	Initial surrounding pressure	MPa	0.1013	[54]
P_e	Holding pressure	MPa		
$P\times$	Critical pressure	MPa	0.192	[76]
Q_1	Heating steam energy	kJ		
Q_2	Heating air energy	kJ		
Q_3	Heating materials energy	kJ		
Q_4	Heating reactor energy	kJ		
Q_5	Radiation energy of reactor	kJ		
Q_t	Total energy consumption of steam explosion process	kJ		
S	Steam deflation passage area	mm^2		
T_0	Initial surrounding temperature	K	293	[54]
T_e	Holding temperature	K	471	[54]
T_t	Temperature of steam after explosion	K	363	[54]
t	Retention time	s	300	[54]
t_0	Gas deflation time	s		
V	Volume of reactor	m^3	0.02	[54]
V_s	Volume of gas contained in the reactor	L		
w	Initial moisture content of materials	%		

(continued)

Table 3.7 (continued)

Parameters	Description	Units	Value	Sources
w_t	Final moisture content of steam-exploded materials	%		
ε	Blackness of reactor		0.6	[66]
ε_p	Porosity inside particles	%		
ε_v	Voidage of materials	%		
κ	Adiabatic exponent		1.33	[76]
ρ'_0	Bulk density of dry material	kg/m^3		
ρ_0	Real density of dry material	kg/m^3		
τ	Gas charge/deflation time constant	s		
Φ	Loading coefficient	kg/m^3		

Reprinted from Ref. [62]. Copyright 2015, with permission from Elsevier

$$m' = \frac{m_g(h_{ge} - h_{f0}) + (C_P k V \rho'_0 + C_w k V \rho'_0 w)(T_e - T_0) + C_r M_r (T_e - T_0) + \varepsilon C_0 (T_e/100)^4 A_r t/1000}{k V \rho'_0 (h_{ge} - h_{f0})} \tag{3.6}$$

According to Eqs. 3.4 and 3.5, the increase of loading pattern k, bulk density ρ_0' and moisture content w increases heating materials energy Q_3, and hence total energy consumption Q_t. As for m', it clearly increases as moisture content increases while declines as loading pattern and bulk density increase. When steam explosion is operated in a given apparatus and holding temperature and time are settled, energy consumed for heating steam and reactor Q_1, Q_4, and reactor radiation energy Q_5 are not varied anymore according to Eq. 3.5. Along with the increase of loading amount caused by loading pattern and bulk density, above three energies shared on per unit mass of materials decreased, resulting in the reduction of m'. Therefore, despite increased loading pattern and bulk density consume high total energy, they decrease m' and hence improve the energy utilization efficiency of per unit mass of dry materials.

To further investigate the influence power of loading parameters on energy consumption, single factor analysis by central composite response surface was conducted on Design Expert 8.0. The analysis is calculated on the proposed equations with parameters in experimental conditions. Results show that the obtained single factor response curves in Fig. 3.13 support above influence trend and provide the influence degree of each parameter: loading pattern > bulk density > moisture content.

Moisture transfer and moisture content of steam-exploded materials The moisture variation during steam explosion process involves (1) water in materials before heating, including initial moisture and added water; (2) condensed water generated in pressure boost stage m_1 for heating materials and the reactor; (3) flash water lost in instantaneous decompression stage m_2 due to sudden phase change of liquid water. Derived from the heat transfer model in our previous work [66], the

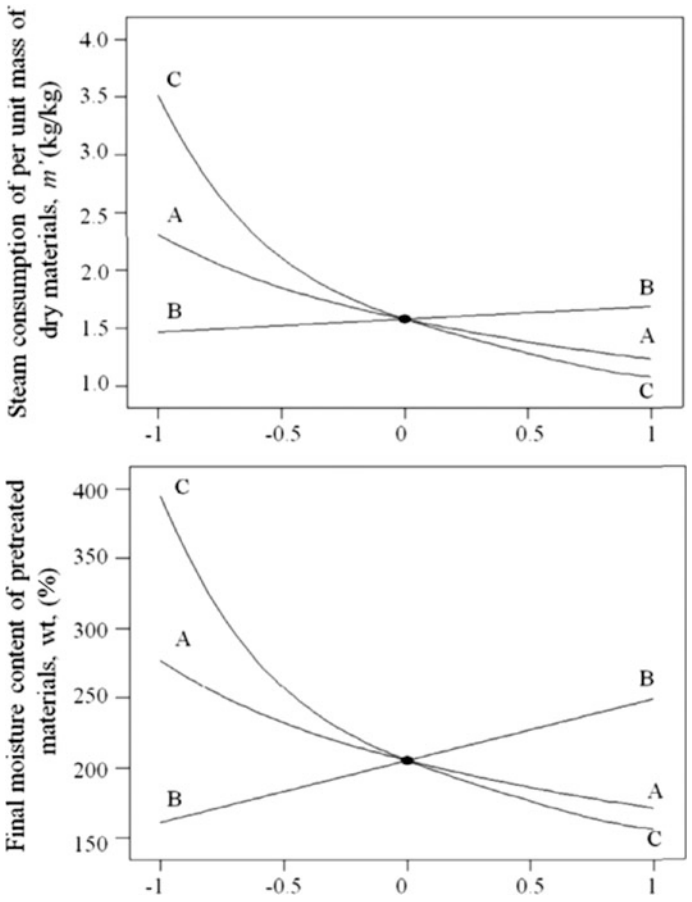

Fig. 3.13 Single factor response curve of steam consumption of per unit mass of dry materials m_0, kg and final moisture content of pretreated materials wt, %. The response is plotted by changing only one factor over its range while holding all the other factors constant [54]. A is bulk density and fixed at 102.35 kg/m^3, B is the moisture content and fixed at 60%, C is loading pattern and fixed at 77.30%. The x axis stands for five levels of each factor in Table 3.8

condensed water m_1 and flash water m_2 under the influence of loading parameters are expressed as

$$m_1 = (C_p kV\rho_0' + C_w kV\rho_0' w + C_r M_r)(T_e - T_0)/h_{fg} \tag{3.7}$$

$$m_2 = (\phi V\rho_0' w + m_1)(h_{fe} - h_{ft})/(h_{gt} - h_{ft}) \tag{3.8}$$

The final moisture content of pretreated materials wt deduced from above equations is written as

$$w_t = (kV\rho_0' w + m_1 - m_2)/(kV\rho_0') = \left[w + (C_p + C_w w)(T_e - T_0)/h_{fg} + C_r M_r (T_e - T_0)/(h_{fg} kV\rho_0')\right](h_{gt} - h_{fe})/(h_{gt} - h_{ft}) \tag{3.9}$$

According to Eqs. 3.7–3.9, loading parameters have obvious impact on all three kinds of water and the final moisture content of pretreated materials wt. As the amount of condensed water exceeds that of flash water lost in sudden explosion according to calculation results, the final amount of pretreated materials is higher than the initial amount of materials. In terms of the final moisture content of pretreated materials wt, it can be inferred from Eq. 3.9 that increasing the moisture of materials before pretreatment certainly leads to the increase of final moisture of pretreated materials, whereas increasing the loading pattern and bulk density do oppositely. The opposite effects of loading pattern and bulk density might be attributed to less condensed water for heating reactor shared on per unit mass of materials. As under the certain apparatus and holding pressure, the amount of condensed water for heating reactor which occupies a large percent of condensed water, is fixed at a certain value. When more materials are loaded by increasing the loading pattern and bulk density, the certain amount of condensed water was contained in more materials, resulting in the decrease of wt.

Results of single factor response curves established on this model in Fig. 3.13 agree with above opinions. The relevant parameters used in calculation are listed in Table 3.7. The curve profile shows the influence sequence of three parameters on wt: loading pattern > bulk density > moisture content, which is similar to that on energy consumption. It is worth noting that the trend occurs under the well-preheating or continuously operational conditions of steam explosion apparatus, which means the initial temperature of the reactor is much higher than the surrounding temperature. If at the initial run time of steam explosion apparatus which means the reactor's initial temperature is low and close to the surrounding temperature, the increased temperature difference between the reactor temperature

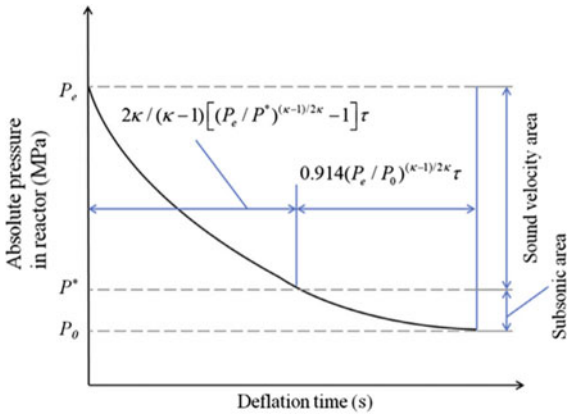

Fig. 3.14 Characteristic pressure–time curve for steam deflation process [54]

and holding temperature would result in a substantial increase of condensed water as shown in Eq. 3.6. Consequently, the influence trend of loading parameters on moisture content of pretreated materials would be more obvious.

Steam deflation process and deflation speed Steam deflation time influences the theoretical explosion power density which represents the severity of the explosion stage, compared with the traditional severity factor which expresses the severity of the cooking stage [75]. It can be calculated with equations describing gas mechanics (adiabatic process), gas flow, and sound velocity of adiabatic process [76], as illustrated in Fig. 3.14. The entire gas deflation time is the sum of the two phases, which involves sonic area and subsonic area and is expressed as

$$t_o = \left\{ \left[(P_e/P^*)^{(\kappa-1)/2\kappa} - 1 \right] 2\kappa/(\kappa-1) + 0.914(P_e/P_0)^{(\kappa-1)/2\kappa} \right\} \tau, \tag{3.10}$$

where P_e represents the holding pressure, P× is the critical pressure with a common value for 0.192 MPa, P_0 is 0.1013 MPa, κ is the adiabatic exponent (1.33 for steam), τ is the gas charge/deflation time constant, s and expressed as

$$\tau = 5.217(V_s/\kappa S)\sqrt{273/T_e}, \tag{3.11}$$

where S is the steam deflation passage area, mm^2; T_e is the holding temperature, K; V_s is the volume of gas contained in the steam explosion reactor, L and written as

$$V_s = (1 - k + \varepsilon_P + \varepsilon_V)V \tag{3.12}$$

When pressure in the reactor > critical pressure P× , steam deflation speed at the discharge port is kept in sound velocity area due to the small deflation amount. It is noticed that the sound velocity under this condition changes with the pressure in reactor, so the gas flow of deflation is variable. When pressure in the reactor < P× , deflation gas flow belongs to the scope of subsonic flow, under this condition, steam deflation speed and flow amount still act in nonlinear variation. As shown in Eqs. 3.10–3.12, loading coefficient has impact on the volume of steam in reactor V_s which influences the gas charge/deflation time constant τ and hence changes the deflation time. With the increase of loading pattern and bulk density, the resulted drop of V_s and τ lead to the decrease of deflation time. The short deflation time which means the instantaneously physical tearing of hydrolyzed materials was thought to benefit the explosion efficiency [77]. In addition to loading parameters, the deflation time is still related to the holding pressure, volume of reactor, and discharge port area according to this model.

Table 3.8 Composition (g/100 g of raw material) of the filtrate and water-insoluble fiber under different pretreatment conditions [54]

Conditions			Filtrate composition					Water-insoluble fiber composition					Total gravimetric recovery
Chip size	Moisture content (%)	Loading pattern (%)	Glucose	Xylose	Acetic acid	HMF	Furfural	Glucan	Xylan	Acid soluble lignin (ASL)	Acid insoluble lignin (AIL)	Ash	□
Milled	40	100.50	3.54	5.26	1.63	2.11	0.09	42.85	3.43	2.25	35.29	0.74	55.90
0.5–0.8 cm	40	100.50	5.78	6.75	1.63	2.13	0.05	44.21	5.65	1.89	29.60	0.75	60.55
1–2 cm	40	100.50	5.72	5.41	1.69	1.88	0.08	45.85	5.71	2.01	32.44	0.99	58.36
3–5 cm	40	100.50	4.08	6.19	3.07	2.15	0.18	45.54	4.37	2.17	33.77	0.67	59.50
5–8 cm	40	100.50	1.78	2.24	1.63	1.90	0.15	46.94	3.57	2.16	40.98	0.80	60.35
5–8 cm	20	100.50	1.31	1.85	2.44	1.72	0.17	46.92	3.01	2.20	41.61	0.66	59.60
5–8 cm	40	100.50	1.78	2.24	1.63	1.90	0.15	46.94	3.57	2.16	40.98	0.80	60.35
5–8 cm	60	100.50	1.72	3.21	2.05	1.82	0.19	50.16	4.39	2.04	38.09	1.07	59.50
5–8 cm	80	100.50	2.13	3.73	1.53	1.68	0.15	50.77	4.12	2.04	40.43	0.34	57.80
5–8 cm	100	100.50	2.12	3.99	1.60	1.52	0.19	51.99	4.51	1.97	36.02	0.61	58.08
5–8 cm	40	30.90	1.28	2.24	1.63	1.77	0.15	46.94	3.57	2.16	40.98	0.80	60.35

(continued)

Table 3.8 (continued)

Conditions			Filtrate composition					Water-insoluble fiber composition					Total gravimetric recovery
Chip size	Moisture content (%)	Loading pattern (%)	Glucose	Xylose	Acetic acid	HMF	Furfural	Glucan	Xylan	Acid soluble lignin (ASL)	Acid insoluble lignin (AIL)	Ash	□
5–8 cm	40	54.10	1.52	2.58	2.38	1.78	0.15	48.66	3.40	2.06	41.20	0.65	62.77
5–8 cm	40	77.30	1.07	1.99	2.94	1.78	0.29	50.00	3.34	2.02	41.81	0.58	62.85
5–8 cm	40	100.50	1.63	2.47	1.80	1.81	0.14	49.14	3.43	2.13	41.30	0.70	59.16
5–8 cm	40	123.70	1.78	2.29	2.07	1.90	0.01	49.58	2.97	2.19	42.77	0.90	60.13

3.3.4.3 Effects of Steam Explosion Loading Parameters on Pretreatment Efficacy of Corn Stalk

Above changes in steam explosion process caused by loading coefficient inevitably influence pretreatment efficiency, which is evaluated by chemical composition and enzymatic hydrolysis performance of pretreated materials. The recovery is defined as the derived sugar in both the filtrate and water-insoluble fiber obtained after steam explosion. The enzymatic hydrolysis yield is expressed as sugar content produced in the hydrolysis of water-insoluble fiber. The overall sugar yield includes the soluble sugars in the liquid from pretreatment and obtained in the enzymatic hydrolysis. All of them are expressed based on the percentage of the theoretically available sugar content in dry materials. And Table 3.8 shows the composition of the filtrate and water-insoluble fiber of steam-exploded materials.

As expected, steam explosion preferentially attracted the hemicellulosic components. The hemicellulose solubilization, which reflected by the residual xylan amount in solid fraction, was found increasing with the increased chip size except for milled chips. The glucan and lignin content in solid fraction increased concurrently due to the removal of xylan. In liquid fraction, there was increased hemicellulosic sugar degradation (mainly xylose) at larger chip size except for milled chips, resulting in the formation of by-products mainly furfural. Therefore, larger chip size improves solubilization and degradation of hemicellulosic sugars compared to smaller chip size at the same pretreatment condition. The recovery of glucose and xylose in both the filtrate and water-insoluble fibers showed a significant increase from milled chips to 5–8 mm chips (Figs. 3.15 and 3.16). When the larger chips were used, the recovery of glucose was more or less constant (approach to 100%), while the recovery of xylose decreased from 84.62 to 36.56%. Previous findings showed that there was a function of higher solubilization and degradation and lower recovery of hemicellulosic sugars during more severe pretreatment [69, 73]. Therefore, it is fair to conclude that corn stalk with larger chip size is subjected to more severe pretreatment than smaller chips. This might be due to the higher pile porosity of corn stalk at larger chip sizes owing to the lower bulk density. High-pressure steam penetrated easier the interior of the pile of corn stalks with larger chip size, making more chips remained contact during pretreatment and available for autohydrolysis and explosion effects [27]. As excessive size reduction sharply increased the surface area of materials and helped to reduce the heat transfer heterogeneity during hydrolysis [73, 77].

The enzymatic hydrolysis yields of glucose and xylose, which reflect the digestibility of pretreated materials, are demonstrated in Figs. 3.15 and 3.16. Both the hydrolysis yield of glucose and xylose increased with increasing chip size except for milled chips. Previous studies have proved that larger chip sizes after steam explosion pretreatment showed the higher specific surface area and lower crystallinity [27], which would contribute to the higher digestibility efficiency of pretreated materials. However, the optimum pretreatment conditions for the maximum recovery and digestibility yield of xylose are not consistent as shown in Fig. 3.16. Hemicellulose required mild severity treatment to be recovered in high

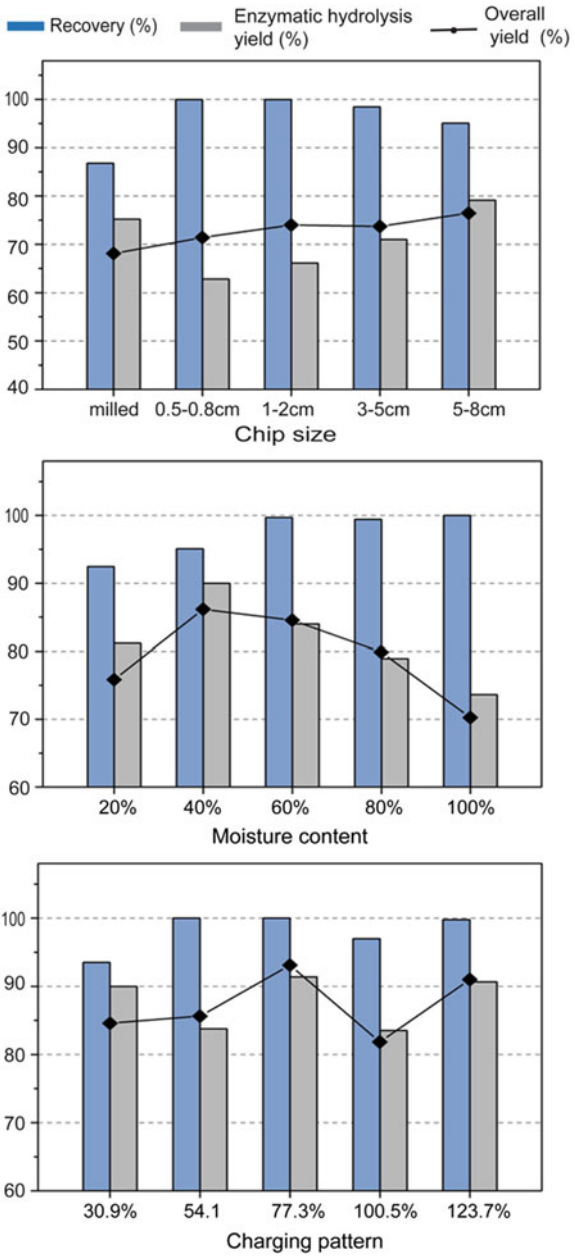

Fig. 3.15 Recovery, enzymatic hydrolysis yield, and overall yield of glucose under different loading parameters [54]

yield but at the expense of decreasing enzymatic hydrolysis yield. To facilitate the comparison of loading parameters on both the recovery and digestibility, the overall yields of glucose and xylose at different chip sizes were investigated. It can be seen

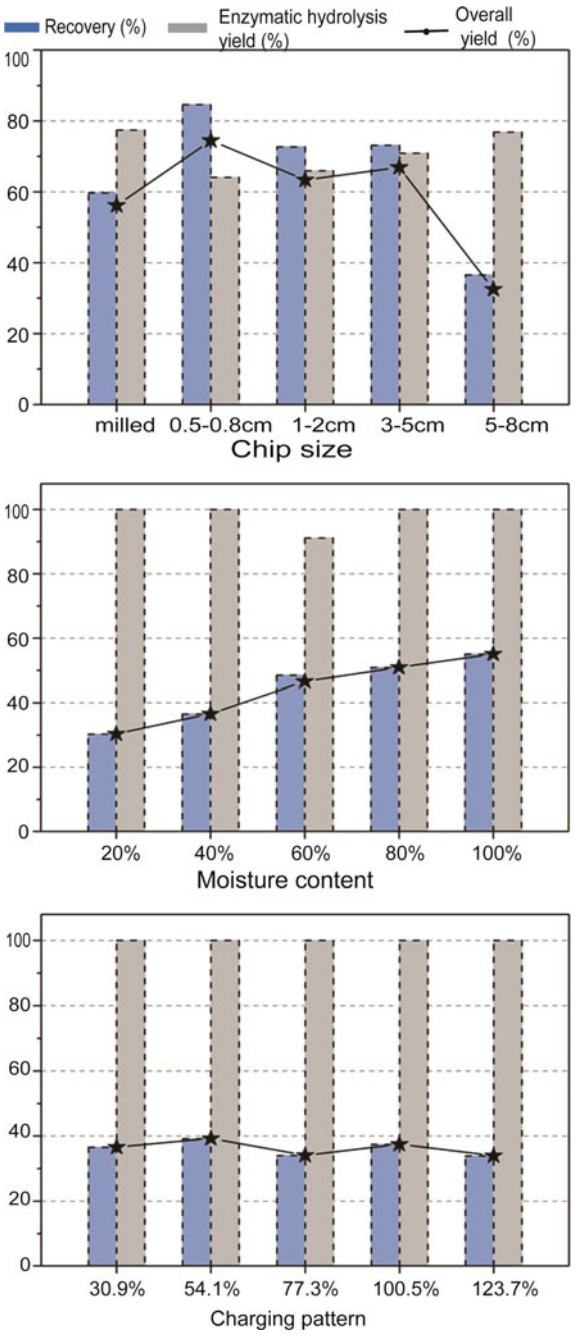

Fig. 3.16 Recovery, enzymatic hydrolysis yield, and overall yield of xylose under different loading parameters [54]

from the asterisk in Figs. 3.15 and 3.16, the total sugar yield reached a maximum of 71.81% at 3–5 cm, which is regarded as the most suitable chip size for pretreatment when considering both glucose and xylose yields. Thus, larger chip size performed better during pretreatment and consequently enzymatic hydrolysis.

Moisture content As illustrated in Table 3.8, the percentage of glucan and xylan in solid fraction increased as moisture content increased, inferring the reduction of sugar solubilization. In liquid fraction, high amount of glucose and xylose obtained at high moisture content with few degraded products HMF also supports the above observation. These indicate that increased moisture content restricted the quantity of carbohydrates that are liberated into the liquid portion and subsequently degraded. Therefore, the recovery of glucose and xylose increased with the rise of moisture content (Figs. 3.15 and 3.16). Previous study showed that solid substrate recovery after steam explosion also presented an upward trend as moisture content increased [69], although no apparent difference observed in this study. Above changes including reduced solubilization and degradation and increased sugar recovery are likely attributed to the weak pretreatment efficacy caused by heat transfer problems at high moisture content [67, 69]. When the moisture content was sufficiently low and the vessels were unblocked by liquid water, heat transfer was thought to be conducted by rapid condensation to give up latent heat of vaporization. If sufficient condensate accumulates to fill the vessels before settled temperature was reached or the moisture was enough high, further heat transfer was by the slow process of conduction. In this regard, the heat transfer through humid materials was slower than dry chips. This "buffer effect" of water presents hurdles for carbohydrate solubilization, decomposition and efficient autohydrolysis due to high heat capacity of water and slow heating rate in the interior of the chips [78, 79]. Thus, it is suggested that high-moisture materials require longer steaming time for development of the maximum digestibility.

As exhibited in Fig. 3.15, the enzymatic hydrolysis yield of glucose first reached a peak of 89.99% at 40% moisture content and then decreased as moisture content increased. This is consistent with previous study that lower moisture led to higher enzymatic digestibility [80]. In Fig. 3.16, the enzymatic hydrolysis yield of xylose showed no difference among different moisture contents. As the combined results of sugar recovery and enzymatic hydrolysis yield, the overall glucose yield decreased with increased moisture content due to the reduction of hydrolysis yield while the overall xylose yield increased resulting from the increase of xylose recovery. The maximum yield of total sugars was still achieved at 40% moisture content. Therefore, low moisture content leads to high pretreatment severity and enzymatic hydrolysis yield, although these improvements are at the expense of slight drop of recovery.

Loading pattern

As shown in Table 3.8, in water-insoluble solids, increasing the loading pattern which means increasing the volume or compaction degree of loading material, resulting in a slight decrease of xylan. This reflects the improved solubilization of hemicellulose at high loading pattern. As a result, glucan and AIL in solid fraction relatively increased. In water-soluble fraction, increased loading pattern prompted

the solubilization and degradation of cellulose, evidenced by the upward trend of glucose and HMF. Changes of xylose, acetic, and furfural were not obvious. Observed variations indicate that the pretreatment severity slightly increased with the increase of loading pattern. This is likely because of the strong shearing force among crowded materials during the sudden explosion and the rapid deflation speed as mentioned in Sect. 3.3.4.2 at compact loading pattern. However, effects of the slight increase of pretreatment severity on the recovery of glucose and xylose were not apparent, as shown in Figs. 3.15 and 3.16.

In relation to enzymatic hydrolysis yield, it also appeared no clear changes with the increase of loading pattern. This might be caused by many reasons including the small distinguish among pretreatment severities and the recalcitrance of lignin [69]. Results of overall glucose and xylose yields at different loading patterns were nearly identical. Therefore, though high steam explosion severity was reached at large loading coefficient, this little increase had almost no effects on the final sugar yield.

3.3.4.4 Optimization Strategy of Steam Explosion Loading Parameters

Taking corn stalk as research subject, simulated calculation and relevant experiments were used to investigate loading parameters' effects on steam explosion process and subsequent hydrolysis performance. Since influence trend of loading parameters varied in several investigated aspects as discussed in Sect. 3.2, their optimization should be balanced among these aspects with the general principle of maximizing products yield and minimizing energy demand to improve the process economy. Influence trends of each loading parameter on pretreatment process, efficacy and batch yield are summarized in Table 3.9.

Table 3.9 Effects of increasing loading parameters on steam explosion process, steam explosion efficiency and batch yield [54]

	Steam explosion process			Steam explosion efficiency		Batch yield of steam-exploded materials
	Energy consumption efficiency	Moisture content of pretreated samples	Deflation rate	Relative severity	Overall sugar yield	
Loading pattern	+	−	+	+	□	+
Moisture content	−	+	□	−	−	□
Chip size	−	+	−	+	+	−

+ = Positive effect
− = Negative effect
□ = Not determined
Reprinted from Ref. [62]. Copyright 2015, with permission from Elsevier

For loading pattern increased from 30.9 to 123.7%, the energy utilization efficiency of steam explosion process is improved and the ultimate moisture content of steam-exploded substrate shows a declining trend which helps to save the power used in subsequent drying process. Compact loading pattern also causes the acceleration of deflation speed, reinforcing physical tearing function in sudden decompression. Experimental analysis reveals that despite the slightly increasing trend of pretreatment severity was obtained at compact loading pattern, the small change did not manifest significant difference in enzymatic hydrolysis performance. However, increasing the loading compaction degree would lead to an increase of handling capacity, consequently a high batch yield of products. Therefore, compact loading pattern is preferable for the aim of maximizing products yield and minimizing process energy consumption. In addition to above aspects, loading pattern still depends on actual transporting, handling and storing capacity and the succession of procedures and equipment.

For moisture content of materials before steam explosion, when it is increased from 20 to 100%, the final moisture content of pretreated materials should increase. Over much moisture consumes large amount of energy, reflected by the increased total energy consumption and reduced energy utilization efficiency. The "buffer effect" caused by extra water provided mild pretreatment to substrate and was responsible for the poor hydrolysis performance. In terms of deflation speed and handling capacity, moisture content is not taken into consideration. Therefore, high moisture content should not be suitable for pretreatment of corn stalk, due to the waste of energy and low enzymatic digestibility. The present study also shows that corn stalk with 40% moisture content generated the maximum enzymatic hydrolysis yield under relatively low water and energy consumption, thereby is possibly the optimum subject.

For chip size ranged from 20 meshes to 5–8 cm, it is clear that smaller corn stalk chips present higher bulk density which corresponds to larger loading amount. The increase of loading amount increased the total energy consumption while improved the energy utilization efficiency, which is similar to the compact loading pattern. The moisture content of pretreated materials exhibited a consistent decreasing trend as chip size decreased. And quick deflation speed would be reached at small chip size, resulting in good physical effects. However, hydrolysis of steam-exploded substrates with smaller chip size showed weaker severity and lower digestibility yields. Therefore, considering the pretreatment energy consumption and processing efficacy, there is a confounding factor caused by different chip sizes. In spite of above mentioned, extra milling energy and batch process yield of small chip size also should be considered. Accordingly, further considerable attention should be taken for selecting a suitable chip size from a compromise between process energy consumption and production yields.

This study stressed the importance of loading coefficient for steam explosion process. Loading coefficient is determined by loading pattern and material property including moisture content and chip size. Both compact loading pattern and low moisture content improved energy efficiency of pretreatment and enzymatic hydrolysis performance of pretreated materials, indicating that they are desirable to

Table 3.10 Summary of literature on thermosensitive compounds and extraction methods [170]

Categories	Compounds	Extraction methods	Reference
Polyphenolic	Chlorogenic acid	Air–steam explosion pretreatment, water extraction	[170]
Alkaloids	Oxymatrine	Ultrasound-assisted extraction	[86]
Saponins	Saponin	Microwave-assisted extraction	[87]
Vitamin	Vitamin C	Vacuum microwave-assisted extraction	[88]
Carotenoids	b-carotene	Supercritical fluid extraction	[79]
Polyphenolic	Chlorogenic acid	Ultrasound-assisted extraction	[89]
Flavonoids	Total flavonoids	Pressurized solvent extraction	[90]
Indican	Anthraquinones	Pressurized hot water extraction	[91]

improve the process economy. Pretreatment of small chip size showed low enzymatic digestibility but high pretreatment energy efficiency, whether the energy demand for pretreatment can be compensated by the process yield, requires techno-economical evaluations.

3.3.5 *Others*

The bioactive compounds from plant materials are widely used in material medical, consumer chemicals, cosmetics, and food industries. The increasing interests in bioactive compounds are accompanied by a need to expand and modify efficient plant-extraction methods [81–83]. Conventional methods for enhancing extraction were characterized by high temperature, lengthy extraction procedures, and decreasing the material size [84, 85]. However, high temperature and lengthy extraction procedures may result in degradation of some thermosensitive compounds. As shown in Table 3.10, there are many thermosensitive compounds, almost involving all kinds of bioactive compounds such as alkaloids, saponins, vitamin, indican, and polyphenolic. In order to reduce the degradation, the thermosensitive compounds are extracted with

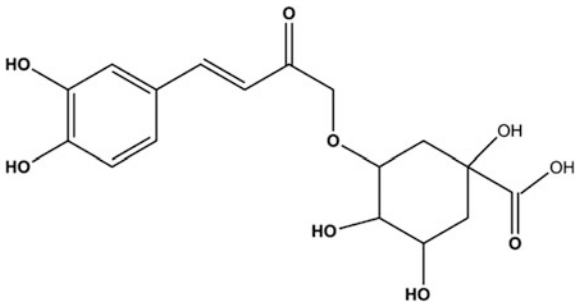

Fig. 3.17 Chemical structure of chlorogenic acid [101]

modern techniques such as supercritical fluid extraction (SFE), pressurized liquid extraction (PLE), vacuum microwave-assisted extraction (VMAE), and ultrasonic-assisted extraction (UAE) [79, 86–91]. These above techniques provide some advantages of faster and efficient extraction processes. However, special equipment is needed in these extraction processes, which requires great financial investments, and the conditions are rigid such as vacuum and high pressure. In order to achieve the desired extraction yield, solid–liquid ratio (w/v) was always kept as 1:6–1:30. Considering the cost efficiency, the large volumes of solvent were challenges for the special equipment and extraction process of these above modern extraction methods. Therefore, an efficient and economical extraction from plant materials is necessary for utilization of thermosensitive bioactive compounds.

Chlorogenic acid is a common thermosensitive polyphenol, which is an ester compound produced by caffeic acid and quinic acid with unsaturated double bond (Fig. 3.17) [92]. Chlorogenic acid is used as antioxidant, antidiabetic, and antihyperglycemic [93–95]. It is also a promising precursor compound for the development of medicine that can resist AIDS virus HIV. The current commercial sources of chlorogenic acid are mainly extracted from plant materials, such as the leaves of *Eucommia ulmoides Oliver* (*E. ulmoides*) that have been used in traditional Chinese medicine [96, 97]. Due to thermosensitivity, the oxidation, hydrolysis, and isomerization can be usually accelerated when chlorogenic acid is subjected to higher temperatures [22]. Therefore, increasing time and temperature is unsuitable for chlorogenic acid extraction. Additionally, the positive effects of decreasing particle sizes of raw materials in chlorogenic acid extraction process have been widely reported [98]. However, *E. ulmoides* is abounded with rigid biopolymers and fibrous long-chain trans^{-1}, 4-polyisoprene (Eucommia-Rubber) [99]. These biopolymers are also accumulated in the leaves of *E. ulmoides*, forming a filament network (Fig. 3.18) [100]. These networks result in the difficulty of size reduction. As chlorogenic acid mainly exists in the cells of *E. ulmoides* leaves, these networks and cell walls are, therefore, considered as barriers for effective extraction. Thus, a rapid and novel method should be developed to achieve the desirable extraction yield of thermosensitive chlorogenic acid.

Steam explosion is a widely employed and environment-friendly pretreatment method for plant materials. Its principle is steam hydrolysis at high temperature, followed by sudden release of high pressure for physically tearing the hydrolyzed materials [26, 101]. Typical results of steam explosion for plant materials include substantial breakdown of the lignocellulosic structure, hydrolysis of hemicellulose compounds, and depolymerization of the lignin compounds. Due to these physicochemical influences on plant materials, steam explosion is employed as pretreatment to effectively extract and separate bioactive compounds [102–104]. Besides, steam explosion is a short-time treatment. As reported, with only one minute of steam explosion, the yield of phenolic compounds from steam-exploded Sasa palmata was 18 times than that from raw materials [101].

Compared with above-enhancing techniques for thermosensitive bioactive compounds used in the extraction process, steam explosion is only a pre-step before extraction [105, 106]. Steam explosion will not consume a large volume of water or other liquid, thus the volume of steam explosion equipment need not to be so large.

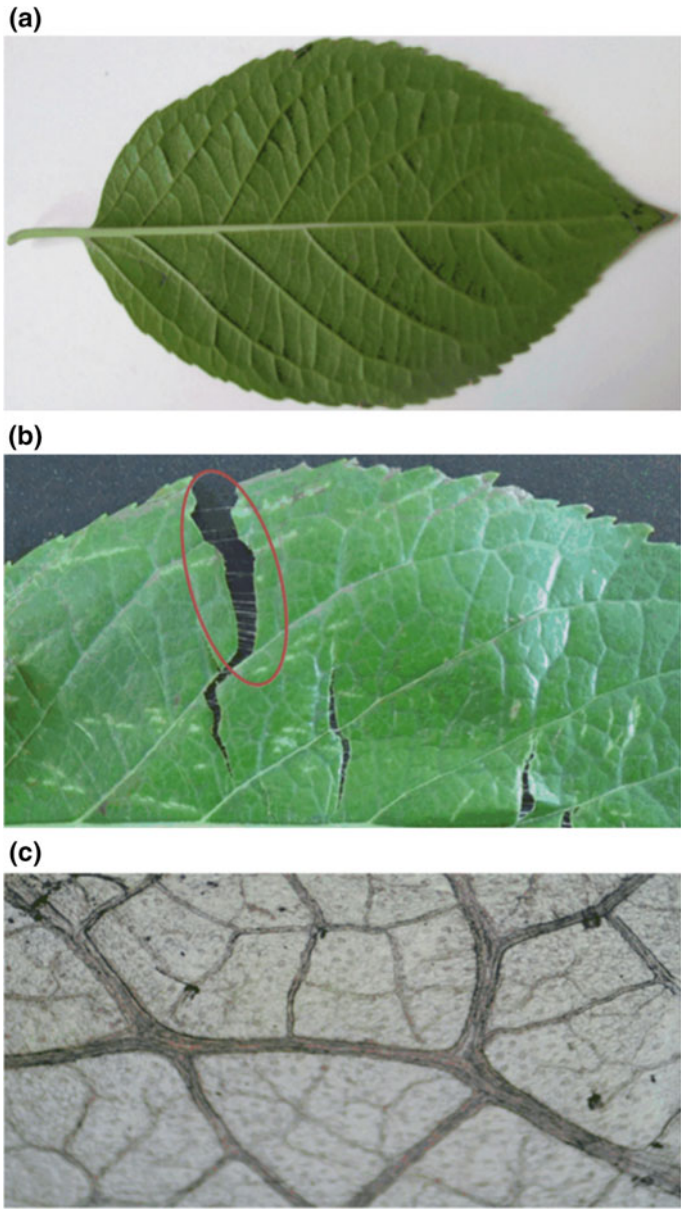

Fig. 3.18 The network and filaments of E. ulmoides leaves (A, whole leaf; B, the filaments of E. ulmoides leaves; C, the network of the nervation). The nervation was produced by the following process: the leaves were soaked with distilled water for 12 h, first decomposed with 1.25 mol/L NaOH, and then decomposed with 1.00 mol/L HCl [101]

Additionally, compared with PLE (the pressure range is 50–1000 MPa), steam explosion is a pretreatment with lower pressure of 0.4–2.0 MPa. As a consequence, steam explosion should be an efficient and cost-effective pretreatment method for improving the extraction efficiency.

The temperature of steam explosion reported in previous literatures was 190–260 °C, which may cause damage to thermosensitive bioactive compounds [102, 103]. Thus, a novel air–steam explosion pretreatment (ASEP) was developed in this study. The correlation of temperature and different partial pressure of air was investigated. The effects of ASEP on physical and chemical structures of Eucommia ulmoidesleaves were also analyzed. In addition, the extraction efficiency and antioxidant capacity of chlorogenic acid from air–steam-exploded samples (ASES) were systematically studied.

3.3.5.1 Correlation of Temperature and Holding Pressure with Air Partial Pressure

Temperature was directly related to the efficiency of steam explosion. The reaction rate of steam explosion was generally improved with the increase of temperature [46]. The degradation rate of hemicellulose within plant materials would increase by 2–4 folds when the temperature increased by 10 °C based on Arrhenius formula. The correlation of temperature and holding pressure with different air partial pressure is as shown in Fig. 3.19. The air partial pressure of 0 MPa represents the saturated steam without air addition.

Figure 3.19 showed that the temperature of gas mixture was decreased compared with that of the saturated steam at the same holding pressure. At the holding pressure of 0.8 MPa with the air partial pressure of 0.15, 0.40 and 0.55 MPa, respectively, the temperature of gas mixture was decreased by 8.04%, 26.69% and 36.31%, respectively, which indicated that the temperature of gas mixture was obviously decreased with the increase of air partial pressure. The more air was

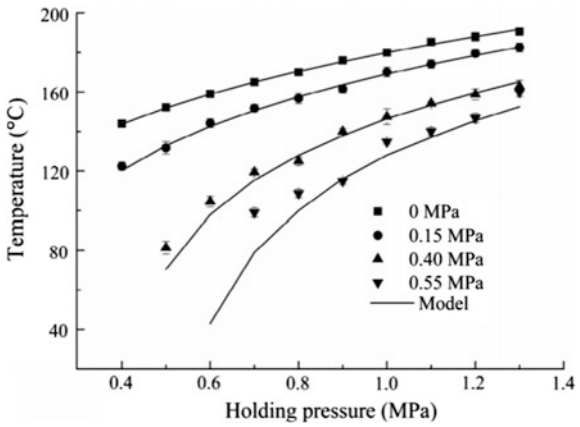

Fig. 3.19 Correlation of temperature and holding pressure with different air partial pressure [101]

added, the lower temperature of gas mixture appeared. However, the temperature was less obviously decreased with the increase of the holding pressure. At the holding pressure of 1.2 MPa with the air partial pressure of 0.15, 0.40 and 0.55 MPa, respectively, the temperature of gas mixture was decreased by 4.47%, 15.53%, and 21.91%, respectively. With the same air partial pressure of 0.55 MPa, the steam partial pressure at the holding pressure of 1.2 MPa was higher than that of 0.8 MPa, which also showed that the low-temperature efficiency was related to the partial pressure of air and steam.

Figure 3.20 shows that the experiment temperature was in good agreement with the calculated temperature at the air partial pressure range of 0–0.40 MPa, which was important to optimize the steam explosion condition in the pretreatment process. However, with air partial pressure increasing to 0.55 MPa, the results became obviously different. These results may be due to the fact that the air–steam mixture process was not considered. The temperature of gas mixture was postulated that it was to be constant in this chapter. However, air was gradually heated and the temperature should be increased with the addition of steam. Moreover, the corresponding steam was reduced with the increasing air mass. The time of temperature reaching uniform was then prolonged at the same pretreatment pressure. In addition, the plant material was a porous media, the heat and mass transfer was more complex in the air–steam mixture process [66, 107]. Thus, the difference between experiment temperature and calculated temperature increased with the increase of air partial pressure.

3.3.5.2 Optimization of Air–Steam Explosion Pretreatment

Due to thermosensitivity and instability of chlorogenic acid, the temperature was important to the pretreatment process of *E. ulmoides* leaves. Lower temperature was helpful for the stability of chlorogenic acid, but it may affect the efficiency of pretreatment and extraction performance. Therefore, it was necessary to optimize the ASEP condition for improving the extraction efficiency. As an efficient pretreatment, steam explosion for plant materials lasted very short time, which was regarded as the process of adiabatic expansion. Thus, the effective power of steam explosion was related to the enthalpy changes of the materials before and after pretreatment [66]. The holding temperature was significant to ASEP. In the same reactor, the main factors related to the holding temperature were the medium, partial pressure, density, and enthalpy, which affected the efficiency of ASEP. The medium was the air–steam mixture in this study, of which the density and enthalpy were constant. Thus, the holding pressure and the partial pressure of air were crucial to the holding temperature.

Effects of the holding pressure of ASEP on the yield of chlorogenic acid were shown in Fig. 3.20a. With the increase of holding pressure, the yield of chlorogenic acid first increased and then decreased when the holding pressure was higher than 1.0 MPa. The yield was 2.74% at the holding pressure of 1.0 MPa with the air partial pressure of 0.55 MPa (gas mixture/air, 1.0 MPa/0.55 MPa), which was 55.68% and 14.64% higher than at 0.6 MPa (gas mixture/air, 0.6 MPa/0.55 MPa) and 1.2 MPa (gas mixture/air, 1.2 MPa/0.55 MPa), respectively. The holding

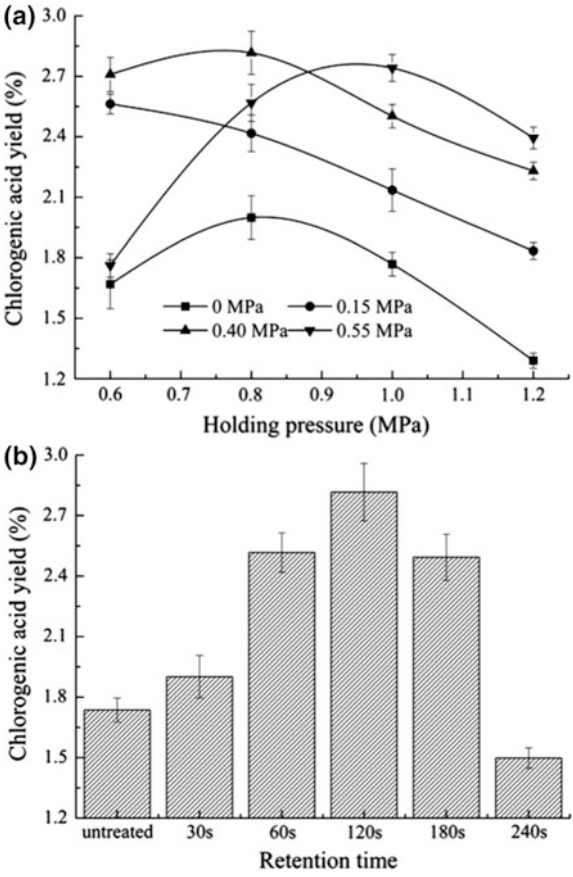

Fig. 3.20 Effect of air–steam explosion on the yield of chlorogenic acid (**a**, air pressure: 0, 0.15, 0.40 and 0.55 MPa, respectively; retention time: 120 s; **b**, air partial pressure: 0.40 MPa, the holding pressure: 0.8 MPa) [101]

pressure was the dynamic source of physical tearing force [46]. With the increase of holding pressure, the temperature also increased with the same partial pressure of air, and hence the effective power improved, which was helpful for improving the extraction efficiency. Gong et al. also reported the similar increase in the phenolic compounds extraction from steam-exploded barley bran [104]. Meanwhile, the decomposition of chlorogenic acid would increase with the increasing temperature. Therefore, the effective low temperature was important for chlorogenic acid extraction with the increase of holding pressure.

As the decrease of temperature with the partial pressure of air increasing at the same holding pressure in Fig. 3.19, the partial pressure of air influenced the holding temperature and then the yield of chlorogenic acid. As seen in Fig. 3.20a, under the same holding pressure, the yield of chlorogenic acid increased with the increasing partial pressure of air. When the sample was pretreated for 120 s at gas mixture/air of 0.8 MPa/0.4 MPa, the yield of chlorogenic acid reached the maximum of 2.82%, which was 62.0% higher than that of raw sample. And the yield of chlorogenic acid was 2.56% when the sample was pretreated for 120 s at gas mixture/air of 0.8 MPa/

0.55 MPa, which was 45.4% higher than that of raw sample. Accordingly, the increasing partial pressure of air was helpful for the stability of chlorogenic acid, but it did not benefit for the efficiency of pretreatment and extraction. As mentioned above, the holding pressure of 0.8 MPa and air partial pressure of 0.4 MPa were optimal and were chosen in the further experiments.

Besides the holding temperature, the retention time was also a major factor affecting the steam explosion pretreatment efficiency. The effects of retention time on chlorogenic acid yield were shown in Fig. 3.20b. Yield of chlorogenic acid increased and reached maximum at 120 s, and then decreased with the increase of retention time. The reaction rate generally increased with the increase of the reaction temperature, while the yield was related to the reaction time. It was widely accepted that the process of steam explosion was divided into two stages [66]. First, the polysaccharides in the cell wall were degraded and depolymerized by the hydrolysis reaction when high-pressure air–steam penetrating into the material during the cooking stage. Second, the samples were disrupted by the joint results of hydrothermal effects and physical tearing force during sudden release of the pressure. Therefore, the retention time was related to the hydrolysis of plant materials and the pervasion of air–steam medium, which was important for the efficiency of pretreatment and the yield of chlorogenic acid extraction.

With the retention time less than 120 s, the cell of plant materials may be not sufficiently filled with the air–steam medium, leading to the decrease of hydrolysis intensity at the cooking stage, which would result in the decrease of steam explosion efficiency. However, with the retention time more than 120 s, the plant materials were subjected to severer pretreatment, which may cause the degradation of bioactive compounds. Therefore, the yield of chlorogenic acid was reduced with longer retention time. According to the discussion mentioned above, the optimum

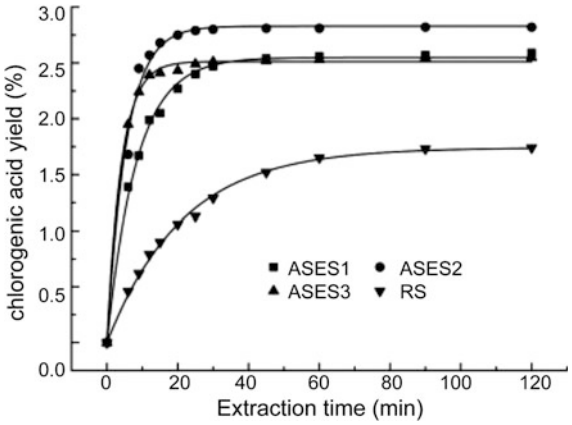

Fig. 3.21 Kinetics of chlorogenic acid extraction before and after pretreatment (ASES1: 0.8 MPa/0.4 MPa/60 s; ASES2: 0.8 MPa/0.4 MPa/120 s; ASES3: 1.0 MPa/0.4 MPa/120 s; RS: raw samples; ASES means the air–steam-exploded sample, 0.8 MPa/0.4 MPa/120 s means that the air–steam explosion condition of the holding pressure, air partial pressure and retention time was 0.8 MPa, 0.4 MPa, and 120 s, respectively) [101]

Table 3.11 Values resulting from kinetic data of chlorogenic acid extraction according to Eq: $Y_t = Y_\infty(1 - \exp(-Kt))$

Sample	Conditions of air–steam explosion			Y_∞(%)	K (min^{-1})	R^2
	Holding pressure (MPa)	Air partial pressure (MPa)	Retention time (s)			
ASES1	0.8	0.4	60	2.550 ± 0.020	0.120 ± 0.004	0.996
ASES2	0.8	0.4	120	2.829 ± 0.034	0.182 ± 0.0012	0.989
ASES3	1.0	0.4	120	2.513 ± 0.011	0.246 ± 0.008	0.998
RS	0	0	0	1.741 ± 0.021	0.047 ± 0.008	0.997

Reprinted from Ref. [113]. Copyright 2007, with permission from Elsevier

ASEP condition was that the holding pressure, air partial pressure and retention time were 0.8 MPa, 0.4 MPa, and 120 s, respectively.

3.3.5.3 Comparison of Extraction Performance Before and After ASEP

In order to evaluate the extraction performance, extraction kinetics test of ASES under different conditions were compared with that of raw sample. Results were shown in Fig. 3.21. The breaking points represent the experimental values and the continuous lines represent the fits with the exponential function from Eq. 3.7. Results showed that the extraction yield of chlorogenic acid from ASES increased significantly at the beginning of extraction and then reached equilibrium. When ASES was pretreated at the same holding pressure of 0.8 MPa, the extraction yield of chlorogenic acid reached the maximum of 2.8% from ASES pretreated for 120 s, which was 10.59% higher than that for 60 s. The maximum yield also was 2.98-fold of the raw sample group. The extraction yield of chlorogenic acid from all ASES reached equilibrium at 15 min, however, that from raw sample at 2 h extraction time. Results demonstrated that the yield of chlorogenic acid extraction from ASES was increased and its equilibrium time was reduced from 120 to 15 min, which was significant to the commercialization of chlorogenic acid extraction from the leaves of *E. ulmoides*.

Table 3.11 showed the specific rate of chlorogenic acid before and after pretreatment based on Eq. 3.7. As seen from Table 3.11, the coefficients of determination (R2) were higher than 0.98, implying that the curves fitted the data well. The specific rate of chlorogenic acid yield (K) from ASES was increased with the increase of steam explosion severity and reached the maximum of 0.246 min^{-1}, which was 5.23-fold of that from raw samples. Therefore, the extraction performance of chlorogenic acid from the leaves of *E. ulmoides* was improved after ASEP.

The improvement of chlorogenic acid yield may result from the characteristics changes of *E. ulmoides* leaves after ASEP. As shown in Fig. 3.22, the specific

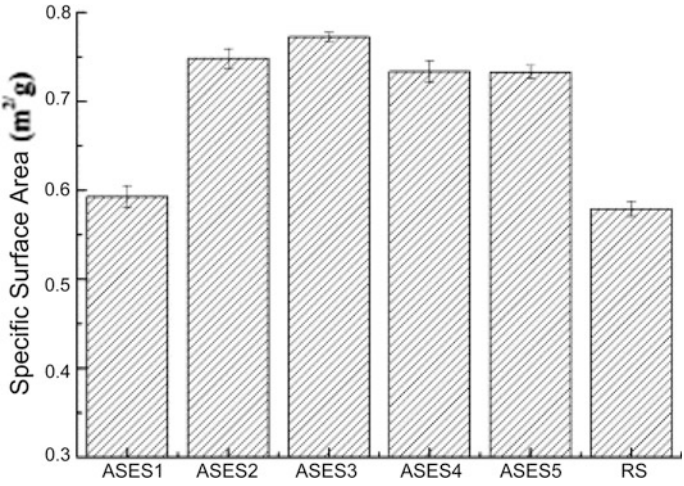

Fig. 3.22 The specific surface area of E. ulmoides leaves before and after air–steam explosion pretreatment (ASES1: 0.6 MPa/0.4 MPa/120 s; ASES2: 0.8 MPa/0.4 MPa/60 s; ASES3: 0.8 MPa/0.4 MPa/120 s; ASES4: 1.0 MPa/0.4 MPa/120 s; ASES5: 1.2 MPa/0.4 MPa/120 s; RS: raw samples; ASES means the air–steam-exploded sample, 0.6 MPa/0.4 MPa/120 s means that the air–steam explosion condition of the holding pressure, air partial pressure and retention time was 0.6 MPa, 0.4 MPa, and 120 s, respectively) [101]

surface area of *E. ulmoides* leaves was improved after ASEP. With the increase of ASEP severity, the specific surface area was first increased and then decreased when the holding pressure was higher than 1.0 MPa. The specific surface area reached the maximum of 0.77 m2/g from ASES pretreated for 120 s at 0.8 MPa (gas mixture/air, 0.8 MPa/0.4 MPa), which was 33.33% higher than that of the raw samples. The specific surface area has a significant influence on mass transfer of active compounds in the extraction process. With the increase of the specific surface

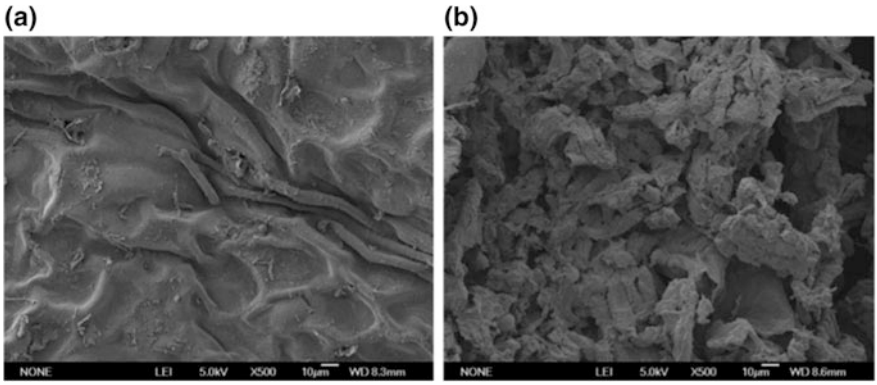

Fig. 3.23 SEM of E. ulmoides leaves (A, raw samples; B, the air–steam-exploded sample pretreated under the condition of the holding pressure, air partial pressure and retention time was 0.8 MPa, 0.4 MPa, and 120 s, respectively) [101]

Table 3.12 pH of the solution for air–steam-exploded *E. ulmoides* leaves

Sample	Conditions of air–steam explosion			pH[a]
	Holding pressure (MPa)	Air partial pressure (MPa)	Retention time (s)	
ASES1	0.8	0.4	60	5.44 ± 0.16
ASES2	0.8	0.4	120	4.92 ± 0.09
ASES3	1.0	0.4	120	4.7 ± 0.15
RS	0	0	0	6.89 ± 0.17

[a]A sample of 10 g of air–steam-exploded *E. ulmoides* leaves was added to 100 mL of distilled water and stirred for 60 min at room temperature. After filtration through filter paper, the filtrate was used for analysis of pH

area, the solvent reached the extraction sites more easily, which resulted in the decrease of internal diffusion resistance [108].

As a result, the solvent accessibility and mass transfer efficiency were improved after ASEP, shown by the increased mass transfer coefficient K and the shortened extraction equilibrium time.

However, the specific surface area was decreased with severer ASEP condition, which may be caused by the changes of pore diameter [108]. Considering that the plant material was a porous media with cell wall and middle lamella as the skeleton, the skeleton may be disrupted due to severer pretreatment, which would result in the close of some pores and then influences the extraction efficiency. Thus, besides the temperature destruction, it may be also a reason that the yield of chlorogenic acid decreased with the increase of ASEP severity.

The physical and chemical changes generated in the steam explosion process [108]. The structure of ASES and raw sample was observed by SEM, as shown in Fig. 3.23. Steam explosion caused breakage and destruction of cell walls, leading to the formation of large cavities and intercellular spaces (Fig. 3.23b), but no pores were observed in the raw sample (Fig. 3.23a). With the air–steam penetrating into the plant material during the cooking stage, the hemicellulose in the cell wall was degraded and depolymerized through the hydrolysis reaction. The conjunction of fibrils was weakened and the space between cellulose fibrils was opened, leading to the increase of porosity. Besides, the removal of hemicellulose made the inter-fibrillar regions less rigid and more capable of softening and rearrangement. Subsequently, the samples were disrupted by the joint results of hydrothermal effects and physical tearing force during sudden release of the pressure. Hence, the barriers of cell wall were destroyed by ASEP.

The dissolution and diffusion of active compounds from plant materials in the extraction process were influenced by the cell wall [109]. The dissolution process was a relatively quick process, but the diffusion process was correlated with both the arrangement of vascular bundles and pits connecting cell walls. Therefore, smaller particles and micropores caused by ASEP weakened the dominant internal diffusion resistance, which was conducive to the chlorogenic acid extraction.

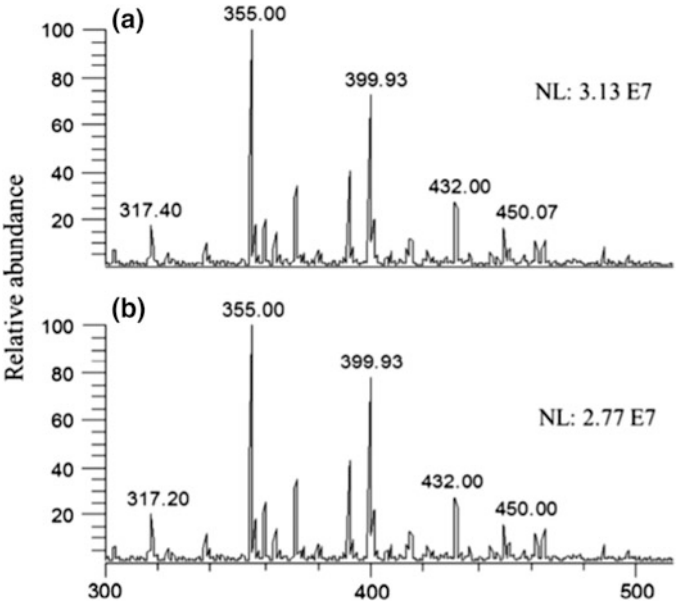

Fig. 3.24 LC-ESI-MS total ion chromatogram of chlorogenic acid extracts (A, raw samples; B, the air–steam-exploded sample pretreated under the condition of the holding pressure, air partial pressure and retention time was 0.8 MPa, 0.4 MPa, and 120 s, respectively) [101]

Besides the improvement of porosities and particles, the acidic condition of ASEP was beneficial to the chlorogenic acid extraction. The organic acids (e.g., acetic acid, formic acid, and levulinic acid) were formed from the biomass itself during the air–steam explosion process [110]. As shown in Table 3.12, the pH was about 4.7–5.5 after ASEP. Moreover, chlorogenic acid was reported to be pH-sensitive with higher stability obtained under acidic conditions [111]. Therefore, the acidic condition of ASEP should improve the chlorogenic acid extraction.

3.3.5.4 Effects of ASEP on Characteristics of Chlorogenic Acid Extracts

The crude extracts of chlorogenic acid before and after ASEP were analyzed by LC–MS. As shown in Fig. 3.24, m/z355 represented chlorogenic acid, which was the major compound extracted from *E. ulmoides* leaves. Fingerprints present no apparent changes of peak profiles, indicating that chemical compositions of chlorogenic acid were not destroyed by ASEP.

To examine the effects of ASEP on the characteristics of chlorogenic acid extracted from *E. ulmoides* leaves, the extracted chlorogenic acid was analyzed by FTIR. The characteristic bands of chlorogenic acid were obvious in Fig. 3.25. The band at

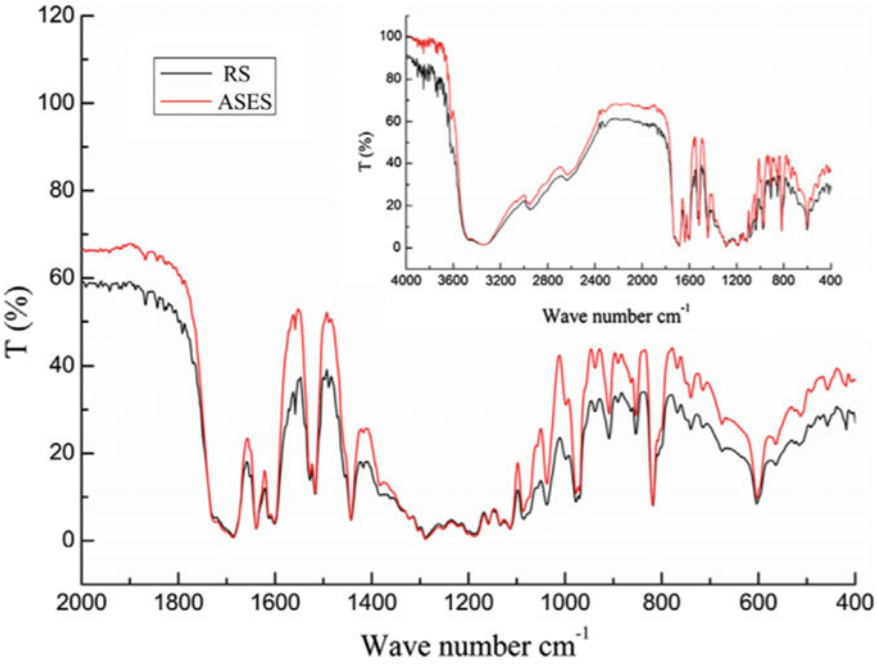

Fig. 3.25 FTIR spectra of chlorogenic acid extracts (RS, raw samples; ASES, the air–steam-exploded sample pretreated under the condition of the holding pressure, air partial pressure and retention time was 0.8 MPa, 0.4 MPa, and 120 s, respectively) [101]

Table 3.13 FTIR spectra of CGA extracts

RS (cm^{-1})	ASES (cm^{-1})	Vibration types and groups	Intensity
3465.84	3461.99	ν_{-OH}	s, b
2952.81	2952.81	ν_{C-H}	m
1685.67	1685.7	ν_{-COOH}	s
1639.38	1639.38	ν_{C-C}	s
1600.81	1600.81	ν_{C-C}(skeletal)	s
1517.87	1515.24	ν_{C-C}(skeletal)	s
1442.66	1442.66	δ_{-CH},δ_{-CH2}	s
1288.36	1288.36	ν_{-COOH}	s
1190	1190	ν_{-C-O}	s
1159.14–1085.85	1159.14–1085.85	ν_{-C-O}	m
1037.63	1037.63	ν_{-OH}	m
970.13	970.13	γ_{C-H}	m
908.41–738.69	909.06–739.01	γ_{C-H}	w

ν, stretching vibration; γ and δ, blending vibration; s, strong absorption peak; m, middle absorption peak; w, weak absorption peak; b, broad peak

Reprinted from Ref. [113]. Copyright 2007, with permission from Elsevier

3465 cm^{-1} was attributed to -OH stretching vibration, and 1159.14–1085.85 cm^{-1} to C–O stretching vibration, which indicated that the compound included alcohol hydroxyl. The band at 2953 cm^{-1} was attributed to C–H stretching vibration, and 1442.66 cm^{-1} to $-CH_2$ and -CH bending vibration, implying that the compound included $-CH_2$ and -CH. 1689.53 cm^{-1} was attributed to ester carbonyl stretching vibration and carboxyl vibration peak was shown at 1685.67 cm^{-1}, 1288.36 cm^{-1} and 1037.63 cm^{-1}. The carbon–carbon double bond and conjugated double bond stretching vibration peak were shown at 1639.38, 1600.81, and 1515.94 cm^{-1}. The characteristic bands of chlorogenic acid from RS and ASES were compared. As shown in Table 3.13, the peak position had no obvious changes, which demonstrated that the chemical structure of chlorogenic acid extract was not destroyed after ASEP.

3.3.5.5 Evaluation of the Antioxidant Capacity of Chlorogenic Acid Extract

In order to evaluate the effect of ASEP on antioxidant capacity of chlorogenic acid, the hydroxyl and superoxide free radical scavenging activity before and after ASEP was compared. As shown in Table 3.14, the OH- and O2- scavenging ratio of raw sample was 15.98% and 87.54%, respectively, while that of ASES increased to 31.10% and 95.85% after pretreated with the holding pressure, air partial pressure and retention time of 0.8 MPa, 0.4 MPa, and 120 s, respectively. Thus, the antioxidant capacity of the chlorogenic acid extract increased after ASEP.

The low temperature and acidic condition of air–steam explosion pretreatment was helpful for the stability of thermosensitive chlorogenic acid. Moreover, the porosities and specific surface area of *E. ulmoides* leaves were improved after pretreatment, resulting in the improvement of solute–solvent accessibility and the internal mass transfer in extraction process. Under the optimal conditions, the yield and antioxidant capacity of chlorogenic acid were both increased, while the equilibrium time of extraction was reduced from 120 to 15 min. Therefore, air–steam explosion was an efficient pretreatment to enhance the extraction performance of chlorogenic acid from the leaves of *E. ulmoides*, which was a promising method to enhance the extraction of thermosensitive bioactive compounds from plant materials.

Table 3.14 Antioxidant activity of the aqueous extracts of chlorogenic acid

Sample	Conditions of air–steam explosion			OH^- scavenging activity[a] (%)	O_2^- Scavenging activity (%)
	Holding pressure (MPa)	Air partial pressure (MPa)	Retention time (s)		
ASES1	0.8	0.4	60	28.77 ± 1.25	90.78 ± 2.97
ASES2	0.8	0.4	120	31.10 ± 2.03	95.85 ± 3.08
ASES3	1.0	0.4	120	33.52 ± 1.86	92.59 ± 2.83
RS	0	0	0	15.98 ± 1.19	87.54 ± 1.75

[a]Data are the mean ± SD (n = 6)

3.4 Novel Process of Fermentable Feedstock Refinery

3.4.1 Novel Steam Explosion Coupling with Mechanical Carding Improving Solid-State Fermentation Performance

Cornstalk is the most distributed lignocellulose biomass in the world and offers renewable low-cost cellulosic fibers [112–114]. The estimated available cornstalk in the world was 75 million ton [114]. Cornstalk is featured by higher hemicellulose and ash content. Cornstalk was heterogeneous biomass, and the central part was the pith, clearly distinguished by its low density, softness and white color from the surrounding harder, denser, light brown fibrous rind. The pith content of cornstalk was approximately 21% and consisted of only small amounts of usable papermaking fiber. Most of its mass consisted of parenchyma cells, used by the plant for storage of water and food. The fine nature of residual pith after pulping significantly reduces the drainage rate of the resulting pulps, making washing and dewatering difficult [115]. Papermaking properties of cornstalk were seriously affected by large quantities of very fine material that made difficult the sheet formation because of their scarce drainability [115, 116]. In addition, heterogeneity of the biomass can result in variation also in the quality of the pulp when the entire plants are used in pulping [117]. Therefore, there is no readily available evidence of current commercial use of cornstalk in the world, and studies on cornstalk dissolving pulp preparation have been rarely reported in the literature to our knowledge. The key factor was lack of the technologies and equipment required in the industrial production.

The rind of cornstalk has numerous fiber vascular bundles, and it is the main source of fiber. The dissolving pulp quality depends both on properties of the raw materials and the pulp processing. Steam explosion and mechanical carding combination pretreatment technology and equipment were patented, it was clean and effective for the separation of lignocelluloses into long fiber fraction and short fiber fraction industrially [118]. The aim of this work is to solve the inhomogeneity, and high hemicellulose and ash content of cornstalk as fiber material to manufacture of dissolving pulp. Steam explosion technology coupling with mechanical carding was used to fractionate cornstalk long fiber, which was used as fiber source for the production of dissolving pulp. The fractionated cornstalk long fiber was subjected to kraft pulping trials, followed by TCF bleaching to manufacture cornstalk dissolving pulp. Cool alkali extraction and xylanase treatment were also used to upgrade low-alpha cornstalk dissolving pulp to high-alpha cornstalk dissolving pulp. The procedure for preparation of cornstalk long fiber and manufacture of cornstalk dissolving pulp was shown in Fig. 3.26 In the present study, the fractionated cornstalk long fiber and prepared cornstalk dissolving pulp were also analyzed and characterized.

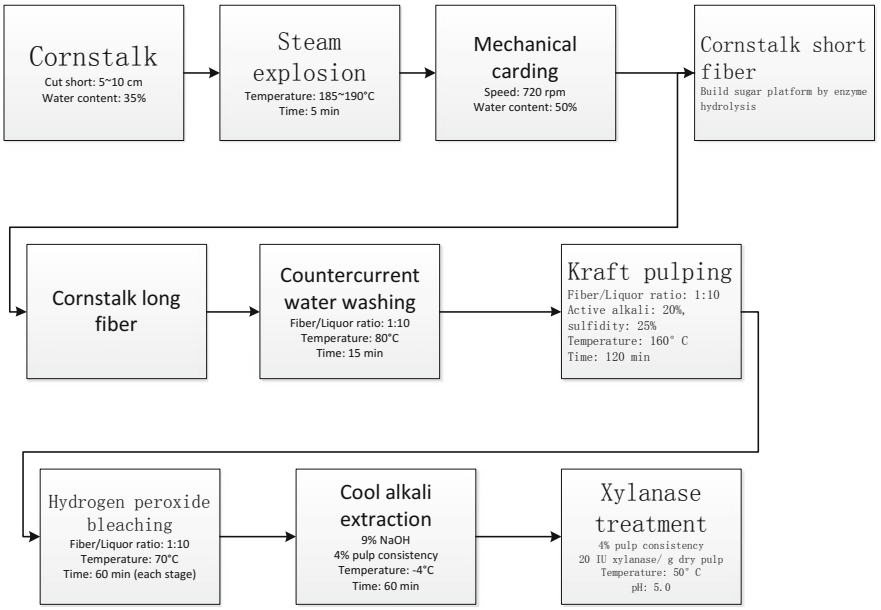

Fig. 3.26 Flow-sheet of the procedure for fractionation of cornstalk long fiber and manufacture of cornstalk dissolving pulp [50]

3.4.1.1 Effects of Steam Explosion Pretreatment on Cornstalk Chemical Components and Structure

In the production of high-purity dissolving pulps, both lignin and hemicelluloses must be extensively removed [119, 120]. Hemicelluloses are undesirable impurities in dissolving pulps, and the undesirable effects of hemicelluloses in dissolving pulps are well established. Hence, it is necessary to add a pre-hydrolysis stage with the kraft process to reduce the hemicellulose content and produce pulps with a cellulose content up to high-grade [121, 122]. Unlike cellulose with a high molecular weight linear homopolymer organized in a crystalline state, hemicellulose is noncrystalline, highly short and branched with a degree of polymerization of 70–200 [123, 124]. Hemicellulose is much more prone to be hydrolyzed into its constituent monomers. Therefore, it is necessary to introduce a pre-hydrolysis stage prior to the kraft pulping to help to produce pulp with a satisfactorily high content of cellulose and with low hemicellulose content [121, 122, 125].

Steam explosion is an effective environmental-friendly technology, in which water is the only necessary reagent for processing the raw material. In this method, biomass is treated with high-pressure saturated steam, and then the pressure is suddenly reduced, which makes the materials undergo an explosive decompression.

Steam explosion is typically initiated at a temperature of 160–200 °C for several a few minutes (Vapor Cooking Process) before the material is exposed to atmospheric pressure (Blasting Process). In the vapor cooking process, the hydronium ions are generated from water by autohydrolysis, but the generation of acetic acid by acetyl groups hydrolysis from hemicellulose provides most to the catalytic species involved in the subsequent hemicellulose degradation. In addition, the hemicellulose-lignin bonds are cleaved, which all promote hemicellulose hydrolysis (autohydrolysis) to soluble sugars [26].

As shown in Table 3.15, all the components of cornstalk were degraded in the steam explosion process. The degradation rate of cellulose, hemicelluloses, lignin, and ash was 6.93%, 69.22%, 8.25%, and 48.86%, respectively. Hemicellulose was depolymerized much faster than cellulose. The vast majority of cornstalk hemicellulose was degraded, and cellulose decreases slowly. Lignin is also depolymerized during the steam treatment, and a significant fraction is solubilized during the water washing. These results were consistent with the above discussion. The soluble carbohydrates mainly from hemicelluloses and soluble lignin could be extracted with hot water from steam-exploded cornstalk, which achieving the fractionation of hemicelluloses from cornstalk. In addition, a great decrease in the ash content of the cornstalk was observed, showing that a significant fraction of the ash was formed of water-soluble components that were easily removed during the washing stage. The extract from steam-exploded cornstalk could be used for other applications, such as microbial oil [126]. After steam explosion followed by water washing, the content of the components of cornstalk varied significantly as shown in Table 3.15. Cellulose content and lignin content of steam-exploded cornstalk increased from 38.81% and 15.74% to 55.08% and 22.02%, respectively. The hemicellulose and ash content of steam-exploded cornstalk decreased from 22.50% and 1.59% to 10.56% and 1.10%

Table 3.15 Compostion and yield of untreated and treated cornstalk fibers and pulps. Composition values reported on material dry basis (%). Yield reported on a dry weight basis at each stage and overall (%)

Samples	Cellulose	Hemicellulose	Lignin	Ash	Yield[b]	Yield[c]
Untreated cornstalk	38.81	22.50	15.74	1.59	100.00	100.00
Steam-exploded cornstalk	55.08	10.56	22.02	1.24	65.58	65.58
Cornstalk long fiber	56.17	8.34	23.97	1.10	42.63	27.97
Long fiber kraft pulp	89.68	4.14	3.10	0.92	57.66	16.12
Long fiber bleaching pulp	93.10[a]	3.96	0.46	0.13	77.20	12.44
Alkali-treated dissolving pulp	96.20[a]	3.52	0.37	0.11	90.39	11.25
Alkali-xylanase-treated dissolving pulp	97.10[a]	2.86	0.36	0.10	89.89	10.11

[a]Represented the content of α-cellulose
[b]The yield on a dry weight basis at each stage
[c]The yield on a dry weight basis overall
Reprinted from Ref. [58]. Copyright 2012, with permission from Elsevier

in the native cornstalk. Therefore, cellulose and lignin were accumulated, while hemicelluloses and ash were reduced after steam explosion, which benefitted for the cornstalk fiber to prepare dissolving pulp.

In the blasting process, rapid flashing to atmospheric pressure and turbulent flow of the material cause fragmentation of the material by mechanical shear, and make the material fiberized. In the vapor cooking process, lignin became plasticized, which made the steamed material easily fiberized. Therefore, steam explosion pretreatment weakened the lignocellulosic structure, opened up the cellulose fibers for further reactions, increased the extractability of lignin during the subsequent kraft pulping process, and thus substantially reduce the lignin and ash contents [125, 127]. Due to the blasting and tearing effect, the native cornstalk was fragmented and fiberized, the structure of steam-exploded cornstalk became loose and porous, and the surface area of steam-exploded cornstalk increased, which all promoted the accessibility of chemicals to cornstalk.

3.4.1.2 Preparing Long Fiber from Steam-exploded Cornstalk Using Mechanical Carding Fractionation

Lignocellulosic materials were used for various applications depending on their composition and physical properties [113]. Cornstalk had much pith, which almost only consisted of parenchyma cells usable papermaking fiber [115]. Therefore, it was necessary to remove cornstalk pith. Cornstalk pith mainly consisting of parenchyma cells had weak mechanical properties, and was easy to become fragmented in the steam explosion process. While cornstalk rind mainly consisting of fiber cell had strong mechanical properties, and was prone to become fiberized in

Table 3.16 Fiber cell dimensions of different plants

Plant fiber materials	Length (mm)	Diameter (lm)
Cornstalk long fiber (this work)	1.79 ± 0.16	15.64 ± 4.2
Cornstalk pulp [156]	0.77	38.0
Cornstover stem [113]	0.8 ± 0.3	27 ± 8.9
Kenaf (bark) [157]	2.32 ± 0.21	21.9 ± 4.6
Reed (internodes) [157]	1.22 ± 0.07	17.3 ± 2.4
Sorghum stem [128]	1.3 ± 0.7	15.8 ± 7.2
Sorghum leaf [128]	1.7 ± 0.8	7.6 ± 2.4
Eulaliopsisbinata [158]	2.05	13.53
Sugarcane bagasse [159]	1.51	21.4
Bamboo [160]	2.5	13.83

Reprinted from Ref. [58]. Copyright 2012, with permission from Elsevier

the steam explosion process. Depending on the different geometry of cornstalk pith and rind after steam explosion, the steam-exploded cornstalk was fractionated into long fiber fraction and short fiber fraction by mechanical carding. The steam-exploded cornstalk long fiber and short fiber were separated into single cells by maceration. The long fiber was rich in fiber cells, while the short fiber was rich in non-fibrous cells. Compared with 35% fiber cell in area in cornstalk, the cornstalk long fiber contained 85% fiber cell in area, which was higher than those of hardwood and bamboo. The dimensions of the fiber cells in steam-exploded cornstalk long fiber were given in Table 3.16. The lengths of fiber cells were 1.79 ± 0.16 mm, and the widths of the fiber cells were 15.64 ± 4.2 μm. The lengths of steam-exploded cornstalk fiber cells were longer than those used by Kadam et al. and Reddy and Yang, and the widths of steam-exploded cornstalk fiber cells were narrower than those used by Kadam et al. and Reddy and Yang [112, 128]. These differences may be caused by the species of cornstalk, but the standard errors of lengths and widths of steam-exploded cornstalk fiber cells were smaller than those used by Reddy and Yang, which indicated that the steam-exploded cornstalk long fiber contained uniform slender fiber cells [128]. It also can be seen in Table 3.16 that the lengths of cornstalk fiber cells were shorter than kenaf, Eulaliopsis binata, and bamboo, but longer than sorghum, reed and sugarcane bagasse.

Cellulose can form very tightly packed crystallites due to intra- and intermolecular hydrogen bonding. The characteristic peaks of Cellulose I appeared at 2θ about 16.3°, 22.6°, 34.8° [129, 130]. X-ray diffraction analysis of cornstalk showed a little loss in the degree of crystallinity of steam-exploded cornstalk long fiber, and the cellulose retained its basic crystalline structure (Cellulose I). This demonstrated that the crystalline destruction during steam explosion process. However, the present investigation is not consistent with Tanahashi's conclusion. Their X-ray diffraction patterns of wood showed that the degree of crystallinity increased by steam explosion treatment [130].

In addition, compared with steam-exploded cornstalk, the cornstalk long fiber fractionated from steam-exploded cornstalk had higher cellulose content and lower hemicelluloses and ash content (as shown in Table 3.15). Based on the above analysis, cornstalk long fiber fractionated from steam-exploded cornstalk was one kind of high-quality long fiber.

3.4.1.3 Preparing Low-Alpha Dissolving Pulp Using Kraft Pulping and Hydrogen Peroxide Bleaching

Dissolving pulp is a chemically refined bleached pulp with high cellulose (α-cellulose > 90%), relatively low hemicellulose (2–4%), and trace amounts of lignin and mineral content [121, 125]. Both lignin and hemicelluloses were considered as contaminants and were to be removed. Otherwise, high hemicelluloses and lignin content in dissolving pulps would result in poor cellulose processability (e.g., fiber swelling, filterability, and xanthation) and a negative effect on properties of the

cellulose-end products [120]. Compared to paper-grade pulps, preparing dissolving pulp needed extensive pulping and bleaching [125]. The cornstalk long fiber fractionated from steam-exploded cornstalk by mechanical carding were composed of single fiber cells that were held together in the form of a bundle by binding substances such as lignin and pectin, and there was a layer of deposits on the fiber surface. This surface layer was probably composed of water-insoluble materials, such as waxes, lignin, and other binding materials [128]. The purposes of pulping and bleaching process were to separate the fiber bundle into single fiber cells and remove the lignin, hemicelluloses, ash and the water-insoluble materials on the fiber surface extensively. The quality of dissolving pulp also depended on the production process. In the present study, kraft pulping and hydrogen peroxide bleaching was used to prepare dissolving pulp.

Cornstalk was easily delignified by alkaline treatment than hardwood or softwood species to reach pulps with equal Kappa numbers [127]. The results of kraft pulping were shown in Table 3.15. After kraft pulping, lignin was removed mostly, and the content of lignin decreased significantly from 23.97% in cornstalk long fiber to 3.10% in cornstalk kraft pulp. Hemicellulose and ash were also removed in the kraft pulping process, and the content of hemicellulose and ash decreased from 8.34% and 1.10% in cornstalk long fiber to 4.14% and 0.92% in cornstalk kraft pulp, respectively. Cellulose was insoluble solid in the kraft pulping process, and the content of cellulose increased from 56.17% in cornstalk long fiber to 89.68% in cornstalk kraft pulp.

The peroxide treatment substantially reduced the hemicellulose, lignin, and the ash content of the cornstalk pulp (as shown in Table 3.15). The resulting bleached cornstalk kraft pulp has a high-purity cellulose with an α-cellulose content of 93.10%, low hemicellulose content of 3.96%, and the lignin and ash content of only 0.46% and 0.13%, respectively (as shown in Table 3.15). In addition, the brightness of bleached cornstalk kraft pulp was 78.70%, and the dynamic viscosity of bleached

Table 3.17 Characteristics of cornstalk long fiber dissolving pulps

Index	L–DP	Alkali-L–DP	Alkali-xylanase-L–DP	FZ/T 51002-2006	FZ/T 51001-1998
α-cellulose/%	93.10	96.20	97.10	≧94.0	≧88.0
Brightness/%	78.70	81.69	82.29	≧74	≧85
Viscosity/mPa·s	23.96	15.46	14.37	9.0 ± 1.1	19–23
Xylan/%	3.96	3.52	2.86	–	≦4
Ash/%	0.13	0.11	0.10	≦0.16	≦0.13

Note L–DP was low-alpha dissolving pulp; Alkali-L–DP was alkali-treated low-alpha dissolving pulp; Alkali-xylanase-L–DP was alkali and xylanase synergistic treated low-alpha dissolving pulp. FZ/T 51002-2006 was the standard of "Bamboo Dissolving Pulp for Viscose" and the values after the ± signs confidence intervals. FZ/T 51001-1998 was the standard of "Wood Dissolving Pulp for Viscose"

cornstalk kraft pulp was 23.93 mPa·s (as shown in Table 3.17). Compared with viscose-grade wood pulp (FZ/T 51001-1998) and viscose-grade bamboo pulp (FZ/T 51002-2006), the characteristics of bleached cornstalk kraft pulp were between viscose-grade wood pulp and viscose-grade bamboo pulp, therefore, bleached cornstalk kraft pulp could be used as cellulose materials for the preparation of viscose. Because of the α-cellulose content of bleached cornstalk kraft pulp < 96%, the bleached cornstalk kraft pulp belonged to low-alpha dissolving pulp.

3.4.1.4 Preparing High-Alpha Dissolving Pulp by Collaborative Effect of Cold Alkali Extraction and Xylanase Treatment

Dissolving pulps can be divided into low-alpha dissolving pulps (α-cellulose: 90–96%) and high-alpha dissolving pulps (α-cellulose: 97–98%) based on the standard of Lenzing Group. Low-alpha pulps were used as cellulose materials for the production of viscose, lyocell, and so on. High-alpha pulps were used as cellulose materials for the production of acetate, nitrates, and ethers. The synergistic effect of alkaline extraction and xylanase treatment could upgrade the paper-grade pulps to dissolving pulps. Hyatt et al. utilized a sequence of caustic extraction, xylanase treatment, and caustic extraction to remove most of the xylan for upgrading paper-grade wood pulp to dissolving grade pulp which is suitable for use in the preparation of viscose rayon, cellulose ethers and cellulose ester such as cellulose acetate [131]. It was feasible to upgrade eucalyptus and birch paper kraft pulps to dissolving pulps by combining alkaline extraction with xylanase and endoglucanase treatments. These treatments were investigated and optimized on flax, hemp, sisal, abaca and jute soda/AQ paper-grade pulps for the same purpose [121]. In this chapter, cool alkali extraction and xylanase treatment were used to boost cellulose levels and upgrade the cornstalk low-alpha dissolving pulp to high-alpha dissolving pulp.

Alkaline extraction could be a feasible alternative to achieve lower xylan content. Special alkaline purification treatments can boost cellulose levels up to 98% for the kraft process [122]. After cool alkali extraction, the cellulose content of cornstalk dissolving pulp increased significantly from 93.10% to 96.20%, and the hemicellulose, lignin and ash content all decreased future, which reduced from 3.96%, 0.46%, and 0.13% to 3.52%, 0.36%, and 0.11%, respectively. In addition, after alkali extraction, the brightness increased from 78.70 to 81.69%, and the dynamic viscosity decreased from 23.96 to 15.46 mPa·s. It indicated that alkali extraction could increase the brightness of pulps and reduce the cellulose degree of polymerization.

Cornstalk pulps were also subjected to a xylanase treatment for reduction of hemicellulose content. It was seen from Table 3.18, the removal efficiency of hemicellulose was low when only using xylanase to treat cornstalk dissolving pulp. The removal efficiency of hemicellulose was high when the cornstalk dissolving pulp treated with alkali extraction followed by xylanase treatment and was more than four times of that only using xylanase. It was also shown in Table 3.18,

Table 3.18 Components of degraded products from low-alpha cornstalk long fiber dissolving pulp treated with alkali extraction and xylanase treatment (g/l)

Treatment	Cellobiose	Glucose	Xylose	Arabinose	Removal efficiency of hemicellulose (%)	Removal efficiency of total sugars (%)
X	0.0305	0.0740	0.1070	0	0.357	0.705
A–X	0.0654	0.1322	0.4649	0	1.550	2.208

Note X was the xylanase treatment; A–X was the cool alkali extraction followed by xylanase treatment. Removal efficiency of hemicelluloses = $(C_{Xylose} + C_{Arabinose})/C_{Pulp}$. Removal efficiency of total sugars = $(C_{Cellobiose} + C_{Glucose} + C_{Xylose} + C_{Arabinose})/C_{Pulp}$. Cellobiose was the cellobiose concentration (g/l). C_{Glucos}e was the glucose concentration (g/l)
C_{Xylose} was the xylose concentration (g/l). $C_{Arabinose}$ was the arabinose concentration (g/l). C_{Pulp} was the dissolving pulp concentration (30 g/l)
Reprinted from Ref. [58]. Copyright 2012, with permission from Elsevier

the xylanase used in this study contained the cellulase activity, and the cellulase activity removed the cellulose with low degree of polymerization, which had the reverse effect similar to hemicelluloses affecting the degree of swelling of pulp, xanthation reaction, and other required characteristics in the viscose process [132]. As shown in Tables 3.15 and 3.17, after the synergistic effect of alkali extraction and xylanase treatment, the resulting cornstalk pulp had a high α-cellulose content up to 97.10%, low hemicelluloses, lignin and ash content (2.86%, 0.37%, 0.10%, respectively), the brightness was up to 82.29%, and the dynamic viscosity was decreased to 14.47 mPa·s. The α-cellulose content was up to 97.10%, therefore the low-alpha cornstalk dissolving pulp was upgraded to high-alpha cornstalk dissolving pulp by the synergistic effect of alkali extraction and xylanase treatment.

The fiber cells surface morphology of the cornstalk pulps was studied by cool field emission scanning electron microscopy (FE-SEM). The fiber cells surface of bleached cornstalk kraft pulp appeared relatively rough and uneven, and the primary cell wall was not destroyed completely, only little secondary cell wall was exposed. After alkali extraction, the primary cell wall of fiber cells was removed almost, and the major part of the secondary cell wall was exposed. But there showed a fibrillation from the surface in certain regions of the fiber cells. After xylanase (containing cellulase activity) treatment, the fibrillar material was eliminated completely. The secondary cell wall was exposed completely, and the microfiber orientation parallelled to the fiber axis direction. This modified surface let to a greater accessibility to reagents and therefore an enhancement of cellulose reactivity [121].

The diffraction peaks of cellulose I appear at 2θ about 16.3°, 22.6°, 34.8°, and for cellulose II they appear at 2θ about 12.1°, 19.8°, and 22.0° [129]. Cellulose I has a parallel chain orientation, but the chains are antiparallel in cellulose II, which can be converted from cellulose I by strong alkali treatment or by cellulose regeneration. X-ray diffractograms were taken for cornstalk dissolving pulps with different treatment. The bleached cornstalk kraft pulp and the alkali-treated cornstalk

dissolving pulp were also assigned to cellulose I, although they were both subjected to alkali treatment (the alkali content was 2% in kraft pulping process, and 9% in alkali extraction process), it inferred that the low concentration of alkali was not enough to convert the cellulose crystalline types. But when the cornstalk dissolving pulp was subjected to 17.5% alkali treatment (the first step for preparing viscose), the cellulose I was converted to cellulose II.

The yields of cornstalk or cornstalk pulps at each step were listed in Table 3.15. After steam explosion and water washing, 69.22% hemicellulose was removed. The hemicellulose reduced and cellulose was concentrated in steam-exploded cornstalk, resulting in the high yield of 57.66% kraft pulp in the kraft pulping process. After a series of treatment, the yields of low-alpha cornstalk dissolving pulp and high-alpha cornstalk pulp were 12.44% and 10.11% respectively. In comparison to the 30–35% yields of wood dissolving pulp, the yield of cornstalk dissolving pulp was lower. Therefore, the integrated refinery of cornstalk different fractions was necessary. Many works about the conversion of cornstalk different fractions into potential products industrially have been done by our group. For example, the hemicellulose extracted from steam-exploded agriculture residues was used to produce single cell protein, microbial oil, xylose, xylitol, and furfural. Acid precipitated lignin was used to produce adhesive without formaldehyde and replace partial phenolic to manufacture phenolic resin. The short fiber fraction was used to build sugar platform by enzyme hydrolysis, or produce cellulase by solid-state fermentation. All these can increase revenue and reduce the production cost of cornstalk dissolving pulp [26, 133, 134].

Due to the disadvantages of cornstalk as fiber materials to manufacture dissolving pulp industrially, such as poor homogeneity, and high hemicellulose and ash content, the patented combination pretreatment technology of steam explosion and mechanical carding was used to fractionate cornstalk long fiber. The cornstalk long fiber is uniform with low hemicellulose and ash content, which can be used to manufacture cornstalk dissolving pulp. The prepared cornstalk dissolving pulp has high pure cellulose with high viscosity, which can meet the qualities of dissolving pulps required for the different end products. The chapter provides a feasible process to manufacture cornstalk dissolving pulp commercially.

3.4.2 Novel Two-Step Steam Explosion Improving Fermentable Feedstock Utilization

The effects of inhibitors on subsequent fermenting microorganisms have become one of the main bottlenecks for lignocellulose bioconversion processes. Effective measures must be taken to reduce or to eliminate the inhibitors. A number of detoxification methods have been proposed to transform inhibitors into inactive compounds or to reduce their concentration [36]. For example, specific enzymes (laccase and peroxidase enzymes) or microorganisms were used to perform

oxidative polymerization of low-molecular-weight phenolic compounds [135]. Physical detoxification methods include vacuum drying enrichment, activated carbon adsorption, ion exchange adsorption, and so on [36, 136]. Chemical methods include the use of various alkali (e.g., NH_4OH and NaOH) and excess lime to treat hydrolysates [36, 136]. In addition, water washing of pretreated materials is a simple and commonly used method for detoxification [137]. A combination of two or more kinds of methods can achieve better detoxification effects [134, 135].

Additional detoxification steps will generally add cost burdens and complexity to the process and generate additional waste products [135, 138]. Screening of highly resistant strain, which promotes tolerance to high concentration of fermenting inhibitors, is regarded as a practical method [139–142]. Genetic engineering is not a proposal based on the generation and nature of inhibitors, and it could not prevent formation of inhibitors. Therefore, the most fundamental method of reducing inhibitors is to optimize the hydrolysis process and control inhibitor formation from the origin [36, 135].

Lignocellulosic material possesses the characteristics of a complex, heterogeneous, and multi-level structure. From the cell composition perspective, it includes fiber cells and parenchyma cells (including catheters, thin-walled cells, and epidermal cells). Different pretreatment conditions are required due to the differences in structure and in morphology between the two cell types. Fiber cells, with high degree of lignification and compact structure, have high heat and mass transfer resistance and are hard to break. On the other hand, thin-walled cells are sensitive to heat and mass transfer and are easily torn physically. Pretreatment conditions for the different tissues and cells should be optimized accordingly to achieve the best hydrolysis effect and to minimize simultaneously side reactions. This suggests two-step steam explosion pretreatment, with the first step performed under mild conditions to hydrolyze parenchyma cells and fiber cells, and the second step, where just difficult-to-hydrolyze fiber cells from the first step is pretreated again under normal conditions to increase the enzymatic hydrolyzation and reduce the generation and concentration of inhibitors.

In literatures [140, 141, 143–145], two-step steam explosion pretreatment, with the first step performed at low severity to hydrolyze the hemicellulose and the second step, where the solid material from the first step is pretreated again, at higher severity, can result in higher sugar yields than one-step steam pretreatment. In the present study, two-step steam explosion combined with an intermediate separation of fiber cells (ISFC) was proposed to optimize fermentation of corn straw hydrolysates. The conditions in the first pretreatment step were chosen to give a high recovery of hemicellulose-derived fermentable sugars and a low conversation of inhibitors in the liquid. In the second step, fiber cells from the first step with an intermediate separation by a separation device were pretreated again under normal conditions to enhance the enzymatic digestibility. The two-step steam explosion combined with ISFC process was optimized with respect to the total inhibitor conversion, enzymatic hydrolyzation of materials, and conversion ratio of 2,3-butanediol (2,3-BD).

3.4.2.1 Feasibility Analysis of Two-Step Steam Explosion with ISFC Process

The pretreatment conditions and utilization approaches of different tissues and cells vary because of their heterogeneity in natural lignocellulosic materials [28]. In the steam explosion process, the steam penetration (steam as solvent in high-temperature cooking as well as power source for physical tearing) and tear resistance of cells both affect the steam explosion. Except for external factors, such as chip size and packing coefficient of materials, the cell wall thickness and size of cell lumen are the main factors that affect steam infiltration. Cell wall thickness is also a major factor in resisting cell tear. In view of the differences in morphology and structure between fiber cells with thick wall and small lumen and thin-walled cells with thin wall and large lumen, steam infiltration in parenchyma cells is easier than that in fiber cells, and parenchyma cells are torn easily.

As is shown in Fig. 3.27a, in the holding pressure process, the rehydration performance is different between fiber cells and parenchyma cells. The rehydration capacity of parenchyma cells is larger than that of fiber cells because parenchyma cells have a larger absorption amount and reach the equilibrium point earlier than fiber cells. Figure 3.27b shows that the moisture content of materials pretreated by steam explosion is different. The moisture content in parenchyma cells is higher than that in fiber cells. Figure 3.27 shows that because of the differences in morphology and structure between fiber cells and parenchyma cells, the steam infiltration varies. In addition, steam, the heat carrier, and power source in the steam explosion process, will certainly affect the degradation and tear of fiber cells and parenchyma cells. Therefore, in the case where the whole corn straw is considered as raw material and the classification and heterogeneity of the tissues are not considered, the raw material is bound to intensify steam explosion conditions, resulting in high hemicellulose degradation yield, high increasing rate of the surface

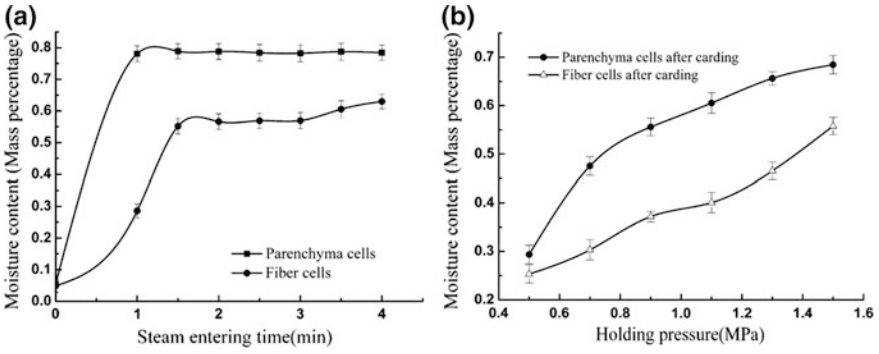

Fig. 3.27 Comparison of the fiber cells and parenchyma cells rehydration rates in the steam explosion process: **a** moisture content of fiber cells and parenchyma cells at different holding time and **b** moisture content of fiber cells and parenchyma cells after steam explosion and ISFC process [50]

area, and low raw material entrainment yield. The parenchyma cells will be excessively degraded in this situation, increasing the possibility of inhibitor generation.

Therefore, fiber cells and parenchyma cells should be pretreated under appropriate steam explosion conditions to achieve the best pretreatment effect for both. In Fig. 3.27, the steam explosion technology contributes to the uniform rehydration of fiber cells and parenchyma cells. Jin and Chen reported that steam explosion helps improve fiber cells and parenchyma cells separation. In the novel method proposed in the present chapter, the first-step steam explosion under milder condition aims to attain uniform rehydration [133]. Based on the principle of weight classification on centrifugal air classifier, fiber cells with low moisture content can be separated from parenchyma cells with high moisture content. The separated fiber cells will then be pretreated under appropriate conditions by steam explosion. Through this new method, enzymatic hydrolyzation of fiber cells will increase, and the parenchyma cells will not be excessively degraded, which is beneficial not only to improve the pretreatment effect but also to reduce inhibitor content. Therefore, the design of the method is reasonable and practical.

3.4.2.2 Effects of Two-Step Steam Explosion with ISFC Process on Inhibitor Content

As is shown in Fig. 3.28, the inhibitor content in parenchyma cells is larger than that in fiber cells after the first-step steam explosion and ISFC process. The inhibitor content in FSSEM with no ISFC process is in the middle, indicating that under the same steam explosion conditions, the degree of degradation of parenchyma cells is larger than that of fiber cells. Hence, the structural heterogeneity of lignocellulosic material determines the difference and selectivity of its pretreatment conditions, which also indicates the necessity of classification and selection of pretreatment for the lignocellulosic material. In the second-step steam explosion, except for the inhibitor content of 1.5 MPa in one group that is higher than the PCG (1.2 MPa/8 min), the inhibitor content in the other groups are lower than the PCG, with the lowest at 1.1 MPa. This result arises because fiber cells and parenchyma cells achieve the best separation (the separation degree is shown in Fig. 3.29) at 1.1 MPa. In this situation, the content of the thin-walled cells of the materials, which participates in the second-step steam explosion, is the lowest, resulting in the lowest inhibitor content. From 0.5 to 0.9 MPa, the inhibitor content gradually increases. Material degradation yield and the by-products increase with increasing steam explosion strength. From 0.5 to 0.9 MPa, the fiber cells and the parenchyma cells fail to achieve a good separation. From 1.3 to 1.5 MPa, although the fiber cell and parenchyma cell separation is good, the intensity is too severe, thus increasing the inhibitor content. Figure 3.28 and 3 show that under 1.1 MPa/4 min-ISFC^{-1}.2 MPa/4 min conditions, where the separation degree of the corn stalks is 1.6, the inhibitor conversion is the lowest at 0.0397. In Fenske et al. research, total phenols conversion of corn stalk was 0.11 by acid steaming

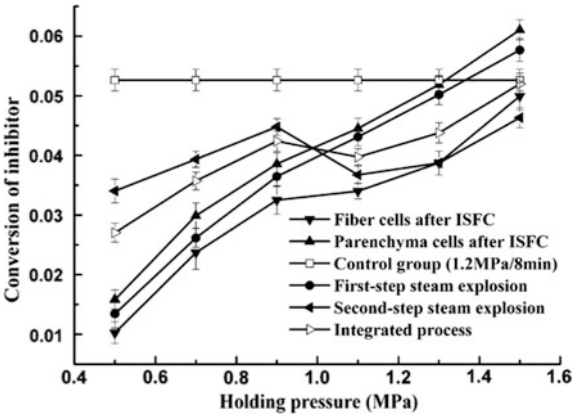

Fig. 3.28 Effects of different steam explosion processes on inhibitor conversion [50]

pretreatment (180 °C, 1% (w/w) H_2SO_4, 1 min) [29]. Du et al. reported that total inhibitor conversion of corn stalk were 0.067 and 0.0473 by 0.7% H_2SO_4 and wet oxidation at 180 °C for 8 min, respectively [30]. The inhibitor conversions in their works were higher than the two-step steam explosion with ISFC process, which may be due to pretreatment conditions adopted by them were more severe than ours and the materials were not fractionated.

3.4.2.3 Effects of Two-Step Steam Explosion with ISFC Process on Enzymatic Hydrolyzation

As is shown in Fig. 3.30, the parenchyma cell enzymatic hydrolyzation is larger than that of the fiber cells after the first-step steam explosion and ISFC process. The enzymatic hydrolyzation of FSSEM with no ISFC process is in the middle, which indicates that under the same conditions of steam explosion, the degree of degradation of parenchyma cells is larger than that of fiber cells. In the first-step steam explosion, from 1.1 to 1.5 MPa, the enzymatic hydrolyzation of all materials is higher than that of the control group. In the second-step steam explosion, except for the group with 0.5 MPa, the enzymatic hydrolyzation of the other groups are higher than that of the control group. With the increase in steam explosion intensity, the enzymatic hydrolyzation likewise shows an increasing trend. It can be seen from Fig. 3.28–4 that the optimal condition for the steam explosion process is from 1.1 MPa/4 min-ISFC–1.2 MPa/4 min. In this case, the fibrous tissue can be moderately degraded, whereas the parenchyma cell can avoid excessive degradation. Inhibitors are consequently produced when the pretreatment reaches the lowest. Compared with the PCG (1.2 MPa/8 min), the enzymatic hydrolyzation of MIP under optimal conditions is 74.35%, which increases by 12.82%.

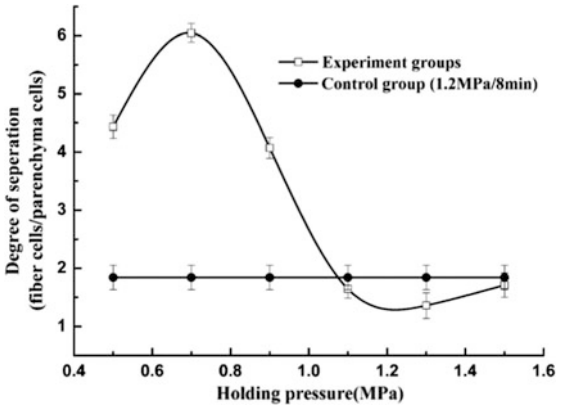

Fig. 3.29 Degree of separation of different steam explosion conditions [50]

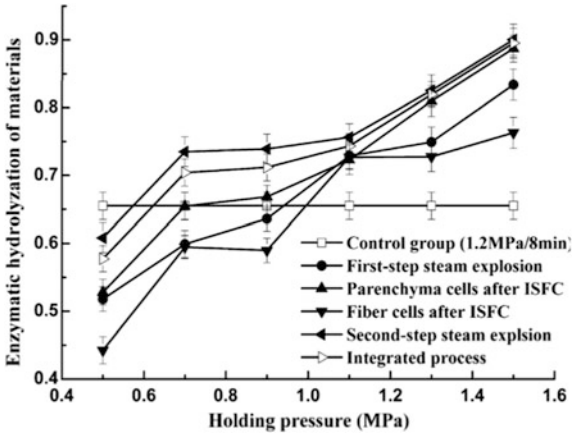

Fig. 3.30 Effects of different steam explosion with ISFC process on enzymatic hydrolyzation [50]

3.4.2.4 Effects of Two-Step Steam Explosion with ISFC Process on the Conversion Ratio of 2, 3-BD

As shown in Fig. 3.31, the inhibitor conversion is the lowest and the concentration of 2,3-BD is the highest in the experimental group (1.1 MPa/4 min-ISFC-1.2 MPa/4 min). Compared with the PCG (1.2 MPa/8 min), the inhibitor conversion in the experimental group is lower by 33%, and the content of the fermentation product 2, 3-BD increases by 209%. Compared with the FCG, which employs glucose as the sole carbon source, the content of 2, 3-BD in the experimental group is higher than that in the fermentation control group. However, the 2, 3-BD content in the other groups is lower than that in the FCG. Thus, the inhibitors generated (1.75 g/L)

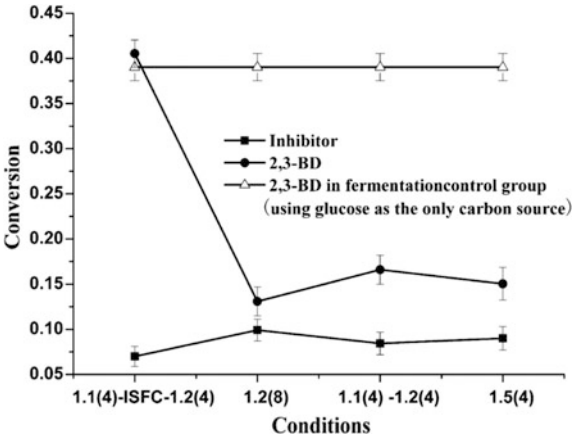

Fig. 3.31 Effects of the two-step steam explosion with ISFC process on the conversion ratio of 2, 3-BD (1.1(4)-ISFC-1.2(4) is the experimental group, and the others are the control groups) [50]

under the experimental group conditions do not inhibit the production of 2, 3-BD but promote its conversion. Meanwhile, the inhibitors in all the other groups, which contents are larger than 1.75 g/L, inhibit the conversion of 2, 3-BD.

The two-step steam explosion with ISFC process was developed because of lignocellulosic materials with structural heterogeneity producing inhibitors for fermenting microorganisms under uniform pretreatment conditions. This process is beneficial not only in achieving a moderate degradation of fiber cells but also in avoiding excessive degradation of parenchyma cells, where the generation of inhibitors can be controlled from the origin and detoxification unit operations can be omitted. In addition, the two-step steam explosion with ISFC process, which separates the fiber cells from the parenchyma cells, provides a new way for multi-level conversion of lignocellulosic resources.

3.4.3 Establishment of Fermentable Feedstock Refinery Platform Based on Steam Explosion Technology

Due to heterogeneity of biomass and the limitation of steam explosion, it is hard to effectively separate the three main components of biomass. At the component level, steam-explosion-solvent extraction pretreatment technology was established for fractionation of cellulose, hemicellulose, and lignin and other main component. This technology includes steam explosion and ethanol extraction composed pretreatment, steam explosion and high boiling solvent composed pretreatment, steam explosion and ironic liquid composed pretreatment and steam explosion and

alkaline hydrogen peroxide combined pretreatment. At the cellular level, steam explosion and wet shattering combined pretreatment technology was established for fractionation. At the organization level, the author combined two-step steam explosion with combing technology for fractionation of fibrous tissue and parenchyma. All above technologies are composed pretreatment system based on steam explosion. By combining the system and transformation of intermediates and purification, we build a refining platform which takes SE technology as a core. And through this platform, we developed a set of cost-effective biorefinery technologies which can be adjusted to some different products like bio-based energy, bio-based chemicals, bio-based material and other bio-based products.

According to the above theories, the author integrated technology and equipment and multidiscipline to establish a poly-generation industrial chain which takes straw as the raw material. The products cover bio-based energy, bio-based chemicals, bio-based materials and other bio-based products, including butanol acetone and ethanol. At present, the author has built a number of multiproducts refining industry chains in Shandong, Jilin, Henan, Jiangxi, Hubei, and other places and cost-effective and large-scale biomass industry which brought good economic and social benefits to the local. These industry chains successfully verified the practical guiding role of anti-seepage and verified the rationality and reliability of taking biomass as raw materials to produce bio-based energy, bio-based chemicals, and bio-based materials. In September 2010, the author collaborated with Jilin Laihe limited company and installed a "300 thousand tons straw biomass refining industry production line". It is the world's first large-scale production line with economic benefits. The production line abandoned the traditional ideas which degraded the straw into the reducing sugar and then be fermented into butanol. The author takes advantages of the fact that fermentation strains of butanol can use pentose. This technology makes full use of straw to produce butanol hemicellulose, and at the same time, it also produced a new kind of raw material for high-purity lignin, cellulose and other excellent biomass chemical or biological materials, finally produced organic acid, furfural, pulp, polyether polyol, protein feed, microcrystalline cellulose and other products. The capacity of the production line is 50 thousand tons of solvent including butanol, acetone, and ethanol. Lignin and cellulose in straw were separated by fractionation, which produces 30 thousand tons of high-purity lignin (producing 20 thousand tons of phenolic resin adhesive) and 12 million tons of high-purity cellulose (producing 50,000 tons of bio-polyether polyols). This created new straw refining industrial model which use steam explosion technology to produce hemicellulose, long fiber, and lignin and use multicellular enzyme to hydrolyze this carbon source. What is more, it broke through the technical and economic problems that have hindered the biomass industry for a long time.

References

1. Chen HZ, Sui WJ (2015) Problems of biomass refining engineering: anti-seepage. Biotechnol Bus 3:69–76
2. Cho HM, Gross AS, Chu JW (2011) Dissecting force interactions in cellulose deconstruction reveals the required solvent versatility for overcoming biomass recalcitrance. J Am Chem Soc 133:14033–14041
3. Himmel ME, Ding SY, Johnson DK et al (2007) Biomass recalcitrance: engineering plants and enzymes for biofuels production. Science 315:804–807
4. Pu YQ, Hu F, Huang F et al (2013) Assessing the molecular structure basis for biomass recalcitrance during dilute acid and hydrothermal pretreatments. Biotechol Biofuels 6:1–13
5. Ding SY, Liu YS, Zeng YN et al (2012) How does plant cell wall nanoscale architecture correlate with enzymatic digestibility. Science 338:1055–1060
6. Meng X, Ragauskas AJ (2014) Recent advances in understanding the role of cellulose accessibility in enzymatic hydrolysis of lignocellulosic substrates. Curr Opin Biotech 27:150–158
7. Liu L, Qian C, Jiang L et al (2014) Direct three-dimensional characterization and multiscale visualization of weat straw deconstruction by white rot fungus. Environ Sci Techol 48:9819–9825
8. Chan CH, Yusoff R, Ngoh GC (2014) Modeling and kinetics study of conventional and assisted batch solvent extraction. Chem Eng Res Des 92:1169–1186
9. Zhao JY, Chen HZ (2013) Correlation of porous structure, mass transfer and enzymatic hydrolysis of steam-exploded corn stover. Chem Eng Sci 104:1036–1044
10. Chundawat SPS, Donohoe BS, da Costa Sousa L et al (2011) Multi-scale visualization and characterization of lignocellulosic plant cell wall deconstruction during thermochemical pretreatment. Energ Environ Sci 4:973–984
11. Ciesielski PN, Matthews JF, Tucker M et al (2013) 3D electron tomography of pretreated biomass informs atomic modeling of cellulose microfibrils. ACS Nano 7:8011–8019
12. Yu MG, Xu P, Zhou MQ et al (2014) Fractal porous media transport. Science Press, Beijing
13. Zhao YS (2010) Multi field coupling of porous media and its engineering response. Science Press, Beijing
14. Alvira P, Tomás-Pejó Ballesteros M et al (2010) Pretreatment technolo1es for an efficient bioethanol production process based on enzymatic hydrolysis: a review. Bioresour Technol 101:485l–486l
15. Chen HZ, Li GH, Li HQ (2014) Novel pretreatment of sream explosion associated with ammonium chloride preimpregnation. Bioresour Technol 153:154–159
16. Deindoerfer FH (1957) Calculation of heat sterilization times for fermentation media. Appl Microbiol 5(4):221
17. Liu XL, Zhou WR, Wu YH et al (2013) Effect of sterilization process on surface characteristics and biocompatibility of pure Mg and MgCa alloys. Mat Sci Eng C 33 (7):4144–4154
18. Pandey A (2003) Solid-state fermentation. Biochem Eng J 13(2):81–84
19. Li GH, Chen HZ (2014) Synergistic mechanism of steam explosion combined with fungal treatment by Phellinus baumii for the pretreatment of corn stalk. Biomass Bioenerg 67 (11):1–7
20. Liu L, Zhuang DF, Jiang D et al (2013) Assessment of the biomass energy potentials and environmental benefits of *Jatropha curcas* L. in Southwest China. Biomass Bioenerg 56 (5):342–350
21. Zhang RX, Xue G, Zhang CJ et al (2007) A device for discharging of spherical digester used in pulping. China Patent 200720079330. X
22. Lund D (1988) Effects of heat processing on nutrients. In: Karmas E, Harris RS (eds) Nutritional evaluation of food processing. Springer, Netherlands, pp 319–354

23. Mann A, Kiefer M, Leuenberger H (2001) Thermal sterilization of heat-sensitive products using high-temperature short-time sterilization. J Pharm Sci 90(3):275–287
24. Mei LH, Yao SJ, Lin DQ (1999) Biochemical production and processes. Science Press, Beijing
25. Kjellstrand P, Martinson E, Wieslander A (1995) Development of toxic degradation products during heat sterilization of glucose-containing fluids for peritoneal dialysis: influence of time and temperature. Periton Dial Int 15(1):26–32
26. Chen HZ, Liu LY (2007) Unpolluted fractionation of wheat straw by steam explosion and ethanol extraction. Bioresour Technol 98(3):666–676
27. Liu ZH, Qin L, Jin MJ (2013) Evaluation of storage methods for the conversion of corn stover biomass to sugars based on steam explosion pretreatment. Bioresour Technol 132:5–15
28. Chen HZ, Li HQ, Liu LY (2011) The inhomogeneity of corn stover and its effects on bioconversion. Biomass Bioenerg 35(5):1940–1945
29. Fenske JJ, Griffin DA, Penner MH (1998) Comparison of aromatic monomers in lignocellulosic biomass prehydrolysates. J Ind Microbiol Biotechnol 20(6):364–368
30. Du B, Sharma LN, Becker C et al (2010) Effect of varying feedstock–pretreatment chemistry combinations on the formation and accumulation of potentially inhibitory degradation products in biomass hydrolysates. Biotechnol Bioeng 107(3):430–440
31. Heitz M, Capekmenard E, Koeberle PG et al (1991) Fractionation of Populus tremuloides at the pilot plant scale: optimization of steam pretreatment conditions using the STAKE II technology. Bioresour Technol 35(1):23–32
32. Iroba KL, Tabil LG, Sokhansanj S et al (2014) Pretreatment and fractionation of barley straw using steam explosion at low severity factor. Biomass Bioenerg 66(7):286–300
33. Overend RP, Chornet E, Gascoigne JA (1987) Fractionation of lignocellulosics by steam-aqueous pretreatments. Philos T R Soc A 321(1561):523–536
34. Zhu SM, Naim F, Marcotte M et al (2008) High-pressure destruction kinetics of Clostridium sporogenes spores in ground beef at elevated temperatures. Int J Food Microbiol 126(1–2):86–92
35. Rajan S, Pandrangi S, Balasubramaniam VM et al (2006) Inactivation of Bacillus stearothermophilus spores in egg patties by pressure-assisted thermal processing. LWT-Food Sci Technol 39(8):844–851
36. Palmqvist E, Hahn-Hagerdal B (2000) Fermentation of lignocellulosic hydrolysates. II: inhibitors and mechanisms of inhibition. Bioresour Technol 74(1):25–33
37. Wang L, Chen HZ (2011) Increased fermentability of enzymatically hydrolyzed steam-exploded corn stover for butanol production by removal of fermentation inhibitors. Process Biochem 46(2):604–607
38. Negro MJ, Alvarez C, Ballesteros I et al (2014) Ethanol production from glucose and xylose obtained from steam-exploded water-extracted olive tree pruning using phosphoric acid as catalyst. Bioresour Technol 153(153C):101–107
39. Wang LP, Shen QR, Yu GH et al (2012) Fate of biopolymers during rapeseed meal and wheat bran composting as studied by two-dimensional correlation spectroscopy in combination with multiple fluorescence labeling techniques. Bioresour Technol 105 (2):88–94
40. Nada AAM, Yousef MA, Shaffei KA et al (1998) Infrared spectroscopy of some treated lignins. Polym Degrad Stabil 62(1):157–163
41. Wang GH, Chen HZ (2014) Carbohydrate elimination of alkaline-extracted lignin liquor by steam explosion and its methylolation for substitution of phenolic adhesive. Ind Crop Prod 53(53):93–101
42. Fu XM, Zhao SM, Liang YX et al (2010) The optimization of solid-state fermentation process for high-yield spore production of a feeding bacillus subtilis. Feed Ind 22:014
43. Joshi S, Bharucha C, Desai AJ (2008) Production of biosurfactant and antifungal compound by fermented food isolate Bacillus subtilis 20B. Bioresour Technol 99(11):4603–4608

44. Langan P, Petridis L, O'Neill HM et al (2014) Common processes drive the thermochemical pretreatment of lignocellulosic biomass. Green Chem 16(1):63–68
45. Pei JX, Ping QW, Tang AM et al (2012) Chemistry of plant fiber. China Light Industry Press, Beijing
46. Chen HZ (2013) Steam explosion technology and biomass refinery. Chemical Industry Press, Beijing
47. Chen HZ, Qiu WH, Wang L (2014) Selective separation of biomass raw materials-functional economic utilization. Eng Sci 16(3):27–36
48. Chen HZ, Liu ZH (2014) Multilevel composition fractionation process for high-value utilization of wheat straw cellulose. Biotechnol Biofuels 7(1):137
49. Chen HZ, Liu ZH (2015) Steam explosion and its combinatorial pretreatment refining technology of plant biomass to bio-based products. Biotechnol J 10(6):866–885
50. Zhang YZ, Fu XG, Chen HZ (2012) Pretreatment based on two-step steam explosion combined with an intermediate separation of fiber cells-optimization of fermentation of corn straw hydrolysates. Bioresour Technol 121(2):100–104
51. Alvira P, Tomás-Pejó E, Ballesteros M et al (2010) Pretreatment technologies for an efficient bioethanol production process based on enzymatic hydrolysis: a review. Bioresour Technol 101(13):4851–4861
52. Chen HZ, Liu ZH (2014) Multilevel composition fractionation process for highvalue utilization of wheat straw cellulose. Biotechnol Biofuels 7(1):137
53. Liu ZH, Chen HZ (2015) Xylose production from corn stover biomass by steam explosion combined with enzymatic digestibility. Bioresour Technol 193(OCT):345–356
54. Sui WJ, Chen HZ (2015) Study on loading coefficient in steam explosion process of corn stalk. Bioresour Technol 179C:534–542
55. Selig MJ, Thygesen LG, Felby C (2014) Correlating the ability of lignocellulosic polymers to constrain water with the potential to inhibit cellulose saccharification. Biotechnol Biofuels 7(1):159
56. Selig MJ, Hsieh CWC, Thygesen LG et al (2012) Considering water availability and the effect of solute concentration on high solids saccharification of lignocellulosic biomass. Biotechnol Prog 28(6):1478–1490
57. Berry SL, Roderick ML (2005) Plant-water relations and the fibre saturation point. New Phytol 168(1):25–37
58. Sun BH, Wang MX (2012) Research on the moisture state and mobility in wood during microwave drying by LF-NMR. J Inner Mong Agric Univ 33:205–210
59. Browning BL (1963) The chemistry of wood. Interscience, New York, USA, pp 405–439
60. Stamm AJ (1964) Wood and cellulose science. In: Wood and cellulose science. Ronald, New York
61. Engelund ET, Thygesen LG, Svensson S et al (2013) A critical discussion of the physics of wood-water interactions. Wood Sci Technol 47(1):141–161
62. Tsuchida JE, Rezende CA, de Oliveira-Silva R et al (2014) Nuclear magnetic resonance investigation of water accessibility in cellulose of pretreated sugarcane bagasse. Biotechnol Biofuels 7(1):127
63. Panshin AJ, Zeeuw CD (1980) Text book of wood technology. Mc Graw-Hill Book Co, New York
64. Christensen GN, Kelsey KE (1965) The sorption of water vapor by the constituents of wood. Forest Products Laboratory
65. Roderick ML, Berry SL (2001) Linking wood density with tree growth and environment: a theoretical analysis based on the motion of water. New Phytol 149(3):473–485
66. Sui WJ, Chen HZ (2014) Multi-stage energy analysis of steam explosion process. Chem Eng Sci 116(40):254–262
67. Brownell HH, Yu EKC, Saddler JN (1986) Steam explosion pretreatment of wood: Effect of chip size, acid, moisture content and pressure drop. Biotechnol Bioeng 28(6):792–801

68. Ferreira LC, Nilsen PJ, Fdz-Polanco F et al (2014) Biomethane potential of wheat straw: influence of particle size, water impregnation and thermal hydrolysis. Chem Eng J 242 (8):254–259
69. Cullis IF, Saddler JN, Mansfield SD (2004) Effect of initial moisture content and chip size on the bioconversion efficiency of softwood lignocellulosics. Biotechnol Bioeng 85(4):413–421
70. Kumar L, Chandra R, Saddler J (2011) Influence of steam pretreatment severity on post-treatments used to enhance the enzymatic hydrolysis of pretreated softwoods at low enzyme loadings. Biotechnol Bioeng 108(10):2300–2311
71. DeMartini JD, Pattathil S, Miller JS et al (2013) Investigating plant cell wall components that affect biomass recalcitrance in poplar and switchgrass. Energy Environ Sci 6(3):898–909
72. Vivekanand V, Olsen EF, Eijsink VGH et al (2013) Effect of different steam explosion conditions on methane potential and enzymatic saccharification of birch. Bioresour Technol 127(1):343–349
73. Ballesteros I, Oliva JM, Navarro AA et al (2000) Effect of chip size on steam explosion pretreatment of softwood. Appl Biochem Biotech 84–86(1):97–110
74. Ballesteros I, Oliva JM, Negro MJ et al (2002) Enzymatic hydrolysis of steam-exploded herbaceous agricultural waste (Brassica carinata) at different particule sizes. Process Biochem 38(2):187–192
75. Yu ZD, Zhang BL, Yu FQ et al (2012) A real steam explosion: the requirement of steam explosion pretreatment. Bioresour Technol 121(121):335–341
76. Wang BG, Liu SY, Huang WG (2005) Gas dynamics. Beijing Institute of Technology Press, Beijing
77. Monavari S, Galbe M, Zacchi G (2009) Impact of impregnation time and chip size on sugar yield in pretreatment of softwood for ethanol production. Bioresour Technol 100(24):6312–6316
78. Foody P (1982) Steam explosion as a pretreatment for biomass conversion. Final Report to Midwest Research Institute. Solar Energy Division, Kansas City
79. Macıas-Sánchez MD, Mantell C, Rodrıguez M et al (2005) Supercritical fluid extraction of carotenoids and chlorophyll a from *Nannochloropsis gaditana*. J Food Eng 66(2):245–251
80. Ewanick S, Bura R (2011) The effect of biomass moisture content on bioethanol yield from steam pretreated switchgrass and sugarcane bagasse. Bioresour Technol 102(3):2651–2658
81. Tan Z, Wang C, Yi Y et al (2014) Extraction and purification of chlorogenic acid from ramie (*Boehmeria nivea* L. Gaud) leaf using an ethanol/salt aqueous two-phase system. Sep Puri Technol 132(132):396–400
82. Memon AA, Memon N, Bhanger MI et al (2010) Micelle-mediated extraction of chlorogenic acid from *Morus laevigata* W. leaves. Sep Puri Technol 76(2):179–183
83. Karabegović IT, Stojičević SS, Veličković DT et al (2013) Optimization of microwave-assisted extraction and characterization of phenolic compounds in cherry laurel (*Prunus laurocerasus*) leaves. Sep Puri Technol 120:429–436
84. Azmir J, Zaidul ISM, Rahman MM et al (2013) Techniques for extraction of bioactive compounds from plant materials: a review. J Food Eng 117(4):426–436
85. Dai J, Mumper RJ (2010) Plant phenolics: extraction, analysis and their antioxidant and anticancer properties. Molecules 15(10):7313–7352
86. Guihua S, Quancheng Z (2008) Ultrasonic-assisted extraction of oxymatrine from Sophorae tonkinesis. Trans Chin Soc Agric Eng 24(3):291–294
87. Kerem Z, German-Shashoua H, Yarden O (2005) Microwave-assisted extraction of bioactive saponins from chickpea (*Cicer arietinum* L). J Sci Food Agric 85(3):406–412
88. Xiao X, Song W, Wang J, Li G (2012) Microwave-assisted extraction performed in low temperature and in vacuo for the extraction of labile compounds in food samples. Anal Chim Acta 712(2):85–93
89. Xu JK, Li MF, Sun RC (2015) Identifying the impact of ultrasound-assisted extraction on polysaccharides and natural antioxidants from Eucommia ulmoides Oliver. Process Biochem 50(3):473–481

90. Liu CM, Zhu JJ, Zhang SQ et al (2005) Study on extraction total flavonoids in Epimedium koreanum using high pressure technology. China J Chin Mater Med 30(19):1511–1513
91. Pongnaravane B, Goto M, Sasaki M et al (2006) Extraction of anthraquinones from roots of Morinda citrifolia by pressurized hot water: Antioxidant activity of extracts. J Supercit Fluid 37(3):390–396
92. Bakowska A, Kucharska AZ, Oszmiański J (2003) The effects of heating, UV irradiation, and storage on stability of the anthocyanin–polyphenol copigment complex. Food Chem 81 (3):349–355
93. Mussatto SI, Ballesteros LF, Martins S (2011) Extraction of antioxidant phenolic compounds from spent coffee grounds. Sep Puri Technol 83(1):173–179
94. Xu JG, Hu QP, Liu Y (2012) Antioxidant and DNA-protective activities of chlorogenic acid isomers. J Agric Food Chem 60(46):11625–11630
95. Ong KW, Hsu A, Tan BKH (2013) Anti-diabetic and anti-lipidemic effects of chlorogenic acid are mediated by ampk activation. Biochem Pharmacol 85(9):1341–1351
96. Wang Z, Clifford MN, Sharp P (2008) Analysis of chlorogenic acids in beverages prepared from Chinese health foods and investigation, in vitro, of effects on glucose absorption in cultured Caco-2 cells. Food Chem 108(1):369–373
97. Chai X, Wang Y, Su Y et al (2012) A rapid ultra performance liquid chromatography–tandem mass spectrometric method for the qualitative and quantitative analysis of ten compounds in Eucommia ulmodies Oliv. J Pharm Biomed Anal 57(1):52–61
98. Pinelo M, Zornoza B, Meyer AS (2008) Selective release of phenols from apple skin: mass transfer kinetics during solvent and enzyme-assisted extraction. Sep Puri Technol 63(3):620–627
99. Bamba T, Fukusaki EI, Nakazawa Y et al (2002) In-situ chemical analyses of trans-polyisoprene by histochemical staining and Fourier transform infrared microspectroscopy in a rubber-producing plant, Eucommia ulmoides Oliver. Planta 215(6):934–939
100. Sun Z, Li F, Du H et al (2013) A novel silvicultural model for increasing biopolymer production from Eucommia ulmoides Oliver trees. Ind Crop Prod 42(1):216–222
101. Kurosumi A, Sasaki C, Kumada K (2007) Novel extraction method of antioxidant compounds from Sasa palmata (Bean) Nakai using steam explosion. Process Biochem 42 (10):1449–1453
102. Chen G, Chen H (2011) Extraction and deglycosylation of flavonoids from sumac fruits using steam explosion. Food Chem 126(4):1934–1938
103. Yuan YT, Chen HZ (2006) Application of steam explosion in ephedrine extraction. J Chin Pharm Univ 36(5):414–416
104. Gong L, Huang L, Zhang Y (2012) Effect of steam explosion treatment on barley bran phenolic compounds and antioxidant capacity. J Arg Food Chem 60(29):7177–7184
105. Pavlović MD, Buntić AV, Šiler-Marinković SS (2013) Ethanol influenced fast microwave-assisted extraction for natural antioxidants obtaining from spent filter coffee. Sep Purif Technol 118(6):505–510
106. Soria AC, Villamiel M (2010) Effect of ultrasound on the technological properties and bioactivity of food: a review. Trends Food Sci Technol 21(7):323–331
107. Zhang YZ, Chen HZ (2012) Multiscale modeling of biomass pretreatment for optimization of steam explosion conditions. Chem Eng Sci 75(25):177–182
108. Sui W, Chen H (2014) Extraction enhancing mechanism of steam exploded *Radix Astragali*. Process Biochem 49(12):2181–2190
109. Chatain D, Rabkin E, Derenne J et al (2001) Role of the solid/liquid interface faceting in rapid penetration of a liquid phase along grain boundaries. Acta Mater 49(7):1123–1128
110. Li H, Chen H (2008) Detoxification of steam-exploded corn straw produced by an industrial-scale reactor. Process Biochem 43(12):1447–1451
111. Wrolstad RE, Putnam TP, Varseveld GW (1970) Color quality of frozen strawberries: effect of anthocyanin, pH, total acidity and ascorbic acid variability. J Food Sci 35(4):448–452
112. Reddy N, Yang Y (2005) Biofibers from agricultural byproducts for industrial applications. Trends Biotechnol 23(1):22–27

113. Reddy N, Yang Y (2005) Structure and properties of high quality natural cellulose fibers from cornstalks. Polymer 46(15):5494–5500
114. Hurter RW, Eng P (2010) Non-wood fibre-2010 and beyond prospects for non-wood paper production in Asia Pacific. In: Appita Asia symposium
115. Byrd M, Hurter R (2005) A simplified pulping and bleaching process for pithcontaining nonwoods: trials on whole corn stalks. In: 2005 TAPPI engineering, pulping and environmental conference
116. Capretti G (2003) Suitability of non-wood fibres for the paper industry. In: Experimental station for cellulose and paper
117. Saijonkari-Pahkala K (2008) Non-wood plants as raw material for pulp and paper. Agric Food Sci 10(1):1–101
118. Chen HZ, Fu XG (2011) A method and equipment for the fractionation of biomass into long fiber fraction and short fiber fraction in dry condition. China Patent 201110233853.6
119. Patrick K (2011) Dissolving pulp gold rush in high gear. Paper 360:8–12
120. Ma X, Huang LL, Cao S et al (2012) Preparation of bamboodissolving pulp for textile production. Part 2. optimization of pulping conditions of hydrolyzed bamboo and its kinetics. BioResources 7(2):1866–1875
121. Ibarra D, Köpcke V, Larsson PT et al (2010) Combination ofalkaline and enzymatic treatments as a process for upgrading sisal paper-grade pulp to dissolving-grade pulp. Bioresour Technol 101(19):7416–7423
122. Patrick K (2011) Dissolving pulp gold rush in high gear. Paper 360:8–12
123. Saha BC (2003) Hemicellulose bioconversion. J Ind Microbiol Biotechnol 30(5):279–291
124. Ragauskas AJ, Williams CK, Davison BH et al (2006) The path forward forbiofuels and biomaterials. Sci 311(5760):484–489
125. Behin J, Zeyghami M (2009) Dissolving pulp from corn stalk residue and wastewater of Merox unit. Chem Eng J 152(1):26–35
126. Peng XW, Chen HZ (2011) Hemicellulose sugar recovery from steam-exploded wheat straw for microbial oil production. Process Biochem 47(2):209–215
127. Montane D, Farriol X, Salvado J et al (1998) Application of steam explosion to the fractionation and rapid vapor-phase alkaline pulping of wheat straw. Biomass Bioenergy 14 (3):261–276
128. Reddy N, Yang Y (2007) Structure and properties of natural cellulose fibers obtained from sorghum leaves and stems. J Agric Food Chem 55(14):5569–5574
129. Isogai A, Usuda M, Kato T et al (1989) Solid-state CP/MAS carbon- 13 NMR study of cellulose polymorphs. Macromolecules 22(7):3168–3172
130. Tanahashi M (1990) Characterization and degradation mechanisms of wood components by steam explosion and utilization of exploded wood. In: Wood research, vol 79. Bulletin of the Wood Research Institute Kyoto University, pp 49–117
131. Hyatt JA, Fengl RW, Edgar KJ et al (2000) Process for the co-production of dissolving-grade pulp and xylan. US Patent 6,057,438
132. Christov L, Akhtar M, Prior B (1996) Impact of xylanase and fungal pretreatment on alkali solubility and brightness of dissolving pulp. Holzforschung 50(6):579–581
133. Jin SY, Chen HZ (2006) Superfine grinding of steam-exploded rice straw and its enzymatic hydrolysis. Biochem Eng J 30(3):225–230
134. Chen HZ, Qiu WH (2010) Key technologies for bioethanol production from lignocellulose. Biotechnol Adv 28(5):556–562
135. Mussatto SI, Roberto IC (2004) Alternatives for detoxification of diluted-acid lignocellulosic hydrolyzates for use in fermentative processes: a review. Bioresour Technol 93(1):1–10
136. Almeida JRM, Bertilsson M, Gorwa-Grauslund MF et al (2009) Metabolic effects of furaldehydes and impacts on biotechnological processes. Appl Microbiol Biotechnol 82 (4):625–638
137. Yu B, Chen HZ (2010) Effect of the ash on enzymatic hydrolysis of steam-exploded rice straw. Bioresour Technol 101(23):9114–9119

138. Liu ZH, Qin L, Jin MJ et al (2013) Evaluation of storage methods for the conversion of corn stover biomass tosugars based on steam explosion pretreatment. Bioresour Technol 132C (2):5–15
139. Ostergaard S, Olsson L, Nielsen J (2000) Metabolic engineering of Saccharomyces cerevisiae. Microbiol Mol Biol R 64(1):34–50
140. Li H, Zhang X, Shen Y et al (2009) Inhibitors and their effects on Saccharomyces cerevisiae and relevant countermeasures in bioprocess of ethanol production from lignocellulose-a review. Chin J Biotechnol 25(9):1321–1328
141. Li J, Gellerstedt G, Toven K (2009) Steam explosion lignins; their extraction, structure and potential as feedstock for biodiesel and chemicals. Bioresour Technol 100(9):2556–2561
142. Hahn-Hägerdal B, Wahlbom C, Gárdonyi M et al (2001) Metabolic engineering of Saccharomyces cerevisiae for xylose utilization. Metab Eng 73:53–84
143. Tengborg C, Stenberg K, Galbe M et al (1998) Comparison of SO_2 and H_2SO_4 impregnation of softwood prior to steam pretreatment on ethanol production. Appl Biochem Biotechnol 70–72(1):3–15
144. Söderström J, Pilcher L, Galbe M et al (2002) Two-step steam pretreatment of softwood with SO_2 impregnation for ethanol production. Appl Biochem Biotechnol 98–100(1):5–21
145. Brodeur G, Yau E, Badal K et al (2011) Chemical and physicochemical pretreatment of lignocellulosic biomass: A review. Enzyme Res 2011:1–17
146. Zhao ZM, Wang L, Chen HZ (2015) A novel steam explosion sterilization improving solid-state fermentation performance. Bioresource Technol 192(9):547–555
147. Sui WJ, Chen HZ (2016) Effects of water states on steam explosion of lignocellulosic biomass. Bioresour Technol 199(1):155–163
148. Halpern JM, Gormley CA, Keech MA et al (2014) Thermomechanical properties, antibiotic release, and bioactivity of a sterilized cyclodextrin drug delivery system. J Mater Chem B 2:2764–2772
149. Mei LH, Yao SJ, Lin DQ (1999) Biochemical production and processes. Science Press, Beijing
150. Wang ZM (2003) Choice of disinfection and sterilization methods. Pharm Eng Des 24:39–46
151. Jeng DK, Kaczmarek KA, Woodworth AG et al (1987) Mechanism of microwave sterilization in the dry state. Appl Environ Microb 53:2133–2137
152. Rai R, Tallawi M, Roether JA et al (2013) Sterilization effects on the physical properties and cytotoxicity of poly (glycerol sebacate). Mater Lett 105:32–35
153. Verma N, Kumar V, Bansal MC (2012) Utilization of egg shell waste in cellulase production by *Neurospora crassa* under wheat bran-based solid state fermentation. Pol J Environ Stud 21:491–497
154. Wang XS, Chen JP (2009) Biosorption of Congo red from aqueous solution using wheat bran and rice bran: batch studies. Sep Purif Technol 44:1452–1466
155. Yao MY, Huang FL, Chen CG et al (2006) Principles of chemical engineering. Tianjin Science and Technology Press, Tianjin
156. Kadam KL, Chin CY, Brown LW (2008) Flexible biorefinery for producing fermentation sugars, lignin and pulp from corn stover. J Ind Microbiol Biotechnol 35(5):331–341
157. Ververis C, Georghiou K, Christodoulakis N et al (2004) Fiber dimensions, lignin and cellulose content of various plant materials and their suitability for paper production. Ind Crops Prod 19(3):245–254
158. Tang J, Chen K, Huang F et al (2012) Characterization of the pretreatment liquor of biomass from the perennial grass, Eulaliopsis binata, for the production of dissolving pulp. Bioresour Technol 129(10):548–552
159. Agnihotri S, Dutt D, Tyagi C (2010) Complete characterization of bagasse of earlyspecies of Saccharum officinerum-Co 89003 for pulp and paper making. Bioresources 5(2):1197–1214
160. Ma X, Huang LL, Chen Y (2011) Preparation of bamboo dissolving pulp for textile production; part 1. Study on prehydrolysis of green bamboo for producing dissolving pulp. BioResources 6(2):14281439

Chapter 4
Microbe and Multienzyme Systems of High-solid and Multi-phase Bioreaction

Abstract Biocatalysts (microbe and enzymes) are sensitive to environmental factors. In high-solid and multi-phase bioprocess system, high-solid loading leads to special colony structure and "microbial ecosystems". It is necessary to screen microorganisms and enzymes which have high osmotic tolerance and substrate-capturing ability. In this chapter, based on feature of high-solid and multi-phase process, suitable screening principles and methods of microorganisms and enzymes are discussed. *Clostridium acetobutylicum* with high butanol productivity is taken as an example to carry out the engineering practice of rational selection of strains and construct the domestication microbial system and enzyme catalysis systems.

Keywords Strain breeding · Microbial ecosystems · Heterogeneous enzyme catalytic system

4.1 Microbial Breeding Methods

4.1.1 Special Requirement for Strain Breeding in High-solid and Multi-phase Bioprocess System

Industrial strain breeding plays a vital role in the fermentation industry, which determines the industrial values of the fermentation products and the economic feasibility of the fermentation process. The rapid development of modern fermentation industry is generally attributed to two main reasons. One is the update of the fermentation technologies and fermentation equipment. The other is the development of strain breeding technologies, which provides people with various mutants, leading to new products including antibiotics, enzymes, amino acids, organic acids and microorganism, nucleotide, hormones, pigments, alkaloids, unsaturated fatty acids, and other bioactive substances. Therefore, strain breeding plays a significant role in improving the quality and qualification of fermentation products and exploring microbial resources and development of new fermentation goods.

H. Chen, *High-solid and Multi-phase Bioprocess Engineering*,
Green Chemistry and Sustainable Technology,
https://doi.org/10.1007/978-981-10-6352-7_4

The strains used for industrial production should exhibit the following characteristics: (1) High hereditary stability; (2) Easy to produce vegetative cells, spores, or other propagules; (3) Pure strains; (4) Seeds grow fast and vigorously; (5) Short production phrase; (6) The products are easy to be separated and purified; (7) Exhibiting self-protection mechanism and good ability to resistant strain pollution; (8) High economic feasibility; and (9) Stability in producing the targeted product.

Strains with above characteristics can ensure the quality and quantity of the fermentation production, forming the fundamental requirement of industrial strains. However, the high-solid system possesses unique characteristics, which can be summarized as "solid effect" and "absorbance effect". In the following part, discussion will be carried out on the special requirements of the two characteristics on strain breeding.

Due to the transfer limitation of high-solid and multi-phase fermentation, cells were limited in particular space region, contributing to high level of cell activity. Therefore, high concentration strain cells can be harvested and the dilute rate of fermentation can be improved. High-solid and multi-phase system provides stable environment for cell with nutrition.

Together with these advantages, high-solid and multi-phase system also supplies special requirements for the cell breeding, including the low homogeneity of transfer and high osmotic pressure. Therefore, cells in this system should be good at capturing substrate and resisting high osmotic pressure.

In the following part, screening of high butanol producing strain for high-solid multi-phase system is taken as example to set up the breeding strategies based on the "special requirements". The main object of this part is not to make an encyclopedic summary of the strain breeding methods, but to show improve strategies based on unique requirement.

4.1.2 Strain Breeding

So far strain, breeding methods can be divided into three categories, including artificial mutation, species domestication, and metabolic engineering [1].

4.1.2.1 Induced Mutation

Most of the strains employed for industrial production were adopted by induced mutation. Even the gene-modified strains were usually obtained from the mutated strains. Induced mutation has obvious advantages on easy operation and low equipment requirement.

The main process of induced mutation includes (1) the selection of original strains; (2) the preparation of pore suspension; (3) the determination of mutagenic

agent and its dosage; (4) the mutation process; and (5) the purification of mutated strains.

(1) The selection of original strains

The selection of original strains plays a key role in the determination of mutation result. Long time study on strain breeding proves that it is essential to select the suitable starting strain and obtain the adequate knowledge on the strain characteristics, especially on the genetic background, stability, homogeneity, colonial morphology, and physiological–biochemical characteristic. All these knowledge could help to improve the mutation effect.

The requirement on the original strains includes the following: (1) Being sensitive to mutant factors and showing high variation range and positive mutant, even with low production ability; (2) Stable production ability during the industrial fermentation process; (3) Showing beneficial characters (e.g., fast growth rate, low requirement on the nutrition, and produces spores easily and with large number); (4) Because some mutated strains can be more sensitive to other mutative solvent, they can be used as the ideal original strains for further mutation; (5) Adopting the "Mutator strains" which are more sensitive to the mutation treatment than the original strains; and (6) When breeding the strains for production of nucleotide or amino acid, it is better to choose the strains which can accumulate one or several precursors and shows increase in the production after each round of mutation.

The treatment method is the first link should be paid attention to. The treatment methods can be divided into single-factor treatment and multifactor treatment. Single-factor treatment is that treating the strains with only one external factor. It is generally thought that single-factor treatment is not as good as multifactor treatment, which had been proved by many studies. However, if some mutation factor is really effective for some strains, it also can be employed singly and generate positive mutation. Multifactor mutation means induce mutation using two or more mutation solvents at the same time. Different mutation factors own different working mechanisms and different acting sites. Therefore, several solvents of mutants can work together and produce a better result by synergy effects.

The multiple treatments can be divided into several methods as mentioned below: (1) Two or more factors used at the same time; (2) Two or more factors used by turns; (3) One mutation factor was used repeatedly; and (4) Mutation and rehabilitation were carried out by turn.

To increase the mutation effect with multiple factors, it should pay adequate attention to their synergistic effects. Generally, it is better to apply the violent factors after the weak factors. Otherwise, the mutation rate will be decreased. Therefore, the design of the mutant experiments should be based on preliminary experiment or previous experience of the experiments.

Taking the breeding of high butanol producing strains as example, Qureshi N et al. obtained a strain named *C. beijerinckii* BA101 by N-methyl-N-nitro-N-nitrosoguanidine mutation treatment, which produced 19 g/L butanol and 29 g/L total solvents [2]. Lee et al. [3] applied multi-mutation treatment on *C.*

Table 4.1 Artificial mutation methods and the working mechanisms

Mutation type	Mutation method	Working mechanism	Reference
Physical mutagenesis	Ultraviolet ray	① cause crosslinking between DNA and protein ② DNA breakage ③ generating pyrimidine dimer	[4]
	Ionizing radiation	① gene mutation ② chromosome aberration	[5–7]
	Ion implantation	① chromosome Duplication, translocation, inversion, missing	[5–7]
Chemical mutagenesis	Base analog	① swapping between Pyrimidine and purine ② gene transfer; ③ frame shift ④ gene large deletion	[2–4, 8, 9]
	Alkylating agent		
	frameshift mutation solvent		
	Other mutation solvent		
Biological mutagen	Bacteriophage	① gene transduction ② transposo ectopia	[9]

acetobutylicum ATCC 824 and obtained a strain named BKM19, whose butanol production was increased by 30.5%. When cultivated in the airlift fermentation, it produced as much as 10.7 g/L butanol and 21.1 g/L total solvents, which is the highest level been reported so far. Table 4.1 [2–9] summarizes the mutation methods and their working mechanism. It also should be noted that the induced mutation method suffers from low mutation rate and hereditary stability of the obtained strains. The mutation usually occurs randomly and heavily relies on labors. In order to make up for the shortcomings, the induced mutation has been developed into strain adaptation method.

4.1.2.2 Repetitive Domestication

Repetitive domestication is a method that enhances the production ability of targeted strains through repetitively mutation and selection through artificial simulation of the real environment in industrial production. It does not require the depth understanding of the high-production mechanism and exhibits advantages of high mutation rate and hereditary stability [10]. Until now, the repetitive demonstration can be mainly divided into two kinds: continual demonstration and intermittent demonstration. The continual demonstration is also called "soaking method", where the strains are cultivated in the demonstration conditions from the beginning to the end [10]. Until now, the reports on the continuous demonstration were quite limited. It is mainly because that strains after mutation processing, even the positive mutants, are always get hurt and need a good environment for rejuvenation. In the

Table 4.2 The researching process of repetitive domestication

Strains	Strategies	Improved strains/control	Reference
E. coli KO11	Hydrolysates from ammonia fiber expansion treated corn stover	Ethanol yield: 0.51 g/g	[12]
S. cerevisiae Y5	Hydrolysate of softwood	Ethanol production: 20 g/L Ethanol yield: 0.4 g/g	[13]
S. cerevisiae (YYJ 003)	Exposing to furfural, phenol, acetic acid	Tolerating 1.3 g/L furfural, 0.5 g/L phenol and 5.3 g/L acetic acid	[14]
C. acetobutylicum D64	Exposed to butanol	Tolerating 4% (v/v)	[10]
C. acetobutylicum JB200	Exposed to butanol	Butanol production: 20 g/L	[11]
Saccharomyces cerevisiae	Exposed to butanol	Ethanol yield: 0.38 g/g hexoses	[15]
P. guilliermondii	Exposing to furfural, phenol, acetic acid	Ethanol production: 35 g/L Ethanol yield: 0.45 g/g	[16]

continuous demonstration cases, the strains tend to be killed because of no chances for rejuvenation. Yu et al. [10] obtained a butanol-tolerant strain *C. acetobutylicum* T64 through repetitive evolutionary domestications, which could withstand 4% (v/v) (compared to 2% of the wild type) butanol and was accompanied by the increase of butanol production from 12.2 to 15.3 g/L using corn meal as substrate. Fermentation was also carried out to investigate the relationship between butanol tolerance and ABE production, suggesting that enhancing butanol tolerance could increase butanol production but unlikely improve total ABE production. These results also indicated that the ABE would be an available and feasible method used in biotechnology for enhancement of butanol tolerance and production. Yang also obtained a high butanol producing strain named *C. acetobutylicum* JB200, which could produce as much as 20 g/L [11].

Table 4.2 [10–16] summarizes the achievements in recent years on the strains development on biomass bioconversion. Though the advantages of this method have been proved by many researches, it also faces some challenges with screening as the biggest one. In other words, screening method is the key of strain simulation.

4.1.2.3 Metabolic Engineering

The application of induced mutation is timing consuming because of the random mutation direction. By contrast, metabolic engineering is very rational, which helps

Table 4.3 Reprinted from Ref. [1]. Copyright 2013, with permission from Elsevier

Strain	Strategy	Engineered strain/control	Reference
C. acetobutylicum ATCC 824	SolR-inactivated, plasmid-encoded copy of the *aad* gene	Butanol: 17.6/11.7 g/L Acetone: 8.2/4.9 g/L Ethanol: 2.2/0.7 g/L	[22]
C. acetobutylicum ATCC 824	Antisense RNA against adc	Butanol: 8.7/10.3 g/L Acetone: 2.9/4.6 g/L Butanol/acetone: 2.34/1.75	[23]
	Antisense RNA against *ctfB*	Butanol: 0.2/1.1 g/L Acetone: 0.0/0.5 g/L	
C. acetobutylicum ATCC 824	Promoters for enhanced *adhE*, *thl* overexpression, and *ctfB* downregulation	Butanol: 13.2/13.0 g/L Acetone: 3.5/6.3 g/L Ethanol: 14.0/0.9 g/L	[24]
C. acetobutylicum 2018(p)	Disruption of *adc* gene by TargeTron technology	Butanol: 7.4/13.6 g/L Acetone: 0.21/2.83 g/L Ethanol: 1.66/2.7 g/L Butanol/acetone: 35.2/4.8	[18]

to modify the strains exactly. Therefore, this method is widely employed. The researches mainly focus on three aspects: (1) To guide the intracellular metabolic flux, reducing power and energy for butanol biosynthesis, (2) To manipulate the metabolic behaviors, and (3) To get deep insight in the working mechanism of metabolite and reactions.

The main strategy for improvement of butanol production by metabolite flux manipulation is to enhance the central carbon metabolism and inhibit the production of by-products (Fig. 4.3). *pta*, *ack*, *ptd*,and *buk* are the most employed gene targets for manipulation. Harries deleted the *buk* gene and improved the butanol production by 42%, however, when the deletion of *buk* and expression of *add* gene had on influence on the butanol production [19]. When deleting *pta* and *buk* simultaneously, the production of acetone was increased to 0.36 mol/mol glucose [20]. Increasing the production of acetyl-CoA and butyryl-CoA through manipulating central carbon metabolism is also a very efficient method. By knockout *adc* gene of *C. acetobutylicum* EA201, Jiang et al. [21] improved the butanol ratio from 70 to 80%. Similarly, by manipulation of the *adhE1* and *ctfAB* gene to intensify the metabolic flux among butanol biosynthesis pathway and enhance the transfer of acetyl-CoA to acetate and butyrate, the butanol ratio was increased from 0.57 of the wild strain to 0.84. Jiang et al. found that butanol biosynthesis efficiency from acetyl-CoA and butyryl-CoA is higher than that from butyrate and acetate. They deleted *pta* and *buk* genes and amplified *adhE1*, increasing the butanol production to 18.9 g/L, and butanol ratio to 71%. 95% butanol was from the acetyl-CoA pathway [20]. Table 4.3 [18, 22–24] summarized the latest research progress of gene engineering on butanol modification (Figs. 4.1, 4.2, and 4.3).

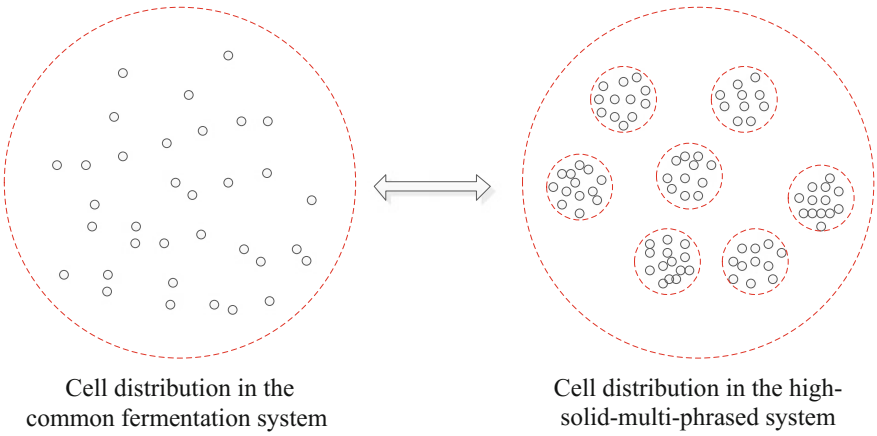

Fig. 4.1 Comparison of the distribution status of cells in different fermentation systems

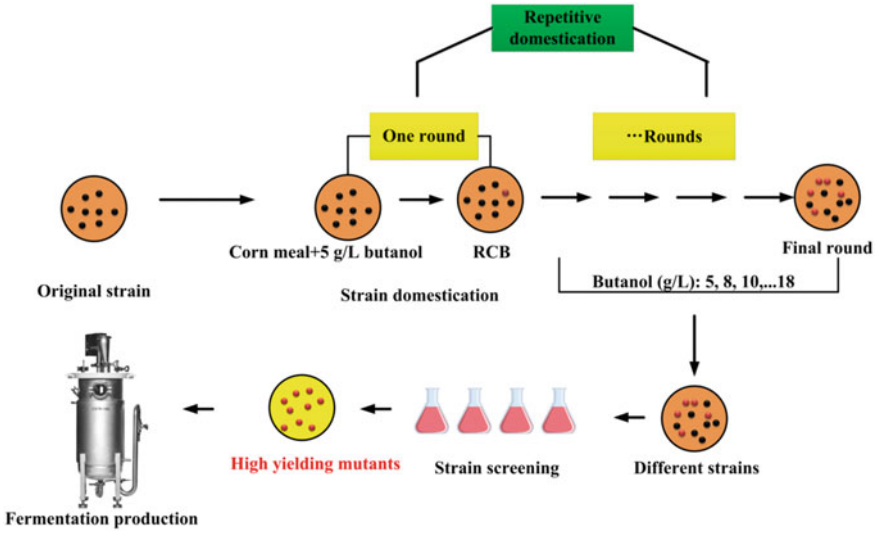

Fig. 4.2 Illustration of repetitive domestication methods [17]

4.1.2.4 The Practice of Strain Breeding in Author's Lab

The selection of breeding method must be based on metabolic characteristics of the target strain.

(1) The determination of breeding method

It is not ideal for the results of the transformation of metabolic engineering because the butanol metabolism involves three complex periods of acid synthesis,

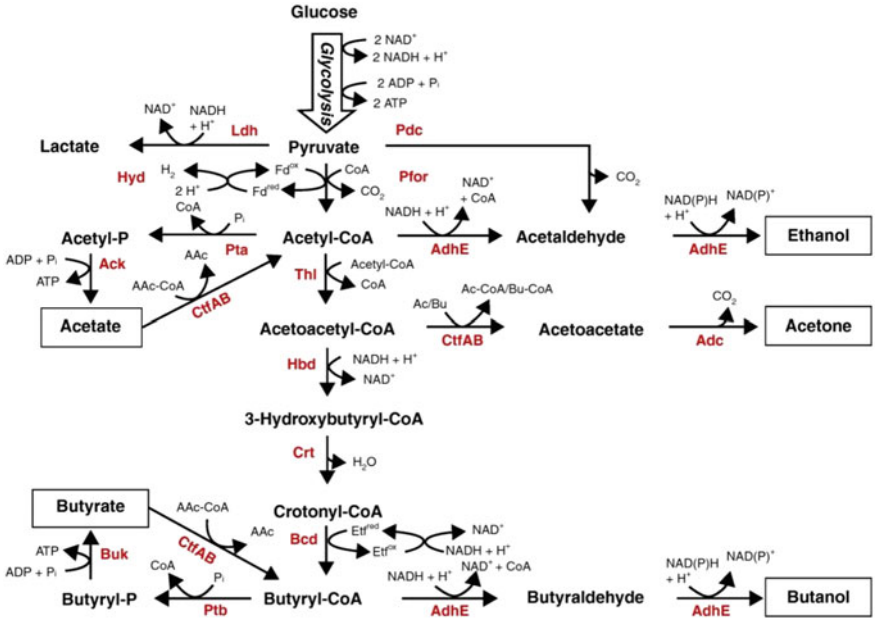

Fig. 4.3 The metabolic pathway of *C. acetobutylicum* ATCC 824 for butanol fermentation. Reprinted from Ref. [18]. Copyright 2009, with permission from Elsevier

solvent synthesis, and sporogenesis. Moreover, it is hard to control the bacterial metabolism exactly through changing one point or one path due to the interaction of different pathways at different times. The interactions between acid production pathway and solvent pathway and four different physiological periods in *Clostridium* are shown in Fig. 4.4.

Through the above analysis, strain domestication is the best way for excellent strains at present, that is, to make up for its non-directional of artificial mutation. Moreover, domesticated strains perform obviously superior to metabolic engineering on bacteria stability and adaptability to the practical production (Fig. 4.5).

Therefore, determination was used to breeding a desired strain which was operated as shown in Fig. 4.6.

(2) The design of objectives filtering

To determine *Clostridium acetobutylicum* selection marker, 200 single colonies (randomly selected) were fermented separately. Bacteria reducing power, product, and substrate utilization in fermentation broth were recorded at 24, 36, 48, and 96 h. These butanol fermentation parameters and yield were analyzed by partial least squares regression and the results are shown in Fig. 4.7. Partial least squares regression (PLS) is a monitoring correlation analysis class with multiple linear regression, canonical correlation analysis, and principal component analysis function [25].

As can be seen from Fig. 4.7, glucose utilization is the most important indicator of the ability to characterize the metabolism of alcohol. For bacterial cells, the

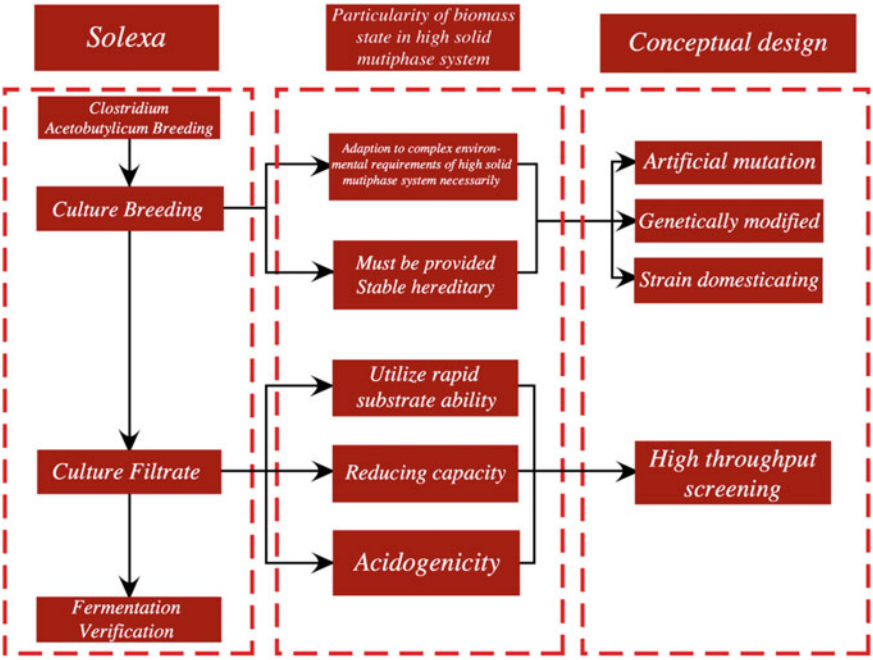

Fig. 4.4 Species breeding and technical route design of high yield *Clostridium acetobutylicum* in high-solid and multi-phase system

higher the speed of sugar utilization, the stronger the ability to synthesize butanol. Reducing ability is determined by examining cell reassuring reduction speed. Reassuring is a nontoxic blue dye which can pass through the cell membrane and used as a redox indicator. The faster the reassuring color change indicates the stronger the reducing ability of cells [26]. After entering into the production phase, small molecule acids were converted into solvent, consuming reducing power. Therefore, reducing power production is directly related to the concentration of the solvent [27]. PLS shows that butanol yield at 48 h, the solution acid, acetic acid, and pH are closely related. When the acid is accumulated to a sufficient concentration, the cell cannot continue to maintain the pH concentration differential across the membrane, resulting in cell growth stop [28]. The acids were converted into a solvent to reduce the toxic effects of acid on bacteria [29, 30]. Thus, in production phase, this behavior can be seen as a protective mechanism.

Acids at 48 h can be grouped into three functions: (1) at stage of acid production, acid is accompanied by ATP synthesis and promotes cell growth [31–33]; (2) accumulation of acid could induce solvent synthesis [27]; and (3) acid is the material for solvent synthesis [34]. Large amounts of acids accumulation lead to "acid crash" phenomenon, resulting in fermentation failure [35]. OD values were used to characterize the cell growth parameters and PLS showed that the higher OD values were usually accompanied with the higher butanol production at 48 h, which

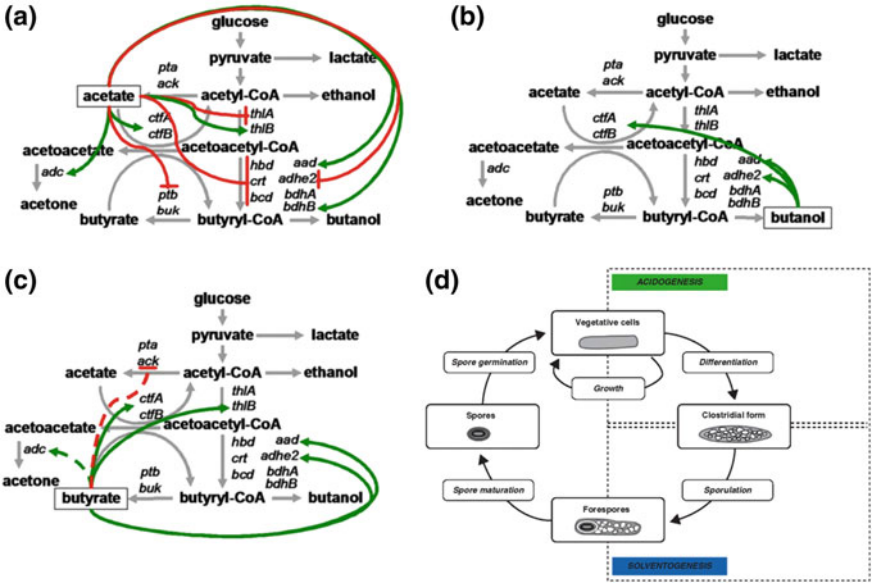

Fig. 4.5 Complexity of acetone–butanol–ethanol fermentation pathway. **a**–**c** show the relationship between sub-pathways, **d** shows the life cycle of *Clostridium acetobutylicum*

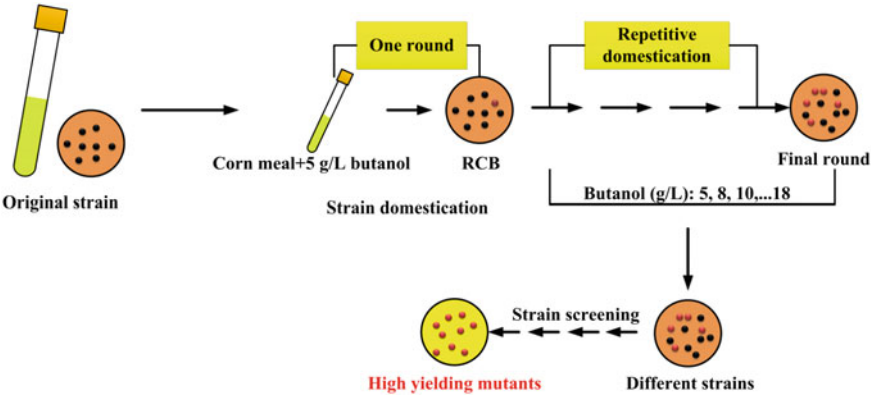

Fig. 4.6 Schematic diagrams of bacteria domestication

is consistent with results of Liu et al. [36]. Considering the complex parameters of detection methods, glucose, pH, and reducing capability are the best screening models. Additionally, for the longer incubation time, disturbance from outside environment to the results of microplate culture becomes greater (e.g., serious solution evaporation and contamination). Therefore, screening time was set at 48 h.

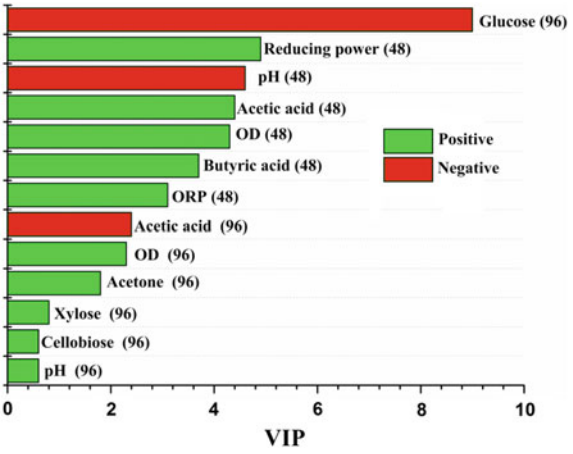

Fig. 4.7 Correlation analysis on fermentation parameters with butanol production using partial least squares method

The relationship among parameters is very complicated, and not a single one of the traits of high yield strain clearly differentiated because discriminant model must be established according to these subtle differences selectable marker. Three most popular methods for solving the problem, including nonlinear fitting, the feasibility of artificial neural networks, and support vector machines, were investigated.

The real value of the 200 samples is connected into a curve from small to large in Fig. 4.8, while splashes to the corresponding predicted values, where the accuracy of three methods is support vector machine (79.8%), artificial neural network (76.4%), and nonlinear fitting (56.3%) in the order.

$$Bu\ \tan\ ol = a(pH - b)^2(\mathbf{60} - Glu\ \cos\ e)(c - R) + d \tag{4.1}$$

Nonlinear fitting is the most commonly used and is one of the simplest operations. The accuracy of this method depends on the selection of expression model. Unfortunately, so far, there have been no unified standard methods used for the expression of the model of optimization design. Combining with the filter data, a prediction model was put forward (e.g., Eq. 4.1). The predictive results of the method are not ideal. Strains of production capacity are very complex variables. Its correlation with selection markers is very complicated, which cannot accurately summarize with conventional formula.

Artificial intelligence is a hot topic in current researches, which has been widely applied to materials [37], chemical engineering [38], automation, face recognition [39], and many other fields. As a kind of adaptive nonlinear statistical data modeling tool, the complex relationship between input and output can be excavated automatically [40]. Through Fig. 4.8, the prediction results (76.4%) of artificial neural network are significantly superior to that of nonlinear fitting (56.3%). Additionally, compared with the neural network, support vector machine is more suitable for small sample modeling, where strains of the predicted results also could indicate the highest accuracy of support vector machine (79.8%).

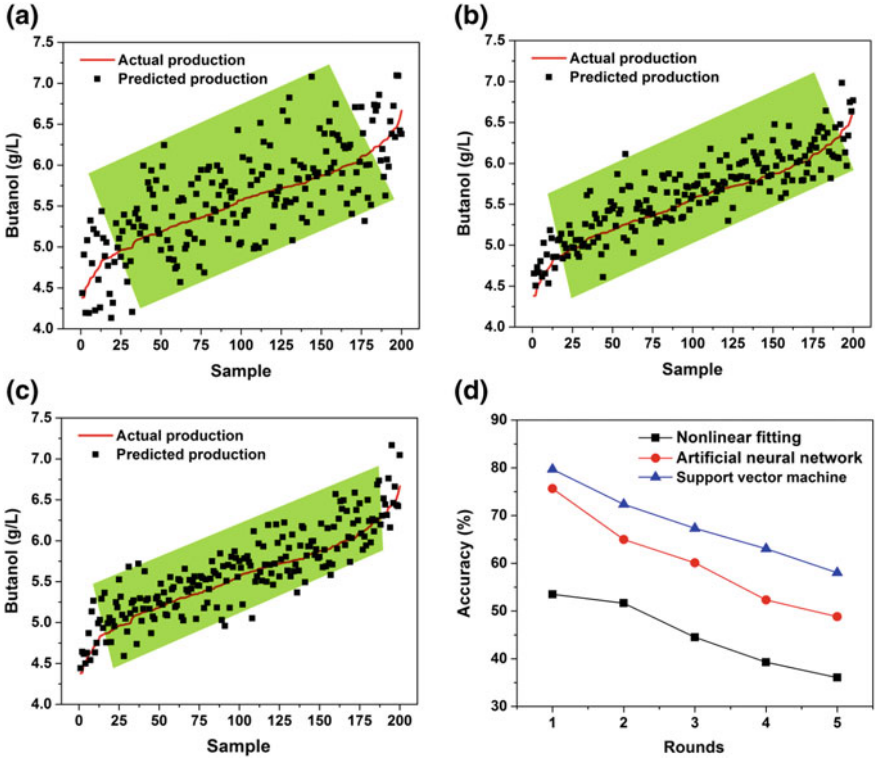

Fig. 4.8 Prediction performances with different prediction models

In order to validate the stability of the model, the trained model is applied to five generations of continuous prediction. And with the emergence of new species, the accuracy of the three models is dropped. One of the most obvious is the nonlinear fitting, dropped from 56.3 to 38.5% at the beginning. Neural network and support vector machine drop to 65.3% and 65.3%, respectively, indicating a better stability. Above all, no matter in accuracy and stability, the support vector machine is the best model for bacterial selection.

At present, biochemists try to use quantitative method to describe the biochemical phenomenon and study biochemical problem in the category of "quantitative" and "mathematics" [41–43]. Unfortunately, a lot of problems, including strains filtration, are still staying in the qualitative description. For example, there are no effective tools of converting biochemical phenomenon to digital information, while the feasibility of image processing in the biochemical quantitative research is proved in this chapter.

In order to improve the work efficiency, automatic equipment for screening is set up (Fig. 4.9). This equipment is mainly composed of cabinet, industrial tablets, and flat plate type of light and digital cameras. Cabinet and flat lamp provide a stable

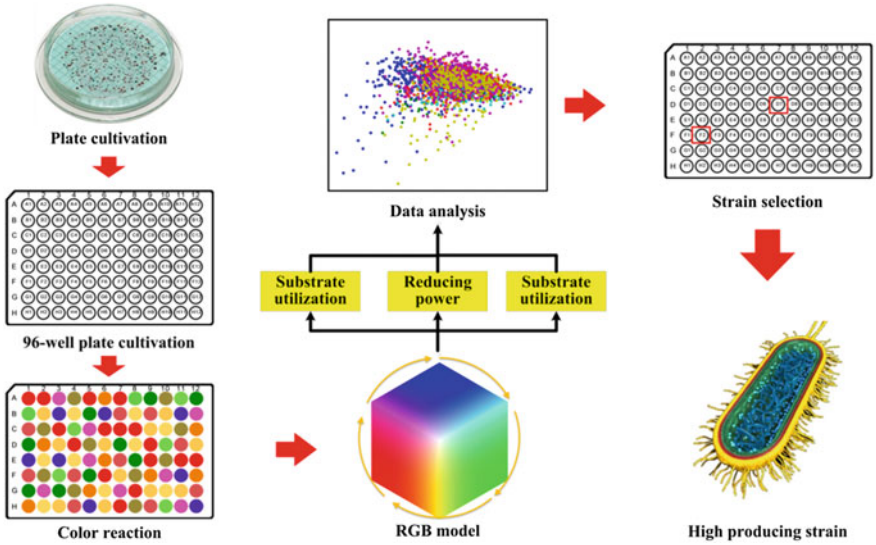

Fig. 4.9 The screening procedure for high butanol producing *C. acetobutylicum* strain

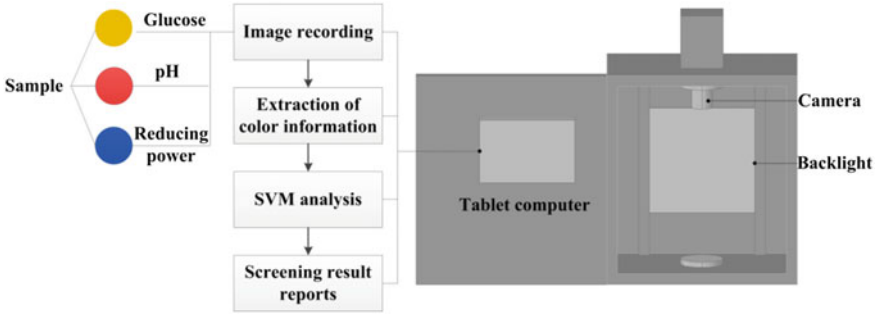

Fig. 4.10 Schematic of the automated equipment used for strain screening [44]

environment to avoid the disturbance of external light source. Digital cameras are connected to the industrial tablets and directly controlled by computer operation, which could strictly control the sample reaction time and effectively reduce the human error. Industrial tablets are installed with automatic analysis program based on Java language. The program mainly includes image, image preprocessing, color information extraction, and test results report. Among them, the image preprocessing image is integrated with automatic extraction algorithm, which could automatically extract vision from samples (Fig. 4.10).

Table 4.4 shows the comparison of high-pressure gas chromatography method and discoloration circle method [44]. Taking selection of 1000 strains, for example, the traditional gas chromatography requires at least 10.5 days and works

Table 4.4 Comparison of the existing methods for screening of 1000 butanol producing strain [44]

Method	Screening time	Material consumed
GC	10.4 d	3L hydrogen, 7.5 L nitrogen
Color-changing circle	4 d	Culture medium 12 L; Plate 200;
Ion beam implantation	1 h	Indicator solution 0.6 L, Microwell plate 11

continuously (each sample testing time is about 15 min), consuming at least 3 L hydrogen (0.2 mL/min), and 7.5 L nitrogen gas (0.5 mL/min). He et al. [44] had put forward a way to screening of acetone butanol clostridium with color ring rapid method. The method estimates the potential output of screening strains by detecting the size of the color ring. This method includes many steps (e.g., production of plate and holes, fermentation liquid transfer, and measurement of color ring) and labor intensive. Therefore, the method proposed in this chapter has obvious advantages with the help of automation process analysis. It takes only one hour when scanning 1000 strains, which is the 1/250 of HPGC and about 1/100 of discoloration method.

After seven gradients of butanol domestication, eventually pick out one individual strain of good traits, named *IPE-005*, compared with the fermentation character of the original strain, and the results are shown in Fig. 4.11.

It can be seen that there are obvious differences between *IPE-005* and the originals during metabolic process. The utilization of glucose has increased from 75.5 to 91.4%. Bacteria concentration increased from 2.2 to 3.5 g/L with 59.1% increase. Final concentration of butanol increased from 6.1 to 10.9 g/L with 78.6% increase, and total solvent increased from 13.4 to 17.5 g/L with 38.1% increase. The results proved the accuracy of this screening method. Seven batches consecutively have been made to verify the stability of the *IPE-005* strains, and the fermentation results are shown in Fig. 4.12. The variation coefficient of the total yield of *IPE-005* and butanol production were 5.56% and 5.48%, respectively, indicating that strain can be used as an original strain in further research with better mitotic stability.

4.2 Microbial Selection Methods for Intensifying Inhibitor Tolerance

Microorganism cannot survive or play a well function in an unsuitable environment with inhibitors. In generally, inhibitors refer to both chemical and physical factors. Chemical factors mainly refer to chemicals, which have a negative effect on microbial growth. For example, high concentration ethanol inhibits yeast growth, resulting in fermentation process to stop. Physical factors include osmotic pressure, temperature, etc. High-solid and multi-phase bioprocess system is a typical system with high osmotic pressure. Microbe in this system should have high osmotic

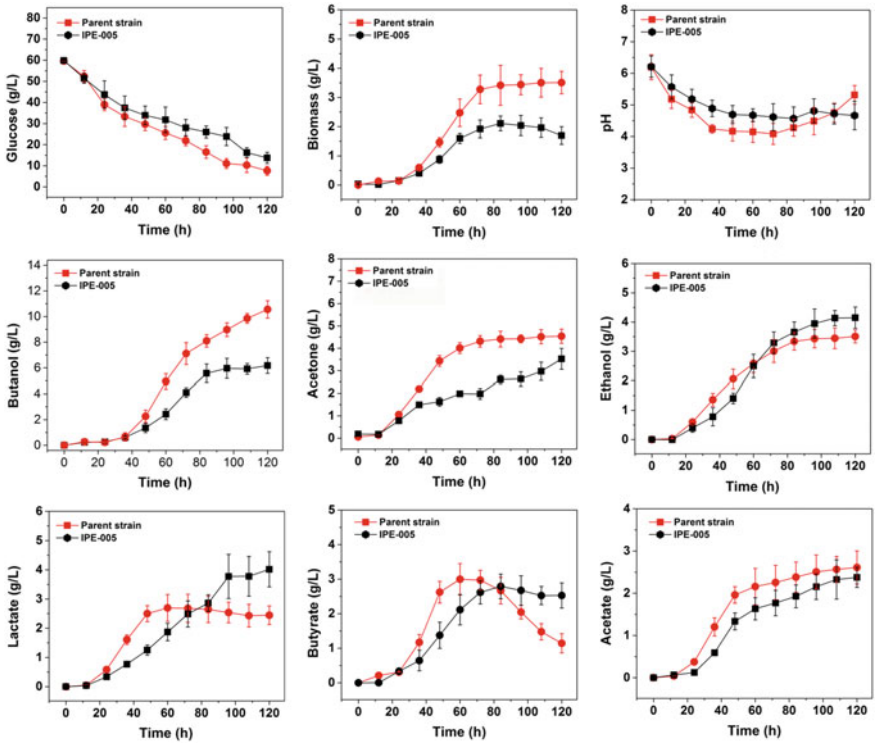

Fig. 4.11 Comparison of *IPE-005* and the parent strain for butanol fermentation [34]

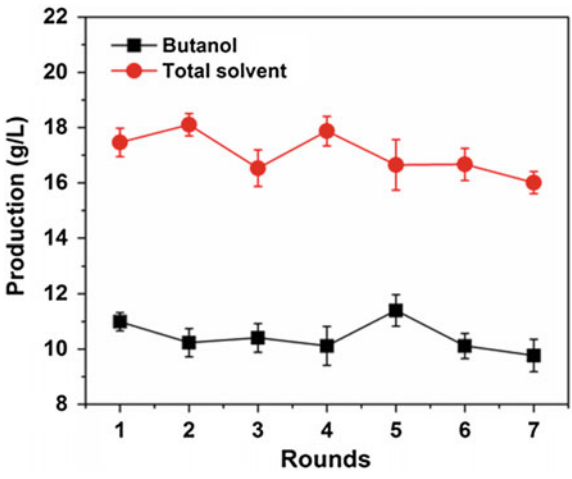

Fig. 4.12 The validation of *IPE*-005 for generation stability [17]

pressure tolerance. In fact, traditional breeding methods can be used to screen desired microbes or enzyme. In later part of the chapter, a popular and efficient method of enzyme directed evolution will be discussed.

4.3 Enzyme Directed Evolution Methods

4.3.1 Special Enzyme Requirements in High-solid and Multi-phase System

Compared with the traditional chemical catalyst, enzyme preparations have the incomparable advantages (e.g., high efficiency, substrate specificity, and mild reaction conditions). Therefore, enzyme preparations gradually play an important role in many fields. Enzyme is sensitive to external environment (e.g., pH and temperature). Differences between the actual reaction conditions and the physiological environment of organism easily result in enzyme inactivation phenomenon in practical application. Therefore, characteristics of enzyme greatly limit its industrial applications. Comparison of enzymes immobilization in the traditional system and that in high-solid and multi-phase is shown in Fig. 4.13.

Enzyme in high-solid and multi-phase system has the following advantages: (1) There is no need for the separation and purification of enzyme, reducing the energy loss and total cost; (2) Multiple enzyme reactions can be done without adding a cofactor. The immobilized cells cannot only play a role as a single enzyme but take advantage of the bacteria in the composite enzyme system to complete a series of catalytic reactions. (3) For cells, the original state of enzyme can maintain and show a strong resistance to unfavorable factors.

However, new requirements on enzyme in the high-solid and multi-phase include the tolerance of high osmotic pressure. At the same time, due to the

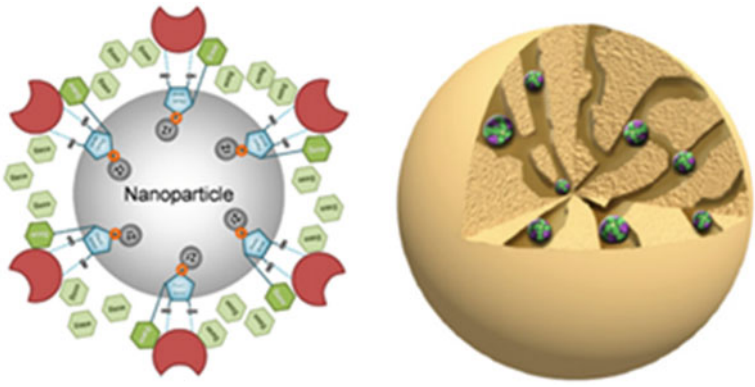

Fig. 4.13 Traditional enzyme immobilization and that in high-solid and multi-phase system

uniformity of the system, mass and heat transfer are weaker than that of the traditional reaction system.

4.3.2 Directed Evolution of Enzyme

Directed evolution is an effective new strategy of protein molecules modification, featured by stimulating natural evolution process in the laboratory. It is randomly induced by mutagenesis of genes which code protein, guided by DNA reorganization, random recombination, and staggered extension methods to recombine mutation gene in vitro. Design high-throughput screening methods to choose the need of mutant strains through the methods of error-prone PCR and mutagenic strain. This method not only can quickly produce new industrial useful enzyme, but also can be significant to the study the relationship between of protein structure and function.

With a long period of natural selection, countless proteins produced in nature show an ideal biology function [45]. Most traditional industrial catalyst cannot be compared to the catalytic efficiency and specificity of an enzyme, and thus enzyme application is becoming more commonl in every field [46]. However, chemical engineers that design industrial technology with enzymes have often encountered problems. For example, enzyme could play very specific biological functions in organism internal energy after hundreds of millions years of evolution while unexpected features show outside the body [47]. Biological process usually requires the following types of enzymes which could maintain stability of active enzyme for long time, remaining highly active enzyme in extreme environments or accept different substrates (including the substrate not existing in nature) [48]. Proteins with new features and properties can be gained through two ways including finding unknown species and transforming existing known proteins or enzymes in natural. The later way may be more appropriate in selecting proteins without natural evolution characteristics [49]. In early 1980s, protein-engineering technology arises based on concept that analyzing three-dimensional structure of protein so as to find out the relationship between the structure and function. Changing individual amino acid residues to generate new traits of protein with site-directed mutagenesis method. Therefore, this attempt is known as the rational design [46]. As the relationship of protein structure and function is very complicated, understanding of this relationship is still very superficial at present. In fact, through different channels (e.g., random mutagenesis screening), and a large number of successfully transformed enzyme, some changes of amino acids are often outside the area according to protein model prediction [46].

Fixed point mutation of proteins becomes helpless when the research is focused on molecular structure [50]. Therefore, people begin to consider method-directed evolution that seems to be irrational [51].

4.3.2.1 Basic Ideas of Protein Directed Evolution

Natural evolution is one spontaneous slow process of reproduction and survival of the whole organisms [49]. Evolution by natural selection contributes to the developmental direction of biology. The diversity of environment and adjustment mechanism of biology determine the diversity of the evolutionary direction. Key steps of the natural evolution can be imitated in the lab including mutation, recombination, and selection, and effectively transform protein and complete the long evolution process in a short time [45], making it possible to meet the demand of human beings. Unlike natural evolution, directed evolution strategy has a clear goal that is usually the specific properties of a particular protein. Directed evolution technique makes it possible for us to understand a few protein molecules, looking for the needless function in natural environment. It is an irrational design because the directed evolution does not require protein structure information.

The following features of proteins must be paid attention to when considering experiment scheme. (1) Protein sequence space is usually huge. One protein composed of 300 amino acids in series may have 20300 kinds of arrangements, among which the vast majority of arrangements have no response function. (2) Desired mutations are scarce and the combinations of beneficial mutations are rare. The characteristics illustrate that completely random sampling way is hard to get what we need. It is best to choose a character similar to the target protein. Besides, the ideal state is that only a single amino acid mutation occurs once in every protein sequence [45].

What directed evolution needs is to produce mutations library that contains a large number of trace beneficial mutants that could express functions in vivo of appropriate microorganisms (e.g., *E. coli* or yeast) [49]. Sensitive screening method must be developed to cognize small increase of expected traits by a single amino acid replacement [48].

Performance of directed evolution in solving particular problem greatly depends on the state of the behavior modified by natural evolution. If a feature (e.g., catalytic activity) has already been under pressure from natural selection for long time, the probability of further change will be relatively small in the lab. In general, desired performance which has not been selected by natural is easy to improve. Enzyme activity of a natural substrate seems to be easily improved [49] when characteristics of biological functions are never needed.

4.3.2.2 Conventional Methods of Protein Directed Evolution

The amount of mutant, the simplicity of establishment of mutation gene library, and the operability of establishment of mutant gene library greatly affect the efficiency of evolution. With irreplaceable advantages of the directed evolution technique than other methods in the field of enzyme molecule modification, researchers designed a variety of methods to establish a mutant gene library. According to different

methods of creating mutant gene library, it can roughly be divided into the non-recombinant and recombinant.

(1) Error-prone PCR

Error-prone PCR refers to the amplifying gene bases and induces mismatch simultaneously, leading to random mutations. However, it is difficult to obtain satisfactory results through one mutation, promoting development of sequential error-prone PCR strategy. It is a PCR amplification where useful mutations are used as the template of the next PCR amplification, accumulating small mutation and obtaining desired mutations. Chen et al. used this strategy on directed evolution activity of *bacillus subtilis* proteinase E in nonaqueous phase (dimethylformamide, DMF). The results showed that catalytic efficiency of the mutant PC_3 was 471 times higher than wild enzyme in 60% DMF [50, 52].

Error-prone PCR method was designed and reported at the first time in 1985 by Leung et al., and improved by Cladwell and Joyce in 1992 [53]. It is a method of establishing non-recombinant mutant library. TaqDNA polymerase has no activity of 3'–5' excision enzyme. Some base mismatch inevitably occurs in the amplification process. Changing the factors in the amplification system (e.g., Mg^{2+} concentration or using Mn^{2+} instead of Mg^{2+} as activation agent of DNA synthetase), could increase the mismatch rate. In this method, the genetic changes just occur within a single molecule, belonging to asexual evolution. The same type base conversion is easy to appear when using this method. Error-prone PCR could only make the original protein sequence of a small space mutation, thus applicable to smaller segments (<800 bp). However, for new researchers in directed evolution, error-prone PCR can be regarded as an effective and practical evolution method indeed [54].

(2) DNA reorganization and exon reorganization

DNA reorganization, also known as sexual PCR, is to sexually recombine genes at molecular level. The method was introduced to the protein directed evolution process by Stemmer in 1994 and has successfully transformed dozens of protein with industrial applications. Through altering the original nucleotide sequence of a single gene or gene family, the method creates new genes and endow expression product with new features. DNA reorganization strategy aims to create the mutation in the gene group of parent as much combination as possible, leading to greater variation and finally obtaining the best combination of mutation enzyme. It is superior to "repeat oligonucleotide induced mutagenesis" and "continuous error-prone PCR". Through DNA reorganization, we can not only accelerate the accumulation of beneficial mutations but also can make the enzyme endowed with optimized properties of two or more.

Exon shuffling is similar to DNA reorganization where individual fragment exchange occurs. However, exons reorganization relies on the same kind of intermolecular introns homology while the DNA reorganization is not subject to any restrictions and occurs in the entire history of the gene. Exon reorganization is

more suitable for eukaryotes and makes sure that various sizes of random peptide library be obtained.

With the deepening study, the DNA reorganization technology is also undergoing improvement [55]. At present, DNA reorganization has successfully evolved coding β-lactamase, β-glycosidase enzymes, green fluorescent protein, alkyltransferase, benzyl lipase, and t-RNA synthetase single gene and the whole operon encoding the arsenic acid salt or atrazine degradation enzyme. Two main disadvantages of DNA reorganization are stated as follows: (1) the reorganization background clone recovers to the cloned child; and (2) higher sequence homology of parent gene is demanded (usually no less than 90%). Family reorganization technology [55–57] has been developed where single-stranded DNA is used as the template, making up for the traditional shortcomings of DNA reorganization method.

4.4 Construction of Microbial System High-solid and Multi-phase Bioprocess

4.4.1 Features of Microorganism System in High-solid and Multi-phase Bioprocess

High-solid and multi-phase system is featured by high-solid loadings. Interaction between microorganism and matrix occurs through energy, matter and information exchange, forming a unique community structure, and microbial ecosystems. Efficient microbial reaction system can be built by recognizing the specificity of this biological system and comprehensive utilization.

Although there are few related studies, broad predictions can be made that high-solid and multi-phase systems provide the best growth environment because diversity of colony microbes and the variety of metabolic types co-exist in the system.

As shown in Fig. 4.14, the high-solid and multi-phase system has features of concentrated substrate and high concentration of bacteria. To be specific, significant adsorption effect on the surrounding culture medium makes the nutrients highly enriched in the matrix and results in a “concentrated substrate” effect. Besides, high-solid and multi-phase bioprocess limits microbe to a specific area, increasing the effective removal of cells and substrates and accelerating the growth rate of bacteria and then achieve high concentration of cell culture.

As shown in Fig. 4.15, differed from the traditional fermentation system, the interaction between the bacteria in the high-solid and multi-phase system is more intense with larger mass, energy, and signal flow. This interaction constitutes a complete ecosystem with higher stability and catalytic conversion capacity. Therefore, a hybrid microbial in high-solid and multi-phase system can be established and applied to sewage treatment, biodegradation, and other occasions.

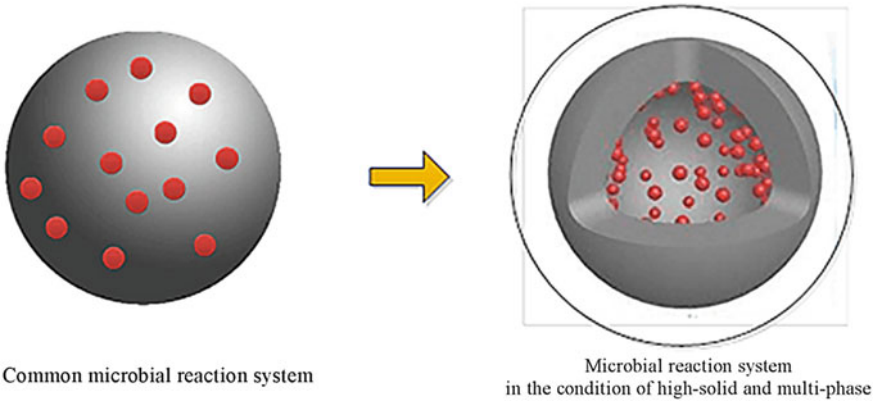

Fig. 4.14 Two effects in high-solid and multi-phase bioprocess microorganism system: substrate concentration and high concentration cultivation of bacteria

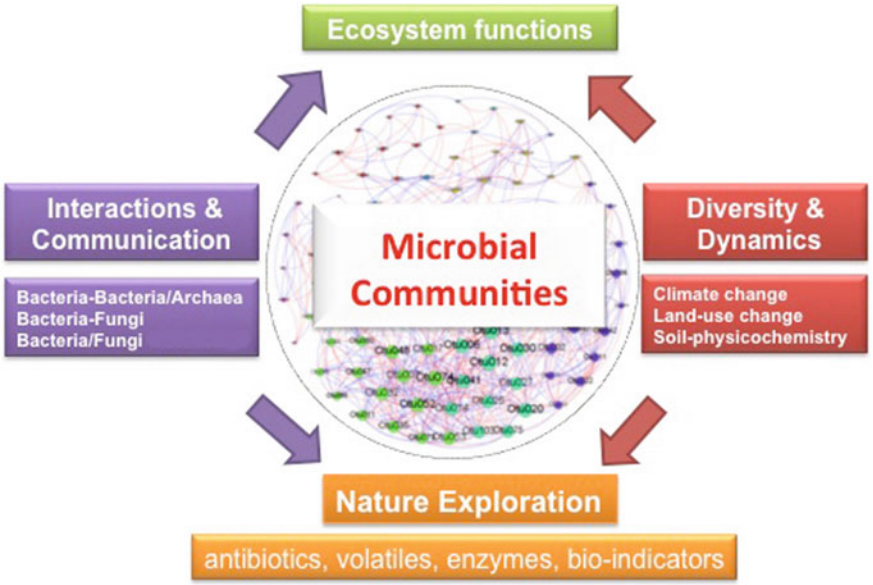

Fig. 4.15 The "ecosystem" formed by microbial–matrix interactions in high-solid systems

4.4.2 Construction Method of Microorganism System in High-solid and Multi-phase Bioprocess

"Domestication of microflora" is an effective method of constructing high-solid biological reaction system. High-solid and multi-phase systems are complex and

bio-diverse micro-ecological systems. Biodiversity is the basis of domestication, and acclimation conditions are the selection of microorganisms. The microorganism which adapts to the environment will survive, while the others will be inhibited or eliminated. In addition, the microorganisms in the high-solid heterogeneous system can take the initiative to adapt acclimation conditions by phenotypic adaptation and evolutionary adaptation. This is a process of redistribution and adjustment of the microbial niche in the ecosystem, conforming to the principle of "selection and adaptation" of ecology.

Diversity of microbial species in high-solid and multi-phase reaction system is the base of domestication. In the process of acclimation, the biological diversity of the system showed a decreasing trend. The more the extreme conditions of domestication, the smaller the microbial diversity. Therefore, the high-solid and multi-phase domestication aims to use desired condition for selecting the microbial species. In the process of acclimation, the microbial community succession also appeared in the high-solid and multi-phase microbial community. The dominant species at low concentration will be replaced by another population at high concentrations. This should be caused by the abundance of functional microorganisms. When a variety of microorganisms have the same metabolic function, the phenomenon of dominant population substitution occurs.

4.5 Construction of Enzyme Catalysis System in High-solid and Multi-phase Bioprocess

4.5.1 Specificity of Heterogeneous Enzyme Catalytic System

Most of the enzymes are proteins with a special three-dimensional conformation, which catalyze extensive and specific reactions in vivo. In recent years, especially with the development of biochemical technology, enzyme-catalyzed reactions, especially catalytic asymmetric synthesis reactions, are increasingly used by organic chemists. Optically active compounds or synthetic products have been used in medicine, pesticides, food additives, spices, daily chemicals, and other fine organic synthesis.

Different from the traditional enzyme reaction system, there is a complex interaction (including enzyme–matrix, matrix–matrix, and enzyme–enzyme) in the high-solid and multi-phase system. Since the enzymes are confined to a fixed region, the high-solid and multi-phase system constitutes a natural complex enzyme reaction system. Different enzymes can be added into high-solid system sequentially. The product in previous reaction is used as the substrate for the enzyme, and the reactions were connected in sequence, constituting a metabolic pathway or a part. Synergetic function of the enzymes can enhance enzymatic hydrolysis efficiency.

Multienzyme complex catalytic system is easy to form in high-solid and multi-phase enzyme. In vivo, many cascade enzyme reactions are carried out in the form of highly ordered multienzyme complexes. Multienzyme catalytic complex generally consists of three or more enzymes through the affinity of the composition which is a certain configuration of the complex. At present, the channeling effect in substrate has been found in many pathways of organism (e.g., the glycolytic pathway [58], the tricarboxylic acid cycle [59], and the mevalonate pathway [60]). In light of this phenomenon, the authors attempted to increase the reaction rate in vitro by using some existed or artificially constructed multienzyme catalytic complexes. Compared with intracellular reaction, the advantages are concluded as follows: (1) Reaction system is easy to control; (2) Higher product yields can be achieved in vitro synthesis, where some new multienzyme catalytic systems can be constructed; (3) In in vitro synthesis, there is no cell membrane obstruction, contributing fast mass transfer and improving reaction efficiency; and (4) The in vitro multienzyme catalytic system can withstand some toxic intermediates and the reaction condition is not as severe as it in vivo [61]. Obviously, the high-solid and multi-phase enzymatic reaction system also has similar advantages.

Figure 4.16a shows the catalytic effect of three synergistic enzymes. Figure 4.16b shows the distribution of three catalytic enzymes in the conventional

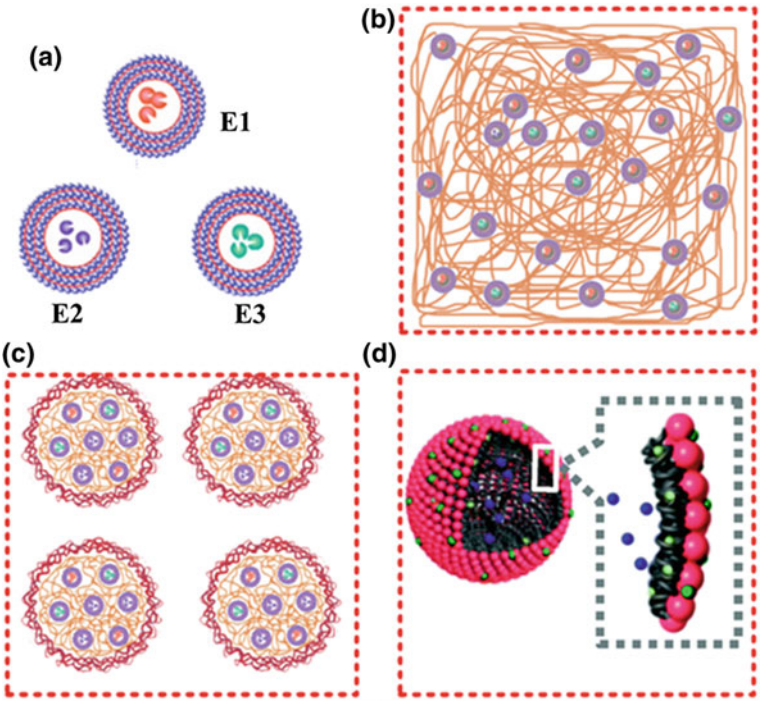

Fig. 4.16 Comparison of the enzyme-catalyzed system in high-solid and multi-phase system and that in conventional enzyme-catalyzed system

catalytic system. The three enzymes were randomly distributed and could not form a good synergistic reaction, and there is a long distance between enzyme and substrate, resulting in low catalytic efficiency. Figure 4.16c, d reflects the distribution of the enzyme in the high-solid and multi-phase system. Strong adsorption effect exits in high-solid and multi-phase for the being of solid, fixing the enzyme in a certain region and increasing effective contact between enzymes and the substrate. Therefore, a number of independent catalytic units are formed and play their roles synergistically in the high-solid and multi-phase system.

4.5.2 *Construction of High-solid and Multi-phase Enzymatic Hydrolysis System*

High-solid enzymatic system has many similar characteristics with single immobilized enzyme methods. Structure and function of each enzyme should be taken into account. Reasonable protective measures should be taken to maintain the highest overall enzyme activity.

Establishment of high-solid and multi-phase enzymatic system could be summarized as follows: (1) Choosing the varieties of enzyme according to the main functions; (2) Optimizing proportion of individual enzyme in compound and providing physical and chemical conditions; and (3) The unit volume of matrix in high-solid and multi-phase system should be calculated according to the dose of enzyme.

References

1. Xue C, Zhao XQ, Liu CG et al (2013) Prospective and development of butanol as an advanced biofuel. Biotech Adv. 31(8):1575–1584
2. Qureshi N, Blaschek H (2000) Butanol production using Clostridium beijerinckii BA101 hyper-butanol producing mutant strain and recovery by pervaporation. In: Twenty-first symposium on biotechnology for fuels and chemicals. Humana Press, Colorado, pp 225–235
3. Jang YS, Malaviya A, Lee SY (2013) Acetone–butanol–ethanol production with high productivity using Clostridium acetobutylicum BKM19. Biotech Bioeng 110(6):1646–1653
4. Bowring SN, Morris J (1985) Mutagenesis of Clostridium acetobutylicum. J Appl Microbiol 58(6):577–584
5. Borden JR, Papoutsakis ET (2007) Dynamics of genomic-library enrichment and identification of solvent tolerance genes for Clostridium acetobutylicum. Appl Environ Microb 73 (9):3061–3068
6. Glass JI, Alperovich N, Assad-Garcia N et al (2005) Estimation of the minimal Mycoplasma Gene set using global transposon mutagenesis and comparative genomics. In: Genomes to life contractor-grantee workshop III, February 6–9
7. Robey-Bond SM, Barrantes-Reynolds R, Bond JP et al (2008) *Clostridium acetobutylicum* 8-Oxoguanine DNA Glycosylase (Ogg) differs from Eukaryotic Oggs with respect to opposite base discrimination. Biochemistry-us 47(29):7626–7636

8. Allcock ER, Reid SJ, Jones DT et al (1981) Autolytic activity and an autolysis-deficient mutant of Clostridium acetobutylicum. Appl Environ Microb 42(6):929–935
9. Dreyfus-Fourcade M, Sebald M, Zavadova M (1972) Restriction and modification of phage r by Clostridium perfringens NCTC 8798 and its mutants. Ann Inst Pasteur 122:1117–1127
10. Liu XB, Gu QY, Yu XB (2013) Repetitive domestication to enhance butanol tolerance and production in Clostridium acetobutylicum through artificial simulation of bio-evolution. Bioresource Technol 130:638–643
11. Xue C, Zhao J, Lu C et al (2012) High-titer n-butanol production by clostridium acetobutylicum JB200 in fed-batch fermentation with intermittent gas stripping. Biotechnol Bioeng 109(11):2746–2756
12. Lau MW, Dale BE, Balan V (2008) Ethanolic fermentation of hydrolysates from ammonia fiber expansion (AFEX) treated corn stover and distillers grain without detoxification and external nutrient supplementation. Biotechnol Bioeng 99(3):529–539
13. Tian S, Zhu J, Yang X (2011) Evaluation of an adapted inhibitor-tolerant yeast strain for ethanol production from combined hydrolysate of softwood. Appl Energ 88(5):1792–1796
14. Ding MZ, Zhou X, Yuan YJ (2010) Metabolome profiling reveals adaptive evolution of Saccharomyces cerevisiae during repeated vacuum fermentations. Metabolomics 6(1):42–55
15. Wallace-Salinas V, Gorwa-Grauslund MF (2013) Adaptive evolution of an industrial strain of Saccharomyces cerevisiae for combined tolerance to inhibitors and temperature. Biotechnol Biofuels 6(1):151
16. Fan C, Qi K, Xia XX et al (2013) Efficient ethanol production from corncob residues by repeated fermentation of an adapted yeast. Bioresource Technol 136:309–315
17. Xia ML (2016) Digital image analysis for rapid detection and fermentation process intensification by periodic-peristole agitation. Graduate University of the Chinese Academy of Sciences (Institute of Process Engineering)
18. Jiang Y, Xu C, Dong F et al (2009) Disruption of the acetoacetate decarboxylase gene in solvent-producing Clostridium acetobutylicum increases the butanol ratio. Metab Eng 11(4–5):284–291
19. Harris LM, Desai RP, Welker NE et al (2000) Characterization of recombinant strains of the Clostridium acetobutylicum butyrate kinase inactivation mutant: need for new phenomenological models for solventogenesis and butanol inhibition? Biotechnol Bioeng 67(1):1–11
20. Jang YS, Lee J Y, Lee J et al (2012) Enhanced butanol production obtained by reinforcing the direct butanol-forming route in Clostridium acetobutylicum. MBio, 3(5):e00314–12
21. Ou J, Ma C, Xu N et al (2015) High butanol production by regulating carbon, redox and energy in Clostridia. Front Chem Sci Eng 9(3):317–323
22. Harris L, Blank L, Desai R et al (2001) Fermentation characterization and flux analysis of recombinant strains of Clostridium acetobutylicum with an inactivated solR gene. J Ind Microbio Biot 27(5):322–328
23. Tummala SB, Welker NE, Papoutsakis ET (2003) Design of antisense RNA constructs for downregulation of the acetone formation pathway of Clostridium acetobutylicum. J Bacteriol 185(6):1923–1934
24. Sillers R, Al-Hinai MA, Papoutsakis ET (2009) Aldehyde–alcohol dehydrogenase and/or thiolase overexpression coupled with CoA transferase downregulation lead to higher alcohol titers and selectivity in Clostridium acetobutylicum fermentations. Biotechnol Bioeng 102 (1):38–49
25. Mahesh S, Jayas D, Paliwal J et al (2015) Comparison of partial least squares regression (PLSR) and principal components regression (PCR) methods for protein and hardness predictions using the near-infrared (NIR) hyperspectral images of bulk samples of Canadian wheat. Food Bioprocess Tech 8(1):31–40
26. Elshikh M, Ahmed S, Funston S et al (2016) Resazurin-based 96-well plate microdilution method for the determination of minimum inhibitory concentration of biosurfactants. Biotechnol Lett 38(6):1015–1019
27. Liu C-G, Xue C, Lin Y-H et al (2013) Redox potential control and applications in microaerobic and anaerobic fermentations. Biotechnol Adv 31(2):257–265

28. Huang H, Liu H, Gan Y-R (2010) Genetic modification of critical enzymes and involved genes in butanol biosynthesis from biomass. Biotechnol Adv 28(5):651–657
29. Grimmler C, Janssen H, Krausse D et al (2011) Genome-Wide Gene Expression Analysis of the Switch between Acidogenesis and Solventogenesis in Continuous Cultures of Clostridium acetobutylicum. J Mol Microb Biotech 20(1):1–15
30. Grupe H, Gottschalk G (1992) Physiological events in Clostridium acetobutylicum during the shift from acidogenesis to solventogenesis in continuous culture and presentation of a model for shift induction. Appl Environ Microb 58(12):3896–3902
31. Lee J, Yun H, Feist AM et al (2008) Genome-scale reconstruction and in silico analysis of the Clostridium acetobutylicum ATCC 824 metabolic network. Appl Microbiol Biot 80(5):849–862
32. Alsaker KV, Paredes C, Papoutsakis ET (2010) Metabolite stress and tolerance in the production of biofuels and chemicals: gene-expression-based systems analysis of butanol, butyrate, and acetate stresses in the anaerobe Clostridium acetobutylicum. Biotechnol Bioeng 105(6):1131–1147
33. Lütke-Eversloh T, Bahl H (2011) Metabolic engineering of Clostridium acetobutylicum: recent advances to improve butanol production. Curr Opin Biotech 22(5):634–647
34. MlL Xia, Wang L, Yang ZX et al (2015) Periodic-peristole agitation for process enhancement of butanol fermentation. Biotechnol Biofuels 8(1):1
35. Maddox IS, Steiner E, Hirsch S et al (2000) The cause of "acid crash" and "acidogenic fermentations" duping the batch acetone-butanol-ethanol (ABE) fermentation process. J Mol Microb Biotech 2(1):95–100
36. Liu H, Huang D, Wen J (2016) Integrated intracellular metabolic profiling and pathway analysis approaches reveal complex metabolic regulation by Clostridium acetobutylicum. Microb Cell Fact 15(1):1
37. Ozyurek D, Kalyon A, Yildirim M et al (2014) Experimental investigation and prediction of wear properties of Al/SiC metal matrix composites produced by thixomoulding method using Artificial Neural Networks. Mater Design 63:270–277
38. Mikulandric R, Loncar D, Boehning D et al (2014) Artificial neural network modelling approach for a biomass gasification process in fixed bed gasifiers. Energ Convers Manage 87:1210–1223
39. Hore S, Bhattacharya T, Dey Net al (2016) A real time dactylology based feature extractrion for selective image encryption and artificial neural network. In: Image feature detectors and descriptors. Springer International Publishing, pp 203–226
40. Wang SC (2003) Artificial neural network. In: Interdisciplinary Computing in Java Programming. Springer, US, pp 81–100
41. Thompson KV, Chmielewski J, Gaines MS et al (2013) Competency-based reforms of the undergraduate biology curriculum: integrating the physical and biological sciences. Cbe-Life Sci Edu 12(2):162–169
42. Vale RD, DeRisi J, Phillips R et al (2012) Interdisciplinary Graduate Training in Teaching labs. Science 338(6114):1542–1543
43. Bialek W, Botstein D (2004) Introductory science and mathematics education for 21st-century biologists. Science 303(5659):788–790
44. Jin XQ, Zhou H, Wu XM et al (2008) A rapid screening method of producing strain in acetone-butanol fermentation. Chin J Process Eng 6:1185–1189
45. Strategy AE (1998) Design by directed evolution. Acc Chem Res 31(3):125–131
46. Fu AY, Chou HP, Spence C et al (2002) An integrated microfabricated cell sorter. Anal Chem 74(11):2451–2457
47. Arnold FH, Moore JC (1997) Optimizing industrial enzymes by directed evolution. In: New enzymes for organic synthesis. Springer, Berlin, pp 1–14
48. Arnold F (1998) In IBC directed enzyme evolution. San Diego CA
49. Zhang JH, Dawes G, Stemmer WP (1997) Directed evolution of a fucosidase from a galactosidase by DNA shuffling and screening. Proc Natl Acad Sci 94(9):4504–4509

50. Chen K, Arnold FH (1993) Tuning the activity of an enzyme for unusual environments: sequential random mutagenesis of subtilisin E for catalysis in dimethylformamide. Proc Natl Acad Sci 90(12):5618–5622
51. Zhao H, Arnold FH (1997) Combinatorial protein design: strategies for screening protein libraries. Curr Opin Struc Biol 7(4):480–485
52. Chen K, Arnold FH (1991) Enzyme engineering for nonaqueous solvents: random mutagenesis to enhance activity of subtilisin E in polar organic media. Nat Biotechnol 9 (11):1073–1077
53. Cadwell RC, Joyce GF (1992) Randomization of genes by PCR mutagenesis. Genome Res 2 (1):28–33
54. Wu WT (2004) Protein engineering technology and design of novel biocatalysts. Pharm Biotechno 11(1):1–6
55. Kikuchi M, Ohnishi K, Harayama S (2000) An effective family shuffling method using single-stranded DNA. Gene 243(1):133–137
56. Crameri A, Raillard SA, Bermudez E (1998) DNA shuffling of a family of genes from diverse species accelerates directed evolution. Nature 391(6664):288–291
57. Kikuchi M, Ohnishi K, Harayama S (1999) Novel family shuffling methods for the in vitro evolution of enzymes. Gene 236(1):159–167
58. You C, Chen H, Myung S et al (2013) Enzymatic transformation of nonfood biomass to starch. P Natl Acad Sci USA 110(18):7182–7187
59. Wang J, Chen X, Zhu H et al (2003) Relationship between aging and renal high-affinity sodium-dependent dicarboxylate cotransporter-3 expression characterized with antifusion protein antibody. J Gerontol A-Biol 58(10):B879–B888
60. Dueber JE, Wu GC, Malmirchegini GR et al (2009) Synthetic protein scaffolds provide modular control over metabolic flux. Nat Biotechnol 27(8):753–759
61. Jandt U, You C, Zhang YP et al (2013) Compartmentalization and metabolic channeling for multienzymatic biosynthesis: practical strategies and modeling approaches. In: Fundamentals and application of new bioproduction systems. Springer, Berlin, pp 41–65

Chapter 5
Periodic Intensification Principles and Methods of High-solid and Multi-phase Bioprocess

Abstract High-solid and multi-phase bioprocess is an interactive process among microorganism and environmental factors. Various environmental stimulations will affect microbial growth and metabolism in high-solid and multi-phase bioprocess. In this chapter, periodic intensification principle is proposed based on microbial physiology and biochemistry properties. Novel periodic intensification methods such as periodic peristalsis and gas double dynamic (GDD) were used in high-solid and multi-phase bioprocess to improve microbial performance, and mechanisms of the two intensification methods are systematically analyzed. Based on the analysis, it is concluded that periodic peristalsis and gas double dynamic can effectively intensify microbial growth and target products formation.

Keywords Periodic intensification · Periodic peristalsis · Gas double dynamic

5.1 Principle of Periodic Stimulation in High-solid and Multi-phase Bioprocess

5.1.1 Universality of Periodic Phenomena

Cyclical phenomenon is very common. Periodic rotation of cosmic objects, periodically running of the sun, the moon, and the earth causing seasonal changes in temperature, light, circadian turnover. Atmospheric gravity, laser ray ionization, ultrasonic radiation, and geomagnetic field result in month and day rhythm of organism reaction. Flowering, migratory birds, and fish are all biological circadian rhythm. Long-term cyclical organisms adapt to external environmental stimuli, and rhythmic oscillation occurs in individual cell, organs, constitution, and even molecular level, such as animal digestive EEG activity, electrocardiographic glycolytic, and molecule cell cycle change structure phenomena. Farmers make plant listen to music can promote growth. From the viewpoint of systems biology, genome replication and division, cell proliferation, and growth all occur with cyclical changes; the cycle of protein phosphorylation and

H. Chen, *High-solid and Multi-phase Bioprocess Engineering*,
Green Chemistry and Sustainable Technology,
https://doi.org/10.1007/978-981-10-6352-7_5

translation and eventually be degraded. Because of autocatalytic and allosteric effectors cyclical effect of the plasma membrane transport, oscillate always occurs in cell metabolism. Take Chinese medicine theory as an example, course of medication treatment is equivalent to a periodic intensification treatment, and the improved condition is a response to the stimuli; acupuncture in different parts of body the dredge meridians through periodic blood circulation. Systems biology and traditional Chinese medicine theory taught us to consider from the whole because the whole is often greater than sum of its parts [1].

Nature microbial species are widely distributed and easy to breed fast variation in environmental. They show a different response to the cyclical stimuli. Even in extreme environments, there are various extremophiles bacteria. Porous surface soil is the compound of liquid, gas, and solid matter. During microbial solid-state fermentation, periodic changes of airflow on the soil surface accelerate heat transfer, resulting in change of oxygen and CO_2 partial pressure, contributing to microbial metabolism. Less microbial species exist in deeper of the ground with inactive metabolism. This provides biomimetic basis for the periodic gas double-dynamic solid-state fermentation (GDDSSF) reactor. Organism with the long-term external stimuli has an inherent rhythm, which should be able to take place in the external force changes. For example, flowers under the lights come out early.

5.1.2 Periodic Oscillations in Biological System

In the natural sciences, a gap has always existed between the life sciences and nonlife sciences, entropy increase principle of Kelao Hughes and natural evolution of the law divided the nature law into two opposing camps: one proposes a unordered nature and the other is tend to an ordered nature. In 1940s, Schrodinger, one of the pioneers in quantum mechanics, wrote a book to explore the essence of life and presented the concept of negative entropy cybernetics in open systems. The formation of information theory and systems theory thought in the late 40s is the bridge established over the gap. The bridge was finished until the early 1970s when dissipative structure theory was proposed. Based on nonequilibrium thermodynamic theory, dissipative structure theory rigorously proved that in an open system which is far from thermodynamic equilibrium, complex nonlinear characteristics of the process can naturally form stable self-organizational behavior, and an ordered structure can be evolved from disordered space and time. In early 1980s, chaotic dynamics was co-founded by a group of mathematicians and physicists, which further proved that the conversion between disorder and order at different levels is the universal law of the nonlinear and complex process in nature. Periodic oscillation behavior is a typical example.

5.1.2.1 Calcium Oscillations in Biological Cells

Biological cells calcium oscillations are important biological rhythms phenomenon at a cellular scale. Calcium is also known as the "life and death signal" because it plays an important role in the numerous processes. It is well known that Ca^{2+} in cell solution is an important second messenger substance of cell [2, 3], transient release of Ca^{2+} is a major cellular response to bail signal, this change can exhibit strong spatiotemporal organization, and it is often in intracellular Ca^{2+} oscillations in the form of calcium called oscillation [4]. Cell solution of calcium oscillations plays an important role in information transmission between cells and the regulation of intracellular and in which the transmission of information and the regulation of many physiological processes are closely related, for example, muscle contraction, cell fertilization, and gene expression.

The mechanism of calcium oscillation is related to cell type. For excitable cells, it generally considered that cells calcium oscillations are related to the cytoplasmic membrane depolarization and channel of voltage-dependent Ca^{2+}. For non-excitable cells, such as liver cells, calcium oscillations occur regularly after stimulation by agonist but no spontaneous calcium oscillations occur. At present, the theory of the calcium oscillation mechanism which is more favorable is that: intracellular Gα subunit of the G protein is activated after agonist binding to the G protein-coupled receptors on the cell membrane in the extracellular, which further activate phospholipase C; the activated phospholipase C catalyzed hydrolysis of membrane lipid inositol diphosphate into inositol triphosphate and diacylglycerol; then inositol triphosphate bond to specific receptors in the endoplasmic reticulum membrane, leading to intracellular calcium Ca^{2+} channel opening, causing large amount of Ca^{2+} release from calcium pool and higher cytosolic Ca^{2+} concentration; Ca^{2+} release at initial stage can promote open of Ca^{2+} channel on the plasma membrane, causing inflow Ca^{2+} influx of extracellular; Ca^{2+} channels are blocked when Ca^{2+} concentration in cytosolic rises to a certain extent; and Ca^{2+} in cytoplasm is pumped out of the cell by calcium pump located on the plasma membrane or pumped into the Ca^{2+} pool in the endoplasmic reticulum, resulting in decrease of cytosolic Ca^{2+} concentration. This periodic change of Ca^{2+} in cytoplasm is called the Ca^{2+} oscillations. However, there are still many unknown aspects of this theory. For example, how the Ca^{2+} channel on the plasma membrane is opened at the initial stage of Ca^{2+} release, the characteristics of the channel and intracellular channels regulation mechanism need further study.

5.1.2.2 Glycolytic Oscillations

Another typical example is the reaction of biological oscillations glycolytic oscillations. The process that glucose and fructose-1,6-diphosphate by 3-phosphoglycerate degrade pyruvate and ATP generation is called glycolysis.

Under certain conditions, many glycolytic intermediate compounds during the reaction process and the concentration of enzyme involved may vary with the time period. In 1964, Chance et al. [5] observed oscillation of metabolic intermediates in yeast cell under the condition of limited oxygen and glucose. At the same time, the researchers found their glycolytic oscillations in cell extracts. When glucose is added to the extract at a steady rate, glycolytic intermediates oscillation with a certain frequency can be observed.

Regardless of cell or cell extraction, there is the same phase difference in oscillation glycolytic intermediates with phosphofructokinase as the core of oscillation, and the oscillation before and after the intermediate product has 180° phase angle difference. AMP is a conformational change in the regulator, and glucose-6-phosphate there is oscillation phase angle difference of 90°. High AMP concentration was accompanied by high phosphofructokinase activity, resulting in accumulation of fructose-6-phosphate and the consumption of fructose-1,6-diphosphate. On the contrary, fructose-1,6-diphosphate will be consumed and fructose-6-phosphate been accumulated.

5.1.2.3 Characteristics of Biological System

Essential difference between biological response to conventional chemical reactions is that the living organisms have sensitivity to the external environment, self-adjusting, and adaptive capacity, which are the natural properties of nonlinear complex systems. When the application period stimulation, biological experience self-adaptive adjustment, if repeated for a long term, this new adaptation will enter the genetic memory of the organism, to the next generation. In the above example, advanced plants and animals were studied everywhere. Many normal activities of organisms are cyclical characteristics, such as feeding and respiration. From complex systems engineering cybernetics perspective, fixed point is effective for the optimal control of linear systems but not for nonlinear systems. Nonlinear dynamic response cycle in regulation system to achieve optimal control strategy in the chemical system also began to gain attention. Biological reaction system at the cellular level, this adjustment period should be a universal input of optimization control. This stimulation cycle may be temperature, concentration, pressure, light, electricity, magnetism, and sound. For example, plants grow in nature and may be subject to various external stimuli such as mechanical strength, light, sound waves, and the growth and metabolism of organisms to external stimuli, and these relations have been the issue which physicists and biologists are concerned.

With a large value of V, stochastic simulation method is close to deterministic limit, and the system is still in the steady state (Fig. 5.1a; when the size of the system is very small, in a dominant position within the noise in the system, chaotic oscillations Fig. 5.1c); and if the system is in a medium size, the system shows random Ca^{2+} oscillations (as shown in Fig. 5.1b). Due to internal disturbances, Ca^{2+} can continue to maintain the oscillation in a wider range of parameters.

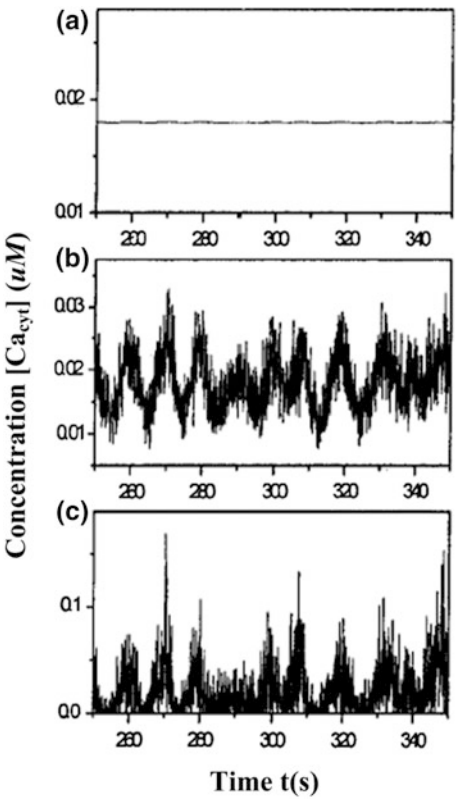

Fig. 5.1 Time sequence of [Cacyt] with different volumes. (**a** V = 106 μm^3, **b** V = 104 μm^3, **c** V = 102 μm^3)

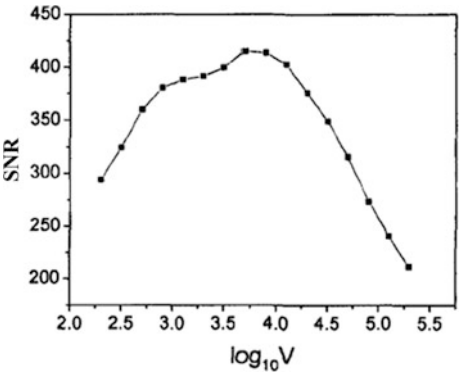

Fig. 5.2 Relationship between SNR and cell volume

In order to quantitatively describe the random oscillatory behavior, signal-to-noise ratio was defined [6]. Since the noise level is proportional to $1/\sqrt{v}$, therefore, the dependency of signal-to-signal noise ratio to cell volume is showed in Fig. 5.2, i.e., signal-to-noise ratio and the dependence of the noise. A similar

resonance behavior is showed, that is, system size resonance behavior. In a limited volume within the dominant noise signal-to-noise ratio is small. The signal-to-noise ratio increase with increased V and reaches the maximum when V is 103.7 μm^3. The volume of real-life in vivo cell volume and the same order of magnitude, indicating that the system of life has learned how to optimize the use of internal noise Ca^{2+} oscillatory behavior. Finally, as a further increase in volume, signal-to-noise ratio reduced, indicating that if the size of the system is very large, the noise inside the system is difficult to induce random oscillations. In a certain amount of excitation agonists, calcium oscillation does not occur even in a deterministic system, the cells will be automatically adjusted by internal disturbances induced calcium oscillations, and thus the signal transfer.

5.1.2.4 Theory Analysis of Metabolic Periodic Oscillations: Nonequilibrium and Nonlinear Theory

Nonequilibrium and nonlinear theory in chemical reaction can be used to explain biological oscillations, biological chaos, and self-organized phenomena in biological systems. Wang et al. [7] reviewed biological temporal oscillation analysis methods and characteristics, which are based on dissipation structure and temporal oscillations, emphasizing advance of enzyme oscillation, calcium oscillation, and the oscillation of glycolysis in cellular metabolism analysis.

In nature, snow and other ordered crystal structure are balanced structure. It can be maintained even in the isolated environment and under equilibrium conditions without exchange energy with the environment and material, which can be explained by Boltzmann principle. However, the macroscopic spatiotemporal structure, such as biological system, must be maintained by energy and matter exchange with the surrounding environment in an open nonequilibrium conditions. In fact, cells of living creature can only survive by continuous exchange materials with the environment to get nutrient supply. Order structure showed by living body in an open and nonequilibrium condition cannot be explained by Boltzmann principle, because the cells are not only the organic molecules which could be synthesized in the laboratory but also a highly organized whole with a clear spatiotemporal organization. Even the formation of a particular protein molecule with one hundred amino acids (all kinds of amino acids) will take more than 3×10^{116} years according to the probability formula. Why does the highly complex and macroscopic ordered structural in biological system which is spontaneous formed exist? Nonequilibrium thermodynamics [8], which was proposed by Prigogine, is a big leap in human understanding. For life activities, cells must generate an unbalanced situation in their environment, and open and nonequilibrium conditions are necessary for life generation and all life sustaining. In addition, the biological order is not only reflected in the space ordered but also in the time ordered. The generation, development, reproduction, and death of living organisms occur in a time order. In cellular metabolism, glycolysis reaction, clock, brain waves, and other

biological oscillations are all examples of time ordered behaviors. Spatiotemporal order is the primary nature of biological systems.

Organism is a highly complex, self-renewing, and highly self-autonomous system. Its structure has clear boundaries, such as semipermeable film which enables the organism to connect outside in an unimaginable way. Organisms absorb low entropy ordered protein, fat, and starch from outside and excrete high entropy disordered water and CO_2. The introduction of negative entropy flow from the outside can offset its own entropy production so that the total entropy of the system gradually reduced from small biological systems to highly ordered structure with long-term sustainability, even to a more complex and orderly evolution and development.

Living organisms maintain life in a "steady state" through metabolism, which is a nonequilibrium state. Life processes in nonequilibrium state is an irreversible process. Because the irreversible process of nonequilibrium state is represented by the generated entropy, the relationship between the force and flow is linear or nonlinear.

When there is a system in thermodynamic force X (temperature gradient, concentration gradient, potential gradient, and reaction affinity driving force), there will be an irreversible process and the introduction of entropy production. The total entropy production rate of thermodynamics stream (heat flow, material flow, charge flow, and chemical reactions) produce under these thermodynamic forces should be as follows:

$$\dot{S} = \frac{d_i S}{dt} = \sum_k J_k X_k > 0. \tag{5.1}$$

There is a linear relationship between the force and flow in equilibrium or near equilibrium in nonequilibrium zone

$$Jk = \sum L_{\mathrm{kl}} X_i, \tag{5.2}$$

where L_{kl} is phenomenological coefficient [9].

$$\begin{aligned} \dot{S} &> 0; \\ \frac{d_i S}{dt} &< 0; \\ \frac{d_i S}{dt} &= 0. \end{aligned} \tag{5.3}$$

If the system is an isolated system, the force and flow in the system tend to zero after a free development and eventually reach a steady equilibrium state. If some restrictions are imposed on the system, the system will eventually reach a nonequilibrium state which cannot change with time. When the system is steady, the entropy production rate is minimal.

When the system is in a steady state, where perturbation or fluctuation occurs and steady state departs from the minimal entropy production rate, the entropy of the system spontaneously reduces until returning to the original state.

Therefore, in a nonlinear region of the nonequilibrium state, the system never can be transferred into a new steady state and ordered structures cannot form. In contrast, it tends to destroy any orderly but increase in disorder.

If the system is far away from equilibrium thermodynamic, the function of flow and force is expressed in Taylor style, and the balance state is used as a reference state:

$$J_k = J_k(0) + \sum \left(\frac{\partial J_k}{\partial X_l}\right) 0X_1 + \frac{1}{2}\sum \left(\frac{\partial J_k}{\partial X_l X_m}\right) 0X_l X_m + \cdots \tag{5.4}$$

Showing a nonlinear relationship between the force and flow, the system is in a nonequilibrium nonlinear region. It is not necessarily being a minimum value for entropy production at this steady state.

Deterministic view is that, under constant control conditions, a chemical reaction system experienced a long enough time and finally reached an ultimate state which cannot be changed with time and space. However, people have long known that chemical components concentration change and show oscillation in some autocatalytic or self-organized chemical open system.

5.1.3 Biological Periodic Rhythm and Regulation of Metabolic Network

5.1.3.1 Effect of Biological Periodic Rhythm and External Stimuli on Biological Periodic Rhythm and Regulation of Metabolic Network Biology

Plants grow in nature subject to a variety of external environment, including mechanical stress stimulation, so the relationship between growth and stress has been an issue which biologist and physicist are concerned. It has long been recognized that mechanical intensification has a significant effect on plant growth. The most obvious examples are climbing plants, which recognize the environment and stretch along a path through contact-sensitive stems, petioles, tendrils, petioles, and roots. In addition, people also observed the following phenomena: (1) some plants are struck by thicker stems shorter; (2) the plant stem synthesizes ethylene affected by friction, then the stem becomes thicker shorter; and (3) the root growth will be hampered within a few hours after being struck. In addition, it was found that the cyclical vibration caused by the wind had a significant effect on plant morphogenesis. In general, vibration can make the stem thicker and shorter, thus to resist vibration.

In addition, as a special form of alternating stress, strong sound waves have a significant impact on plant growth. Many scientists at home and abroad have studied the impact of music on plant growth. They found that a certain intensity of music stimuli can significantly promote the growth of certain plants. All of these results showed that the mechanical stress signal has a certain influence on plant growth and development. Sun et al. [10] studied the effects of alternating stress on tobacco callus cells, using the strong acoustic generator to generate alternating stress field, and using differential scanning calorimetry to study changes of thermodynamic phase behavior of tobacco cells after alternate stress with different intensities and frequencies. The results showed that the effect of the alternating stress was closely related to the frequency and intensity of the stress. The alternating stress in the range of frequency and intensity can reduce the phase transition temperature of the plant cell obviously, while the high-frequency stress stimulus increase cell transformation temperature. Cell thermodynamics phase transition reflects the cell wall membrane fluidity, and low phase transition temperature indicates increased cell wall membrane fluidity, which is related to the growth and division of cells provides a convenient condition. Therefore, it is a meaningful attempt to study the effect of alternating stress on plant growth and development from the cellular and molecular level and its mechanism.

The importance of physical forces in regulating the macroscopic growth of tissues has been recognized in scientific research. Recent studies showed that, in vitro, direct mechanical disturbances can alter the metabolism of many cells with different types [11]. The cytoskeleton system provides a molecular pathway for cell conduction and integration of mechanical signals [12]. The rapid growth and proliferation of tumor cells make the cytoskeleton depolymerization, polymerization, and other functional activities. Stimulating tumor cells with mechanical intensification and analyze its effect on growth behavior of tumor cells, which is meaningful to understand the regulation of tumor proliferation.

5.1.3.2 Mechanism of Biological Periodic Rhythm

From the 1970s, people began to reveal the mechanism of spontaneous oscillation (periodic rhythm) molecular loop in cells with genetic and molecular biology methods, and what is the role of light, temperature, and other external signals in molecular oscillator.

The present experimental method is able to screen the mRNA expression patterns of all rhythm-related genes at genomic level. It is found that about 10% of the genes of mRNA in higher eukaryotes can be accumulated with rhythm. Fluorescence or bioluminescence probe imaging techniques allow people to observe the operation of the self-oscillating oscillators at the single-cell level. Periodic oscillations are common in single cell. However, these rhythmic oscillations have noises, i.e., their periods are not strictly constant, but are fluctuating from

one cycle to the next [13]. With the absence of cell–cell interactions, these cellular rhythms are non-synchronized and exhibit rhythm disorders at the population level. On the other hand, a sufficiently strong oscillating coupling action counteracts this chaos and ensures the synchronization of cell population.

5.1.3.3 Biological Periodic Rhythm and Regulation of Metabolic Network

Microorganisms are generally single-celled organisms, and microbial growth, cell metabolism, and reproduction have a fixed cycle, which is closely related to biosynthesis. In general, single-cell algae breed one generation every 3–6 h, 2–4 h for yeast, and 0.5–1 h for bacteria. Microbial growth curve is divided into lag, exponential, stable, and decay phases. This is the periodic rhythm of microbial population growth.

Lag phase. When the cells were introduced into the fresh liquid medium, the volume of the cells increased rapidly in the initial culture stage, and the synthesis of the inducible enzymes was increased. The protoplasm of the cells was homogeneous, but the cell concentration did not change significantly, the curve is gentle. Cells in this period are in the new physical and chemical environment of the adaptation period, and are preparing for rapid growth and reproduction. The duration of the lag phase change with microbial species or strains and culture conditions. The practice proved that the delay can range from a few minutes to several hours, days, or even months. If there is a long lag phase, it will lead to lower utilization of equipment, water consumption resulting in increase of production costs and lower labor productivity, and economic benefits. Only shorten the delay period can improve economic efficiency. Therefore, it is very important to be aware of the formation mechanism of lag phase and provide theoretical basis for shortening or lengthening the lag period, which is very important for its application in industry, agriculture, medicine, environmental microbiology, and its application. Therefore, in the practice of microbial applications, strong strains usually in rapid growth and reproduction state should be taken.

Exponential phase. In the logarithmic growth phase, due to strong metabolism, rapid growth, generation stability, individual morphology, chemical composition, and physiological characteristics are more consistent. Therefore, in microbial fermentation production, using logarithmic phase cells as the seed can shorten the lag phase and improve labor productivity and economic benefits. Cell in logarithmic growth phase is also the excellent material for studying microbial growth, metabolism, and genetic regulation of biological basic characteristics. The growth rate of exponential growth phase is affected by environmental conditions (composition of culture medium, culture temperature, pH value, and osmotic pressure), which is also a reflection of the genetic characteristics of microbial strains under certain conditions. In general, prokaryotic microbial cells grow faster than eukaryotic

microbial cells and smaller eukaryotic microorganisms grow faster than the larger eukaryotic microorganisms.

Stationary phase. In this period, there must be some factors inhibit cell growth and reproduction. In general, the main factors which restrict the logarithmic growth are as follows: (1) the depletion of essential nutrients in the medium or the concentration cannot meet the needs of maintaining the growth of the index to become growth limiting factor; (2) large cell effluent in the medium of inhabit the growth of bacteria; and (3) changes in the physical and chemical environment inside and outside the cell caused by above two main factors, such as the ratio of nutrients, pH, and redox potential changes. Although these factors do not occur at the same time, once one factor exists, cell growth rate will be reduced, affecting the combined effect of growth factors. And then, cell death and growth achieve balance, which is the stable period of population growth. During the stable phase, the number of cells does not fluctuate greatly, and the growth rate constant is substantially equal to zero. At this point, the cells grow slowly, and some even die, but energy metabolism and a number of other biochemical reactions continue. Storage substances, such as glycogen, heterochromatin granule, and adipose granule, accumulate in the cells at stable phase, and most of the spore-forming bacteria also form spores at this stage. The number of viable bacteria reaches the highest level at stable growth. At the stable phase, the accumulation of metabolites began to increase, and gradually reach to the peak.

Decay phase. When microorganisms reach the stable growth stage, the cell death rate gradually increased in the population due to the continued deterioration of the growth environment and the shortage of nutrients, so that the number of dead bacteria gradually exceeded the number of new bacteria. Abnormal cell shape and size appear in the decay phase. Many intracellular metabolites and intracellular enzyme release to external. Growth curve of microorganisms reflects growth and reproduction and death of the law in a certain environment (such as test tubes, shake bottles, fermenters). It can be used as a theoretical research index to investigate effects of nutrient and environmental factors on growth and reproduction, and can also be a basis for regulation of the growth and metabolism of microorganisms and guide the practice of microbial production. In the microbial metabolic process, various metabolites will produce, which can be divided into primary metabolites and secondary metabolites according to the relationship between metabolites and microbial growth and reproduction. Primary metabolites are essential metabolites generated by the microorganisms for their growth and reproduction, such as amino acids, nucleotides, polysaccharides, lipids, and vitamins. In different microbial cells, the primary metabolite products are basically the same. In addition, the synthesis of primary metabolites happened during all the fermentation process, any obstacles to product synthesis will affect the normal microbial life activities, and even lead to death.

Secondary metabolites refer to the microbial growth at a certain stage. Their chemical structure is very complex and has no obvious physiological function, or is

not necessary for microbial growth and reproduction of substances such as antibiotics, toxins, hormones, and pigments. Different microorganisms produce different secondary metabolites. They may accumulate in the cell or be released to the external environment. Among them, antibiotic is a class of organic compounds with function of specific inhibition and bactericidal effect. The commonly used antibiotic are streptomycin, penicillin, and erythromycin and tetracycline.

The period of generation and accumulation of different metabolites is different. For example, the primary metabolites of microorganisms are synthesized in large amounts during the lag phase, while large amounts accumulate in the logarithmic phase. Strong division of cells produced more primary metabolites because the primary metabolites of microorganisms provide material basis for microbial growth and development. The secondary metabolites of microbes are synthesized and accumulated in stable phase, and the yield changes with time, in order to remove the product feedback inhibition, monitor, and isolation of the product in real time should be done.

The growth of certain microorganisms and the conditions required for fermentation products are different; in the early stages of fermentation, appropriate conditions should be provided for microbial growth and microbial mass reproduction. And then, the products are synthesized in new environment. In addition, the external signal stimuli can also change the microbial cell cycle, such as shorten or extend the life stage of the accumulation of metabolites. By the external factors on the role of microbial cells, intracellular metabolic network flow changes in different ways, thereby increasing the carbon source to the target product flow accumulation and reducing the flow of by-products to obtain more target products. From the view of complex system engineering control theory, the optimal control of fixed point is only effective for linear system and not for nonlinear system. The periodic control of the nonlinear reaction power system is achieved, and the chemical reaction system has been paid more and more attention. For a bioreactor system at the cellular level, this periodic input adjustment should be a general optimization control. Such periodic stimuli can be temperature, concentration, pressure, light, electricity, magnetic, sound and other physical factors. In addition, it can also be substrate, product concentration, and other chemical factors. Microbial cells exposed to external stimuli factors, that is, impose a new cycle of perturbation to the cell cycle. The use of cell rhythm oscillator adaptability and plasticity to change the metabolic circuit or biological clock, by the transcription level, translation level or phosphorylation cycle response to strengthen the inherent cycle of the cell rhythm or produce a new rhythm oscillation phenomenon, regulation of intracellular metabolic network so that it is beneficial to the fermentation engineering practice for biochemical reaction engineering, which has broad prospects for development.

5.1.3.4 Propose of Periodic Intensification in High-solid and Multi-phase Bioprocess

Based on the above analysis, it was assumed that the fermentation process to improve the microbial biomass by periodic external stimulus to accelerate their

metabolism in the fermentation process is line with the law. Microbes are highly adaptive, appropriate intensification cycle will magnify fermentation efficiency and enable the microorganism to play a quick and efficient role and service humanity. Our practice has proved that the application of periodic intensification in bioreactor design showed a great advantage.

The living organism itself, called cell factory should be optimal bioreactor structurally. Since ancient times, humans have used this natural gift along with many limitations. Now, biotechnology requires more efficient way to produce large quantities of the desired biological products, which is the object of study biological reaction engineering. Although advances in genetic engineering for the construction of the plant cell have been made great progress, people have not totally controlled the modified microbes. People still need to adjust the external environment to achieve goals that genetic engineering cannot achieve. Build an excellent artificial bioreactor is not easy in bioprocess engineering. At present, the mechanical stirred tank is commonly used. However, damage caused by mechanical mixing tank on cells is always difficult to solve, and it is difficult to be scale up industrially. Therefore, more ideal new artificial bioreactor has become one of the modern biotechnology industry research major research directions.

From modern bioreactor engineering literature, it can be easily found that the contents of the bioreactor, the theory, and method almost simply transplant general chemical reactor theory. However, in vivo, biological response is a complex network system simultaneously nonlinear material, energy and information conversion differences on the molecular level with a level of a chemical reaction with the conventional. So simply transplant chemical reactor theory and method may not work. Li [6] proposed to strengthen bioreactor rate and mass transfer principles by periodic external stimuli based on new developments in the life sciences, mathematical sciences, such as dissipative structure theory and chaotic dynamics theory. Based on the principle, an airlift loop bioreactor and GDDSSF bioreactor have been designed, and achieved good results, showed a broad development vision of universal significance.

Reconsidering theory and methods of liquid–solid mass transfer in modern chemical industry, it is the basic means to enhance the relative movement of the two-phase liquid–solid interface between mixed. In either two-film theory, penetration theory, or surface renewal theory, tangential friction momentum transfer and mass transfer strengthen on the interface. In nonbiological systems, this maximum tangential force cause damage to solid phase, which is benefit to the reactivity. However, in terms of the living organism, increasing the shear force will affect cellular metabolism and cause injury and even death. Therefore, tangential force (in traditional chemical liquid–solid mass transfer of methods and tools) cannot fully meet the requirements of living cells culture. Based on this understanding, we propose concept and methods that strengthen mass transfer by normal force.

Biological cell is a hierarchy with basic reproductive ability. Cell membrane separates the cell from outside environment, and the structure and function of the cell membrane are still the most cutting-edge areas of biological research today. The most representative model of fluid mosaic model proposed by Singer et al. [14] was that a two-dimensional solution globulin and lipids orientation. Membrane lipids and membrane proteins are constantly lateral movement. Cells and the surrounding environment through the cell membrane continuous exchange of substances, modes of transport have to wear membrane transport and membrane package transport. Microbial cells are different from animal cells, cell wall outside the cell membrane, and have a unique shape to withstand high osmotic pressure within the cell. Due to the high concentration of internal metabolites, causing the osmotic pressure of up to 20 atmospheres. Cell walls are macromolecules with more tough and slightly flexible bags, and cells shrink in hypertonic solution and enlarge in a hypotonic solution, which is related to toughness and flexibility of the cell wall. If artificially increasing external pressure, making it much more than the body pressure that exceeds the tolerance range of the cell wall will rupture the cells to achieve the purpose of sterilization.

In the bioreactor, there are three important processes, namely, thermodynamics, kinetics, and microstructure transfer process. The former two has nothing to do with zoom in theory. However, with the change of reactor size, momentum transfer within the system change, especially stirrer shearing of biological cells increased with the increase of reactor size, not only affects the dispersed state of the cells, such as flocculation suspension and forming clumps, but serious cases will lead to shear cell injury.

Transfer process is significantly affected by system size, which should be the core issues of enlarged reactor. In the transfer process in the bioreactor, it depends on two factors: convection and diffusion. Secondary phenomenon related to this, namely, mixed fluid shear, mass transfer, heat transfer, and the macroscopic reaction rate, may be important factors in the amplification process. Internal rules of the bioreactor system and its influencing factors, focused on solving related to mass transfer, momentum transfer and heat transfer problems, in order to maintain the growth rate of biological cells as possible in the amplification process of the reactor, the rate of formation of metabolites, which would be object the of enlarged bioreactor [15].

There is a long history although the bioreactor engineering disciplines are relatively new. In ancient, European filled cow stomach with milk, and microbes in cow stomach converted milk into cheese. This is original artificial cow stomach bioreactor. Production of Chinese wine began in the Zhou Shang Dynasty; airtight container of wine is an early bioreactor [16]. Bioreactor major innovation occurred in the 1940, it would have been a chemical reactor knowledge transplanted to the fermentation industry. A deep mechanically stirred bioreactor for fermentation production of penicillin has been developed to

achieve pure mass culture (50–150 m^3). Three transport and one reaction theory in traditional chemical engineering have been used in following 30-years research, and bioreactor did not change fundamentally. Since the development of genetic engineering and cell engineering in 1970s, fermentation engineering is not simply a natural microorganism, but involving the bacteria, animal and plant cell culture genetic engineering. This demands new efficient diverse and large-scale requirements.

Our previous works focused on nonlinear dynamics properties of the principles in life and living cells enzymatic reaction network system, which affect the structure of the functional properties of the membrane material and information transfer. Gradually clear understanding should be based on the normal cell cycle to force a power source, to increase the rate of cell membrane bioreactor mass transfer rate. "Strengthen the mass transfer rate by outside periodic stimulation" in bioreactor design was proposed and a (kinetics of biological reaction) structural framework of "four transfer" (momentum, quality, energy, information) in biological reaction engineering was formed. With the principle, a 100 m^3 double loop airlift bioreactor for glutamate production and a 100 m^3 GDDSSF reactor have been successfully developed [17].

5.2 Analysis of Bioprocess Principle of Periodic Intensification for High-solid and Multi-phase System

5.2.1 Macro-Effect of Periodic Intensification on Fermentation Process

5.2.1.1 Effect of Periodic Gas Intensification on Solid Medium

Li [18] observed solid medium in gas double-dynamic system. QuickCam ® 8.0 camera and industrial endoscope were used as image acquisition device. The observed sample was placed on the material support inside the reactor. After adjusting light source and the focal length of the camera, the reactor was closed and the air pulse program was run. At the same time, the material change was recorded under air pulse. The range of air pressure pulsation used in the test is 0–0.2 MPa.

No obvious movement of normal fermentative solid medium (steam-exploded straw (4): wheat bran (1)) was observed during air pulsation. However, intensive air flow in solid medium can be felt (Figs. 5.3, 5.4 and 5.5).

The volume of compressible objects in the reactor changed significantly. In this section, the morphological changes of a large block of foam in GDD were observed. Observations showed that the volume decreased as the pressure increases and returns to its original size when the pressure decreased.

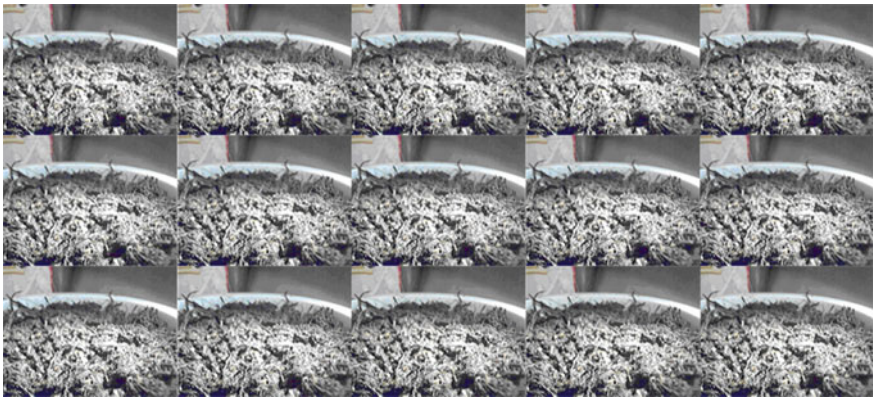

Fig. 5.3 Solid medium in high pressure

Fig. 5.4 Solid medium in low pressure

The strength of GDD was observed by using small mass and low-density objects. The materials used were ion exchange resins, foam particles and cotton fibers. The results showed that the tangential force of the gas phase intensification is very weak, and it cannot make the tiny resin particles and the fine cotton fibers move while normal force is strong, which can make obvious compression deformation of the foam granules.

The effects of gas phase intensification on the liquid were observed. Also, as an incompressible material, no appreciable change in water was observed under GDDSSF.

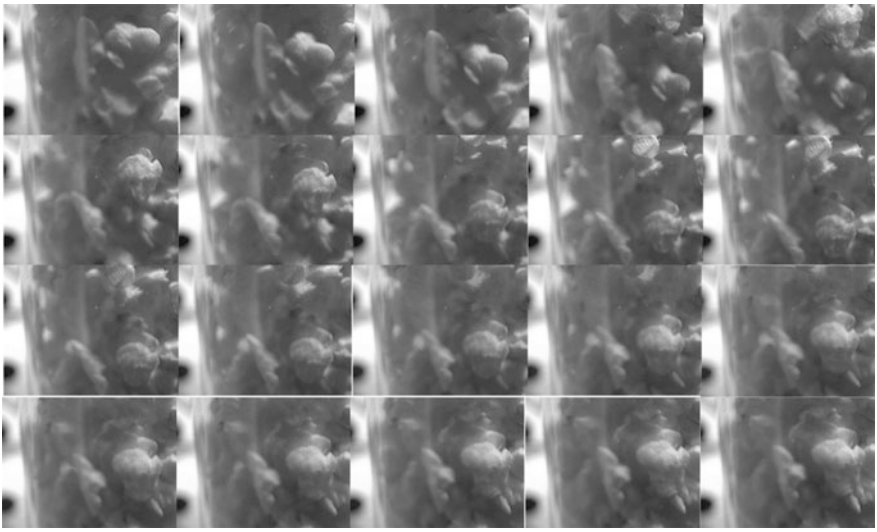

Fig. 5.5 Change of foam under GDDSSF

5.2.1.2 Effect of Magnetic Field on Microbial Growth

Magnetic field effects on organisms are multilayered and have been reported at the cellular, with a primary focus on animal and microbial cells.

The first study about the role of magnetic field on the biological start from the microorganisms, there have been reports in the magnetic field culture of bacteria, yeast, filamentous bacteria, colony that no major changes occur. Later, people extend the study of microorganisms to a variety of biological and magnetic fields and found different phenomena when studying the relationship between microbe and magnetic field. Microorganisms are mostly single-celled organisms, and the role of magnetic field on microorganisms can be seen as a direct role of the magnetic field on the typical cell. Therefore, in the study of the relationship between cells and the magnetic field, the microorganism is the best material.

In view of the wide range of microorganisms, the role of the magnetic field effects is not the same. With the advancement of applied physics, the application of superconducting materials in electromagnetic fields has made it possible to produce high magnetic fields (100,000 times of the geomagnetic field). Biologists have begun to notice the effects of high magnetic fields. A new technique of controlling the biological response using a high magnetic field is proposed. The most recent results are the increase in the amount of cells in the initial logarithmic growth of *E. coli* at T7 under the high magnetic field. This facilitation is more obvious in the heterogeneous 5.2–6.T magnetic field, and the amount of *E. coli*

*c*ells increased by two- to threefold, making it possible to increase the yield of the product in *E. coli*.

The physiological and biochemical indexes including growth curve and enzyme activity between the treatment group and geomagnetic control group were compared to study the effect of dynamic magnetic field on microorganisms. It was found that the growth of two strains of bacteria was affected by dynamic magnetic field. In the treatment group, *B. subtilis* was inhibited in the exponential phase, the alkaline protease activity increased, the activity of neutral protease was decreased, and the protease expression was not different. The dynamic magnetic field treatment group of *Salmonella typhimurium* delayed the lag phase.

5.2.1.3 Effect of pH Pulsation on Microbial Growth

Huang et al. [19] optimized fermentation performance using pH pulsation.

The researchers found that the composition of the by-products were significantly different when producing 1,3-propanediol via *Klebsiella pneumoniae* fermentation using glycerol at different pH. The main by-product of lactic acid when the pH was 7.1–8.0 while the main by-product was 2,3-butanediol when the pH was 5.0–6.0. Aimed at the different stress effects of cell metabolism on the outside, the regulation strategy of pH fluctuation was adopted in the feeding process. The pH of the fermentation broth was controlled between 6.3 and 7.3 by controlling the ratio of glycerol to ammonia and the flow rate. Two control schemes (A and B) were adopted. The fluctuation periods of the two regimens were different. The protocol A was 4 h and the protocol B was 8 h (Table 5.1).

The final concentration of 1,3-propanediol in the final fermentation broth reached 70 g/L, which not only effectively inhibited the production of 2,3-butanediol and lactic acid but also reduced the conversion rate of the two main by-products. The concentration of residual glycerol in the final fermentation broth reduced the difficulty in the separation and extraction of 1,3-propanediol.

5.2.1.4 Effect of Ultrasonic Wave on Microbial Fermentation

Ultrasonic wave is a kind of physical energy. Under the low intensity and proper frequency, its special cavitation forms turbulence and vortex-type ultrasonic action,

Table 5.1 pH regulation strategy and fermentation performance

	A	B
Period of fluctuations/h	4	8
Time/h	28	72
Propylene glycol concentration/($g.L^{-1}$)	55	70
Propylene glycol yield/($mol.mol^{-1}$)	0.63	0.60
Convert rate/($g.L^{-1}.h^{-1}$)	1.96	0.97
Residual glycerinum concentration/($g.L^{-1}$)	1.1	0.5

which caused the local temporary to be the negative pressure area and produce unstable vacuoles. Ultrasonic wave propagated in the medium, making the particles enter the vibration state of the media, which occurs mainly in the interface layer, membrane or cell wall in the vicinity and in the cell fluid. Ultrasound can increase the biofilm and cell wall mass transfer speed. Liquid circular motion around the bubble is benefit to the mass transfer of, substrate into the active site of the enzyme and the product into the media, thereby enhancing the rate of biological reactions [20].

Ultrasound in biochemistry in the earliest application is to crush the cell wall to release its content. However, with the application of ultrasound in life science, it was found that low-intensity ultrasound can accelerate the growth of microbial cells and promote the synthesis of beneficial metabolites. Gao et al. [21] found that, with the frequency of 32.5 kHz, power of 30 w ultrasound irradiation of beer yeast, cell growth rate increased in the logarithmic phase, indicating that the appropriate frequency and intensity of ultrasound can improve the cell growth.

5.2.2 Effect of Periodic Intensification on Expressed Proteins in Microorganism

5.2.2.1 Effect of GDD Periodic Intensification on Microbial Proteins in Solid-State Fermentation

Fu et al. [22] studied the effect of GDDSSF on the expression of microbial proteins in solid-state fermentation. FPA activity, CMCase activity, and β-glucosidase activity were determined after extracting the protein from the static solid-state fermentation and gas double-dynamic solid-state fermentation. Comparison of the protein quality extracted from dry mass (Fig. 5.6), FPA activity (Fig. 5.7), and CMCase activity (Fig. 5.8) during the 7 d fermentation cycle of the two fermentation modes) and β-glucosidase activity (Fig. 5.9).

Figure 5.6 shows that the amount of protein extracted from per unit dry mass was the highest in the 7 d fermentation cycle, and the amount of protein produced at 6 d fermentation was the highest. The mass of the extracellular protein extracted from the dry mass of the microbes after 6 d of solid-state fermentation was 5.31 mg and 9.09 mg, respectively, which were 34.63 and 17.75% higher than those obtained from static conventional fermentation. So the GDDSSF improved the quality of the fermenting microbial protein. The microorganisms extracted from the gas double-dynamic solid-state fermentation for 5 days had the same quality as those extracted from the solid-state fermentation for 6 days. The GDDSSF improved the fermentation condition and shortened the fermentation cycle.

Figures 5.7 and 5.8 show the same enzyme activity trend in the two fermentation systems. The results showed that the activity of extracellular protein was increased,

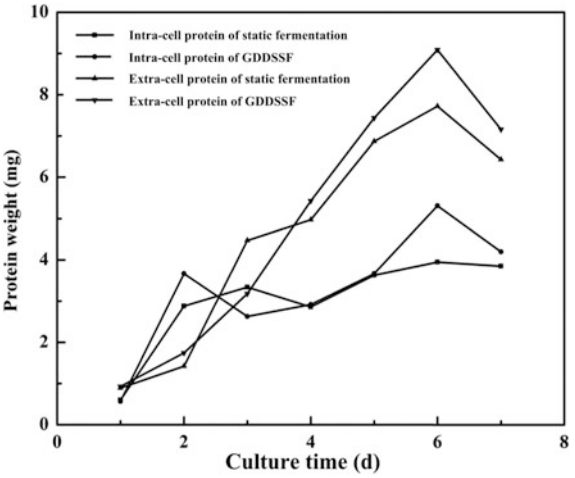

Fig. 5.6 Effect of GDD stimuli on microbial protein quality of solid-state fermentation

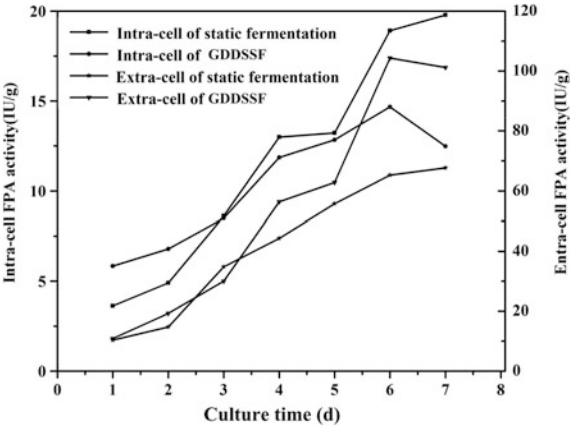

Fig. 5.7 Effect of GDD stimuli on FPA activity of solid-state fermentation

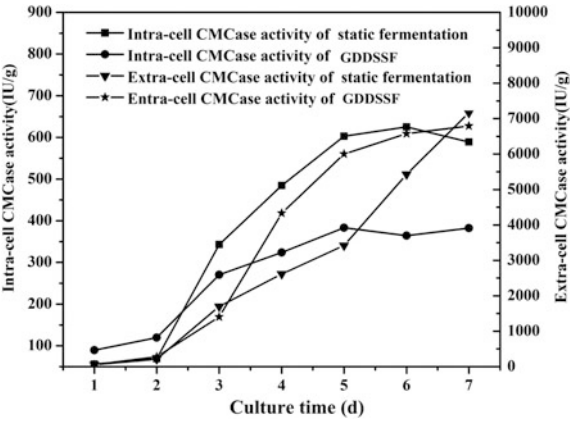

Fig. 5.8 Effect of GDDSSF on CMCase activity

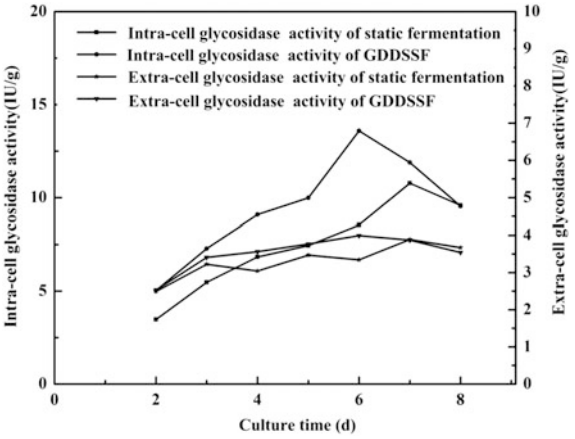

Fig. 5.9 Effect of GDDSSF on β-glycosidase activity

but the activity of intracellular protein was slightly decreased. The activities of extracellular FPA and CMCase of the dry mass of the enzyme were 104.34 IU•g^{-1} and 6575.52 IU•g^{-1}, respectively, and the activities of intracellular FPA and CMCase activity were 14.7 IU•g^{-1} and 383.52 IU•g^{-1}, respectively. The activity of the extracellular protein in GDDSSF at 5 d was similar to that in the static solid-state fermentation at 7 d. And it increased by 21.17% at 6 d compared with the former one. In addition, the determination of the enzyme activity verifies that the protein extraction and purification methods are feasible.

Figure 5.9 shows that β-glucosidase activity is higher than that of extracellular in the fermentation. The β-glucosidase activity in gas double-dynamic solid-state fermentation was higher than the conventional static solid-state fermentation. At sixth day, the intracellular and extracellular β-glucosidase activity of the dry mass of the enzyme was 13.586 IU/g and 3.99 IU/g, respectively. However, the intracellular and extracellular β-glucosidase activity per unit mass of the conventional static solid- The activity of extracellular β-glucosidase was 8.54 IU/g-1 and 3.34 IU/g, respectively, and reached the highest level at the seventh day of fermentation, which were 10.77 IU/g and 3.89 IU/ g.

SDS-polyacrylamide gel electrophoresis (SDS-PAGE) is an economical, rapid and reproducible method for the quantification, comparison and characterization of proteins. SDS-PAGE analysis of proteins before and after purification (see Fig. 5.10) was performed to compare the difference between the purified solid-state fermentation microbes and GDDSSF microbes, and the SDS-PAGE electrophoresis curves were used to calculate the molecular weight size.

It can be seen in Fig. 5.10, compared with the control group, microbial protein composition changes in GDDSSF reduce the relative molecular mass of about 80,400 components, but increase the relative molecular mass of about 28520 components.

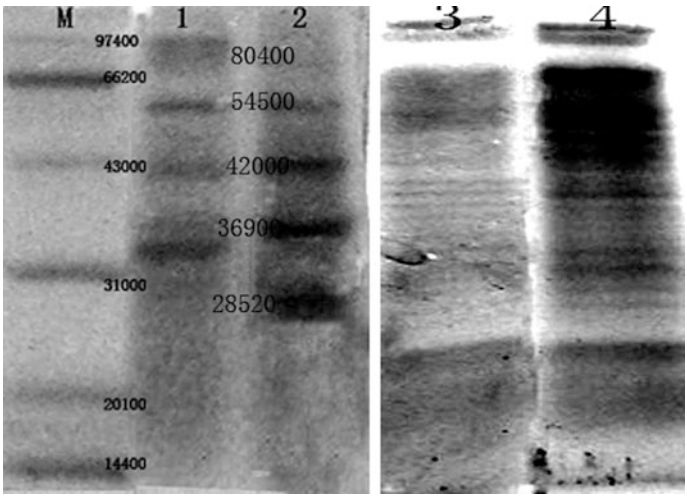

Fig. 5.10 SDS-PAGE image of protein (1. protein in static culture after purification, 2. protein in GDDSSF after purification, 3. protein in static culture before purification, 4. protein in GDDSSF before purification, and 5. standard protein)

Changes in the external environment may promote the proteins in the body to spontaneous assemble, such as rotation to change its original conformation, or spontaneous generation of the corresponding stress proteins to adapt to changes of the external environment. For example, heat shock proteins (HSPs) were stress protein induced by high temperature, hypoxia, starvation, heavy metal ions, and other adverse environmental factors. They are very important in cell signal transduction. Under adverse conditions, both bacteria and humans can induce the synthesis of some proteins to protect cells from further damage.

Under the two different fermentation modes, the microbial protein changed in the yield, the enzyme activity and the composition. Compared with the conventional static solid-state fermentation, the GDD becomes a different periodic intensification source. In order to adapt to this different cycle of stimulation, the composition of the protein in microorganisms changed. Some protein synthesis may be inhibited, reflected by decreased activity of intracellular protease, and some specific proteins were induced synthesis, reflected by increased activity of intracellular protease. However, from the increase of fermentation yield, it can be seen that the induced protein by this intensification was beneficial to the growth of microorganisms and the fermentation yield is improved. SDS-PAGE also confirmed the differences in protein components between the two fermentation methods. However, the specific properties and functions of these differential proteins still need further studies.

5.2.2.2 Effect of Dynamic Magnetic Field on Microbial Protease Expression

The effect of dynamic magnetic field on protease expression during the cultivation of *Bacillus subtilis* was investigated. The effect of dynamic magnetic field on the growth of *Bacillus subtilis* was studied based on the static magnetic field generated by the superconducting magnets. The growth curve, sprouting rate, protease expression, and protease activity were studied by static magnetic field microbial traits. The results showed that the strong magnetic field could affect the spore formation rate of *Bacillus subtilis* and inhibit the death of the vegetative body. The content of protease and the activities of alkaline protease and neutral protease were measured, and it was found that the protease content change did not occur before and after magnetic field treatment. The activity of alkaline protease in the treatment group was significantly higher than that in the control group, while the activity of neutral protease was lower than that in the control group.

5.2.3 Effect of Gas Double Dynamic on Key Enzyme in Microorganism

Glucose glycolysis occurs in the first step catalyzed by hexokinase, which is the first enzyme in sugar metabolism and has a strong impact on the metabolism of microorganisms [23]. Li et al. [24] studied the relationship between hexokinase activity and lincomycin biosynthesis rate. The results showed that with the increase of hexokinase activity, the rate of product synthesis increased gradually. At the later stage of fermentation, the activity of the enzyme began to decrease and the synthesis of the product began to decrease with the aging of the cell and the decrease of the cell concentration. Thus, the hexokinase maintained a high activity during the synthesis of the product and kept the pentose phosphate metabolism in a higher metabolic flux, which is conducive to product biosynthesis.

Biological cells have corresponding sensory, regulatory and adaptive mechanisms for external stimuli and environmental stresses [25, 26]. Previous studies showed that ATPase plays a key role in the process of microbial perception of the environment [27], while ATPase hydrolyses ATP to produce energy, producing transmembrane proton gradients and ion gradients that provide the driving force for cell growth, transmembrane transport, such as sugars and amino acids [28]. Heat shock proteins, which are commonly found in biological cells, are responsible for cellular resistance to stress conditions during microbial cell adaptation to external stimuli. The heat shock protein and ATPase activity changes also have some obvious relationship [29].

5.2.3.1 Effect of Gas Double Dynamic on Hexokinase Activity

It can be seen from Fig. 5.11 that the effects of gas double-dynamic culture on hexokinase and microbial respiratory metabolism were similar: at the initial stage of fermentation, samples in the gas double-dynamic solid-state fermentation and the static fermentation had higher enzyme activity. However, with the fermentation progressed, the activity of hexokinase of *Trichoderma viride* cultivated in GDDSSF decreased rapidly after maintaining for a while; while the activity of hexokinase of *Trichoderma viride* was decreased significantly, there was a remarkable recovery stage. The reason of this recovery may be that the statically cultured microorganisms use cellulase to obtain new fermentation substrate in the later stages of fermentation, while the gas phase double-action is that the microorganisms can use these substrates in the early and middle stages of the fermentation. The determination of reducing sugar concentration in culture medium also showed that the concentration of reducing sugar in the medium of gas double-dynamic culture was lower, taking the high activity of cellulase in pulsating culture medium and the ability of producing reducing sugar into consideration. As a matter of fact, it is known that under the pulsation culture condition, the uptake ability of the microorganism to the reducing sugar in the culture medium is stronger than that in the static culture.

In addition, the high frequency of intensification also has a greater impact on hexokinase of *Trichoderma viride*. At the end of the incubation, the enzyme activity was measured immediately after extraction. The results showed that the activity of hexokinase was increased to 0.034 IU/ mg, and the amplitude increased by 30.7% compared with the static culture in short time.

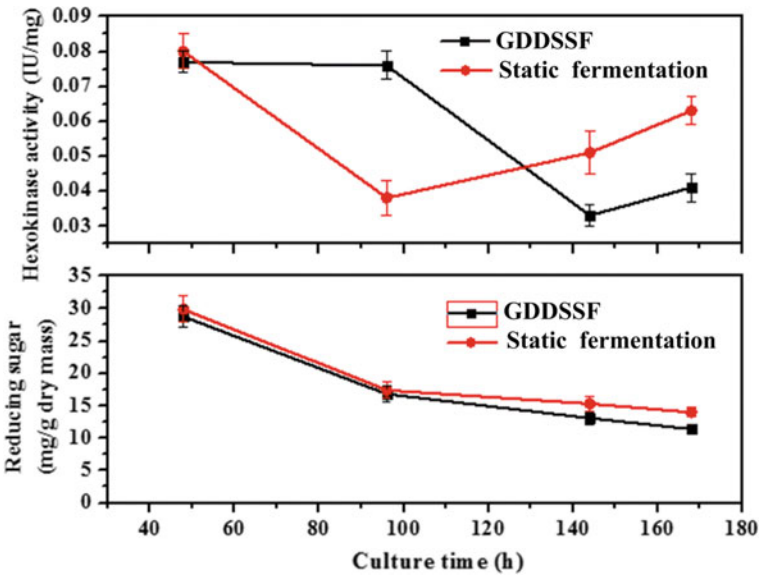

Fig. 5.11 Effect of culture time in GDDSSF system on hexokinase activity and reducing sugar

5.2.3.2 Effect of Periodic Stimuli on ATPase

(1) Effect of GDD on ATPase in *T. reesei*

Although short time (1–2 h) cultivation has a light effect on microbial metabolism, Fig. 5.12 showed that longtime cultivation in GDDSSF had significant effects on ATPase activity. Results showed that the changes of ATPase activities were complicated and different during the fermentation process. During the period of 6 days cultivation, ATPase activity under static state cultivation went down continuously from the first day to the end. And the final ATPase activity was low to 2.23 IU/mg with the initial value of 25.5 IU/mg. During the period from the first to the third day, the ATPase activity under GDDSSF decreased to the nearly identical value of 5.7 IU/mg compared with static SSF. However, the activity changed to rise strongly at the third day, and the ATPase activity was up to the level of 14.16 IU/mg at the fifth day. Then the ATPase activity decreased. The period from the third to the fifth day was the stationary phase of microbe, but there appeared to be an increase of ATPase activity during GDDSSF. It indicated that GDDSSF helped stimulate the metabolism of *T. reesei* YG3 in the stationary phase, regarding the increase of ATPase activity at the day of third to fifth. Then, the microbial key enzyme activity of ATPase has declined fundamentally to the degree of initial. The stationary phase during the microbial growth was the main period when the amount of microbe reached to the peak, and numerous intracellular metabolites accumulate. Meanwhile, the ATPase plays significant roles in hydrolyzing ATP to produce energy for synthesis and regulating metabolism. As a result, the increase of ATPase activity may strengthen metabolism activities like the cellulase production.

(2) Relationship between ATPase and weight loss

In the fermentation process, the accumulation of cellulase and the weight loss of the medium were also detected. As shown in Fig. 5.13, the periodic gas intensification

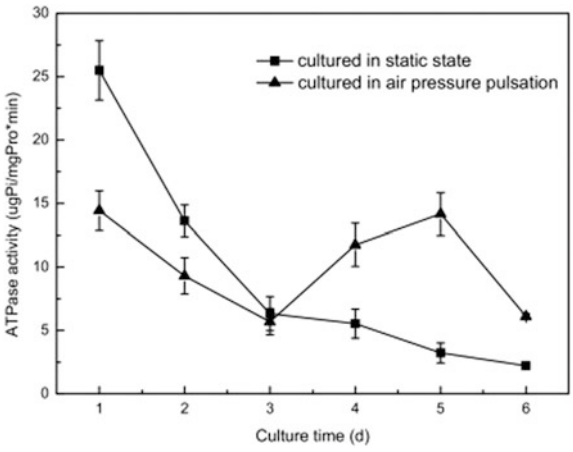

Fig. 5.12 Effect of GDDSSF on ATPase activity of *T. reesei* YG3

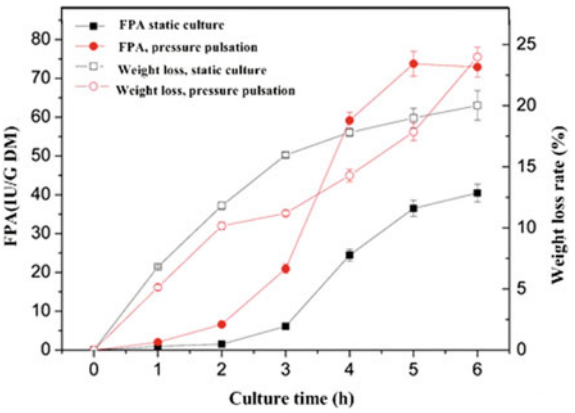

Fig. 5.13 FPA of cellulase weight loss of the medium in GDDSSF (0–0.2Mpa, 20 min, 2.5 m/s) and static culture system

had a significant effect on the accumulation of cellulase during the fermentation. The cellulase activity of *Trichoderma viride* reached the highest value at the fifth day of fermentation. Cellulase activity increased obviously at the sixth day, and the highest activity was 82% higher than that of the static culture under the gas double-dynamic solid-state fermentation. However, the effect of double-dynamic gas on the weight loss of fermentation medium was not regular. Obviously, the relationship between the weight loss rate and the change of ATPase activity in the fermentation process was observed after the weight loss data is transformed into weight loss rate. Figure 5.14 showed a linear relationship between ATPase activity and weight loss rate in two different fermentation modes, which was more obvious during pulsation culture. Loss of weight basically reflects the amount of CO_2 produced by microbial metabolism during fermentation, and the weight loss rate is the rate of CO_2 production, representing the metabolic rate of microorganisms. The fact that the linear relationship between the weight loss rate and ATPase activity was significant, suggesting that the gas phase intensification exerted an influence on the metabolism of *Trichoderma viride* to some extent, which was mediated by the ATPase system.

5.2.3.3 Effect of Intermittent Ventilation on Key Enzyme Activities in Microorganism

Cao et al. [30] studied the effects of intermittent ventilation on key enzymes and coenzymes in the production of 1,3-propanediol from *Klebsiella pneumoniae*. Researchers of Tsinghua University designed three kinds of ventilation to investigate the effect of intermittent ventilation on *Klebsiella pneumouniae* key enzyme activity.

Results showed that the activity of glycerol dehydrogenase was promoted by air in the early stage of fermentation. The activity of glycerol dehydrogenase increased by sevenfold in the first 4 h of air exposure in the experimental group, while the control group increased by only 1. The glycerol dehydrogenase enzyme activity in

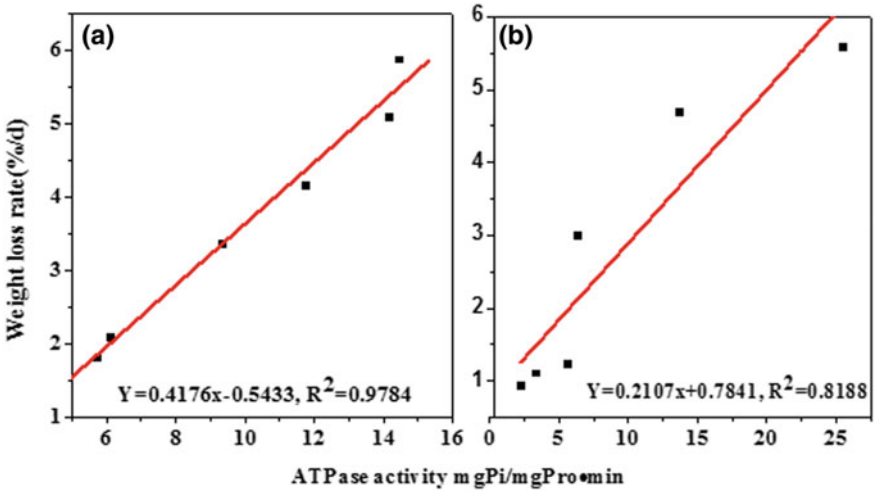

Fig. 5.14 Effect of ATPase activity and weight loss of medium in the solid-state fermentation (**a** GDDSSF and **b** static culture)

the shake flask was 2.5 times higher than that in the control, and the intermittent access to air could not only inhibit the glycerol dehydrogenase enzyme activity of glycerol anaerobic fermentation (dioxyacetone) system. It greatly promoted the fermentation of glycerol dehydrogenase in the early stage of fermentation but was not obvious at the end of the fermentation. The glycerol dehydrogenase activity of the control group was higher than that in the control group after long-term adaptation to anaerobic environment. The activity of 1,3-propanediol oxidoreductase was significantly decreased after air exposure, but the enzyme activity could be recovered within 4 h. The activity of 1,3-propanediol oxidoreductase was 14% higher than that before ventilation and increased by 18% compared with the control group after the first ventilation. At the end of the second pass, the 1,3-propanediol oxidoreductase activity in the flasks was higher than that in the control group at the end of the second pass, indicating that the 1,3-propanediol oxidoreductase had some adaptability to intermittent air. Through the metabolic regulation, the cells could reduce and rapidly repair the oxygen and the activity of 1,3-propanediol oxidoreductase was decreased by 48 h at the end of fermentation. The activity of 1,3-propanediol oxidoreductase was reduced to 50% after air exposure for 1 h.

5.2.4 Effect of Periodic Stimuli on Microbial Respiration

Microbial respiration in fermentation process is the overall performance of microbial metabolic activity. O_2 is an important substrate in aerobic fermentation process. The supply of O_2 in liquid fermentation determines the fermentation performance [31]. During the solid-state fermentation, the supply of O_2 is not the

decisive factor of fermentation, but the consumption of O_2 could also reflect the growth rate and metabolic activity of the microorganism. CO_2 is the end product of respiration and catabolism, and almost all of the fermentation produces large amounts of CO_2. Dissolved CO_2 in the fermentation broth affects the synthesis of on the amino acids, antibiotics and other fermented. The CO_2 production curve is an accurate and sensitive indicator of microbial metabolic activity. Saucedo-Castaneda et al. [32] developed the automatic control system of tail gas in packed bed solid-state fermentation reactor. It was concluded that effective microbial physiological state information can be obtained by real-time analysis of exhaust. During the cultivation of aerobic microorganisms, the specific growth rate of the microbial growth can be estimated from the measurement data of the exhaust gas concentration.

5.2.4.1 Respiration Characteristics of Microorganisms in Forced Ventilation Solid-State Fermentation

The process of produce cellulase by solid-state fermentation of *Penicillium obliquus* was first used to study microbial respiratory metabolism. Medium with different dosage was incubated with spores and cultivated in GDDSFB. The temperature was set at 30 °C and the air flow rate was 0.5 L/min. The results showed that concentration changes of O_2 and CO_2 in exhaust have an inverse tendency, but are different in detail (Fig. 5.15).

After a brief lag at the beginning of the fermentation, *Penicillium obliquus* entered into the logarithmic growth phase which lasts for 25 h. After logarithmic growth phase, the microbial respiratory strength began to decline and the subsequent changes in the process began to slow down, during which cellulase begins to accumulate. A long time in this process can accumulate a large number of cellulase, but also have a negative impact that the fermentation process is extended. Load factor is low in solid-state fermentation, and the reactor production capacity will be

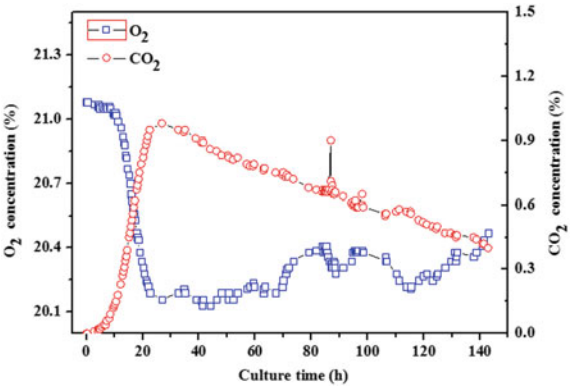

Fig. 5.15 Exhaust curve of force ventilation

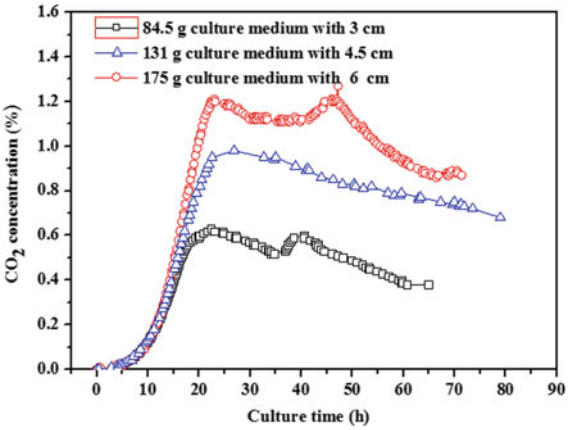

Fig. 5.16 Concentration of the exhaust in the fermenter with different loading factors

significantly reduced, reducing production economy if the fermentation cycle is extended.

Figure 5.16 shows the concentration of the exhaust in the fermenter with different loading factors in the fermenter. The results show that the logarithmic time of the fermentation process increased with the increase of the culture medium, which can be obtained from Fig. 5.17. Although the overall respiratory intensity is basically the same, there are significant differences in the emergence of peak and late respiratory strength under different loading factors. In the case of high loading factors, the peak appeared late, but in the later stages of enzyme production, the respiration rate was relatively low. Microbial growth in solid-state fermentation was an asynchronous process, which could be concluded from the data of respiration intensity.

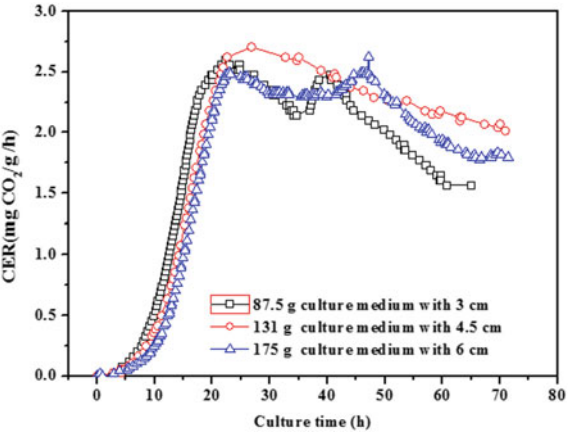

Fig. 5.17 CER of *Penicillium obliquus* with different medium loading factors

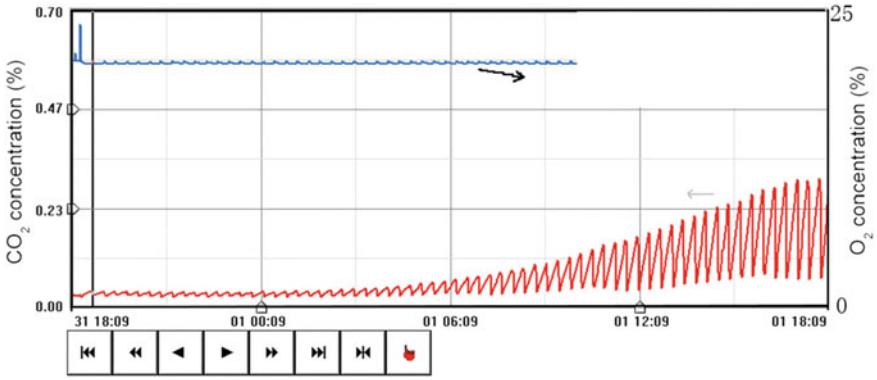

Fig. 5.18 Exhaust carve in GDDSSF

5.2.4.2 Respiration Characteristics of Microorganisms in GDDSSF

Figure 5.18 shows the exhaust carve in GDDSSF system, which is different from Fig. 5.15. The concentration of CO_2 in the exhaust has a periodic fluctuation in the course of gradual increase, and the O_2 also has a periodic recovery in the process of gradual decline.

CO_2 release can be calculated according to the data. Figure 5.19 is the comparison of force ventilation, GDDSSF, and periodic air exchange. The results showed that gas double dynamic was obvious benefit to microbial respiration which could be reflected by CO_2 release rate. CO_2 release rate was 5.48 mg/g/h in GDDSSF while 2.52 mg/g dry medium/h and 1.2 mg/g dry medium/h were obtained in force ventilation and periodic air exchange system, respectively. The CO_2 release rate curve in gas double-dynamic solid-state fermentation decreased rapidly after reaching the peak value, while the curve in periodic air exchange solid-state fermentation and force ventilation solid-state fermentation showed flat peak and double peak. The appearance of flattened peaks and bimodal peaks indicated that the unsynchronized phenomena in solid-state fermentation are more serious. There is no means to increase mass transfer as that in GDDSSF due to lack of stirring in the latter two fermentation modes. Microorganisms cannot enter into deep solid medium when the process reaches a certain level, resulting in a lower peak intensity of respiration and a longtime respiratory intensity after reaching the peak.

The three curves in Fig. 5.19 were processed by integrating so as to obtain the total production curve of CO_2. The results are shown in Fig. 5.20. It can be seen that growth rate of the curve is different at 15 h. At the end of 70 h fermentation, the total amount of CO_2 production was 220 mg/g dry medium in GDDSSF, 230 mg/g dry solid medium in force ventilation, and 78 mg/g in periodic air exchange.

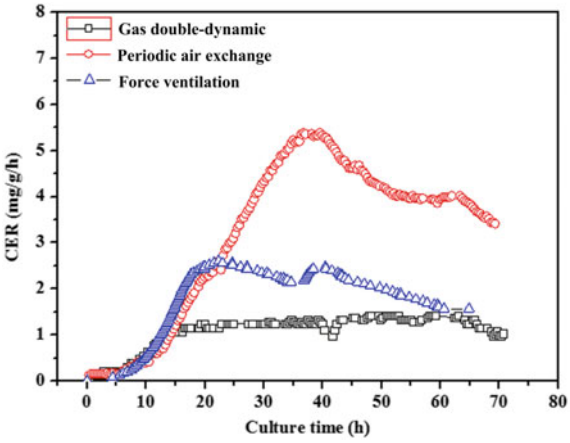

Fig. 5.19 Comparison of respiration intensity of different fermentation strategies

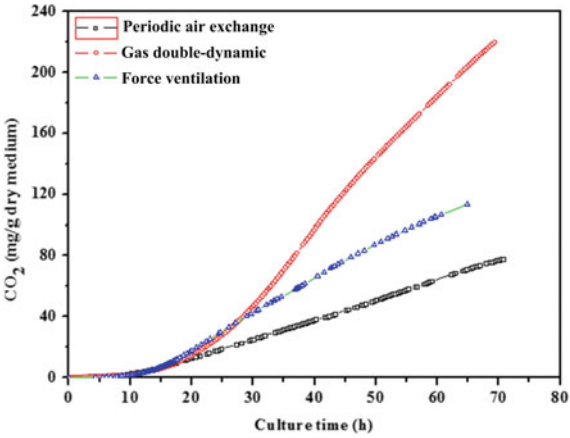

Fig. 5.20 Comparison of total CO_2 of different fermentation strategies

5.2.4.3 Effect of GDDSSF on Microbial Respiration Intensity

(1) *Trichoderma viride*

Figure 5.21 showed the effect of varying the pulsation amplitude of the GDD process on the CO_2 production rate. It can be seen that the choice of fluctuation amplitude is important, and the effect of pulsation amplitude on the CO_2 production rate curve has two main aspects: first, the amplitude of the pulse had influence on the peak value of the curve, 0–0.1 MPa, 0–0.2 MPa, and 0–0.3. And the peak at 0.3 MPa was 3.15, 5.39, and 4.47 mg/h/g dry medium, respectively. Moreover, the shape of the curve also changed significantly. When the pulse amplitude was 0.1 MPa, the respiration intensity reached the peak rapidly, and then maintained at a relatively high position until the end of the fermentation, which was similar to the curve of periodic air exchange solid-state fermentation and respiration rate was

higher than the latter. It can be inferred that the reason for this curve is that the growth of microorganisms quickly reached the substrate limit level although more substrate is not used due to medium agglomeration, particle radius, and other factors. Increasing the amplitude of the pulsation favors the use of the substrate, and still did not achieve the optimum conditions. As the pulse amplitude increased from 0–0.2 MPa to 0–0.3 MPa, the respiration intensity of the microorganisms began to decrease, reflected by the total amount of produced CO_2 (Fig. 5.22), the difference was also significant, while the observed peak time of the postponing and logarithmic growth rate of slowing. This phenomenon and the emergence of microorganisms on the high pressure is not suited to the appropriate GDD to stimulate the metabolism of microorganisms, which make the microorganisms have an adaptive process, while there is a limit to adapt.

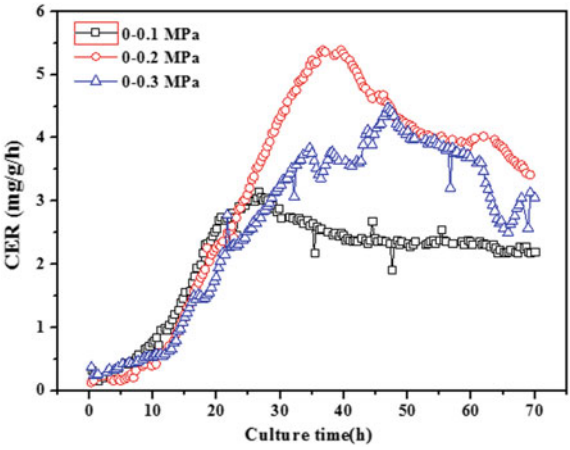

Fig. 5.21 Effect of amplitude of pressure pulsation on CO_2 release rate

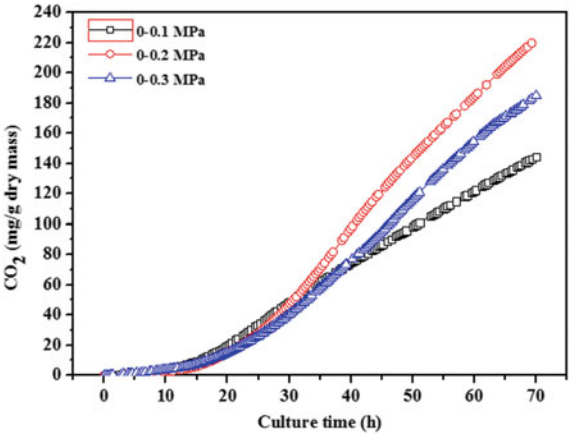

Fig. 5.22 Comparison of total CO_2 with different amplitudes in GDDSSF

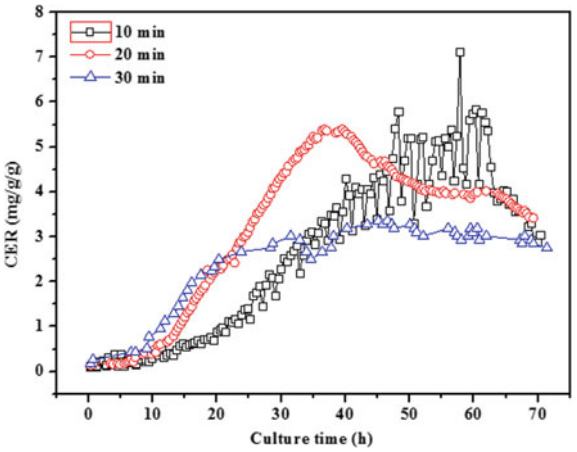

Fig. 5.23 Effect of pulsation cycles on microbial respiratory metabolic intensity

Figures 5.23 and 5.24 show the effect of pulsation cycles on microbial respiratory metabolic intensity. As can be seen from the figure, pulsation cycle and pulsation amplitude microbial respiratory metabolism to some extent have a certain degree of similarity. Increasing the pulsation amplitude and decreasing the pulsation period are the intensities of the pulsation operation. Here, the intensity is understood as the energy required for the GDDSSF operation. Then, the product of the pulsation frequency (the reciprocal of the pulsation period) and the pulsation amplitude (gauge pressure) was the same.

(2) *Mortierella ramanniana*

Peng et al. [33] compared respiration intensity (in terms of the increase of CO_2 concentration in the exhaust gas) during gas double-dynamic solid-state fermentation and static fermentation. Static air-displacement static fermentation was

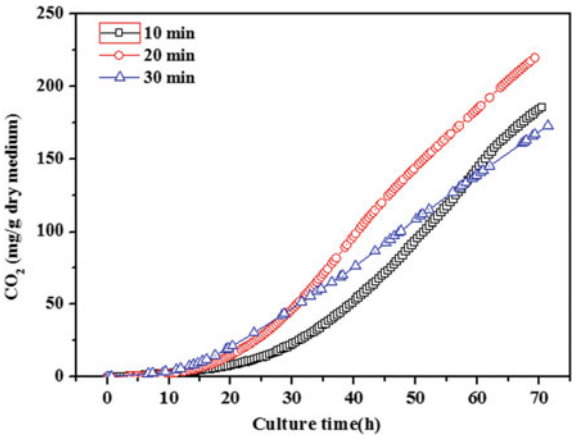

Fig. 5.24 Comparison of total CO_2 with different pulsation cycles

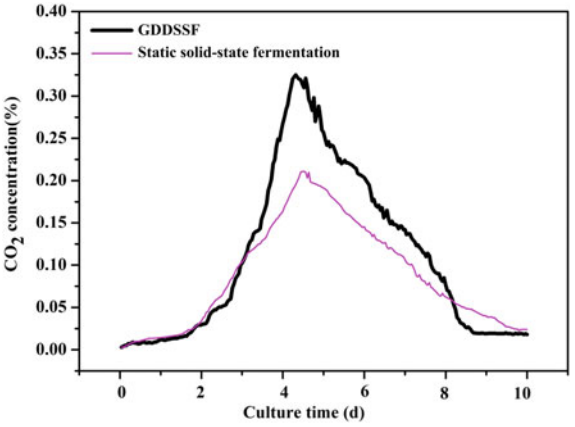

Fig. 5.25 Respiration intensity curve in GDDSSF and static fermentation

carried out in a solid-state fermentation tank. Figure 5.25 shows the change in CO_2 concentration (respiration rate) during static fermentation by GDDSSF s and air displacement. It can be seen that the maximal respiration (respiration intensity) was 0.32%, while the latter was 0.21%. The intensity of respiration decreased rapidly after the GDDSSF reached the maximum, while the static fermentation call intensity reached its maximum value. The decrease of respiration intensity was relatively stable, which indicated that the microbial metabolism was enhanced under the GDDSSF, which enhanced the respiration and shortened the fermentation cycle. The production of polyunsaturated fatty acid remained basically unchanged, indicating that in the GDDSSF, the metabolic pathway of lipid accumulation was not changed.

(3) *Sclerotium sp.*

The exhaust analysis in the fermentation process was carried out using the online monitoring and control system of ExxonMaxhak (Beijing) Instrument Co., Ltd., and the carbon dioxide and oxygen concentration of the exhaust in the reactor were automatically recorded by the industrial control software. The change of CO_2 concentration in the fermenter can be recorded in real time by computer.

Figure 5.26 shows the trends of CO_2 (a) and O_2 (b) in the growth of *Sclerotium sp*. under in GDDSSF cycle and periodic air exchange without high-pressure pulse. It can be seen that in GDDSSF, the CO_2 production of *Sclerotium sp*. reached the maximum at 42 h which was the highest respiratory metabolic intensity, and then decreased rapidly. However, the CO_2 production of *Sclerotium sp.* was slower than that of *Sclerotium sp*. and reached its maximum at 72 h and then decreased slowly. Figure 5.27 shows the effect of pressure intensification on *Sclerotium sp*. respiratory metabolism.

The amount of CO_2 produced within 20 min was obtained by subtracting the CO_2 concentration at the end of atmospheric pressure from the initial concentration of atmospheric pressure. Since CO_2 produced in the reactor and the consumption of

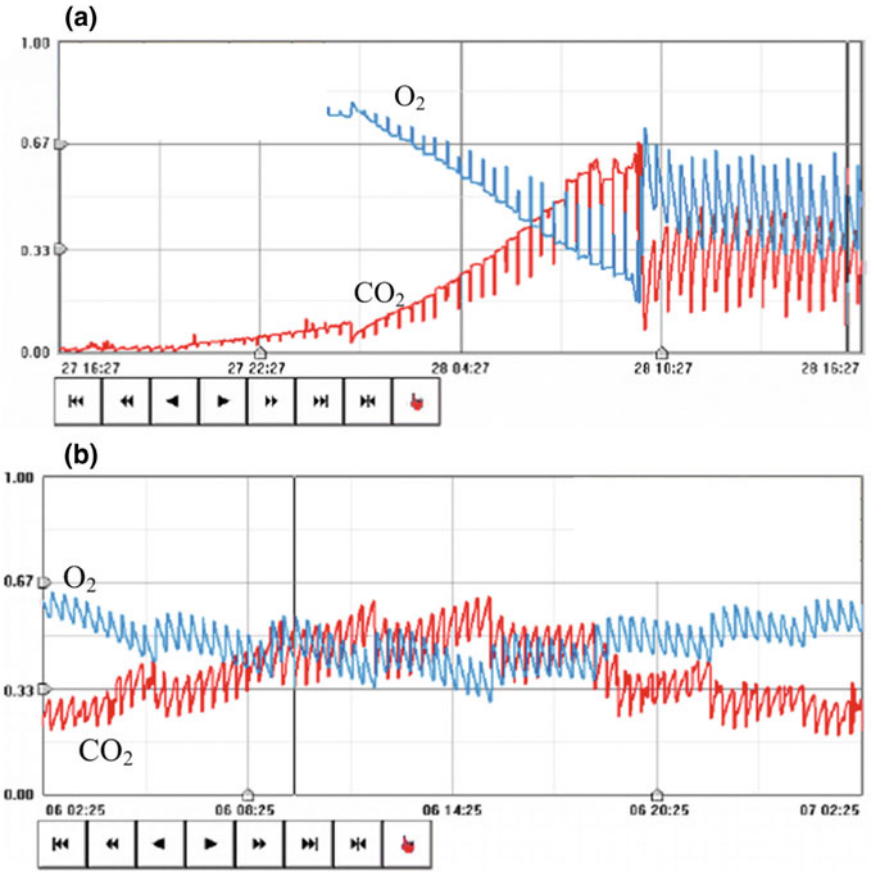

Fig. 5.26 Exhaust curve in different culture systems. **a** GDDSSF; **b** periodic air exchange

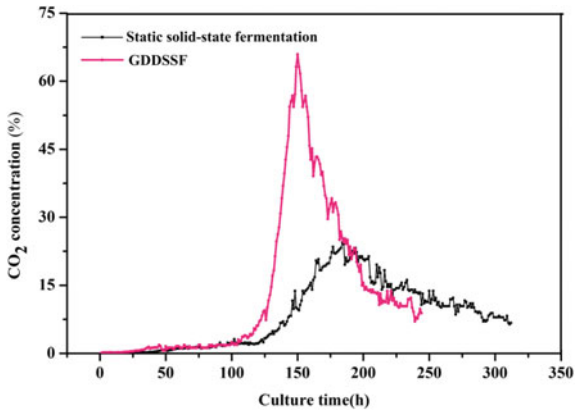

Fig. 5.27 Respiration intensity curve in GDDSSF and static fermentation

O_2 were almost the same for most of the time, the CO_2 produced at this time also reflected the metabolic activity of the microorganisms within 20 min. Figure 5.27 compares the change in CO_2 concentration during the metabolic process of *Sclerotium sp.* in a pressure pulsating solid-state fermentation reactor under both GDDSSF intensification and air exchange only. In the two modes, the CO_2 produced by *Sclerotium sp.* was the same, and reached the maximum at the second day of fermentation. However, the concentration of CO_2 in the two modes was different. In GDDSSF, CO_2 concentration was about 66%, while the static air replacement fermentation condition was about 25%. However, in GDDSSF, the CO_2 concentration began to decrease after a short time when the CO_2 concentration reached its maximum, while under the static culture, the CO_2 concentration remained stable for about 6 days. GDDSSF may stimulate the growth of microorganism and enhance its metabolism, thus increasing the concentration of CO_2, while shortening the fermentation cycle of the bacteria.

(4) *Aspergillus niger*

Zeng et al. [34] studied the respiration characteristics of *Aspergillus niger* under periodic gas stimulation. The changes of O_2 and CO_2 concentration in gas double-dynamic solid-state fermentation and conventional solid-state fermentation were investigated. The gas circulation in the fermenter was detected by an exhaust detection system. The results were shown in Figs. 5.28 and 5.29.

As shown in Fig. 5.28, the O_2 concentration gradually decreased during the initial phase. The concentration of O_2 in the solid-state fermentation of GDDSSF was lower than that of static solid-state fermentation. After 48 h fermentation, the lowest O_2 concentration in the solid-state fermentation was 20.4881%, which was 0.3881% higher than that in the traditional static solid-state fermentation (20.1%). In Fig. 5.29, the CO_2 concentration increased with the fermentation time before 48 h, but the CO_2 concentration in GDDSSF was smaller than that of the traditional static solid-state fermentation. At 48 h of fermentation, the maximum CO_2

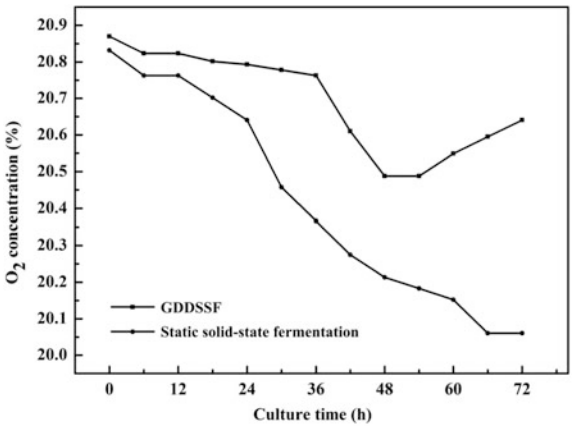

Fig. 5.28 Variation of O_2 concentration in GDDSSF and static solid-state fermentation

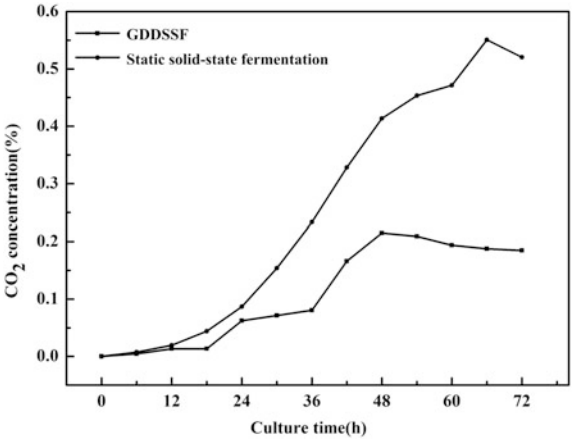

Fig. 5.29 Variation of CO_2 concentration in GDDSSF and static solid-state fermentation

concentration reached 0.21% in gas double-dynamic solid-state fermentation system, which was 0.34% lower than the traditional static solid-state fermentation (0.55%).

Figures 5.28 and 5.29 showed that, despite the O_2 depletion due to bacterial growth, CO_2 was reduced and the concentration of CO_2 is reduced, and the GDDSSF solid-state fermentation facilitates the rapid exchange of gas from the fermentation tank with the outside air, reducing the concentration of O_2 and CO_2 concentration changes. It indicated that GDDSSF can provide more O_2 than conventional static solid-state fermentation, and more CO_2 produced by the strain during the fermentation process can be released effectively Moreover, the GDDSSF can greatly improve the O_2 and CO_2 transfer during the fermentation process.

In GDDSSF, the respiration rate at different GDD cycles was calculated by subtracting the CO_2 concentration at the beginning of the cycle from the CO_2 concentration at the end of the cycle. In traditional static solid-state fermentation, the same method is used to calculate the respiration rate in the same fermentation cycle.

As shown in Fig. 5.30, before 40 h, the respiration intensity increased with the increase of the fermentation time, and then decreased gradually, which was consistent with the growth status of the strain. Figure 5.29 showed that microbial growth in GDDSSF is better than that of conventional static solid-state fermentation, because the intensity of respiration can be used to represent the strength of the metabolism. That is to say, the GDDSSF greatly promoted the growth of the strain. Both of the GDDSSF and the conventional static solid-state fermentation have a wave-like respiratory intensity curve, which may due to the periodic regularity of the growth and metabolism of microorganisms. This phenomenon needs further study.

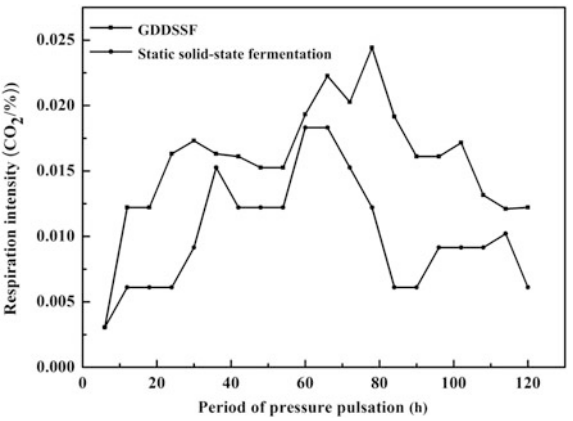

Fig. 5.30 Respiration intensity in GDDSSF and static solid-state fermentation

5.3 Mechanism Analysis of Periodic Stimulation in High-solid and Multi-phase Bioprocess

5.3.1 Principle of Fermentation Process Optimization

New biological products development and more economical production mode are two main aims of biotechnology research, and the latter is vital to biotechnological industrialization and creating social value further. The key factors which restrict the industrialization process of fermentation products are desired product yield, the target product productivity, and the rate of consumption of the substrate because high products yield is benefit to products extraction while a high productivity is advantageous to reduce raw material costs. Based on a clear knowledge of microbial metabolic mechanism, process optimization techniques could reach the uniform of high yield, high productivity, and high production intensity of the target products by changing and optimizing microbial physiological function. Therefore, it is of great importance for industrial biotechnology with the core of fermentation engineering.

The aim of fermentation process optimization is to simplify the complex interaction among cell physiological adjustment, cell environment, reactor features, technological condition, and reactor operation, so as to fit the fermentation process. However, microorganisms are living creatures, and microbial behavior could change a lot, resulting in process parameters are difficult to be detected. Therefore, combining modeled conception and basic question of microbial physiological has been one of the main focuses of process optimization research.

Based on nonlinear dynamics properties of biological cells in vivo enzymatic reaction network system, it is the base and direction of periodic process optimization to use the periodic force to strengthen the role of genetic expression. In terms of microbial requirement in biology and physical, periodic strategies cover periodic material supply, cultural environmental strengthen or weaken, and variable

environmental stimulating. All the technological operation covers several factors which affect microbial metabolic flow. Establishment of mathematical model among those factors and the common target products is important to process optimization.

5.3.2 Periodic Process Optimization Covers the Following Research Aspects [35]

(1) Cell growth process: understanding the physiological and biochemical characteristics of intracellular microbial cells, a clear knowledge of microbial nutrient intake, as well as the whereabouts of nutrients through the metabolic pathway transformed from a nonbiological nutrient medium, and the distribution of different environments metabolites.
(2) Chemometrics in microbial reaction: the advantages of chemometrics of microbial reaction were that the probable optimization method could be established without microbial metabolic documents by applying metabolic flow method with the chemometric relationship.
(3) Bioreaction dynamics: studying the relationship between bioreaction rate (intrinsic dynamics) and influential factors (concentration of substrate, temperature, and solvent).
(4) Bioreactor engineering: bioreactor and parameters detection and control. Style and structure of the reactor, operation mode, material flow and mixing status, and transfer features are important influence factors which could affect macrodynamics of bioreaction. Parameters detection and control are the basic methods in fermentation process optimization. Timely detection and adjust substrate concentration ensure a favorable environment for bioreaction.

In terms of periodic stimulating process, a clear knowledge of microbial physiological and biochemical characteristics is the premise of process optimization. Based on perceptual knowledge about periodic stimulating, combining chemometrics and reaction dynamics of microbial reaction, we establish mathematical model between process parameters and target metabolites, which could be guidance for process optimization.

5.3.3 Periodic Operation Optimization Based on Substrate Requirement

Multi-period and fed-batch fermentation also called repeatedly fed-batch fermentation refers to in the cultural process, removing a volume of culture medium, while adding an equal volume of medium in the same time interval. In this way, the culture, the culture fluid volume, and dilution rate will undergo periodic changes in

the specific growth rate and metabolism as well as other relevant parameters. Compared with traditional fed-batch fermentation, repeatedly fed-batch fermentation has the following advantages:

(1) Remove substrate, production, and catabolite repression.
(2) Reduce the viscosity of the fermentation broth which is caused by rapid microbial growth because of rich nutrient.
(3) Increase the proportion of spore germination.
(4) To be the research method and provide experimental basis for favorable auto control.

For an industrial strain and its cultivation stage, it is necessary to give the necessary nutrients for growth, including carbon source, nitrogen source, inorganic salt, and auxin. In addition, various special nutrients which act as precursors and accelerators must be given for products formation. Especially, for nongrowth-coupled fermentation, medium compositions are different during the main stage of growth and product formation. For example, the production of antibiotic should be the main stage, the special substrate which inhabits antibiotics formation must be strictly controlled (such as auxin) so as to obtain more antibiotics and the ideal component.

5.3.3.1 Periodic Supplement of Carbon and Nitrogen Source

Reducing carbon compounds are usually used to culture cells and form products. Apart from glucose, other natural organic compounds (ethanol, glycerol and lactose) can be used as carbon sources for microbial growth and metabolites production. Carbon source concentration in the culture medium is very important. If the carbon source concentration in the medium exceeds by 5%, the growth of the bacteria begins to decline due to dehydration of the cells. Yeasts or molds can tolerate higher glucose concentrations, up to 200 g/L, due to their low water dependency. Also, at a given concentration, the carbon source blocks one or more enzymes responsible for the synthesis of the product, which is termed carbon catabolite repression. One approach to avoid catabolite repression is to make the rate of the carbon source equal to its rate of consumption, and another approach is to use non-repressive carbon sources such as monosaccharides, oligosaccharides, polysaccharides, or oils other than glucose. Nitrogen source includes peptone, soybean meal, peanut cake, corn steep liquor, yeast extract and urea, and other organic nitrogen sources.

It is important to select the appropriate feed time after determining the contents of the feed. For example, during the production process of glutathione by fermentation of baker's yeast, sugar was added 4 h after the fermentation, and the final cell concentration and intracellular glutathione were 0.878 g/L and 136 mg/L, respectively. The total amount of glutathione in the solution reached 1194 mg/ L, and the cell conversion rate was 0.335 g/g. The fermentation process of all the

indexes was significantly improved compared with before or after feeding. It can be seen that the timing of sugar supplement has a great influence on the products yield. Early sugar supplementation will stimulate the growth of the cells, thereby accelerating the utilization of sugars. The yield of the fermentation product at the same saccharide rate was significantly lower than that of the appropriate sugar addition time. The timing of sugar supplementation cannot be simply based on the culture time, but also according to the basic medium carbon source type, dosage and consumption rate, pre-fermentation conditions, strain characteristics and seed quality, and other factors. So, it is favorable to make the judge according to metabolic changes such as residual sugar content, pH, and hyphal morphology. In determining the time after the start of sugar supplement, the way sugar and control indicators also should be paid attention to. For example, in the process of glutathione fermentation, when the initial sugar concentration is lower than 12 g/L, the cell can keep high glutathione synthesis ability for a long time while it keeps growing. However, as long as the total sugar concentration is more than 25 g/L, regardless of whether the sugar, glutathione production will decline.

Ja et al. [36] studied the effect of supplemental glucose on the production of pristinamycin by *Streptomyces pristinaespiralis XC 416* in shake flask and 5 L fermentor. The results showed that the initial glucose concentration was 40 g/ L, the biomass could be increased by 23–31% by addition of 20 g/L glucose in the logarithmic growth phase, and the yield of pristinamycin could be increased by 20–36%; the addition of 20 g/ L glucose in the stationary phase has little effect on biomass, but it can significantly enhance the ability of bacterial synthesis of antibiotics, and the yield of pristinamycin increased by 56–76%. In the middle and late growth stages and the stabilization period, by addition of 10 g/L of glucose twice, the yield of pristinamycin was increased by 1.92 times. Results of 5 L fed-batch fermentation showed that in the logarithmic growth phase and the initial synthesis of antibiotics in the first three times, a total of 36 g/L glucose not only effectively extends the synthesis of antibiotics but also improves the antibiotic synthesis of bacteria capacity and product yield. And the yield of pristinamycin was increased by 1.02 times. Zhao et al. [37] studied the β-glucosidase preparation via liquid fermentation of *Aspergillus niger*. The amount of feeding and the number of feeding affect the β-glucosidase secretion. After adding 1% sterile bran dry powder for four times, the β-glucosidase activity in fermentation broth increased from 1.72 to 5.07 U/mL, which was nearly three times higher. Moreover, the addition of bran extract can achieve the same effect.

5.3.3.2 Periodic Supplement of Mineral Salts

Inorganic salts are indispensable substances for microbial growth and metabolism. Its main function is to constitute the bacterial component, as part of the enzyme, enzyme activator or inhibitor, regulating osmotic pressure, pH value, and the redox potential. Sulfate, phosphate, chloride and potassium, sodium, magnesium, and iron compounds are common inorganic salts which are needed for the growth of

microorganism. Copper, manganese, zinc, molybdenum, iodine, and bromine are trace elements for microbial growth. Little inorganic salts are required by microorganisms, but they have a great impact on the cell growth and product formation.

Phosphorus is the most important element in the synthesis of nucleic acid, phosphoric acid, some important coenzymes (NAD^+, $NADP^+$, and CoA) and high-energy phosphate compounds (ADP, ATP). In addition, phosphate is the composition of the buffer solution, which has a great impact on pH adjustment of the environment. Phosphorus required by microorganisms is mainly from inorganic phosphorus compounds, such as KH_2PO_4 and K_2HPO_4. Phosphorus concentration has great influence on glutamic acid fermentation. High phosphorus concentration leads to the synthesis of valine while low phosphorus concentration results in worse growth of cell.

Magnesium is the constituent of the chlorophyll of certain bacteria. Although not involved in the composition of any cell structure material, magnesium ionic is the activator of many important enzymes, such as hexose phosphorylase, isocitrate dehydrogenase, and carboxylase. Low magnesium ion content affects the oxidation of the substrate. Sulfur in the protein of the cell is a constituent of sulfur-containing amino acids. Sulfur is the active group of some enzymes [38].

Most metal ions, especially inorganic phosphates, repress the biosynthesis of several secondary metabolites. In phosphate biosynthesis of pseudocillin, phosphate represses at least one enzyme, p-aminobenzoic acid synthase [39].

5.3.3.3 Periodic Supplement of Special Nutrient Content

Many microorganisms require special nutrients and growth factors that they cannot synthesize, such as amino acids, purines, pyrimidines, vitamins, and biotin, which are essential to the growth of many yeasts and molds [39].

Growth factors are necessary trace organic compounds for microbial regulation of normal metabolism, which cannot be synthesized by microorganism. Various microorganisms require different growth factors. In general, growth factors include vitamins, amino acids, purines and pyrimidines and their derivatives, porphyrins and their derivatives, sterols, amines and fatty acids. The main function of growth factors is to provide microbial important chemical substances (proteins, nucleic acids and lipids), cofactors (coenzyme and prosthetic) components and participate in metabolism. All kinds of microorganisms need different growth factors, as well as the dosage. The addition of certain components of the fermentation medium helps to regulate the formation of the product without promoting the growth of microorganisms such as precursors, suppressors and promoters (including inducers and growth factors). Precursor refers to certain compounds added to the fermentation medium, which can be directly bond to the product molecules by microorganisms in the biosynthesis process. The product yield increases due to adding of precursor while its own structure and did not change much. Precursor must be added in some amino acids, nucleotides and antibiotics fermentation system in

order to obtain higher yields. Some substances such as phenylacetic acid, propionic acid, and other high concentrations of the bacteria will produce toxic. At the same time, bacteria also have the ability to oxidative decomposition of precursor. Therefore, in order to reduce the toxicity of the production and increase the utilization of precursors, the precursor should be added often with small dosage. The total amount of each product can be added into the molecule, the number of precursor molecules, according to the amount of such substances calculated the amount of precursor in the total amount of calculation should also take into account the part of the cell oxidative decomposition precursor [38]. For example, phenylacetic acid showed stronger toxicity in acidic environment (pH5.5) (at this time phenylacetic acid in the fermentation broth is not dissociated), it must be added into penicillin broth 12–15 h after inoculation when pH slightly increased. Penicillin-producing bacteria oxidation of phenylacetic acid quickly, phenylacetic acid should not be too much but continuously. The optimum concentration is usually 0.08–0.1%. Generally start with 0.05%, after every 12 h added 0.05–0.1 or 0.2% per day, which is a small number of times or continuous flow way to add. In addition, when two precursors are present, sometimes strong precursors preclude the action of the weak precursors, sometimes with the aid of a synergistic effect. For example, phenylacetic acid lauryl alcohol vinegar is superior to phenylacetic acid, but has slow hydrolysis of the characteristics of the release of precursors which leads to the lack of phenylacetic acid. 1.2% of phenylacetate lauryl alcohol vinegar and 0.1% phthalide amine mixture can make a substantial increase in penicillin fermentation units [40].

Promoter or stimulant is the matter which could improve fermentation performance. For example, in the fermentation process of enzyme preparation, adding some inducers, surfactants, and some other enzyme-producing accelerator can greatly increase the amount of enzyme production. The addition of a small amount of the promoter to the medium can greatly increase the yield of certain microbial enzymes. Commonly used promoters are some surfactants (detergent, Tween 80, and phytic acid), ethylenediaminetetraacetic acid, soybean oil extract, ferrocyanide, and methanol [38].

5.3.4 Periodic Intensification in Microbial Fermentation Environment

5.3.4.1 Variable Pressure Operation

Pressure intensification can affect heterogeneous catalytic reactions in at least two ways. For porous medium and gas or gas–liquid systems, pressure intensification can increase the mass transfer rate within the structure, which is more obvious when both the gas and liquid phases are present. Therefore, for mass transfer-limited reaction systems, pressure intensification is very important. This is the first and most important application of pressure intensification. The second effect is

important in situations where the catalyst contains close active sites, while the adsorbed reactants and products are strongly inhibited. The following are several practical examples of industrial application cycle operation. When the supply of H_2 and N_2 is switched over in the cycle of several seconds, the synthesis rate of ammonia is increased by a factor of a thousand, in the case of ammonia synthesis using a ruthenium catalyst. When air and water are present, SO_2 is oxidized on an activated carbon catalyst. If the high-frequency switch operates the inlet valve, the oxidation rate of SO_2 is increased by 50% relative to constant flow. In the reaction of propylene with acrolein partially oxidized with Sb-SnO as catalyst, the production rate of acrolein is doubled if the feed of air and propylene is switched in different proportions.

Many biochemical reactions, particularly microbial fermentation, occur in the flocculent structure, and the process of mass transfer through the flocculent structure is a limiting step in the enzymatic reaction. Thus, increasing the mass transfer rate through the flocculent structure without having an impact on the flocculent structure has a very large attraction. Experimental results showed that the rate of bioreaction can be greatly increased by pressure modulation at sub-acoustic frequencies. The increase rate depends on the air contained in the mycelium.

Li et al. [18] studied internal temperature and humidity changes in gas double-dynamic solid-state fermentation bioreactor. The results showed that the temperature and air humidity in the reactor are changed periodically with the fluctuation of air pressure. The amplitude of the pressure fluctuation was significantly correlated with the pressure amplitude of the pulsation. The pressure fluctuation range is 0–0.2 MPa, the variation of the air temperature in the reactor reaches 4–5 °C, and the variation of the air humidity is RH 20%. The changes of temperature and pressure have an important effect on biological process strengthening, and this study provides an important database for future model research. Effect of periodic gasification, forced ventilation, and GDDSSF on microbial respiratory metabolism has also been compared. The results showed that the gas phase had a significant effect on the respiratory metabolism of microorganisms. The ratio of CO_2 respiration intensity was 1: 2.1: 4.57, and the ratio of total CO_2 production was 1: 1.45: 2.82. The analysis of the respiratory quotient also showed that the state of the gas phase had an effect on the status and peak of the respiratory quotient curve. Periodic gas stimulus not only strengthened the heat and oxygen transfer increase of oxygen but also changed the metabolic pathways of microorganism. In addition, the effect of pressure intensification on cell membrane permeability and the activities of key enzymes in the metabolism of two microorganisms have been studied, and the following conclusions were obtained: (1) periodic intensification source used in GDDSSF for microbes was moderate. The air pressure cycle intensification of 0.2 MPa had no significant effect on cell membrane permeability of *Trichoderma viride*. (2) The activity of hexokinase was increased by 30.7% after a short period of high-frequency gas phase stimulation. But no significant effect of long-term gas phase double-dynamic culture on hexokinase was observed. This indicated that the microorganisms are adapted to this periodic stimulus under long-term GDDSSF [18].

Tao et al. speeded transport into *Bacillus* by GDDSSF with the beer grains as raw materials. The results showed that it can effectively improve the virulence potency of biological pesticides [41]. GDDSSF was also used to stimulate the production of acid protease of *Aspergillus niger* with the pressure range of 0.05–0.25 MPa, low pressure maintained for 5 min and high pressure maintained for 10–60 min. The results showed that the GDDSSF could stimulate the activity of the acid protease [42]. The effect of GDD on the microbial protein in solid-state fermentation was studied by Fu et al. The protein extracted in GDDSSF cycle was improved compared with the protein extracted from the microorganism without stimulated by the periodic stimulation. The activities of FPA and CMCase were increased by 17.175%, 60108% and 21.117%, respectively, while the activities of FPA and CMCase were reduced by 38% and 34%, respectively. The enzymatic activity of microbial extracellular protein in the 5d solid-state fermentation was similar to that in the static solid-state fermentation for 6 days, and the fermentation cycle was shortened. GDDSSF changed the composition of the protein, reducing the fraction of the molecular weight of about 80,400 but increasing the molecular weight of about 28,520 components [22]. Xu et al. produced cellulase in a 50 L gas double-dynamic solid-state fermentation with a reactor. Compared with the traditional solid-state fermentation, enzyme activity can be increased by 1 times, the cycle shortened by 1/3. The results showed that the microbial growth of the upper, middle, and lower layer of 9.0 cm layer was uniform; the substrate was loose; and the microorganism entered the rapid growth phase in a short time. In gas double-dynamic solid-state fermentation system, spore was produced at third day, and the enzyme activity was 20.36 U/g while in static solid-state fermentation system, spore was produced at fourth day, and the enzyme activity was 10.82 U/g [43–47] Xu et al. [48] cultivated *Beauveria bassiana* in a 20 m^3 gas double-dynamic reactor. Results showed that fermentation cycle of *Beauveria bassiana* can be shortened by 28%, and the amount of sporulation increased by 65%, to 20 billion/g. Industrial production of *Beauveria bassiana* by GDDSSF reactor is feasible. GDD has a positive effect on promoting the metabolism of *Beauveria bassiana*.

5.3.4.2 Variable Temperature Operation

Because of the exponential relationship between reaction constants and temperature, periodic temperature intensification is also attractive to researchers. In 1960s and 1970s, this type of incentive has been the concern of researchers. For reactors operated below 500 °C, if the temperature can vary cyclically over a range of 10 °C, the average reaction rate increases by 7.4% for a chemical reaction with an activation energy of 83.6 kJ/mol. For a reaction with higher activation energy (418 kJ/mol), the average reaction rate increases by 266%. If the amplitude is increased to 20 °C, the average reaction rate in the above activation energy range will increase by 30-2300%. Early periodic temperature intensification experiments were not successful because of the thermal inertia of the catalyst bed or reactor. With the

emergence of micro-reactor, study of periodic temperature intensification comes back again. In addition, a significant increase in reaction rate observed in the three-phase drip bed reactor of the interrupted liquid phase flow is now considered to be due to the cyclical variation of the temperature. In conclusion, the theoretical analysis and simulation all agree that the periodic temperature excitation will increase the yield obviously, but need further experimental support. Fortunately, with the advent of new reactors such as micro-reactors, above expectations are likely to arise [18].

For nonfilamentous fermentation, the maximum rate of its product formation period is in the exponential phase, i.e., cell growth is the main behavior before the end of the exponential growth. Products formation rate reached the maximum value in and part growth coupling microorganism reach to the maximum, while the growth coupling type did not start to produce the product until the cell growth was negative. Therefore, the optimal temperature should be determined according to the different fermentation stages of the enzyme characteristics. The optimum temperature and optimum pH value of the enzymes synthesized from cell material of cell synthesis and fermentation product could be different, reflecting different optimum temperatures and optimum pHs for the main stage of fermentation process and the main stage of product formation. Therefore, the optimum temperature should be determined separately for each fermentation stage. The optimum temperature for the main growth stage maximizes the specific growth rate so as to facilitate the rapid growth and reproduction of the cells. The optimum temperature for the production of the product should be the temperature that maximizes the rate of product formation. This temperature will advantageously result in faster and more product formation. One of the required fermentation conditions to maintain the microbial growth and process is temperature. Both microbial growth and product synthesis are carried out at suitable temperatures.

1. Effect of temperature on product synthesis
   In process optimization, it should be aware that the effect of temperature on growth and production is different. In general, increasing the fermentation temperature can improve enzyme reaction rate, accelerated metabolism and shorten production. However, the enzyme activity will be reduced due to overheating, which is reflected by the aged microorganism and shortened fermentation period, affecting the final yield. Temperature not only affects reaction rate in system but also the physical properties of the fermentation broth (such as the solubility of oxygen, substrate mass transfer rate, and nutrient decomposition and absorption rate) which indirectly affect product synthesis. Temperature also affects the direction of biosynthesis. For example, chlortetracycline can be produced during tetracycline fermentation of *Streptomyces aureus*. Below 30 °C, *Streptomyces aureus* has the strong ability of synthesis of chlortetracycline. The proportion of tetracycline increased with increasing temperature, and tetracycline is the only product at 35 °C.

2. Choice of optimum temperature
   Optimum temperature of different strains, culture conditions, and growth stage are not the same. Only one optimum temperature is not necessarily good for the whole fermentation period. The temperature which is suitable for bacterial growth is not necessarily suitable for the synthesis of the product. The choice of temperature should also refer to other fermentation conditions neatly. For example, the effect of increasing the erythromycin fermentation temperature in corn steep liquor medium is not as good as in soybean meal flour medium, since the temperature is favorable for the assimilation of soybean meal [39].

5.3.4.3 pH Adjustment

pH is also one of the main fermentation parameters. With the determination of optimum temperature, the determination of the optimum pH should also be carried out on the basis of the kinetic principle of the enzyme action, that is, the optimum pH value for the major enzymes of the different fermentation stages. The optimum pH value of different enzymes may be different, and different fermentation stages of the best pH may also be different. The optimum pH for the main phase of growth is the pH which maximizes the growth rate, and the optimum pH for the main phase of the product formation is the pH that maximizes the conversion [40].

Changes in the pH of the fermentation broth will have a significant effect on the fermentation. (1) It will lead to changes in microbial cell protoplast membrane charge. The protoplast membrane has a colloidal property, and the protoplast membrane can be positively charged at a certain pH, while the protoplast membrane is negatively charged at another pH. This change in charge can also cause changes in the ion permeability of the protoplast membrane, thus affecting the absorption of nutrients and metabolites in the culture medium, and impede the normal metabolism of the metabolism, such as *Penicillium chrysogenum* cell wall thickness decreased with increasing pH, and the mycelium diameter is 2–3 μm at pH6.0 and is 2–18 μm at pH7.4. (2) pH changes also affect the direction of cell metabolism. In the case of recombinant human serum albumin produced by the genetic engineering *Pichia pastoris*, protease production is the least desirable. At pH5.0 or lower, the protease activity increased rapidly and was superior to the albumin production. When the pH value was above 5.6, the activity of protease was very low, which could avoid the loss of albumin. Moreover, the change of pH will affect the activity of various enzymes and the utilization rate of bacteria on the substrate, which will affect the cell growth and the synthesis of the product. Therefore, in industrial fermentation to maintain growth and product synthesis, the optimal pH is one of the key parameters to the success of the production. (3) pH change affects the synthesis of metabolites.

Zhang et al. [49] investigated the effect of intermittent pH adjustment on hydrolysis and acidification of steam-exploded cornstalks by microbial community. Owing to lower degradation rate of steam-exploded cornstalk, the concentrations of water-soluble metabolites were lower with intermittent pH adjustment to 6.0 or

10.0, and acetate and propionate were also found to be the major water-soluble metabolites at pH 7.0, 8.0, and 9.0. The total concentrations of acetate and propionate reached peak values after 84 h of fermentation, which is increased accompanied by the pH increase, from 1.86 g/ L (pH 7.0), 2.04 g/L (pH 8.0) to 3.32 g/L (pH 9.0). Interestingly, the concentration of acetate after 84 h of fermentation increased as pH increases from 7.0 to 9.0, which was opposite to that of propionate. In addition, compared with that only initial pH adjustment, the total concentrations of acetate and propionate increased by 33% with intermittent pH adjustment to 8.0, respectively. After fermentation for 84 h, both concentrations of acetate and propionate decreased at all pH levels, which might be consumed by the obtained microbial community itself. During the fermentation process, the concentrations of other water-soluble metabolites such as ethanol, butyrate, glucose, and lactate remained at low levels. Based on the above results, it was found that intermittent pH adjustment was effective to enhance the acidification of SEC and regulate the distribution of organic acids.

The results of DGGE analysis showed that pH had remarkable effects on shifts in microbial community structure, which might further result in the change in fermentation patterns. Intermittent pH adjustment was considered to be a useful way to enhance hydrolysis and acidification of lignocellulose and regulate the distribution of organic acids by the enriched microbial community.

5.3.4.4 Variable Rate of Oxygen Supply

From the perspective of microbial growth and oxygen dynamics, the change of oxygen during growth depends on the oxygen consumption or oxygen uptake rate and the amount of dissolved oxygen. Oxygen changes during the production process also depend on oxygen consumption and oxygen dissolution. The oxygen consumption in the growth stage depends on the number of bacteria and bacterial respiration. In the exponential phase, the specific growth rate was the largest, as well as the respiratory intensity and the number of cells increased in a geometric progression. In the stable phase, the specific growth rate is almost equal to zero and the number of viable cells no longer increase, so the unit cell weight per unit of time in the oxygen consumption (breathing intensity) is basically unchanged. Since the consumption of oxygen by bacteria are different at different stages, in order to meet the needs of cell reproduction and production of products, the provision of dissolved oxygen should also be different. For example, the critical oxygen concentration in the growth phase of the production of the taxamycin is greater than the critical oxygen concentration of the product formation phase which are 13% and 5%, respectively, whereas the growth of the ampicillin producing stage is less than the critical dissolved oxygen concentration, which are 5% and 10%–20%, respectively.

Oxygen consumption is not only different at different fermentation period but also in different stages of the same period. For example, citric acid produced by *Aspergillus niger* in the 3 days before and after the acid absorption of oxygen is about 3: 2. In the cell growth stage of the fermentation process, the number of

bacteria is constantly changing (curve growth), and the oxygen consumption changes are more complex, but always gradually increasing. Therefore, in order to meet the oxygen consumption needs of bacteria in different stages of different periods, oxygen should be adjusted timely. The oxygen balance (oxygen demand rate, NA) was in equilibrium with the dissolved oxygen per unit volume of culture medium (OTR). The dissolved oxygen concentration at this time is the optimum dissolved oxygen concentration selected.

When the concentration of dissolved oxygen is below the critical value in the growth phase, oxygen is the limiting growth factor, and if it is above the critical value, the growth proceeds smoothly and reaches the maximum rate. According to the linear relationship between oxygen transfer driving force (oxygen partial pressure difference between gas phase and liquid phase) and the microbial, it can be seen that microbial growth is accelerated and finally reached the maximum specific growth rate with the increase of dissolved oxygen concentration which is the best dissolved oxygen concentration (critical value). Only the concentration of dissolved oxygen in the fermentation broth is always maintained at the optimal concentration or critical concentration in each period, so that the growth rate or product formation rate can be maximized. For example, cephalosporin C is produced with *Acremonium versicolor*, and the oxygen concentration for of the product formation is 20% of the saturation value. Below this value, the accumulation of intermediate penicillin N (PENN) and the formation of repressive cephalosporin C were caused, whereas a higher concentration of dissolved oxygen in the culture medium produces more cephalosporin C, with a maximum of cephalosporin C at the critical value [40].

5.3.5 Periodic Intensification Optimization Based on Environmental Stress

The traditional fermentation process has become increasingly difficult to meet the needs of modern fermentation engineering, forcing people to improve the fermentation process with new methods. Therefore, people began to explore the effect of some physical quantities (such as light, electricity, and heat) on biological characteristics of the fermentation process (such as enzyme activity) [50]. There are two periodic action modes of the physical factors in the fermentation process: one is the periodic intensification of the constant field, and the other is the continuous action of the high-frequency field.

5.3.5.1 Principle and Optimization of Periodic Effects of Low-Speed Ultrasound

(1) Principle of ultrasound on fermentation process

Ultrasound used in biological fermentation engineering can be divided into power ultrasonic and ultrasonic detection. Power ultrasound is mainly used to improve the

fermentation process or to improve the fermentation process. The mechanism of action is divided into heat, cavitation and mechanical mass transfer, the strength of the role and the frequency and intensity of ultrasound. The thermal effect is mainly used for sterilization while cavitation and mechanical mass transfer can promote cell cycle mass transfer. Cavitation is the propagation of ultrasonic waves in the medium, the average distance of molecules in the liquid changed with the molecular vibration. When it exceeds the role of maintaining the liquid critical molecular spacing, the cavitation is formed. At macroscopic level, cavitation is reflected by growth, shock, and collapse of a series of microbubbles in liquid (often called the cavitation of the nucleus).

From the perspective of cell stress, ultrasound is a periodic longitudinal wave, in a vibration cycle, the biological pressure on the moment changes according to a certain law. Forces imposed on cells can be divided into normal component and tangential component. Part of the normal force enters into the cytoplasm through the cell membrane, and the other part forms a normal pressure. The pressure will produce the normal direction of deformation because the cell membrane is an elastomer. Two effects can be caused by the deformation which are increased area and compressed cell volume. The former stretched the cell membrane to reduce the local thickness, which squeezed the cell body to increase its internal pressure. Displacement of cell membrane in tangential direction is caused by tangential force, which has no impact on cell volume. However, it will make local cell membrane become thin and increase microporosity, which increases the permeability of the local cell membrane and accelerate the exchange of material on both sides of the cell membrane. At the same time, the cell membrane plays an important role in the life activities such as cell division, differentiation, and metabolism regulation, in addition to maintaining the stability of intracellular environment, regulating the transport of internal and external substances, cell recognition, transmembrane transmission, and cellular immunity. Changes in permeability are bound to affect cell life activities [20].

Ultrasonic applied to the fermentation process is usually low-intensity ultrasound, relying on mechanical vibration and steady-state cavitation effect of the mass transfer boundary layer thinning, and to accelerate the movement of solute particles, which reacts into the enzyme or active site and product. The low-intensity ultrasonic waves applied to plant and animal cells will produce intracellular microfluidic, endoplasmic rotation, and eddy current movement, and improve the cell membrane and cell wall penetration. These effects can improve the cell's metabolic function.

(2) Process optimization with ultrasound

There are two aspects to optimize the ultrasonic stimulation. One is the nature of the ultrasound which is closely related to the fermentation effect, and the most important parameters are the intensity (frequency) and the timing of the ultrasonic wave. Changes in other parameters of the fermentation environment (such as changes in optimum pH and temperature) are caused by ultrasound. Through optimization of these parameters, the yield of the product can be improved significantly.

5.3.5.2 Principle and Optimization of Periodic Effects of Alternating Magnetic Field

There is a very close relationship between magnetic and biological original life. On the one hand, magnetic exist in various materials, life activities in the electron transfer, and ion motion will produce a weak biological magnetic field. Biomagnetism and the interaction of magnetic field and external magnetic field produce various effects on the organism. The biological effect of magnetic field not only occurs at the biological, tissue, and cellular level but also at molecular level and ion level in vitro experiments. Therefore, it is possible to combine the magnetic theory and explore the mechanism of the biological magnetic effect [51].

Magnetic field strengthwork when the intensity reach to a certain threshold. There is some biological sensitivity to the distribution of the magnetic field. Therefore, the magnetic gradient and magnetic field and gradient product on biological impact research have got attention. In addition to the threshold, cumulative effect also exits in biological and magnetic fields. In some biological magnetic effect, exposure to the magnetic field irradiation will produce biological response in a long time although the magnetic field strength is not high.

Most of the microbial cells are single-cell organisms, and the role of magnetic field on microorganisms can be seen as a direct role of the magnetic field for the typical cell. Microorganisms are the best material to study the relationship between magnetic field and cells.

5.3.5.3 Alternating Electric Field

Environmental electric field of biological substances in the microbial body influence distribution arrangement and movement of the charge, thus affecting the biological activities of life. In addition, the electric field also affects physical and chemical properties of the medium (e.g., water) (such as refractive index, conductivity, dielectric constant, surface tension, viscosity, and infrared absorption spectra), thereby affecting the biological organism reaction process.

Periodic steady electric field and continuous high-frequency electric field are two main electric intensification strategies for fermentation process. The results showed that the two strategies both improved microbial growth and metabolic process. Alternating electric field improved cellulase production with when lignocellulose was used as the fermentation substrate, and the electric field was enhanced by electric field of 2.86 V/cm. The change period of the electric field direction was 12 h, and the cellulase activity could be increased by 10%. In the process of fermented bean curd, salt water on the role of mucor protease inhibition. Li et al. [52] found that within a certain range of high-frequency electric field activation of the role of protease, protease solution by the electric field strength of 10 V/cm (the frequency of about 2500 Hz, 5 min) and the enzyme activity increased 20%. In

addition, it was found that high-frequency electric field can passivate the enzyme. The fermented bean curd fermented with fermented bean curd was treated by high-frequency electric field. It was found that the high-frequency electric field did have some ripening effect, which could shorten the post-fermentation period by 25%, but the total content of amino acid in fermented bean curd decreased, and its composition changed. This indicated that the effects of high-frequency electric field on the microbes and enzyme systems of post-fermentation were complex and may activate certain microorganisms or enzyme systems within the selected electric field treatment range while inactivating other microorganisms or enzymes.

At present, the application of electric field in the fermentation process is less, but the above research shows that the high-frequency electric field of suitable intensity has obvious effect on the fermentation and post-fermentation process, but its mechanism is still needed to be further studied. As an effective optimization operation mode, long period electric intensification will undoubtedly promising.

5.4 Novel Methods of Periodic Intensification of High-solid and Multi-phase Bioprocess

5.4.1 Periodic Peristalsis: A New Strategy for Process Enhancement of Butanol Fermentation

It has been reported by Doremus et al. [53] that the agitation rate plays a significant role in controlling the metabolism of *C. acetobutylicum* because agitation favors butyric acid productivity during the acid phase and hinders the butanol biosynthesis in the solvent phase. It has been proved by Lamed et al. [54] that agitation can dramatically affect the level of dissolved hydrogen gas and solvent ratio by *Clostridium thermocellum*. Most of the research verified that the effect of agitation on butanol was inhibition rather than promotion due to the adverse effect of agitation [53, 55]. Therefore, new agitation type with less shear force is urgently required for the biofuel engineering [56], which can be achieved only by full understanding of the undergoing agitation-associated mechanism.

The concept of periodic peristalsis agitation was derived from the illumination of stomach and intestine. By expanding and contracting periodically, stomach and intestine can mix the food and digestive juices (mostly digestive enzymes) efficiently. This process is usually called “periodic peristalsis”, which has great potential in fermentation process enhancement.

5.4.1.1 Metabolite Profiles Comparisons Among Periodic Peristalsis Group, the Traditional Rushton Impeller Group, and the Stationary Group

Metabolites are direct indication of the fermentation process. Xia et al. [57] have compared metabolites difference in PPG, TIG, and SG. Table 5.2 shows the result of Student's t-test of metabolites in the three groups, which indicates there is obvious difference in cell growth, substrate utilization, and product synthesis of IPE-005.

The fermentation process of ABE can be divided into two phases: the acidogenic phase and solventogenic phase [58]: the acidogenic phase was observed during the first 60 h when cell biomass was rapidly produced (Fig. 5.31). During this period, biomass in PPG and TIG was 2.75- and 1.47-fold of that in SG, suggesting agitation could promote cell growth in this phase. During 96–120 h (the solvent-producing phase), however, biomass in the TIG decreased sharply, and obvious cell autolysis was observed. It should be noted that butanol concentration in TIG was only 6.4 g/L (2.1 g/g biomass), which is much lower than the threshold (16.2 g/L) of cell tolerance [59]. Therefore, the cell autolysis in TIG was probably mainly the result of hydrodynamic mechanical stress. Strain in PPG consumed the most glucose in the media at 110 h. However, there were 9.4 and 15.3 g/L glucose remained in TIG and SG until the end of the fermentation (120 h), indicating periodic peristalsis could promote glucose utilization. At the same time, production profiles under different agitation types were quite different: PPG produced more butanol and acetone while TIG had higher concentration of butanol, lactate, butyrate, and acetate.

5.4.1.2 Comparison of Shear Force in Different Agitation Systems

Eddy length is the most commonly used criterion to scale shear stress in bioreactor, which is based on the classical effect of agitation on cell growth. Figure 5.32b shows the relationship between eddy length with agitation rate in TIG and peristole

Table 5.2 Metabolite profiles comparisons between periodic peristalsis group (PPG), the traditional Rushton impeller group (TIG), and the stationary group (SG) by Student's t-test [57]

Materials	P values		
	PPG-SG*	PPG-TIG*	SG-TIG*
Biomass	0.00051	0.0016	0.89
Glucose utilization	0.00025	0.00072	0.15
Acetone production	0.00011	0.00019	0.00085
Butanol	0.0067	0.0107	0.0187
Butyrate	0.00062	0.10	0.019
Lactic acid	0.48	0.00036	0.000032
Ethanol	0.00027	0.00055	0.0014
Acetic acid	0.11	0.00026	0.00093
Hydrogen	0.00020	0.00080	0.021

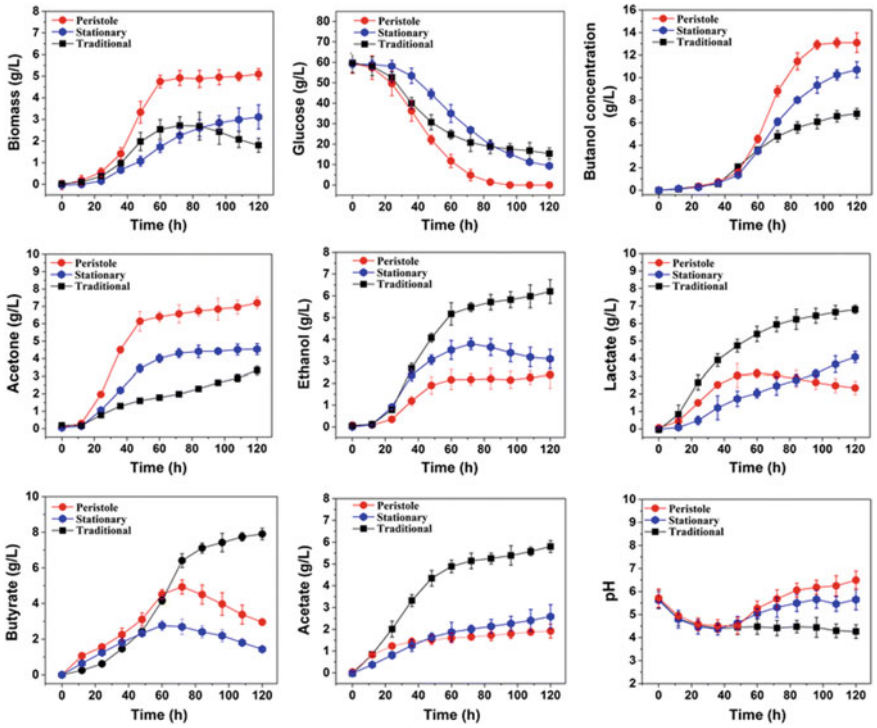

Fig. 5.31 Time course profiles of key fermentation parameters (dry cell weight, glucose, butanol, acetone, ethanol, lactate, butyrate, acetate, and pH) from PPG, TIG, and SG. PPG represents periodic-peristole group, TIG represents traditional Rushton impeller agitation group, and SG represents stationary culture group [57]

rate in PPG. It can be found that the inhibition effect of agitation on cell growth gets more severe with the decreasing eddy length. The critical point of the eddy length is 120 μm for *C. acetobutylicum* ATCC824, below which the damage becomes visible. In our experiment, the eddy length in PPG is 128 μm and is 95.4 μm in TIG, indicating that the shear force in PPG is only 74% of that in TIG. Figure 5.32c and d show the relationship of eddy length with turbulence intensity and velocity. In the case of same eddy length, PPG always owns higher turbulence intensity (more than 20-fold of that in TIG in the whole range) and lower velocity (less than 60% of that in TIG in the whole range). This characteristic makes periodic peristalsis agitation different from the existing agitation methods. It enhances mass transfer by high turbulence intensity instead of high velocity, in other words, running under a mild condition. Therefore, this novel agitation causes less hydrodynamic damage to cells.

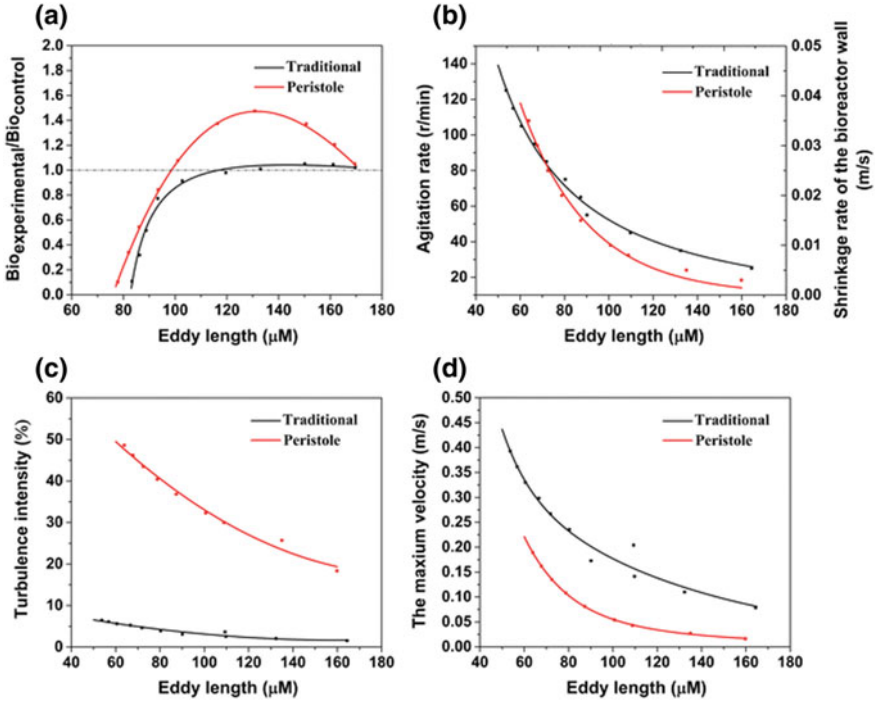

Fig. 5.32 Hydrodynamics parameters in periodic-peristole agitation group and traditional *Rushton* impeller group. **a** shows the relationship between eddy length and cell growth enhancement rate. Cell growth enhancement rate was calculated by dividing biomass in the reference group (stationary culture group) by that in the experimental group at 120 h; **b** shows the relationship between eddy length and agitation velocity; **c** shows the relationship between eddy length and turbulence intensity; and **d** shows the relationship between the eddy length and the maximum velocity [57]

5.4.1.3 Analysis of Metabolic Flux in Periodic Peristalsis Group, the Traditional Rushton Impeller Group, and the Stationary Group

(1) Embden–Meyerhof–Parnas (EMP) pathway

Glucose was first converted into G6P and channeled into the EMP pathway and the PPP at this branch point. Then, 90% of the glucose was further converted into pyruvate through the EMP pathway. At 48 h (Fig. 5.33), the EMP pathway showed a flux toward pyruvate in PPG and TIG to 84.2 and 88.5%, respectively, compared with that in SG, suggesting that this flux contributed to increased cell growth through the PPP [60]; however, at 96 h, the EMP pathway showed a flux toward pyruvate in PPG and TIG to 154.6 and 229.3%, respectively, compared with that in SG, implying that the EMP pathway flux was significantly stimulated by agitation.

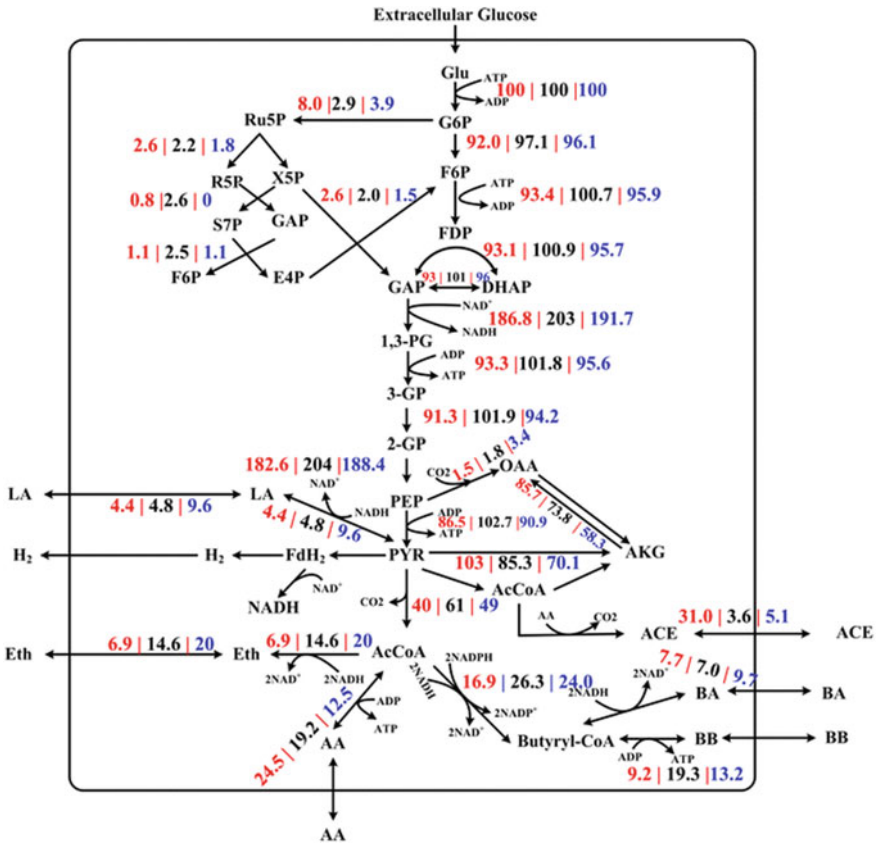

Fig. 5.33 Flux distributions at 48 h from three cultivation models. *Abbreviations*: AKG, α-ketoglutarate; OAA, oxaloacetate; BA, butyrate; Eth, ethanol; LA, lactate; AA, acetate; AcCoA, acetyl-CoA; X5P, xylulose-5-phosphate; S7P, d-sedoheptulose-7-phosphate; E4P, d-erythrose-4-phosphate; FDP, d-fructose-1, 6 bisphosphate; G6P, glucose-6-phosphate; ICIT, isocitrate; CIT, citrate; PYR, pyruvate; PEP, phosphoenolpyruvate; 2GP, 2-phospho-d-glycerate; 1,3GP, 3-phospho-d-glyceroyl phosphate; 3GP, 3-phospho-d-glycerate; GAP, glyceraldehyde-3-phosphate; R5P, d-ribose-5-phosphate; ACE, acetone; D6PAH3U, d-arabino-6-phospho-hex-3-ulose; and Ru5P, d ribulose-5-phosphate [57]

The EMP pathway was the main source of ATP and NADH [60]. As shown in Fig. 5.34, the EMP pathway of cells in PPG and TIG generated 1.25-fold and 2.41-fold ATP, respectively, compared with that of SG at 96 h. Furthermore, the NADH generation rate from the EMP pathway of cells in PPG and TIG was 1.22-fold and 1.56-fold, respectively, than that of SG. These results indicated that cells produced more ATP and NADH through the EMP pathway following both types of agitation in the solvent-producing phase.

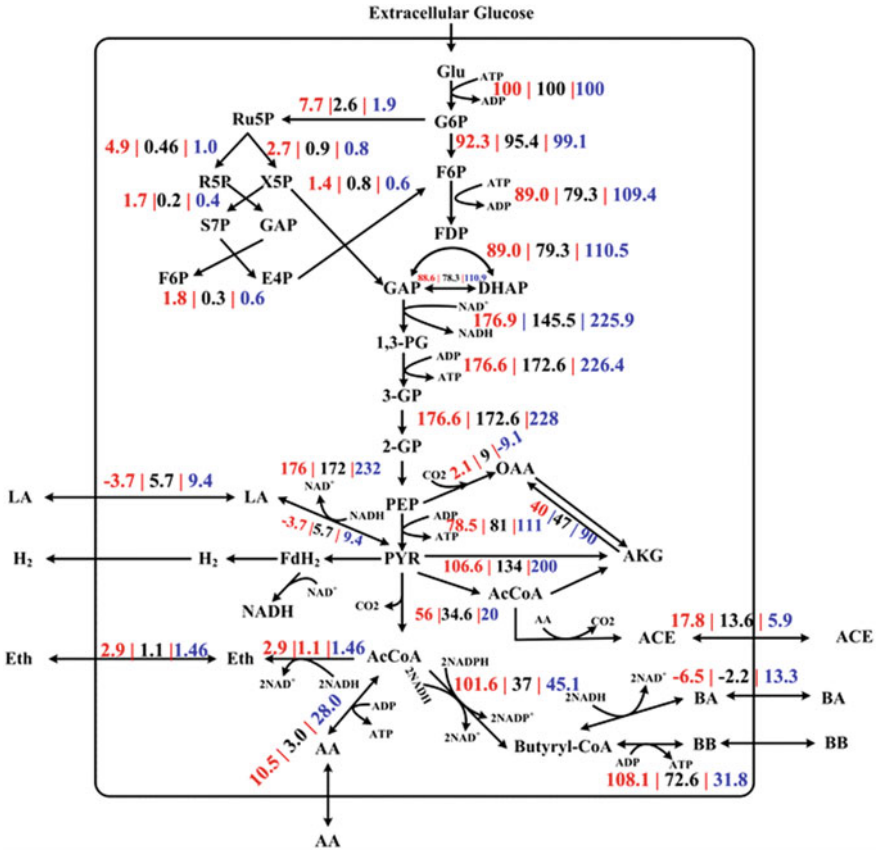

Fig. 5.34 Flux distributions at 96 h from three cultivation models. *Abbreviations*: AKG, α-ketoglutarate; OAA, oxaloacetate; BA, butyrate; Eth, ethanol; LA, lactate; AA, acetate; AcCoA, acetyl-CoA; X5P, xylulose-5-phosphate; S7P, d-sedoheptulose-7-phosphate; E4P, d-erythrose-4-phosphate; FDP, d-fructose-1, 6 bisphosphate; G6P, glucose-6-phosphate; ICIT, isocitrate; CIT, citrate; PYR, pyruvate; PEP, phosphoenolpyruvate; 2GP, 2-phospho-d-glycerate; 1,3GP, 3-phospho-d-glyceroyl phosphate; 3GP, 3-phospho-d-glycerate; GAP, glyceraldehyde-3-phosphate; R5P, d-ribose-5-phosphate; ACE, acetone; D6PAH3U, d-arabino-6-phospho-hex-3-ulose; and Ru5P, d ribulose-5-phosphate[57]

(2) Pyruvate metabolism

After the EMP pathway, the flux enters the pyruvate metabolic pathway. Pyruvate is a key intermediate in cellular metabolic pathways. The glycolysis flux is converted to lactate or acetyl-CoA and CO_2 through the pyruvate node. Acetyl-CoA is further converted to other end products such as butyrate, butanol, and acetate. It was clear that phosphoenolpyruvate (PEP), pyruvate, and acetyl-CoA form three main key nodes in the flux distribution. PLS analysis showed that butyrate, lactate and acetate inhibited butanol production (Fig. 5.35).

The inhibition effect of butyrate might be because of the competition for the precursor, butyryl-CoA. There are no significant differences in the levels of butyrate among PPG, TIG, and SG at 48 h. However, at 96 h, the flux toward butyrate biosynthesis (2 AcCoA + 2NADH → BA) in PPG and SG was −6.5 and −2.2%, respectively, suggesting that butyrate was being absorbed for butanol synthesis [61]. By contrast, butyrate in TIG continued to be produced at a flux rate of 13.3%, competing for butyryl-CoA with butanol biosynthesis [62].

The difference in the flux distribution of acids (acetate, butyrate, and lactate) among the three groups may be strongly associated with the intercellular energy state. Acids producing pathways (acetate, butyrate, and lactate) and substrate-level phosphorylation form the main sources of ATP generation [63, 64]. In the solvent-producing phase, the accumulation of butanol inhibits glucose uptake, thus inhibited energy generation, which is compounded by an independent drop in intracellular ATP levels [64]. To compensate for the ATP shortage, cells usually increase the flux toward acids synthesis.

(3) TCA cycle

In our MFA model, oxaloacetate (OAA) and α-ketoglutarate (AKG) are the key metabolites that contribute to biomass production [60, 65]. Strikingly, they are listed as the most unfavorable metabolites for butanol synthesis (VIP of AKG and OAA were −9.3 and −3.8, respectively). In the solvent—producing phase, the flux toward AKG in PPG and TIG was 0.85- and 1.62-fold, respectively, that of SG at 96 h. The inhibition effect of these two metabolites is likely probably due to the consumption of acetyl-CoA competing with butanol biosynthesis. Based on previous studies [61], cells should cease to grow in the solvent-producing phase and distribute the flux toward butanol synthesis, just as seen with SG. Therefore, understanding this abnormality required further investigation into the metabolic network. It is known that the TCA cycle can provide the low redox potential of the internal anaerobic environment of *C. acetobutylicum*, as well as generate ATP [66]. Lee et al. [62] found that *C. acetobutylicum* M5 facilitates the biosynthesis of amino acids by altering the flux in the TCA cycle. Hence, the increased TCA flux in cells likely compensated the energy and amino acid pool.

(4) Amino acids metabolism

Amino acids are key metabolites that reflect the intercellular energy status. Studying on amino acids may aid our understanding of cell behavior. Therefore, intracellular amino acids from the three agitation modes were dynamically detected, as shown in Fig. 5.36.

Figure 5.36a shows the synthetic pathway for amino acids. From Fig. 5.36c, d, it was evident that in TIG, the availability of some amino acids was exhausted during the solvent-producing phase, including isoleucine, tryptophan, and histidine. Given the energetic costs for amino acid biosynthesis (shown in Fig. 5.36b), these amino acids are the most energetically expensive ones. This further indicates that a reduced availability of metabolic energy might be involved in the reduced supply of the "expensive" amino acids [67]. To validate our hypothesis, intracellular $NADPH/NADP^+$, $NADH/NAD^+$, and ATP were detected (as shown in Table 5.2).

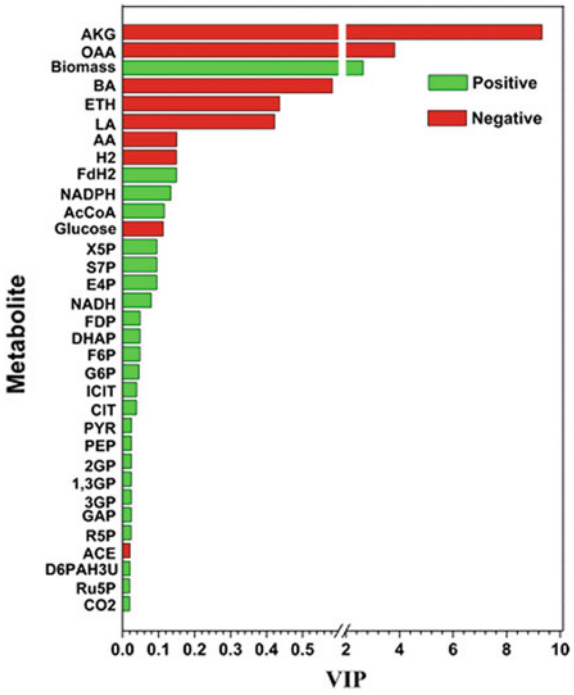

Fig. 5.35 The VIP plots of the PLS model for butanol biosynthesis. *Abbreviations*: AKG, α-ketoglutarate; OAA, oxaloacetate; BA, butyrate; Eth, ethanol; LA, lactate; AA, acetate; AcCoA, acetyl-CoA; X5P, xylulose-5-phosphate; S7P, d-sedoheptulose-7-phosphate; E4P, d-erythrose-4-phosphate; FDP, d-fructose-1, 6 bisphosphate; G6P, glucose-6-phosphate; ICIT, isocitrate; CIT, citrate; PYR, pyruvate; PEP, phosphoenolpyruvate; 2GP, 2-phospho-d-glycerate; 1,3GP, 3-phospho-d-glyceroyl phosphate; 3GP, 3-phospho-d-glycerate; GAP, glyceraldehyde-3-phosphate; R5P, d-ribose-5-phosphate; ACE, acetone; D6PAH3U, d-arabino-6-phospho-hex-3-ulose; and Ru5P, d ribulose-5-phosphate [57]

The intracellular concentrations of NADPH/$NADP^+$, NADH/NAD^+, and ATP at 96 h in TIG were 48.4, 19.5, and 37.6%, respectively, of those in TIG at 48 h, and were 48.3, 40.0, and 57.6%, respectively, of those in PPG at 96 h. These findings confirmed the "energy starvation" status of cells in TIG during the solvent-producing phase.

The "energy starvation" status may strongly correlate with the solvent-resistance mechanism and agitation. In the presence of solvents, *Clostridia* increase branched-chain amino acids and branched-chain fatty acids to improve membrane structure stability, a process known as "*homeoviscous adaptation*" [68, 69]. Simultaneously, the hydrodynamic damage of the cell membrane caused by agitation also triggers the synthesis of tolerance protein [56, 70]. This process requires high quantities of ATP because amino acid synthesis is energetically expensive. To maintain a high-energy status, which is also one of the central requirements for

cellular metabolism [71], cells have to rearrange their metabolism (acid biosynthesis in our study) toward enhanced ATP synthesis [72].

(5) Fatty acids metabolism

Fatty acids have long been recognized as signaling molecules that have the capacity to trigger profound physiological responses [73]. Table 5.3 shows the dynamic profiling of fatty acids during the fermentation process. TIG possessed a high level of total unsaturated fatty acids, 0.15-, 0.3-, and 0.6-fold higher than that of PPG at 48, 96, and 108 h, respectively. However, the total amount of saturated fatty acids in TIG was

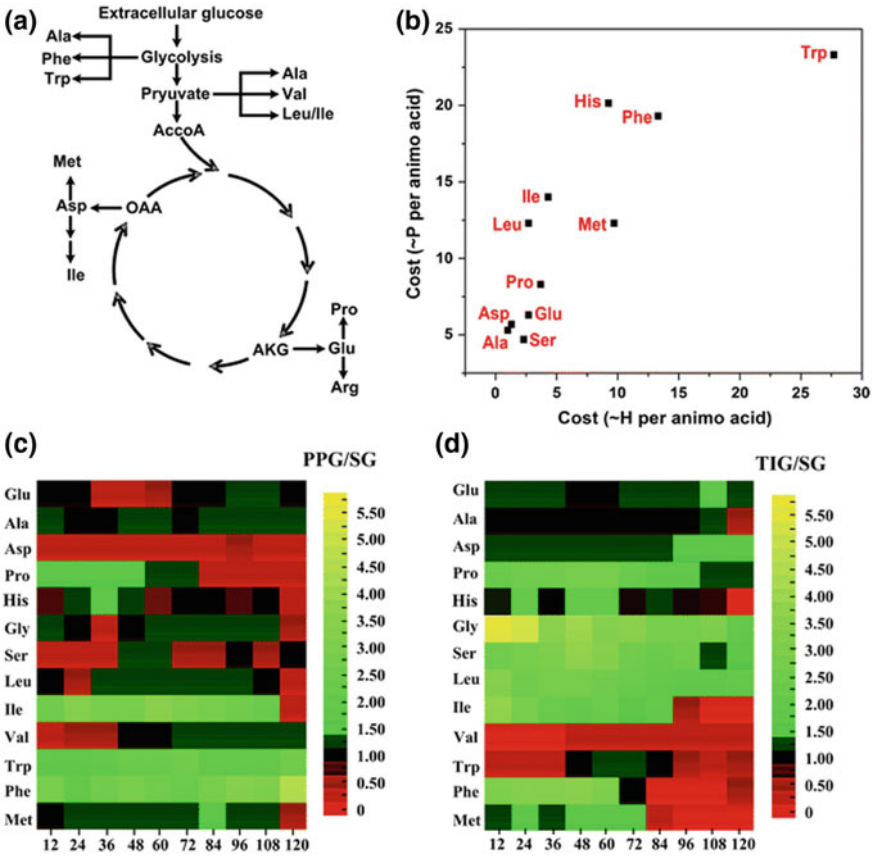

Fig. 5.36 The comparison of the intracellular amino acids under traditional and normal stirring groups. **a** Was the synthesis pathways of the amino acids; **b** the energetic costs for amino acid biosynthesis; **c–d** were the heat map visualizing the intracellular amino acids contents during fermentation from normal and traditional groups. The color code indicates an increased (green) or a decreased (red) availability under the two conditions as compared to the reference process as indicated by the color legend as aside the graph. The full amino acid data set is given in the supplementary material 3. Availability for each amino acid was calculated as ratio of the concentration to that at reference group. The data given reflect a period of 12 ~ 120 h [57]

Table 5.3 The dynamic changes of the important metabolites [57]

Time (h)	36 h	48 h	96 h	108 h
NADH/NAD$^+$	0.16 ± 0.056^a	0.24 ± 0.079^a	0.1 ± 0.026^a	0.07 ± 0.012^a
	0.12 ± 0.017^b	0.17 ± 0.069^b	0.06 ± 0.01^b	0.05 ± 0.020^b
	0.15 ± 0.037^c	0.21 ± 0.092^c	0.04 ± 0.02^c	0.02 ± 0.011^c
NADPH/NADP$^+$	4.2 + 1.5^a	10.32 + 1.8^a	5.67 + 1.6^a	2.21 + 1.83^a
	3.45 + 0.98^b	7.64 + 2.91^b	3.46 + 1.79^b	1.14 + 0.31^b
	3.98 + 1.7^c	5.65 + 1.79^c	2.74 + 1.49^c	0.67 + 0.38^c
AcCoA**	1.37 ± 0.68^a	2.10 ± 0.14^a	1.90 ± 0.26^a	0.07 ± 0.02^a
	1.06 ± 0.42^b	1.65 ± 0.11^b	2.33 ± 0.17^b	0.11 ± 0.03^b
	1.34 ± 0.69^c	2.17 ± 0.19^c	1.84 ± 0.43^c	0.03 ± 0.02^c
ATP**	3.54 ± 0.82^a	3.86 ± 0.23^a	2.34 ± 0.14^a	1.45 ± 0.15^a
	4.27 ± 0.17^b	2.88 ± 0.47^b	1.93 ± 0.13^b	1.11 ± 0.10^b
	3.31 ± 0.21^c	3.59 ± 0.56^c	1.35 ± 0.09^c	0.863 ± 0.16^c
	27.2 ± 1.9^a	28.5 ± 2^a	39.8 ± 2.8^a	25.3 ± 1.3^a
Oleic acid**	25.7 ± 1.8^b	25.7 ± 0.8^b	32.4 ± 2.6^b	27.2 ± 2.1^b
	34 ± 2.4^c	35.2 ± 1.4^c	49.9 ± 2.5^c	46.2 ± 3.6^c
	23.6 ± 0.9^a	35.1 ± 2^a	31.8 ± 2.2^a	28.3 ± 1.4^a
Stearic acid**	25.5 ± 1.3^b	36.7 ± 1.9^b	29.4 ± 1.2^b	29.9 ± 2.1^b
	26.1 ± 0.8^c	37.2 ± 1.6^c	21.2 ± 1.9^c	11.7 ± 1.6^c
Linoleic acid**	35.9 ± 0.6^a	15.7 ± 0.9^a	18.3 ± 1.1^a	19.4 ± 1.4^a
	32.9 ± 1.0^b	13.4 ± 0.4^b	15.5 ± 0.5^b	15.9 ± 0.8^b
	32.8 ± 0.9^c	13.8 ± 1.1^c	21.6 ± 1.5^c	23.5 ± 1.2^c
Arachidonic acid**	42.1 ± 1.5^a	38.5 ± 1.5^a	30.1 ± 1.2^a	23.3 ± 1.3^a
	34.8 ± 2.1^b	41.4 ± 2.1^b	35.6 ± 1.3^b	33.3 ± 1.8^b
	45.4 ± 3.6^c	46.2 ± 2.8^c	43.1 ± 4.4^c	41.5 ± 4.5^c

Note

*Stands for the formation rate at the corresponding time point, (mol/L)

**Stands for the specially concentration at the corresponding time point, (mol/g); which is calculated by the concentration/biomass

^{a}Stands for the normal force model

^{b}Stands for the stationary culture model

^{c}Stands for the shear force model

lower than that of the other groups, being 106.3, 66.1, and 41.3% of that in the PPG and 101, 72.1, and 39.1% of that in the SG at 48, 96, and 108 h, respectively.

The cell membrane is a flexible structure composed of a lipid bilayer and proteins, and its fluidity is determined by the fatty acid composition. When under agitation, cells adjust fatty acid metabolism to resist the adverse effects of shear force by improving cell membrane fluidity. Bhagyalakshmi et al. [74] found that endothelial cells activate phospholipid turnover and enhance the biosynthesis of arachidonate under fluid shear stress. In our study, the high levels of unsaturated fatty acid in TIG may arise for a similar reason: during the acid-producing phase, shear forces may upregulate the synthesis of unsaturated fatty acids to increase cell

membrane fluidity. Because suffering more serious shear force than the other two groups, cells in TIG own the highest content of unsaturated fatty acids. However, in the solvent-producing phase, the accumulation of solvents, especially n-butanol, began to disrupt the phospholipid bilayer of the cell [75], a phenomenon enhanced by shear stress. To exacerbate this, cells in TIG were unable to synthesize saturated fatty acids rapidly enough to inhibit the flow of organic solvent into the cell because of "energy starvation", leading to autolysis. By contrast, in PPG, the hydrodynamic damage was not as pronounced as in TIG because the relatively higher energy status enabled cells to redistribute their flux and initiate the tolerance mechanism efficiently.

5.4.1.4 Mechanism Analysis of Periodic Peristalsis Strategy for Enhancing Butanol Fermentation

The effects of agitation on metabolic distribution in *C. acetobutylicum* are summarized in Fig. 5.37. Based on our findings, we proposed a possible mechanism by

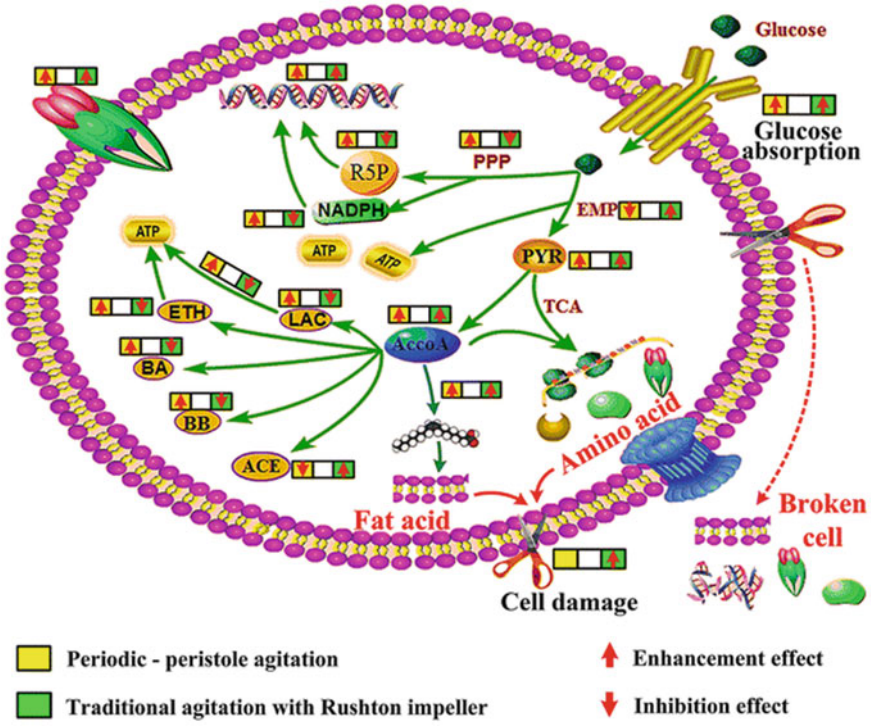

Fig. 5.37 Effects of agitation on metabolic distribution of *IPE*-005 and the corresponding enhancement strategy for butanol production [57]

which *C. acetobutylicum* cells respond to agitation. The high mixing efficiency in PPG enhances the PPP flux, providing more precursors for nucleotide synthesis and promoting both cell growth and butanol tolerance. Furthermore, the high reducing power and increased carbon flux promote butanol biosynthesis. By contrast, traditional agitation leads to higher levels of hydrodynamic damage on cells. To resist shear forces, cells increase the levels of unsaturated fatty acids and amino acids to modulate membrane fluidity. To achieve this, cells rearrange their metabolism toward enhanced ATP synthesis, which results in enhancing the flux through glycolysis and acid synthesis at the expense of the pentose phosphate pathway. This effect of hydrodynamic damage is intensified by the chemotropic effects of solvents on the cell membrane.

In conclusion, the enormous differences impacted by agitation are obviously associated with three issues, which result in significant changes in cell metabolic behaviors: first, a rebalanced redox status; second, the energy (ATP) acquirement and consumption; and third, the tolerance mechanism of the cell for survival of solvent (homeoviscous adaptation).

5.4.2 GDDSSF for Process Enhancement of Solid-State Fermentation

Solid-state fermentation has been considered as the technology with the characteristics of backward, low level, and hard to be scaled up. Since the mid century of 20th, especially in 1970s, when the concept of biochemical proposed, scholars have done great attempts to tackle the problems, and many solutions have been proposed. Scholars in Institutes of Process Engineering, Chinese Academy of sciences have focused on solid-state fermentation reactors research since 1984. They concluded that for better performance of the reactors, thoughts for reactor design must be changed from the basic theory. In 1991, GDDSSF technology was proposed, which based on the new principle of reactor design that intensifies transfer of the mass and thermal in and outside of the cells by periodic intensification and the normal force as the power source.

In traditional chemical industry, mass and heat transfer of the solid substrate is generally resolved through mechanical stirring (shear force) with the purpose that the particles are mixed well, accelerating the reaction between the gas phase molecules or solid matter and changing molecular diffusion into convective diffusion around the solid particles. Mechanical stirring is easy to be realized and can make the gas phase well mixed. However, mechanical stirring results in mycelium damage and restrict microbial growth. In addition, mechanical stirring has the disadvantages of energy-extensive consumption, complex structure, microbiological contamination, and agglomeration. Moreover, mechanical stirring cannot make mixed scale of the solid particles as that in liquid phase because mass inside of the particle is not affected by macro-stirring. Therefore, mechanical stirring shows no

function in microscale and cannot realize homogeneous of temperature, humidity, and oxygen supply in the solid-state fermentation system [76].

5.4.2.1 Mechanism of GDDSSF

GDDSSF is static in terms of solid particle while it is dynamic in terms of gas phase. Gas has the advantage of better capability of pervasive. Increasing pressure in reactor change the gas molecular from molecular diffusion into convective diffusion at the particle level, getting the thermal and humidity mixed in microscale and enhancing oxygen supply and dioxide emission. In the pressure discharge process, gas phase inside of the particle expansion due to pressure of the solid particles contributes to loosen the matrix bed, which is favorable for mycelium growth because of adequate oxygen supply and the large population of mycelium expansion space. Therefore, the fermented mycelia are very plump inner and outer of the matrix. Microorganisms must live in moisture surroundings both in a liquid medium and in a solid because matter, energy, and information exchange occur in moisture through the cell membrane, and then, exchange occurs among solid, gas, and liquid phase. Bacteria are stretchable pouch-like living body. Gas pressure pulsation cycle will soon cause a variety of methods to force the liquid film layer. Since the liquid film is thin, this method boosts the transfer rate quickly and more sensitively [76].

Reactor with GDDSSF has the advantages of simple mechanical structure, easily sew, less sterile air, and low energy consumption (power of circulating fan and air consumption are 10 and 20% of that required for mechanical stirring). Solid medium is generally 2–5 cm in shallow tray fermentation system in which the temperature and humidity are easy to be controlled and scaled up. Matrix temperature can be adjusted by circulating air while the humidity was adjusted by controlling pulsation frequency. Application of solid-state fermentation reactor GDDSSF cellulase fermentation, pressure pulsation two to three times higher than the constant pressure operation, and fermentation time can generally be shortened 1/3. Riboflavin fermentation can be shortened from 12 to 7 days. Live fermented bassiana spores reach to more than 50 billion/g.

5.4.2.2 Variable Pressure Pulsation Frequency Optimization in Gas Double-Dynamic Solid-State Fermentation

Carbon dioxide is important indicator reflecting microorganism growth. Zhao et al. [77] investigated microbial metabolism characteristic by carbon dioxide evolution under different pressure pulsation frequencies in GDDSSF. The experimental results showed that when the frequency increased from 1/30 to 1/20 min^{-1}, the carbon dioxide evolution increased apparently, demonstrating that the microbial metabolism was enhanced. While the frequency continued to increase from 1/20 to 1/10 min^{-1}, the carbon dioxide evolution became less especially at the beginning of

the fermentation. The lag phase of *Penicillium decumbens* JUA10 under the frequency of 1/10 min^{-1} prolonged for nearly 10 h than that under the frequency of 1/20 min^{-1}, which may owe to that the microbes required more time to adapt the unnatural environment with high frequency, high pressure. Previous literatures also studied the effect of pressure pulsation frequency on the microbial metabolism. It was suggested that the high frequency of air pressure pulsation with high frequency meanwhile requires lots of power energy especially in the large-scale production. The power energy consumption can be expressed by the number of pressure pulsation cycles. Therefore, concerning the variable heat generation regularity in GDDSSF process and energy conservation, the optimal GDDSSF frequencies were determined with the same energy consumption of the conventional preferred constant.

To evaluate the fermentation performance under the optimal variable pressure pulsation frequencies, experiments involving heat removal efficiency and fermentation production were carried out. Results showed that the medium temperature increased extent under the optimal variable frequencies was lower than that under the conventional constant frequency of 1/20 min^{-1}. The maximum medium temperature was 32.5 °C under the optimal variable frequencies while that was 34.2 °C under the conventional constant frequency both at 48 h. Additionally, the medium temperature under the optimal variable frequencies during fermentation time of 36–96 h was lower than that under the conventional constant frequency of 1/20 min^{-1} correspondingly, revealing that the variable frequencies matching with the metabolic heat generation regularity removed heat more effectively. Although the medium temperature under the optimal variable frequencies during fermentation time of 0–24 h and 108–120 h was little higher than that under the conventional constant frequency owing to the frequencies were lower than 1/20 min^{-1} during these two stages, it would not affect the fermentation production much. One reason was that the temperature difference was small enough to neglect. The other reason was that the microbes did not metabolize vigorously and barely produced enzyme during these two stages. As a result, the cellulose activities under the optimal variable frequencies reached the maximum (21.3 IU/g dry medium) due to the enhanced heat removal efficiency while that was 19.5 IU/g dry medium under the conventional constant frequency of 1/20 min^{-1}. The results indicated that the optimized variable frequencies matching with metabolic heat generation regularity improved heat removal efficiency and thus increased the fermentation productivity compared with the conventional constant frequency with same energy consumption, demonstrating the significance of the pressure pulsation frequency optimization based on heat balance. GDDSSF for biopesticide production using *Bacillus thuringiensis* CM-l was conducted and the pressure pulsation frequency was optimized based on extensive investigations. The results showed that the optimized frequency was also variable. At the beginning of fermentation, the frequency was lowest, which was 1/60 min^{-1}. While during the active stage of metabolism, the frequency was largest, reaching 1/10 min^{-1}. The maximum medium temperature under the optimized frequency was lower by 7 °C than that under the conventional trays fermentation, which demonstrated the enhanced heat removal under the

optimized frequency in GDDSSF. These results indicated that the optimized variable frequency was beneficial to remove the metabolic heat timely, which was consistent with the present study. It was concluded that the variable frequency was the preferred operation mode than the constant one in GDDSSF. And the optimization method established by the heat balance model was proved efficient and practical.

5.4.2.3 Mass Distribution in GDDSSF

Knowing mass distribution in substrate of solid-state fermentation is benefit to conduct a comprehensive analysis and enhancement of the SSF performance. Chen et al. [78] determined the distributions of water, biomass, and fermentation product in different medium depths of SSF using near-infrared spectroscopy and the developed models. Based on the mass distribution regularity, the effects of gas double dynamic on heat transfer, microbial growth and metabolism, and product distribution gradient were systematically investigated. Results indicated that the maximum temperature of substrate and the maximum carbon dioxide evolution rate were 39.5 °C and 2.48 mg/(h•g) under static aeration solid-state fermentation and 33.9 °C and 5.38 mg/(h•g) under GDDSSF, respectively, with the environmental temperature for fermentation of 30 ± 1 °C. The fermentation production (cellulase activity) ratios of the upper, middle, and lower levels were 1:0.90:0.78 at seventh day under SASSF and 1:0.95:0.89 at fifth day under GDDSSF. Therefore, combined with near-infrared spectroscopy analysis, gas double dynamic could effectively strengthen the solid-state fermentation performance due to the enhancement of heat transfer, the intensification of microbial metabolism, and the increase of the homogeneity of fermentation products.

References

1. Liang JX, Weng SH, Chen JH (2006) Chaos theory and modernlization of chinese medical. J Guangzhou Univ Tradit Chin Med 23(3):186–189
2. Ghosh A, Greenberg ME (1995) Calcium signaling in neurons: molecular mechanisms and cellular consequences. Science 268(5208):239
3. Berridge MJ, Taylor C (1988) Inositol trisphosphate and calcium signaling. In: Cold spring harbor symposia on quantitative biology. Cold Spring Harbor Laboratory Press, pp 927–933
4. Thomas A, Bird G, Hajnoczky G, Robb-Gaspers L, Putney J (1996) Spatial and temporal aspects of cellular calcium signaling. FASEB J 10(13):1505–1517
5. Chance B, Hess B, Betz A (1964) DPNH oscillations in a cell-free extract of *S. carlsbergensis*. Biochem Biophy Res Co 16 (2):182–187
6. Li H, Hou Z, Xin H (2005) Internal noise stochastic resonance for intracellular calcium oscillations in a cell system. Phys Rev E 71(6):061916
7. Wang J, Liu ZH, Cai RX et al (2006) Current development of analytical methods based on biological spatiotemporal oscillators. Process Chem 18 (1)

8. Nicolis G, Prigogine I (1977) Self-organization in nonequilibrium systems, vol 191977. Wiley, New York
9. Li RS (1986) None-equilibrium thermodynamics and dissipative structure. Tsinghua University Press
10. Sun KL, Cai GY (1999) The effect of alternative stress on the thermodynamical properties of cultured tobaccco cells. Acta Biochemica et Biophysica 15(3):578–583
11. Ingber DE, Folkman J (1989) Tension and compression as basic determinants of cell form and function: utilization of a cellular tensegrity mechanism. In: Cell shape: determinants, regulation, and regulatory role, pp 3–31
12. Ingber DE (1997) Tensegrity: the architectural basis of cellular mechanotransduction. Annu Rev Physiol 59(1):575–599
13. Li ZH (1993) A new principle of bioreactor design. In: Proceedings of the 5th National Conference on Biochemistry
14. Singer S, Nicolson GL (1972) The fluid mosaic model of the structure of cell membranes. In: Day SB, Good RA (eds) Membranes and viruses in immunopathology, pp 7–47
15. Yin JZ, Chen SJ, Jia LY et al (2009) Research on scale up factors and methods. Chem Equip Technol 30(1):22–27
16. Wang ZH (1982) History of microbial industry in China. Chin J Sci Techn Hist 4:98–98
17. Chen HZ, Li ZH (1998) Bioreactor engineering advances. Biotechnology 18(4):46–49
18. Li HQ (2008) Study on cellulase solid-state fermentation with gas periodic stimulation
19. Chen PS (1979) History of microbial industry in China. Light Industry Press
20. Dai CY, Wang BC (2003) Development of high-speed rectangle burner used in baked aluminum reduction cells. J Chongqing Univ (Nat Sci) 26 (2):15–17
21. Gao DW, Gao WH (1999) effect of linear ultrasonic wave irradiation on the growth of *SaccharomYCES cerevisiae*. J South China Univ Technol (Nat Sci) 27(12):34–37
22. Fu XG, Chen HZ, Li HQ et al (2006) Study of microorganism protein and mechanism in solid state fermentation with periodical dynamic changes of air. J Bejing Univ Chem Technol (Nat Sci)
23. Wang JY, Zhu SG, Xu CF (2002) Biochemistry. Higher Education Press, Beijing
24. Li WQ, Chen HJ, Chen CH et al (2007) The influence of Key enzyme in glucose metabolism on lincomycin biosyhthesis. Pharm Biotechnol 14(6):424–428
25. Spano G, Massa S (2006) Environmental stress response in wine lactic acid bacteria: beyond *Bacillus subtilis*. Crit Rev Microbiol 32(2):77–86
26. Kültz D (2005) Molecular and evolutionary basis of the cellular stress response. Annu Rev Physiol 67:225–257
27. Serrano R (1988) Structure and function of proton translocating ATPase in plasma membranes of plants and fungi. Biochemica et Biophysica Acta (BBA)-Rev Biomembr 947 (1):1–28
28. Portillo F (2000) Regulation of plasma membrane H + -ATPase in fungi and plants. Biochimica et Biophysica Acta (BBA) Rev Biomembr 1469 (1):31–42
29. Piper P, Talreja K, Panaretou B et al (1994) Induction of major heat-shock proteins of *Saccharomyces cerevisiae*, including plasma membrane Hsp30, by ethanol levels above a critical threshold. Microbiology 140(11):3031–3038
30. Du CY, Liu M, Rao Z et al (2005) Effect of alternative aeration on key enzymes and coenzyme in 1,3-propanediol prodction by *Klebsiella pneumoniae*. Chin J Process Eng 5 (5):540–544
31. Xie MD, Liu DH, Zhang Y et al (2000) Enhancement of fermentative gltcerol yield with heat shock treatment. Chin J Biotechnol 16(3):384–386
32. Saucedo-Castañeda G, Trejo-Hernández M, Lonsane B et al (1994) On-line automated monitoring and control systems for CO_2 and O_2 in aerobic and anaerobic solid-state fermentations. Process Biochem 29(1):13–24
33. Peng XW (2008) Production of single cell oils from steam-exploded straw in solid-stated fermentation and pyrolysis of fermented mass for producing biodiesel. university of chinese academy of sciences. Institute of Process Engineering, Chinese Academy of Sciences

34. Zeng W (2008) Solid state fermentation of feruloyl esterase and synergistic effect with cellulase. Institute of Process Engineering, Chinese Academy of Sciences
35. Chen J, Liu LM, Du GC (2009) Optimazation principle and technology of fermentation process. Chemical Industry Press, Beijing
36. Jia B, Jin ZH, Mei LH (2008) Influence of glucose feeding on pristinamycins fermentation process of *Streptomyces pristinaespiralis*. Chin J Antibiot 33(2):75–79
37. Zhao LG, Wang P, Ni H et al (2008) β-glucosidase production by Aspergillus niger with fed-batch fermentation. Ind Microb 38(6):13–16
38. Xie MY, Bie ZX (2007) Fermentation technologies. Chemical Industry Press, Beijing
39. Ming Y (1998) Optimization control of fermentation engineering. Jiangsu Science and Technology Press
40. Shi TH, Liu XL, Liu H et al (2005) Effect factors and control of microbial fermentation. Poult Sci 2:45–48
41. Tao YG, Tang B, Huang W, Xu XL (2003) The environmental conditions of producing *Bacilus thr.ingiensis* in the pressure pulse bioreactor. J Huazhong Agric Univ 22 (5):466–468
42. Tao YG, Xiang SG, Zhou DC (2003) Study on solid-state fermentation conditions of producing acid proteinase feed in pressure pulsation. Cereal Feed Ind 3:23–24
43. Chen HZ, Qiu WH (2007) The crucial problems and recent advance on producing fel alcohol by fermentation of straw. Process Chem 19(7):1116–1121
44. Xu FJ, Chen HZ, Li ZH (2002) Gas double dynamic solid state fermentation of cellase. Environ Sci 23(3):53–58
45. Xu FJ, Chen HZ, Shao MJ et al (2002) Scanning electron microscopic observation on solid-state Fermentation of Cellulase. J Chin Electron Microsc Soc 21(1):25–29
46. Li ZH, Chen HZ (2001) Key technology of ecological Industry for straw. Trans CSAE 17 (2):1–4
47. Xu FJ, Chen HZ, Li ZH (2002) Effect of periodically dynamic changes of air on cellulase production in solid-state fermentation. Enzyme Microb Tech 30(1):45–48
48. Xu XL (2003) Studies on the technology for industrial production of *beauveria*. J Zhejiang Univ Technol 31(5):520–523
49. Zhang X, Qiu WH, Chen HZ (2012) Enhancing the hydrolysis and acidification of steam-exploded cornstalks by intermittent pH adjustment with an enriched microbial community. Biores Technol 123:30–35
50. Lv XF, Y HL, Wang W (2001) The application of ultrasonic in fermentation engineering. Lett Biotechnol 12 (4):310–313
51. Lin Y (1997) Effect of magnetic field on the cells growth and inulinase biosynthesis of *Kluyveromyces fragili*. South China Univ Technol
52. Li GJ, He X, Gao DW (2000) Study of forced ripening fermented bean curd with high frequence electric field. China Brewing 19(6):13–14
53. Doremus MG, Linden JC, Moreira AR (1985) Agitation and pressure effects on acetone-butanol fermentation. Biotech Bioeng 27(6):852–860
54. Lamed R, Lobos J, Su T (1988) Effects of stirring and hydrogen on fermentation products of *Clostridium thermocellum*. Appl Environ Microb 54(5):1216–1221
55. Qureshi N, Singh V, Liu S et al (2014) Process integration for simultaneous saccharification, fermentation, and recovery (SSFR): production of butanol from corn stover using *Clostridium beijerinckii* P260. Bioresour Technol 154:222–228
56. Han PP, Yuan YJ (2009) Metabolic profiling as a tool for understanding defense response of Taxus cuspidata cells to shear stress. Biotechnol Progr 25(5):1244–1253
57. Xia ML, Wang L, Yang ZX et al (2015) Periodic-peristole agitation for process enhancement of butanol fermentation. Biotechnol Biofuels 8(1):1
58. Lee J, Yun H, Feist AM et al (2008) Genome-scale reconstruction and in silico analysis of the *Clostridium acetobutylicum* ATCC 824 metabolic network. Appl Microb and Biotechnol 80 (5):849–862

59. Janssen H, Grimmler C, Ehrenreich A et al (2012) A transcriptional study of acidogenic chemostat cells of *Clostridium acetobutylicum*—solvent stress caused by a transient n-butanol pulse. J Biotechnol 161(3):354–365
60. Castro J, Razmilic V, Gerdtzen Z (2013) Genome based metabolic flux analysis of *Ethanoligenens harbinense* for enhanced hydrogen production. Int J Hydrogen Energy 38 (3):1297–1306
61. Ezeji T, Milne C, Price ND et al (2010) Achievements and perspectives to overcome the poor solvent resistance in acetone and butanol-producing microorganisms. App Microbiol Biotechnol 85(6):1697–1712
62. Lee JY, Jang YS, Lee J et al (2009) Metabolic engineering of Clostridium acetobutylicum M5 for highly selective butanol production. Biotechnol J 4(10):1432–1440
63. Alsaker KV, Paredes C, Papoutsakis ET (2010) Metabolite stress and tolerance in the production of biofuels and chemicals: gene-expression-based systems analysis of butanol, butyrate, and acetate stresses in the anaerobe *Clostridium acetobutylicum*. Biotechnol Bioeng 105 (6):1131–1147
64. Lütke-Eversloh T, Bahl H (2011) Metabolic engineering of Clostridium acetobutylicum: recent advances to improve butanol production. Curr Opin Biotech 22(5):634–647
65. Cai G, Jin B, Saint C et al (2010) Metabolic flux analysis of hydrogen production network by *Clostridium butyricum* W5: effect of pH and glucose concentrations. Int J Hydrogen Energy 35(13):6681–6690
66. Amador-Noguez D, Feng XJ, Fan J et al (2010) Systems-level metabolic flux profiling elucidates a complete, bifurcated tricarboxylic acid cycle in *Clostridium acetobutylicum*. J Bacteriol 192(17):4452–4461
67. Korneli C, Bolten CJ, Godard T et al (2012) Debottlenecking recombinant protein production in Bacillus megatherium under large-scale conditions—targeted precursor feeding designed from metabolomics. Biotechnol Bioeng 109(6):1538–1550
68. Jones SW, Paredes CJ, Tracy B et al (2008) The transcriptional program underlying the physiology of clostridial sporulation. Genome Biol 9(7):1
69. Alsaker KV, Papoutsakis ET (2005) Transcriptional program of early sporulation and stationary-phase events in *Clostridium acetobutylicum*. J Bacteriol 187(20):7103–7118
70. Han PP, Yuan YJ (2009) Lipidomic analysis reveals activation of phospholipid signaling in mechanotransduction of *Taxus cuspidata* cells in response to shear stress. FASEB J 23 (2):623–630
71. Chapman AG, Fall L, Atkinson DE (1971) Adenylate energy charge in *Escherichia coli* during growth and starvation. J Bacteriol 108(3):1072–1086
72. Ball W, Atkinson DE (1975) Adenylate energy charge in *Saccharomyces cerevisiae* during starvation. J Bacteriol 121(3):975–982
73. Zhao S, Huang D, Qi H et al (2013) Comparative metabolic profiling-based improvement of rapamycin production by *Streptomyces hygroscopicus*. App Microbiol Biotechnol 97 (12):5329–5341
74. Bhagyalakshmi A, Berthiaume F, Reich K et al (1992) Fluid shear stress stimulates membrane phospholipid metabolism in cultured human endothelial cells. J Vasc Res 29(6):443–449
75. Zhao Y, Hindorff LA, Chuang A, Monroe-Augustus M et al (2003) Expression of a cloned cyclopropane fatty acid synthase gene reduces solvent formation in *Clostridium aceto-butylicum* ATCC 824. Appl Environ Microb 69(5):2831–2841
76. Chen HZ, Li ZH (2001) Microbial solid fermentation reactor. Chem Technol Mark 24(2):25–27
77. Zhao ZM, Wang L, Chen HZ (2015) Variable pressure pulsation frequency optimization in gas double-dynamic solid-state fermentation (GDSSF) based on heat balance model. Process Biochem 50(2):157–164
78. Chen HZ, Zhao ZM, Li HQ (2014) The effect of gas double-dynamic on mass distribution in solid-state fermentation. Enzyme Microb Technol 58–59(9):14–21

Chapter 6
Design and Scale-up of High-solid and Multi-phase Bioprocess

Abstract The rheological properties in high-solid and multi-phase system are different from that of ordinary fluids because of the high solid content. Thus, there is new requirement for solid-state reactor and large-scale solid materials conveyor devices. In this chapter, the rheological characteristics of high-solid enzymatic hydrolysis system were analyzed and the transfer and seepage laws in the porous solid medium were revealed. Agitation and intensification methods for the high-solid and multi-phase system were also studied. Based on the above, the high-solid and multi-phase reactor and corresponding large-scale conveyor devices were developed, and prospect for the engineering application and development direction of the high-solid and multi-phase bioprocess in the future were provided.

Keywords Rheological characteristics · Mass transfer and seepage
Solid-state reactor · Mixing and strengthening method · Large-scale conveyor devices

6.1 The Rheological Properties of High-solid and Multi-phase Bioprocess

6.1.1 The Rheological Properties of Solid-State Medium in Bioprocess

Rheology is a branch of mechanics, which refers to deformation and rheological properties of material under the effect of stress, strain, temperature, humidity, and other conditions. In high-solid enzymatic hydrolysis process, studying rheological properties will be beneficial to process optimization and reactor development. Rheological properties of high-solid enzymatic hydrolysis system are mainly depended on the material characteristics and solids content. When the solid–liquid ratio of the lignocellulose system is higher than 15%, mixture presents solid state, not slurry. Rheological models such as Bingham model, Herschel–Buckley model, Wildemuth–Williams model, and Casson model of solid enzyme hydrolysis have

H. Chen, *High-solid and Multi-phase Bioprocess Engineering*,
Green Chemistry and Sustainable Technology,
https://doi.org/10.1007/978-981-10-6352-7_6

been proposed by scholars [1, 2]. Roche et al. [3] studied the change of solid particles concentration and rheological yield stress in enzymatic hydrolysis process of corn straw pretreated by acid with 20% (w/w) solid–liquid ratio, it was found that when the total conversion rate of biomass was near to 40%, at a suitable enzyme loading, corn straw reached mobile point (τ_y < 10 Pa) after two days saccharification. Wildemuth–Williams semiempirical rheological model was used to describe the relationship of rheological yield stress (τ_y) and the volume fraction (ϕ) [1]

$$\tau_y(\phi) = [\ (\phi/\phi_{m0} - 1)/(1 - \phi/\phi_{m0})]^{1/\mathrm{m}}, \tag{6.1}$$

where ϕ_{m0} was the maximum volume fraction without shear stress; ϕ_m was the maximum packing fraction under limiting shear stress; "*A*" and "*m*" were related to microstructure changes of system under mechanical shearing. In solid enzymatic hydrolysis process, the yield stress decreased with decrease of volume fraction. Through the establishment of material balance and semiempirical model, solid enzymatic hydrolysis process was correlated with solid particles concentration and yield stress to provide guidance for the process design and optimization. Dasari et al. [4] studied influence of several partials diameter $33\ \mu m < x \leq 75\ \mu m$, $150\ \mu m < x \leq 180\ \mu m$, $295\ \mu m < x \leq 425\ \mu m$, *and* $590\ \mu m < x \leq 850\ \mu m$ on the analysis of enzymatic hydrolysis rate and rheological properties of saw dust. With smaller initial particle size, a higher initial hydrolysis rate and a higher final conversion ratio of cellulose were obtained. The results showed that enzymatic hydrolysis systems had small viscosity with small particle size, which contribute to shortening the reaction time, reduce power and energy consumption of agitator, and increase solid–liquid ratio and reduce reactor size in mass production. Zhang et al. [5] found that when the solid–liquid ratio increased from 15% to 30%, energy consumption of agitator increased rapidly increased from 79.5 MJ/t to 1009.2 MJ/t, and energy consumption increased by an order of magnitude, while half of energy used for agitator mixing in spite of solid enzymatic hydrolysis process increased product concentration. Viamajala et al. [6] studied the relationship among rheological properties change, the initial solid concentration, pretreatment level (xylan removal), and particle size in enzymatic hydrolysis system of corn straw with dilute acid pretreatment. The results showed that enzymatic hydrolysis of corn stover system exhibited shear thinning properties, which can be described by Casson model

$$\tau^{0.5} = \tau_{Cy}^{0.5} + K_C\gamma^{0.5}, \tag{6.2}$$

where $_{Cy}$ is apparent Casson yield stress, Pa;$\gamma$is the rate of shear; K_C is a Casson constant, Pa^2s^2. The results showed that the yield stress and apparent viscosity increase with solid–liquid ratio; under the same condition of solid–liquid ratio, dilute acid pretreatment lead to smaller yield stress and viscosity, while a smaller particle size could produce smaller viscosity and yield stress as well. These researches confirm that solids content (the opposite is water content) determines the

rheological properties of enzymatic hydrolysis systems. With the increase of solid–liquid ratio, the interaction between the particles results in increase of apparent viscosity and yield stress in system. In addition, the rheological properties are closely related to solid component composition and physical properties (such as porosity) [6]. Um and Hanley [2] studied the relationship among viscosity, shear stress, and shear rate with 10–20% solid–liquid ratio. In 10%, 15%, and 20% solid–liquid ratio enzymatic hydrolysis system, the viscosity was 0.0418-0.0144, 0.233-0.0348, and 0.292-0.0447 Pa•s, respectively. Enzymatic hydrolysis systems exhibited pseudoplastic behavior, and rheological analysis showed that the solid–liquid ratio is closely related to apparent viscosity [2]. The above researches showed that the increase of solid–liquid ratio significantly affects the rheological properties of the enzymatic hydrolysis system, which has brought new challenges to process design and optimization. Simultaneously, rheology analysis of high-solid enzymatic hydrolysis system will contribute to seek new effective strategies to change the rheological properties to improve the high-solid enzymatic hydrolysis efficiency.

6.1.2 Strengthening of High-solid and Multi-phase Bioprocess

During high-solid enzymatic hydrolysis of lignocellulose, the rheological properties of system are the key factors influenced enzymatic hydrolysis efficiency. In addition, researches about rheological properties of mixture system and lignocellulose mechanical characteristics are the foundation of reactor design and strengthening process [1, 3]. Rheological properties of mixture system can be influenced by physical and chemical properties of particles such as size and distribution, fibers flexibility, matrix skeleton elasticity, and material compositions [1]. Rheological properties of mixture can be influenced by the water state significantly. Some models have been already established to describe the rheological properties of high-solid enzymatic hydrolysis process. Um and Hanley [2] studied rheological properties in enzymatic hydrolysis process of the mixture under 15–20% solid–liquid ratio and found it conform to the pseudoplastic fluid model. Knutsen and Liberatore [7] and Szijarto et al. [8] found that the enzymatic hydrolysis yield stress was effectively reduced with the addition of surfactant, and the addition of surfactant and temperature raise could reduce viscosity to a certain extent. Increase of solid–liquid ratio could significantly influence the rheological properties of system, thus affecting the material concentration, product removal, and heat transfer. In addition, the rheological variation requires higher agitator power and energy consumption. Therefore, new strengthen strategies which can change rheological properties is still needed to improve the efficiency of solid enzymatic hydrolysis.

6.2 Transfer and Reaction Characteristics in High-solid and Multi-phase Bioprocess

6.2.1 Cognition of Transfer Behavior in High-solid and Multi-phase Bioprocess

The main factor influencing high-solid enzymatic hydrolysis efficiency is mass transfer limitations [5, 9]. Sufficient contact of substrate (cellulose and hemicellulose) and enzyme (cellulose enzyme, β-glycosidase, and xylanase), and active diffusion of product (e.g., glucose, xylose) is an important guarantee for high efficient enzymatic hydrolysis. Roche et al. and Zhao et al. [3, 10]. However, with the increase of solid content, free water content reduced in reaction system. When solid–liquid ratio is higher than 15%, water turns into combined water and capillary water bounded by lignocellulose, with nearly no free water existed, which is called "water binding effect" [11–13]. Water binding effect is closely related with lignocellulose materials species, pretreatment, chemical composition, and physical structure of solid materials (pore size distribution, bending, and porosity). Rapid decrease of free water could significantly affect the mass transfer efficiency of enzymatic hydrolysis process and rheological properties of system. On one hand, water is not only the diffusion media of enzymes or product, but also participated in the enzymatic hydrolysis process as a substrate, and decrease of free water could reduce product dissolution and transfer efficiency of enzymes in enzymatic hydrolysis; on the other hand, low free water content could reduce system viscosity and increase energy consumption of agitation [11, 12, 14]. Roberts et al. [13] and Felby et al. [14] found that high solid–liquid ratio increased the physical bondage between water and lignocellulose system, where water binding effect tends to increase with the addition of glucose and mannose. Addition of monosaccharide increase water binding capacity showed the same trend, and cellobiose was not found in bioprocess, which indicated that monosaccharide reduced the saccharification efficiency by increase water bound, before the inhibition of enzyme activity. In addition,there was a positive correlation between water binding effect and the diffusion of monosaccharide and enzymes. However, the increased viscosity caused by the interaction of water and cellulose as well as water and soluble substances leads to increase of diffusion resistance and the decrease of enzymatic hydrolysis efficiency. With the solids content increased from 5% to 20%, effective diffusion coefficient of BSA showed a decrease of nearly two-thirds, and intrinsic diffusion coefficient dropped by nearly half [13, 14]. Selig et al. [15] researched the relationship between high molecular weight polymers in lignocellulose (hemicellulose, pectin, and lignin) and water binding effect as well as inhibition of enzymatic hydrolysis. It was found that T_2 (from relaxation time curve of low-field nuclear magnetic resonance measurement) of system was soon dropped to zero with the addition of polymer, and the efficiency of cellulose enzymatic hydrolysis also decreased; and the trend of water bondage was consistent with that of enzymatic hydrolysis conversion rate, which proved the high-solid enzymatic hydrolysis

efficiency can be reduced by bound water. Selig et al. [16] investigated the influence of water accessibility and soluble substances on lignocellulosic enzymatic hydrolysis at high solid content, which indicated that soluble substances produced in this process could influence water accessibility, thus had determinative effect on enzymatic hydrolysis. In addition, Hodge et al. [17] studied enzymatic hydrolysis of corn stalk with dilute acid pretreatment, mass transfer became the main limited factors of enzymatic hydrolysis conversion rate when solids content higher than 20%, mainly due to the low efficiency of mass transfer before the liquefaction of solid-state system. Additionally, low water content limited sugar spread from enzyme active sites, which has limited saccharification and make enzyme unreachable to new catalytic sites. Lignocellulose species, pretreatment, physical structure, and chemical composition of solid materials affect water states and distribution, thus affect the mass transfer efficiency [18–20]. Above analysis indicated that enzymatic hydrolysis efficiency is significantly affected by mass transfer in high-solid enzymatic hydrolysis process, so new strategy to remove mass transfer limitations are needed to realize high efficient conversion in high-solid enzymatic hydrolysis of lignocellulose.

6.2.2 *Seepage Law in Solid-State Medium*

6.2.2.1 Darcy's Law

(1) Darcy's law

Experimental conditions: constant head, constant flow, and homogeneous sand. The groundwater in one-dimensional uniform motion, the value and direction of seepage velocity, and hydraulic gradient was the same along the flow. Expression of Darcy's law (in 1856):

$$Q = KAJ = KA\frac{H_1 - H_2}{L} \tag{6.3}$$

$$V = \frac{Q}{A} = KJ \tag{6.4}$$

In this equation, Q—seepage discharge (exit flow), that is, the flow through water cross section A (sand column section) (m^3/d), K—the seepage coefficient of porous media (m/d); A—cross sectional area of the flow (m^2), H_1, H_2—the water head of upstream and downstream in water section (m); L—seep age path way (m), J—hydraulic gradient ($J = (H^1–H^2)/L$), the hydraulic head pressure difference between two sections to divide L, which is head loss per unit length in seepage pathway.

The differential form of Darcy's law:

$$v = KJ = -K\frac{dH}{dn} \tag{6.5}$$

$$v_x = -K\frac{dH}{dX}, v_{y=} - K\frac{dH}{dy}, v_{z=} - K\frac{dH}{dz} \tag{6.6}$$

$$J = -\frac{dH}{dn} = -grad\mathrm{H} \tag{6.7}$$

The vector form of Darcy's law:

$$\vec{v} = v_x\vec{i} + v_y\vec{j} + v_z\vec{k} \tag{6.8}$$

(2) Discussion about Darcy's law

Darcy's law reflects the energy conversion and conservation.

V makes direct proportion to first power of *I*; and when *K* is determined, head pressure difference increases with the increase of V, which indicates that more mechanical energy losses is converted into heat energy much more in unit seepage pathway, that is *V* is directly proportional to mechanical energy loss; When *V* is determined, the greater the hydraulic head pressure difference, the *K* becomes smaller, that to say, *K* is inversely proportional to mechanical energy loss.

(3) Scope of application of Darcy's law [21, 22]

Re < 1–10, laminar flow, applicable, low-speed movement of groundwater, viscous force is in dominant;

Re > 10–100, laminar flow, not applicable, groundwater flow rate increases, the transition zone, laminar flow with the dominant of viscous force turns into that with the dominance of inertial force;

Re > 100, turbulent flow, and it is improper.

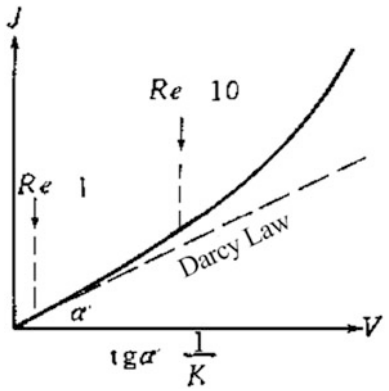

Fig. 6.1 Relationship between seepage coefficient and hydraulic gradient

The lower bound of Darcy's law: there is an initial hydraulic slope J_0 when groundwater moves in the cohesive soil. When hydraulic slope $J < J_0$, there is almost no movement (Fig. 6.1).

6.2.2.2 Seepage and Water Conductivity

(1) Seepage coefficient (K)

$V = KI$. *When* $I = 1$, $V = K$, value of K is equal to that of seepage velocity, with the unit of speed, which is also called hydraulic conductivity coefficient, reflecting the coefficient of water-bearing media to seepage resistance. Common unit: m/d or cm/s.

Seepage coefficient is the index reflecting rock seepage performance, which can classify rock seepage according to the value of the seepage coefficient (Table 6.1).

Influence factors of K: ① the properties of rock such as grain size, composition, particle arrangement, filling condition, structural fissure, and development degree, ② the physical properties of fluid: Volume, weight, and viscosity [23, 24].

(2) Intrinsic permeability

Darcy's law can be expressed as

$$v = \frac{k\rho g}{\mu}\frac{dH^*}{ds} \tag{6.9}$$

In this expression,ρ—liquid density; g—acceleration of gravity; μ—dynamic viscosity of fluid; k—constants describing the permeability of porous media, which does not change with the physical and mechanical properties of infiltration liquid, only depends on the properties of rock, not related to properties of the liquid. Its unit is cm^2 or D, and $1\ D = 9.8697 \times 10^{-9}\ cm^2$.

Piezometric head:

$$H^* = z + \frac{P}{\gamma} \tag{6.10}$$

Table 6.1 Partition of rock seepage

Permeability coefficient K (cm/s)	10^{-2}	10^{-3}	10^{-6}	10^{-7}
K (m/d)	8.64	0.864	0.000864	0.0000864
Water permeability	Permeable	Weak permeable	Water insulation	
Aquiclude	Good	Poor	No water	

Pipe flow formula:

$$u = \frac{\rho g b^2}{32\mu} J \tag{6.11}$$

Slit flow formula:

$$u = \frac{\rho g b^2}{12\mu} J \tag{6.12}$$

Porous media:

$$v = \frac{nd^2}{32} \frac{\rho g}{\mu} J \tag{6.13}$$

Fissure media:

$$v = \frac{nd^2}{12} \frac{\rho g}{\mu} J \tag{6.14}$$

Then,

$$K = \frac{nd^2}{32} \frac{\rho g}{\mu} = k \frac{\rho g}{\mu} \tag{6.15}$$

or

$$K = \frac{nd^2}{12} \frac{\rho g}{\mu} = k \frac{\rho g}{\mu} \tag{6.16}$$

$$K = \frac{\rho g}{\mu} k = \frac{g}{\mu} k\prime \tag{6.17}$$

The definition of Darcy (D): the permeability of rock sample at flow rate of 1 cm^3/s through a sample with 1 cm^2 area, 1 cm length when the dynamic viscosity of the liquid is 0.001 Pa·s and the pressure difference is 101325 Pa.

Scale effect refers to that permeability coefficient related to the test range, and increases with the increase of test range, expressing as $K = K(x)$, the long pumping time and large drawdown "s" of group drilling pumping test, the "K" is larger.

(3) Water transmissivity [25]

$$Q = KMBJ \tag{6.18}$$

$$Q = Q/B = KMJ = TJ \tag{6.19}$$

In this equation, $T = KM$, called water transmissivity, the hydrogeological parameters of water reflecting water yield capacity of aquifer, whose physical significance is, unit discharge through the aquifer when hydraulic gradient is 1. It is defined as hydrogeological parameters in one-dimensional or two-dimensional flow, unit: m^2/d (Fig. 6.2).

6.2.2.3 Seepage Continuity Equation

The value and direction of seepage velocity at each point of seepage field are different. Continuity equation in differential equation form in three-dimensional space needs to be established to reflect the relationship of mass conservation of liquid movement.

Select one arbitrary point *P (x, y, z)* in seepage field arbitrarily, and then select one tiny hexahedron along rectangular axes with *P* as center, whose volume is $\Delta x\Delta y\Delta z$, called haplont [25]. Hypothesize, the haplont infinitely small to pass through skeleton and gap of media (Fig. 6.3).

Setting v_x, v_y, v_z as the seepage velocity of the point *X, Y, Z* direction, respectively. The midpoint of plane (*a, b, c, d*) is

$$P_1 = (x - \frac{\Delta x}{2}, y, z) \tag{6.20}$$

which flow into along the *X* axis

$$M_{xi} = \rho V_{x_1} = \rho V_x \left[x - \frac{\Delta x}{2}, y, z\right] \Delta y \Delta z \Delta t \tag{6.21}$$

and flow out

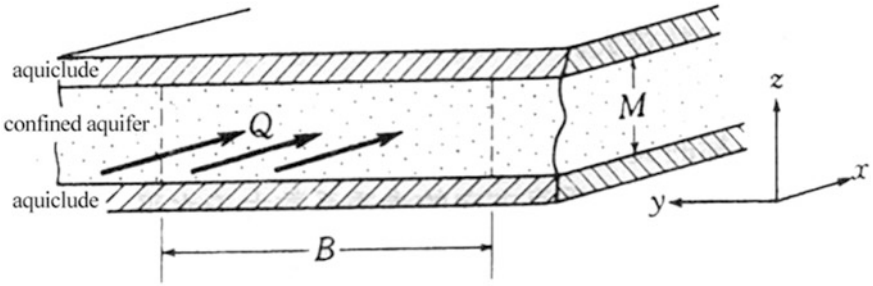

Fig. 6.2 The conception of coefficient of transmissibility

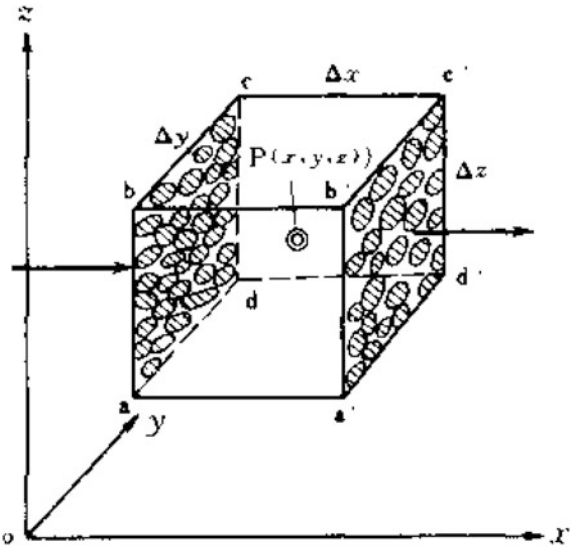

Fig. 6.3 Haplont of seepage area

$$M_{xo} = \rho V_{x2} = \rho V_x \left[x + \frac{\Delta x}{2}, y, z \right] \Delta y \Delta z \Delta t \tag{6.22}$$

With Taylor series expansion, leave out higher order term more than the second derivative, then

$$\begin{aligned} \Delta M_x = M_{xi} - M_{x0} &= \left[\rho v_x - \frac{1}{2} \frac{\partial(\rho v_x)}{\partial x} \Delta x \right] \Delta y \Delta z \Delta t - \left[\rho v_x + \frac{1}{2} \frac{\partial(\rho v_x)}{\partial x} \Delta x \right] \Delta y \Delta z \Delta t \\ &= -\frac{\partial(\rho v_x)}{\partial x} \Delta x \Delta y \Delta z \Delta t \end{aligned} \tag{6.23}$$

and

$$\Delta M_y = -\frac{\partial(v_x \rho)}{\partial x} \Delta x \Delta y \Delta z \Delta t \tag{6.24}$$

$$\Delta Mz = -\frac{\partial(v_z \rho)}{\partial z} \Delta x \Delta y \Delta z \Delta t \tag{6.25}$$

The water quality variation of haplont in Δt time is

$$\Delta M = \frac{\partial(\rho \eta \Delta x \Delta y \Delta z)}{\partial t} \Delta t, \tag{6.26}$$

where ρ is the liquid density. Seepage flow continuity equation could be obtained through the law of mass conservation:

$$\Delta M_x + \Delta M_y + \Delta M_z = \Delta M - \left[\frac{\partial(\rho v_x)}{\partial x} + \frac{\partial\left(\rho v_y\right)}{\partial y} + \frac{\partial(\rho v_z)}{\partial z} + \right]\Delta x\Delta y\Delta z = \frac{\partial(\rho\eta\Delta x\Delta y\Delta z)}{\partial t}\Delta t \tag{6.27}$$

or

$$-div(\rho v)\Delta x\Delta y\Delta z = \frac{\partial(\rho\eta\Delta x\Delta y\Delta z)}{\partial t} \tag{6.28}$$

Above equation is the continuity equation of unsteady flow, which showed that the volume difference of water quality of inflows and outflows of any volume aquifer in the seepage field is identical to the variation volume of water quality. It expresses the law of mass conservation which any "section" in the seepage zone must meet. If the aquifer is regarded as rigid body (ρ and n are constant), which means water and media without elastic deformation or seepage is steady flow, then the seepage equation of continuity can be expressed as

$$div(v) = \frac{\partial v_x}{\partial x} + \frac{\partial v_y}{\partial y} + \frac{\partial v_z}{\partial z} = 0 \tag{6.29}$$

It indicates that the water volume into and out the haplont is equal at the same time the volume conservation. Continuity equation is the basic equations of groundwater movement, and various differential equation studies on groundwater movement are based on the continuity equation and law of mass conservation [26].

6.2.2.4 Application of Seepage Principle in the High-solid Biomass Refining

Mass transfer in low- and high-solid biomass systems

Fluid deferring to Newton's law of viscosity is called Newtonian fluid. On the contrary, others are known as non-Newtonian fluid. All gas and most low molecular weight liquid belong to Newtonian fluid.

Newton's law of viscosity:

$$\tau = -\mu\frac{du_x}{dy} \tag{6.30}$$

In this equation, τ is shear force or internal friction, μ is dynamic viscosity of fluid, hereinafter is viscosity, $\frac{du_x}{dy}$ is velocity gradient. Fluid which is not in conformity with the Newton's law of viscosity are called non-Newtonian fluid. And

polymer solution or melt body, fat, and starch solution belong to pseudoplastic fluid, which is satisfied with the relation:

$$\tau = K\left|\frac{du_x}{dy}\right|^{n-1}\frac{du_x}{dy}, \tag{6.31}$$

wherein apparent viscosity of pseudoplastic fluid increases with the increase of shear rate. Some wet sands, aqueous solution containing potassium silicate, arabic gum all belong to pseudoplastic fluid. There is a yield shear stress when some liquids such as grease, toothpaste, paper pulp, and sludge flow. When shear stress is lower than it, the liquid will not move anymore; when the shear stress is higher than it, the liquid starts to flow, which is called Bingham plastic fluid.

Mass transfer in low solid system In low solid biomass conversion system, the influence of solid on the properties of the liquid often ignored due to low solid content. In the chemical process, the fluid is in motion state, when mass transfer occurs between the move fluid and walls or two miscibility fluids, which is called convective mass transfer. Therefore, convective mass transfer is mass transfer method in low solid biomass conversion system, which could meet the requirement of mass transfer by agitation reinforcement in the reaction. When the fluid is moving, there are two different patterns of flow, laminar flow and turbulent flow. Reynolds number can be used for judgment of fluid flow form, and the dimension of the Reynolds number (Re) is 1:

$$\mathrm{Re} = \left[\frac{d\rho u}{\mu}\right] \tag{6.32}$$

In this equation, Reynolds number is the ratio of the fluid inertia and viscosity. Results indicate that when the fluid is flowing in pipe, the flow is laminar flow when Re is less than 2000; the flow is turbulence flow when Re more than 4000; and the flow is in transition stage when Re between 2000–4000 [27, 28].

Mass transfer in high-solid system With the content of solid biomass increase, system characteristics change, fluid was bound both in and out the biomass, which does not meet the Newton's viscosity law in biomass conversion. The most important thing is that because the biomass is porous media with skeleton structure and porous characteristics, due to the irregular shape and intertwine of biomass particles, there are many pores in system. Necessary condition for porous media: small aperture, large specific surface area, and pore connectivity, which are all reflected in high -solid biomass conversion system. Therefore, percolation theory can be used for research, description, and explanation of fluid flow behavior and mass transfer characteristics of high-solid biomass refining process [29, 30].

The seepage principle of high-solid biomass refining

Construction of mathematic model Because of the complexity, the high solid reaction system needs to be studied by mathematical model. The partial differential equation represents the movement law of whole categories water, and for the

aquifer with different boundary properties, different boundary shape, water distribution is different. And for the partial differential equation, the equation does not contain all information to reflect the specific conditions of seepage area, there may be many solutions. If the only special solution corresponding to the specific regional conditions need to be obtained from a large number of possible solutions, the information reflecting the characteristics of the specific area must be provided. The information mainly includes the following:

(1) Only when the parameters T, μ^*, W aredetermined, the differential equation can be determined.
(2) Seepage zone and shape: Only when the differential equation of the area is identified, the equation can be solved.
(3) Boundary conditions: It represents the conditions of seepage zone boundary, to express the boundary conditions which head H (or seepage flow q) in the seepage area should satisfy. It is the restriction relationship between water seepage zone and surrounding environment.
(4) Initial conditions: It expresses the initial state of the seepage area, which is the distribution of seepage zone head H at a selected initial moment ($t = 0$).

Boundary conditions and initial conditions known as definite condition, and the differential equation and the definite condition together form the mathematical model of seepage field. Mathematical model is used to describe a mathematical equation of water flow movement in the study area and its definite solution conditions constitute a representation of the mathematical structure of a practical problem, which based on physical model, with a concise mathematical language, namely a set of mathematical relationship to depict its quantitative relation and spatial form, to reflect the research hotspot, reaction conditions and the basic characteristics of the water movement and copy or reproduce a practical water system basic state. Among the differential equation of water flow law, definite condition shows the specific environmental conditions the object—the true state of the water. In fact it is mathematical physical problems that given equation and corresponding definite condition. Models refer to the establishing mathematical model.

Definite condition Definite condition refers to the change law of seepage flow elements such as water head and flow rate on the flow field boundary, which is caused by the external conditions of flow field. However, it constantly influences the seepage process of the internal flow field, and it plays a role during the whole process. Definite condition includes boundary conditions and initial conditions.

Boundary conditions are boundary conditions of seepage area, to express the water head H (or seepage flow q) in seepage area which should satisfy the boundary conditions, that is, the water seepage zone and its surrounding environment restriction relationship to each other.

(1) The first kind boundary condition (Dirichlet conditions): If the border (set as S_l or Γ_1) and the head of each point in every moment is known, this boundary can

be called as the first kind of boundary or the boundary of the given head, which could be expressed as the following:

$$H(x,y,z,t)|_{S_1} = \varphi(x,y,z,t), \quad (x,y,z) \in S_1 \tag{6.33}$$

Or

$$H(x,y,z,t)|_{\Gamma_1} = \varphi(x,y,t), \quad (x,y,) \in \Gamma_1 \tag{6.34}$$

While the given head boundary is not always the boundary of fixed water level.

(2) The second class boundary conditions (Neumam conditions): When (out is negative) inflow q of per unit area of boundary (set to S_2 or Γ_2) (two-dimensional space as the unit width) is given, it is known as the second boundary or boundary of the given flow. The corresponding boundary condition is expressed as

$$K\frac{\partial H}{\partial n}|_{S2} = q_1(x,y,z,t), \quad (x,y,z,t) \in S_2 \tag{6.35}$$

Or

$$T\frac{\partial H}{\partial n}|_{\Gamma 2} = q_2(x,y,t), \quad (x,y,) \in \Gamma_2 \tag{6.36}$$

In this equation, n is outside normal direction of boundary S_2 or Γ_2. The *q1* and *q2* are known function, show the lateral recharge of per unit area of S_2 and the width of Γ_2, respectively.

(3) The third boundary condition: A linear combination of the boundary on the H and $\frac{\partial H}{\partial n}$ are known.

That is,

$$\frac{\partial H}{\partial n} + \alpha H = \beta \tag{6.37}$$

which is also called mixed boundary conditions.

The weak permeable layer is that boundary (seepage coefficient K_1, thickness or width m_1).

$$\sigma' = \frac{m_1}{K_1}, \quad K\frac{\partial H}{\partial n}| = \frac{K_1}{m_1}(H_m - H) = q(x,y,z,t) \tag{6.38}$$

On s_3,

$$K\frac{\partial H}{\partial n}|_{S_3} - \frac{H_n - H}{\sigma'} = 0 \tag{6.39}$$

On Γ_3,

$$T\frac{\partial H}{\partial n}|_{\Gamma_3} - M\frac{H_n - H}{\sigma'} = 0 \tag{6.40}$$

The boundary conditions of infiltration curve:

$$K\frac{\partial H}{\partial n}|_{c_2} = q \tag{6.41}$$

When infiltration curve descending, per unit area flow from infiltration curve boundary flow into seepage is q,

$$q = \mu\frac{\partial H^*}{\partial t}\cos\theta \tag{6.42}$$

In this equation, μ is specific yield, and θ is the angle between infiltrations curve outward normal and the vertical line.

Initial conditions: the distribution of seepage zone head H at a certain initial moment ($t = 0$).

$$H(x, y, t)|_{t=0} = H_0(x, y, z), \quad (x, y, z) \in D \tag{6.43}$$

Or

$$H(x, y, t)|_{t=0} = H(x, y), \quad (x, y, z) \in D \tag{6.44}$$

In this equation, H_0 is the known function of D.

Classification of seepage mathematical model (1) Linear and nonlinear model: Linear model is composed of linear equation such as homogeneous isotropic confined two-dimensional flow equation. Nonlinear model is composed of nonlinear equation such as the diving model Eq. (6.2) Static and dynamic model: It based on the relationship between the unknown variables and time in the model. If the unknown variables are not related to time, such as steady flow model, that is called static model, otherwise is dynamic model. (3) Lumped, distributed parameter model: Lumped parameter model has no space coordinates variable, such as the experience formula between the pumping well flow and drawdown and the distributed parameter model contains space coordinate variables. (4) Deterministic and stochastic model: Deterministic model is models where variables have clear and strict mathematical relationships. Stochastic model contains one or more random variables in mathematical relationship.

Main points of the construction of mathematical models (a) The determination of range of the study area and the boundary of the seepage; (b) The determination of hydraulic characteristics of the seepage (containing burial conditions, the seepage state, and media characteristics); (c) The determination of boundary conditions of the seepage area; (d) The determination of source-sink term of the seepage area; (e) Selection of differential equation; and (f) The determination of the initial conditions of the seepage.

The solution of seepage flow mathematical model (a) Analytical method. It is a method that could solve the mathematical model directly by parameter analysis and integral transform method. Its solution is exact solution, easy to use, but has certain limitations, which is only applicable to aquifer, simple equations, single boundary conditions cases. Analytical solution is also known as exact solution, which uses analytic method to solve mathematical problems of analytic expression. (b) Numerical method. It is a method that uses numerical method (discretization method) to solve the mathematical model, of which solution is approximate solution. It is the main method to solve the large groundwater flow problem. The whole seepage area can be divided into a number of small units with regular shape. Each small unit approximately is treated as a homogeneous unit, and then established the relation about groundwater flow of each small unit, which could transfer the irregular shape and inhomogeneous problems to regular shape and homogeneous problems. The number of unit division is determined according to research, and then unsteady flow is divided by time frame. Finally, integrate parts together and add the definite condition. Numerical solution is approximate solution obtained by numerical method. (c) Simulation. Due to the similarity of physical phenomena and flow, simulation method can be used in the laboratory.

6.2.3 Characteristics of Capillary Flow in Solid-State Media

Lignocellulosic biomass is porous media with different pores in micron scale. In high-solid reactions process, the study of fluid flow in micron-scale porous media is the basis of efficient process strengthening. Currently, the distribution and saturation of multiphase fluid in porous media, the relation of capillary pressure and fluid saturations in porous media, the fluid infiltration in porous media are the focus and hot spots of engineering fluid flow study [22, 31, 32].

6.2.3.1 Model of Multi-phase Flow in Porous Media

The flow of multi-phase fluid in porous media is a complex physical process. Various flow patterns exist simultaneously or not, but there is no perfect theory on fluid flow in porous media because of lack of physics principle and mathematical description [32, 33]. Different models were established to study the fluid flow in porous media by researchers, which are given as follows:

Network model Network model is widely used for study of displacement process of different fluid in simple or ideal fluid porous media. The conceptions of seepage are introduced from single-phase fluid flow, where study is on two type seepage behavior dominated by capillary seepage. Another extreme behavior of two-phase flow is dominated by viscous force, refers to viscous phenomena happens in the pore-scale when high viscosity fluid displaces low viscosity fluid. Considering the effect of fluid viscosity and capillary pressure on the flow behavior, a dynamic network model was developed.

Bundle model vascular bundle model can accurately calculate the location of phase interface and velocity of the fluid as time goes on which is driven by water. There are two typical vascular models, one is a parallel bundle model, vascular diameter of this model is uniform, but cannot guarantee that all bundle diameter is exact the same, and the other is a continuous bundle model, the tube diameter randomly or periodically changed in driven direction. In above models, tube bundles are independent. The flow direction of fluid in tube bundles is same. In order to better represent the true morphology of the fluid, capillary bundles model with multiple interacting developed.

6.2.3.2 Movement Laws of Gas–Liquid Mixture Phase Fluids of Capillary Tube

The imbibition process occurs when appropriate wettability of liquid phase on capillary inner wall, where the process of the liquid drive gas which based on Newton's second law. In this process, the acceleration of the liquid is directly proportional to resultant force, inversely proportional to mass, direction of acceleration and force is the same, then:

$$ma = F + F_c + f \tag{6.45}$$

In the formula, "m" is the quality of liquid, "a" is the fluid acceleration, "Fc" is the resultant force that capillary pressure effects on the fluid, "f" is the friction force caused by the viscosity of liquid and tube wall, and "F" is the acting force besides capillary force and friction.

At certain moment, the fluid enters the capillary from one side to the other side, where the length could be to x.

$$\rho va = \Delta p \pi r^2 + p_{c(l-g)} \pi r^2 = 2\pi r \tau (x + dx) \tag{6.46}$$

In the formula, "ρ" is density of liquid; "v" is volume of fluid; "r" is capillary radius; "$P_{c(l-g)}$" is the capillary pressure caused by the interface of liquid and gas; Δp is external pressure on both ends of the capillary; τ is viscous shearing stress from the wall to fluid.

And the above formula ignored the friction. Then:

$$\rho\pi r^2 x\frac{dx^2}{dt^2} = \pi r^2\left(\Delta p + p_{c(1-g)}\right) - 2\pi r\frac{4\eta}{r}(x + dx) \tag{6.47}$$

Average velocity of the fluid (u_m) can be expressed as differential expression:

$$u_m = \frac{dx}{dt} \tag{6.48}$$

And then,

$$\rho r^2 x\frac{dx^2}{dt^2} = r^2\left(\Delta p + p_{c(1-g)}\right) - 8\eta\frac{dx}{dt}(x + dx) \tag{6.49}$$

Through integration what can be gained is

$$X^2 = \frac{r^2(\Delta p + p_{c(l-g)})}{4\eta}t \tag{6.50}$$

Due to

$$u_m = \frac{dx}{dt} \tag{6.48}$$

Then,

$$u_m = \frac{r^2(\Delta p + p_{c(l-g)})}{4\eta x} \tag{6.51}$$

The formula is mathematical expressions for the motion law of gas and liquid two-phase fluid.

6.2.3.3 The Movement Laws of Liquid–Liquid Mixture Phase Fluids of Capillary Tube

Seepage of liquid–liquid in the capillary filtration has got widely attention, for example, based on the Newton's second law, the displacement of oil–water two-phase is analyzed, the acceleration the liquid is directly proportional to resultant force, inversely proportional to mass, direction of acceleration and force is the same, then according to Eq. (6.45).

$$ma = F + F_c + f \tag{6.45}$$

At some point, fluid enters into one side of the capillary from another side to reach the length of x, then:

$$(\rho_w v_w + \rho_o v_o)a = \Delta \mathrm{p}\pi r^2 + \mathrm{p}_{\mathrm{c(w-o)}}\pi r^2 + 2\pi r[\tau_w(x+dx) + \tau_o(L-x-dx)] \tag{6.52}$$

In the formula, "ρ" is density of liquid; "V" is volume of fluid; "w" and "o" represent water and oil, respectively; "r" is capillary radius; "$p_{c(w-o)}$" is the capillary pressure caused by the interface of liquid and gas; "Δp" is external pressure on the both ends of the capillary; "τ" is viscous shearing stress from the wall to fluid.

From Eq. 6.48, which can be gained is as following:

$$\begin{aligned} &\mathrm{r}^2(\rho_w \mathrm{x} + \rho_o(L-x))\frac{\mathrm{dx}^2}{\mathrm{dt}^2} + 8[\eta_w(x+dx) + \eta_o(L-x-dx)]\frac{dx}{dt} \\ &= r^2\left(\Delta \mathrm{p} + \mathrm{p}_{\mathrm{c(w-0)}}\right) \end{aligned} \tag{6.52}$$

Then,

$$u_m = \frac{r^2(\Delta p + p_{c(w-o)})}{8(\eta_w x + \eta_o(L-x))} \tag{6.53}$$

6.2.3.4 Law of Interaction Force Between Capillaries

In high solid substrate reaction, liquid between particles can be regarded as the force between capillaries, called suction stress, which refers to combined effects of negative pore water pressure and surface tension on the skeleton of unsaturated granular particles. Suction stress is performed as tensioning action at macro level, but the particles close together within the scope, similar to the particle has the overload stress or additional pressure.

By considering the combination of unsaturated particles in the ideal condition, the micro forces between particles method to estimate the suction stress. When saturation degree of pore water is low, pore water in gas–liquid–solid inter face meniscus has effect forces with particles. The figure of meniscus can be decreased by particle radius r_1 and r_2, particle radius R, and fill angle θ. Related system forces on free body are air pressure, pore water pressure, surface tension, and external forces or overload force.

The total force caused by the air pressure is equal to the product of the air pressure and gas–solid interface area.

$$F_a = u_a(\pi R^2 - \pi r^2) \tag{6.54}$$

The resultant force generated by surface tension effect on the perimeter of the meniscus is expressed as follows:

$$F_t = -T_s 2\pi r^2 \tag{6.55}$$

The projection in the vertical direction of the total force caused by the pore water pressure is given as follows:

$$F_w = -u_w 2\pi r^2 \tag{6.56}$$

The resultant force of capillary is the sum of the above three forces. Assume that the air pressure is the only external force, then according to the mechanical equilibrium, the following expression of interatomic forces of particles caused by interface interactions:

$$F_e = u_a \pi R^2 - (u_a - u_w)\pi r^2 - T_s 2\pi r^2 \tag{6.57}$$

6.2.3.5 Application of Molecular Dynamics Simulation in Capillary Seepage

Computer simulation is the mathematical–physical model describing the motion law by computer programming visualization process. If the mathematical–physical model was verified that it can describe the movement law conformed to the actual situation, then model can be used to calculated the motion state and predict the unknown state which are difficult to get by detection means.

Based on the Born–Oppenheimer, molecular mechanics method proposed that energy could be regarded as the space coordinates of each atom composed of molecules approximately, where molecular conformation determines value of molecular energy and the movement of the nucleus and electronics can be considered distinctively. Molecular mechanics, the functional of describing the relationship between molecular energy and the molecular space structure is called molecular potential energy, ignored coordinates and movement of electron, considered as the interaction among the nucleus.

The precision of molecular mechanic calculation is high under the appropriate condition. Classical molecular dynamics is a calculation method based on molecular mechanics, describe the interaction between the atoms by molecular potential energy, get position and velocity of each constituent atom in system by integrating Newton's equations of motion, and then determine the system state. Molecular dynamics method can describe the dynamics of the system and get the evolvement law of position and velocity with time. Molecular dynamics simulation can be used to simulate the displacement process of liquid and liquid, gas and liquid, so as to indicate the direction for complex system to obtain function law which is consistent with actual process.

6.3 Material and Energy Balance in High-solid and Multi-phase Bioprocess and Integration

Conservation of mass and energy is the universal law of nature. The equations only can be formed based on accurate knowledge of the bioprocess. In particular, it is significant in studying the quantitative relationship between substrate and product, as well as the energy consumption in microbial metabolism. Therefore, it is a favorable strategy in process study.

Conservation of mass and energy is the universal law of nature. The equations can be formed based on accurate knowledge of the bioprocess. It is significant in studying the quantitative relationship between substrates and products, as well as the energy consumption in microbial growth and metabolism. Therefore, it is a favorable strategy in process study.

There are obvious differences in bioprocess and chemical reaction process. In bioprocess, cells are the catalyst, which requires more nutrients to ensure a normal growth and metabolism. The metabolic process is usually complicated and can be affected by environmental factors. Nutrients (carbon source, nitrogen source, oxygen, and inorganic salts) are converted to new cells, metabolites, and dioxide. Carbon source is vital substrate in bioprocess. The flux of carbon source includes maintaining cell living and producing metabolites. Cell yield is the proportion of cell weight to substrate consumption, which is an important indicator for bioprocess. Energy consumption is based on the oxidation enthalpy of organics and effective electron transfer. The released energy of carbon source and nitrogen source is used by microbes through ATP. Electron transfer always exists in oxidation of organics, which is called effective electron transfer.

6.4 Economic Analysis and Evaluation of High-solid and Multi-phase Bioprocess

In high-solid and multi-phase bioprocess, total cost includes two parts which are production cost and waste treatment cost. Production cost including equipment, energy, water, establishment of the industry, and other indirect cost. High-solid loading in the system contribute to high products concentration, resulting in decrease of cost in separation process. Effective pretreatment technology reduces energy cost in raw material treatment. Less waste discharge in high-solid and multi-phase system reduces waste treatment cost. The details for economic analysis will be shown in Chap. 8 with industrial demonstration.

6.5 Mixing Apparatus in High-solid and Multi-phase Bioprocess

Aiming at problems existing in high-solid and multi-phase bioprocess, specifically the agitated mixing problems. Based on the particularity of lignocellulose refining system, first, the conception, purpose, and application of mix in chemical engineering are discussed. Second, principle and power of agitation equipment often used in different fields, chemical strengthens process in the new field and systems are introduced, the scale-up of agitation is also discussed. Finally, based on the particularity of mixture, summarizes the development of new agitation method, the application, and prospect in lignocellulose refining.

6.5.1 Introduction of Mixture

6.5.1.1 Conception of Mixture

The unit operation which makes two or more different materials dispersed in each other to achieve uniform distribution called stir, agitation or mixture. Agitation mixing is one of the most common operational processes in chemical engineering, petrochemical engineering, pharmaceutical, food industry that aims to make two or more media that could achieve the maximum contact, so as to complete the mixing, mass transfer, heat transfer, and reaction or more than two processes at a certain time. Liquid, gas or solid may be involved in the agitation, but liquid is dominated [27, 34, 35].

6.5.1.2 Purpose of Mixture

Agitation could make the material flow in a flow pattern within the mixing tank to make material mix or disperse evenly by agitator. Agitation generally has the following functions: (1) Getting the mixed uniformly material; (2) Making immiscible material dispersed or suspended commendably, including gas phase uniformly dispersed in liquid phase, solid particle uniformly suspended in liquid phase, liquid phase uniformly suspended or full emulsified in another liquid phase; (3) Strengthening heat or mass transfer. Focusing on the above function, agitation is widely used in industrial production, especially in chemical production.

6.5.1.3 Classification of Mixture

According to the species of the materials, agitated mixing of fluid media can be divided as agitated mixing of liquid–liquid, liquid–solid, gas–liquid, and gas–gas

agitated mixing. For solid media, which contains agitated mixing of solid powder, solid grain, and kneading of paste material.

6.5.1.4 Application of Mixture in Industry

As an independent unit, agitated mixing operation could achieve uniform mixing, dispersion, suspension, emulsion of the materials. In the large crude oil storage tank of the petroleum oil industry, due to different components in the crude oil, density of various components are different, the distribution of components in the crude oil tank is inhomogeneous, so agitated mixing operation must be done consistently in order to make the crude oil evenly from top to bottom. In order to improve the quality of gasoline, diesel oil, lubricating oil or guarantee quality stability or meet the requirements of a certain standard, additional processing of the product from oil refining equipment must be carried out, the operation is mainly completed by agitated mixing operation. As a separate unit operation, agitated mixing operation can be widely used in field of wastewater treatment, fuel, chemical building materials, paint, food and other industries.

Agitated hybrid equipment can be used as the reactor in many cases. As we all know, fully mixing and contact is the premise of chemical reaction, while the purpose of mixing is to make materials disperse uniformly. So, mixing can provide a good prerequisite for the chemical reaction, especially for heterogeneous chemical reaction, such as the reaction between liquid–liquid, liquid–solid–liquid, mixing is of great significance to the normal of reaction. In addition, mixing is of great significance to reaction. For exothermic reaction, mixing operation can enhance heat transfer, prevent material from local overheating or coking, and ensure the quality of product. In the production of synthetic rubber, synthetic plastics, and synthetic fiber, mixer accounts for 90% of the total. Reactions such as sulfonation and nitration reaction in organic chemical industry, silicon aluminum reaction, barium reaction, barium acidification reaction, and alkylation reaction are accomplished by agitated reactor. In the chemical production, mixing operation is commonly used to improve the efficiencies of heat transfer and mass transfer of the process such as dissolution of solid, crystallization of supersaturated solution and gas absorption [27, 34, 35].

6.5.2 Configuration of Mixing Agitator

Due to different purposes of agitation and the diversity of the agitation media, there are many kinds of agitators. Typical mechanical agitators contain paddle agitators, turbine agitators, propeller agitators, anchor agitators, frame agitators, propeller agitators, and screw agitators. According to the paddle shape, agitators can be divided into three kinds: straight blade, folding blade, and spiral blade. Paddle

shapes of turbine anchor and frame agitators are straight or folded blade, while paddle shape of pusher or screw agitators is spiral blade.

According to the flow direction of drainage in the agitation operation (also known as the flow pattern), and types of impeller agitator can be divided into two kinds: runoff and axial flow. Flat blade paddle and turbine are radial flow type, push type and screw type of spiral type belong to axial flow type, while the folding paddle is between radial flow type and axial flow type, generally, it is believed more close to the axial flow type.

In order to achieve the specific purpose, agitators can be improved and combined, fast and slow types of blades can be combined together to adapt to the mixing process with large change of viscosity. For the mixing process of high viscosity fluid, screw and screw conveyor can be combined together to make the central and peripheral of stirring tank fully agitated, so as to achieve the effect of agitated mixing.

With the rapid development of measurement and control technology, and wide application of computer, agitation technologies also developed rapidly. Development trend of agitation equipment is high efficiency, energy saving, mechatronics and intelligentized, and gradually introduced the computer-aided design (CAD), computer-aided drawing (CAG), and computer-aided manufacturing (CAM) into the development of agitation equipment [35, 36].

6.5.3 Calculation of Agitation Power

The power consumption of agitation should be divided into two aspects. On the one hand, the power required to maintain the normal rotate of agitator at a constant speed. On the other hand, power required to achieve the purpose of mixing operation, which is called agitator power. These two kinds of power are overlapped, not independent.

6.5.3.1 Influencing Factors of the Agitator Power

The agitator power relates to the state of fluid flow in the agitator tank. Therefore, all factors that affect fluid flow state can also be the influencing factors of agitator power, mainly the following factors are included geometrical parameters, (such as shape and size of blade, blade number, the installation height of the blades), operation parameters of agitator (such as rotational speed), geometry parameters of agitator tank (such as the inner diameter of the agitator tank, the width of the baffle), the physical parameters of agitating media (such as fluid density, viscosity).

There are many factors which can influence the agitator power. These factors can be summed up to geometric parameters of paddle and tank, the operating parameters of paddle and physical parameters influencing power.

6.5.3.2 The Basic Method to Calculate the Agitation Power

Theoretically, agitation power could be divided as agitator power and mixing operation power. But in practice, the agitator power is only considered or mainly considered. Mixing operation power is hard to calculate precisely then agitation operation power generally is satisfied by setting the rotational speed.

Factors that affect the agitator power are very complex. Generally, calculation equation of agitation power is difficult to directly obtain by theoretical analysis. Therefore, experimental methods combine with theoretical analysis is the only way to calculate the agitation power.

The dimensionless equation can be obtained from Navier–Stokes equations and its dimensionless form:

$$N_P = \frac{P}{\rho N^3 D_j^5} = F(\mathrm{Re}, Fr), \tag{6.58}$$

where Np is the power characteristic number, Fγ is the Froude number, Fγ = N2di/g, P is the agitation power.

Re(Re) reflects the ratio of inertia force and viscous force of the fluid, Froude number(Fγ) reflects the ratio of the fluid inertia force and gravity. Experimental results showed that when Re is higher than 300, Fγ impacts the agitation power slightly. Fγ number has almost no effect on the agitation power in laminar flow and turbulent flow. Fγ number has little influence on most of the agitator blades in the excessive flow state when Re > 300. Thus, in engineering, the power factor expressed as a function of Re directly, without considering the influence of the Fγ.

Due to the agitator rotational speed, the blade diameter, density, and viscosity of fluid contained in the Re, so the other factors must be determined in a laboratory, and then determine the relationship between power characteristics number and Re. It can be seen that all the curve or equation of Re and power characteristic parameters which are obtained by experiments can only be used in certain conditions. For different types of paddles, curves of the power characteristic number and Re are different. Even for the same type of blade, their correlation curve of Np-Re will be also different for the difference in ratio of blade width and diameter.

6.5.3.3 Power Characteristic Number of High-Speed Blade

Rushton et al. made a lot of experiments on blade type, structure size, rotate conditions of common agitator, Np-Re relation curves when liquid viscosity was 1.0×10^{-3} Pa•s, Re below 10^6 are given. If blade type of agitator included in the Rushton curve, calculated agitation power by Np-Re relation curves will be very convenient. First, calculating the Re by the known blade diameter, rotational speed, the fluid density, and viscosity, power characteristic number can be checked out from corresponding curve, then the power can be calculated as

$$P = N_p \rho N^3 D_j^5 \tag{6.59}$$

In the laminar flow, when the Re is less than 10–30, relationship between the power characteristics of blade number and Re is logarithmic linear. While in turbulence area, power characteristic number is a constant, not changing with Re. In excessive flow zone, Np-Re curve of the blade is varied. And with the same Re, power characteristics of propeller agitator is smallest, and that of radial flow type of disc turbine agitator is the largest.

In engineering design, Bates chart can be used to determine the power characteristics for open type turbine with wide application because the width and dip angle of blade has distinctly effected on the power characteristics, the choose of conditions need to be paid attention to. In addition, using curve need to meet full-baffle conditions and the following geometry size: dj/D = 1/3; ratio of liquid height and agitation tank diameter H/D = 1; the ratio of blade distance from the tank bottom and the tank inner diameter c/D = 1/3.

6.5.3.4 Power Characteristic Number of Low-Speed Blade or Without Baffle Blade

Most curves in Rushton's figure and all curves in Bate's figure can be only suitable for various quick blade agitators under full-baffle conditions. Powers consumed by blade blender under the no baffle condition can be calculated with empirical formula is as follows:

$$Np = \frac{P_0}{\rho n^3 d^5} = \frac{A}{\mathrm{Re}} + B \times \left(\frac{10^3 + 1.2 \times \mathrm{Re}^{0.66}}{10^3 + 3.2 \times \mathrm{Re}^{0.66}}\right)^p \left(\frac{H}{D}\right)^{(0.35 + \frac{b}{D})} (\sin\theta)^{1.2} \tag{6.60}$$

A, B refers to a coefficient, and *p* is an exponential.

$$A = 14 + \left(\frac{b}{D}\right)\left[670(\frac{d}{D} - 0.6)^2 + 185\right] \tag{6.61}$$

$$B = 10\left[1.3 - 4(\frac{d}{D} - 0.5)^2 - 1.14(\frac{d}{D})\right] \tag{6.62}$$

$$p = \left[1.1 + 4(\frac{b}{D}) - 2.5(\frac{d}{D} - 0.5)^2 - 7(\frac{b}{D})\right] \tag{6.63}$$

In this equation, *b* is the width of agitator blade; *H* is the depth of liquid; *D* is the agitator tank inner diameter; *d* is propeller diameter of agitator; θ is angle of blade, and $\theta = 90°$ for oars.

The empirical formula is based on the relationship between semi-diameter of "cylindrical raceway" formed by flow liquid and fluid resistances of agitator blade,

and then the formula of power characteristics corrected by experiment. Although the formula is for double paddle agitator, but through the experimental verification in turbulence area, blades with same oar diameter, as long as blade width is same, so that the agitator power consumption is equal.

(1) Anchor agitator and fram agitator

As empirical formula could be applied in anchor agitator and fram agitator with high viscosity fluid, with the height of blade h could be considered as the width of blade b introducing into the empirical formula equations. The second item of this formula can be ignored when in high viscosity fluid, then the following can be obtained:

$$Np = \frac{A}{\mathrm{Re}} \tag{6.64}$$

And when blade diameter is very close to the diameter of inner agitation tank (*di/D* > *0.9*), value A could be obtained with Bochner formula as below:

$$A = 82\left[\frac{2D}{D - d_j}\right]^{0.25} \tag{6.65}$$

(2) Helical ribbon agitator

Helical ribbon agitator used for high viscosity fluid is generally operated in laminar flow. The power number could be also calculated with empirical formula, where value of A can be calculated as below:

$$A = 66z\left(\frac{d_i}{s}\right)\left(\frac{h}{d_i}\right)\left(\frac{b}{d_i}\right)\left(\frac{D - d_i}{2d_i}\right)^{-0.6} \tag{6.66}$$

In this equation, z is the helical ribbon index; h is the helical ribbon height; and s is screw pitch.

(3) Screw agitator

According to the measurement results, when screw pitch S = di of screw agitator with diversion barrel, its power characteristics is the same as of ribbon agitator in same size. Therefore, empirical formula can be used for screw agitator.

6.5.4 New Agitators of High-solid and Multi-phase Bioprocess

6.5.4.1 Process Intensification

There are various definitions of process intensification. Process intensification is regarded as a design concept. Meet the chemical and physical requirement by fluid

dynamics design, so as to make the reaction carry on at best rate. According to its definition, process intensification is integration of chemistry and chemical processes. This can be illustrated in the S—curve in Fig. 6.4. Process performance can improve until limit point of chemical process, with the improvement of the equipment performance (e.g., increase of mixture rate). An optimized chemical process intensification design means the design of chemical process has been achieved (without limitation of equipment) the desired performance, and then through the equipment design achieve the peak point of the curve S, then curve became horizontal. If the operation point by right means excessive design results in increase of investment and operating costs [37–39].

Above all, the process intensification is to realize the matching of the following:

(1) Mixing rate and reaction rate.
(2) The heat transfer performance and heat generation.
(3) The retention time and the reaction time.
(4) The flow pattern and reaction diagrams.

6.5.4.2 Mixing of High Viscosity Fluid

High viscosity fluid generally refers to fluid in which the viscosity is higher than 2.0 Pa•s. Flow property of high viscosity fluid is quite different from which of low viscosity fluid. High viscosity fluid in engineering generally is difficult to achieve the turbulent state, but only flow in the condition of laminar fluid. In the area where agitator blade cannot reach, dead zone will be easy to form with the effect of viscous force due to the high viscosity of the fluid. Working in high viscosity fluid,

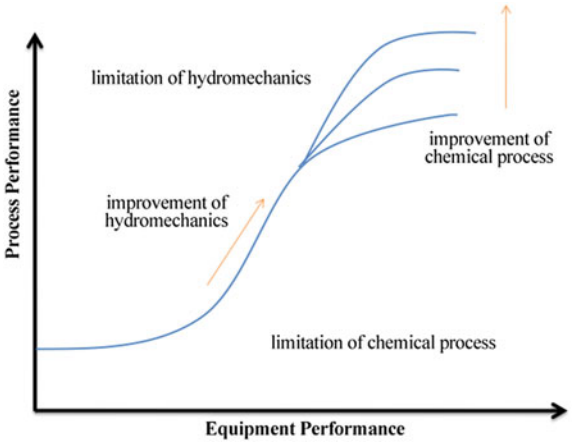

Fig. 6.4 S-curve of factory performance and process performance

fluid volume discharged by agitator blade is small and fluids slightly away from blades become inert. Channeling formed when agitator rotational speed is too high. Therefore, for high viscosity fluid which is in laminar flow state, only try to expand the agitation range, the dead zone can be as small as possible.

6.5.4.3 The Choice of Agitator

Many factors should be considered when choosing the agitator. The most basic factor is the viscosity of media, the purpose of mixing process, and flow state caused by the agitator. Choose the agitator according to the viscosity of mixing media is a basic method due to the fluid viscosity has a great influence on mixing status. Generally, with the increase of viscosity, the agitator used in order is promoted type, turbine, paddle, anchor, screw conveyor, and screw.

Select the agitator according to the purpose of the mixing process is a basic method. Low viscosity homogeneous fluid mixing is the smallest viscosity with low power consumption, easy circulation, it is difficult only when the agitation tank is very big and mixing time is very short. Propeller agitator is the best choice due to the large circulation capacity and low power consumption. And power consumption of turbine agitator is large, it has high shear capacity, but it is not necessary for combination process. So it is not reasonable to mix in large container. Paddle agitator is still widely used in small container fluid mixing for its simple structure. But when it refers to agitator in a large container, its circulation ability is insufficient.

In the dispersing and emulsifying process, in spite of agitator having large circulation ability, it is supposed to have high shear capacity. The turbine agitator has this characteristic. It is usually used in the situation that straight blade turbine agitator is more suitable due to the shear stress of which is larger than folding blades and curved blade. Shear stress of pusher and paddle agitator blades smaller than straight blade and turbine agitator. Therefore, they can only be used in liquid with small amounts. And the paddle agitator is rarely used in dispersion process. The dispersive mixing process, baffles are installed in the mixing tank to strengthen shear effect (Table 6.2).

Dissolution of solids requires that the agitators have strong ability of shear stress and circulation, so the turbine agitator is the best choice. The circulation capacity of propeller agitator is high, but the shear stress is low, so it can only be used for dissolving process in small containers. Paddle agitator needs a baffle to improve circulation ability, usually used the dissolution of easily suspended particles.

Gas absorption process, the disc turbine agitator in the most suitable condition, the shear capacity is strong, and the bottom of the disc can hold some gas to make the dispersion of the gas more stable. Open turbine agitator does not have these

Table 6.2 Type and trial conditions of mixer

	Flow state			Agitation purpose									Capacity range of agitator tank	Range of speed	Highest viscosity
Type of agitator	Convectional circulation	Turbulent diffusion	Shear flow	Mixture of low viscosity stationary liquid	Heat transfer and reaction of mixture of high viscosity stationary liquid	Dispersion	Dissolution	Solid particle suspension	Gas absorption	Crystallization	Heat transfer	Liquid phase reaction			
Turbo type	√	√	√	√	√	√	√	√	√	√	√	√	1–100	10–300	50
Paddle	√	√	√	√	√		√	√		√	√	√	1–200	10–301	2
Push type	√	√		√		√	√	√		√	√	√	1–1000	100–500	50
Anchored concrete	√				√		√						1–100	1–101	100
Screw type	√				√		√						1–50	0.5–50	100
Ribbon type	√				√								1–50	0.5–50	100

Note "√" is appropriate, blank is inappropriate or unknown

advantages. Paddle and propulsion agitator cannot be used for gas absorption process, only used in absorption of small amount of gas with a high dispersion degree is not high.

For agitation crystallization process, it is generally needed agitator with small diameter and high speed, such as turbine agitator, suitable for particle crystallization process. And the agitators with big size and slow speed such as paddle agitator are suitable for crystallization process of particles in large size.

Turbine agitators are widely used for suspension operations of solid particles, and among them, the open turbine agitator is the best choice. There is no disc in the middle of open the turbine agitator, the mixing of upper and lower fluid will not be hindered, and curved turbine type agitator has the advantages of the turbine is more outstanding, its performance is good, blade is not easy to wear, so it is more suitable for suspension of solid particles. The speed propeller agitators are low, it can be only applied to the occasion of small solid particles, small solid–liquid density difference, high-solid concentration, low settling velocity solid particles.

6.5.4.4 Strengthening Methods and New Agitators of High-solid and Multi-phase Bioprocess

Effective mix depends on the geometry of the agitation blade. The shape of the agitation blade resulting in the difference of agitation rate and shear stress. Zhang et al. [5] studied the impact of spiral impeller agitator on performance of high-solid enzymatic (30%) by vertical reactor. It was found that spiral impeller agitator reduce power by four-fifth than conventional Rushton impeller, which indicates that the paddle of helical impeller is more suitable for mixing of high viscosity non-Newtonian fluid. Moreover, the geometry of the impeller plays a vital role in efficient mixing. Wang et al. [40] studied the influence of frame impeller agitator and double curved blade impeller paddle on high-solid enzymatic of sweet sorghum with hydrothermal pretreatment. Compared with double curved blade impeller agitator, frame impeller paddle increases glucose yield by 10%, which indicates that the geometry of the impeller can affect agitation efficiency. Frame impeller agitator produced a larger uniform mixing zone at different depths in the reactor, in order to facilitate mass transfer. Zhang et al. [41] studied the effect of Nail—shaped agitator on the high-solid enzymatic hydrolysis of hardwood biomass. The results showed that compared with the shaking flask, the conversion rate of the enzymatic hydrolysis under the 20% solid–liquid ratio by Nail—shaped agitator was higher, the liquefaction time of the non-bleached hardwood pulp reduced, thus improved the efficiency of mass transfer. In addition, the rotating speed, the size of the agitator, the ratio of the reactor diameter to size can also affect the mass transfer efficiency of the high-solid solution process. The above researches showed that developing new mixing mode is an effective strategy to improve the efficiency of high-solid enzymatic hydrolysis.

New reactor for high-solid enzymatic hydrolysis has been studied. Jørgensen et al. [29] studied the impact of rotary drum reactor mix by free fall on the

performance of high-solid enzyme. When the initial solid–liquid ratio was 40%, around 10 h, wheat straw particles pretreated liquefied into paste. When the mixing rate at 24 h was at 3.3–11.5 rpm, there was no obvious effect on the enzymatic hydrolysis efficiency. After 96 h, the glucose concentration reached 86 g/kg with the condition of 7 FPU/g dry matter and 40% solid to liquid ratio. Roche et al. [3] investigated horizontal reactor mixed by gravity or free fall, compared with the traditional vertical mixing reactor, the new reactor has many advantages, such as minimized the particle sedimentation and partial product accumulation, made the enzyme distribution more uniform. Under the 20% solid–liquid ratio conditions, the free fall mixture of the rotating bottle reaction system makes the high-solid solution rate reach 80–85%. Dasari et al. [4] found that compared with the vertical reactor, with 25% solid–liquid ratio, the conversion rate of the horizontal reactor increased by more than 10%, and the power of the horizontal reactor was significantly lower than that of the vertical mixing. Sun et al. [42] compared steel ball impact oscillation, shaking and static on steam explosion solid enzymatic efficiency at the 10% solid–liquid ratio, it was found that during the oscillation, the stainless steel ball "squeezed" the steam exploded straw continuously, made the adsorption capacity of enzyme increased, and can improve the accessibility of substrate, increased adsorption desorption efficiency of cellulase, thus increased the enzyme efficiency. Chen and Liu [43, 44] invented device of high-solid enzymatic hydrolysis coupled with liquid fermentation to produce ethanol from cellulose, which consists of vertical concentric inner tube and the outer tube, the outer tube cavity, inward in lignocellulose and cellulase enzymatic hydrolysis liquid by the pump into the inner cylinder by yeast fermentation. The device overcomes the shortcomings such as the enzyme hydrolysis product feedback inhibition and high-solid–liquid ratio, which is not conducive to the rapid fermentation of ethanol. The amounts of the cellulase was reduced by 20–40% when being used this device. The device has been scale up to 110 m3, which is used to produce 3000 t straw ethanol every year.

6.5.5 *The Application Prospects of Seepage Theory in High-solid and Multi-phase Reaction Engineering*

High-solid multi-phase reaction process has the advantages such as high substrate concentration, high production efficiency, environmental-friendly, it will help improve products concentration and reduce the cost of product separation. High-solid multi-phase reaction is the inevitable requirements of industrialization of lignocellulosic ethanol. However, the industrial applications of lignocellulose still need technical breakthrough. Researches of high-solid multiphase reaction process should first focus on inhibitor and product inhibition effects, changes in the rheological properties and mass transfer efficiency. And the influences of intrinsic properties (such as chemical composition, porosity, mechanical property, heterogeneity, resistance ability) of lignocellulosic on limiting factors should be revealed.

Moreover, the effect of key technologies which can improve the efficiency of high-solid multi-phase reaction process (such as washing operation, fed hydrolysis, multi-enzyme system) on process economy should be discussed and studied. Reactors for high-solid multiphase reaction should be developed and scaled up. Based on the intrinsic characteristics of lignocellulose, taking limiting factors into consideration, in-depth study and analysis of assumptions, derivation used in model establishment and the rationality of experimental data is an effective way to correctly understand the percolation law of the high-solid multi-phase reaction process. In addition, based on the basic seepage law of porous media, studying flow characteristics of the fluid in and out of the pore in the high-solid multi-phase reaction process of lignocellulose is meaningful. The further analysis of the high-solid multi-phase reaction process is an effective way to realize the industrialization of the solid-state enzyme hydrolysis. The advantage of solid-state enzymatic hydrolysis is a guarantee of economic benefit of lignocellulose refining.

6.6 Large-Scale Transport for High-solid and Multi-phase Bioprocess

6.6.1 Methods and Measures of Large-Scale Transport in High-solid System

Transport method of material in high-solid system can be divided into two kinds: mechanical conveying and pneumatic conveying. Mechanical conveying equipment include belt conveyor, bucket elevator, screw conveyor, vibrating conveyor. The pneumatic conveying ways include: pneumatic suction transport, low pressure, medium pressure and high-pressure deliver, pulse transporting, suction—pressure transportation, circular conveyor [45, 46]. Here are the mass transport equipment and measures of high-solid material.

6.6.1.1 Manual Transport

Fermented grains in liquor factories are still artificially transported by cart. The intensity of labor is high. More opportunities for touching materials resulting in microbial contamination [47].

6.6.1.2 Belt Conveyor

Belt conveyor uses ribbon to convey material, not only used to transport the fine powder and granular materials but also used to transfer material with a large volume. It has advantages of large production capacity, low power consumption, and

simple structure, easy to maintain, loading and unloading of whole fuselage. The deficiency is that it can only transport straight, material loss and environmental pollution caused by material are easy to float into the sky when conveying light-weight material, only applicable to transport in horizontal or small inclination angle.

6.6.1.3 Air Cushion Belt Conveyor

Air cushion belt conveyor (or air cushioning machine) is a kind of new continuous conveyor equipment with air cushion replacing the roller bearing. It brings a series of advantages, the principle changing from gas–solid friction to rolling friction, then friction resistance reduced by 50–70% [48].

Operation principle Operation principle of air cushion belt conveyor is shown in Fig. 6.5 [5].

When air cushion machine works, pressure fan 7 makes air flow into the air chamber 5 via 8 air vent, gas film formed between conveyor belt 3 and the upper plate slot arc plate with air chamber 5, supporting the tape bearing materials. And when the machine operates, it just needs to overcome the gas resistance of cushion to convey material.

Advantages of air cushion belt conveyor Replacing roller bearing with air cushion, air cushion machine, solid friction of air cushion belt conveyor becomes fluid friction, thus it can overcome the disadvantages such as high resistance, high energy consumption, easy to deviation, and a heavy work load in maintenance, then brought a series of advantages. (1) Belt operates smoothly, safely, and reliably.

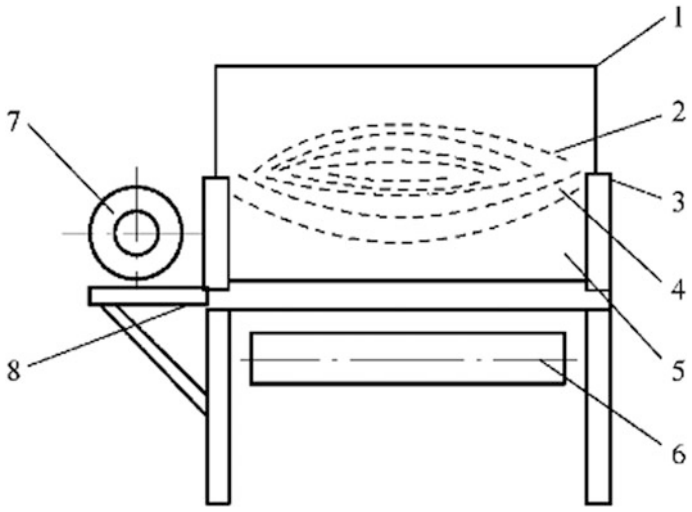

Fig. 6.5 Schematic diagram of air cushion type of belt conveyor. *Note* 1—cover; 2—material; 3—conveyor belt; 4—air cushion; 5—air chamber; 6—return roller; 7—pressure fan; 8—air vent

(2) Belt operation without off-tracking. (3) Low power consumption. (4) A light work load in maintenance. (5) High transmission efficiency. (6) Light tape could be chosen and prolong service life. (7) Could be used in layout of large dip angle. (8) Low noise and little dust. (9) Easy to close.

6.6.1.4 Tubular Belt Conveyor

Principles of tubular belt conveyor Tubular belt conveyor is a kind of continuous bulk material conveying machine which bears by tape, except the tape rolled into tubes in the operational area, the rest are very similar with ordinary belt conveyor. Tubular belt conveyor has guide chute in the feed area, with guide roller, the tape transit from flat tape to U-shaped finally curled into a tube shape. In the unloading area, the tape transit from the tube shape to the U-shaped, transition from U-shaped to flat again, finally discharge. Tubular belt conveyor in the operational area is supported by two groups of hexagon roller.

Characteristics of tubular belt conveyor In addition to the characteristics of ordinary belt conveyor, the tubular belt conveyor also has the following features: ①Enclosed conveying material. Due to the material running inside the duct tape, the effective transportation process is carried out in a closed environment. Therefore, this will overcome the mass loss and the pollution to the environment in transportation. ② Conveyor space curve layout could be realized. Because the tape could be curled up into a tube to reduce the lateral stiffness, which can make the tape arbitrarily bent with small radius, expand the application range of the belt conveyor. ③ Sharp inclination transportation. Tape curled up into a tube, increase contact area and the friction between material and material, material, and tape, conveying angle can be raised from 18° of the ordinary belt conveyor to 30°.

6.6.1.5 Bucket Elevator

Bucket elevator can lift materials vertically, suitable for loose, small granular materials, such as barley, wheat, rice, corn, sorghum. By using tape or chains as traction, screw the hopper on the traction, traction driven by the drum tight and run. Material put into the hopper from the bottom of the elevator, and hopper is upraised to the top by traction, when hopper bypass active rotary drum, material removed from the bucket, so as to set the materials to a high location. To prevent flow out of dust, components (except the motor and gearbox) are installed in the casing. There are observation ports in the appropriate location. Revolving drum at the top is driving wheels, which are connected with reducer, motor. Revolving drum at the bottom is driven wheels, usually is also a tension wheel, with a screw or a heavy tensioning device [45].

6.6.1.6 Screw Conveyor

Function and scope of screw conveyor Screw conveyor is transport machinery widely used in biological chemistry, which is suitable for loose, small granular materials (barley, wheat, rice, corn, sorghum) and sticky materials with high water content (fermented grains and wet brewer mash).

Principle and structure of screw conveyor Screw conveyor is mainly composed of shell, a rotating spiral chute and a rotating device (Fig. 6.6) [45]. When the shaft rotates, materials move along the chute by screw conveyor. Spiral consists of rotating shaft and the blades on the shaft. Blades commonly used in the factory are vane and belt type. The vane has simple structure, large thrust and conveying capacity, high efficiency [49].

Screw shaft is made of round steel or steel pipe. Spiral plate is mainly composed of thin steel plate. The speed of the screw is usually 50–80 r/min, screw pitch is generally 0.5–1.0 times of the diameter of screw. There is a certain gap between the screw and material, generally 5–10 mm. Gap e factory are vane and bie factory are vane and bs small but transport efficiency is high. Chute can be divided into two kinds: the circular chute and semicircular chute. The circular chute is screw concentric circular tube, its diameter is larger than that of spiral plate by 10–20 mm. Semicircular chute below shaft center is concentric semicircle. Chute usually made by pipe or steel. Inlet open at the top of a chute, above the inlet, is funnel, outlet open at the bottom of the other chute. When installed, the direction of the screw rotation should be paid attention to.

The advantages of screw conveyor are simple and compact structure, easy to seal and unloading. But energy consumption is high. The conveyor is often used for short distance transportation, or transportation with angle no more than 20°.

6.6.1.7 Vibration Conveyor

Vibration conveyor use vibrator to make chute vibrate along the tilt direction, realize the movement of material. Its advantages are simple structure, easy to adjust, and easy to realize automatization. Vibration conveyor has been widely used in

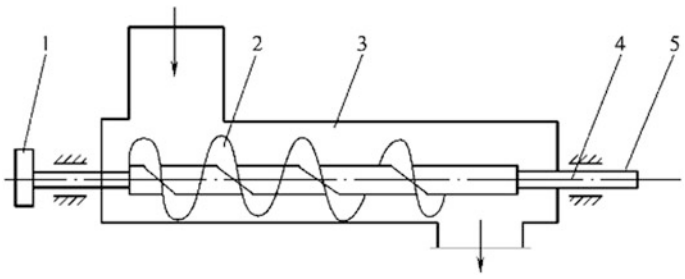

Fig. 6.6 The schematic diagram of screw conveyor. *Note* 1, belt pulley; 2, helix; 3, shell; 4, bearing; 5, axle

food industry, such as transportation of sugar, salt, packaging of chocolate particles, hard candy [50]. However, the vibration conveyor makes large noise and vibration, and it causes congestion easily especially for material with high viscosity.

Long-term production practice proved that machinery transmission mode has the following defects in the field of solid particles and powder material conveying: (1) Mechanical conveying equipment is huge, complex, and arrangement is not flexible; (2) The component of machinery (such as guide rail, idler pulley, shaft,) usually run in a dusty environment with poor lubrication condition, wear-seriously, a high failure rate; (3) Uneven load, the electrical system is easy to damage; (4) Sealing performance is poor, the material leakage will cause environmental pollution and material loss; (5) There area heavy workload and high cost in maintenance.

Due to the above disadvantages, mechanical transmission method has begun to be partly replaced by pneumatic conveying.

6.6.1.8 Pneumatic Conveyor

Pneumatic conveyor system is conveyor equipment which uses flow with a certain energy in the pipe to make the suspended powder or granular materials move and to separate gas and material by separator. According to the different power, sources can be divided into negative pressure suction (vacuum conveying) and pressure feed (positive pressure conveying) and attract pressure combined transport. According to solid particles concentration in gas, pneumatic conveyor system can be divided into the dilute phase, dense phase (fluidization), and super dense phase [51, 52].

Suction conveying process Suction air transport is also called the vacuum transport. The process is to install fan at the end of the whole system, using the fan extract gas from the pipeline system, make the gas pressure in the pipeline is lower than the atmospheric pressure, to complete the delivery process in a state of negative pressure. Because of air pressure difference of inside and outside the whole pipeline, and the material and gas is dragged into feeding tube through suction nozzle, then separated after go through the cyclone separator, the material discharged from the bottom of the cyclone separator discharger, the gas containing small material and dust go into the bag filter, and then discharged into the atmosphere. Dust will not leak out because the conveying system is vacuum. Therefore, suction conveying system can avoid the leakage of material and dust, keep a clean environment.

Pressure conveying process Pressure conveying process is also called the positive pressure conveying, the fan installed in the front of system when the fan works, the air is pressed into the pipe, the pipe pressure is higher than the atmospheric pressure, the pipe in positive pressure condition. Material flows down from hopper, mix with air through pipes, then sent to the separator, in the separator, material discharged from the bottom of the separator, air goes into purifier, then discharge into the atmosphere. Pressure conveying can cause large pressure

difference, so it can be used to in wet materials transportation, transportation distance, and height are larger than suction conveying.

The mixed air conveying process Mixed air conveying process is a combination of vacuum and pressure conveying. The fan is usually installed in the middle of the whole system. In front of fan, it is called suction segment, materials are transported by negative pressure within the pipe. After the fan, it is called pressure section, materials are transported by positive pressure. The mixed air conveying process has the characteristics of suction and pressure conveying, it can convey materials from several places to a far, higher place. But because of the change from suction conveying process to pressure conveying process, the structure of device is complex, and work conditions of fan is poor [45].

6.6.2 *Special Requirements of Project Conveying in High-solid and Multi-phase Bioprocess*

Bioprocess usually needs to keep sterile [53]. Thus, in high-solid and multi-phase bioprocess, the delivery not only needs to be considered about chemical transfer characteristics but also the biological characteristics. Due to the particularity of high-solid multi-phase bioprocess system, the mass transport should meet the following requirements: (1) to overcome the poor fluidity solid material, realize effective transport of materials; (2) ensure that sterility of conveying process, avoid bacterium contamination; (3) improve the mechanization level of mass transport process and reduce the labor intensity.

6.6.3 *Large-scale Material Transport of High-solid and Multi-phase Bioprocess Engineering*

Large-scale transportation of materials in high-solid and multi-phase bioprocess should avoid bacterial infection, so closed systems with less manual operation is best choice. On one hand, reduce the labor intensity; on the other hand, reduce the risk of bacterium contamination. For this purpose, learn from other industries.

The docking mechanism of the Shenzhou spacecraft is the homologous structure peripheral (flip-in type) docking mechanisms. The major advantages of this docking mechanism is tracking aircraft and target aircraft adopting the same docking mechanism, so there is no distinction between active and passive, which benefit to orbital recovery; and all components of the docking mechanism are placed on the surroundings, while the center position of the spacecraft is set aside as a transitional passage, which ensures rapid evacuation when fault occurs; the guide plate is in flip-in type, with the advantages such as compact structure, high stiffness, large carrying. The docking mechanism is mainly used for docking of space shuttle and

space station, the international space station. It is the most advanced docking mechanism currently [54].

The whole docking process includes contact, capture, buffering, adjustment, closing, locking of space craft (a shown in Fig. 6.7) [54], keep the docking state and the separation of spacecraft.

(1) Aircraft close. GNC system control two aircraft close to each other, until the docking mechanism contact with each other.
(2) Contact. The docking ring of two spacecraft contact and collide with each other, then docking process begins.
(3) Capture. Docking mechanisms gradually eliminate the initial deviation and establish a flexible connection to complete the capture of the two aircraft.

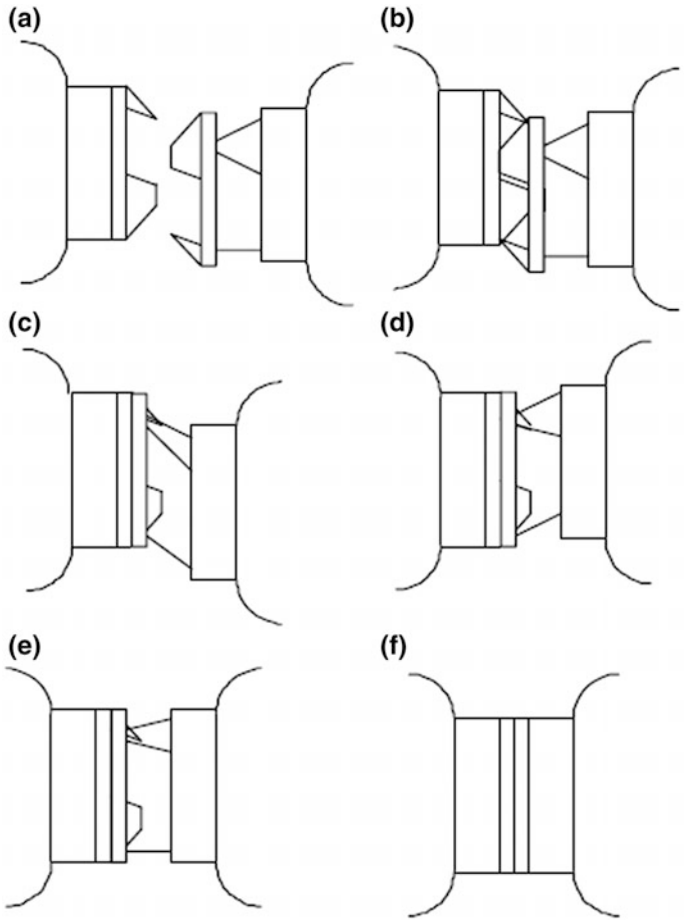

Fig. 6.7 Space docking process. a- Aircraft close to; b-touch; c-capture; d-The buffer and correction; e-zoom in; f-locking and seal

(4) Buffering and adjustment. Buffering system of docking mechanisms works, buffer, and consume the collision energy, gradually decay oscillation between the two spacecraft docking. Under the effect of restoring force of elastic element, auto correction of aircraft could be realized. Complete the force adjustment of flight attitude by the axial alignment of two aircraft or push docking ring beyond the limit position.
(5) Closing. Active docking mechanism makes aircraft close, achieve precise alignment by guide pin set of docking box surface.
(6) Locking. When the docking boxes surface of two aircrafts come close, lock two aircraft by the docking lock system, complete the rigid connection, and finally seal the docking mechanism by double sealing ring of docking box surface.

The aircraft with rigid connection take a joint flight, docks mechanism keep completion status to ensure the seal of docking channel. After the joint fight mission, docking mechanism receives the separation command, open docking lock, then two aircrafts separate by the push rod [54].

In 1954, the American scholar George Devol created the world's first programmable manipulator, manipulator has developed three generations. First, teach the robot movement, then input program, manipulator automatically repeat theaction is known as the first generation of manipulator, and manipulator controlled by sensors is known as the second generation of manipulator, intelligent robot is the third generation of manipulator. Many countries such as American and Japan have put huge amounts of manpower and material resources into manipulator, but it is still developing. In China, manipulator development starts from the fixed-action manipulator in the 1950s. After experiencing numerical control manipulator in the 60s, it starts to be applied since 1978. Nowadays, industrial robots and intelligent robots have gotten more attention, has been included in high-tech and the technology development plan. In general, the research focused on kinematics of manipulator begin from early 1990s, with a wide range to consider, most research focused on computational efficiency and singularity of redundancy manipulator equation. The establishment of the manipulator dynamics model is necessary for effective control and reasonable design of manipulator, so researchers always focus on manipulator dynamics. Nowadays, calculate mechanical efficiency, elastic dynamics of the manipulator, dynamic stability of force is a hot spot in the manipulator dynamics researches. At the same time, due to the depth research of manipulator dynamics, flexible manipulator developed, thus improve flexibility of manipulator, bring a problem in stability control of manipulator, so research about these aspects will be the top priority in manipulator dynamics control.

Picking up the material smoothly, quickly, accurately, and complete the removal action is the most basic requirements of material handling manipulator. This requires high accuracy, certain capacity, enough operation space, flexibility, and operation stability. Designing the material handling manipulator must according to the action to select appropriate mechanical structure, determining the time allocation and action order, explicate weight and size of handling material as well as the demand of environmental accuracy, to determine the requirements for operation

control of manipulator. Take generality and specificity into consideration, and select standard components to realize the modularization of the manipulator.

To complete the function of material handling, material handling manipulator needs to complete the following actions: (1) Horizontal extend (mechanical arm should extend 70 mm in horizontal direction to reach the area above material); (2) Vertical downward (manipulator can be downward 60 m min the vertical direction to make terminal actuators reach horizontal position with the material); (3) Clamping material (manipulator terminal actuator clamp materials to make the material does not drop); (4) Vertical rise (after ensure the material being clamped, manipulator vertical upward 60 mm, the manipulator terminal actuator make materials stay in situ); (5) Horizontal Contraction (mechanical arm contract 70 mm in a horizontal direction to make the manipulator terminal actuators back to the initial position); (6) Retrograde (manipulator move anticlockwise to horizontal direction for 90°, so manipulator can reach the terminal of material); (7) Vertical drop (manipulator downward 60 mm in the vertical direction to make material smoothly move to terminal); (8) Release material (hand clamping mechanism quickly release materials); (9) Vertical rise (after the material placed rightly, manipulator upward 60 mm in the vertical direction, back to the initial limit position); (10) Clockwise rotation (manipulator move clockwise in horizontal direction for 90° to make the manipulator back to the initial position). The above is all the action need to be completed.

According to the movement and speed of material handling manipulator, time for a complete transport could preset as 6 s, the movements, and time allocation are as below: horizontal extend and horizontal contraction of manipulator occupy 0.5 s respectively, vertical rise and vertical drop occupy 0.6 s respectively, twice rotation occupy 1s respectively, clamping and release occupy 0.3 s respectively [55]. Due to the particularity of high-solid bioprocess system, learn from relevant ideas, integrated innovation, make a series of progress.

6.6.3.1 High-pressure Pneumatic Conveying

Sterilization of solid materials can use steam explosion as sterilization method. And steam explosion is a process of high-temperature short time which can be divided into two stages. First, cooking materials by water vapor of high-pressure and high-temperature change material properties. Second, decompress immediately after maintaining a certain time, materials rapidly undergo from high-pressure environment into the low pressure or atmospheric environment. When solid media is sterilized by steam explosion, it is found that steam explosion could not only achieve sterilization of material but also change the state of media.

After steam explosion sterilization, the material can be conveyed by high-pressure steam in the tank. Steam explosion sterilization has the following advantages: (1) Compared with the conventional steam sterilization, cooling time after pressure maintenance was saved, and efficiency of sterilization raise; (2) Avoiding heating of the sterilization tank, thus saving energy. (3) Taking advantage of high-pressure steam could realize the sterility pneumatic conveying of solid material [56].

6.6.3.2 Telescopic Pipe

Steam sterilization tank connects with the seed mixer through telescopic pipe, and the telescopic pipe is controlled by cylinder. Then, a closed sterile environment was established to make solid sterile materials go through. When seeding begin, the casing pipe shrinks with its entrance closed by a valve at the same time, cut off connection between the sterilization tank and seed tank, therefore the seed process and subsequent operations will not be affected

6.6.3.3 Feed Cylinder

The function of stuff canister is to achieve the sterile convey of the material in double cones seed tank into the plate, discharge gate diameter of double cones seed tank is 400 mm, the opening diameter of feeding tube is 500 mm, the casing size is 470 mm × 600 mm, casing is driven by pneumatic cylinders and sealed by sealing ring. To avoid curdling of material and to control blank ingrate, the bottom of feed cylinder is designed in shape of mace (Table 6.3).

Parameter of feed cylinder apparatus is showed as following:

6.6.3.4 Automatic Tray Filling System

The material after seeding falls from feed cylinder to plate machine, then automatic tray filling system plate automatically by manipulator structure.

First, charging car fully filled with empty plates are placed at automatic tray filling system, and automatic hydraulic unit will control height of empty plate and conveyor belt, followed by pushing plate to conveyor belt by push rod. When the plate is transmitted to the region below the stuff canister, electromagnetic sensor of stuff canister sensed plate, motor drives the mace to rotate, then feeding starts.

Table 6.3 Designing parameter of stuff canister apparatus

Apparatus	Stuff canister
Volume	1.6 m^3
Apparatus texture	Stainless steel SUS304
Heat preservation	Glass wool, around the tank
Design pressure of tank	0.3 Mpa
Working pressure of tank	0.2 Mpa
Design temperature of tank	143 °C
Operating temperature of tank	133 °C

When the plates go to the receiving area, receiving device will put plate filled with material into the charging car automatically. Finally, charging car is full of plate, then transport by revolving car.

The automation system adopts hoist lifting and positioning plate automatically, pushing mechanism automatically pushes the plate to the conveyor belt. Receiving plate hoist automatically collect plate, once plate move to the receiving area, the products position could be sensed by sensor automatically, and then pushing device pushes the product to charge car automatically. All operations interlock with each other to prevent wrong operation.

6.6.3.5 Electric Revolving Cars

The height of the charging car orbiting fermentation tanks is 680 mm, revolving car is designed to realize the transport of charging car.

Charging car is transported to the fermentation tank by revolving car, then charging car is pushed into the fermentation tank by remote control car after the docking of revolving car and the orbit of fermentation tank.

The conveying system mentioned above could effectively improve the mechanization level of solid-state fermentation. On one hand, it could reduce the labor intensity and save labor; on the other hand, it reduces the opportunities of direct contact of the human and material, thus, the probability of bacterium contamination decrease, which will satisfy the requirements of large-scale sterile conveying in solid-state fermentation.

6.7 Design and Scale-up of High-solid and Multi-phase Bioprocess Reactors

6.7.1 Design Ideas for High-solid and Multi-phase Bioreactors

Bioreactor is the device using biological catalyst to produce bio-products, and link the raw materials and products, which plays a key role in the reaction. The goal of bioreactor is to control the activity of biological catalyst at the best level, which will improve the bioprocess efficiency, production quality and technical and economic level. Therefore, the following factors should be considered when bioreactor is designed: (1) Biological factors. Well biocompatibility; (2) Chemical factors. Enough retention time for reaction and satisfy the reaction kinetics; (3) Mass transfer factors. Diffusion rate of reactants often becomes the limiting factor of the heterogeneous reaction, therefore the requirements of the mass transfer must be satisfied; (4) Heat transfer factors. Heat can be removed or added any time in the process to ensure there is no overheated spot; (5) Security factors. The reactor

should have excellent anti-pollution ability; (6) Operational factors. Easy to operate and maintain [57].

Bioreactor design and operation is very important in biological engineering and has great influence on the cost and quality of product [58]. The main functions of bioreactors is provided space for the cultivation, growth and metabolic control of biological cells and make structure and operating process conditions satisfy the specific conditions required by biological engineering technology; most different from the other industrial equipment is the high requirement of purebred cultivation, any carelessness will cause irreparable losses of enterprise. Thus, the rigor and high running reliability of bioreactor are the marked characteristics of biological industry [59].

The microorganism in cow stomach turned the milk into cheese, where the cow stomach was the original bioreactors. The Chinese alcohol production started from Shang and Zhou dynasty, where the airtight container used for the wine production was also a kind of early bioreactor. And major innovations of bioreactor occurred in 40s of this century, and then the chemical reactors applied to the fermentation industry, deep mechanical agitation bioreactors had been developed for penicillin fermentation production and realized the large-scale pure culture (50–150 m^3). Traditional chemical engineering of "three transmissions and one reaction" is still using and no fundamental change of bioreactors in the thirty years' research. Genetic engineering and cell engineering developed in the 70s make fermentation engineering not just for natural microbe but extend to culture of genetic engineering bacteria, animal and plant cell, and new requirements for bioreactor are put forward at the same time.

In the early 70s, Pregaussian logically proved the dissipative structure theory that from the nonequilibrium thermodynamic theory, in open systems far from thermodynamic equilibrium, the complexity of the process can naturally result in stable self-organizing behavior, developed temporal and spatial ordered structure from disorder structure. In early 80s, mathematics and physics created the chaotic dynamics which further proved that the conversion of chaos and orderly nature at different levels was the universal law of nonlinear complex processes [60]. The development of nonlinear scientific made people recognize that bioprocess had essential differences with conventional chemical reactions, then"three transmissions and one reaction" theory of chemical engineering was not suitable for bioreactor. The researchers of Chinese Academy of Sciences Institute of Process Engineering focus on life principles and nonlinear dynamic properties of the enzymatic reactions network system in living cells, the structure and function of cell membrane, and influence on transmission of matter and information. What has been gradually realized that the normal cycle forces of the cell membrane should be considered as the source of power to enhance the bioprocess rate and mass transfer rate of cell membrane, and the design principle of bioreactor—"strengthen bioprocess and cell membrane mass transfer rate by external cycle stimulus" was first proposed, formed the framework of "four transfer" (momentum, mass, heat and information) and "one reaction" (bioprocess kinetics) in bioprocess engineering. The direction trend of bioreactor is large-scale, highly automatic and diversification. The largest volume

of West Germany's single cell protein production reactor is 2300 m^3 (60 m in height, 7 m in diameter) and the input power is 7 Mw; the biggest volume of wastewater treatment reactor was 27000 m^3 in Britain, and the volume of domestic biggest bioreactor mainly between 100–200 m^3. Although amplification reactor volume could reduce the operation costs, certain technical problems still exist in large reactor design [58]. And some bioreactors with special purpose and performance also rapidly applied and developed. For example, animal and plant cell culture reactors, solid-state fermentation reactor and coupling reactors of fermentation and separation have been developed in vary degrees [53].

Air is considered as the continuous phase in high-solid bioprocess system, while the thermal conductivity is very low, which is just about 1/23 of the water. Therefore, besides oxygen, heat transfer is more important in the design of solid-state fermentation bioreactor. In addition, due to the tolerance of mycelium to shear stress in bioprocess system, the traditional chemical idea of strengthening heat transfer by shear stress is not applicable, so new strengthen methods are needed

6.7.2 Gas Double-Dynamic Solid-State Fermentation Bioreactor

Solid-state fermentation (SSF) plays an important role in industrial fermentation. Compared with the traditional submerged fermentation (SmF), it solves the problem of solid wastes disposal. SSF is defined as the fermentation with solids in the absence (or near absence) of free water. However, substrate must contain enough water to ensure growth and metabolism of microorganisms. SSF has advantages of low energy requirement, high product concentration, and little wastewater production. What is more, it is environment-friendly. However, the substrates used in SSF always are agro-industrial wastes with low thermal conductivities and low heat removal rate. Thus, the over-heat problem in fermentation media has become the bottleneck of SSF technological development. To strengthen heat transfer and avoid the damage of microbial mycelium, the researchers of Institute of Process Engineering, Chinese Academy of Sciences, proposed newly designed principles of bioreactor that using normal pressure as power source of outside cycle pulsation to stimulate the fermentation process. Based on the characteristics of raw materials and the biological characteristics of microbes, Chen Hongzhang designed pressure pulsation solid-state fermentation technology which owned completely independent intellectual property rights. In 1998, the large-scale solid-state pure culture fermentation demonstration was built. And the results showed that economic indicators of this technology were better than the traditional submerged fermentation. On this basis, the gas double-dynamic solid-state fermentation technology gradually developed as one of the modern solid-state fermentation technologies.

In the traditional solid-state fermentation process, the transfer of heat and mass were usually enhanced by mechanical agitation, which the gas phase was fixed and

the solid phase was agitated continuously in order to mix the solid substrate particles completely and to strengthen the connection within the particles or gas molecules. First, during the agitation of solid-state fermentation process, the growth of microbes would be damaged by the shearing force. Second, the equipment is difficult to be sealed, and the energy consumption is high. Third, the sticky wet materials are easily stuck to fermentation tanks, which cause the dead angle in the fermenter. If the agglomeration of media cannot be completely avoided, the efficiency of heat and mass transfer would be influenced. These shortcomings of traditional solid-state fermentation can be overcome by gas double-dynamic solid-state fermentation. The mass and heat transfer can be improved and the concentration gradient of temperature, O_2 and CO_2 can be reduced. At the same time, the microbial metabolism can be promoted by high-pressure pulse circle.

The gas double-dynamic solid-state fermentation bioreactor consists of horizontal solid-state fermentation tank, built-in circular duct, cooling pipes, blowing devices, air circulation system. The device can be divided into two kinds with a single vessel or double vessels. The characteristics of gas double-dynamic solid-state fermentation can be summarized as follows: (1) No mechanical agitation device. The mass and heat transfers are achieved by the air circulation. (2) The bioreactor is easy to be sealed, and structure is simple. (3) The fermentation tank is a pressure-resistant container, which can be sterilized by steam pressure. (4) In the fermentation process, the pressure of the fermenter always maintains at a closed stage, which is easy to keep sterile. (5) The microbial metabolism could be enhanced by cycle stimulation. (6) The temperature and humidity in the bioreactor are easy to be controlled. (7) The fermentation process is automatic [61].

The gas double-dynamic solid-state fermentation technology is developed from tray solid-state fermentation. Pressure pulsation in the gas double-dynamic solid-state fermentation is accomplished by supercharging and decompression of sterile air. One cycle of pressure pulsation consists of stamping stage, decompression stage, maintaining stage. The time of supercharging stage is long and the curve rises gently. The time of decompression is as short as possible, usually from a few seconds to one minute, to make the solid substrate expanded suddenly. The time of high-pressure stage and maintaining stage can be set according to fermentation process. The pressure pulsation circulation is frequent in microbial logarithmic growth period, and in the delay growth period and stable period, the circulation is infrequent. The circle time ranges from 15 min to 150 min. The wet solid particles are rapidly loosened by the rapid expansion of gas, which enhances the heat and mass transfer [62, 63].

The gas double-dynamic solid-state fermentation technology has groundbreaking significance both in theory and industrial applications. Based on the results of experiment and practice, the technology can be applied to the culture of a wide range of microorganisms, such as bacteria, fungi or actinomycetes.

Gas double-dynamic solid-state fermentation technology breaks the monopoly of submerged fermentation technology in the modern fermentation industry. Due to the unique advantages of this fermentation, liquid fermentation technology could be replaced by gas double-dynamic solid-state fermentation technology to produce

pesticides, cellulase, pectinase, and riboflavin. A lot of new products can be produced by gas double-dynamic solid-state fermentation such as cellulosic ethanol and bioorganic fertilizer. Compared to traditional solid-state fermentation technology, gas double-dynamic solid-state fermentation technology can shorten fermentation time by one third. In addition, it could also be used in the mixed culture fermentation, such as Chinese traditional liquor brewing, and flavor food production. At present, gas double-dynamic solid-state fermentation has been scaled up to 100 m^3.

6.7.3 Silo Composting Reactor

Compost is an important treatment method of organic solid waste [64]. Composting reactor can improve and promote the metabolism of microbes. In the fermentation process, turns heaps, aeration, stirring, mixing, and assisted ventilation facilities are needed to control the temperature and moisture content of the pile. At the same time, the problems of material movement, discharging need to be solved in the composting reactor to improve the fermentation rate, shorten the fermentation period, realize mechanization production. The silo composting reactor is commonly reactor in compost, whose system is a kind of compost silo that the feed input from the top and product discharge from the bottom, mix raw materials by a rotating blade or shaft. This typical composting period is about 10 days, and the volume of composting taken out or raw material repacked every day is about 1/10 of the silo's volume. Due to raw material stacked vertically in the silo, the space this compost system needed is very small. However, composting still need to overcome problems such as compaction, temperature control, and ventilation, and raw material must be mixed evenly before entering the silo for not fully mixed in warehouse.

6.7.4 Normal Force Operation of Packed Bed Reactor

As important representative of normal force, electric and magnetic drew much attention in fermentation. Although there are no industrialization examples currently, research on function and development of the reactor always been active. Sanromán et al. [65] studied the immobilized yeast fermentation to produce ethanol by packed bed reactor. In general, packed bed reactor faces engineering problems that difficult to overcome, such as delivery restrictions, escape of gas taking up the reactor volume, rill flow and pressure from the material gravity. In order to solve these problems, Sanromán et al. [65] introduced continuous pulse operation in packed bed reactor, greatly improved the efficiency of ethanol production without improving microbial immobilized activity.

In addition to the application in the ethanol fermentation, the fluid mechanics characteristics and operation of reactor also discussed. Pulse operation can make

material mixing inside the reactor, improve turbulent degree and the axial dispersion coefficient, these effects are more obvious in high viscosity fluid [66].

6.7.5 *Design of Bioreactor Coupled with Magnetic Field*

Magnetic field is invisible and impalpable special material, which has radiative characteristics of wave-particle. And the magnetic field of magnet is considered as a media for the interaction of magnet [61]. The existence of the magnetic field can affect physiology of organisms, and the influence can be positive stimulus or growth inhibition [62]. Therefore, many researchers tried to use magnetic fields to strengthen bioprocess and obtain ideal effects [63]. For example, Moore [62] used magnetic fields to strengthen growth of Saccharomyces cerevisae. The research showed that magnetic field made biomass accumulation increased by 2.5 times, and ethanol concentration was 3.4 times of the control group, glucose consumption also increased greatly, under the condition of pH 4–5. Perez et al. [67] designed electromagnetic bioreactor. The reactor contains two sets of magnetic field generators, including a set of magnets and a group of helical coil electromagnetic generator. The yield of ethanol fermented by the device is 17% higher than that of control group.

References

1. Modenbach AA, Nokes SE (2013) Enzymatic hydrolysis of biomass at high-solids loadings-a review. Biomass Bioenergy 56(38):526–544
2. Um BH, Hanley TR (2008) A comparison of simple rheological parameters and simulation data for Zymomonasmobilis fermentation broths with high substrate loading in a 3-L bioreactor. Appl Biochem Biotechnol 145(1):29–38
3. Roche CM, Dibble CJ, Stickel JJ (2009) Laboratory-scale method for enzymatic saccharification of lignocellulosic biomass at high-solids loadings. Biotechnol Biofuels 2(1):28
4. Dasari RK, Dunaway K, Berson RE (2008) A scraped surface bioreactor for enzymatic saccharification of pretreated corn stover slurries. Energy Fuels 23(1):492–497
5. Zhang J, Chu DQ, Huang J et al (2010) Simultaneous saccharification and ethanol fermentation at high corn stover solids loading in a helical stirring bioreactor. Biotechnol Bioeng 105(4):718–728
6. Viamajala S, Mcmillan J, Schell D et al (2009) Rheology of corn stover slurries at high solids concentrations-Effects of saccharification and particle size. Bioresour Technol 100(2):925
7. Knutsen JS, Liberatore MW (2010) Rheology modification and enzyme kinetics of high-solids cellulosic slurries: an economic analysis. Energy Fuels 24(12):6506–6512
8. Szijártó N, Horan E, Zhang JH et al (2011) Thermostableendoglucanases in the liquefaction of hydrothermally pretreated wheat straw. Biotechnol Biofuels 4(1):2
9. Zhang Y, Liu YY, Xu JL et al (2011) High solid and low enzyme loading based saccharification of agriculutural biomass. BioResources 7(1):0345–0353

10. Zhao XB, Zhang LH, Liu DH (2012) Biomass recalcitrance. Part I: the chemical compositions and physical structures affecting the enzymatic hydrolysis of lignocellulose. Biofuel BioprodBior 6(4):465–482
11. Modenbach AA, Nokes SE (2012) The use of high-solids loadings in biomass pretreatment-a review. Biotechnol Bioeng 109:1430–1442
12. Koppram R, Tomás-Pejó E, Xiros C et al (2013) Lignocellulosic ethanol production at high-gravity: challenges and perspectives. Trend Biotechnol 32(1):46–53
13. Roberts KM, Lavenson DM, Tozzi EJ et al (2011) The effects of water interactions in cellulose suspensions on mass transfer and saccharification efficiency at high solids loadings. Cellulose 18(3):759–773
14. Felby C, Thygesen LG, Kristensen JB et al (2008) Cellulose–water interactions during enzymatic hydrolysis as studied by time domain NMR. Cellulose 15(5):703–710
15. Selig MJ, Thygesen LG, Felby C (2014) Correlating the ability of lignocellulosic polymers to constrain water with the potential to inhibit cellulose saccharification. Biotechnol Biofuels 7(1):1–10
16. Selig MJ, Hsieh CW, Thygesen LG et al (2012) Considering water availability and the effect of solute concentration on high solids saccharification of lignocellulosic biomass. Biotechnol Progr 28(6):1478–1490
17. Hodge DB, Karim MN, Schell DJ et al (2008) Soluble and insoluble solids contributions to high-solids enzymatic hydrolysis of lignocellulose. Bioresour Technol 99(18):8940–8948
18. Berry SL, Roderick ML (2005) Plant–water relations and the fibre saturation point. New Phytol 168(1):25–37
19. Zhang H, Thygesen LG, Mortensen K et al (2014) Structure and enzymatic accessibility of leaf and stem from wheat straw before and after hydrothermal pretreatment. Botechnol Biofuels 7(1):74
20. Elder T, Labbé N, Harper D et al (2006) Time domain-nuclear magnetic resonance study of chars from southern hardwoods. Biomass Bioenergy 30(10):855–862
21. Liu W, Fan AW, Huang XM (2006) Theory and application of heat and mass transfer in porous media. Science Press, Beijing (in Chinese)
22. Muralidhar K, Swarup J (2007) Theoretical study of inter phase heat and mass transfer in saturated porous media. Int J Eng Sci 35(2):171–185
23. Gu WC (2000) Seepage calculation principle and application. China Building Material Industry Publishing House, Beijing (in Chinese)
24. Wang XD (2006) Basis of seepage fluid mechanics. Petroleum Industry Press, Beijing (in Chinese)
25. Kong XY (2010) Advanced fluid mechanics in porous media. University Science and Technology of China Press, Beijing (in Chinese)
26. Bear J (2013) Dynamics of fluids in porous media. Courier Corporation, New York
27. Chai CJ, Zhang GL (2000) Flow and heat transfer of chemical engineering fluid. Chemical Industry Press, Beijing (in Chinese)
28. Jia SY, Chai JC (2005) Chemical mass transfer and separation process[M]. Chemical Industry Press, Beijing (in Chinese)
29. Jørgensen H, Vibe-Pedersen J, Larsen J, Felby C (2007) Liquefaction of lignocellulose at high-solids concentrations. Biotechnol Bioeng 96(5):862–870
30. Wyman CE (2007) What is (and is not) vital to advancing cellulosic ethanol. Tends Biotechnol. 25(4):153–157
31. Aris R (2012) Vectors, tensors and the basic equations of fluid mechanics. Dover Publictions Inc., New York
32. Miller EE, Miller RD (1955) Theory of capillary flow: I. Practical implications. Soil SciSoc Am J 19(3):267–271
33. Zhao LG, Chu GZ, Bao CS (2002) Non-equilibrium extrapolation method for velocity and pressure boundary conditions in the lattice Boltzmann method. Chinese Phys C 11(4):366 (in Chinese)
34. Smith R (2005) Chemical process: design and integration. Wiley, New Jersey

35. Chen ZP, Zhang XW, Ling XH (2004) Handbook of stirring and mixing equipment design selection. Chemical Industry Press, Beijing (in Chinese)
36. Towler GP, Sinnott RK (2012) Chemical engineering design: principles, practice and economics of plant and process design. Elsevier, Amsterdam
37. Dautzenberg FM, Mukherjee M (2001) Process intensification using multifunctional reactors. Chem Eng Sci 56(2):251–267
38. Reay D, Ramshaw C, Harvey A (2013) Process Intensification: Engineering for efficiency, sustainability and flexibility. Butterworth-Heinemann, Oxford
39. Stankiewicz AI, Moulijn JA (2000) Process intensification: transforming chemical engineering. Chem Eng Prog 96(1):22–34
40. Wang W, Zhuang XS, Yuan ZH et al (2012) High consistency enzymatic saccharification of sweet sorghum bagasse pretreated with liquid hot water. Bioresour Technol 108(2):252–257
41. Zhang X, Qin WJ, Paice MG et al (2009) High consistency enzymatic hydrolysis of hardwood substrates. Bioresour Technol 100(23):5890–5897
42. Sun ZC, Chen HZ, Wang YH et al (2006) Enzymatic hydrolysis of steam-treated straw using a ball shaker. J B Univ Chem Technol 33(6):26–30
43. Chen HZ, Li GH (2013) An industrial level system with non isothermal simultaneous solid state saccharification, fermentation and separation for ethanol production. Biochem Eng J 74:121–126
44. Chen HZ, Liu ZH (2015) Steam explosion and its combinatorial pretreatment refining technology of plant biomass to bio-based products. Biotechnol J 10:866–885
45. Wu ZQ (2006) Solid state fermentation technology and applications. Chemical Industry Press, Beijing (in Chinese)
46. Marcus RD, Leung LS, Klinzing GE et al (1993) Pneumatic conveying of solids: a theoretical and practical approach. Drying Technol 11(4):859–860
47. Xu GR, Hu WF (2009) Fundamentals, equipment and applications of solid-state fermentation. Chemical Industry Press, Beijing (in Chinese)
48. Wen C, Wen T (2011) The design and innovation of air-cushion belt conveyor. Grain Distribution Technol 05:18–24 (in Chinese)
49. Saravacos GD, Kostaropoulos AE (2002) Handbook of food processing equipment. Springer Science & Business Media, Berlin/Heidelberg
50. Holloway MD, Nwaoha C, Onyewuenyi OA (2012) Process plant equipment: operation, control, and reliability. Wiley, New Jersey
51. Xie ZL (2001) Numerical simulation of pneumatic conveying. J B Univ Chem Technol 28(1):22–27
52. Klinzing GE, Rizk F, Marcus R et al (2011) Pneumatic conveying of solids: a theoretical and practical approach. Springer Science & Business Media, Berlin/Heidelberg
53. Chen HZ (2013) Modern Solid State Fermentation. Springer, Netherlands
54. Zhang CF, Bai HM (2014) Space docking mechanism technology of spacecraft. Sci Sin Tech 44:20–26 (in Chinese)
55. Tan J (2011) Development on the four degree manipulation of the material handling. Wuhan University of Technology Institute of Electrical and Mechanical Services, Wuhan
56. Zhao ZM, Wang L, Chen HZ (2015) A novel steam explosion sterilization improving solid-state fermentation performance. Bioresource Technol 192:547–555
57. Qi YZ, Wang SX (2007) Biological reaction kinetics and reactor. Chemical Industry Press, Beijing (in Chinese)
58. Zhang SL (2001) Study on the fermentation processes at multi-levels in bioreactor and its application for special purposes—ptimization and scaling up of the fermentation process based on the parameter correlation method. Eng Sci 3(8):37–45
59. Asenjo JA (1994) Bioreactor system design. CRC Press, Boca Raton
60. Chen DY (2013) Some theoretical problems and applications of nonlinear dynamic analysis and control. Northwest Agriculture and Forestry University
61. Da MM, Muniz JB, Schuler A, Da MM (2004) Static magnetic fields enhancement of Saccharomyces cerevisaee than olic fermentation. Biotechnol Progr 20(1):393–396

62. Moore RL (1979) Biological effects of magnetic fields: studies with microorganisms Cana. J Microbiol 25(10):1145–1151
63. Ramon C, Martin JT, Powell MR (1987) Low-level, magnetic-field-induced growth modification of Bacillus subtili. Bioelectromagnetics 8(3):275
64. Haug RT (1993) The practical handbook of compost engineering. CRC Press, Boca Raton
65. Sanromán A, Roca E, Núñez MJ et al (1994) A pulsing device for packed-bed bioreactors: II. Application to alcoholic fermentation. Bioprocess Biosyst Eng 10(2):75–81
66. Roca E, Sanromán A, Núñez MJ et al (1994) A pulsing device for packed-bed bioreactors: I Hydrodynamic behavior. Bioprocess Biosyst Eng 10(2):61–73
67. Perez VH, Reyes AF, Justo OR et al (2007) Bioreactor coupled with electromagnetic field generator: Effects of Extremely Low Frequency Electromagnetic Fields on Ethanol Production by Saccharomyces cerevisiae. Biotechnol Progr 23(5):1091–1094

Chapter 7
Online Detection of High-solid and Multi-phase Bioprocess Parameters

Abstract Parameter monitoring is the key in high-solid and multi-phase bioprocess, which is also a core problem to be solved in its industrialization process. While solid-state substrate has the characteristics of heterogeneity, poor mobility, low moisture content, and parameters (temperature, moisture content, biomass) with large gradient, resulting in great difficulties for parameters monitoring and control in reaction process and proposing higher requirements for parameters monitoring and control. This chapter focuses on parameters monitoring and control in solid-state fermentation (SSF) and high-solid enzymatic hydrolysis of biomass, in order to obtain more important parameters, which could provide the guidance for optimizing and regulation of the high-solid and multi-phase bioprocess.

Keywords Parameter detection · Parameter control · Solid-state fermentation

7.1 Detection Principle and Methods of High-solid and Multi-phase Bioprocess Parameters

SSF is a typical process of high-solid and multi-phase bioprocess [1, 2]. So far, from the view of the whole fermentation industry, SSF has only occupied a small share of the market. The main reason is that there is lack of the advanced monitoring and control technologies for SSF. In SSF process, parameters monitoring is the key and also is the core problem to be solved in its industrialization process. The information obtained by the detection can help people better understand the whole process of fermentation, so as to improve the fermentation level. At present, parameter monitoring and control in SSF process is lagging, and fermentation processes are mainly controlled by human experience [2–5]. Disadvantages, such as low level of automation, small scale of production, low product yield and poor consistency in SSF, caused by the lagging monitoring and control technology, have become the significant factors restricting the industrialization process of SSF. Therefore, development of simple, real-time, and high-performance measurement and control technologies is very important for SSF [1, 2].

H. Chen, *High-solid and Multi-phase Bioprocess Engineering*,
Green Chemistry and Sustainable Technology,
https://doi.org/10.1007/978-981-10-6352-7_7

7.1.1 Physical Parameters

The high-solid and multi-phase bioprocess system is a complex gas–liquid–solid three-phase system, wherein the porous solid matrix is the main body, gas is the mobile phase and the liquid film attached with the solid matrix is the stationary phase. In SSF process, for example, determination of the temperature, moisture, substrate structure (porosity), and mechanical properties (matrix strength, springiness, viscosity) is the basis for the exploration of heat and mass transfer during fermentation, which is also of great significance for SSF process optimization and regulation to improve the fermentation level. Thus, the physical parameters, such as the porous structure, moisture state and content, rheological properties, thermal properties and mechanical properties, are key factors to be detected in high-solid multi-phase bioprocess.

At present, the SSF industries are mostly in the extensive operations or in "black box" experiments. A limited number of parameters (CO_2 and O_2, temperature) can be detected online. Substrate porous structure, moisture, and mechanical properties are usually analyzed by offline methods. The porous structure of biomass can be measured by an offline mercury porosimeter [6] (Fig. 7.1a) or a specific surface analyzer (Fig. 7.1b). The moisture content was often measured by the offline sampling and drying method, and moisture distributions and states can be measured by low-field nuclear magnetic resonance imaging (NMR) (Fig. 7.1c) [7]. The mechanical properties can be measured by a texture analyzer (Fig. 7.1d).

During enzymatic hydrolysis of biomass, in addition to the sugar measurement by traditional offline high-performance liquid chromatography HPLC or DNS (3,5 dinitrosalicylic acid) methods, laser particle analyzer was often used offline to measure the dynamic changes of particle size (Fig. 7.1e). The rheometer was often used to measure the rheological properties, such as viscosity and shear stress (Fig. 7.1f) [8–13]. Microscopic photograph technology was used to observe the particles degradation in hydrolysis process [14]. To date, substrate properties (particle size, specific surface), mechanical properties (matrix strength, stress, and strain) in the enzymatic hydrolysis process cannot be real-time captured, and the online control and optimization of the enzymatic hydrolysis process have not been achieved.

7.1.2 Chemical Parameters

The chemical parameters in high-solid and multi-phase bioprocess mainly refer to the substrate and product composition. Determination of the variation of substrate and product composition and content is very important for judging the utilization of the substrate, the product generation, and the fermentation performance.

Near-infrared spectroscopy (NIR) is one of the important online monitoring technologies for SSF (Fig. 7.2) [15, 16]. From the view of principle, NIR can

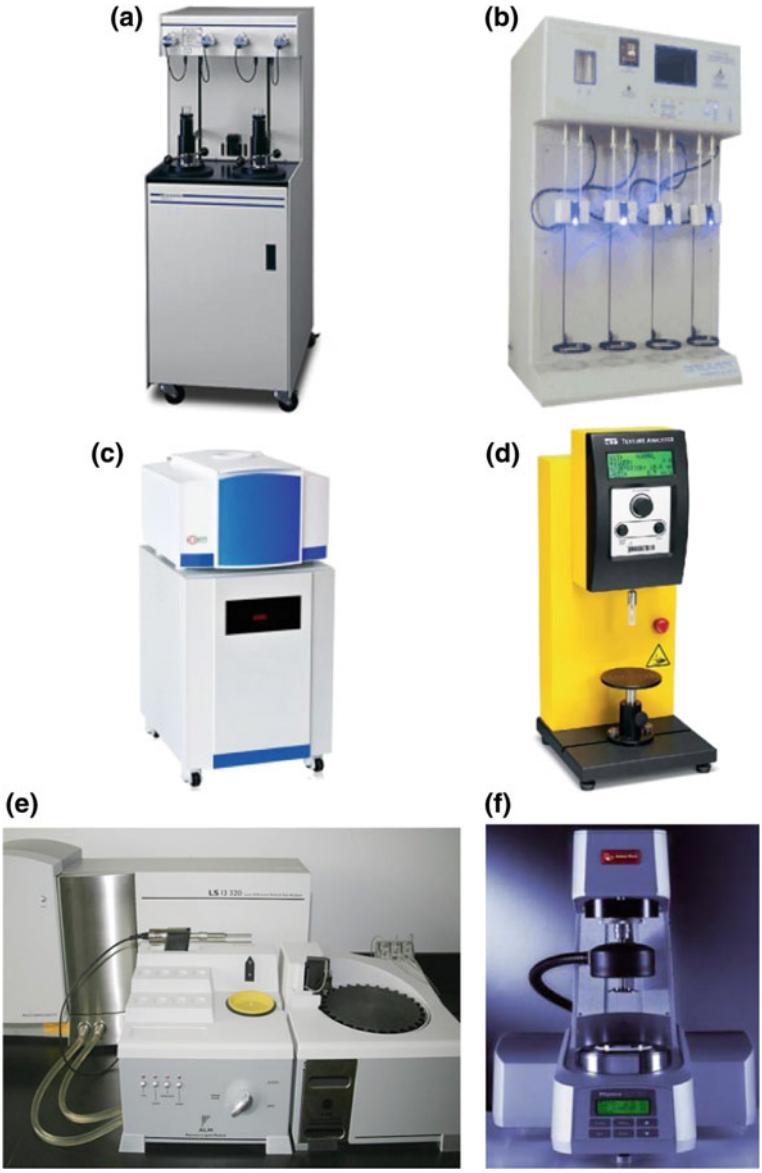

Fig. 7.1 Apparatus for physical parameters detection in high-solid and multi-phase bioprocess **a** Mercury Porosimeter; **b** Ratio surface area analyzer; **c** Low-field NMR and MRI; **d** Texture analyzer; **e** Laser particle size analyzer; **f** Rheometer

predict the chemical parameters, such as biomass, water, ash, volatile matter, fixed carbon, cellulose, hemicellulose, lignin, crude protein, soluble sugar and calorific value, with the advantage of fast and nondestructive, which is favored by the

Fig. 7.2 Near-infrared spectroscopy

majority of scientific researchers. However, this method still has disadvantages, such as high cost, small monitoring scope, and large amount of data needed for calculation of model parameters. Therefore, it has not been widely used in SSF industries.

Ultraviolet spectrophotometry was reported in online determination of enzyme protein in liquid enzymatic hydrolysis [17, 18]. However, this method is limited to liquid reaction system and not applicable to the determination of solid-state substrates. There is lack of effective monitoring of intermediate products or metabolites during the reaction.

7.1.3 Biological Parameters

Determination of biomass variation during SSF is the basis for establishing the kinetics of microbial growth [1, 2]. During SSF, fungal hypha and solid matrix are intertwined with each other, so they are difficult to be separated. Thus, the direct counting method is not suitable for determining the biomass. Subsequently, chemical methods have been developed for estimating biomass based on the amount of carbon dioxide produced by microbial growth and metabolism or the concentration of characteristic components, wherein the former is based on the amount of carbon dioxide, and the latter is according to measuring glucosamine, ergosterol, and other cell wall chemical compositions. Those chemical methods cannot avoid the interference of impurities and cannot obtain the real-time results of biomass. Thus, online monitoring of biomass has been the urgent problem to be solved for SSF.

Therefore, the online monitoring methods and equipment for temperature, moisture, biomass, and substrate physical properties (particle size, porous structure, strength, viscosity, springiness, heat conductivity coefficient, thermal diffusion coefficient) of substrate in the process of SSF and enzymatic hydrolysis are imminent, and they would strengthen the understanding of biochemical conversion. Meanwhile, they might promote the biomass biochemical transformation industry to achieve a real breakthrough.

7.1.4 Analysis and Comparison of Various Nondestructive Testing Technologies

Nondestructive testing consists of a wide group of analysis techniques used in science and technology industry to evaluate the properties of a material, component, or system without causing damage [19]. Because nondestructive testing does not permanently alter the detected objects, it is a highly valuable technique that can save both money and time in product evaluation, troubleshooting, and research. Nondestructive testing is commonly used in mechanical engineering, petroleum engineering, electrical engineering, civil engineering, systems engineering, aeronautical engineering, medicine, and art [19].

Nondestructive testing is an indispensable tool for modern industrial development. Common nondestructive testing methods include ray, ultrasonic, electromagnetic, infiltration, eddy current, microwave, and infrared thermal imaging.

Ultrasonic is a kind of mechanical waves, the frequency of which is 20 kHz–200 MHz. It features high frequency, short wavelength, high energy, good penetrability, and small attenuation in propagation in liquid and solid. Ultrasonic is very important in the fields of geology and medicine. The detection principle of ultrasonic is based on the differences of various acoustic characteristics in the medium. The characteristics such as Doppler shift are generated by reflection, refraction, scattering, diffraction, attenuation, and relative movement when acoustic waves are in two different interfaces, thus the received waves carry various information of the physical and mechanical properties of the measured medium. In addition, other advantages of the ultrasonic nondestructive testing are the low cost of equipment, small size, portable probe with plug and play, shape control and high precision and speed, which meet the needs of industrial production. Ultrasonic diagnostic testing is one of the most widely used methods in nondestructive testing.

From a theoretical perspective, the sound velocity, attenuation, impedance, and scattering characteristics of ultrasonic carry much information of the materials, which can be used in the detection and characterization of the surface morphology, structure and mechanical properties, and are very suitable for the online detection of basic properties such as particle size, porosity, and mechanical properties during SSF process. However, the physical properties of the ultrasonic result in the limitation for application. Ultrasonic cannot pass through the interfaces with very different impedances, such as interface between air and solid as well as air and liquid, and it needs to couple the probe with solid or liquid to discharge the air. On the basis of this, in medical ultrasound detection, coupling agent was commonly used in coupling probe and human skin.

SSF medium is a multi-phase system composed of gas–liquid–solid phases and microorganism. The gas is continuous phase, and the particle size is not uniform, resulting in the various and complex interfaces of medium. Ultrasonic attenuation in such medium is serious, and penetration ability is poor. For example, penetration distance of 50 kHz ultrasonic is not more than 2 mm, so it is difficult for ultrasonic

to deeply scan solid-state substrate. However, based on the principle of ultrasonic reflection, it is possible to characterize the morphology of the SSF medium.

Computed tomography (CT) is commonly used in medical, aerospace, and military industry, which can obtain the three-dimensional imaging of objects by two-dimensional scanning. Based on the high sensitivity and precision, it plays a more and more irreplaceable role in the medical and military fields. However, the biggest obstacle in its promotion and application is the high cost, which is not suitable for large quantities of applications in general industrial production. Therefore, CT is not suitable for online monitoring of the SSF process.

Near-infrared (NIR) spectroscopy is the fastest growing and most spectacular spectroscopic analysis techniques since the 1990s. It can provide the similar information about frequency doubling and frequency absorption of hydrogen as classical mid-infrared spectrum. Compared with the mid-infrared spectrum, NIR has strong penetrating power, which need not sample preparation, does not destroy the sample, is suitable for quantitative analysis, and can achieve long-distance online detection. Because of these characteristics, NIR has become one of the most common detection technologies for SSF in recent years. NIR has been used for the online determination of organic acids, polysaccharides, water, pH, and biomass in SSF processes. However, this method still has the disadvantages of high cost and small monitoring scope, and it has not been applied in large scale in SSF industry.

The development of microwave detection technology is relatively late, while it can pass through the air easily without coupling agent. In recent years, it has been applied to nondestructive testing of nonmetallic materials. The attenuation is large when microwave passes through the metal conductor, while it can penetrate very thick nonmetallic materials, so it can be used to detect the internal structure and defects of nonmetallic materials. The basic principle of microwave detection is the comprehensive interaction of microwave with material. On the one hand, microwave generates reflection, scattering, and transmission at the discontinuous interface. On the other hand, the microwave interacts with the material (polarization), and then the microwave field (amplitude, frequency, and phase) is influenced by two dielectric parameters (dielectric constant and dielectric loss tangent) and geometrical parameters (material size, shape) of materials. It is well known that the dielectric parameters of a material are function of material composition, structure, uniformity, orientation, moisture content, and so on. Therefore, the properties of the material can be inferred from the variation of microwave field.

It can be seen that the microwave detection makes up for the deficiency of ultrasonic detection of nonmetallic porous materials, with characteristics of no coupling agent, noncontact measurement, and fast detection. Microwave detection is very suitable for the detection of parameters of SSF process. The shortcoming is that the microwave detection technology is relatively immature, and the testing equipment and model algorithm is not perfect, so it is not applied in the SSF industry currently.

Infrared thermal imaging detection is out of the conventional nondestructive testing technologies (ray, ultrasonic, electromagnetic, infiltration, and eddy current). However, infrared thermal imaging is developing rapidly, and it has been widely

used in the aerospace, military, power, and many other fields. Infrared thermal imaging has the characteristics of optical scanning, video display, rapid measurement, and online temperature mapping. The detection accuracy of infrared thermal imaging is high up to 0.05 °C, and the resolution is up to nanometer level. Infrared thermal imaging has great advantages and potential in SSF (due to its high resolution and temperature mapping, the real-time growth of microorganism can be achieved).

7.1.5 Development Trend of Detection Technologies

Based on the analysis and comparison of various detection technologies in the Table 7.1, from the view of principle and economy, it can be concluded that SSF process can be online monitored by infrared thermal imaging (which is used to dynamic monitor the surface temperature and hypha distribution), near-infrared absorption spectroscopy (which is used to detect chemical information such as water content, pH, polysaccharide, and cellulose), and microwave detecting technology (which is used to detect physical information such as medium moisture, particle size, and structure).

In addition, based on the dynamic correlations between the physical properties of the medium and the fungus growth, the mechanical properties of the medium, such as hardness, cohesion, viscosity, elasticity and deformation, can be measured online by dynamic strain gauge, which could reflect dynamic changes of medium porosity, strength, viscosity, elasticity, and even water content. The real-time heat transfer characteristics and the medium temperature distribution in SSF process can be obtained by the online thermal conductivity meter and the temperature sensor, which could guide the control of ventilation, spraying water, or other operations.

Owing to the deficiency for current hardware sensor, some important parameters in SSF process cannot be obtained. Therefore, developing soft measurement technology is the trend for monitoring complex process parameters in high-solid and multi-phase bioprocess. The basic idea of soft measurement is to organically combine the theory of automatic control with the knowledge of production process. Computer technology is used to select important variables that are difficult to measure or temporarily unable to measure, and to construct some mathematical relations to infer or estimate, then to replace the function of hardware. Thus, soft measurement technology is important for parameters monitoring and controlling of modern process engineering, which has been used in more and more industrial processes.

In summary, the trend for parameters monitoring and controlling of high-solid and multi-phase bioprocess is developing advanced hardware sensors and novel analytical instruments. Furthermore, development of economical, efficient, real-time, high-throughput soft measurement is urgent to meet the requirements of large-scale industrial production.

Table 7.1 Principle, advantages and disadvantages of various detection technologies

	Technology	Principle	Advantages	Disadvantages	Suitable
Magnetism	Nuclear magnetic resonance	Relaxation time differences of H/C Proton	The qualitative, quantitative and indirect characterization of the structure of material	Difficult to scale up, and high cost	×
Light	Infrared spectroscopy (absorption spectrum)	Vibration and rotation of the molecules group	online nondestructive testing of material composition, structure and mechanical properties, with a portable probe	High cost	√ ?
	Raman spectroscopy (scattering spectra)	Molecular vibration and rotation	Online, nondestructive testing of material composition, structure and mechanical properties, with a portable probe; not affected by water, can achieve qualitative and quantitative spectral analysis of water, powder, block and surface media	High cost	√ ?
	Ultraviolet spectrum (UV) (absorption spectrum)	Electron transition, the selective absorption of spectra		Liquid samples required transparent, not suitable for sample of solid phase	×
	Fluorescence spectrum (absorption spectrum)	Fluorescent light emitted under the irradiation of excitation light			×
	X-ray diffraction (XRD)			Determine the crystal structure	×

(continued)

Table 7.1 (continued)

	Technology	Principle	Advantages	Disadvantages	Suitable
	Ultrasonic inspection	Doppler shift occurs at the two different interfaces by reflection, refraction, scattering, diffraction, attenuation, and relative motion	Online, nondestructive, portable, low cost	Large gas–solid, gas–liquid interface attenuation, poor penetration; need coupling agent; difficult to detect small crack(<1 mm)	×
Wave	Microwave Testing	Reflection, scattering, transmission occurred at the discontinuous interface, on the other hand, the microwave can also be polarized with the material being tested, measuring the electrical parameters and geometric parameters	Easy to penetrate the air medium, do not need coupling agent, suitable for nonmetallic porous media measurement, noncontact measurement, fast.	The technology is not yet mature, currently.	√ ?
Machine vision	Ultraviolet microscopy			Imaging system installation conditions is hard; high cost; Less information can be stripped from the image	×
	Fluorescence microscopy				
	Confocal microscopy				
	Scanning electron microscope				
	Atomic Force Microscope				
	Infrared thermography	Transform the invisible infrared radiation into recognizable temperature maps	Noncontact, no damage, high precision, high resolution, fast, can provide more information	Only detect surface	√

7.2 Novel Online Detection Methods of High-solid and Multi-phase Bioprocess Parameters

7.2.1 Imaging Nondestructive Detection Method of High-solid and Multi-phase Bioprocess

Rapid quantifying the concentration of glucose solutions is vital in the process high-solid and multi-phase bioprocess. The development of cheap, fast, and robust standard analysis techniques is of great importance. Nowadays, the colorimetric methods (such as the Anthrone method, phenol–sulfuric acid method and 3,5-dinitrosalicylic acid method) are still widely used, because of their simplicity and low cost. However, the measurement process is carried out in a spectrophotometer, the low throughput of which presents practical difficulties of usage for quick detection [20].

Color is a three-dimensional psychophysical phenomenon [21]. By defining a color space, color information can be transformed into numerical values, color library data, etc., that can be treated as analytical information [22]. By treating colors as digital information, not only the "colors" themselves can be made use of but algorithms also can be applied to mine the numerical values converted from color information [23]. With the help of a camera and data processing software (such as Matlab, R, etc.), the image of thousands of samples can be recorded within seconds and rapidly transformed into a measurement report on a personal computer. Until now, digital color analysis has found applications in the chemical medicine, biological, drug and food analysis fields. Compared to conventional methods, digital color analysis has many fundamental advantages, including (1) a higher throughput, (2) a shorter analysis time, (3) an improved performance and reliability, (4) the potential for in situ operation, and (5) the potential for real-time analysis. Furthermore, the digitized color data are easily integrated with automated algorithms to achieve automated operation.

In the present chapter, we attempted to set up a digital color analysis method to substitute the use of a spectrophotometer in colorimetric glucose detection. The suitable calculation algorithm for glucose detection using color information was investigated. Experimental tests are also performed to compare the accuracy and efficiency of the proposed method with that of the traditional DNS and high-performance liquid chromatography (HPLC) method. The feasibility for the detection of other reducing sugars was also investigated. It is expected to open a new and effective way in the efforts toward material measurement and biochemical analysis [20].

7.2.1.1 Methods Establishment

The Traditional DNS Method In the traditional DNS method, 0.5 mL of the standard glucose solvent with concentrations of 0–3 g/L was added to colorimetric

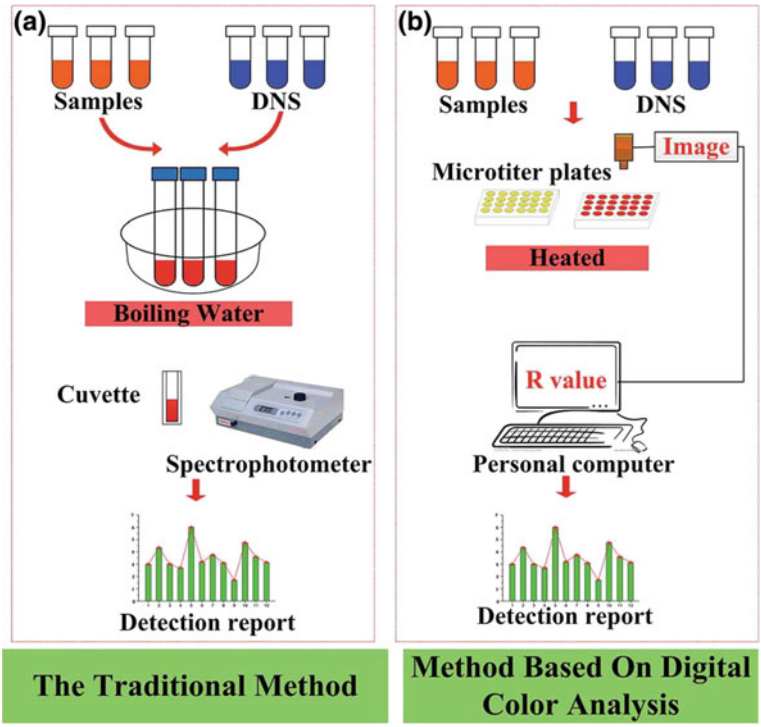

Fig. 7.3 Procedure comparison between the traditional method and digital color analysis method. **a** shows the working procedure of the traditional OD method and **b** shows the working procedure of the digital color analysis method [20]

tubes and diluted with water to 2 mL. Then 2 mL DNS broth was added and kept in the boiling water bath for 2 min. After being cooled in running tap water, the solution was diluted to 10 mL using water and scanned for the absorption spectrum against a blank solution within 3 min using a spectrometer (UV2550, Shimadzu, Japan) at OD540. The experimental procedure of the traditional DNS method was shown in Fig. 7.3a.

Color Development Recording The working procedure of the digital image processing method for measurement was shown in Fig. 7.3b. In this method, glucose samples were detected in a 48-well microtiter plate (as shown in Fig. 7.4a). Each microtiter well was loaded with 1 mL water in advance. 100 mL of the samples and 100 mL DNS were transferred into the 48-well microtiter plate and mixed using a pipette (A0632010, Eppendorf, Germany). The final volume of each well was 1.2 mL. Then, the plate was placed in a thermostat heater (MT70-2, Hangzhou Aipu Instrument and Equipment Co., Ltd, China) at 100 °C for color development. The image of the samples was taken by a digital camera (TP614000B, Hangzhou ToupTek Photonics Co., Ltd, China) after or during the color development. To avoid impact from the environment, the images were taken

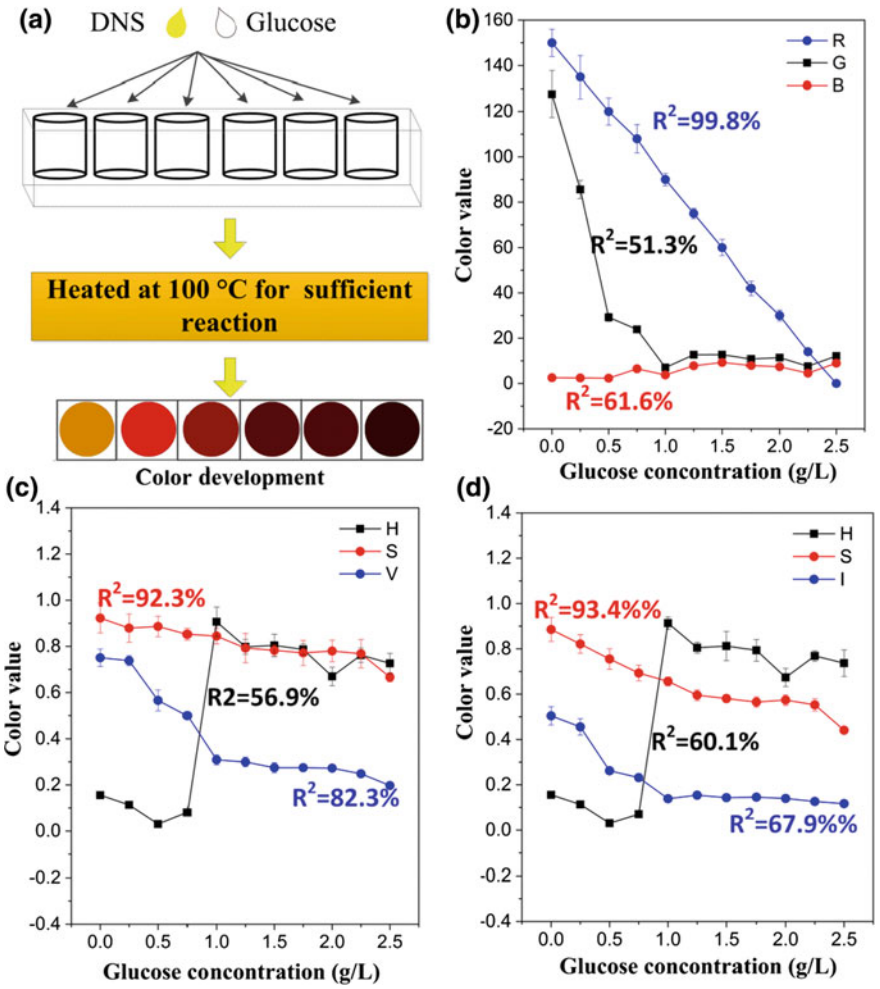

Fig. 7.4 The quantitative relation between primary colors and glucose concentration in the DNS method. **a** shows the color development procedure in the 48-well microplate. **b–d** show the quantitative relation between glucose concentration and the primary colors from the RGB, HSV and HSI color spaces, respectively [20]

in a special box equipped with a light and a microwell plate heater (WS-350P/WS-350B, Shinetek Instruments Co., Ltd, Beijing, China).

Before delving into the work, we shall briefly describe the definitions and differences between the color models we considered.

RGB. Color in the RGB system is produced by any additive or subtractive mixture of the spectra of the three primary colors of red (R), green (G), and blue (B). Their corresponding monochromatic primary stimuli occur at 700, 546, and 436 nm, respectively. On an 8-bit digital system, color is quantified by numeric

tristimulus R, G, B values that range from 0 (darkness) to 255 (whiteness) [24]. The three colors were 3 color matrixes [22]. In our research, the color value is the average value of the corresponding color matrix, which was analyzed by Eq. (7.1).

$$R = \frac{\sum_0^j \sum_0^i R(x, y) \text{ form R color matrixin RGB color space}}{j \times i} \tag{7.1}$$

HSV Hue-saturation-value (HSV) and hue–saturation–intensive (HSI) are the two most common cylindrical coordinate representations of points in an RGB color model. HSV describes colors (hue or tint) in terms of their hue, shade (saturation) and their brightness (value). It was first used to describe colors by Alvy Ray Smith in 1978. Comparing with the RGB system, HSV is a very intuitive way to represent colors in some applications, such as object tracking, human face detection, etc. In the calculation processing, HSV values were first converted from RGB following the method that Ford and Adrian proposed [25], which is achieved in Matlab 2014a (Maths, USA) with the function rgb2hsv from the Image Processing Toolbox. Then the average values of the corresponding color matrix (HSV) were calculated with the function mean [26].

HSI HSI model defines a color model in terms of its components, which refers to the hue, saturation, and color intensity. This space has the ability to separate the intensity of the intrinsic information of color; therefore, it is suitable for processing images that present lighting changes. The hue and saturation in the HSI model are a bit different from those in the HSV model because of the differences in the conversion equations. In the calculation processing, HSI values are first converted from RGB following the method that Ford and Adrian proposed [25]. Then the average values of the corresponding color matrix (HSI) were calculated with the function mean [26].

All the parameters used for color description are dimensionless. The scale of the parameters is summarized as follows: RGB model: R, 0–255; G, 0–255; B, 0–255; HSV model: H, 0.0–1.0; S, 0.0–1.0; V, 0.0–1.0; HSI model, H, 0.0–1.0; S, 0.0–1.0; V, 0.0–1.0.

Based on our research, the R2 (correlation coefficient) values between the primary colors and glucose are: (a) RGB color space: R, 99.8; G, 51.3; B, 61.6%; (b) HSV color space: H, 56.9; S, 92.3; V, 82.3%; (c) HSI color space: H, 60.1; S, 93.4; I, 67.9%.

Nonlinear t Method Figure 7.5 illustrates the colorimetric reaction between the DNS reagent and glucose. As shown, it is the formation of 3-amino-5-nitrosalicylic acid that leads to the color development. According to the law of mass action, the formation rate of 3-amino-5-nitrosalicylic acid was controlled by the concentration of glucose and DNS. Assuming the reaction obeys second-order reaction kinetics, the generation rate of 3-amino-5-nitrosalicylic acid can be determined in accordance with Eq. (7.2):

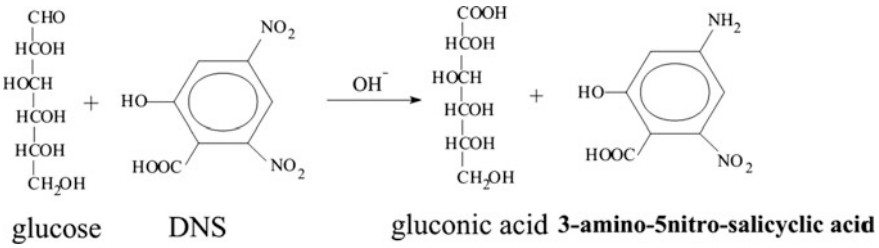

Fig. 7.5 Colorimetric reaction of DNS reagent and glucose [20]

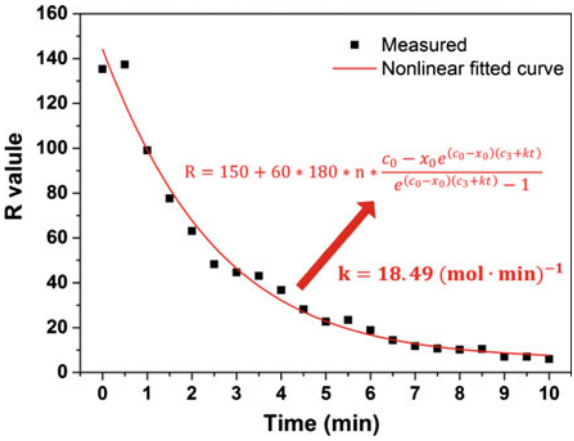

Fig. 7.6 Calculation of k (reaction rate constant) for the color development dynamics model [20]

$$\frac{dc}{dt} = k(x_0 - c)(c_0 - c) \tag{7.2}$$

where c is the concentration of 3-amino-5-nitrosalicylic acid produced (mol/L), x_0 is the initial concentration of glucose before the reaction occurred (mol/L) and c_0 is the initial concentration of DNS before the reaction occurred (which is 0.0276 mol/L in our research). t is the reaction time (min). k is the reaction rate constant calculated by the Arrhenius formula [27] Eq. (7.3):

$$k = k_0 e^{-E_0/TR} \tag{7.3}$$

where k is the reaction rate constant, k_0 is the frequency factor (min^{-1}), E_0 is the activation energy (kJ/mol), R is the universal gas constant, R is 8.314 J/mol/K and T is the reaction temperature, which is set at 100 °C throughout our study. It should be noted that k is a fixed value in a specified reaction under a stable temperature.

Therefore, by integrating Eq. (7.3), the formation of 3-amino-5-nitrosalicylic acid (also the glucose consumption kinetic equation) was achieved as Eq. (7.4):

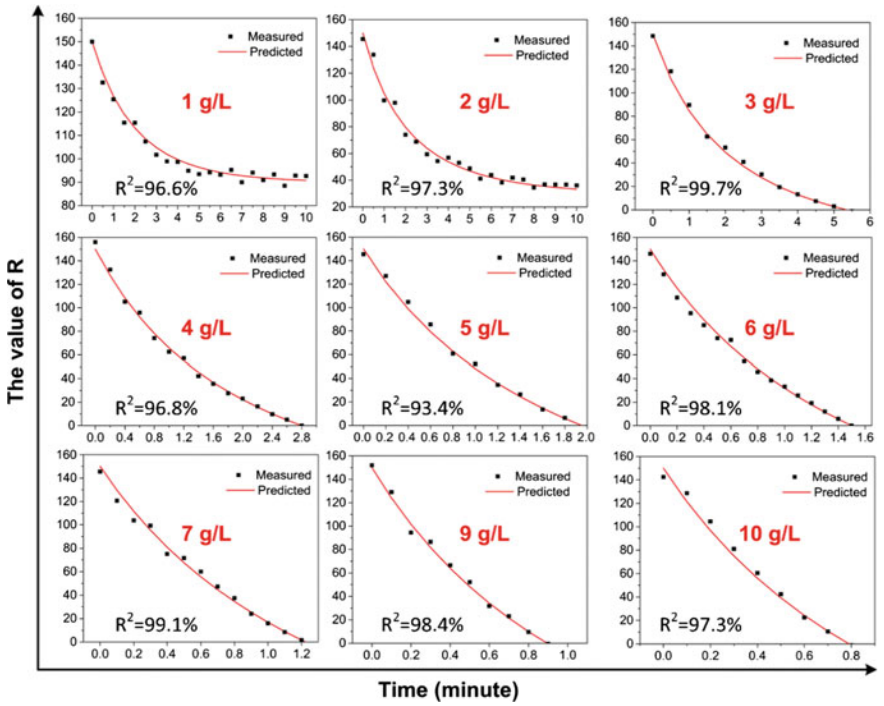

Fig. 7.7 The measured and predicted color development processes of samples with different glucose concentrations at 100 °C. The dots stand for the experimental data and the red lines stand for the predicted values by the kinetic model of color development [20]

$$c = -\frac{c_0 - x_0 e^{(c_0 - x_0)(c_3 + kt)}}{e^{(c_0 - x_0)(c_3 + kt)} - 1}, \tag{7.4}$$

where $c_3 = \frac{In(\frac{c_0}{x_0})}{c_0 - x_0}$ $(c_{t=0} = 0)$.

Our experiments proved that this kinetic model also applies to other reducing sugars including xylose, fructose, and maltose, except for different values of k.

7.2.1.2 The Relationship Between Primary Colors and Glucose Concentration in the DNS Method

Color is commonly measured using a spectrophotometer in the colorimetric methods. However, color can be broken up into different primary colors in different color spaces. Different color models are suitable for different purposes, including descriptive purposes and analysis purposes [24]. The best suited color model(s) can provide the best result. Therefore, to determine the best suited model for the quantitative description of the DNS method, the images of the reacted broth with

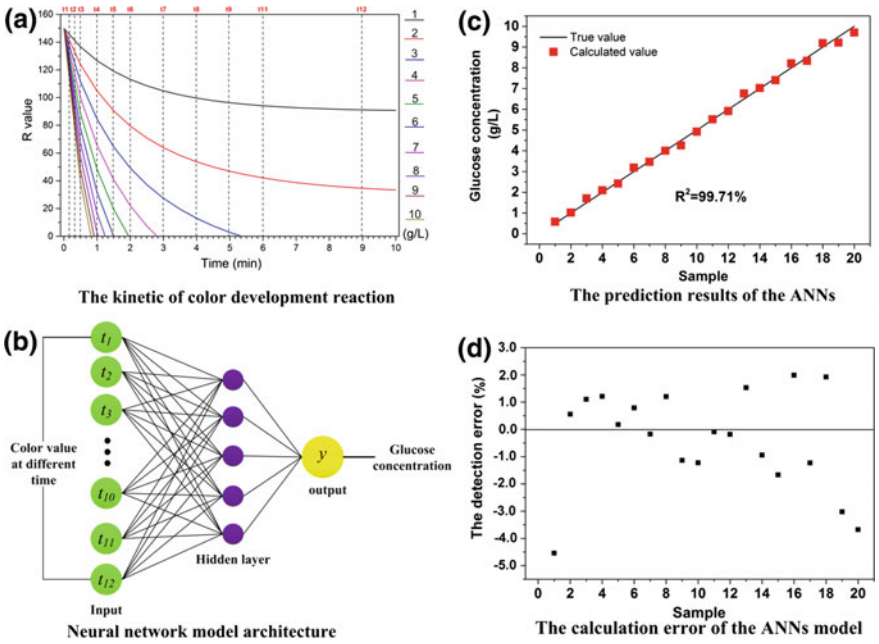

Fig. 7.8 The ANNs model for detection of high concentration glucose. Figure 7.8a showed the kinetics of color development reactions with different glucose concentrations (1–10 g/L); Fig. 7.8b showed the architecture of the neural net model; Fig. 7.8c showed the prediction results of the ANNs (only 20 samples were given). The dots stand for the calculated values by ANNs; Fig. 7.8d showed the calculation error of the ANNs model [20]

different glucose concentrations (0, 0.5, 1, … 2.5 g/L) were analyzed in different color models (RGB, HSV, HSI). The correlationship analysis between the primary color values and glucose is given in Fig. 7.8.

The correlation coefficients range from 51.3 to 99.8% and the best result was achieved by R from the RGB color space (99.8%). A. S. Raja et al. also found that RGB data of a color image of the assay is suitable for blood glucose measurement [28]. As the comparison group, the R^2 (correlation coefficient) value of the traditional method was 99.6% (data not shown). It means that the accuracy of the concentration measurements obtained using R (RGB color space) is comparable to that of the measurements obtained using the traditional method. Furthermore, this parameter is stable, simple to calculate and easily obtained from commercial devices such as scanners and digital cameras.

A fitting process was conducted on the R value and glucose concentration. The result is given in Eq. (7.5):

$$R = 150 - 60 \times Glu, \tag{7.5}$$

where R is the R (or red) value (from the RGB color space) of the reacted broth image and Glu is the glucose concentration of the samples for detection (g/L).

By converting Glu into the true molar concentration in the mixture, Eq. (7.5) can be written as follows:

$$R = 150 - 60 \times 180 \times c, \tag{7.6}$$

where c is the molar concentration of the glucose sample for measurement (mol/L); 180 is the molecular weight of glucose (g/mol).

7.2.1.3 The Calculation Algorithm for the Direct Calculation of a High Concentration of Glucose by Color Analysis

Obviously, samples with less than 2.5 g/L of glucose can be directly calculated by the digital color analysis method Eq. (7.3). However, the R value of any sample with more than 2.5 g/L of glucose falls to zero if the reaction proceeds completely. In other words, the digital color analysis method can only measure the samples with less than 2.5 g/L of glucose in this case. However, how to expand the measurement range seems worth studying. It is because a large detection range can not only liberate the operators from the time-consuming dilution operations, but also avoid some possible human bias in measuring. A large detection range will bring convenience to many bioanalysis applications, such as strain screening [29], fast sugar quantification in food [26] process monitoring [30, 31].

To extend the detection range of color analysis, there are two protocols in the toolbox: a nonlinear t based on color development dynamics and an artificial neural net trained with the experimental data of the R values and glucose. Therefore, the goal of the following part was to find the suitable strategy for the direct detection of a high concentration of glucose.

7.2.1.4 Nonlinear Fit Based on Color Development Dynamics for the Direct Detection of a High Concentration of Glucose

Color development dynamics models are widely employed for chemical measurements [22, 32]. Conventionally, to obtain a sufficiently accurate and robust mathematical model for a color development process is a time-consuming and harsh task, due to the exceeding complexity in the accurate recording of the colors and glucose concentration. However, with the help of a digital camera and Eq. (7.6), this can easily be achieved by: (1) recording the color development process, (2) extracting the color values from the images, and (3) fitting the data to the kinetic equation.

The kinetic equation for the color development was deduced in the experimental section. The color development kinetics Eq. (7.7) can finally be achieved by combining Eqs. (7.4) and (7.6):

$$R = 150 + 60 \times 180 \times n \times \frac{c_0 - x_0 e^{(c_0 - x_0)(c_3 + kt)}}{e^{(c_0 - x_0)(c_3 + kt)} - 1}, \tag{7.7}$$

where n is the dilution factor, which is 12 in our study. $c_3 = {In\left(\frac{c_0}{x_0}\right)}/{c_0 - x_0}$ (calculated from $C_{t=0} = 0$); k was calculated according to the Arrhenius equation [27] Eq. (3). Because the operation is set at 100 °C throughout our study, k is a fixed value.

To determine the parameter k, we recorded the dynamic process of the color development of a 2.5 g/L glucose sample at 100 °C (as shown in Fig. 7.6). The value of k was determined to be 18.49 $(\text{mol.min})^{-1}$ by fitting the experimental data to Eq. (7) in Matlab 2014a (Maths, USA) with the nonlinear regression toolbox. Therefore, the kinetic curves for different concentrations of glucose were given in Fig. 7.7 (shown by the red lines).

For verifying the accuracy of the calculation result, the measured data of glucose samples with different concentrations and the predicted data by the kinetic equation above were compared in Fig. 7.7. All of the correlation coefficients between the measured and predicted data are above 93%, validating the high accuracy and validity of our proposed model.

So, based on the color development dynamics achieved, the calculation of glucose by a nonlinear t method can be achieved by: (1) recording the image at several time points, and (2) fitting the data of the R values (R > 0) from different time points to Eq. (7.7). With the help of commercial digital and data analysis software (Matlab, R, and Origin), the image recording and nonlinear t process can be carried out automatically.

To determine the accuracy of the nonlinear t method, 20 samples were used for evaluation. The R data from nine time points (0.5, 1, 1.5, 2.0, 3.0, 4.0, 5.0, 6.0, and 9.0) for each sample were used for the nonlinear t. R^2 of the measured values and the true values was 91.3%. The measurement error gets larger with the increase in glucose concentration detected, and the maximum error (10.9%) was observed in the detection of samples containing 20 g/L of glucose.

7.2.1.5 Artificial Neural Nets for the Direct Detection of a High Concentration of Glucose

Calculation tasks can be handled with artificial neural net (ANN) techniques without any a priori knowledge requirements on the interdependencies of the process variables, thus offering a direct approach a direct approach [33]. Artificial neural nets have the capability to learn from known input/output vector pairs through iterative training, and to handle highly nonlinear problems [34]. By using ANNs trained with experimental R data at specified given time points, it is possible to obtain the calculation results with high accuracy.

In our experiments, the specified points in time were set at 0.2, 0.4, 0.6, 1, 1.5, 2.0, 3.0, 4.0, 5.0, 6.0, and 9.0 min (Fig. 7.8a). The neural net model architecture is

Table 7.2 Comparison of different calculation algorithms for glucose detection by color analysis [20]

Model name	Detection range (g/L)	Detection precision (g/L)	Formula for data fitting	Number of image needed for calculation	Advantage	Disadvantage
Linear fit	0–2.5	0.07	Eq. 2.7	1	Easy to operate;	Low detection range; Dilution pretreatment is needed for high concentration glucose detection.
Nonlinear fit	0–10	0.20	Eq. 2.8	≥ 3	Precise;	Requirement of knowledge on color development dynamics
ANNs	0–10	0.10	None	≥ 3	Highly precise;	

shown in Fig. 7.8b. 80 samples were used for training and the other 20 were used for testing. Less than 200 iterations were needed for proper learning. The detection results are given in Fig. 6c and d. R^2 was 99.71% and the largest error was 4.7%, implying that empirical models derived from ANN can be used adequately to detect a high concentration of glucose (>2.5 g/L).

The comparison of the three calculation algorithms in this chapter is summarized in Table 7.2. (1) The linear t algorithm is the easiest one, which is also the most widely employed one in traditional colorimetric methods. However, it can only be used for the measurement of a low concentration of glucose (0–2.5 g/L). (2) The nonlinear t method can be applied to the measurement of a higher concentration of glucose (0–10 g/L) with higher accuracy. However, it must be based on the knowledge of color development dynamics. Before application, it is required to carry out sufficient preliminary experiments to set up the suitable kinetic models. This disadvantage hinders its application in the detection of other reducing sugars. (3) ANNs exhibit obvious advantages in practicality, accuracy, and calculation robustness. The training of ANNs is easy and does not require a priori process knowledge, making the ANNs process have great potential for the detection of other sugars.

7.2.1.6 Rapid Detection of Glucose on a 48-Well Plate by Color Analysis

Based on the studies above, we designed the quick and high-throughput measurement method shown in Fig. 1. The method includes three main steps: (1) mix the glucose solution sample with DNS in the 48-well microtiter plate and get them

Table 7.3 Comparison of the detection results using traditional DNS, HPLC and digital color analysis method for glucose measurement [20]

Method	Evaluation criterion	Standard samples						
		0.5 g/L	1 g/L	2 g/L	4 g/L	6 g/L	8 g/L	10 g/L
DNS method	Mean	0.49	0.98	2.15	3.55	3.42	3.64	3.71
	Maximum error	2.62%	3.12%	4.6%	12.29%	55.36%	67.33%	82.38%
	*V-Coefficient	3.42%	4.65%	6.98%	38.96%	44.91%	38.97%	43.63%
HPLC	Mean	0.50	1.02	1.98	3.99	5.96	8.05	9.96
	Maximum error	1.13%	1.56%	4.65%	3.26%	4.36%	4.23%	4.32%
	*V-Coefficient	3.61%	3.64%	4.12%	3.78%	4.12%	3.89%	4.12%
Color analysis method	Mean	0.52	0.98	2.11	4.32	5.81	8.43	9.84
	Maximum error	5.13%	6.23%	8.96%	6.72%	8.88%	8.04%	7.75%
	*V-Coefficient	4.51%	5.92%	6.88%	5.78%	4.97%	7.59%	8.41%

to react for the corresponding optimal reaction time under an appropriate temperature (usually 100 °C), (2) extract the R value of the reacted broth image by image processing, and (3) calculate the glucose concentration by the pretrained ANNs model (readers can also use the linear relationship between glucose concentration and the R value as shown in Eqs. (7.5) or (7.6) for glucose detection. In this case, the dilution process is needed for samples with a high concentration of glucose).

Experimental tests were performed to compare the accuracy of the digital color analysis method with the traditional DNS method and the HPLC method. The results are given in Table 7.3. The detection range of the traditional DNS method was only 0–3 g/L. When the glucose concentration surpasses 3 g/L, the detection error increased sharply. Meanwhile, the colorimetric method was determined by a spectrophotometer, and the samples should be treated one by one, which was time-consuming and labor intensive. HPLC was the most accurate and robust method. Both the maximum error and the variable coefficient are within 5% in the range of 0–10 g/L. However, the measurement of one sample needs at least 15 min, which hinders its application in high-throughput screening. Though not as exact as HPLC, the digital color analysis method can still well meet the requirement of daily analytical: the maximum measurement error of 150 samples was less than 9%. Most importantly, our proposed method owns a significant advantage in throughput and speed. The speed of the digital color analysis method is 150- and 10-fold that of the HPLC and DNS method, respectively (shown in Fig. 7.9). This advanced feature renders this newly developed assay method highly suitable for applications in glucose-related research.

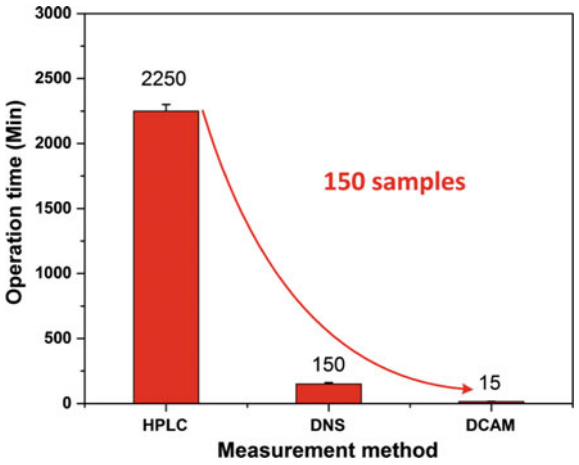

Fig. 7.9 The comparison of the operation time of 150 samples with different measurement methods [20]

7.2.1.7 Expanding the Application of the Digital Color Analysis Method for the Detection of Other Reducing Sugars

In order to expand the application of the digital color analysis method for the detection of other reducing sugars/materials, samples of xylose, fructose, maltose, and ascorbic acid with known concentrations were used for evaluation. The experimental results are shown in Tables 7.4 and 7.5.

Validation experiments showed that the digital color analysis method also applies well to xylose, fructose, maltose, and ascorbic acid. The maximum error of all the experiments was less than 10%, and the detection results for 150 samples are available within 15 min. Most importantly, there is no requirement for knowledge of the color development dynamics of the detected sugars, making the proposed

Table 7.4 Measurement results of xylose, fructose, and maltose by the digital color analysis method [20]

Sugar	Evaluation criterion	Standard samples						
		0.5 g/L	1 g/L	2 g/L	4 g/L	6 g/L	8 g/L	10 g/L
Xylose	Mean (g/L)	0.42	0.94	2.07	3.94	6.06	8.14	10.16
	Maximum error	5.23%	5.63%	7.66%	6.56%	6.91%	7.63%	5.97%
	*V-Coefficient	6.96%	7.65%	8.05%	7.03%	6.01%	8.82%	5.49%
Fructose	Mean (g/L)	0.38	1.12	2.16	4.03	5.87	7.85	9.79
	Maximum error	5.46%	7.65%	6.56%	4.78%	7.86%	5.01%	8.60%
	*V-Coefficient	3.09%	3.67%	5.99%	4.92%	6.83%	6.73%	6.27%
Maltose	Mean (g/L)	0.41	1.16	1.92	4.22	6.07	7.85	9.76
	Maximum error	5.61%	5.90%	5.71%	4.66%	5.98%	6.56%	8.12%
	*V-Coefficient	4.06%	5.83%	4.81%	6.71%	5.26%	5.42%	7.04%

Table 7.5 Measurement results of ascorbic acid by the digital color analysis method [20]

Material	Evaluation criterion	Standard samples (g/L)						
		0.02	0.05	0.1	0.2	0.3	0.4	0.5
Ascorbic acid	Mean (g/L)	0.020	0.048	0.011	0.197	0.304	0.402	0.496
	Maximum error	2.11%	3.6%	4.41%	4.32%	4.24%	4.88%	6.42%
	V-Coefficient[a]	2.64%	4.1%	4.31%	5.34%	4.67%	5.21%	7.66%

[a]V-Coefficient stands for the variable coefficient

method easy to be implemented. Compared with the existing methods, its rapidity and simplicity makes it a very promising alternative for the quick detection of reducing sugars.

In order to make sure whether the method is suitable for measurement of a sugar mixture, we carried out the validation experiments of a glucose–xylose mixture. The results showed that when used for the measurement of a sugar mixture, its measurement accuracy decreases (the measurement error rises from 6% for the single sugar to 10% for mixed sugar), but is still more accurate than the traditional OD method (measurement error was 15%). In summary, the detection power of the digital color analysis method is superior to the traditional OD method both for the detection of a single sugar or a sugar mixture.

The detection limit and range of the digital color analysis method is compared to that of other prevailing methods, including a biosensor, an electrochemical sensor and a surface-enhanced Raman spectroscopy (SERS) sensor (as shown in Table 7.6). With regard to the operability, our proposed method exhibits obvious advantages. It does not require specialized equipment or professional knowledge. Common commercial imaging devices such as digital cameras or desktop scanners are completely satisfactory for the present experiment. The color analysis can easily be achieved using common commercial so ware, such as Matlab (Maths, USA), R (Development Core Team, Austria, http://www.r-project.org), and Photoshop (Adobe Systems, USA). An untrained person can carry out the measurements easily. However, on the contrary, most of these electrodes and surface-enhanced Raman spectroscopy glucose sensors are not available in the common libraries, which hinders their application in common experiments.

In the near future, more work will be done to expand our proposed method in the field where colorimetric methods are being employed, such as the detection of ascorbic acid, erythromycin, and enzyme activities.

This study has presented a sensitive and quick glucose detection method based on color analysis. The red color provides superior precision (99.8%), which is comparable to the absorbance which is used in the traditional typical 3,5-dinitrosalicylic acid (DNS) method. Combined with the ANNs algorithm, it can be used for the detection of a high concentration of glucose with high accuracy. Based on the study above, a microtiter plate (48-well plate) platform based on color analysis was set up, which owns high measurement throughput and speed. The measurement of 150 samples only needs 15 min. It also has wide potential

Table 7.6 Comparison of biosensor, electrochemical sensor, and surface-enhanced Raman spectroscopy sensor for glucose detection [20]

Method	Detection limit	Sensitivity	Linear range	References
Graphene–glucose oxidase biocomposite biosensor	0.1 mM	1.85 μA/(mM × cm^2)	0.1–27 mM	Unnikrishnan et al. [35]
TiO2–Graphene composite biosensor	Not given	6.2 mA/(mM × cm^2)	0–8 mM	Jang et al. [36]
Zinc oxide nanocomb biosensor	0.02 mM	15.33 A/(cm^2 × mM)	0.02–4.5 mM	Sun et al. [37]
Mesoporous platinum electrochemical sensor	0.1 mM	9.6 μA/(cm^2 × mM)	0.0–10.0 mM	Park et al. [38]
Nickel ion implanted-modified indium tin oxide electrode	0.5 μM	0.1895 mA/(mM × cm^2)	1–350 μM	Tian et al. [39]
RGO-Ni$(OH)_2$/GCE	0.6 μM	0.01143 mA/(mM × cm^2)	2–3100 μM	Zhang et al. [40]
Surface-enhanced Raman spectroscopy glucose sensor	0.56 mM	Not given	0–25 mM	Lyandres et al. [41]
Near-Infrared Surface-Enhanced Raman Spectroscopy	0.5 mM	Not given	0.5–44 mM	Stuart et al. [42]
Digital color analysis	0.38 mM	–	0–55.6 mM	Xia et al. [20]

application in measurements of other reducing sugars including xylose, fructose, and maltose. The method proposed does not require specialized equipment or professional knowledge. Its rapidity and simplicity makes it a very promising alternative for the quantitation of other reducing substances [20].

7.2.2 *Near-Infrared Detection Method of High-solid and Multi-phase Bioprocess*

Fermentation has played a major role in the production of food, alcoholic beverages, enzymes, food additives, and supplements for a long period [15, 43]. There are essentially two kinds of fermentation modes, either in solid state or submerged in liquid. In submerged fermentation (SmF), the microorganism and nutrient source are normally suspended or dissolved in a liquid medium and the growth takes place in a dispersed cell suspension [44]. While referring to solid-state fermentation (SSF), it is defined as the growth of microorganisms in absence or near absence of free water [45].

In recent years, SSF has caused much more attention from researchers since SSF offers numerous opportunities in processing of agro-industrial residues. And its processes have environmental friendly advantages of lower energy requirements and less wastewater production [45, 46]. However, since the continuous phase in

SSF is the gas phase with low thermal conductivity and the culture medium is solid phase rather than the liquid phase [1], the heat and mass transfers in SSF medium are more difficult than those in SmF [47, 48]. Thus, the temperature, water, biomass, and product distribution gradients are easily formed in the SSF medium [49, 50]. Gradient phenomena result in unstable product quality and reactor's low production efficiency. At present, much attention to the research of reducing heat and mass distribution gradients is directed toward designs involving mechanical agitation and rotation [51]. However, the mechanical agitation and rotation may also lead to microbial mycelium damage while enhancing heat and mass transfers. Sometimes this negative effect and positive effects of enhancing heat and mass transfers will cancel each other out [52, 53].

In order to reduce the heat and mass gradients and avoid the microbial mycelium damage, a novel SSF bioreactor, gas double-dynamic SSF bioreactor (GDSFB) was devised by our research group [54, 55]. It consists of periodic pulsation of air pressure and internal air circulation. Pressure pulsation occurs through feeding and exhaling sterile air in the reactor, not only promoting evaporation and cooling but also enhancing biological activity by outside periodic stimulation. Internal air circulation is another dynamic process. Its main purpose is to strengthen the internal airflow and circulation [56].

Early studies have proven that gas double dynamic can reduce the temperature gradient in solid-state substrate [54] and the effect of gas double dynamic on cellulase production was studied roughly [57]. However, limited to traditional analytical tools and the complexity and heterogeneity of the solid medium [58], a more in-depth study on the effect of gas double dynamic on mass distribution gradients in medium has not been carried out.

Recently, the development of near-infrared spectroscopy (NIRS) techniques and chemometrics have resulted in rapid detection for chemical components and have been widely applied in the fields of food chemistry [59], pharmaceutical technologies [60], and determination of chemical compositions of straw [61, 62]. Based on the C-H, N-H, and O-H absorption frequencies by functional groups and scattering at specific wavelength in the near-infrared (NIR) region, near-infrared reflectance spectroscopy in the range of 11,000–7000 cm^{-1} has been used for the analysis of protein, oil, and moisture in many agricultural products, such as cereal grains, forage, and rice straw [61, 63–65]. This method is based on the construction of multivariate calibration models combining spectrometric data and traditional chemical composition results obtained with conventional laboratory methods, normally consisting of the following three procedures. First, calibrating models, that is, to construct models or called databases combining NIR spectra properties and conventional analysis results of large numbers of samples using chemometrics. For example, as reference data obtained by conventional methods, moisture content can be measured by the constant weight method, drying at 105 °C [62]. The biomass can be obtained by the chemical analysis of biomass components, glucosamine [66]. Cellulase activity can be determined by filter chapter assay as described by literature [67]. In order to relate the spectral data to the reference data, multivariate analysis could be performed with a commercial spectral analysis

program (TQ Analyst 6.2) and partial least squares (PLS) regression could be used to construct models [62]. Student's t-test, internal validation, and external validation or other validation methods can be performed to check the prediction capacity and robustness of the obtained models. After the models being checked to be efficient, the variables such as moisture content, biomass, and cellulase activity of new samples could be predicted through inputting the collected spectra to the models. In our previous study, the models were developed based on 50 samples for water content, biomass, and cellulase activity determination, giving R^2-value of 0.994, 0.999 and 0.984, respectively [16], and showing the accuracy of NIRS method.

In this study, the distribution gradients of water, biomass, and product (cellulase) at different medium depths in gas double-dynamic SSF (GDDSSF) versus static aeration SSF (SASSF) were studied and compared using NIRS and the developed models. Based on the distribution regularity, the effects of air pressure pulsation and air circulation on microbial growth and metabolism in SSF medium were analyzed and discussed [15].

7.2.2.1 Methods Establishment

A Nicolet Nexus FT-NIR spectrometer (Thermo Nicolet Corporation, USA) was used to obtain NIRS spectra. The system TQ Analyst 6.2 (Thermo Nicolet Corporation, USA) was used for calculation and analysis of the spectra.

Remove the tray at the end of fermentation. As shown in Fig. 7.10, the medium was carefully divided into three layers accordance with the average height. The height of each layer was about 1.5 cm. In each layer, layout 11 × 7, total 77 collection points, the row spacing and line spacing were 2 cm. The fiber-optic probe was pointed directly to the collection point to collect NIR spectra. Reprinted from Ref. [15]. Copyright 2014, with permission from Elsevier.

The settings of the parameters in the experiment were as follows: the spectrum data range was 4000–10,000 cm^{-1}, the number of scans was 64, and the resolution was 4 cm^{-1}. The detector has an integrating sphere to collect scattered radiation. Each sample spectrum was divided by the background spectrum so as to remove the effects caused by the instrument and atmospheric conditions so as to ensure that the peaks in the final spectrum were due solely to the sample (Thermo Nicolet User's Guide). Each sample was scanned twice, and the two spectra were averaged. The averaged spectrum was preprocessed by a Karl Norris Derivative Filter to filter out noise, improving the signal-to-noise ratio of the data. Between samples, the fiber probe was washed with distilled water and then purged to dry. Since the compositions of SSF medium and the settings of the NIRS parameters in present and our previous study were consistent [16], the models or called databases established in the previous study were applicable to the presently studied system. The collected spectra were input the models obtained in our previous in TQ Analyst 6.2 [16], then the average water content, biomass, and product (cellulase) data of the point in the substrate could be obtained. Using the three-dimensional contour map tool

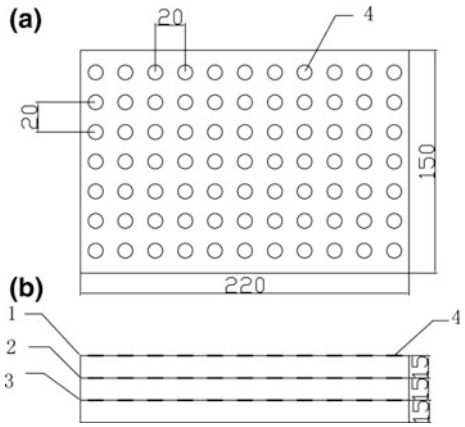

Fig. 7.10 The sketch of the NIRS collection points in medium (**a**, Vertical view; **b**, Side view; 1, Upper level; 2, Middle level; 3, Lower level; 4, NIRS collection points. Reprinted from Ref. [15]. Copyright 2014, with permission from Elsevier

(Coutour B/W line) in OriginPro 8.0 [68], the water content, biomass, and product (cellulase) distribution contour graphs of the different layers were then obtained.

7.2.2.2 Enhanced Heat Transfer in Gas Double-Dynamic SSF

Evaporation cooling is an important means of heat removal in SSF [69, 70]. Figure 7.11 shows the water content distribution and changes in different medium depth and culture time under SASSF and GDDSSF. The data in the figure were water content of medium with a unit of % (w/w). As shown in Fig. 7.11, there were always certain water content gradients under the two fermentation styles, respectively. The general law was that upper layer of substrate had lower water content and lower layer of substrate had higher water content. The water content ratios of the upper, middle, and lower levels of substrate were 71.44%:72.41%:73.05% at seventh day under SASSF and 69.72%:70.03%:70.16% at fifth day under GDDSSF with the initial water contents both were 75.00%, showing that the water contents of the upper, middle, and lower levels of GDDSSF were all lower than those of SASSF accordingly. Water evaporating in medium of GDDSSF was easier than that of SASSF, which was consistent with the previous research by Sheu and Liou that the periodic air pulsation accelerated the evaporation process in moist solid substrate [71]. However, during the SSF process, evaporation cooling is one important means of heat loss [69, 70]. As Fig. 7.11 shows, the maximum temperature of substrate was 39.5 °C under SASSF and 33.9 °C under GDDSSF appeared during the low-pressure stage (0.0 MPa) with the environmental temperature for fermentation of 30 ± 1 °C. This result indicated that gas double dynamic could enhance heat removal from the substrate effectively. Meanwhile, since the thermal conductivity of culture medium in SSF is low, the temperature distribution gradient was formed in the SSF medium which was also shown in Fig. 7.12. In both GDDSSF and SASSF, the metabolic heat was removed by heat exchange of the culture medium with air. For the upper level of medium, it was exposed to the air fully

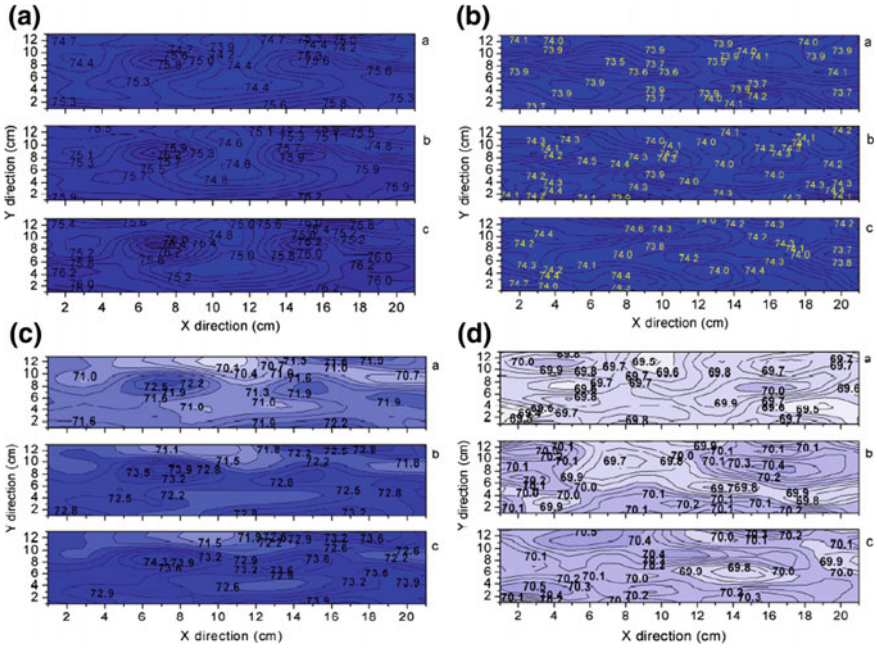

Fig. 7.11 Layered distribution of water in solid-state medium. **a** Layered distribution of water in solid-state medium cultured for 3 days under static aeration solid-state fermentation (SASSF). **b** Layered distribution of water in solid-state medium cultured for 3 days under gas double-dynamic solid-state fermentation (GDDSSF). **c** Layered distribution of water in solid-state medium cultured for 7 days under SASSF. **d** Layered distribution of water in solid-state medium cultured for 5 days under GDDSSF. a, upper level; b, middle level; c, lower level (The X direction represents the long side of the tray while the Y direction represents the short side. The data in this figure with the unit of % (w/w) and the shades of color reflects the water content). Reprinted from Ref. [15]. Copyright 2014, with permission from Elsevier

which increased the area of heat exchange and the water evaporated was more, thus improving the heat removal efficiency. For the lower level of medium, although not exposed to the air and with less evaporated water, it was contacted with the enamel tray with low thermal resistance, thus the metabolic heat generated in the lower level of medium could be transferred relatively timely. While for the middle level of medium, it was surrounded by the upper and lower levels of medium with relatively higher temperature and had common water evaporation. Therefore, the heat transfer driving force was relatively weak, resulting in the higher temperature than that of the upper and lower levels of the medium. However, GDDSSF affected the vertical maximum temperature gradient considerably due to that the water evaporation of the middle and lower levels were accelerated. SASSF resulted in a relatively large temperature gradient of 3.0 °C cm^{-1}, while GDDSSF decreased this gradient to 0.9 °C cm^{-1}, which provided beneficial conditions for microbial growth and metabolism in the middle and lower levels of substrate.

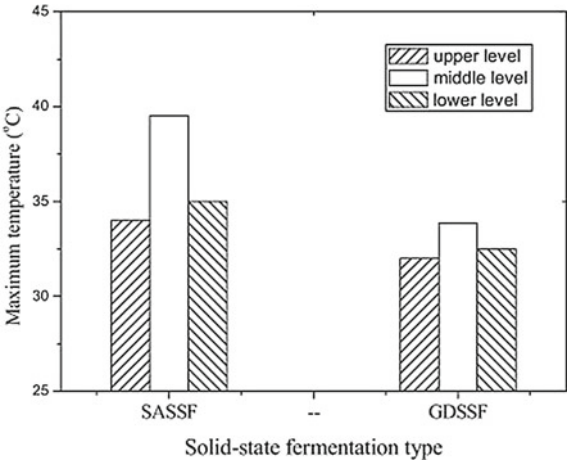

Fig. 7.12 The maximum temperature of different bed heights in gas double-dynamic solid-state fermentation (GDDSSF) versus static aeration solid-state fermentation (SASSF) with the environmental temperature for fermentation of 30 ± 1 °C [15]

7.2.2.3 Microbial Growth and Metabolism Properties in Gas Double-Dynamic SSF (GDDSSF)

To evaluate the effect of GDDSSF on microbial growth, the biomass distributions at different fermentation stages in medium of SASSF and GDDSSF were investigated. As shown in Fig. 7.13, the gas double dynamic affected the microbial growth obviously, which was mainly manifested at the following two aspects. First, it is on the total amount of biomass. Figure 7.13 shows that the biomass ratios of the upper, middle, and lower levels were 43.28:39.12:31.23 on the seventh day under SASSF and 47.90:44.88:43.04 on the fifth day under GDDSSF. Biomass in every level of GDDSSF was more than that of SASSF, resulting in the total amount of biomass increased by 19.53%. Second, it is on the biomass distribution gradients. It was indicated that there was not only vertical distribution gradient (perpendicular to the bottom of the tray) but also horizontal distribution gradient (parallel to the bottom of the enamel tray) under SASSF (Fig. 7.13). While under GDDSSF, the horizontal gradient was not obvious and the vertical distribution gradient significantly decreased from 1:0.90:0.72 under SASSF to 1:0.94:0.90 under GDDSSF. The accelerated effect of microbial growth in GDDSSF was discussed as follows. First, as described above, evaporation cooling was more efficient and it removed more metabolic heat in GDDSSF than in SASSF, which provided suitable temperature for microbial growth in GDDSSF. Second, when air pressure in the fermenter dropped suddenly, the gas phase within substrates would swell and then the swell would loosen the solid substrates in GDDSSF process. The strategy was very beneficial to mycelia due to that the method could not only provide sufficient O_2 but also expand more room for fungal propagation and improve heat transfer within the

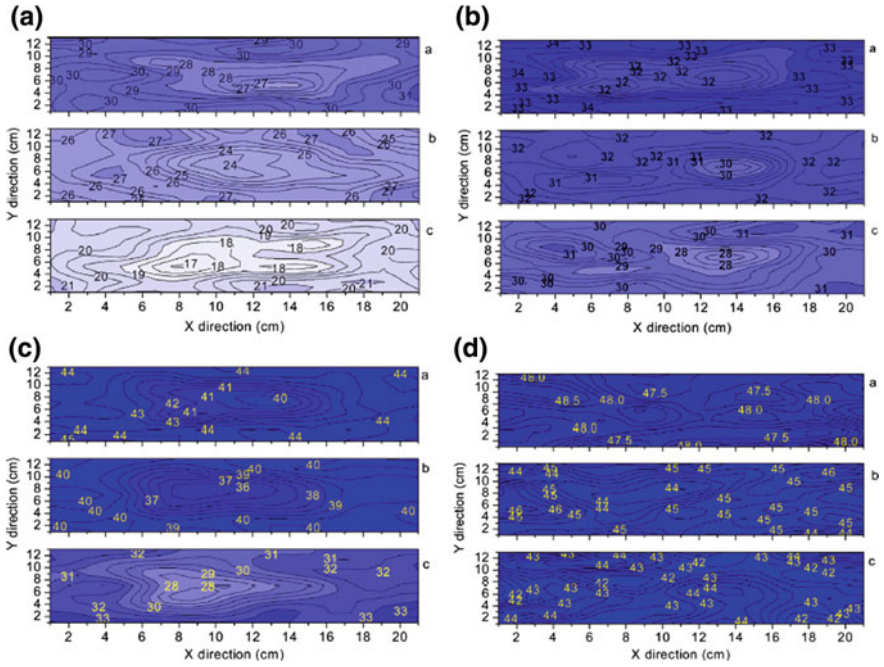

Fig. 7.13 Layered distribution of biomass in solid-state medium. **A** Layered distribution of biomass in solid-state medium cultured for 3 days under static aeration solid-state fermentation (SASSF). **B** Layered distribution of biomass in solid-state medium cultured for 3 days under gas double-dynamic solid-state fermentation (GDDSSF). **C** Layered distribution of biomass in solid-state medium cultured for 7 days under SASSF. **D** Layered distribution of biomass in solid-state medium cultured for 5 days under GDDSSF. (a) Upper level; (b) middle level; (c) lower level (The X direction represents the long side of the tray while the Y direction represents the short side. The data in this figure with the unit of mg biomass/g dry medium and the shades of color reflects the biomass) [15]

substrate [54]. Therefore, the microbial growth in medium, especially in the lower level, was apparently strengthened compared to SASSF and thus the biomass in whole medium was increased while the biomass distribution gradient was decreased in GDDSSF.

In addition to quantitative analysis using NIRS techniques, SEM was used to observe the microbial growth in the substrates at different layers. The results were shown in Fig. 6. Similar results were observed as the NIRS analysis. There were more spores and mycelia in the medium cultured under GDDSSF than those in the medium cultured under SASSF. Addition to the contrast between the two culture styles, the difference between the three layers was studied too. As Fig. 7.14 shows, the biomass distribution gradient under SASSF was more apparent than that under GDDSSF as the quantitative analysis using NIRS techniques, which also confirmed the accuracy of the NIRS method.

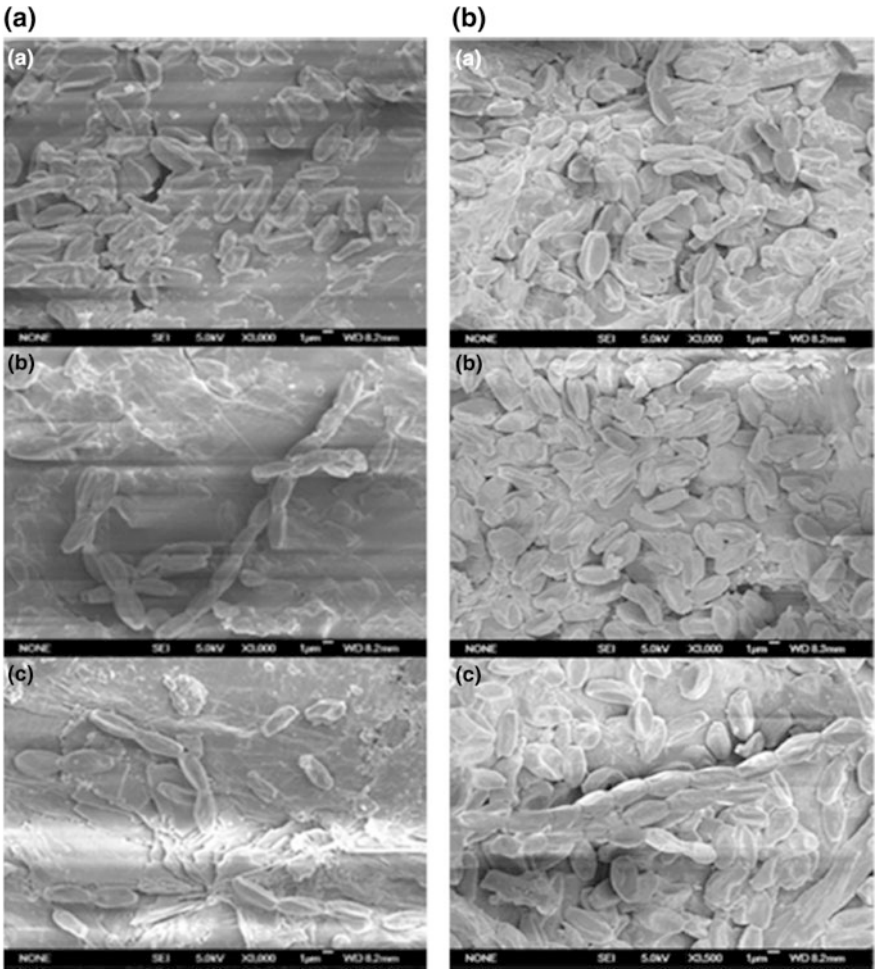

Fig. 7.14 Scanning electron microscope (SEM) analysis of layered distribution of biomass in solid-state medium. **A** Layered distribution of biomass in solid-state medium-cultured for 7 days under static aeration solid-state fermentation (SASSF). **B** Layered distribution of biomass in solid-state medium cultured for 5 days under gas double-dynamic solid-state fermentation (GDDSSF). (a) Upper level; (b) middle level; (c) lower level. Reprinted from Ref. [15]. Copyright 2014, with permission from Elsevier

The results of Figs. 7.13 and 7.14 have indicated that effect of gas double dynamic on growth of *T. reesei* YG3 was enhanced. Not only the total amount of biomass increased but also the biomass distributed more uniformly.

Besides microbial growth, effect on microbial metabolism of gas double dynamic was also studied. It can be calculated from Fig. 5 that after fermentation for 3 days, the biomass under GDDSSF increased by 26.4% than that under SASSF, while cellulase activity increased by 234.3% calculated from Fig. 7.13.

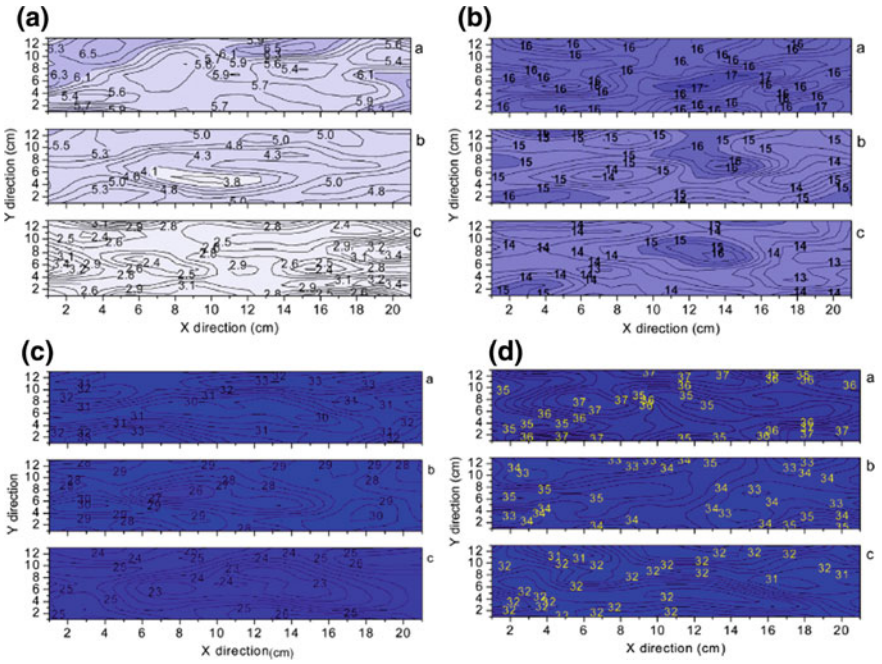

Fig. 7.15 Layered distribution of cellulase activity in solid-state medium. **A** Layered distribution of cellulase activity in solid-state medium cultured for 3 days under static aeration solid-state fermentation (SASSF). **B** Layered distribution of cellulase activity in solid-state medium cultured for 3 days under GDDSSF. **C** Layered distribution of cellulase activity in solid-state medium cultured for 7 days under SASSF. **D** Layered distribution of cellulase activity in solid-state medium cultured for 5 days under GDDSSF. (a) Upper level; (b) middle level; (c) lower level (The X direction represents the long side of the tray while the Y direction represents the short side. The data in this figure with the unit of IU/g dry medium and the shades of color reflects the cellulase activity). Reprinted from Ref. [15]. Copyright 2014, with permission from Elsevier

This phenomenon indicated that microbial metabolism and cellulase production may be stimulated by gas double-dynamic stimulation. Following this thought, microbial respiration rate, which is commonly used as a measure of microbial activity [72], was determined at different culture times under two fermentation styles. As shown in Fig. 7.16, gas double-dynamic stimulation improved microbial metabolism apparently, mainly manifested at the following two aspects: first, on the peak value of CER. It can be seen from Fig. 7.16 that the peak value of CER under GDDSSF was 5.48 mg/g dry medium/h and it was 2.17 times of the peak value of CER under SASSF, indicating that microbial metabolism was enhanced under GDDSSF. Because neither agitation nor pressure pulsation to strengthen heat and mass transfers was included in SASSF, it was hard for microorganisms in the lower level medium to metabolize actively due to relatively high temperature and insufficient oxygen, making the CER peak value of SASSF low. On the other hand, the pressure pulsation in GDDSSF motivated ATPase activity, which plays a

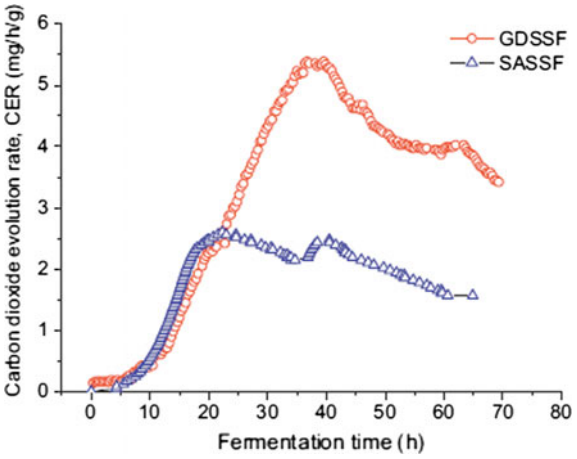

Fig. 7.16 Carbon dioxide evolution rate (CER) curves of gas double-dynamic solid-state fermentation (GDDSSF) and static aeration solid-state fermentation (SASSF) [15]

significant role in the self-regulation that microbial cells feel external environment of adjustment and adaptation [73–77]. In addition, ATPase hydrolyzes ATP to produce energy and provide transmembrane proton and ionic gradients for cells growing thus greatly affecting the microbial metabolism. It was reported that ATPase activity and medium weight loss rate were linearly dependent under GDDSSF with correlation coefficient of $R^2 = 0.9784$ [73], confirming that ATPase activity stimulated the microbial metabolism. Therefore, through increasing ATPase activity in GDDSSF, the microbial metabolism was accelerated, and thus the CER of GDDSSF increased.

Second, on the shape of CER curve, for GDDSSF, CER decreased rapidly after reaching the peak value. While for SASSF, two moderate peaks appeared in the CER curve. The appearance of two peaks indicated that microbial metabolism under SASSF was not centralized in view of time. For GDDSSF, due to the periodic stimulation by pressure pulsation [55], microbe grew and metabolized synchronously, which resulted in the centralization of cellulase production and the shortening of the fermentation period. For SASSF, since the temperature, water content in the substrate were not consistent and there was no outside stimulation, the microbial growth and metabolism were not synchronous, resulting in relatively long-lasting time for the peak value of CER and extending the time for fermentation. This result also could be seen in Fig. 7.15 that cellulase activity under GDDSSF for 5 days exceeded that under SASSF for 7 days by 20.3%.

It could be indicated that gas double dynamic stimulated the metabolism of *T. reesei* YG3, which resulted in that the microbe metabolized vigorously and synchronously and thus shortening the fermentation period.

7.2.2.4 Effect on Product Distribution Gradient of Gas Double-Dynamic Solid-State Fermentation

Product distribution gradient in SSF medium affects the fermentation quality and efficiency, and thus it is a key aspect for evaluation of SSF performance. In the present study, the cellulase productivity distributions at different fermentation stages in medium of SASSF and GDDSSF were investigated. Figure 7.15 indicated that the fermentation type and time affected the cellulase productivity distribution in the substrates apparently. The data showed in the figure were cellulase activity with a unit of IU/g dry medium. Results indicated that cellulase activity gradients appeared in the SSF medium, and this phenomenon occurs more clearly in SASSF (Fig. 7.15). In the SASSF medium, the cellulase productivity ratios of the upper, middle, and lower levels were 1:0.82:0.48 on the third day and 1:0.90:0.78 on the seventh day, respectively. As for the GDDSSF, the ratios were 1:0.94:0.88 on the third day and 1:0.95:0.89 on the fifth day, respectively. These results indicated that at the former stage of fermentation, the cellulase distribution in the whole medium of GDDSSF has already been relatively homogeneous. While for the lower level of SASSF, the microbial metabolism at the former stage was weak. At last, the gas double dynamic reduced cellulase gradient by 20.8% than SASSF. Since the biomass and temperature distribution gradients were reduced by GDDSSF, the amount of biomass in the lower level was larger and the temperature was lower under GDDSSF than those under SASSF, and the microbial metabolism in the lower level under GDDSSF was enhanced, correspondingly. Thus, by promoting more effective utilization of the lower level of SSF medium, the fermentation product (cellulase) distribution gradient in GDDSSF decreased apparently and thus the homogeneity of the fermentation products was improved.

In the present study, the mass distribution in SSF was quantitatively determined using NIRS. The performance of GDDSSF was investigated based on the mass distribution regularity in solid-state substrate.

Our present study clearly showed that gas double-dynamic SSF, featuring periodic pulsation of air pressure and internal air circulation, reduced the mass distribution gradients in substrate and shortened the fermentation period, which obviously enhanced the SSF performance. With advantages of improving product homogeneity and production efficiency, GDDSSF is proved to be an efficient way of SSF [15].

7.2.3 Fractal-Based Digital Image Detection Method of High Solid and Multi-phase Bioprocess

Determination of the fungal growth is essential but always difficult for process control in SSF (SSF) [2]. Since the substrate bed of SSF is complex and heterogeneous, fungal mycelia penetrating the substrate particles are impossible to be

separated, therefore, quantitative recovery of biomass from the matrix is a tough [78]. Indirect methods such as the chemical analysis of biomass components (chitin, glucosamine, ergosterol, protein, nucleic acid) [79–81], measurement of biologic activity (ATP, enzyme activity, respiration rate, immunological activity) [82–85] as well as using artificial SSF systems (membrane culture, amberlite resin) [86, 87] have been applied to determine fungal growth. Among these methods, glucosamine as an indicator of fungal biomass is more reliable [88, 89]. Nevertheless, preparation and determination of the ingredients from SSF samples are destructive and troublesome. Recently, near-infrared spectroscopy using a fiber-optic probe has been put forward to replace chemical methods with its convenience in usage [16]. However, this technique is cost and incapable for online determination of samples with heterogeneous distribution or large surface areas.

Quantitative fractal geometry yield insights into the mechanism whereby spatial organization influences the interaction between the heterogenic porous structure and biotic processes [90]. Combined with high-resolution image capture and image analysis, the calculated fractal geometry has been used to quantify the relationship between the morphology and mycelia growth in agar [91, 92], soil [93, 94] and activated sludge [95, 96], even used in online measurement and process monitoring [97, 98]. Apparently, quantitative fractal geometry provides an optional economic way to indicate fungal growth. Involved in this method, various structured models [99, 100] have been developed, with the main hyphal length and total hyphal length as morphological parameters. However, the existing models are unable to account for many observable growing characteristics in SSF. Most of those models focused on the morphological growth of individual mycelia trees or single colony [92]. In fact, mycelia always entwine each other [101] and wrap the substrate particles [102], rarely grow as individuals undisturbed. Meanwhile, the lignocelluloses substrates (wheat straw, bagasse, and oat hull) are porous and structurally heterogeneous, thus cannot be represented by agar. Therefore, the current quantitative fractal models are mostly improper for mycelia-matrix system in SSF, especially for those having lignocelluloses as substrates. With digital image analysis, this chapter developed a method to determine fungal growth according to the morphological changes of mycelia matrix in SSF. Fractal features of mycelia-matrix during SSF were investigated using image process, and quantified by fractal dimension. Relation between the variation of fractal dimension and fungal growth was reasonably modeled and validated in different fermentation systems. Advantages and the potential use of this method were also discussed [2].

7.2.3.1 Methods Establishment

Images Acquisition of Microbial Cultures At intervals of 24 h, three columned bottles were taken out to be photographed from both the top and bottom sides of the cultures, using a 35 mm Cannon Power shot A650 camera fitted with a 50 mm lens. Images grabbing was performed in 72 bit, 3264 × 2448 pixels matrix. Around 10

digital images were acquired for each sample and stored in JPEG format. In order to keep the focal length and the illumination constant, a foursquare polystyrene plate embodying a central hole was used to fix the camera (Fig. 7.17). Since the central hole of the polystyrene plate and camera lens had the same diameter, the camera could be clipped by the polystyrene plate and kept a fixed distance from the culture. The side length of foursquare polystyrene plate was twice the radius of the bottle, making it large enough to keep the light inside the bottle uniform for photography.

Digital Image Processing An automated image analysis protocol was developed in Matlab 7.1. The schematic representation of image processing procedure is illustrated in Fig. 7.18. The first step of the procedure consisted of the conversion of RGB images into grayscale images and the subsequent background correction. The grayscale images were then enhanced by histogram equalization and denoised by low-pass filtering. In this procedure, function histeq and fft2 provided by Matlab image processing toolbox were applied; the low-pass filter was programmed independently. Once the digital images were enhanced, an adaptive threshold selection named Ostu method [103] was used to get binary images. Ostu can

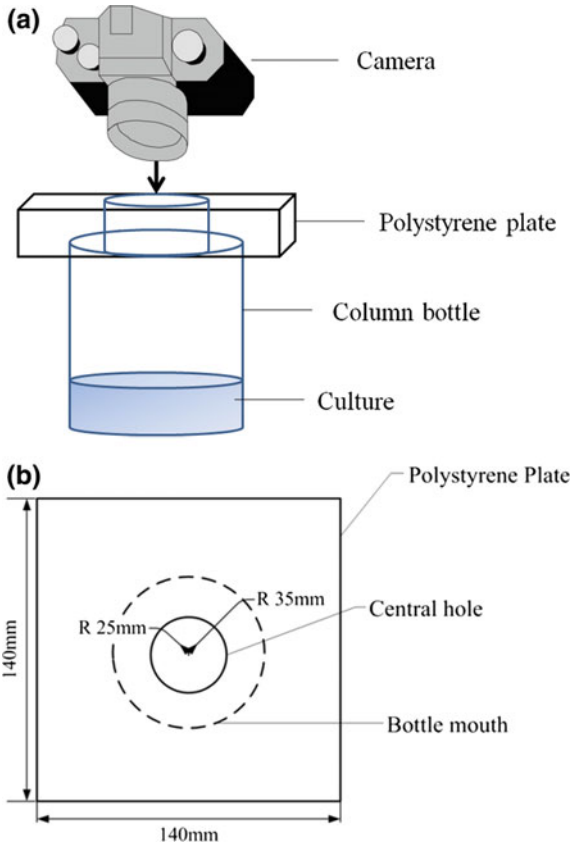

Fig. 7.17 Schematic drawing of the image acquisition method. **a** the tridimensional view of the apparatus; **b** the vertical view of the polystyrene plate covering the bottle mouth [2]

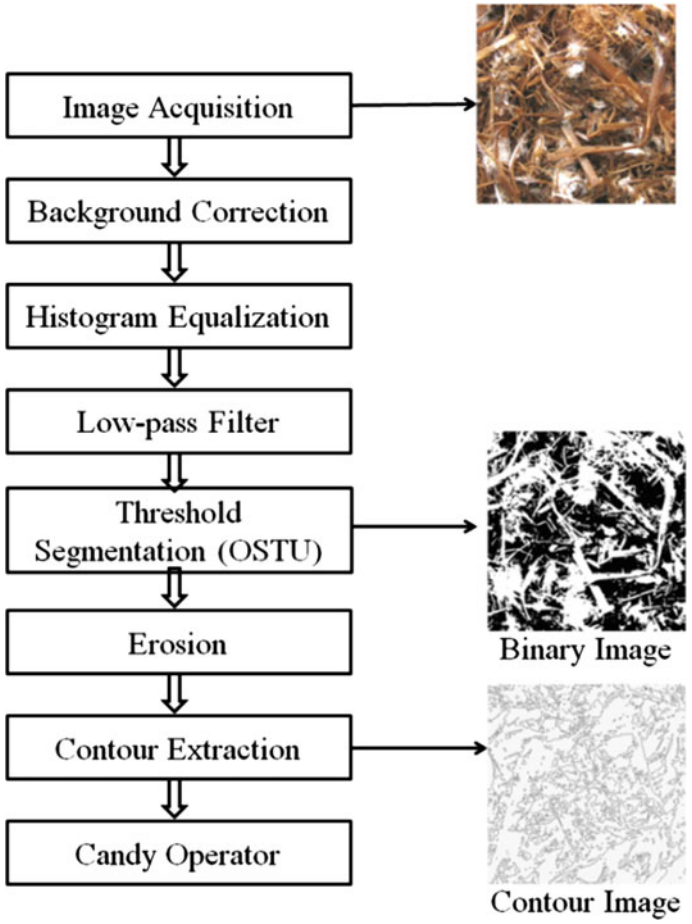

Fig. 7.18 Schematic representation of the image processing procedure [2]

analyze image histograms automatically and obtain the best threshold value in statistics. In this chapter, it was carried out by calling function graythresh from the Matlab image processing toolbox. Then binary images were additionally processed by image erosion, in which function strel and imerode were called. At last, with the function edge, contours of the images were detected by Candy operator [2].

Fractal Dimension Calculation Fractal dimensions of the culture were estimated by the box-counting method according to Theiler [104] with some modification. Essentially, a series of grids of square boxes with the size of 1–1024 pixels were positioned to overlay each electronic image. For a series of boxes of side length s pixels, the number of boxes intersecting the contours of image by the set (N) was counted. Fractal structures obey the power law relation over a range of length scales, such that

$$N(s) = cs^{-DB}, \tag{7.8}$$

where D_B is the box-counting fractal dimension, $N(s)$ is the total number of boxes of side length s that intersect contours of the culture image, and c is a constant. D_B (surface box fractal dimension) is estimated as the negative gradient of a regression line through the linear part of the plot of log$N(s)$ against log s, for a sequence of scales:

$$\log N(s) = \log c + (-D_B)\log s \tag{7.9}$$

7.2.3.2 Changes of Fractal Dimension and Fungal Biomass During SSF

In order to find out the effect of fungal growth on lignocelluloses substrates and changes in the fractal dimension of mycelia matrix, cultures on SEWS-bran were photographed from both the top and bottom sides at 24 h intervals; corresponding pictures were processed to calculate the fractal dimensions (Fig. 7.19). It can be observed that, along with the organism growth, lignocelluloses of the substrates became slender after 72 h and the structure of mycelia matrix turned to be complex (Fig. 7.19a). The contours of corresponding images underwent a decrease and then an increase at around 60 h (Fig. 7.19b).

For quantitative study, biomass and fractal dimension (D_B) of the cultures were both determined. During SSF, fractal dimension of mycelia matrix decreased with the mycelia growth before 60 h, then increased until 132 h when biomass reached the maximum (Fig. 7.20). According to the box-counting method, fractal dimension

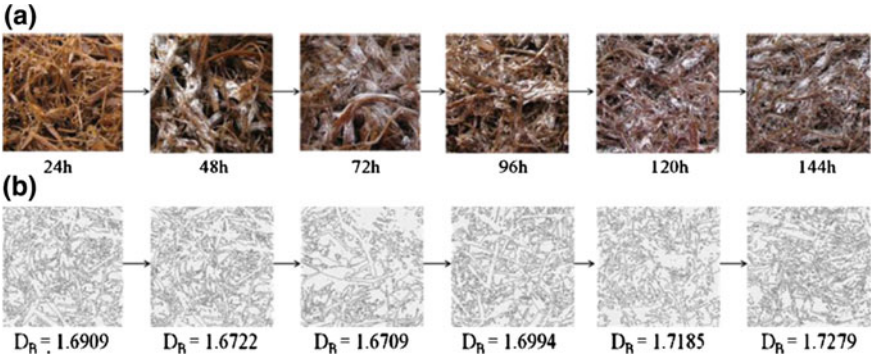

Fig. 7.19 Morphological changes of mycelia matrix in SSF. **a** original pictures of mycelia matrix in SSF; **b** the contours and fractal dimensions of the processed images corresponding to original pictures. Morphological changes of mycelia matrix in SSF. a. original pictures of mycelia matrix in SSF; b. the contours and fractal dimensions of the processed images corresponding to original pictures Reprinted from Ref. [2]. Copyright 2012, with permission from Elsevier

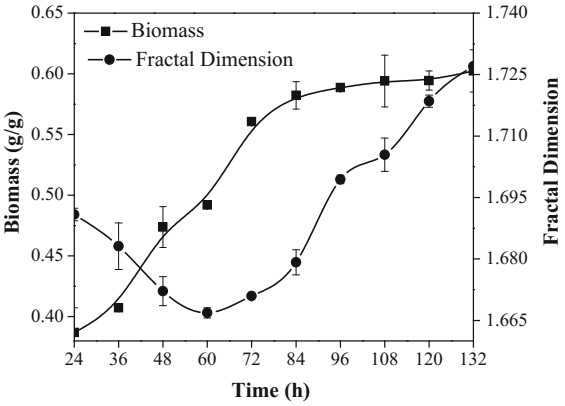

Fig. 7.20 Variation of fractal dimension and biomass during SSF. Reprinted from Ref. [2]. Copyright 2012, with permission from Elsevier

increases when the image contour multiplies or pores in the matrix structure accelerate, and vice versa. Therefore, fungal growth first reduced the porosity of the substrates, and then enhanced it in the later stage.

It should be noted that, in each fermentation periods, relative errors of D_B for different layers of the substrate ranged from 0.001 to 4.42%, the minor difference indicated that mycelia grew equably throughout substrates bed. Therefore, when the bed height was around 4 cm, images of the top side of culture could present the fungal growth in entire bed.

Deduced from the experiment phenomena, the effect of fungal growth on the morphology of mycelia matrix can be explained by a schematic model (Fig. 7.21). Initially, only sparse mycelia grow inside the substrate; the matrix can keep the unbroken porous structure. As the mycelia continue to grow, hypha mainly concentrate in macropores (>10 m) with high space filling efficiency [105]. Then matrix get filled and become less porous than before, but still keep the integrity; outside the pores, hyphae form shells around the pore tubes. Therefore, the morphological edges blur lead to the decrease of fractal dimension. In the late exponential phase, continuous growth of mycelia utilizes the substrate intensively; matrix structure is destroyed and breaks into big pieces, more morphological edges appear in vision and lead to an increased fractal dimension. When microbial growth gets into stationary phase, further breakage of substrates makes the pieces smaller;

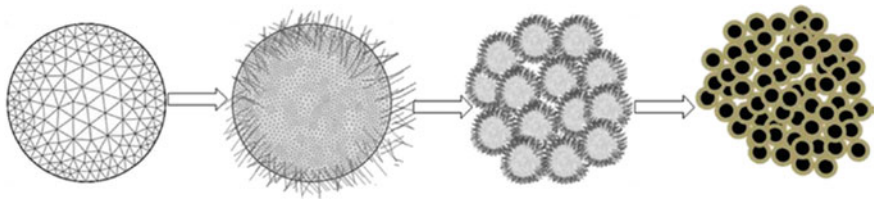

Fig. 7.21 Schematic model of the morphological change in mycelia matrix during SSF. Reprinted from Ref. [2]. Copyright 2012, with permission from Elsevier

as a result, corresponding fractal dimension increases gently. The physical model provided theory basis for the mathematical modeling.

7.2.3.3 Kinetic Modeling Based on the Fractal Character of Mycelia Matrix

Mathematical models were developed to quantify the relations between fungal growth and morphological evolution of mycelia-matrix system. Logistic equation was used to describe the organism growth as it gave the most adequate fit in the majority of reported cases [33].

$$\frac{dX}{dt} = \mu_M X(1 - \frac{X}{X_M}). \tag{7.10}$$

In this equation, X was the biomass content in the solid substrate, X_M was the maximum possible biomass content, and M was the maximum specific growth rate. Because the temperature and water activity within the substrate bed remained constant throughout the entire growth cycle, effects of environmental variables on the growth rate were ignored.

It was assumed that the fractal dimension (D_B) was eigen feature of mycelia matrix and equivalent throughout the substrate bed. Variations of DB shared logistic equation as fungal growth did. Equations 7.11 and 7.12 were constructed to estimate the fractal dimension in different periods of SSF. As observed, D_B underwent a decrease and then an increase along with fungal growth, biomass at this inflection was named as Xg. When $X < Xg$, variation of D_B and biomass presented linear correlation as follows:

$$\frac{dD_B}{dt} = \alpha_M D_B \left(1 - \frac{D_B}{D_{Bm}}\right) = k_1 \alpha_M X \left(1 - \frac{X}{X_M}\right) \tag{7.11}$$

When $X > Xg$, D_B got into the increasing stage. At this time, with the decay of some cells, growth of the mycelia slowed down gently. Therefore, changes in D_B were influenced by both mycelia decay and growth. Equation 7.12 included a biomass declining coefficient $((X/Xg)^{-1})$.

$$\frac{dD_B}{dt} = \beta_M D_B \left(1 - \frac{D_B}{D_{BM}}\right) = k_2 \beta_M \left(\frac{X}{X_g} - 1\right)\left(1 - \frac{X}{X_M}\right) \tag{7.12}$$

In Eqs. 7.11 and 7.12, α_M and β_M respectively represented the maximum specific decreasing and increasing rate of DB. D_{BM} was the minimum fractal dimension at the inflection point, D_{BM} was the maximum fractal dimension; k_1 and k_2 were equivalent factors for α_M and β_M, respectively.

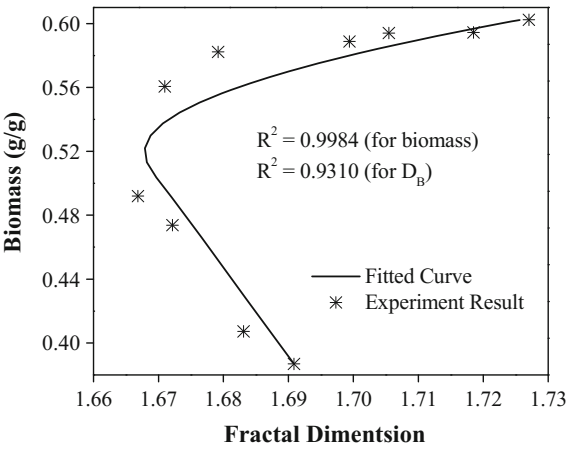

Fig. 7.22 Fitting of the constructed model to original data of biomass and fractal dimension. Reprinted from Ref. [2]. Copyright 2012, with permission from Elsevier

Derived from Eqs. 7.10–7.12, Eqs. 7.13, and 7.14 directly indicated the variation of D_B along with fungal growth, where δ and μ represented equivalent parameters for the decreasing and increasing rate of D_B.

$$\frac{dD_B}{dt} = \frac{dX}{dt}\frac{k_1\alpha_M}{\mu_M} = \frac{dX}{dt}\frac{\delta}{\mu_M}, D_B > D_{Bm} \tag{7.13}$$

$$\frac{dD_B}{dt} = \left[\frac{dX}{dt}\left(\frac{1}{X_g} - \frac{1}{X}\right)\right]\frac{k_2\beta_M}{\mu_M} = \left[\frac{dX}{dt}\left(\frac{1}{X_g} - \frac{1}{X}\right)\right]\frac{\eta}{\mu_M} \tag{7.14}$$

To fit the experimental curve with minimal error, parameters δ, μ, and μ_M must be estimated accurately, therefore, initial values of X_M, X_0, X_g, and DB in equations were needed. For fermentation on SEWS-bran, the best δ, μ, and μ_M were separately −0.006, 0.17 and 0.033, with which the relative error of X and D_B were respectively 0.776% and 0.093%. Excellent goodness of fit (Fig. 7.22) indicated that the kinetic models were quite appropriate for the prediction of X and D_B in SEWS-bran fermentation system.

7.2.3.4 Effect of Substrates Properties on Fungal Growth and Fractal Dimension

In order to investigate the sensitivity and versatility of the constructed models, fermentations on SERS-bran with particle length (PL) of 3.5, 1.5, and 0.4 cm as well as the initial moisture content (MC) of 65, 75 and 85% (w/w) were carried out. The fungal growth and variations of fractal dimension in different fermentation systems were investigated; corresponding parameters (δ, μ, and μ_M) were estimated using the algorithm described above.

As shown in Fig. 7.23 (PL 0.4, 1 and 3 cm), D_B of SERS-bran fermentation systems had similar variations with SEWS-bran system: the fractal dimension of the

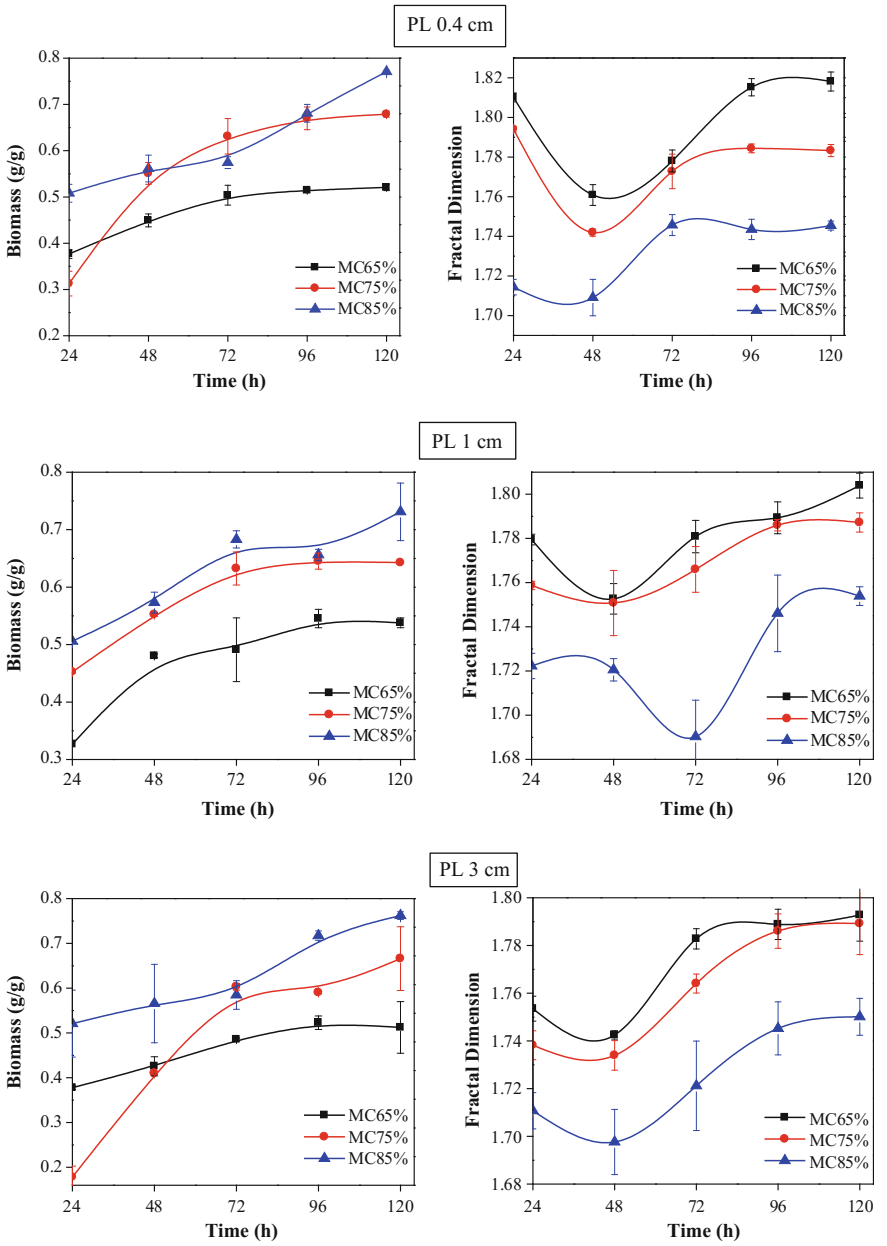

Fig. 7.23 Variation of fractal dimension and biomass on different substrates with particle length (PL) of 0.4, 1, 3 cm and initial moisture content (MC) of 65%(■), 75%(●), 85%(▲) in SSF. Reprinted from Ref. [2]. Copyright 2012, with permission from Elsevier

Table 7.7 Results of the kinetic model fitting. Reprinted from [2]. Copyright 2012, with permission from Elsevier

Sample	δ ($\times$ (-10^{-3})/h)	η ($\times$ 10^{-2}/h)	μ_M ($\times$ 10^{-2}/h)	RE of D_B ($\times$ 10^{-3})	RE of biomass ($\times$ 10^{-2})
A_1B_1	26	19.4	3.82	1.55	3.6292
A_1B_2	14.7	9.9	6.82	0.4544	3.2566
A_1B_3	1.7	4.3	1.52	0.6512	2.7616
A_2B_1	8.7	30.5	5.91	1.6811	5.2203
A_2B_2	3.9	12.8	4.96	1.1957	1.8694
A_2B_3	2.3	32	3.11	1.396	1.5456
A_3B_1	5.4	9.1	3.87	3.8847	2.1083
A_3B_2	1.2	2.3	6.21	1.6141	0.5405
A_3B_3	2.2	5.7	2.73	4.908	3.9831

mycelia matrix initially decreased then increased at a certain time. Differences in DB showed significant specificity for corresponding fungal growth.

The constructed kinetic models fitted these curves well (Table 7.7). The relative errors (RE) of X and D_B among all these systems ranged within 0.541–5.221% and 0.454–3.885%, respectively. Therefore, the constructed models were proved to be reliable.

Differences δ, η, μ_M (Fig. 7.24) reflected the effect of moisture content and particle length on the morphology of mycelia matrix as well as fungal growth. At the stage before inflection ($X < Xg$) (Fig. 7.24a), fractal dimension of mycelia matrix with small substrate particles declined faster than big ones did when the moisture content was below 85% (w/w). However, when the moisture content reached 85%, no significant difference was found among different particles. The reason is that the movement of hyphal tips in the macropore space was greatly affected by both the particles' physical boundaries and the surface tension of the surrounding water films [100].

Because oxygen diffusion in water is only 1/200,000 of that in air, water tension is the foremost factor of hyphae distribution. Since the length of the oxygen diffusion pathways through waterlogged areas restricts hyphae growth, increased moisture content will result in reduced mycelia growth in open pore spaces [105], further lead to DB reduction. Besides, distance between macropores is another key factor. Branching hyphae are commonly concentrated within a 50 m shell around the macropores no matter what size is the substrate particle in [105, 106]. As a 50 m shell owns relative strong impact on the shape of smaller particle than that of big particles, D_B declines faster in substrates with small particles. However, relation between ı and M at this stage was nonlinear as shown. Equation 7.13 gave reasonably explanation, which was, D_{B0} and X_0 at 24 h also affect the two parameters remarkably.

At the stage after inflection ($X > Xg$) (Fig. 7.24b), D_B of substrate with a particle length of 1 cm rises faster than others over all the ranges of moisture content tested,

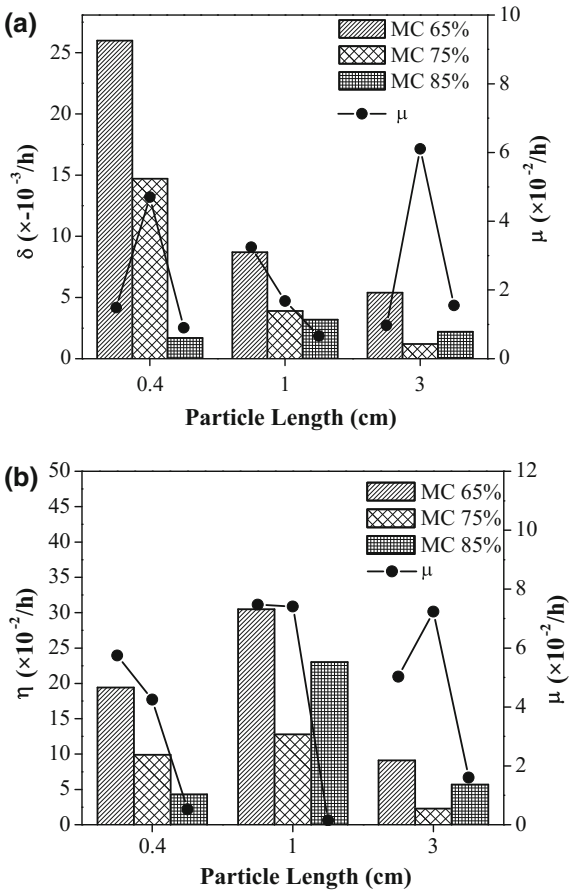

Fig. 7.24 Variation rates of fractal dimension and corresponding maximum specific growth rate of mycelia for fermentation systems with different substrates particle sizes and moisture contents (sub-picture (**a**) and (**b**) respectively shows the decreasing rate δ and increasing rate η of fractal dimension as well as the corresponding maximum specific growth rate of mycelia). Reprinted from Ref. [2]. Copyright 2012, with permission from Elsevier

which meant substrates with 1 cm particles disintegrated distinctly in the field of vision. For larger particle sizes, steric limitations that connected with mass transfer difficulty restrict mycelium growth [107]. Although mycelia owned relative high growth rate, hyphal within a short distance from the particles appeared in aggregates other than branching ones. As a result, changes in fractal dimension of 3 cm particles were not significant. As pores between small particles got more filling with mycelium in the early stage ($X < Xg$), less space and oxygen were available for growth of hyphae [107, 108]. Therefore, substrates with a particle size of 1 cm appeared to have appropriate steric hindrance, nutrient mass transfer as well as oxygen supply for hyphae branching. According to Eq. (7.14), δ and μM at this stage were influenced by Xg and D_{BM}, therefore, relations between the two parameters were nonlinear.

Actually, fractal dimension can specifically reflect the fungal growth in different substrates. Previous researches have confirmed that the growth profiles of *Rhizoctonia solani* in soil [109, 110], *Rhizopus oligosporus* in barley tempeh [111]

and *Physisporinus vitreus* in woods [112] could be described with fractal dimension. Therefore, the image processing and constructed fractal-based kinetic models present the versatility of predicting the growth profile of filamentous fungi in porous structured matrix.

Filamentous microorganisms commonly owned special fractal features, and the analytical system constructed in this chapter was applicable to determine fungi. By photographing the mycelia matrix dynamically with high-resolution camera and image processing, the variation curve of fractal dimension was obtained. Based on the proved kinetic models, parameters can be estimated for calculating the specific growth rate of mycelia. Also, biomass in different periods can be further estimated with reasonable accuracy. Especially, with adjustable focus of image acquisition, this method is applicable for matrixes in various ranges of surface areas.

In conclusion, the coupling of dynamic imaging with kinetic models based on quantitative fractal geometry was proved effective in the determination of fungal biomass in SSF. Because the variation rates of fractal dimension of mycelia matrix in the constructed models presented strong specificity for fungal growth rate, this method could be used universally in various environments. With advantages of reasonable accuracy and low cost, this nondestructive method shows potential in the online determination and further control of SSF, especially for the lignocelluloses substrates [2].

References

1. Chen HZ (2013) Modern Solid State Fermentation. Springer, Netherlands
2. Duan YY, Wang L, Chen HZ (2012) Digital image analysis and fractal-based kinetic modelling for fungal biomass determination in solid-state fermentation. Biochem Eng J 67 (1):60–67
3. Jiang H, Liu GH, Mei CL et al (2012) Measurement of process variables in solid-state fermentation of wheat straw using FT-NIR spectroscopy and synergy interval PLS algorithm. Spectrochimica Acta Part a-Molecular Biomolecular Spectroscopy 97:277–283. https://doi.org/10.1016/j.saa.2012.06.024
4. Jiang H, Liu GH, Mei CL et al (2012) Rapid determination of pH in solid-state fermentation of wheat straw by FT-NIR spectroscopy and efficient wavelengths selection. Anal Bioanal Chem 404(2):603–611. https://doi.org/10.1007/s00216-012-6128-y
5. Jiang H, Liu GH, Xiao XH et al (2012) Monitoring of solid-state fermentation of wheat straw in a pilot scale using FT-NIR spectroscopy and support vector data description. Microchem J 102:68–74. https://doi.org/10.1016/j.microc.2011.12.003
6. Zhao JY, Chen HZ (2013) Correlation of porous structure, mass transfer and enzymatic hydrolysis of steam exploded corn stover. Chem Eng Sci 104:1036–1044
7. He Q, Chen HZ (2015) Comparative study on occurrence characteristics of matrix water in static and gas double-dynamic solid-state fermentations using low-field NMR and MRI. Anal Bioanal Chem 407(30):9115–9123
8. Nguyen TC, Anne-Archard D, Fillaudeau L (2015) Rheology of Lignocellulose Suspensions and Impact of Hydrolysis: A Review. Springer International Publishing
9. Wiman M, Palmqvist B, Tornberg E et al (2011) Rheological characterization of dilute acid pretreated softwood. Biotechnol Bioeng 108(5):1031–1041. https://doi.org/10.1002/Bit.23020

10. Um BH, Hanley TR (2008) A comparison of simple rheological parameters and simulation data for Zymomonas mobilis fermentation broths with high substrate loading in a 3-l bioreactor. Appl Biochem Biotechnol 145(1–3):29–38. https://doi.org/10.1007/s12010-007-8105-z
11. Stickel JJ, Knutsen JS, Liberatore MW et al (2009) Rheology measurements of a biomass slurry: an inter-laboratory study. Rheologica Acta 48(9):1005–1015. https://doi.org/10.1007/s00397-009-0382-8
12. Shobha MS, Tharanathan RN (2009) Rheological behaviour of pullulanase-treated guar galactomannan on co-gelation with xanthan. Food Hydrocoll 23(3):749–754. https://doi.org/10.1016/j.foodhyd.2008.04.006
13. Lavenson DM, Tozzi EJ, McCarthy MJ et al (2011) Yield stress of pretreated corn stover suspensions using magnetic resonance imaging. Biotechnol Bioeng 108(10):2312–2319. https://doi.org/10.1002/Bit.23197
14. Dibble CJ, Shatova TA, Jorgenson JL et al (2011) Particle morphology characterization and manipulation in biomass slurries and the effect on rheological properties and enzymatic conversion. Biotechnol Prog 27(6):1751–1759. https://doi.org/10.1002/Btpr.669
15. Chen HZ, Zhao ZM, Li HQ (2014) The effect of gas double-dynamic on mass distribution in solid-state fermentation. Enzyme Microb Technol 58–59(9):14–21
16. Li H, Chen HZ (2008) Near-infrared spectroscopy with a fiber-optic probe for state variables determination in solid-state fermentation. Process Biochem 43(5):511–516
17. Lindahl S, Liu J, Khan S et al (2013) An on-line method for pressurized hot water extraction and enzymatic hydrolysis of quercetin glucosides from onions. Anal Chim Acta 785(12):50–59
18. Petucci C, Li D, Mcconnell O (2007) Rapid screening of enzymes for the enzymatic hydrolysis of chiral esters in drug discovery. Chirality 19(9):701
19. Cartz L (1995) Nondestructive testing. Society for Nondestructive Testing
20. Xia ML, Wang L, Yang ZX et al (2015) A novel digital color analysis method for rapid glucose detection. Anal Methods 7(16):6654–6663
21. Zou BZ, Yue L, Yan XL et al (2013) Gold nanoparticles based digital color analysis for quinidine detection. Science Bull 58(17):2027–2032
22. Hirayama E, Sugiyama T, Hisamoto H et al (2000) Visual and colorimetric lithium ion sensing based on digital color analysis. AnaCh 72(3):465–474
23. Cantrell K, Erenas MM, De OPI et al (2010) Use of the hue parameter of the hue, saturation, value color space as a quantitative analytical parameter for bitonal optical sensors. Anal Chem 82(2):531–542
24. Rossel RAV, Minasny B, Roudier P et al (2006) Colour space models for soil science. Geoderma 133(3–4):320–337
25. Ford A (1998) Colour Space Conversions. Westminster University, London
26. Vermeir S, Nicolaï BM, Jans K et al (2007) High-throughput microplate enzymatic assays for fast sugar and acid quantification in apple and tomato. J Agric Food Chem 55(9):3240–3248
27. Laidler KJ (1984) The development of the Arrhenius equation. J Chem Education 61(6):494
28. Raja AS, Sankaranarayanan K (2012) Digital image processing technique for blood glucose measurement. Res J Med Sci
29. Tan J, Chu J, Wang Y et al (2014) High-throughput system for screening of Monascus purpureus high-yield strain in pigment production. Bioresources Bioprocess 1(1):1–7
30. Wang L, Xia ML, Zhang L et al (2014) Promotion of the Clostridium acetobutylicum ATCC 824 growth and acetone-butanol-ethanol fermentation by flavonoids. World J Microbiol Biotechnol 30(7):1969–1976
31. Wang L, Chen HZ (2011) Increased fermentability of enzymatically hydrolyzed steam-exploded corn stover for butanol production by removal of fermentation inhibitors. Process Biochem 46(2):604–607
32. Li C, Luo W, Xu H et al (2013) Development of an immunochromatographic assay for rapid and quantitative detection of clenbuterol in swine urine. Food Control 34(2):725–732

33. Eerikäinen T, Zhu YH, Linko P (1994) Neural networks in extrusion process identification and control. Food Control 5(2):111–119
34. Kiviharju K, Salonen K, Leisola M et al (2006) Modeling and simulation of Streptomyces peucetius var. caesius N47 cultivation and epsilon-rhodomycinone production with kinetic equations and neural networks. J Biotechnol 126(3):365–373
35. Unnikrishnan B, Palanisamy S, Chen SM (2013) A simple electrochemical approach to fabricate a glucose biosensor based on graphene–glucose oxidase biocomposite. Biosens Bioelectron 39(1):70–75
36. Jang HD, Kim SK, Chang H et al (2012) A glucose biosensor based on TiO 2–graphene composite. Biosens Bioelectron 38(1):184–188
37. Sun X, Wang J, Wei A (2008) Zinc oxide nanostructured biosensor for glucose detection. J Mater Sci Technol 24(4):649–656
38. Park S, Chung TD, Kim HC (2003) Nonenzymatic glucose detection using mesoporous platinum. Anal Chem 75(13):3046–3049
39. Tian H, Jia M, Zhang M et al (2013) Nonenzymatic glucose sensor based on nickel ion implanted-modified indium tin oxide electrode. Electrochim Acta 96:285–290
40. Zhang Y, Xu F, Sun Y et al (2011) Assembly of Ni $(OH)_2$ nanoplates on reduced graphene oxide: a two dimensional nanocomposite for enzyme-free glucose sensing. J Mater Chem 21 (42):16949–16954
41. Lyandres O, Yuen JM, Shah NC et al (2008) Progress toward an in vivo surface-enhanced Raman spectroscopy glucose sensor. Diabetes technology and therapeutics 10(4):257–265
42. Stuart DA, Yonzon CR, Zhang X et al (2005) Glucose sensing using near-infrared surface-enhanced Raman spectroscopy: gold surfaces, 10-day stability, and improved accuracy. Anal Chem 77(13):4013–4019
43. Rodriguez CS, Sanroman MA (2006) Application of solid-state fermentation to food industry–a review. J Food Eng 76(3):291–302
44. He Q, Chen HZ (2013) Pilot-scale gas double-dynamic solid-state fermentation for the production of industrial enzymes. Food Bioprocess Technol 6(10):2916–2924
45. Pandey A (2003) Solid-state fermentation. Biochem Eng J 13(2–3):81–84
46. Hölker U, Höfer M, Lenz J (2004) Biotechnological advantages of laboratory-scale solid-state fermentation with fungi. Appl Microbiol Biotechnol 64(2):175–186
47. Gowthaman MK, Ghildyal NP, Rao KS et al (1993) Interaction of transport resistances with biochemical reaction in packed bed solid state fermenters: the effect of gaseous concentration gradients. J Chem Technol Biotechnol 56(3):233–239
48. Hamidi-Esfahani Z, Shojaosadati SA, Rinzema A (2004) Modelling of simultaneous effect of moisture and temperature on A. Niger growth in solid-state fermentation. Biochem Eng J 21(3):265–272
49. Nagel FJ, Van AH, Tramper J et al (2002) Water and glucose gradients in the substrate measured with NMR imaging during solid-state fermentation with Aspergillus oryzae. Biotechnol Bioeng 79(6):653–663
50. Raghavarao KSMS, Ranganathan TV, Karanth NG (2003) Some engineering aspects of solid-state fermentation. Biochem Eng J 13(2–3):127–135
51. Mitchell DA, Krieger N, Stuart DM et al (2000) New developments in solid-state fermentation: II. Rational approaches to the design, operation and scale-up of bioreactors. Process Biochem 35(47):1211–1225
52. Chen HZ, Qiu WH, Liu SJ et al (2010) Key technologies for bioethanol production from lignocellulose. Biotechnol Adv 28(5):556–562
53. Krishna C (2005) Solid-state fermentation systems-an overview. Crit Rev Biotechnol 25(1–2):1–30
54. Chen HZ, Jian X, Li ZH (2005) Temperature control at different bed depths in a novel solid-state fermentation system with two dynamic changes of air. Biochem Eng J 23(2):117–122
55. Chen HZ, Li ZH (2007) Gas double-dynamic solid state fermentation technique and apparatus. U.S. Patent 7183074 B2

56. Chen HZ, He Q (2012) Value-added bioconversion of biomass by solid-state fermentation. J Chem Technol Biotechnol 87(12):1619–1625
57. Xu FJ, Chen HZ, Li ZH (2002) Effect of periodically dynamic changes of air on cellulase production in solid-state fermentation. Enzyme Microb Technol 30(1):45–48
58. Bellon-Maurel V, Orliac O, Christen P (2003) Sensors and measurements in solid state fermentation: a review. Process Biochem 38(6):881–896
59. Cen H, He Y (2007) Theory and application of near infrared reflectance spectroscopy in determination of food quality. Trends Food Sci Technol 18(2):72–83
60. Roggo Y, Chalus P, Maurer L et al (2007) A review of near infrared spectroscopy and chemometrics in pharmaceutical technologies. J Pharm Biomed Anal 44(3):683–700
61. Jin SY, Chen HZ (2007) Near-infrared analysis of the chemical composition of rice straw. Ind Crops Prod 26(2):207–211
62. Liu LY, Chen HZ (2007) Prediction of maize stover components with near infrared reflectance spectroscopy. Spectroscopy Spectral Anal 27(2):275–278
63. And SEK, Ii FEB (2002) Near-Infrared analysis of soluble and insoluble dietary fiber fractions of cereal food products. J Agric Food Chem 50(10):3024–3029
64. Bruno-Soares AM, Murray I, Paterson RM et al (1998) Use of near infrared reflectance spectroscopy (NIRS) for the prediction of the chemical composition and nutritional attributes of green crop cereals. Anim Feed Sci Technol 75(1):15–25
65. Shen H, Chen J (2003) Study on the application of near infrared reflectance spectroscopy (NIRS) technique for the prediction of fiber composition and silicification of rice straw. Sci Agric Sin
66. Sakurai Y, Lee TH, Shiota H (1977) On the convenient method for glucosamine estimation in koji. Agric Biol Chem 41(4):619–624
67. IUPAC (2014) Measurement of cellulase activities. Pure Appl Chem 59(2):257–268
68. Edwards PM (2002) Origin 7.0: scientific graphing and data analysis software. J Chem Inf Model 42(5):1270–1271
69. Gervais P, Molin P (2003) The role of water in solid-state fermentation. Biochem Eng J 13 (2–3):85–101
70. Liu J, Li DB, Yang JC (2007) Operating characteristics of solid-state fermentation bioreactor with air pressure pulsation. Appl Biochem Microbiol 43(2):234–239
71. Sheu WJ, Liou NC (1999) Effect of temporal variation of pressure on vaporization of liquid droplets. Int J Heat Mass Transf 42(21):4043–4054
72. Doran G, Zander A (2012) An improved method for measuring soil microbial activity by gas phase flow injection analysis. Revista Brasileira De Ciência Do Solo 36(2):349–357
73. Chen HZ, Shao MX, Li HQ (2013) Effects of gas periodic stimulation on key enzyme activity in gas double-dynamic solid state fermentation (GDD-SSF). Enzyme Microb Technol 56(6):35–39
74. Elmore JM, Coaker G (2011) The role of the plasma membrane H+ -ATPase in plant-microbe interactions. Mol Plant 4(3):416–427
75. Kültz D (2005) Molecular and evolutionary basis of the cellular stress response. Physiology 67(67):225–257
76. Serrano R (1988) Structure and function of proton translocating ATPase in plasma membranes of plants and fungi. ACBB 947(1):1–28
77. Spano G, Massa S (2006) Environmental Stress Response in Wine Lactic Acid Bacteria: Beyond Bacillus subtilis. Crit Rev Microbiol 32(2):77–86
78. Singhania RR, Patel AK, Soccol CR et al (2008) Recent advances in solid-state fermentation. Biochem Eng J 44(1):13–18
79. Koliander B, Hampel W, Roehr M (1984) Indirect estimation of biomass by rapid ribonucleic acid determination. Appl Microbiol Biotechnol 19(4):272–276
80. Matcham SE, Jordan BR, Wood DA (1985) Estimation of fungal biomass in a solid substrate by three independent methods. Appl Microbiol Biotechnol 21(1):108–112
81. Sharma PD, Fisher PJ, Webster J (1977) Critique of the chitin assay technique for estimation of fungal biomass. Trans Br Mycol Soc 69(69):479–483

82. Barak R, Chet I (1986) Determination, by fluorescein diacetate staining, of fungal viability during mycoparasitism. Soil Biol Biochem 18(3):315–319
83. Bengtsson G, Rundgren S (1983) Respiration and growth of a fungus, Mortierella isabellina, in response to grazing by Onychiurus armatus (Collembola). Soil Biol Biochem 15(4):469–473
84. Brezonik PL, Browne FX, Fox JL (1975) Application of ATP to plankton biomass and bioassay studies. Water Res 9(2):155–162
85. Frankland JC, Bailey AD, Gray TRG et al (1981) Development of an immunological technique for estimating mycelial biomass of Mycena galopus in leaf litter. Soil Biol Biochem 13(2):87–92
86. Nopharatana M, Howes T, Mitchell D (1998) Modelling fungal growth on surfaces. Biotechnol Tech 12(4):313–318
87. Richard A, Sergio H, Maurice R et al (1990) Ion exchange resin: a model support for solid state growth fermentation of Aspergillus niger. Biotechnol Tech 4(6):391–396
88. Abd-Aziz S, Gan SH, Hassan MA et al (2008) Indirect Method for Quantification of Cell Biomass During Solid-State Fermentation of Palm Kernel Cake Based on Protein Content. Asian J Sci Res 1(4)
89. Terebiznik MR, Pilosof AMR (1999) Biomass estimation in solid state fermentation by modeling dry matter weight loss. Biotechnol Tech 13(3):215–219
90. Crawford JW, Ritz K, Young IM (1993) Quantification of fungal morphology, gaseous transport and microbial dynamics in soil: an integrated framework utilising fractal geometry. Geoderma 56(1–4):157–172
91. Marín S, Cuevas D, Ramos AJ et al (2008) Fitting of colony diameter and ergosterol as indicators of food borne mould growth to known growth models in solid medium. Int J Food Microbiol 121(2):139–149
92. Camacho DBH, Jiménez AA, Chanonapérez JJ et al (2011) Morphological characterization of the growing front of Rhizopus oligosporus in solid media. J Food Eng 101(3):309–317
93. Donnelly DP, Boddy L, Leake JR (2004) Development, persistence and regeneration of foraging ectomycorrhizal mycelial systems in soil microcosms. Mycorrhiza 14(1):37–45
94. Juge C, Champagne A, Coughlan AP et al (2009) Quantifying the growth of arbuscular mycorrhizal fungi: usefulness of the fractal dimension. Botany-botanique 87(4):387–400 (314)
95. Arelli A, Luccarini L, Madoni P (2009) Application of image analysis in activated sludge to evaluate correlations between settleability and features of flocs and filamentous species. Water Sci Technol A J Int Association Water Pollut Res 59(10):2029–2036
96. Perez Leite YG, Coelho SGF et al (2006) Activated sludge morphology characterization through an image analysis procedure. Braz J Chem Eng 23(3):319–330
97. Amaral AL, Ferreira EC (2005) Activated sludge monitoring of a wastewater treatment plant using image analysis and partial least squares regression. Anal Chim Acta 544(1):246–253
98. Smets I, Banadda E, Deurinck J et al (2006) Dynamic modeling of filamentous bulking in lab-scale activated sludge processes. J Process Control 16(3):313–319
99. Meskauskas A, Mcnulty LJ, Moore D (2004) Concerted regulation of all hyphal tips generates fungal fruit body structures: experiments with computer visualizations produced by a new mathematical model of hyphal growth. Mycol Res 108(4):341–353
100. Boswell GP, Jacobs H, Ritz K et al (2007) The development of fungal networks in complex environments. Bull Math Biology 69(2):605–634
101. Rahardjo YS, Tramper J, Rinzema A (2006) Modeling conversion and transport phenomena in solid-state fermentation: a review and perspectives. Biotechnol Adv 24(2):161–179
102. Mitchell DA, Meien OFV, Krieger N et al (2004) A review of recent developments in modeling of microbial growth kinetics and intraparticle phenomena in solid-state fermentation. ChemInform 17(27):15–26
103. Otsu N (1979) A threshold selection method from gray-level histograms. IEEE Trans Syst Man Cybernetics 9(1):62–66
104. Theiler J (1990) Estimating fractal dimension. J Optical Soc Am A 7(6):1055–1073

105. Schack KH, Wilpert KV, Hildebrand EE (2000) The spatial distribution of soil hyphae in structured spruce-forest soils. Plant Soil 224(2):195–205
106. Viccini G, Mitchell DA, Boit SD et al (2001) Analysis of growth kinetic profiles in solid-state fermentation. Food Technol Biotechnol 39(4):271–294
107. Sun T, Li P, Liu B et al (1997) Solid state fermentation of rice chaff for fibrinolytic enzyme production by Fusarium oxysporum. Biotechnol Lett 19(5):465–467
108. Laukevics JJ, Apsite AF, Viesturs US et al (1985) Steric hindrance of growth of filamentous fungi in solid substrate fermentation of wheat straw. Biotechnol Bioeng 27(12):1687–1691
109. Blackledge J, Barry D (2011) Morphological analysis from images of hyphal growth using a fractional dynamic model. Theory & Practice of Computer Graphics, Warwick, United Kingdom
110. Boswell GP, Hopkins S (2008) Linking hyphal growth to colony dynamics: spatially explicit models of mycelia. Fungal Ecol 1(4):143–154
111. Boswell GP (2008) Modelling mycelial networks in structured environments. Mycol Res 112(Pt 9):1015–1025
112. Feng XM, Olsson J, Swanberg M et al (2007) Image analysis for monitoring the barley tempeh fermentation process. J Appl Microbiol 103(4):1113–1121

Chapter 8
Industrial Application of High-solid and Multi-phase Bioprocess

Abstract In this chapter, two typical high-solid and multi-phase bioprocesses including cellulosic ethanol fermentation and cellulase fermentation are discussed. In cellulosic ethanol production, selective fractionation and oriented conversion of lignocellulose based on steam explosion is the core of the whole technology. Selective fractionation is realized by steam explosion and whole components of lignocellulose are effectively used. Gas double-dynamic solid-state fermentation is employed for cellulase production. Both technological and economic feasibility in the two systems are analyzed. The two demonstration projects prove that high-solid and multi-phase bioprocess have economic and environmental benefits, which can effectively promote Chinese bioindustry development.

Keywords Steam explosion · Selective fractionation · Gas double dynamic Industrial application

8.1 Industrialization Application of High-solid Enzymatic Hydrolysis Coupled with Fermentation Technology

There are many problems in submerged fermentation which are considered as the majority of fermentation industry. Annual wastewater production in submerged fermentation industry is 2.8 billion m^3 which causes environmental pollution because of high concentration of organics produced. Additionally, complex material pretreatment and mechanical agitation result in high energy consumption. Low products concentration lead to high separation cost [1]. Huge pressure from resources and environment have become the bottleneck restricting the sustainable development of bioindustry [2]. At present, the crisis of energy, grain, and environment is becoming more serious. High-solid fermentation technology which is featured by high-solid content and less water can be the solution. In high-solid and multi-phase system, cheap materials (such as corn stover, wheat straw) can be used. Less water is produced in solid-state fermentation and energy cost is low.

H. Chen, *High-solid and Multi-phase Bioprocess Engineering*,
Green Chemistry and Sustainable Technology,
https://doi.org/10.1007/978-981-10-6352-7_8

Therefore, solid-state fermentation could be a solution to energy, food and environmental crisis and the focus in green bioindustry [3].

Lignocellulose is sustainable resources which widely spread on earth [4]. Producing high value-added chemicals from lignocellulose has been the hot topic in various fields around the world. United States Department of Energy has claimed that no less than 10% petroleum-based products will be taken from biomass by 2020 and increase to 50% by 2050. In 2030, biomass will provide 5% electric power, 20% fuels, and 25% chemicals. In China, Laws of Renewable Resource stipulates that 10% primary energy should be taken from renewable energy [5]. No matter from the view of energy demand or environmental protection, producing chemical from lignocellulose (such as corn stover) is beneficial to boosting sustainable development and reducing greenhouse gases.

Bioethanol is a promising biofuel which could be produced from lignocellulose. It has the advantages of environmental friendly and has attracted much attention. Bioethanol can be used as fuels for cars which could reduce exhaust pollution. Therefore, as an environmental friendly industry, it should be greatly encouraged. In the long term, from the perspective of whole ecological balance, it is a great ideal to produce ethanol from agricultural wastes [6–8]. High-solid loading is the necessary condition to reduce total cost in lignocellulose conversion system and has become the hot topic in biorefinery. Most scholars focus on converting cellulose into ethanol while neglecting lignin and hemicellulose in lignocellulose. The single component utilization will inevitably hinder industrialization of ethanol production in economy. Additionally, the unused composition will lead to waste of resources and environmental pollution when released to nature. Selective fractionation and oriented conversion in biorefinery of lignocellulose targets to break the traditional concept of single product with single component. It makes the most use of components and intermediates, realizing whole components usage and achieving the most value of the lignocellulose.

8.1.1 Key Technologies of Producing Bioethanol from Lignocellulose

Ethanol production from lignocellulose has been widely reported at home and abroad. It has stagnated and the reasons are concluded as follows. (1) It is hard for one single technology to take the utilization of cellulose, hemicellulose, and lignin at the same time. Single component usage will cause environmental pollution and waste of resources. (2) Lacking of the breakthrough of key technologies on the conversion of cellulosic materials. Pretreatment of the raw material is premise for lignocellulose conversion. Traditional acid hydrolysis pretreatment could cause high cost and serious environmental pollution. High price of cellulase directly increases total cost in ethanol production. (3) Technology integration for industrial production is deficient [6]. It is difficult to rely on a single technology or take

Table 8.1 Key technical problems and solving strategies during the development of cellulosic ethanol industrialization

Process	Industrialization problems	Key technology
Pretreatment of raw material	Lack of a new, clean, efficient, and less inhibitors existed process to remove biomass recalcitrance naturally	With steam explosion as the core, resolve refining technology system selectively
Bacterial strain for fermentation	Problems about pentose/hexose simultaneous fermentation to ethanol, how to remove the inhibitors in enzymatic hydrolysis liquid glucose efficiently	Strains for pentose/hexose simultaneous fermentation
Enzymatic hydrolysis fermentation pattern	Long process cycle time of a two-step method for enzymatic hydrolysis fermentation	Coordinated enzymatic hydrolysis of multienzyme system; new process of solid phase depolymerization simultaneous fermentation
Comprehensive utilization	How to take higher value applications on each component among raw material	Process of higher value applications of biomass

utilization of one single component to realize the preparation of ethanol from corn stover. Biological properties of the raw materials must be fully understood and methods should be greatly polished. Only by this can the key technological problems can be solved. The key technical problems and solving strategies during the development of cellulosic ethanol industrialization are shown in Table 8.1.

8.1.1.1 Efficient and Clean Technology of Components Selective Fractionation

Steam explosion pretreatment could break down the original organization structure through instantaneous pressure discharge, pressure difference inside and outside the material, and collision force between materials and equipment. Compared with untreated corn stover, porosity and pore size of steam-exploded corn stover increased 10.12% and 3.74 times, respectively. Specific surface area and curvature of steam-exploded corn stover deceased 81.79% and 55.27%, respectively. All changes of the cornstalk proved that steam explosion is an efficient method to break down the intrinsic tight porous structure of the original plant biomass.

Based on the cognition of porous properties of lignocellulose, steam explosion can be an effective solution in selective fractionation of lignocellulose refinery. It can maintain the original macromolecular structure and activate the bioactivity of degradable components. Most of the components can be made the most use after steam explosion treatment. From the perspective of efficiency, economy and cleanness steam is a favorable selective fractionation technology. Based on the properties of lignocellulose, steam explosion realizes selective fractionation of hemicellulose and high-valued usage. The cellulose in lignocellulose has been

maintained. The destroyed biomass recalcitrance is beneficial to the degradation of cellulose and improves enzymatic hydrolytic efficiency. Additionally, reducing inhibitors during pretreatment process can be realized by optimizing steam explosion intensity. The intermediate products can be made the most use. Therefore, selective fractionation technology based on steam explosion is the breakthrough in lignocellulose pretreatment, which builds a firm foundation for the industrialization of ethanol production.

8.1.1.2 Construction and Domestication of Strain Capable of Co-fermenting Pentose and Hexose

The productivity of bioethanol depends on three factors, including strains, fermentation process, and subsequent extraction process. Good industrial strain has great significance on quality, output, and production cost of ethanol fermentation directly. *Saccharomyces Cerevisiae* is a traditional strain for producing ethanol, whose genome has been sequenced completely. *Saccharomyces Cerevisiae* could make use of xylulose. Constructing metabolic engineering strain of *Saccharomyces Cerevisiae* that can make use of the pentose and hexose simultaneously. Steam-exploded corn stover is considered as the substrate to domesticate modified yeast strain. And concentrations of glucose and xylose hydrolysate were 135 g/L and 25.8 g/L respectively in steam explosion corn stover enzymatic hydrolysate. Ethanol production capacity of the naturalized strain on steam-exploded straw hydrolysate was investigated. Results showed that resistance and ability of five-carbon sugar metabolism of the strain were enhanced. Ethanol yield increased significantly when the steam-exploded corn stover hydrolysate was used as substrate. Dynamic domestication may effectively reduce the sensitivity of ATP synthase to H^+ gradient on both sides of cytoplasm membrane of strains. This ensured normal usage of the oxidative phosphorylation in yeast cells and made the glycolysis process smoothly, contributing to improve the cell tolerance ability.

8.1.1.3 Efficient Multienzyme System Enzymatic Hydrolysis and Synergistic Cooperation

It is the key of reducing enzymatic hydrolysis cost and realizing ethanol production industrialization to improve the enzymatic hydrolysis efficiency of lignocellulose. With the development of genetic engineering, the cellulase production also improved significantly. However, genetic engineering is never the only way of solving problems in ethanol production. It must be noticed that lignocellulose is a biomass with complicated chemical composition and physical structure. High content of lignin–hemicellulose complex in lignocellulose can lead to invalid adsorption and shielding effect of cellulase. The author has proposed a new enzymatic technology that takes synergetic advantages among laccase, ferulic acid esterase, helicase, and cellulase. Reducing sugar yield increased 37.9% and ethanol yield increased by 13.8 times in laccase–cellulase

system. Additionally, in synergetic system of ferulic acid esterase and cellulase, enzymatic efficiency of steam-exploded corn stover increased 32%.

8.1.1.4 Enhancing of Depolymerization and Simultaneous Saccharification by High-solid Enzymatic Hydrolysis

High energy consumption and large amount of wastewater discharge is one of the key problems for the economic operation of ethanol industrialization [7]. In order to reduce energy consumption, a new technology was established. High-solid enzymatic hydrolysis was employed to enhance deploymerization, followed by simultaneous saccharification and fermentation of the whole sugar. Steam-exploded corn stover is degraded under the condition of 45–50 °C for 7–9 h with high-solid loading. The pre-degraded substrate was incubated with naturalized yeast for simultaneous saccharification and fermentation. Over 60 g/L ethanol was obtained under the condition of 30–35 °C for 63–65 h. In a 400 m^3 enzymatic bioreactor, over 13% reducing sugar was obtained in high-solid enzymatic system. Compared with step enzymatic and fermentation technology, the period was shortened and sugar in high-solid enzymatic system did not inhabit enzymatic and fermentation process. Compared with regular simultaneous saccharification and fermentation, high initial sugar content improved ethanol productivity and shortened fermentation period, therefore, increasing economy of biomass-based ethanol.

8.1.2 Demonstration Project

In May 2014, based on the above ethanol conversion technology system, a 10,000 ton ethanol production line has been established in Jilin province, China, which has realized the large-scale production of straw ethanol. The technical route is shown as follows (Fig. 8.1).

In this technical route, steam-exploded corn stover was directly subjected to pre-degradation in multienzyme system after steam explosion treatment. There is no need for detoxification so as to simplify the technological process. The naturalized yeast can make use of both pentose and hexose for ethanol fermentation, hence improving the utilization rate of raw materials and reducing the cost of ethanol fermentation. Fermented mash was used to produce marsh methane which could be used in cars after being cleaned and compressed. The residual which was featured by high lignin content was used for thermoplastic composite material production with additionally PVC. The multiproduct technology is simple and has great potential in solving single product in domestic ethanol production market.

The ten-thousand ton ethanol production line includes six steam explosion tanks (50 m^3), eight enzymatic hydrolysis and fermentation bioreactors (400 m^3), and distillation equipment. The line has the production capacity of 20-thousand tons

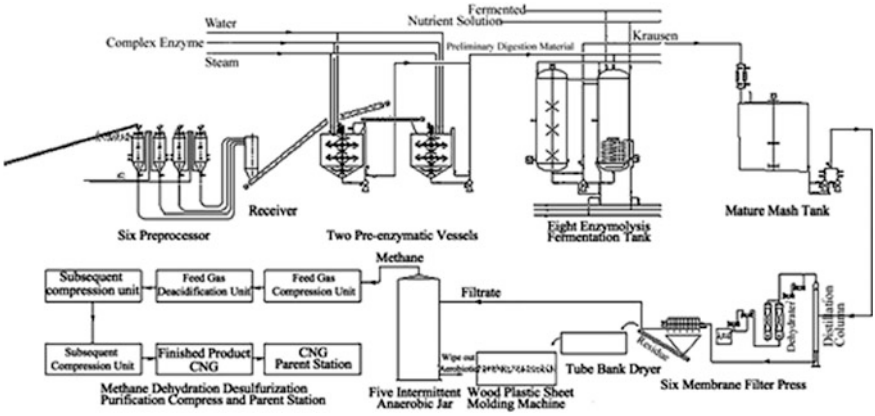

Fig. 8.1 Ton class of straw refinery industrialization of ethanol production line

lignocellulose-based ethanol, 60-thousand tons thermoplastic composite material and one million m^3 CNG.

An assessment on the economic feasibility has been made for this demonstration project, and analysis results are shown in Table 8.2. Ethanol, thermoplastic composite materials, and CNG are 20-thousand tons/year, one million m^3/year, and 60-thousand tons/year, respectively. The total cost of is distributed to the material cost, cost of operating, cost of maintenance, and cost of investment. Product cost of ethanol is mainly affected by the costs of material and investment, the costs of maintenance and operating accounted for less proportion. It can be seen from Table 8.2 that the total cost of ethanol production is 6888 yuan/ton. Material costs accounted for 52.1% of the total cost, including 25.41% of corn stover and 21.78% of enzyme preparations. Since the project for coproduction demonstration project, taking the thermoplastic composite materials and CNG production into account, the comprehensive production cost of cellulosic ethanol is about 5572 yuan/ton, which is similar to grain ethanol.

The coupling technology of high-solid enzymatic hydrolysis and fermentation for ethanol production is the solution to improving enzymatic hydrolytic efficiency and reducing ethanol production cost. This technology has the advantages of less cellulase, lower cost, and less wastewater. Saccharification and fermentation were conducted in separate region of the bioreactor which is beneficial to coordinate the optimum temperature. Additionally, this technology combined saccharification, fermentation, and adsorption separation, which reduced ethanol cost. The established industrial straw refinery technology realized multi-composition utilization and high-value conversion of the materials. It promotes the footsteps of renewable energy development and is beneficial to realize the independence of national energy and reduce environmental pollution. Additionally, the established industrial production line of coproduct can greatly promote the development of biomass-based energy industry and serve human beings.

Table 8.2 Cost of each part in cellulosic production

Name	Cost (¥/ton ethanol)	Product		
		Ethanol	Lignin thermoplastic composites	Compressed natural gas (CNG) fueling for vehicles
Material cost	1750.00	1050.00	525.00	175.00
Enzyme cost	1500.00	1500.00		
Other material costs	357.13	357.13		
Electricity	1135.00	829.20	305.80	
Water	36.33	36.33		
Steam	540.54	540.54		
Wastewater treatment	79.00			79.00
Maintenance operation	200.00	200.00		
Investment	1290.00	1058.4	231.60	
Total cost	6888.00	5571.60	1062.40	254.00

8.1.2.1 Industrialization Application of Gas Double-Dynamic Solid-State Fermentation Technology

With the continuous consumption of fossil fuels and the increasingly serious environmental pollution, the world's energy problem is becoming more and more prominent. In order to alleviate the problem of the shortage of fossil fuels and environmental degradation, people have been focused on looking for renewable energy. Cellulose is the most abundant renewable resource on earth, which accounts for 80% of terrestrial ecosystem biomass. The full utilization of cellulose is of great significance in solving environmental pollution, energy crisis, and food shortage [8]. If cellulose can be economically and effectively converted into fuel ethanol which could produce biodiesel will alleviate the current energy crisis and environmental pollution crisis. Additionally, it will be conducive to human society to achieve sustainable development. Cellulase is an environmental friendly biocatalyst and is one of the most important elements in bioconversion of cellulose materials. However, the cost of cellulase production accounts for about 50–60% of the production cost of cellulose-based fuel ethanol, which directly impacts the industrialization of cellulose-based fuel ethanol production [9]. Therefore, it is of great significance to study the production of cellulase with high yield.

The cellulase is mainly composed of three kinds of enzymes including endo-β-glucanase, exo-β-glucanase, and β-glucosidase. They form the multicomponent enzyme system and play the role through synergy during enzymatic hydrolysis. Endo-β-glucanase and exo-β-glucanase play the role of degrading cellulose into oligosaccharides and cellobiose, and β-glucosidase was used to degrade oligosaccharides and cellobiose into glucose [10, 11].

Cellulase has many advantages such as high specificity, mild reaction condition, and low environmental pollution. However, due to the low efficiency of enzyme production, long produce cycle, poor heat resistance, short life and high cost, which limited industrial production of cellulase. Submerged fermentation has been the main method for cellulose production. Large-scale production of cellulase can be realized by liquid fermentation, but there are some problems limiting the cellulase in industrial applications including low productivity and high production costs. The use of solid-state fermentation for cellulase production has many advantages, such as low cost and higher productivity (2–3 folds yield of submerged fermentation) [12]. In addition, the purity of the enzyme is not demanding for the conversion of cellulose to cellulose-based fuel ethanol, cellulase production by solid-state fermentation can be directly used for enzymolysis of lignocellulose. Cellulase by solid-state fermentation has high content which reduces the concentration steps of downstream, further reducing the cost of cellulose production.

But the large-scale production of cellulase by solid-state fermentation is not rapidly developed, mainly because solid-state fermentation has difficulties in large-scale sterilization, heat transfer, and mass transfer in the solid substrate [13, 14]. Gas is the continuous phase in solid-state fermentation, and due to the low thermal conductivity of gas phase and inhomogeneous heat distribution in the solid matrix, the strict sterilization is usually hard to complete. However, in the heat sterilization process, heat will not only cause damage to microbial cells but also cause damage to the nutrients in the medium. In the research of solid medium sterilization, solid matrix properties should be taken account. In the traditional solid-state fermentation, mechanical agitation was employed to strengthen mass and heat transfer in the solid matrix. However, too much mechanical agitation is harmful to the growth of microorganism, and breaks the mycelium, the shear force caused by agitation is often harmful to the cell. So it is necessary to study new solid-state fermentation technology and reactor to solve the problems of difficult heat transfer and difficult mass transfer in solid matrix of traditional solid-state fermentation.

8.1.2.2 New Method for High Efficient Sterilization of Solid Medium

As a new method of sterilization, steam explosion is used to sterilize solid medium. Steam explosion sterilization could reduce the destruction of nutrients as much as possible under the premise of achieving the sterilization effect. And it improves the utilization of sterilization equipment and enhances production efficiency. Steam explosion operating procedures are described as follows: steam explosion tank is inlet the saturated steam, the pressure can be maintained in a steam explosion tank for a specific period of time while a certain pressure in steam explosion tank is reached, and then suddenly relief pressure in the tank. Then the material is instantaneously excreted with steam [15].

Steam explosion sterilization is feasible and efficient for solid culture medium. Two main processes are included in the steam explosion sterilization, including pressure maintenance stage and pressure discharge stage. During pressure maintenance stage, the steam with high temperature and high pressure in steam explosion tank has the thermal sterilization effect. During pressure discharge stage, the pressure in the tank is suddenly released which will cause the destruction of microbial cell structure. When sterilized by steam explosion at 128 °C for 1 min, the microbial survival rate has reached $10^{-5.1}$, meeting sterilization requirement which is less than 10^{-3}. When the conditions of steam explosion sterilization are at 128 °C for 5 min, microbe was completely killed in this system.

Steam explosion sterilization improves the nutrient content of solid medium and promotes the performance of solid-state fermentation. Under the premise of satisfying sterilization, the glucose content of culture medium by steam explosion sterilized with high-temperature and short-term conditions were 66.7–157.1% higher than that of the conventional steam sterilization at 121 °C for 20 min of the same culture medium, steam explosion sterilization effectively raises the solid-state fermentation level.

Steam explosion sterilization increased the sterilization temperature and which has instantaneous blasting effect could shorten the high-temperature maintenance time and reduce the stage of cooling. Comparing with conventional steam sterilization with batch operation, steam explosion sterilization shortened 69.8% of the sterilization time. The total steam consumption of steam explosion sterilization was 1.66% lower than that of conventional steam sterilization. Steam explosion sterilization is more efficient than conventional steam sterilization in achieving sterilization industrialization, and therefore, promoting solid-state fermentation development [16].

8.1.2.3 Development of New Type Reactor for Solid-State Fermentation Process

The key to the success of the industrialization of solid-state fermentation of cellulase is the reactor. As a new kind of solid-state fermentation reactor, gas double-dynamic solid-state fermentation bioreactor has been applied to the industrial production of cellulase, which has already showed its industrial feasibility. The pulsation and circulation of airflow in gas-phase double-dynamic solid-state fermentation reactor can effectively improve the heat transfer and oxygen transfer in the solid-state fermentation process, which could promote the growth and metabolism of the cell and realize large-scale pure culture of strains. The main features are as follows:

(1) Compared with the traditional solid-state fermentation, the heat transfer and oxygen transfer in the solid bed in the gas-phase double-dynamic solid-state fermentation reactor can be effectively enhanced by pressure pulsation and the circulation rate. Gas-phase double-dynamic solid-state fermentation reactor can eliminate the temperature gradient of the solid bed.

(2) Based on pressure pulsation, air circulation, gas double dynamic (pressure pulsation and air circulation) was formed, which further improves the temperature distribution and humidity distribution of solid-state fermentation, and optimizes the cell growth and metabolism.

(3) Developed a gas double-dynamic solid-state fermentation bioreactor of 100 m^3 production scale, which is the largest solid-state fermentation process for the production of cellulase and other preparations both at home and abroad.

The enhanced effect of the gas double-dynamic state on the solid-state fermentation process is concluded as follows: (1) the gradient of temperature and humidity in the culture medium is reduced [12]; (2) the particles of the medium are loosened, and the space for microbial growth is provided [17]; (3) Medium and heat exchange between the reactor; (4) it can stimulate microorganisms and boost microbial growth [18]. The gas double-dynamic solid-state fermentation effectively enhances the heat transfer and oxygen transfer in the solid bed in the fermentation reactor, and eliminates the temperature gradient in the solid bed. It overcomes the limitations of traditional solid-state fermentation (such as pure microorganism culture in large scale) and greatly broadens the application of solid-state fermentation in modern fermentation industry. Additionally, it changes the idea that solid-state fermentation is an old and backward production method. Compared with the submerged fermentation, the energy consumption was reduced by 87.5%, and a large amount of organic wastewater was eliminated.

8.1.2.4 Application of Gas Double-Dynamic Solid-State Fermentation in the Industrialization of Cellulase

Based on the gas-phase double-dynamic solid-state fermentation, cellulase production line with 800 tons of cellulase annually year has been established in Dongping County, Shandong province, China, and the technical routes which are shown in Fig. 8.2.

In the technical route, straw is pretreated by steam explosion then directly goes to gas double-dynamic solid-state fermentation, which has simplified the process.

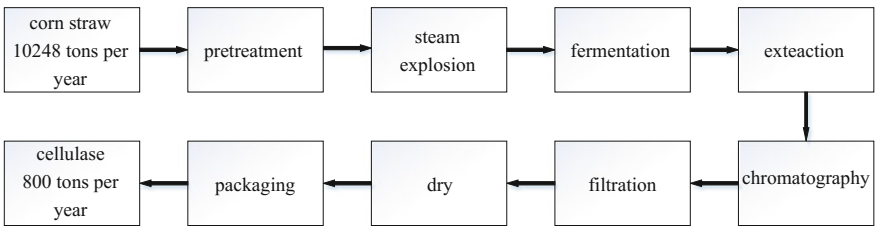

Fig. 8.2 Flowchart of the cellulase procedure

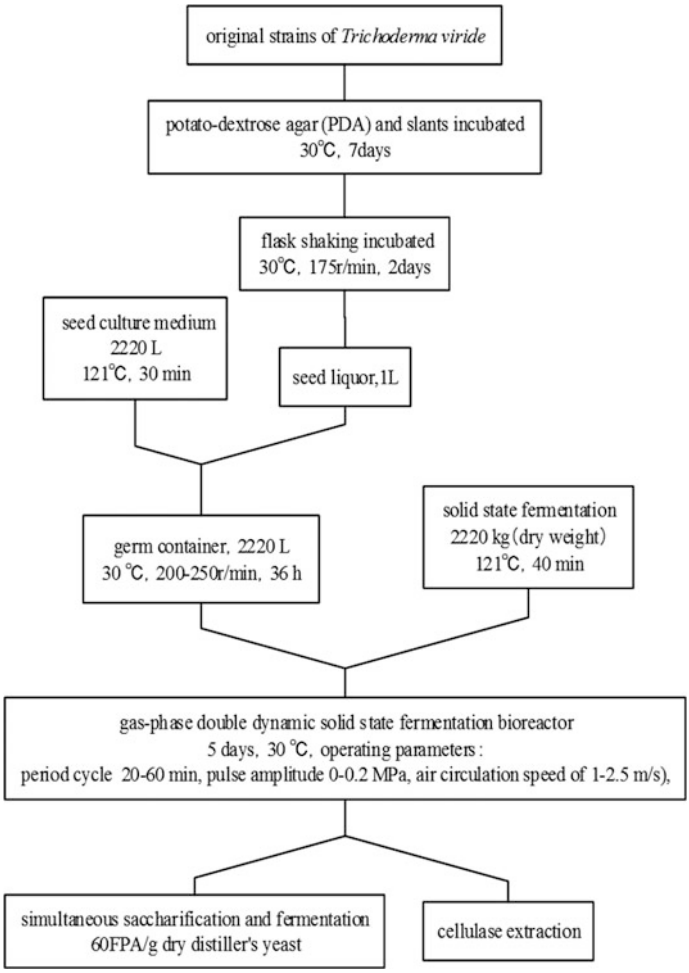

Fig. 8.3 Technical route of cellulase production

Technical route of cellulase production in 100 m^3 gas double-dynamic solid-state fermentation bioreactor is described in Fig. 8.3.

Production of cellulase with steam-exploded corn stover by gas double-dynamic solid-state fermentation not only shortened the fermentation period (The period of traditional solid-state fermentation from 6–7 d to 4–5 d) but also improved the cellulase enzyme activity. After 5 batch experiments, the average activity of cellulase has reached to 120 FPA/g dry medium, which even could reach the highest of 210 FPA/g dry medium.

The cellulase production process by gas double-dynamic solid-state fermentation reactor has the following characteristics: (1) There is no solid layer mechanical stirring device. Gas double dynamic and circulating fan could achieve the

requirement of mass transfer and heat transfer together; (2) The positive pressure is maintained by sterile compressed air so as to strictly meet the requirements of pure microorganism culture; (3) Gas double dynamic could effectively promote microbial metabolism, and strengthen intracellular and extracellular mass transfer, reduce the feedback inhibition of metabolite, thereby shorten the fermentation period and improve the fermentation yield; (4) Air circulation forced by blower ensures the uniformity of temperature and humidity of the reactor.

The cellulase production line has included four steam explosion tanks with the volume of 5 m^3, and five gas double-dynamic solid-state fermentation tanks with the volume of 100 m^3. This production line could produce 800 tons cellulase enzyme every year. And the main equipment and models are shown in Table 8.3.

Figure 8.4 shows the 5 m^3 steam explosion for high efficient sterilization of solid medium. And Fig. 8.5 is the 100 m^3 gas double-dynamic solid-state fermentation reactor applied to the cellulase production.

This product line has been made an economic feasibility analysis, and the analysis results are concluded as follows: production capacity of cellulase is 800 tons per year, and the production cost of cellulase is mainly influenced by raw material cost and the investment cost. From Table 8.4, the total cost of cellulase production is 19,836 yuan/t, and the cost of raw material occupied 19.4% of total costs.

Submerged fermentation for cellulase production will not only produce large amounts of organic wastewater (80 tons of wastewater/per ton of product), but also consume a large amount of energy. With the application of gas double-dynamic solid-state fermentation technology to cellulase production, there is no need to invest in the construction of large organic wastewater treatment plant and save 20 million yuan. Prices of cellulase produced with traditional solid-state fermentation and submerged fermentation technology for cellulase production were 150,000 and 119,000 yuan/t, respectively. However, the factory price of cellulase produced with

Table 8.3 Main equipment and models

No	Equipment and model	Size	Quantity
1	Solid-state fermentation reactor	V100 m^3	5
2	Steam explosion tank	V5 m^3	4
3	Steam braising tank	V3 m^3	2
4	Germ container	V1 m^3 N7.5KW	4
5	Air purifier	Q120Nm^3/min	4
6	Extraction tank	V25 m^3	4
7	Filter	5 m^3/h	2
8	Ultrafilter	hollow fiber	2
9	Plate tank	1.5 m^3	2
10	Vacuum drying oven	28 kg/h N10KW	2
11	Water ring vacuum pump	2SK-A N7.5KW	2

Fig. 8.4 5 m^3 steam explosion tank

Fig. 8.5 100 m^3 gas double-dynamic solid-state fermentation tanks

gas double-dynamic solid-state fermentation technology is 72,800 yuan/t, considering all aspects of the production process included. Cellulase price is dropped substantially which means the biofuel could make a breakthrough in the future.

Table 8.4 The production cost of cellulase with capacity of 800 tons per year

Items	Cost (yuan)
Main material costs	3.0744 million
Building investment costs	7.1808 million
Water and electricity costs	0.6917 million
Steam costs	7.41 ten thousand
Investment in environmental	One million
Maintenance and depreciation costs	1.8475 million
Labor and manufacturing costs	2 million
Total costs	15.8685 million

The production line has established 5 sets of 100 m^3 gas double-dynamic solid-state fermentation tanks. The annual profit could reach 32.1208 million and 10.28004 million yuan of tax.

References

1. Chen HZ, Peng XW (2009) Bioprocess engineering and fermentation industry-research progress of raw material substitution and cleaner production in fermentation Industry. In: China Fermentation Industry Association Member Congress, 2009
2. Chen HZ, Xu J (2004) Principle and application of modern solid state fermentation. Chemcial Industry Press, Beijing
3. Shi Y (2008) Study on spore production of Verticillium lecanii in solid-state fermentation. Zhejiang SciTech University
4. Li ZQ, Xu L, Xu P (2013) Analysis of international development situation of lignocellulose biorefinery. Biotechnol Bus 4:36–39
5. Chen HZ, Qiu WH, Xing XH et al (2009) Development of the biomass material refining process for the next generation biological and chemical industries. China Basic Sci 11(5):34–396
6. Chen HZ, Qiu WH (2007) The crucial problems and recent advance on producing fuel alcohol by fermentation of straw. Prog Chem 19(z2):1116–1121
7. Qu YB (2014) Status and prospect of non-grain biomass refining technology industrialization. Biotechnol Bus 2:20–24
8. Doelle HW, Mitchell DA, Rolz C (2009) Solid Substrate Cultivation. Elsevier Appl Sci, London and New York
9. Ji CX, Du FG, Shi JP et al (2007) Research advance in the use of cellulsae to produce fibrous ethanol. Liquor Mak Sci Technol 7:118–121
10. Liu JL, Wang J (2008) Research progress in cellulase excreted from biology. Chem Bioeng 25(12):9–12
11. Li YL, Lin KC (2016) Research advances of cellulase production. J Jinan Vocat Coll 2:99–101
12. Xu FJ, Chen HZ, Li ZH (2002) The solid-state fermentation with double dynamic of gas phase for celluloses. Chin J Environ Sci 23(3):53–58
13. Ghildyal NP, Ramakrishna M, Krishnaiah MM (1992) Scale-up strategies for solid state fermentation systems. Process Biochem 27(92):259–273
14. Ryoo D, Murphy VG, Karim MN et al (1991) Evaporative temperature and moisture control in a rocking reactor for solid substrate fermentation. Biotechnol Tech 5(1):19–24

15. Zhao ZM, Wang L, Chen HZ (2015) Physical structure changes of solid medium by steam explosion sterilization. Bioresour Technol 203 (Mar):204–210
16. Zhao ZM, Wang L, Chen HZ (2015) A novel steam explosion sterilization improving solid-state fermentation performance. Bioresour Technol 192(5):547–555
17. Xu FJ, Chen HZ, Shao MJ et al (2002) Observation of solid-state fermentation process of cellulase by enviromental scanning electron microscopy(ESEM). J Chin Electron Microsc Soc 21(1):25–29
18. Li HQ, Chen HZ (2005) The periodic change of environment factors in solid state fermentation and effect on microorganism fermentation. Chin J Biotechnol 21(3):440–445